UiT The Arctic University of Norway

Faculty of Health Sciences
Department of Pharmacy

Advanced topical delivery systems for membrane-active antimicrobials

Exploring nature to improve antimicrobial wound therapy

Lisa Myrseth Hemmingsen

A dissertation for the degree of Philosophiae Doctor - August 2022

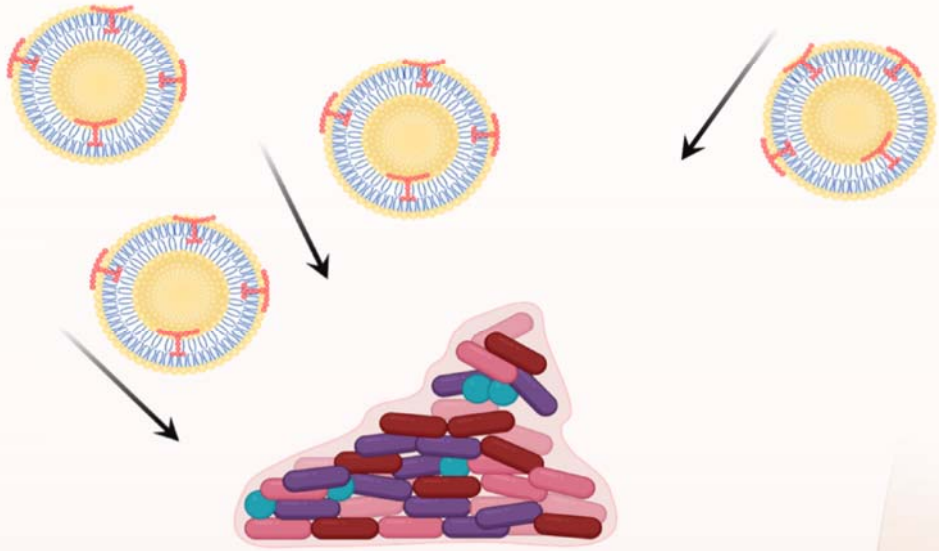

A dissertation for the degree of Philosophiae Doctor

Advanced topical delivery systems for membrane-active antimicrobials

Exploring nature to improve antimicrobial wound therapy

Lisa Myrseth Hemmingsen

Tromsø, 2022

Drug Transport and Delivery Research Group

Department of Pharmacy

Faculty of Health Sciences

UiT The Arctic University of Norway

Norway

The front page was created with BioRender.com.

Strength does not come from physical capacity.

It comes from an indomitable will.

- Mahatma Gandhi

Acknowledgements

The work presented in this thesis was carried out at the Drug Transport and Delivery Research Group, Department of Pharmacy, UiT The Arctic University of Norway from November 2018 to August 2022. I am grateful to UiT The Arctic University of Norway for financing this project. The project was part of the interdisciplinary research project Lead-to-drug development of amphipathic scaffolds targeting multi-resistant bacteria – *LEADScAMR* supported by the thematic strategic priorities at UiT. I would also like to take the opportunity to express my deepest gratitude to everyone that have supported, encouraged, and helped me over these years.

First of all, I would like to express my sincere gratitude to my main supervisor, Professor Nataša Škalko-Basnet. Your continuous support, everlasting encouragement, and excellent guidance have improved me both as a person and in the world of research. I wish and hope that every PhD student is as lucky as me to have a supervisor with genuine care and dedication to everyone. I really appreciate that you spent your valuable time supervising and guiding me through all stages of my wonderful PhD journey. It has been a privilege to be your student and a part of this project. To my co-supervisor, Professor Gøril Eide Flaten, thank you for your encouragement and support throughout my project. You have not only guided me in the project and world of research, but also sheared your outstanding knowledge about public engagement and outreach. I appreciate your open-door policy, knowing that you were always available when I needed you.

I am grateful to the project leader of the *LEADScAMR* project, Professor and Vice-dean of Research and Innovation Morten B. Strøm. I want to thank you for allowing me to be a part of this interesting and promising project, and for all inputs and support. Your dedication to research is truly inspiring.

I am very grateful to all my collaborators for wonderful collaborations and support. Thanks to Professor Purusotam Basnet, Associate Professor Mona Nystad, Maddhusja Sritharan Nalliah, and Nora Hersoug Nedberg for teaching me how to work in the cell lab, allowing me to work in your labs, and assisting me when I needed it. Furthermore, I would like to thank Associate Professor Beatrice Vitali and Dr. Barbara Giordani from the Department of Pharmacy and Biotechnology at the University of Bologna for great collaboration in the antimicrobial work and fruitful discussions. I would also like to extend my gratitude to Professor Mona Johannessen and Dr. Kjersti Julin from the Research Group for Host-Microbe interaction (HMI) for allowing me to work in your labs, assisting me in antimicrobial work, and for valuable contributions and discussions. Thanks to Associate Professor Željka Vanić from the Department of Pharmaceutical Technology at the University of Zagreb for your contribution in performing membrane-elasticity studies and for valued inputs and discussions. Moreover, I would like to thank Professor Annette Bayer, Dr. Marianne H. Paulsen, and Manuel K. Langer for performing compound synthesis and great contributions to our manuscripts. I would like to thank the people at The Advanced Microscopy Core Facility, especially Randi Olsen, Augusta Hlin Aspar Sundbø, and Tom-Ivar Eilertsen for all help and guidance in acquiring TEM images. I am truly grateful to all my collaborators for your valuable contributions and support throughout my whole PhD journey.

Thanks to all my wonderful former Erasmus and master students, Ann Kristin Pettersen, Luquman Mian Ahsan, Svenja Stomberg, Virginia Panzacchi, Luca Boracchia, Mari Salamonsen, and Pimmat Panchai for your excellent contributions to my PhD project. I really appreciate your intensive and hard work, and I feel that I have learned much from all of you. I am happy that I got the opportunity to work with you.

I want to thank all former and current colleagues at the Department of Pharmacy and especially the head of the department Guro Forsdahl for creating a thriving and nice environment. I appreciate all social interactions and scientific discussions between the research groups. You have all made my time here at IFA wonderful.

A special thanks to former and current colleagues in my research group, Drug Transport and Delivery Research Group. I have truly enjoyed my time here and I will never forget all wonderful times I have spent with you. My journey would never have been the same without brilliant chats, lutefisk, and lunches. Thanks to Associate Professor May Wenche Jøraholmen for collaborations, enlightening discussions, and support. Your patience and inclusiveness are admirable. I appreciate all I have learned from you. Thank you, Associate Professor Ann Mari Holsæter, for all support, great conversations, and guidance in teaching. Thanks to Cristiane de Albuquerque Cavalcanti Jacobsen, Skjalg Nyheim Solum, Kirill Jefimov and Martin Skipperud Skarpeid for encouragement and support in all technical and bureaucratic problems. A warm thanks to Dr. Sybil Obuobi for sharing your incredible knowledge in the field and all valuable discussions. I am enthused by your dedication to research, and I really appreciate your support. Maxim Bril'kov and Elena Markova, thanks for greetings and conversations around the coffee machine. Thanks to the person I have seen more than any other person over the last years, Laura Victoria Schulte-Werning. I am going to miss you as my office mate. I truly am grateful for our friendship, your patience with all ups and downs of my journey, and that I always have had someone I could talk to about everything. Thank you, Dr. Jennifer Cauzzo, for the support and all great conversations. I highly appreciate that someone as knowledgeable and thorough as you have had such a great impact on my journey. Your broad knowledge and perfectionism are admirable. Thanks to Alexandra Sofia Antunes de Sousa, for always being positive and showing up with a smile on your face. Even in the morning, however that might have appeared from my side. I am grateful for your kindness, stamina, and ability to always see the best in people. Thank you, Eirik André Lindeløff Rustad for always lifting the mood with witty remarks and jokes. Your brilliant mind has brightened many days and you have a unique ability to understand people. Thank you, Silje Mork, interesting conversations and fun stories. Lunches would never have been the same without you, and I really enjoyed the time we spent together at the Nordic POP conference. I would also like to thank Dr. Margherita Falavigna for welcoming me with open arms when I started my PhD journey. I highly appreciated our lunches and social gatherings. I am not only impressed by you work, but also your incredible cooking skills.

To all of my friends here in the high north and the rest of Norway. I am really grateful for your support and friendships. I appreciate all of you and looking forward to more fun times. I also want to thank my amazing football team, Stakkevollan IF, all team members, and everyone connected to the team. You have helped me disconnect from work and recharge my batteries throughout the whole journey.

Finally, a million thanks to my incredible family. Mom, I really appreciate your dedication to the family and me, and your endless support through my PhD project and my entire life. You are always a solid rock we all can lean on, and I know that I can always count on your support and advice. Dad, thank you for always supporting me and believing in my capabilities. I also highly appreciate your ability to lighten the mood and put me into a positive state mind. I know that I can contact you for guidance whenever I need. Katrine, my incredible and sweetest little sister, you are the most caring person in the world and the person that always knows what I think and how I feel. You are always there for me when I need you, and you are always a ray of sunshine that brightens up my day. I really appreciate how close we are to each other, and I really appreciate you. To all of my family, I hope you know how much I appreciate and love you.

Tromsø, August 2022

Lisa Myrseth Hemmingsen

Table of Contents

Abstract

Chronic wounds are currently a major burden for health care providers and patients; their management is becoming increasingly challenging especially because of the rise of resistant bacteria. The prevalence of chronic wounds in the general population is approximately 2%, however, due to an aging population and heightened disease burden, an upsurge of cases is expected. To overcome the currently limited wound management, eradication of wound bacteria and bacterial biofilms is crucial. There are many innovative wound therapy strategies in preclinical stages today, however, the clinical pipeline is still rather unsuccessful. We posed the question: "Could we learn from nature and the human body's own toolbox to improve the therapeutic outcomes?" Many of nature's habitants utilize antimicrobial compounds with fast onset of action and independence from metabolic activity as protection from intruders. Membrane-active antimicrobials (MAAs), such as antimicrobial peptides (AMPs), synthetic mimics of antimicrobial peptides (SMAMPs), and other compounds targeting bacterial membranes, could epitomize attractive alternatives to conventional strategies. However, these compounds bear limitations, such as toxicity and instability. We proposed that these drawbacks could be circumvented or limited by utilizing pharmaceutical innovations represented by drug delivery systems and scaffolds.

In the current project, we aimed to develop delivery systems based on liposomes and chitosan for SMAMPs to improve treatment of infected chronic skin wounds with focus on antimicrobial and anti-inflammatory activities. To find the optimal combination of liposomes and chitosan, we tailored chitosomes, chitosan-containing liposomes, chitosan-coated liposomes, and liposomes-in-chitosan hydrogel using chlorhexidine (CHX) as a model MAA.

The CHX-containing lipid-based vesicles and liposomes-in-hydrogel were optimized for topical skin therapy. Furthermore, *in vitro* release, anti-inflammatory properties, cell compatibility, and antimicrobial and anti-biofilm activities were assessed. We found that liposomes and chitosan inserted within the liposomal bilayers, as a coating, and as a hydrogel exhibited promising biological properties and antimicrobial activities. However, liposomes-in-chitosan hydrogel was deemed the most suitable system, and therefore selected for further development of delivery systems for two novel SMAMPs, namely 7e-SMAMP or 7a-SMAMP.

The 7e-SMAMP is the most potent membrane-active SMAMP and is therefore expected to interact strongly with liposomal bilayers. To confirm that liposomes were stable upon their association with 7e-SMAMP, and that we could maintain or improve the biological and antimicrobial properties of 7e-SMAMP incorporated in liposomes, we performed a thorough investigation of 7e-SMAMP-liposomes without chitosan hydrogels. From this study we confirmed that novel liposomes were stable, able to imprint anti-inflammatory properties, and were highly biocompatible. Furthermore, the anti-biofilm activities of 7e-SMAMP against *Staphylococcus aureus*, *Escherichia coli*, and *Pseudomonas aeruginosa* improved upon its incorporation in liposomes.

To approach more multitargeted wound management, 7a-SMAMP was co-entrapped with chlorogenic acid (CGA) in the dual liposomes-in-chitosan hydrogel system. The 7a-SMAMP is not as highly membrane-active as 7e-SMAMP, however, it is substantially more biocompatible. Therefore, we investigated the ability of SMAMP and delivery systems to improve other aspects of wound treatment such as cell migration. A more rigorous evaluation of cell compatibility was performed as well as an evaluation of the effect of CGA/7a-SMAMP-liposomes on cell migration. The CGA was also evaluated and compared to vitamin C and E for its anti-oxidative properties, highly relevant in wound therapy. We confirmed that the novel dual system had strong anti-inflammatory activity, good cell compatibility, and could potentially improve cell migration and anti-oxidative effects.

Overall, the MAA-comprising liposomes-in-hydrogel systems were proven to be suitable formulations with good biocompatibility and enhanced anti-inflammatory, antimicrobial, and anti-biofilm properties. The novel delivery system comprising SMAMPs bears great potential as a platform in the therapeutic management of infected chronic skin wounds.

List of Abbreviations

AMP	Antimicrobial peptide
AMR	Antimicrobial resistance
B3M-liposomes	Bacterial Membrane-Mimic Liposomes Models
CCK-8	Cell counting kit-8
CGA	Chlorogenic acid
CHX	Chlorhexidine
DAMP	Damage-associated molecular pattern
EE	Entrapment efficiency
EPS	Extracellular polymeric substance
IL	Interleukin
LPS	Lipopolysaccharide
MAA	Membrane-active antimicrobial
MDR	Multidrug resistant
MIC	Minimal inhibitory concentration
MLC	Minimal lethal concentration
MMP	Matrix metalloproteinases
MRSA	Methicillin-resistant *S. aureus*
MSSA	Methicillin-sensitive *S. aureus*
M_w	Molecular weight
NO	Nitric oxide
PAMP	Pathogen-associated molecular pattern
PEG	Polyethylene glycol
PI	Polydispersity index
ROS	Reactive oxygen specie
SEM	Scanning electron microscopy
SMAMP	Synthetic mimic of antimicrobial peptide
SWF	Simulated wound fluid
TEM	Transmission electron microscopy
TNF-α	Tumour necrosis factor-alpha

List of Publications

Paper I

Hemmingsen, L.M., Giordani, B., Pettersen, A.K., Vitali, B., Basnet, P., Škalko-Basnet, N., 2021. Liposomes-in-chitosan hydrogel boosts potential of chlorhexidine in biofilm eradication in vitro. Carbohydr. Polym. 262, 117939. doi: https://doi.org/10.1016/j.carbpol.2021.117939.

Paper II

Hemmingsen, L.M., Julin, K., Ahsan, L., Basnet, P., Johannessen, M., Škalko-Basnet, N., 2021. Chitosomes-In-Chitosan Hydrogel for Acute Skin Injuries: Prevention and Infection Control. Mar. Drugs 19, 269. doi: https://doi.org/10.3390/md19050269.

Paper III

Hemmingsen, L.M., Panchai, P., Julin, K., Basnet, P., Nystad, M., Johannessen, M., Škalko-Basnet, N., 2022. Chitosan-based delivery system enhances antimicrobial activity of chlorhexidine. Front. Microbiol. 13, 1023083. doi: https://doi.org/10.3389/fmicb.2022.1023083.

Paper IV

Hemmingsen, L.M., Giordani, B., Paulsen, M.H., Vanić, Ž., Flaten, G.E., Vitali, B., Basnet, P., Bayer, A., Strøm, M.B., Škalko-Basnet, N., Tailored anti-biofilm activity – liposomal delivery for mimic of small antimicrobial peptide.

Under review

Paper V

Hemmingsen, L.M., Salamonsen, M., Paulsen, M.H., Basnet, P., Nystad, M., Bayer, A., Strøm, M.B., Škalko-Basnet, N., Towards multitarget approach in chronic wound healing – Synthetic mimic of antimicrobial peptide combined with polyphenol in liposomes-in-hydrogel dressing.

Manuscript

1. Introduction

1.1 Antimicrobial resistance, persistence, and rising prevalence of chronic wounds

Currently, antimicrobial resistance (AMR) is emerging as the leading cause of death worldwide and jeopardizing our health care systems both directly and indirectly (Murray et al., 2022). The principal drivers for this crisis are the overuse of antibiotics in agriculture, inappropriate prescription practices along with a decelerated pipeline of antimicrobial compounds with new targets limiting novel treatment strategies reaching the patients (Hemmingsen et al., 2021a; Murugaiyan et al., 2022). The resistivity in bacteria to antimicrobial treatment could derive from both the resistance and persistence, even though these terms are, correctly, separated in literature. Resistance refers to the ability of bacteria to resist antibiotic treatment through e.g., antibiotic degradation or modification of antibiotic targets. The bacteria are able to grow during antibiotic exposure, and the resistivity is heritable. While persisters are usually susceptible to the antibiotic treatment, however, subpopulations of these bacteria are able to sustain during the antibiotic treatment. These bacteria are not actively growing and often exist in a state of dormancy (Jung et al., 2019; Levin-Reisman et al., 2019). In this thesis, persistence is generally subsumed into the term resistance since both are the factors influencing bacterial survival (Reygaert, 2018). It is imperative that novel antimicrobial compounds or smart strategies for microbial and biofilm eradication are established and optimized to mitigate the challenges of resistant pathogens and alleviate both direct and indirect impacts of AMR (Erdem Büyükkiraz and Kesmen, 2022; Murugaiyan et al., 2022). Currently, the development of antimicrobial compounds is slower than both the emerge of resistant microorganisms and the increase in infection rates. The lack of antimicrobial compounds with new targets points to the need for multidisciplinary efforts, that can utilize full arsenal to improve the current situation and address the issues limiting the success of compounds approaching the clinical pipeline (Rubey and Brenner, 2021).

In parallel, treatment of wounds become a growing challenge due to these resistant pathogens along with the limited treatment options, leading to chronic or non-healing wounds. The prevalence of chronic wounds in the general population is about 2% with a 5-year mortality rate of approximately 50% (Sharifi et al., 2021). Furthermore, it is expected to

rise because of an aging population with appended conditions, such as diabetes, and obesity. These numbers call for attention and underline the importance of advancements in the current strategies for prevention and treatment of infected skin and skin wounds (Sen, 2021). Nature has clever ways to survive and resist pathogens; all its habitants have evolved in fascinating manners to overcome the challenges and ensure survival in their respective environment. The habitants exist in harsh environments, from the deep, cold oceans to the scorching deserts, that could be a threat to their existence. Moreover, even human cells have developed remarkable mechanisms to survive. The natural question is then: "Could we learn from nature and our own bodies to improve our arsenal against the pathogens including the therapy of infected skin wounds?"

The inherent defence and barrier function of the skin are highly effective in both protecting the host from commensal organisms and fighting off intruding bacteria. In exploring and learning from nature, and the human body, antimicrobial peptides (AMPs) emerge as promising candidates in the battle against resistant bacteria and management of chronic wounds. These compounds possess several attractive biological properties, ranging from broad antimicrobial to immunomodulating activities (Divyashree et al., 2020). Interestingly, the AMPs were first discovered in skin wounds (Yamasaki and Gallo, 2008). To exploit this potential solution, I structured the thesis by introducing our brilliant natural defence, explaining the ways the healing cascade operates and fails, leading to the path utilizing synthetic mimics of antimicrobial peptides (SMAMPs) and other membrane-active antimicrobials (MAAs) and their promise in treatment of chronic wounds. However, I attempted to highlight both the potential and challenges, as well as a need for more innovative strategies to fully utilize these compounds as valid therapeutic options.

1.2 Skin and its defence

To understand and address the challenges and complexity of skin therapy, we should gain a deeper insight on both its function and structure. The skin is our primary barrier to the surrounding environment and the first line of defence against pathogens and toxic substances (Benson et al., 2019; Lin et al., 2021). Additionally, the skin is maintaining important functions

such as thermoregulation, sensation, water balance, absorption, and synthesis of vitamin D (McKnight et al., 2022). Structurally, the skin is composed of three layers, namely epidermis, dermis, and hypodermis (Figure 1.1). Epidermis, including *stratum corneum*, is the outermost layer and the closest to outside environment, serving as the first barrier of defence. In addition to skin's role as a physical barrier, the skin protection mechanisms also arise from an immunological aspect, where skin and immune cells work together to provide protection (McKnight et al., 2022). This additional immunological aspect of defence is crucial to protect the body from both cutaneous and systemic infections. Once the skin barrier is damaged or breached, the immune system initiates a whole cascade to protect the body and fight off intruders (Coates et al., 2018).

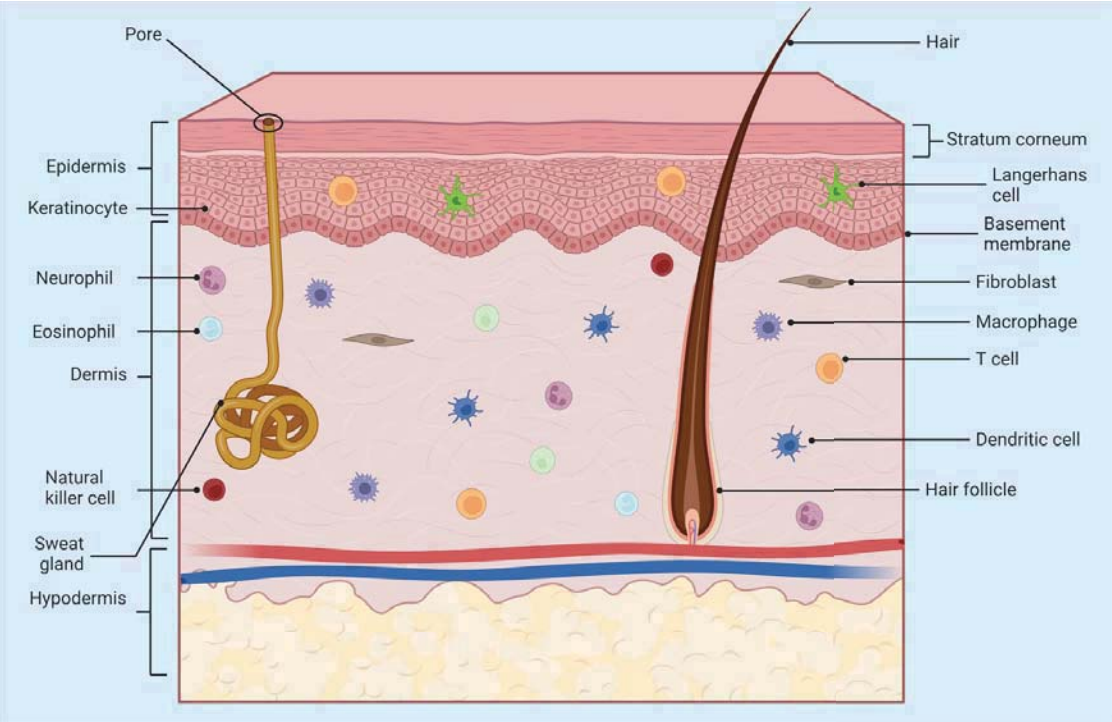

Figure 1.1. Structure of the skin with three main layers; epidermis, dermis, and hypodermis. Selected important skin and immune cells are also included. The presentation is based on the work of Kwiecien *et al.* (Kwiecien et al. 2019). Created with BioRender.com.

The skin's immune response involves various processes that occur within the different skin layers, involving numerous cells (Figure 1.1). The epidermis mainly consists of keratinocytes in different differentiation levels, from the basal keratinocytes to the

corneocytes at the surface (Chessa et al., 2020). Together with the Langerhans cells, T-cells, and other immune cells, these cells contribute to a vast immune response upon injuries. In the dermis, fibroblasts are the principal cell type and highly important for the closure of wound gaps. In this section of the skin, the dermal dendritic cells, dermal macrophages, natural killer cells, eosinophils, mast cells, neutrophils, and T-cells partake in the immune response (Nguyen and Soulika, 2019). The deeper skin layers contain nearly all immune cells and are considered more immunologically active than previously anticipated (Chen et al., 2019). Upon a skin injury, the cells recognise the tissue damage through the damage-associated molecular patterns (DAMPs), and pathogen-derived molecules, referred as pathogen-associated molecular patterns (PAMPs). Subsequently, the inflammatory mediators and chemokines are released for recruitment of the neutrophiles, macrophages, and activated T-cells. Langerhans cells are also triggered to migrate to the lymph nodes to activate more T-cells (Piipponen et al., 2020). Furthermore, compounds that directly kill pathogens, modulate immune responses, and support the wound healing are also released. The AMPs are among these compounds; the human keratinocytes produce at least nine different types of AMPs (Chessa et al., 2020). Neutrophiles that infiltrate wounds are also expressing AMPs (Yamasaki and Gallo, 2008). Contrary to earlier belief that the skin barrier function was its only or main protection mechanism, the responses to skin injuries are both vast and complex.

1.2.1 Wounds and wound healing – when the skin is breached

For most people, the skin's defence and healing cascade operate in a normal and well-regulated manner; the skin will return to its normal functional and anatomical integrity within a relatively short time after an injury. The wound healing process is a tightly regulated and temporal process divided into four phases as depicted in Figure 1.2A: the haemostasis, inflammation, proliferation, and remodelling phase (Öhnstedt et al., 2019). As derived from its Greek name, haemostasis, *haíma* = blood and *stasis* = halting or stopping, the main purpose of this phase is the prevention of extensive blood loss and formation of a clot to close the injured area (Pourshahrestani et al., 2020). The blood vessels contract due to neuronal reflexes, and for a period, this is a most often sufficient to partly or completely stop blood loss until the formation of the clot. However, after a few minutes, hypoxia, and acidosis in the wall cause overturing of constriction. If the clot is not properly formed by then, bleeding will

resume (Velnar et al., 2009). In the formation of the clot, platelets are exposed to vascular subendothelial matrix and activated, leading to the formation of a platelet plug. Next, fibrinogen is converted to a fibrin mesh that interacts with the platelet plug and forms the clot. This clot is vital for the initial stop of blood loss, but it also serves as a scaffold for infiltrating cells and a seal from the surroundings (Rodrigues et al., 2018).

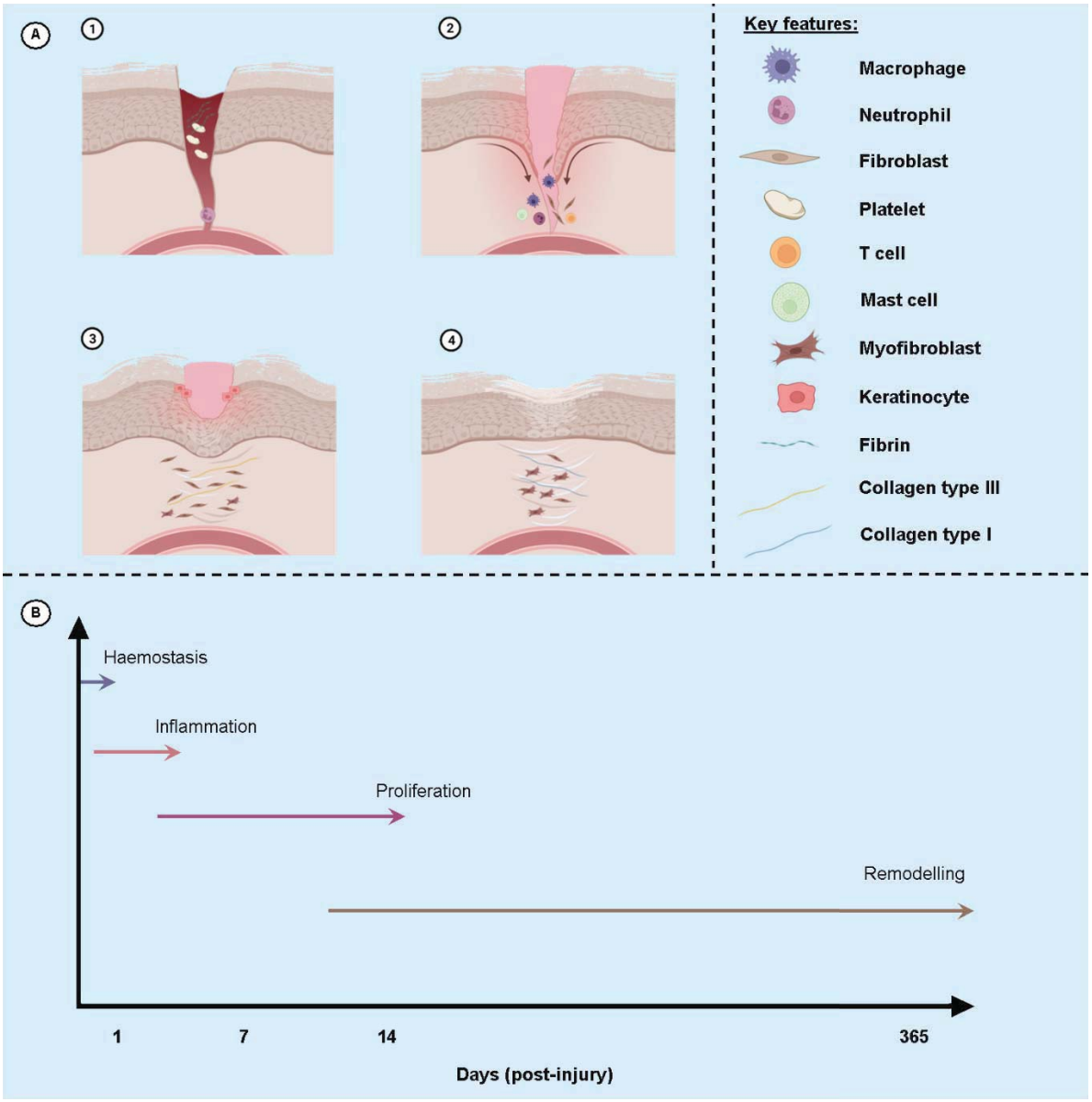

Figure 1.2. A) Four stages of wound healing: 1) haemostasis, 2) inflammation, 3) proliferation, and 4) remodelling. B) Timeline of normal wound healing, based on Las Heras *et al*. and Velnar *et al*. (Las Heras et al., 2020; Velnar et al., 2009). Adapted from "Wound Healing", by BioRender.com (2021). Retrieved from https://app.biorender.com/biorender-templates.

The second stage of the wound healing cascade is the inflammatory phase, where the skin's defence plays the major role (Figure 1.2 A2). First, the DAMPs and PAMPs lead to infiltration of the resident Langerhans cells, mast cells, macrophages, and T-cells and subsequent release of cytokines and chemokines (Las Heras et al., 2020). Furthermore, release of growth factors and chemokines from the activated platelets in the clot leads to recruitment of neutrophiles to the wound bed. In the wound bed, these cells kill bacteria through different means, such as production of reactive oxygen species (ROS) and antimicrobial substances, and release of lytic enzymes and matrix metalloproteinases (MMPs). Additionally, the neutrophiles activate the resident hematopoietic cells, macrophages, dendritic cells, B-cells, T-cells, and natural killer cells through crosstalk involving cytokines, chemokines, and angiogenic factors (Cañedo-Dorantes and Cañedo-Ayala, 2019). After the infiltration of neutrophiles, monocytes enter the wound bed, and predominantly transform into M1-type macrophages to intensify the inflammation response. The macrophages remove debris, kill bacteria, and produce nitric oxide (NO), ROS, interleukin-1 (IL-1), IL-6, IL-8, IL-12, tumour necrosis factor-alpha (TNF-α) and MMPs (Arango Duque and Descoteaux, 2014; Las Heras et al., 2020). Later in the inflammatory response, the M2-type macrophages become predominant. These cells release vascular endothelial growth factor, platelet-derived growth factor, insulin growth factor 1, fibroblast growth factors, transforming growth factor, and IL-10 to promote migration, proliferation, and matrix formation (Arango Duque and Descoteaux, 2014; Las Heras et al., 2020). Furthermore, both T-cells and mast cells play important roles in the healing cascade; the T-cells in the initial response and resolving the inflammatory cascade and mast cells in the initial recruitment of neutrophiles through release of histamine (Wilkinson and Hardman, 2020).

The third stage of the wound healing cascade is the proliferation phase characterized by formation of granulation tissue (Figure 1.2 A3). Fibroblasts are the cells responsible for the formation of the new extracellular matrix. Moreover, formation of new blood vessels, angiogenesis, and re-epithelialization occur in this stage (Rodrigues et al., 2018). Upon re-epithelialization, the resurfacing of wounds, keratinocytes migrate and proliferate in the wound bed to cover and strengthen the barrier (Las Heras et al., 2020; Rousselle et al., 2019). The last stage of the wound healing cascade, remodelling phase (Figure 1.2 A4), is initiated

about three weeks after the skin breach and could last for over a year (Tottoli et al., 2020). This stage revolves around the strengthening of the wounded area where the granulation tissue is remodelled to scar tissue. Fibroblasts differentiate into myofibroblasts that strengthen the scar due to contraction of the area. Collagen type III is degraded, while levels of collagen type I are increased due to its increased tensile strength (Li et al., 2022). In addition to collagen type I, the clot is also replaced with hyaluronan, fibronectin, and proteoglycans. The remodelling phase is ended when macrophages, endothelial cells, and fibroblasts leave the area or undergo apoptosis (Wilkinson and Hardman, 2020).

The wound healing cascade is a complex process that stretches over a significant time (Figure 1.2B); however, in most cases this cascade is finely tuned and transpire without any considerable interruptions resulting in a timely healing. Nevertheless, if the process is disrupted or haltered, the non-healed wound turns chronic.

1.2.2 Chronic wounds

Wounds are often defined as chronic or non-healing if the breach has not closed within a period of 4-6 weeks or 3 months, depending on literature as well as aetiology (Drago et al., 2019; Teot and Ohura, 2021). In contrast to wounds following the normal healing cascade, the chronic wounds are characterized by prolonged inflammation and extended presence of inflammatory cells, such as M1-type macrophages, as well as increased levels of ROS and inflammatory cytokines (Matar et al., 2022). These wounds are haltered in the inflammation phase and the healing cascade is hampered. Among chronic wounds, the most common wound types are the diabetic, pressure, and vascular ulcers that often occur in patient with neuropathy, venous insufficiencies, and limited movement. However, the common denominator for all these wounds is that they are arrested in the inflammatory phase (Firlar et al., 2022). The situation is yet more complex and involves the typical immune cells, keratinocytes, and fibroblasts (Darwin and Tomic-Canic, 2018). Nevertheless, one of the major burdens in these wounds is the microbial load, especially the biofilm-embedded bacteria, the most common reason for treatment failure (Wu et al., 2019).

1.2.3 Bacterial biofilms in wounds

It is estimated that the prevalence rate of biofilms in chronic wounds is approximately 78%; increasing the complexity of treating those wounds (Malone et al., 2017). Biofilm-embedded bacteria are up to 1000-fold more resistant than planktonic cells; together with the general resistance patterns in bacteria and polymicrobial nature of biofilms, their eradication remains challenging (Ciofu et al., 2022; Hemmingsen et al., 2021a).

The *Staphylococcus aureus* and *Pseudomonas aeruginosa* are recognized as strong contributors to biofilm formation, especially in wounds (Gajula et al., 2020). This biofilm formation is often divided into four stages, namely the attachment, formation of microcolonies, biofilm maturation, and detachment (Wu et al., 2019). A brief summary is offered in Figure 1.3 A. In the first stage, bacteria either reach the surface passively, as *S. aureus*, or actively through pili or flagella, as *P. aeruginosa* (Joo and Otto, 2012). Upon reaching the surface, bacteria non-covalently attach to human proteins through bacterial binding proteins. Utilizing bacterial signalling, the biofilm formation is initiated, followed by maturation of the extracellular polymeric substances (EPS) or the biofilm matrix (Wu et al., 2019). During detachment, the last stage of biofilm formation, bacteria detach from the main structure of the mature biofilm and disperse into the environment (Ballén et al., 2022). The detachment could either be through an active dispersion or a passive detachment (Rumbaugh and Sauer, 2020). The biofilm matrix will provide structure, support, and protection of bacteria embedded in the matrix. This protection offers a supplementary mechanism in addition to the more classical resistance mechanisms presented in Figure 1.3 B.

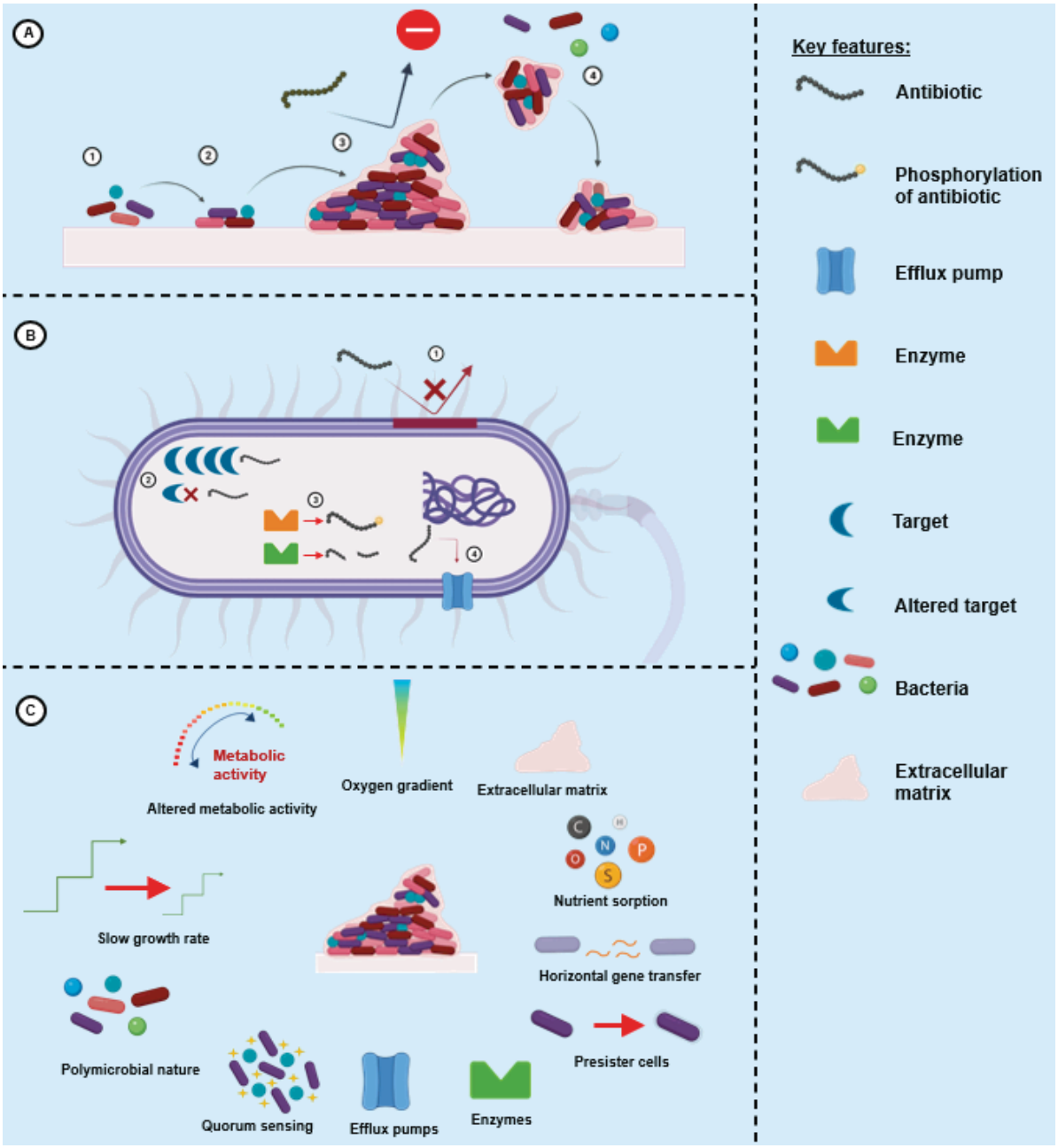

Figure 1.3. A) Four stages of biofilm formation: 1) attachment 2) formation of microcolonies, 3) biofilm maturation, and 4) detachment. B) General resistance mechanisms: 1) decreased penetration of antibiotics, 2) alteration or amplification of target, 3) enzymatic alteration or destruction of antibiotic, and 4) increase in efflux pumps. C) Common factors found in biofilms leading to resistance or increased bacterial survival in the biofilm community. Adapted from "Polymicrobial Biofilm 2", by BioRender.com (2021). Retrieved from https://app.biorender.com/biorender-templates.

Increased resistance and enhanced bacterial survival in the biofilm communities are orchestrated by several driving forces (Figure 1.3 C). As mentioned previously, biofilm matrix serves as a physical barrier for the penetration of antimicrobial compounds. Additional mechanisms involve i) persistent or dormant bacteria, decelerated growth rate and altered metabolic activity, due to nutrients and oxygen gradient in the matrix leading to network heterogenicity; ii) increased horizontal gene transfer and therefore increased resistance mechanisms such as efflux pumps and enzymes altering the antimicrobial compounds and iii) increased nutrient sorption allowing the matrix to harvest resources. Additionally, enhanced communication through quorum sensing is reported (Flemming et al., 2016; Römling and Balsalobre, 2012).

All these mechanisms lead to more resistant and resilient bacteria within the biofilm, that further hampers normal wound healing. Additionally, the complexity of these wounds plays a role. Moreover, the situation could turn grimmer due to the increasing resistance to conventional antimicrobials (Mahmoudi and Gould, 2020). Among promising arsenal to tackle resistant bacteria and bacteria in biofilm communities, MAAs with their anti-biofilm activities (Dias and Rauter, 2019; Zhang and Ma, 2019) need to be further exploited.

1.3 Antimicrobial and anti-biofilm strategies

1.3.1 Current therapies of infected chronic wounds

The treatment of infected wounds is complex and dependent on the severity of the wound, microbial picture, and pathogen's susceptibility. Furthermore, the current treatment options do not address all the issues and needs in management (Guimarães et al., 2021b). In addition to the bacterial burden, the pain, odour, exudate, and other factors affecting the patients' quality of life need to be considered (Eriksson et al., 2022). Besides, the diagnosis and treatment plans are often inaccurate or inappropriate leading to unhealed, chronic wounds. To address the treatment challenges, diagnostic tools like TIME (tissue, infection/inflammation, moisture balance, and edge of the wound) principles and TIME CDST (TIME clinical decision support tool) were developed to help clinicians to decide on the

treatment strategy (Moore et al., 2019). Along with antimicrobial therapy, the needs for debridement, wound bed preparation, compression, or surgery need to be discussed (Frykberg and Banks, 2015). For milder wound infections, topical antimicrobial treatment options are often desired because of higher local and lowered serum drug concentrations. Mupirocin, metronidazole, and silver sulfadiazine are among the most common topical treatment options for wounds (Ciofu et al., 2017). The evidence for using topical antimicrobial therapies is limited and their effect is often not sufficient (Williamson et al., 2017). In more severe cases, systemic administration is often the only viable alternative to achieve treatment goals; however, it should not be used indiscriminately (Falcone et al., 2021). The choice of antimicrobial for systemic treatment should be based on the evidence, microbial burden, resistance patterns, and other clinical conditions. Furthermore, National Institute for Health and Care Excellence (NICE) has developed guidelines for treatment of diabetic foot ulcers and leg ulcers. The relevant treatments are summarized in Table 1.1.

Table 1.1. Summary of NICE guidelines for antimicrobial treatment of diabetic foot ulcers and leg ulcers in adults.

Condition	**Mild cases**		**Moderate to severe cases**
	Antibiotic	Comment	Antibiotic
Diabetic foot ulcers	Flucloxacillin	First choice.	Flucloxacillin with/without Gentamicin and/or Metronidazole
	Clarithromycin	In cases of penicillin allergies or if appropriate.	Amoxicillin + clavulanic acid with/without Gentamicin
	Erythromycin	In cases of penicillin allergies or if appropriate. In pregnancy.	Trimethoprim + sulfamethoxazole with/without Gentamicin and/or Metronidazole
	Doxycycline	In cases of penicillin allergies or if appropriate.	Ceftriaxone with Metronidazole
Leg ulcers	Flucloxacillin	First choice.	Flucloxacillin with/without Gentamicin and/or Metronidazole
	Doxycycline	Alternative first choice. In cases of penicillin allergies or if appropriate.	Amoxicillin + clavulanic acid with/without Gentamicin
	Clarithromycin	Alternative first choice. In cases of penicillin allergies or if appropriate.	Trimethoprim + sulfamethoxazole with/without Gentamicin and/or Metronidazole
	Erythromycin	Alternative first choice. In cases of penicillin allergies or if appropriate. In pregnancy.	Piperacillin with tazobactam
	Amoxicillin + clavulanic acid	Second choice.	Ceftriaxone with/without Metronidazole
	Trimethoprim + sulfamethoxazole	Second choice.	

Treatment alternatives are based on NICE guidelines "Diabetic foot problems: prevention and management" NG19 (NICE guideline, 2015) and "Leg ulcer infection: antimicrobial prescribing" NG152 (NICE guideline, 2020). The summary does not include recommendation for methicillin-resistant *S. aureus* (MRSA) or *P. aeruginosa* infections.

1.3.2 Novel antimicrobial strategies

In spite of extensive guidelines for treatment of wounds, the success rate remains low; the market lacks products that improve healing, while biofilms often remain an underlying reason for healing failure (Verma et al., 2022; Wu et al., 2019). The strategies used today in biofilm eradication are rather ineffective, therefore prevention of biofilm formation is often regarded the most suitable method (da Silva, et al., 2021) The US Food and Drug Administration (FDA) has also recognized the lack of effective strategies and marketed products for chronic wounds (Verma et al., 2022). Several novel treatment strategies are being investigated with various degrees of promise, innovative solution, or translational potential. To retain focus, I mention only a few of these emerging strategies briefly; the phage therapy has received attention as a promising option in different infections, including wound infections. Furthermore, it has also exhibited promising results against biofilms (Chang et al., 2022). Alternatively, lysins could also be used as therapeutic agents against bacterial infections (Ghosh et al., 2019). Another assessed strategy is treating bacteria and bacterial biofilms with antibodies (Raafat et al., 2019). Finally, AMPs, their mimics, and other small MAAs have garnered much attention both because of their antimicrobial activities as well as their wound healing potential. In the era of AMR, these compounds are attractive due to their lowered potential for evoking resistance in addition to their activity against persister cells (Bi et al., 2021; Miao et al., 2021).

1.3.3 Membrane-active antimicrobials

The antimicrobial activity of MAAs is independent of metabolic activity, allowing their potential to evade the bacterial resistance mechanisms. The MAAs often exhibit non-specific action with broad activities and fast onset leading to wide applicability and, so far, lower resistance rates (Zhou et al., 2020). The cationic elements of these compounds enable the interaction with bacterial membranes, mainly through an interaction with teichoic acids in gram-positive bacteria and lipopolysaccharide (LPS) in gram-negative bacteria (Figure 1.4 A), further leading to destabilization of the membrane and subsequent bacterial death (Gera et al., 2021).

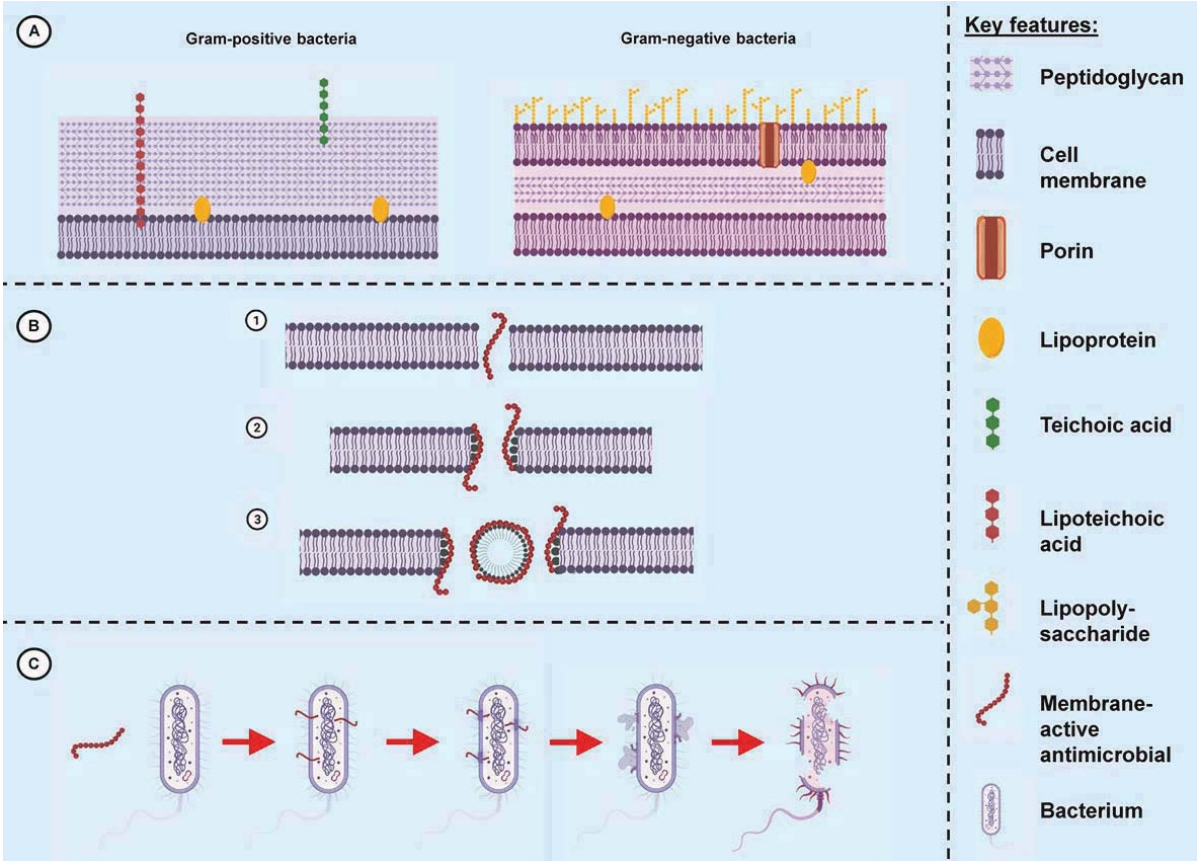

Figure 1.4. A) Illustration of gram-positive and gram-negative bacterial membrane. B) Common mechanisms of antibacterial activity of membrane-active antimicrobials (MAAs): 1) barrel-stave model, 2) toroidal pore model, and 3) carpet model. C) MAAs' effect on bacterial membrane. Adapted from "Structural Overview of a Bacterial Cell", by BioRender.com (2021). Retrieved from https://app.biorender.com/biorender-templates.

There are several antimicrobial mechanisms of action described for these AMPs or MAAs; however, the main mechanisms are presented in Figure 1.4 B and referred to as the barrel-stave, toroidal pore, and carpet models (Zhou et al., 2020). The cationic elements of MAAs induce interaction with membranes, while the hydrophobic regions induce penetration and disruption of bacterial membranes (Figure 1.4 C). However, effects on more discrete membrane proportions are also proposed (Rzycki et al., 2021). Therefore, it is highly important to better understand their mechanisms and targets. Since the transport and penetration into or through membranes are complex and dynamic, we need multiple methods to determine their antimicrobial effects. Among others, exploiting artificial membranes, or Bacterial Membrane-Mimic Liposomes Models (B3M-liposomes), could expand our knowledge on the

relationship of MAAs and bacterial membranes, indirectly indicating the relevant mechanisms (Pinheiro et al., 2019; Sun et al., 2015).

1.3.3.1 Antimicrobial peptides and synthetic mimics of antimicrobial peptides

MAAs comprise a wide choice of promising antimicrobials, however the AMPs and SMAMPs seems to be particularly promising. The AMPs are found in many kingdoms on the planet; and can be utilized as antimicrobial compounds to treat infections (Ron-Doitch et al., 2016; Vanzolini et al., 2022). However, to address their toxicity, degradation, and instability, development of the SMAMPs or peptidomimetics has been the popular approach (Vanzolini et al., 2022). SMAMPs are synthetic molecules with tuneable architecture mimicking the key structural elements of AMPs, mainly charge and hydrophobicity (Mojsoska et al., 2015; Sgolastra et al., 2013). These synthetic compounds could be classified into three groups according to their size: macromolecular, oligomeric, and small molecules. The small molecules could be favourable due to ease of synthesis, diversity of biological activities, permeability, and tuneability of the molecules (Ghosh and Haldar 2015; Sgolastra et al., 2013). Therefore, I chose to focus on the smaller molecules in this project. In addition to their antimicrobial properties, the AMPs along with SMAMPs could serve as multitargeting compounds exhibiting anti-inflammatory and immunomodulatory properties as well as neutralizing effects on endotoxins (Erdem Büyükkiraz and Kesmen, 2022), highly relevant to assist in chronic wound healing. Several AMPs and SMAMPs are currently under clinical investigations or in clinical trials (Dijksteel et al., 2021). The optimism around AMPs and their mimics also stems from their potential activity against multidrug resistant (MDR) pathogens and biofilm-embedded bacteria, a crucial issue in the post-antibiotic era we are facing now (Song et al., 2021). However, a few resistance mechanisms are also revealed for the AMPs. Among these, the alterations of the bacterial membrane surface, production of proteases or sequestering proteins, production of anionic polysaccharide capsule as a physical barrier around the bacterial cells, and expression of efflux pumps have been reported so far (Gan et al., 2021).

1.3.4 Membrane-active antimicrobials and biofilms

The MAA compounds can be of natural or synthetic origin, comprising a broad spectrum of compounds ranging from plant-originated, such as polyphenols and cannabinoids, common antiseptics, such as chlorhexidine (CHX), and small AMPs or SMAMPs. Regardless of their origin, all exhibit ability to destabilize and disrupt bacterial membranes. A few MAAs are enlisted below to highlight their anti-biofilm potential.

Among plant-originated, Akhtar *et al.* evaluated the anti-biofilm activity of a polyphenol, curcumin, against clinical isolates of biofilm-producing vancomycin-resistant *S. aureus*. Free curcumin (non-formulated) was able to eradicate 37% of the pre-formed biofilm; however, when applied as a photosensitizer, 68% of the biofilm was eradicated with a decrease in EPS of 48% compared to 14% for free curcumin. Additionally, scanning electron microscopy (SEM) confirmed bacterial cell rupture (Akhtar et al., 2021). Vipin *et al.* investigated the anti-biofilm activity of quercetin against clinical isolates of *P. aeruginosa*. Quercetin was able to inhibit the biofilm formation in both reference strains and clinical isolates up to 100% at the highest tested concentration (500 µg/mL). Moreover, the authors confirmed the effect of quercetin on quorum sensing controlled virulence factors. Quercetin also significantly affected twitching motility in the bacteria (Vipin et al., 2019). Farha *et al.* reported anti-biofilm activity of cannabinoids, especially cannabigerol, which was able to inhibit biofilm formation and eradicate pre-formed biofilm produced by methicillin-resistant *S. aureus* (MRSA). Furthermore, cannabinoids increased permeabilization of bacterial membranes and eradicated persister cells (Farha et al., 2020). It was suggested that the chemical modifications of quinoline structures could lead to molecules exhibiting strong anti-biofilm potential. Frapwell *et al*. assessed the quinoline derivative, HT61, against *S. aureus* biofilms. The anti-biofilm activity of HT61 was found to be superior to vancomycin. Furthermore, the authors confirmed upregulation of genes responsible for both the cell wall biosynthesis and DNA maintenance at minimal inhibitory concentration (MIC) of HT61. This effect was seen in both planktonic and biofilm-embedded bacteria, however, was more muted in biofilm-embedded bacteria (Frapwell et al., 2020).

The small AMPs and SMAMPs exhibit excellent inhibition of biofilm formation, eradication of pre-formed biofilms, and bacterial membrane rupture. For example, Konai *et al*. demonstrated that mimics of AMPs significantly improved biofilm eradication in MRSA, compared to vancomycin and fucidic acid. Additionally, the AMPs eradicated *S. aureus* and *Escherichia coli* in both stationary phase and persister cells (Konai et al., 2020). *P. aeruginosa* biofilm formation inhibition at low sub-MIC was confirmed for another small AMP, AMP 1037. Additionally, the authors found that genes related to swarming motility were downregulated, while genes responsible for twitching motility were upregulated in treated biofilm-embedded bacteria. This could increase removal of bacteria from surfaces and induce fast movement on surfaces, subsequently hampering colonisation. Other genes related to biofilm formation were also downregulated upon treatment with this novel AMP (de la Fuente-Núñez et al., 2012). Recently, Wang *et al*. synthesised scorpion-like peptidomimetics that displayed biofilm formation inhibition in both MRSA and *E. coli* in a dose-dependent manner. The authors confirmed that the bacterial membrane integrity was indeed disrupted using both fluorescent and transmission electron microscopy (TEM). Moreover, AMPs and SMAMPs are also known to be less prone to resistance development. For example, MRSA and *E. coli* were subjected to 14 passages of treatment with a scorpion-like peptidomimetic or ciprofloxacin and the alterations in their MIC values were assessed. The MIC values remained the same throughout all 14 passages for the scorpion-like peptidomimetic, while the MIC values of ciprofloxacin significantly increased (Wang et al., 2021a). Dey *et al*. tailored small antibacterial molecules with structural similarities to AMPs or SMAMPs to eradicate MRSA biofilms. The most potent molecule reduced the biofilm mass in pre-formed biofilms by 60-80%, whereas vancomycin reduced the mass by only 10%. The authors confirmed both the membrane permeabilization and depolarization. The small antibacterial molecules also displayed activity towards metabolically inactive bacteria, an effect that was superior to the one of vancomycin (Dey et al., 2019).

The mechanisms behind the anti-biofilm actions of MAAs are, as described above, many and complex. The main mechanisms discussed above are summarized in Figure 1.5, however, other mechanisms are also described in literature.

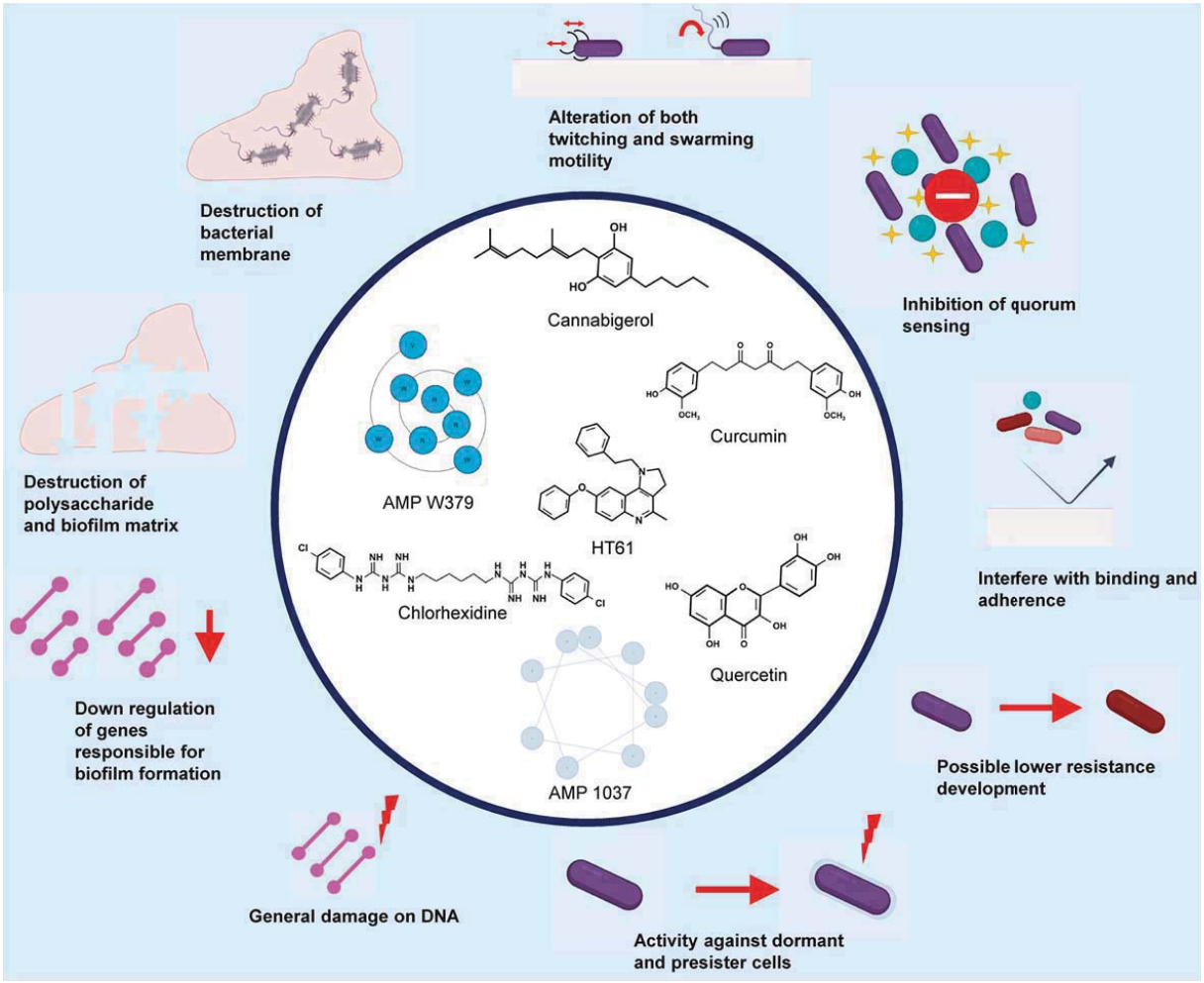

Figure 1.5. The mechanisms of action of membrane-active antimicrobials (MAAs) in biofilm-embedded bacteria and biofilm matrices. Created with BioRender.com.

Although highly promising, these novel antimicrobial strategies are not without limitations. Some of the drawbacks linked to full utilization of MAAs could be addressed utilizing nanotechnology and drug delivery strategies to improve their bioavailability, ability to reach the desired site of action, and offer protection against degradation (Gera et al., 2021; Mascarenhas-Melo et al., 2022). Furthermore, by the smart selection of nanomaterials that also exhibit antimicrobial properties along with anti-inflammatory activity, we could further improve the promise of utilizing nanotechnology and drug delivery technologies to improve the therapy of infected, chronic wounds (Díez-Pascual, 2020). Moreover, the translational journey into the clinics bears opportunities for exciting pharmaceutical innovations that can be received as a driving force for drug development.

1.4 Pharmaceutical innovations

The translation of MAAs, especially the AMPs or SMAMPs, into clinics, has been rather limited up to now (Dey et al., 2019). The pharmaceutical technological innovations open up possibilities for targeted therapy that could improve the application, retention, and release of MAAs (Aiello et al., 2021; Hemmingsen et al., 2021a; Ong et al., 2017; Su et al., 2020). The space does not permit enlisting all promising pharmaceutical innovations proposed or studied for improved delivery of MAAs. Only the representative selection is enlisted here. The delivery systems and scaffolds are categorized based on the origin of MAAs.

Aiello *et al.* investigated the anti-biofilm activities of a polyphenol resveratrol, entrapped in glycosylated liposomes, targeting clinical MRSA biofilms. The liposome-entrapped resveratrol eradicated the biofilm at sub-MICs (Aiello et al., 2021). Ong *et al*. encapsulated propolis in chitosan nanoparticles and challenged *Acinetobacter baumannii* biofilms. The propolis-nanoparticles outperformed the extract alone in both the biofilm inhibition and eradication; however, higher concentrations were required for biofilm eradication. Using SEM and fluorescent microscopy, the authors confirmed biofilm disruption. Furthermore, the genes associated with biofilm virulence factors were found to be downregulated. In addition to providing prolonged release of propolis, the authors postulated that the nanoparticles were able to penetrate the biofilm, contributing to stronger effects (Ong et al., 2017).

Many different strategies for delivery of small AMPs and SMAMPs were evaluated against biofilm-producing bacteria. Neff *et al*. used chitosan hydrogel as delivery system for small AMPs, namely ASP-1 and ASP-2, against MRSA, *P. aeruginosa* and *A. baumannii* biofilms. In the *ex vivo* biofilm assay, the AMPs in hydrogel were able to eradicate biofilms of all three strains completely or almost completely. The hydrogel prolonged the release of the AMPs for several days (Neff et al., 2020). Rozenbaum *et al*. utilized monolaurin lipid nanocapsules to improve the anti-biofilm activity of the small AMP DPK-060 against MRSA and *S. aureus* biofilms. The AMP was adsorbed onto lipid nanocapsules and challenged against pre-formed biofilms. The AMP alone did not reduce the biofilm-embedded bacteria; however, the lipid

nanocapsules-adsorbed AMP significantly reduced the number of bacteria in the biofilm (Rozenbaum et al., 2019). Microneedles that can penetrate the biofilm could be a solution to the biofilm penetration challenges. Su *et al*. utilized core-shell nanofibers on microneedles loaded with the AMP W379 against MRSA biofilms. In the *ex vivo* biofilm model, the novel delivery system significantly improved biofilm eradication in the tested strains. The *ex vivo* polymicrobial biofilm, comprising MRSA and *P. aeruginosa*, was found to be bacteria-free after 72 hours. Moreover, the authors confirmed the *ex vivo* results in an *in vivo* murine wound model (Su et al., 2020). The potential advantages of utilizing drug delivery systems and scaffolds in MAA treatment of wounds are summarized in Figure 1.6.

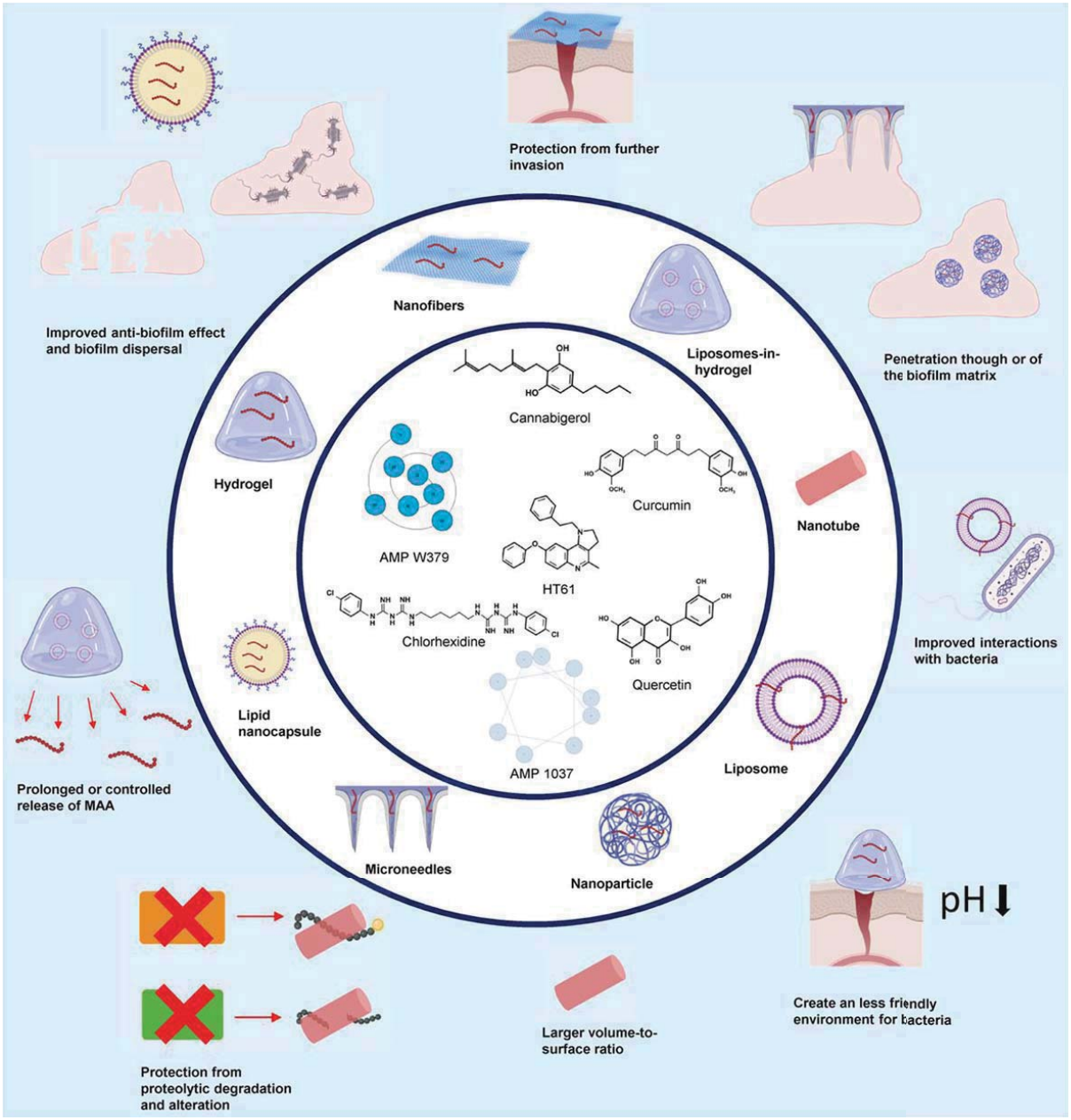

Figure 1.6. Pharmaceutical innovations to improve membrane-active antimicrobial (MAA) therapy. Portrayed with potential drug delivery systems and scaffolds summarizing the advantages of respective pharmaceutical technologies. Created with BioRender.com.

Deeper insight into MAAs' mechanism of action as well as understanding the microbial targets are needed to permit tailoring delivery systems for specific interventions. When designing drug delivery systems and scaffolds, we should further explore nature regarding active yet safe materials with beneficial inherent properties that would act in synergy leading to efficient wound therapy. The arsenal of potential materials exhibiting such properties is

rather broad, however, the materials should be safe and biocompatible, exhibiting additional activities impacting wound healing.

1.4.1 Role of chitosan in infected skin wounds

Considering tailoring the delivery systems for the topical route, chitosan is frequently used as an important building block (Parhi, 2020). Chitosan is a natural polymer composed of (1→4)-2-amino-2-deoxy-β-D-glucan and (1→4)-2-acetamido-2-deoxy-β-D-glucan units (Figure 1.7) that is derived from deacetylated chitin found in crustaceans, insects, and fungi (Liu et al., 2021a). As a material in pharmaceutical formulations, it is highly important that chitosan is confirmed to be biocompatible, biodegradable, and non-toxic (Riaz Rajoka et al., 2019). However, chitosan's biological properties are linked to its molecular weight (M_w) and degree of deacetylation and should always be considered in the development of new delivery systems (Kou et al., 2022). Although Wiegand *et al*. reported the M_w-dependent toxicity of chitosan in an *in vitro* study on keratinocytes (Wiegand et al., 2010), most studies have deemed chitosan generally safe for topical administration (Hao et al., 2022; Hemmingsen et al., 2021c; Intini et al., 2018; Rata et al., 2021).

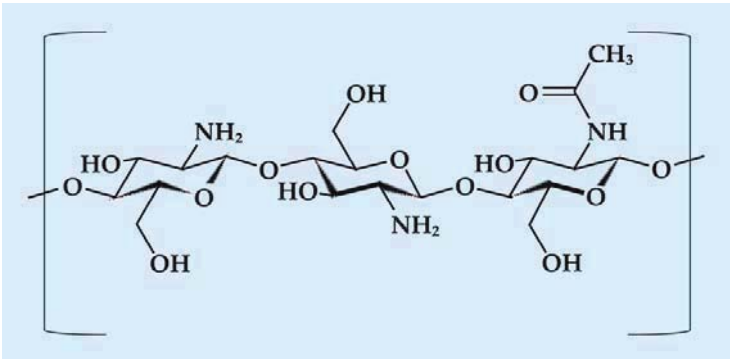

Figure 1.7. Structure of chitosan.

In addition to its safety, the optimism around this polymer stems from its numerous biological activities. Chitosan is proposed to possess antibacterial, antifungal, antiviral, anti-inflammatory, anti-oxidative, haemostatic, and wound healing properties (Parhi, 2020; Xia et al., 2022). Additionally, chitosan has also bioadhesive properties, often beneficial for wound

dressings (Hamedi et al., 2022). In this project, the focus was placed on chitosan's inherent antimicrobial, anti-inflammatory, and wound healing properties. There are several proposed mechanisms for the antimicrobial action of chitosan, however, the complete antimicrobial mechanism is not yet fully understood. The first and most commonly proposed mechanism relies on the interaction between positively charged chitosan with negatively charged bacterial membrane, causing the enhanced permeability and destabilization of bacterial membrane, further leading to bacterial cell lysis (Matica et al., 2019). The second antimicrobial mechanism involves its ability to form an envelope on the bacterial membrane leading to reduced nutrient and oxygen uptake and bacterial growth (Matica et al., 2019). These two mechanisms complement role of MAAs in destruction of bacterial membrane, leading to stronger bacterial eradication. The third proposed mechanism involves chitosan complexation with bacterial DNA affecting the mRNA and protein synthesis (Fuster et al., 2020). Finally, the fourth mechanism, utilizes chitosan's ability to chelate metal cations, leading to growth inhibition and hampering of membrane integrity (Fuster et al., 2020). Moreover, the mechanisms of action are also dependent on M_w of chitosan, namely the higher M_w chitosans are more likely to form an envelope on the bacterial membrane, while chitosans with lower M_w are more likely to penetrate into the bacteria and interact with intracellular components (Matica et al., 2019).

Considering the wound healing properties of chitosan, chitosan offers additional benefits regarding the healing process, especially in the haemostasis, inflammation, and proliferation stages (Feng et al., 2021). It is suggested that chitosan could act as a haemostatic agent, able to promote platelet adhesion and aggregation, while prevent fibrinolysis (Feng et al., 2021). In the inflammatory stage, chitosan participates in several processes involving both innate and adaptive immune system. Chitosan reportedly could increase the infiltration of polymorphonuclear neutrophils and augment functions of macrophages (Barbosa et al., 2010; Kou et al., 2022). The anti-inflammatory properties of chitosan derive from downregulation of different pro-inflammatory factors, like ILs and TNF-α. Additionally, it could also regulate different immune cells leading to altered immune responses (Xia et al., 2022). Yet, the immunomodulating effects of chitosan are rather wide, and could include both the pro- and anti-inflammatory responses (Fong and Hoemann, 2017). Nevertheless, the anti-inflammatory

effects have been confirmed in rodent wound models (Chen et al., 2018; Shen et al., 2020). In the proliferation stage, chitosan has been proven to affect the fibroblast proliferation and migration through stimulated secretion of cytokines (Feng et al., 2021; Ribeiro et al., 2021; Sandri et al., 2019). It has also been proven that chitosan promotes both the proliferation and migration of keratinocytes (Romanova et al., 2015).

There are already some marketed products comprising chitosan for wound therapy, however, most of these products are rather simple formulations including bandages, gels, or sprays approved for haemostatic applications (Hemmingsen et al., 2021b). Even though marketed chitosan-based wound dressings are scarce, chitosan has been extensively studied as an active material or excipient in different formulations, drug delivery systems, or scaffolds aimed at multitargeted wound therapy (Shariatinia, 2019). Among these, the nanoparticles, films, sponges, hydrogels, nanofibers, and other scaffolds are the most common (Hemmingsen et al., 2021b; Xia et al., 2022).

1.4.1.1 Chitosan as the excipient and coating material for liposomes

Chitosan has also been extensively studied as a bio- and mucoadhesive material in formulations destined for different applications routes (Hemmingsen et al., 2021b). The main consequence of its bio- and mucoadhesiveness is a prolonged retention at the administration site. It is also known that the formulation type, or the mode that chitosan is incorporated in pharmaceutical formulation, can tailor its antimicrobial properties (Jøraholmen et al., 2020). In this project, we selected two approaches to incorporate chitosan in the delivery systems for our MAAs. First approach was based on using chitosan as a coating material or excipient in liposomal formulations. In the second approach, the chitosan hydrogels were utilized as a secondary vehicle for liposomes as the primary MAAs carriers.

Chitosan-coating or chitosan-insertion within liposomes could be exploited to improve the stability of liposomes, provide bioadhesive properties, prolong the release of the active compound, and improve the antimicrobial activity of the formulation (Bochicchio et al., 2021;

Jøraholmen et al., 2015). Several studies have proven superior antimicrobial activity of liposomes comprising chitosan. For instance, Wang *et al.* reported the enhanced bacteriostatic activity against *S. aureus* for the chitosan-coated liposomes with cinnamaldehyde as compared to non-coated liposomes. Additionally, the authors demonstrated that both the active compound and chitosan affected the bacterial membrane (Wang et al., 2021b). In another study, Hassan *et al.* tailored lipid-chitosan hybrid vesicles loaded with vancomycin against MRSA biofilms *in vitro*. The hybrid vesicles improved biofilm eradication compared to control. Furthermore, the novel system lowered the bacterial burden of planktonic MRSA by 95-fold as compared to vancomycin alone, in an intradermal MRSA infection mice model (Hassan et al., 2020). Oligo-chitosan-coated liposomes with curcumin significantly improved wound healing and scar repair in mice, as compared to free curcumin (Nguyen et al., 2019).

1.4.1.2 Chitosan hydrogel

Chitosan hydrogel could exert an inherent antimicrobial effect as well as serve as a delivery system for antimicrobial compounds entrapped within the hydrogel structure (Figure 1.8). Additionally, chitosan provides required moisture balance in the wound bed, offers protection from external contaminants and bacteria, and allows gas exchange (Liu et al., 2018). These are crucial requirements from ideal wound dressings (Stoica et al., 2020). Moreover, the three-dimensional network created by the swelling of the polymer permits cell migration and nutrient uptake or diffusion, further enhancing wound healing (Pellá et al., 2018; Shahzadi et al., 2020).

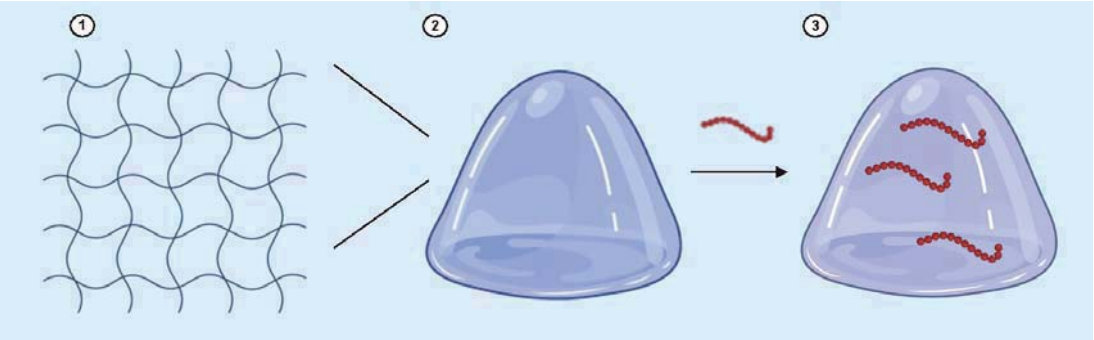

Figure 1.8. Representation of chitosan hydrogel. Graphical depiction of 1) empty hydrogel network, 2) empty hydrogel, and 3) hydrogel loaded with antimicrobial compound. Created with BioRender.com.

Chitosan hydrogels have been reported able to enhance wound healing both in animals and small-scale studies in humans. Ribeiro *et al.* confirmed improved fibroblast survival and wound healing in rats treated with chitosan hydrogel (Ribeiro et al., 2009). In another study, a novel chitosan hydrogel loaded with the AMP LL-37 significantly reduced the wound area after 21 days, furthermore, epidermal and subepidermal layers were better defined and organized as compared to the control group mice (Yang et al., 2020). Rodríguez-Acosta *et al.* developed chitosan hydrogel loaded with silver nanoparticles and calendula extract that was applied in two diabetic patients. The wounds of both patients healed within two to four months (Rodríguez-Acosta et al., 2022). Guo *et al.* tailored a quaternized chitosan hydrogel loaded with tannic acid and ferric iron that significantly improved healing of full-thickness mouse wounds infected with *S. aureus* compared to the control. The effect was enhanced in combination with near-infrared radiation (Guo et al., 2022). In another study, Wang *et al*. prepared multifunctional hydrogels comprising chitosan quaternary ammonium salt and polyacrylamide loaded with litmus and evaluated the formulation against *S. aureus*-infected full-thickness skin wounds in mice. The hydrogel not only reduced the wound area but also pus, redness, and swelling. Furthermore, the epidermal layer was found to be thicker as compared to the control group (Wang et al., 2022). Fasiku *et al*. treated MRSA biofilm-infected wounds in mice with a chitosan hydrogel loaded with hydrogen peroxide and an AMP. The novel formulation significantly reduced the bacterial wound load at the same time as decreasing the wound area (Fasiku et al., 2021).

Examples discussed earlier confirm that chitosan hydrogels are promising delivery system in the treatment of infected wounds, however, there are a few limitations to their wider use that need to be considered. One of the limitations is an initial fast as well as uncontrolled release of the active compound. Additionally, not all active compounds are suitable for loading into hydrogel networks since it is a highly hydrophilic medium that can destabilize sensitive compounds. Improved stability can often be achieved by using a primary carrier to protect the sensitive active compounds; those carriers can be easily incorporated into the hydrogel network, forming so called dual delivery systems, resulting in the liposomes-in-hydrogels systems (Hemmingsen et al., 2021a; Peers et al., 2020).

1.4.2 Liposomes and liposomes-in-hydrogel as formulations for infected skin wounds

Since the discovery of liposomes about 60 years ago, they have been widely studied in drug delivery and biomedical field (Bangham and Horne, 1964; Ferreira et al., 2021; Hua, 2015; Ibaraki et al., 2020; Liu et al., 2021b; Municoy et al., 2021). Liposomes are spherical structures comprising phospholipid bilayers (Figure 1.9). These self-assembled membrane structures comprise one or several layers surrounding aqueous cores. The phospholipids are arranged with their head groups either facing the cores or surrounding aqueous phase, while tails are accommodated within the bilayers (Guimarães et al., 2021a).

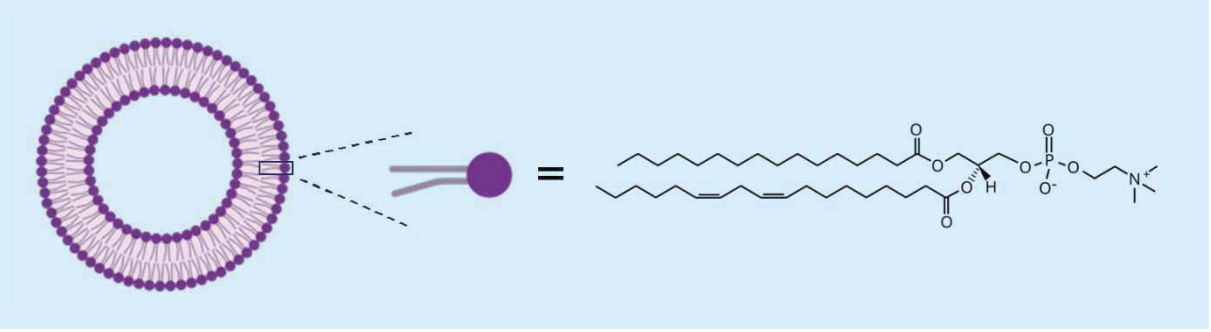

Figure 1.9. A graphical representation of liposome with highlighted phospholipid and phosphatidylcholine structure. Created with BioRender.com.

Liposomes are versatile delivery systems, with numerous liposome-based formulations on the market, for various therapies that include, for example, AmBisome®, comprising an antifungal drug, Doxil®, comprising a chemotherapeutic drug, and Arikayce®, against *Mycobacterium avium* complex lung disease (Large et al., 2021). Their promise relies on their biocompatibility, biodegradability, and generally low toxicity and immunogenicity (Antimisiaris et al., 2021). Furthermore, the versatility of these carriers is often attractive for formulation developers as liposomal surface can be tailored/modified for specific targets. Due to the amphiphilic nature of liposomes, the hydrophilic, lipophilic, and amphiphilic compounds could be entrapped or associated with liposomes. However, the clinical success of liposomal formulation is influenced by the preparation method applied in their manufacturing, liposomal characteristics as well as the physiochemical properties of the incorporated active compound or compounds (Guimarães et al., 2021a).

The use of liposomes for skin delivery has increased since the first report on entrapment of triamcinolone in liposomes that were applied to rabbit skin in 1980 (Mezei and Gulasekharam, 1980). Due to the similarity of their and skin compositions, liposomes are an attractive delivery system for skin administration. By allowing liposomal lipids to interact with skin lipids, leading to accumulation of active compounds in the intended skin site or acting as a skin reservoir for an active compound, liposomes are widely studied as skin delivery system (Hua, 2015; Jain et al., 2017). However, in wounds, the skin structure is impaired therefore the deposition of a compound can be altered (Hua, 2015). Liposomes could also provide prolonged release of an active compound, leading to reduced application frequency and prolonged, continuous exposure of an active compound to skin targets (Carita et al., 2018). Their potential in improving the wound therapy has also gained optimism and remains to be further exploited (Nwabuife et al., 2021; Wang et al., 2019).

There are several advantages of lipid-based systems in antimicrobial therapy. Liposomes allow for local delivery of the antimicrobial compounds, which is often the ideal administration mode in localized infections (Huh and Kwon, 2011). Local delivery of antimicrobial compound could provide high local concentration at the infected site, reduce

resistance development due to limited systemic exposure, and therefore also improve patient safety (Hemmingsen et al., 2021b; Lam et al., 2018). The fact that liposomes could interact with other lipid membranes could also be utilized for the eradication of bacteria. Liposomes could interact or fuse with bacterial membranes and therefore deliver a higher payload into the bacterial cell (Montefusco-Pereira et al., 2020; Wang et al., 2020). Moreover, liposomes with cationic surfaces could further improve the interaction (Wang et al., 2020). This interaction and higher local concentration could translate into lower total dose of the antimicrobial compound given to the patients, reducing the probability of systemic effects and resistance development (Gonzalez Gomez and Hosseinidoust, 2020; Rukavina and Vanić, 2016). Moreover, studies have proven better anti-biofilm effects of compounds/drugs incorporated in liposomes. Ibaraki *et al.* confirmed enhanced permeation and retention of cationic and anionic liposomes in *P. aeruginosa* biofilms. Liposomes comprising polyethylene glycol (PEG) enhanced permeation, while liposomes without PEG improved retention (Ibaraki et al., 2020). Ferreira *et al.* also reported the therapeutic potential of rifabutin loaded liposomes against *S. aureus* biofilms (Ferreira et al., 2021).

However, there are some limitations linked to these carriers. The disadvantages that hamper their wider use in skin antimicrobial therapy include low stability, drug leakage, and low viscosity and retention at administration site, especially for conventional liposomes (Maja et al., 2020; Rukavina and Vanić, 2016). These limitations could be addressed by using a secondary vesicle, such as hydrogel. Moreover, to improve the antimicrobial potential of the formulations, chitosan hydrogels could be great candidates (Rukavina and Vanić, 2016). Employing a combination of liposomes and hydrogels, both the burst release from the hydrogel network and leakage from liposomes could be avoided. This dual system, liposomes-in-hydrogel (Figure 1.10), possesses promising features suitable for treatment of wounds. Hurler *et al.* reported that novel mupirocin-liposomes-in-hydrogel were superior formulation to treat burns in mice (Hurler et al., 2013). Furthermore, Değim *et al.* confirmed that the rats treated with epidermal growth factor in liposomes-in chitosan hydrogel exhibited faster wound healing and increased epidermis thickness (Değim et al., 2011). Gao *et al.* tailored pH-sensitive gold nanoparticle-stabilized liposomes-in-hydrogel against *S. aureus*. The authors proved pH-dependent fusion with the bacteria and therapeutic potential of the novel

formulation (Gao et al., 2014). All these results assure the potential of liposomes-in-hydrogel and chitosan-containing liposomes as suitable delivery systems for infected chronic wounds. Moreover, utilizing the nature-derived MAAs as an active antimicrobial compound, we could explore nature to boost the potential of innovative solutions and advanced topical delivery systems.

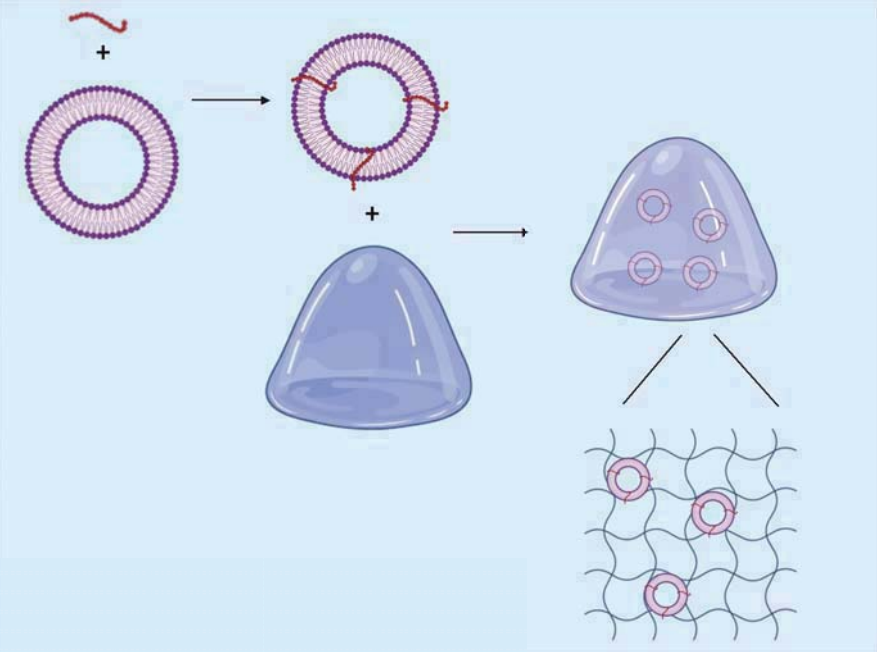

Figure 1.10. Concept of liposomes with antimicrobial compound incorporated into the chitosan hydrogel network (liposomes-in-hydrogel). Created with BioRender.com.

1.5 Our approach – antimicrobial compounds and delivery systems

The MAAs bear great potential in antimicrobial, topical therapy. However, the synthesis and purification of AMPs and SMAMPs is often time-consuming and expensive, with rather limiting yield considering a large-scale production (Erdem Büyükkiraz and Kesmen, 2022). Therefore, to gain time and assure accessibility, in the first stage of the development of novel drug delivery systems, we used a model MAA, namely CHX (Figure 1.11 A). CHX is a broad-spectrum divalent cationic biguanide antiseptic, often used to treat or prevent skin infections, with known activity against gram-positive and gram-negative bacteria (Williamson et al., 2017). The most frequently described antimicrobial mechanism of action of CHX is reportedly

its ability to bind to negatively charged components of the bacterial membrane, destructing the membrane, and consequently causing leakage and bacterial death (Zheng et al., 2022). At lower concentrations, CHX causes leakage and precipitation of proteins and nucleic acids, while at higher concentrations the bacterial membrane is disrupted (Hoang et al., 2021). Moreover, we chose to work with CHX base because of its lowered water solubility compared to the salts (Farkas et al., 2001) to better mimic the lowered water solubility of MAAs approaching the clinical pipeline. However, we were concern regarding the safety of CHX since it is often debated. While some data indicate that CHX can cause skin irritation, and that it exhibits toxicity against common skin cells, other reports claim that skin toxicity is not common (Abdel-Sayed et al., 2020; Barrett et al., 2022; Chiewchalermsri et al., 2020; Hirschman et al., 2012). However, to both assure the CHX safety and improve its antimicrobial effects, several studies reported successful CHX incorporation in drug delivery systems; also, the drug delivery systems comprising chitosan (Al-Obaidy et al., 2021; Kettel et al., 2017; Kutsevol et al., 2021; Rossi et al., 2007; Song et al., 2016). Therefore, we tailored drug delivery systems for CHX as a model MAA aiming at improving its antimicrobial effects.

After optimizing the delivery systems for CHX (papers I-III), we utilized the gained knowledge to tailor drug delivery systems for model SMAMPs (papers IV-V). Paulsen *et al*. synthesised novel SMAMPs mimicking eusynstyelamides isolated from the bryozoan *Tegella cf. spitzbergensis*. These amphipathic guanidine barbiturates exhibited promising antimicrobial activity against a panel of bacteria, making them promising candidates against various infections, MDR bacteria, and biofilm-embedded bacteria. The SMAMPs caused destruction of bacterial membranes, similar to CHX (Paulsen et al., 2021). From these promising SMAMPs we selected two, namely 7e-SMAMP and 7a-SMAMP (Figure 1.11 B and C, respectively). The 7e-SMAMP was selected for its strong antimicrobial activity, while 7a-SMAMP was selected due to its safety profile against human erythrocytes (Paulsen et al., 2021). To pursue a multitargeting approach to wound healing, we also utilized chlorogenic acid (CGA, Figure 1.11 D) in combination with 7a-SMAMP. The CGA was mainly added to implement anti-oxidative effects (Feng et al., 2016; Xu et al., 2012). However, CGA is also linked to other biological effects, such as antimicrobial (Kabir et al., 2014; Li et al., 2014; Lou et al., 2011), wound healing (Bagdas et al., 2015; Moghadam et al., 2017), and anti-

inflammatory properties (Schröter et al., 2019). Furthermore, Chen *et al*. proved good wound healing and anti-oxidative properties of topically applied CGA in a rat excision wound model, revealing encouraging actions of CGA in wound therapy (Chen et al., 2013).

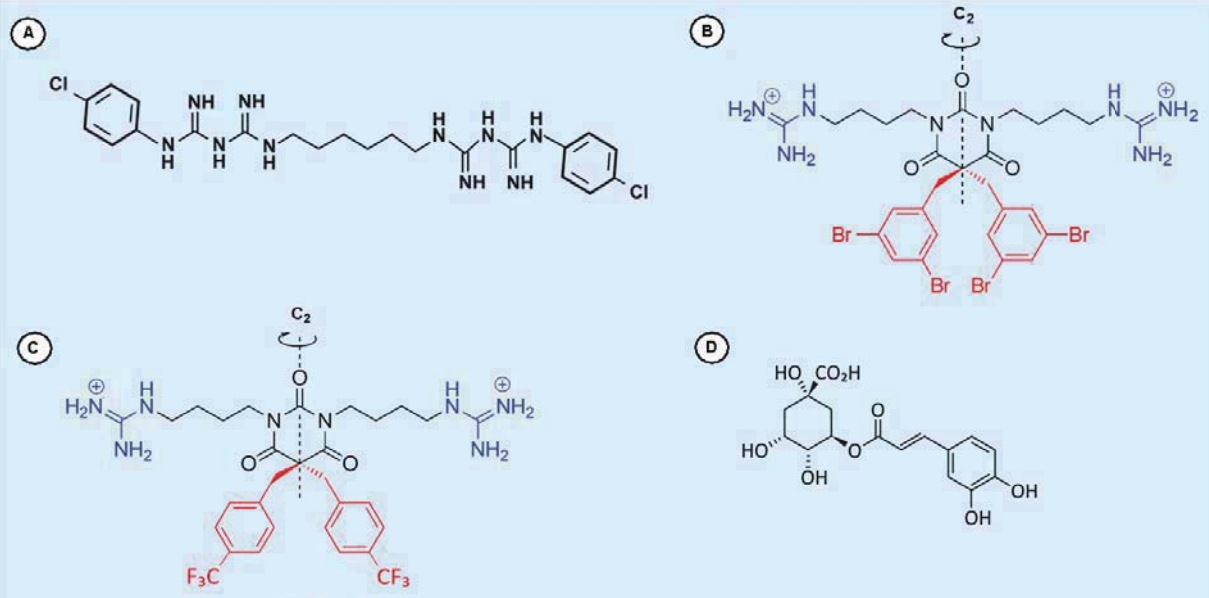

Figure 1.11. Molecular structures of active compounds used in this project. A) chlorhexidine (CHX), B) 7e-SMAMP, C) 7a-SMAMP, and D) chlorogenic acid (CGA).

To improve the antimicrobial activities and safety of these compounds, we tailored liposomes and chitosan in different formulations. In the first part of the project, we developed a primary carrier for our MAAs using CHX as a model compound. Various vesicles were prepared, namely the conventional liposomes and chlorhexidine-liposomes (CHX-liposomes, paper I), chitosomes and chlorhexidine-chitosomes (CHX-chitosomes, paper II), chitosan-containing liposomes and chlorhexidine-chitosan-containing liposomes (CHX-chitosan-containing liposomes), and chitosan-coated liposomes and chlorhexidine-chitosan-coated liposomes (CHX-chitosan-coated liposomes, paper III, Figure 1.12). Furthermore, liposomes (papers I, IV, and V), plain vesicles (paper II), and lipid carriers (paper III) corresponding to plain liposomes were prepared, however, due to various production procedures we used different nomenclatures to distinguish them. All vesicles were optimized regarding wound healing potential. Additionally, we produced chitosan hydrogels as a secondary vehicle and optimized a mode of chitosan incorporation in the novel formulations.

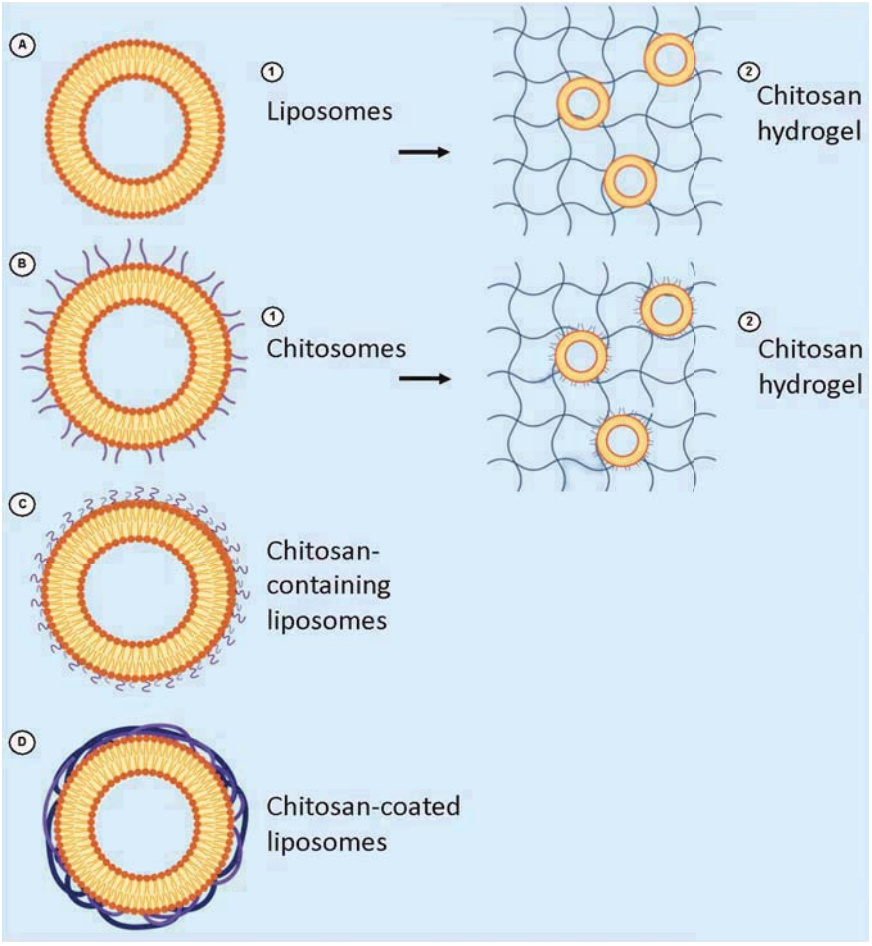

Figure 1.12. Summary of delivery systems used in this project. A) 1) liposomes, 2) chitosan hydrogel, B) 1) chitosomes, 2) chitosan hydrogel, C) chitosan-containing liposomes, and D) chitosan-coated liposomes. Created with BioRender.com.

In the second part of the project, we tailored the delivery systems for the novel SMAMPs based on the optimization of formulations for CHX. The conventional liposomes and liposomes-in-chitosan hydrogel were deemed the most suitable systems for biofilm-infected chronic wounds (Figure 1.12 A). We therefore tailored liposomes for 7e-SMAMP (7e-SMAMP-liposomes) and liposomes-in-hydrogel for 7a-SMAMP (7a-SMAMP-liposomes-in-hydrogel).

2. Aims of the thesis

The overall aim of the PhD project presented in this thesis was to tailor and optimize delivery systems for MAAs, especially SMAMPs, intended for treatment of infected skin wounds. The goal was to optimize the antimicrobial and anti-inflammatory properties of the antimicrobial compounds and delivery systems. To achieve this, novel delivery systems comprising combinations of liposomes and chitosan were developed and optimized to assure improved antimicrobial and anti-inflammatory effects of incorporated active compounds.

The specific aims were as following:

- Optimize conventional liposomes, chitosomes, chitosan-containing liposomes, and chitosan-coated liposomes loaded with CHX, confirming their suitability as delivery systems for improved therapy of skin wounds. Further, finding the most suitable system to the SMAMPs.
- Translate the optimization of CHX-liposomes into liposomal delivery systems for novel antimicrobials, the SMAMPs.
- Tailor chitosan hydrogels and liposomes-in-hydrogels for topical skin wound application.
- Assure that the novel systems provide the sustained release of active compounds as well be considered the patient-friendly dressings.
- Confirm anti-inflammatory activity of the formulations.
- Confirm the cell compatibility of the formulations in relevant cell lines, e.g., keratinocytes, fibroblasts, and macrophages.
- Confirm the antimicrobial and anti-biofilm effect of formulations in relevant bacteria and biofilms, e.g., *S. aureus*, *Staphylococcus epidermidis, P. aeruginosa,* and *E. coli*.

3. Summary of papers

Paper I - Liposomes-in-chitosan hydrogel boosts potential of chlorhexidine in biofilm eradication in vitro

In the first paper, we utilized CHX as a model compound for MAAs and SMAMPs. The synthesis of AMPs and SMAMPs is often a small-scale production and both costly and time-consuming. On the other hand, CHX is a cheap, well-known, and widely available antimicrobial drug that presents a pharmaceutical challenge considering its applicability in wound dressings. Novel formulations able to improve its biological properties could be highly beneficial in management of chronic wounds. The aim was to develop a liposomes-in-chitosan hydrogel system to improve antimicrobial properties and assure biocompatibility of CHX.

The CHX-liposomes prepared by the thin-film hydration method and manual extrusion, were further incorporated into a chitosan hydrogel network to create a formulation optimized for skin delivery. The liposomes were characterized for their size, size distribution, zeta potential, pH, and entrapment efficiency while the hydrogel and liposomes-in-hydrogel were characterized by texture analysis. The *in vitro* drug release, bioadhesion, anti-inflammatory properties, biocompatibility, and antimicrobial and anti-biofilm activities were assessed.

The optimized phosphatidylcholine liposomes bearing CHX were around 300 nm in size with relatively narrow size distribution suitable for delivery of CHX onto/into the skin while allowing its penetration into biofilms. Additionally, the cationic surface charge (45.5 mV) assured a strong interaction with bacterial membranes and biofilm matrices. The novel liposomes-in-hydrogel system provided prolonged release of CHX, produced a significant reduction in inflammatory responses in macrophages, and exhibited proliferative effects on keratinocytes. Since the chronic wounds are arrested in an inflammatory phase, the confirmed anti-inflammatory properties could help further progression of the healing cascade without inducing toxicity to the cells needed for proper healing.

Finally, we assessed the antimicrobial and anti-biofilm activities of the formulation in *S. aureus* and *P. aeruginosa*. In the planktonic bacteria, non-formulated CHX exhibited the fastest eradication, however, both CHX-liposomes and CHX-liposomes-in-hydrogel were able to completely eradicate bacteria even when challenged in the simulated wound environment.

This delayed eradication can be contributed to the prolonged CHX release. To evaluate the anti-biofilm effects, we focused on two mechanisms, namely the inhibition of biofilm formation and eradication of pre-formed biofilm. The free CHX had moderate effect on both inhibition and eradication, while the novel liposomes-in-hydrogel system was able to completely inhibit biofilm formation and eradicated 82-98% and 64% of *S. aureus* and *P. aeruginosa* biofilms, respectively.

This study demonstrated that CHX-liposomes-in-hydrogel could serve as a novel platform in the development of wound dressings for chronic wounds. Furthermore, we confirmed that chitosan hydrogel boosts the effects of the liposomally-associated CHX.

Paper II - Chitosomes-In-Chitosan Hydrogel for Acute Skin Injuries: Prevention and Infection Control

In the second paper, we continue to focus on intrinsic antimicrobial properties of chitosan by investigating whether the chitosan's activities are affected by the way chitosan was accommodated in the formulation. We were particularly interested in the properties of CHX-liposomes if we inserted chitosan within the liposomal bilayers. We therefore utilized the one-pot method, a modified version of solvent injection, to prepare chitosomes. The CHX was again used as a model MAA.

Both CHX-vesicles and CHX-chitosomes were prepared by the one-pot method followed by probe sonication. Due to the promising results from the first paper, we also included chitosan hydrogels in this study. After optimizing novel delivery systems for skin administration, we additionally quantified the surface-available chitosan as well as evaluated the rheological behaviour of the hydrogels. The antimicrobial activity of these formulations was evaluated against *S. aureus* and *S. epidermidis*. The biocompatibility assessments were also extended to include the hydrogel, even though the safety of chitosan hydrogels has been previously thoroughly investigated.

We determined that both CHX and chitosan were accommodated on the surface of the CHX-chitosomes. Considering antimicrobial therapy, this finding could clearly be an advantage since both molecules could interact with the bacterial membrane to assert their antimicrobial effects. The hydrogels and vesicles-in-hydrogel exhibited pseudoplastic flow with shear thinning behaviour; the viscosity and shear stress decreased upon increasing temperature, which is considered beneficial for formulations intended for skin applications.

All formulations were biocompatible with keratinocytes, important cells considering the healing cascade. Furthermore, the chitosan was once again proven to enhance the antimicrobial effects of the active compound. Chitosomes were more effective than the plain lipid vesicles, however, the antimicrobial effects of the hydrogel formulations were the strongest. The CHX-chitosomes-in-chitosan hydrogel could be a suitable formulation for both the prevention and infection control of skin injuries, particularly for therapy of acute skin injuries.

Paper III - Chitosan-based delivery system enhances antimicrobial potential of chlorhexidine

Encouraged by the findings in paper II, in the third paper, we further exploited the mode of inserting chitosan in the liposomal bilayers, namely we challenged the chitosan-coated versus chitosan-containing liposomes. CHX was used as a model MAA. Contrary to the second paper, we used chitosan of lower M_w since it is more often used as a coating polymer. This enabled us to also assess the effect of its M_w.

Lipid carriers and chitosan-containing liposomes with and without CHX were formed through the thin-film hydration method, followed by probe sonication and manual extrusion. Chitosan-coated liposomes were prepared by coating the plain lipid carriers with chitosan solutions. We evaluated three different types of vesicles, namely the lipid carriers, chitosan-containing liposomes, and chitosan-coated liposomes. All vesicles were characterized as in papers I and II. We particularly focused on the surface-available chitosan, cell compatibility, anti-inflammatory activity, and antimicrobial effect.

All vesicles, except the CHX-chitosan-coated liposomes, had mean vesicle populations between 300 and 350 nm (cumulative size ≤80%). The CHX-chitosan-coated liposomes were larger, however, still with a mean cumulative size below 400 nm. The size distribution was still deemed suitable for topical administration. The surface charge of CHX loaded chitosan-containing-liposomes and chitosan-coated liposomes were significantly higher than for the CHX-chitosomes in our previous paper, indicating that more CHX and/or chitosan was available at the surface of the vesicles. We confirmed that more chitosan was surface available to potentially interact with bacteria.

The cell compatibility of these vesicles was evaluated in three different cell lines, namely keratinocytes, fibroblasts, and macrophages. The vesicles exhibited excellent biocompatibility; no toxicity was observed for any of the vesicles throughout the whole concentration range in any of the cells. Furthermore, the reduction of NO production, indicating that the anti-inflammatory response was strong. Finally, the same trends that were observed for the chitosomes in the previous study were confirmed in this study. The CHX induced a strong antimicrobial effect, that was further enhanced by chitosan. The

combinations of CHX and chitosan in CHX-chitosan-containing liposomes and CHX-chitosan-coated liposomes exhibited strong antimicrobial activity against *S. aureus*.

We confirmed that both chitosan-containing and chitosan-coated liposomes could serve as potential platforms for the delivery of MAAs exhibiting improved antimicrobial activity against *S. aureus* and therefore potentially enhancing healing of chronic wounds.

Paper IV - Tailored anti-biofilm activity – liposomal delivery for mimic of small antimicrobial peptide

Among the MAAs, AMPs and SMAMPs have attracted more attention for their broad and fast antimicrobial action together with other beneficial biological properties. In the fourth paper, we focused on novel amphipathic guanidine barbiturates modelled after eusynstyelamides isolated from *Tegella cf. spitzbergensis*, a marine bryozoan. The eusynstyelamides comprise two cationic groups, either amine or guanidine groups, and two lipophilic groups coupled with a five-membered ring. To mimic this structure, the novel SMAMPs consist of two cationic guanidine groups and two lipophilic groups with bromine or trifluoromethyl substituents coupled with barbiturate ring to fulfil the pharmacophore of small AMPs. These mimicked SMAMPs have previously exhibited excellent antimicrobial activity, however, we aimed to further enhance the antimicrobial action of the novel SMAMP as well as improve other biological properties, as achieved for CHX in the first part of the project (paper I). The selected SMAMP, 7e-SMAMP, was especially interesting due to its strong antimicrobial activity. Conventional liposomes were selected as a primary carrier for 7e-SMAMP. Since 7e-SMAMP exhibits a strong membrane activity, we focused both on improved antimicrobial effects of liposomally-associated 7e-SMAMPas well as potential effects this novel compound may have on liposomal properties.

At first, we needed to assure that the 7e-SMAMP was stable in relevant fluids, especially a simulated wound fluid (SWF). The 7e-SMAMP was proven to remain stable at three different storage temperatures, namely 4, 25, and 32 °C for up to 7 days.

We than prepared liposomes by the thin-film hydration method using manual extrusion. To make sure that liposomes were indeed formed, stable, and in desired size range, we determined the size, size distribution, zeta potential, phospholipid content, membrane elasticity, morphology, and *in vitro* 7e-SMAMP release profile. The 7e-SMAMP-liposomes in a size range of around 250-300 nm maintained their stability over a period of 12 weeks. The surface charge (59 mV) suggested that 7e-SMAMP was accommodated within or onto the surface of liposomes assuring its accessibility to interact with bacterial membranes. The 7e-SMAMP-liposomes also exhibited prolonged release of 7e-SMAMP, indicating their potential to prevent bacterial regrowth without need for multiple applications, thereof improving patient compliance.

Next, we evaluated the cell compatibility and anti-inflammatory activity of the 7e-SMAMP-liposomes. We confirmed that 7e-SMAMP-liposomes (50 μg/mL lipid) significantly reduced the NO production in murine macrophages, indicating strong anti-inflammatory activity. Furthermore, we confirmed the safety of 7e-SMAMP-liposomes in both keratinocytes and macrophages. Moreover, 7e-SMAMP-liposomes (50 μg/mL lipid) also exhibited proliferative effects in the keratinocytes, similarly to empty liposomes.

Lastly, we evaluated the antimicrobial activity of 7e-SMAMP-liposomes. To investigate the mechanism of their activity, we utilized an indirect approach. We tailored B3M-liposomes to mimic the membrane of *S. aureus* and *P. aeruginosa*. First, we loaded these B3M-liposomes with FITC-dextrans and measured their leakage upon exposure to non-formulated or formulated 7e-SMAMP. Only the 7e-SMAMP-liposomes were able to induce leakage of high M_w FITC-dextran from *P. aeruginosa* B3M-liposomes. We further investigated fusion between the inner and outer layer of B3M-liposomes by labelling the inner leaflet and monitoring possible lipid flip-flop induced by membrane stress. In *S. aureus* B3M-liposomes, 7e-SMAMP-liposomes induced strong fusion at the highest concentration, while non-formulated 7e-SMAMP induced fusion at all tested concentrations. In *P. aeruginosa* B3M-liposomes, 7e-SMAMP-liposomes induced the strongest fusion in all concentrations. These results indicated that both 7e-SMAMP and 7e-SMAMP-liposomes exerted their activity on mimics of bacterial membranes.

The most abundant wound bacteria, namely *S. aureus*, *P. aeruginosa*, and *E. coli* were used in the antibacterial challenges. In an environment comprising SWF, both non-formulated and formulated 7e-SMAMP completely eradicated all bacteria, except *S. aureus* SO2 and *P. aeruginosa* ATCC10145. The effect was delayed in 7e-SMAMP-liposomes, corresponding to release data.

Encouraged by a strong antibacterial effect, the final challenge focused on the anti-biofilm effects exhibited through both the inhibition of biofilm formation and eradication of pre-formed biofilm. The 7e-SMAMP-liposomes were more effective than non-formulated 7e-SMAMP in both inhibition and eradication of biofilm. These results suggest that 7e-SMAMP-liposomes could be utilized both in prevention and treatment of infections, confirming their potential in chronic wound therapy.

Paper V - Towards multitarget approach in chronic wound healing – Synthetic mimic of antimicrobial peptide combined with polyphenol in liposomes-in-hydrogel dressing

After confirming that liposomes enhance antimicrobial action of highly potent SMAMP, we evaluated another SMAMP, the 7a-SMAMP is a less potent antimicrobial but could exhibiting several beneficial properties regarding wound healing. We developed liposomes-in-hydrogels for 7a-SMAMP. Furthermore, we co-entrapped 7a-SMAMP with the polyphenol chlorogenic acid (CCA), a known antioxidant and anti-inflammatory compound, to develop a dressing able to achieve multitargeted activities in wound healing. We were particularly interested in improved healing.

Liposomes containing 7a-SMAMP and/or CGA were produced via thin film hydration method and their size optimized using manual extrusion. The liposomes were characterized for their size, size distribution, surface charge, entrapment efficiency, and *in vitro* release, and incorporated in chitosan hydrogels. The hydrogels were characterized for their texture properties, rheological behaviours, and *in vitro* release. The radical scavenging activity of CGA was confirmed and compared to the activities of vitamin C and E.

We performed assessments of the anti-inflammatory activity, cell toxicity, and effects on cell migration in cells treated with the novel formulations. More specifically, we measured the NO production in murine macrophages, and evaluated potential toxicity in the murine macrophages, keratinocytes, and fibroblasts. Moreover, we assessed the effects of liposomes and CGA/7a-SMAMP-liposomes on keratinocyte and fibroblast cell migration to gain insight on wound closing potential of novel formulation.

Liposomes containing 7a-SMAMP and/or CGA were of approximately 200 nm in size with a narrow size distribution. The surface of CGA-liposomes was neutral but increased upon incorporation of 7a-SMAMP, indicating that 7a-SMAMP is associated with the bilayers of liposomes. Interestingly, the entrapment efficiency increased when both compounds were entrapped in the liposomes. The liposomes provided prolonged release of 7a-SMAMP. The CGA exhibited similar or stronger anti-oxidative effects compared to vitamin C and E. The hydrogels and liposomes-in-hydrogels, except the ones containing CGA, demonstrated stable texture properties, while the hardness and cohesiveness increased for hydrogels containing

CGA. Furthermore, the hydrogel, 7a-SMAMP-liposomes-in-hydrogel, and CGA/7a-SMAMP-liposomes-in-hydrogel exhibited temperature-dependent pseudoplastic flow and were therefore deemed suitable for topical skin application. Interestingly, the liposomes-in-hydrogel had an initial faster 7a-SMAMP release rate than the liposomes, however, release was still suitable for treatment of infected wounds.

All liposomal formulations and hydrogels, except the liposomes containing CGA, exhibited strong dose-dependent anti-inflammatory activity. Even though that CGA is described in literature as being an anti-inflammatory compound, the opposite effect was seen in the macrophages treated with CGA-liposomes and CGA/7a-SMAMP-liposomes. No significant toxicity was observed in any of the cells treated with either liposomal formulations or hydrogels. There was a small reduction in the viability of murine macrophages treated with hydrogel or CGA/7a-SMAMP-liposomes-in-hydrogel, however, viability remained above 70% and therefore the formulations were deemed non-toxic. The CGA/7a-SMAMP-liposomes improved keratinocyte migration after 24 and 30 hours. In fibroblasts, the migration was not affected by the treatment.

The result highlighted that liposomes-in-hydrogel containing CGA and 7a-SMAMP could address the challenges of inflammation and improve wound closure in chronic wounds.

4. Experimental section

The methods utilized in this project are described in depth in papers I-V, however, in this section a very brief overview of selected methods is given.

Three studies were designed to evaluate the characteristics and *in vitro* properties of liposomes, chitosomes, chitosan-containing liposomes, and chitosan-coated liposomes with CHX (Figure 4.1). The method descriptions for liposomes and secondary vehicles are found in papers I-III. To evaluate the characteristics of both the vesicles and secondary vehicles, different methods were employed as described in papers I-III.

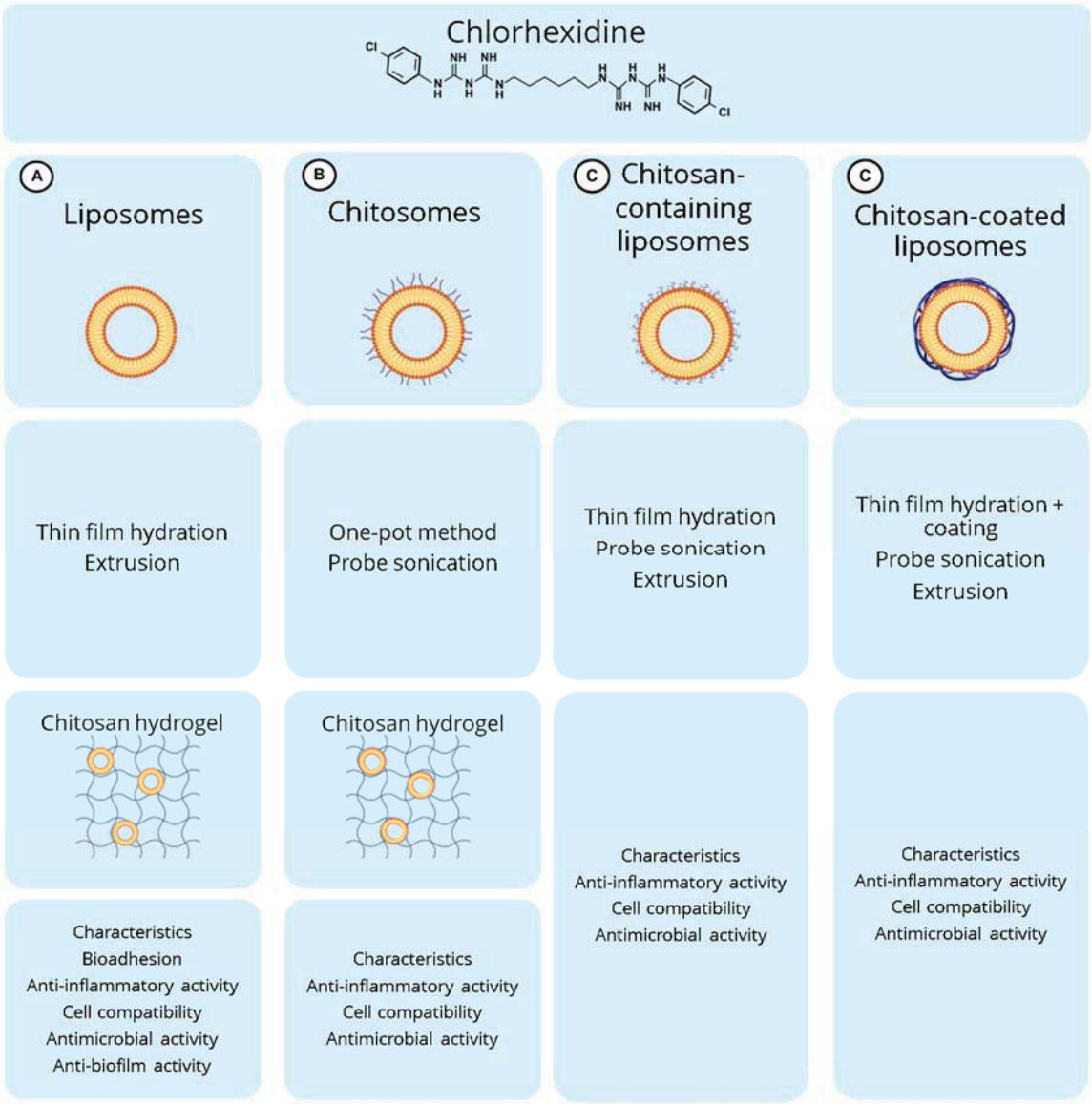

Figure 4.1. Overview of primary and secondary delivery systems prepared with chlorhexidine (CHX) as a model compound. Preparation and characterization methods included in the different studies are also specified. A) Paper I, B) paper II, and C) paper III. Created with BioRender.com.

Based on the evaluation of the various carriers for CHX, conventional liposomes incorporated into chitosan hydrogel were selected as the optimal dual delivery system for the second model MAAs, the newly patented SMAMPs (Strøm et al., 2018). The selection was based on a shorter production time, relative ease of the procedure, bilayer structure and characteristics, biological activities, and potential for upscaling. However, prior to SMAMP-liposomes incorporation in hydrogels, we deemed it necessary to initiate more thorough

evaluations of the liposomes comprising novel SMAMPs synthesised for this project. Therefore, two separate studies were designed. In the first study, we aimed to perform a rigorous evaluation of 7e-SMAMP associated with liposomes (7e-SMAMP-liposomes, Figure 4.2 A, paper IV), whereas in the second study, we tailored 7a-SMAMP-liposomes-in-chitosan hydrogel (Figure 4.2 B). Furthermore, CGA was co-entrapped with 7a-SMAMP to provide a multitarget approach to wound heling, contributing with the anti-oxidative properties (paper V).

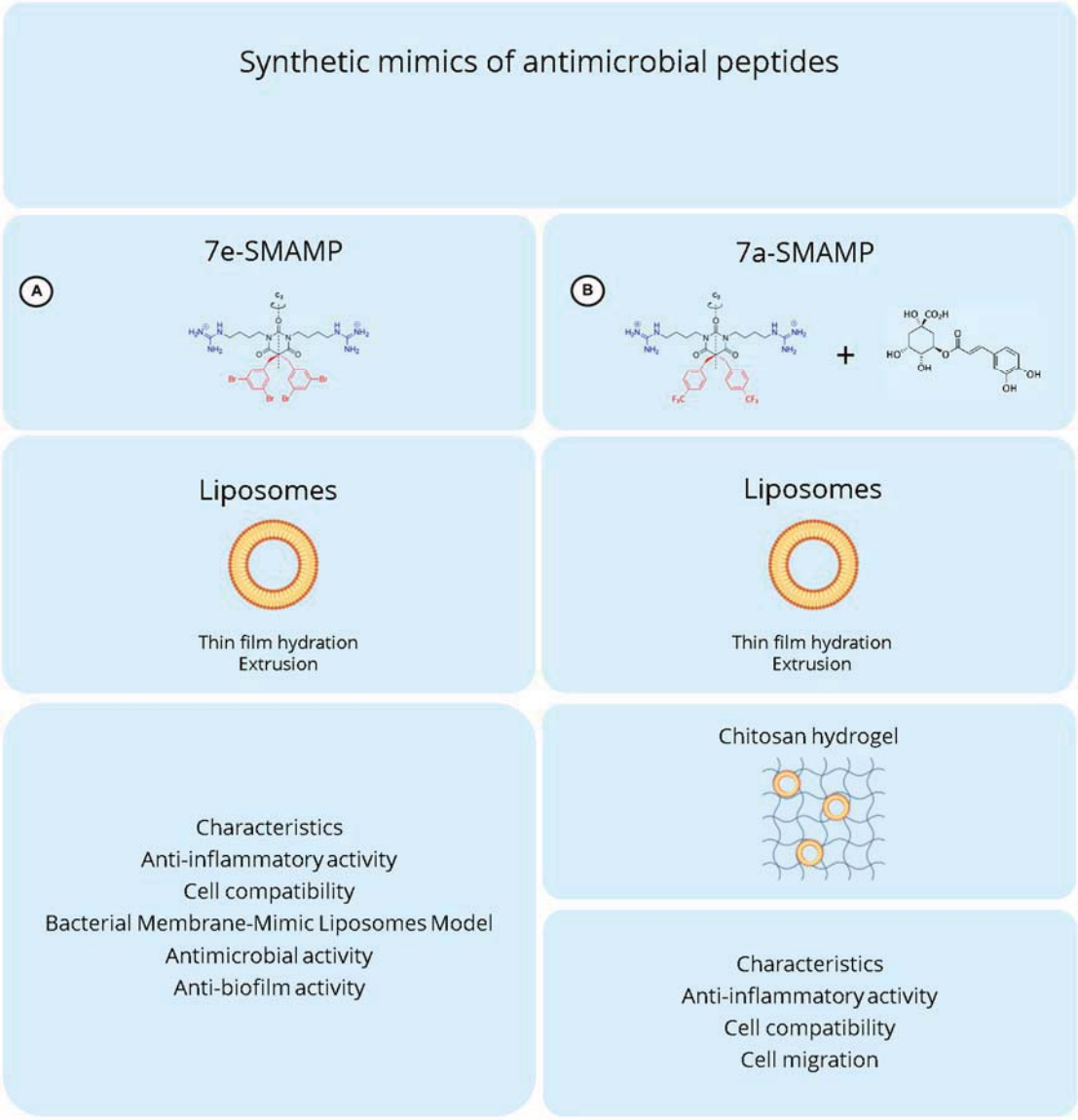

Figure 4.2. Overview of primary and secondary delivery systems for synthetic mimics of antimicrobial peptides (SMAMPs). Preparation and characterization methods included in the different studies are also specified. A) Paper IV and B) paper V. Created with BioRender.com.

In the following subsections the methods applied to evaluate the activities of novel delivery systems are briefly described; however, full method descriptions can also be found in papers I-V.

4.1 Cell experiments (papers I-V)

The murine macrophages (RAW 264.7) were cultured in RPMI, while keratinocytes (HaCaT) and fibroblasts (HDF-neo) were cultured in DMEM high glucose. In both cases, the media was supplemented with fetal bovine serum (10%, v/v) and penicillin-streptomycin. Cell compatibility was assessed in all three cell lines; the cell migration was evaluated for HaCaT and HDF-neo cells, whereas the anti-inflammatory activity in RAW 264 cells.

4.1.1 Cell compatibility (papers I-V)

Potential cytotoxicity of the formulations was assessed as described previously by Cauzzo *et al.* using the cell counting kit-8 (CCK-8), a colorimetric assay for determination of cell viability (Cauzzo et al., 2020). Cells were seeded (1 x 10^5 cells/mL, 90 µL) in 96-well plates and incubated (37 °C, 5% CO_2) overnight. To evaluate the compatibility of formulations, either liposomes, hydrogels, or liposomes-in-hydrogel, were added to the wells (lipid concentrations of 1, 10, and 50 µg/mL or the corresponding concentration of hydrogels). After 24 hours incubation, 10 µL of the CCK-8 reagent was added to each well and the cells were incubated for another 4 hours. The reduction of the CCK-8 reagent by dehydrogenases to formazan, was evaluated on a UV-vis plate reader (Tecan Trading AG, Switzerland); the absorbance was measured at 450 nm and referenced at 650 nm.

4.1.2 Anti-inflammatory activity (papers I-V)

The anti-inflammatory activity was determined by inducing NO production in RAW 264.7 cells with LPS as previously reported (Giordani et al., 2019). Cells were seeded (5 x 10^5 cells/mL, 1 mL) in 24-well plates and incubated (37 °C, 5% CO_2) overnight. Complete medium was replaced with medium containing LPS (1 µg/mL) to induce NO production. The cells were

treated with either liposomes, hydrogels, or liposomes-in-hydrogel (lipid concentrations of 1, 10, and 50 µg/mL or the corresponding concentration of hydrogels). Cells treated with only LPS containing medium or complete RPMI served as controls. Afterwards, the cells were incubated for another 24 hours. Finally, the NO production was evaluated on the UV-vis plate reader (Tecan Trading AG, Männedorf, Switzerland) with Griess reagent (1:1, v/v; 2.5% phosphoric acid with 1% sulphanilamide and 0.1% N-(-1-naphthyl)ethylenediamine) at 540 or 560 nm.

4.1.3 Cell migration – *in vitro* scratch assay (paper V)

Prior to the experiments, 6-well plates were coated with fibronectin (2.1 µg/cm^2) as previously reported (Liang et al., 2007). Cells were seeded in the pre-coated 6-well plates and incubated (37 °C, 5% CO_2) to attain a confluent cell monolayer (Borges et al., 2017). A scratch was created in the cell monolayer with a p200 pipette tip and debris was removed by washing with Dulbecco's phosphate buffered saline (pH 7.4). Fresh medium containing treatment (2 mL, liposomes or CGA/7a-SMAMP-liposomes, lipid concentrations of 1, 10, or 50 µg/mL) was added to the wells. Complete medium served as control. The cells were incubated (37 °C, 5% CO_2) and evaluated under an Eclipse Ts2 inverted microscope (Nikon Corporation, Tokyo, Japan) coupled to an HDMI microscope camera (DeltaPix, Smorum, Denmark) after 4, 7, 24, and 30 hours. The images were analysed using ImageJ (Schneider et al., 2012) with the Wound_healing_size_tool plugin developed by Suarez-Arnedo *et al.* according to the instructions provided by the authors (Suarez-Arnedo et al., 2020).

4.2 Bacterial Membrane-Mimic Liposome Models (paper IV)

4.2.1 Preparation of bacterial membrane-mimic liposomes

The B3M-liposomes mimicking *S. aureus* or *P. aeruginosa* were prepared by the thin film hydration and extrusion using DOPG and cardiolipin (molar ratios of 58:42) or DOPE, DOPG and cardiolipin (molar ratios of 65:23:12), respectively (Epand et al., 2008; Lombardi et al., 2017; Sun et al., 2015). The lipid films were hydrated with FITC-dextrans of average M_ws

of 4400 or 20 400 Da in HEPES buffer (10 mM, pH 7.4) with 100 mM NaCl and 1 mM EDTA sodium or HEPES buffer, respectively.

4.2.2 FITC-dextran leakage

The B3M-liposomes were diluted (20-fold) and treated with non-formulated or formulated 7e-SMAMP (concentrations corresponding to 0.5, 2, and 5 μg/mL of the 7e-SMAMP). Fluorescence intensity was measured at excitation wavelength 485 nm and emission wavelength 530 nm. Triton X-100 served as control (Sun et al., 2015; Xiong et al., 2005).

4.2.3 Lipid flip-flop

The B3M-liposomes mimicking *S. aureus* or *P. aeruginosa* membranes for the lipid flip-flop assay were tailored in the same manner as for the FITC-dextran leakage assay; however, C6-NBD-PG was added at 0.5 mol% together with the other lipids. The B3M-liposomes were treated with sodium dithionite in 1 M HEPES buffer (pH 7.4) and incubated for 15 min at 24 °C to ensure C6-NBD-PG quenching in the outer leaflets. The B3M-liposomes were diluted (50-fold) and treated with non-formulated or formulated 7e-SMAMP (concentrations corresponding to 0.5, 2, and 5 μg/mL of the 7e-SMAMP). Sodium dithionite was added, and flip-flop activity was monitored with excitation and emission wavelengths of 460 and 520 nm, respectively, for 650 sec. Triton X-100 or buffer served as respective controls (Orioni et al., 2009; Yamamoto and Tamura, 2010).

4.3 Antimicrobial evaluation

The antimicrobial activities of the formulations were tested against common skin-associated bacteria, namely *S. aureus*, *S. epidermidis*, *P. aeruginosa*, and *E. coli* (Lam et al., 2018).

4.3.1 Broth microdilution (papers I-IV)

Broth microdilution was performed either as described in the CLSI guidelines or according to EUCAST guidelines (Balouiri et al., 2016; EUCAST—the European Committee on Antimicrobial Susceptibility Testing, 2020). The two guidelines are very similar (Balouiri et al., 2016). In brief, bacterial inocula were prepared in broth (Mueller Hinton or nutrient broth). Non-formulated or formulated MAAs were diluted two-fold in 96-well plates, bacterial inocula added to the wells, and the 96-well plates incubated (37 °C, 24 hours). After incubation, results were recorded either on a plate reader or spotted on agar plates (blood or nutrient agar plates), incubated overnight, and counted (Balouiri et al., 2016; Hemmingsen et al., 2021a).

4.3.2 Time-kill assay (papers I and IV)

To investigate the antimicrobial activities of the formulations in planktonic bacteria in the presence of simulated wound fluid (SWF, bovine serum albumin 2% w/v; $CaCl_2$ 0.02 M; NaCl 0.4 M; Trizma base 0.05 M (Cerchiara et al., 2020)), the time-kill curves were determined. Non-formulated or formulated MAAs were diluted in SWF and inoculated with bacterial suspensions. Viable bacteria were counted on plates at inoculation time and after 3, 6, 8, and 12 or 24 hours of incubation (Hemmingsen et al., 2021a).

4.3.3 Anti-biofilm activities (papers I and IV)

The anti-biofilm activities were determined both as the activities against biofilm formation as well as eradication of pre-formed biofilms. For the biofilm formation evaluation, bacterial suspensions and non-formulated or formulated MAAs (equal volumes) were incubated in 96-well plates for 48 hours to allow biofilm formation. In the biofilm eradication assay, bacterial suspensions were incubated for 48 hours to form biofilms. After the initial biofilm formation, the biofilms were treated with non-formulated or formulated MAAs for 24 hours. To quantify the biofilms in both assays, crystal violet staining was utilized, and the absorbance recorded at 595 nm (Hemmingsen et al., 2021a).

5. Results and discussions

The aim of this project was to tailor drug delivery systems for MAAs, particularly SMAMPs, to improve antimicrobial and wound healing therapy of infected chronic wounds. However, due to SMAMP synthesis costs and production time, we utilized CHX as a model MAA in the first part of the project. As discussed previously, due to their similarity to the skin and bacterial membranes as well as their diversity, liposomes were chosen as the primary carrier for these antimicrobial compounds (Wang et al., 2020). Since conventional, neutral liposomes do not exhibit antimicrobial properties (Ternullo et al., 2019), chitosan was added to the formulations to improve biological and antimicrobial potential (Arora and Nanda, 2019; Hamedi et al., 2018). Further, we intended to assess the *in vitro* biological properties, particularly the cell compatibility and antimicrobial efficacy, of various delivery systems in respect to the accommodation of model MAAs, CHX, within novel delivery system. The approaches used for papers I-III are presented in Figure 5.1.

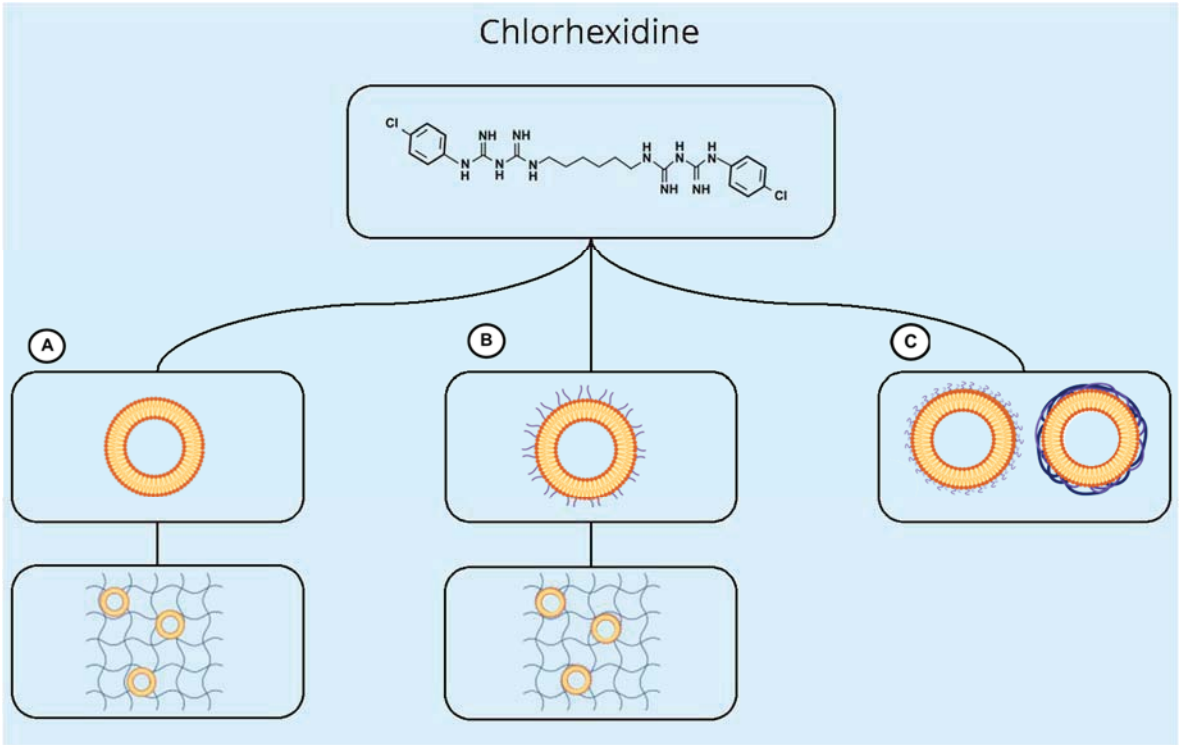

Figure 5.1. Schematic representation of delivery systems in the first part of the project. A) Paper I, B) paper II, and C) paper III. Created with BioRender.com.

5.1 Model membrane-active antimicrobial, CHX, and liposomes (papers I-III)

Even though CHX was selected as a model compound, its potential as a drug to be included in wound dressing is clear. In addition to its antimicrobial efficacy, it is also rather cheap, available, and well-known compound. We aimed to further improve its efficacy by incorporating it in delivery systems. Using delivery systems to repurpose older antimicrobials is often considered a great strategy in overcoming some of the challenges in the AMR patterns seen today. Many perceive the repurposing or reviving of old antibiotics as a viable strategy to ease the challenges of AMR (Karaiskos et al., 2019; Theuretzbacher et al., 2015). Development of novel antimicrobial compounds with new targets is both expensive and challenging, therefore repurposing could improve both the financial and time aspects (Farha and Brown, 2019). It is not a secret that development of novel antimicrobial compounds is a rather low-margin venture where expenses and revenue might not harmonize (Roope, 2022). Liposomes have previously exhibited promising features as a carrier for antimicrobial compounds in wound therapy and could therefore represent a suitable option to improve older antimicrobial compounds (Hajiahmadi et al., 2019; Sinsinwar and Vadivel, 2021).

5.1.1 Chlorhexidine-liposome characteristics (papers I-III)

Since this project aimed to tailor drug delivery systems for topical skin therapy, the target vesicle size was around 300 nm (Table 5.1, paper I) to achieve a depot effect of formulations (du Plessis et al., 1994). Yet, the optimal size of systems depends on the physiochemical properties of the specific system and condition intended to treat. Nevertheless, in a study by Meers *et al.*, the authors demonstrated improved biofilm penetration of liposomes of around 300 nm (Meers et al., 2008). Unfortunately, there is little agreement in literature regarding the optimal carrier size for biofilm penetration; moreover, biofilm penetration also depends on other properties, like the surface change, shape, and bacterial species (Liu et al., 2019). Additionally, we achieved a polydispersity index (PI) that is considered suitable for lipid-based carriers intended for topical therapy (Danaei et al., 2018). The size was confirmed with TEM, where also the morphology of liposomes was assessed, and the successful preparation of liposomes was confirmed (Figure 5.2).

Table 5.1. Liposome and CHX-liposome characteristics: mean diameter, polydispersity index (PI), zeta potential, entrapment efficacy (EE%), and pH in aqueous medium.

	Mean diameter (nm)	PI	Zeta potential (mV)	EE (%)	pH
Liposomes	271 ± 16	0.33 ± 0.07	−0.4 ± 0.3	-	6.9 ± 0.2
CHX-liposomes	318 ± 9[¥]	0.24 ± 0.03[¥]	45.5 ± 1.3[¥]	94.7 ± 0.7	8.0 ± 0.1

Results are expressed as means with their respective SD (n = 3, [¥] n = 6). The mean diameter represents the weight-intensity distribution of the liposomes.

Adapted from Hemmingsen *et al.* (2021a), reproduced under Creative Commons Licence (CC BY).

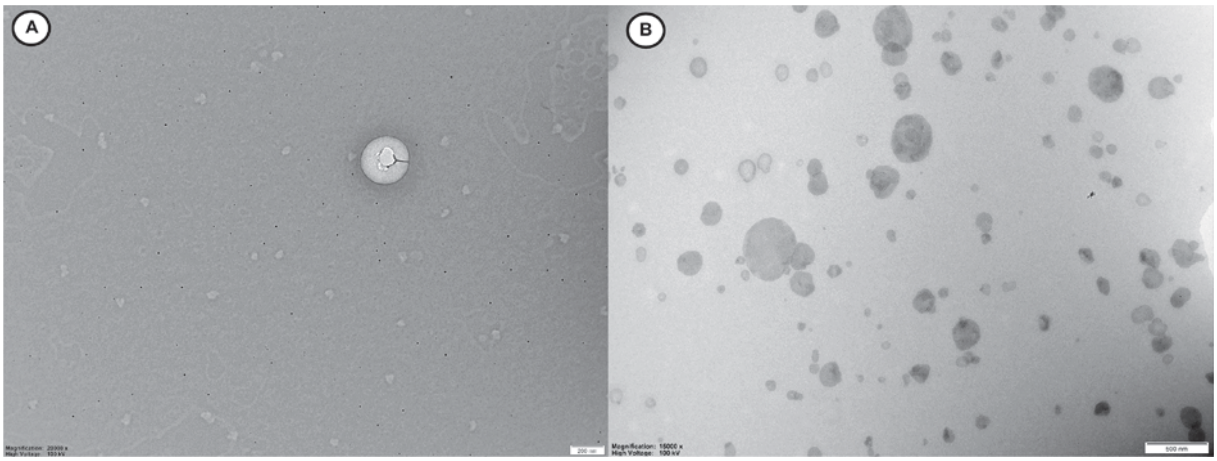

Figure 5.2. TEM-image of CHX-liposomes. A) Scale bar: 200 nm, prepared uranyless. B) Scale bar: 500 nm, prepared utilizing uranyl acetate and methylcellulose.

Adapted from Hemmingsen *et al.* (2021a), reproduced under Creative Commons Licence (CC BY).

The liposomes were prepared from phosphatidylcholine, a zwitterionic lipid, to attain neutral surfaces of empty liposomes (Table 5.1). Many MAAs display selectivity towards negatively charged membranes due to the positively charged groups on the compounds. Therefore, we aimed to avoid membrane disruption in the liposomal bilayer by selecting lipids that formed neutral liposomes. The surface charge of the CHX-liposomes suggests that CHX, an amphiphilic molecule, is accommodated on the bilayers or stretched with its hydrophobic

parts from within the liposomes exposing the hydrophilic parts to the aqueous surroundings or cores. The cationic character of the liposomes might improve interactions with the negatively charged bacterial cells and penetration into biofilm matrices (Rukavina and Vanić, 2016), of relevance for our aims.

Following the promising characteristics of the CHX-liposomes, we further investigated whether inclusion of chitosan within liposomal bilayers by formation of chitosomes as primary carrier for the membrane-active CHX, could affect liposomal properties. We selected the method originally reported by Andersen *et al.* (Andersen et al., 2013) to produce chitosomes comprising medium M_w chitosan (paper II). The medium M_w chitosan was initially selected due to the proposed antimicrobial mechanism of membrane attack and the potential to form an envelope on the bacterial membrane (Hemmingsen et al., 2021b). Additionally, this M_w was also selected for the chitosan hydrogel for the CHX-liposomes in the stage of the first part of this project (paper I).

As seen in Table 5.2, both chitosomes and vesicles (corresponding to liposomes in paper I) prepared through the one-pot method and probe sonication had a multimodal distribution of the vesicle populations, with a higher PI as could be expected based on the preparation methods. We had to use probe sonication for size reduction due to the enhanced rigidity of the membranes upon insertion of chitosan in the chitosome bilayers. However, both plain CHX-vesicles and CHX-chitosomes were in an acceptable size range, also confirmed with TEM (Figure 5.3). Interestingly, the CHX and chitosan seemed to co-accommodate within and on the chitosome bilayers, suggesting that both molecules exist on the chitosome surface and are available to interact with bacteria to assert their activities. The entrapment efficiency was slightly lower and surface charge slightly higher for the vesicles and chitosomes produced through the one-pot method and probe sonication (paper II) compared to the CHX-liposomes produced with the thin film hydration and extrusion (paper I). Furthermore, the combination of CHX and chitosan provided an even higher surface charge than the two constituents alone; a finding that suggests improved potential of chitosomes to interact with bacterial

membranes. The increase in surface charge could potentially also increase the cytotoxicity (Rukavina et al., 2018).

Table 5.2. Chitosome characteristics: mean diameter, polydispersity index (PI), zeta potential, entrapment efficacy (EE%), and pH in aqueous medium.

	Mean diameter (nm)			**PI**	**Zeta potential (mV)**	**EE (%)**	**pH**
	Peak 1	**Peak 2**	**Peak 3**				
	%	**%**	**%**				
Plain, empty vesicles	31 ± 9 5 ± 3	62 13	169 ± 18 90 ± 4	0.18 ± 0.01	0.6 ± 0.0	-	5.6 ± 0.0
Empty chitosomes	14 ± 4 5 ± 4	41 ± 4 30 ± 12	150 ± 3 65 ± 16	0.22 ± 0.01	11.5 ± 0.3	-	4.4 ± 0.0
Plain, CHX-vesicles	16 ± 7 2 ± 1	66 ± 15 16 ± 5	243 ± 13 81 ± 6	0.32 ± 0.03	53.6 ± 2.0	68 ± 5	7.0 ± 0.3
CHX-chitosomes	14 ± 1 3 ± 1	79 ± 5 29 ± 15	260 ± 3 69 ± 16	0.30 ± 0.00	79.0 ± 3.7	74 ± 2	5.5 ± 0.1

Results are expressed as means with their respective SD (n = 3). Mean diameter denotes the mean diameter of each peak in a multimodal representation of the liposome populations, and the intensity (%) of each peak (weight-intensity distribution).

Adapted from Hemmingsen *et al.* (2021c), reproduced under Creative Commons Licence (CC BY).

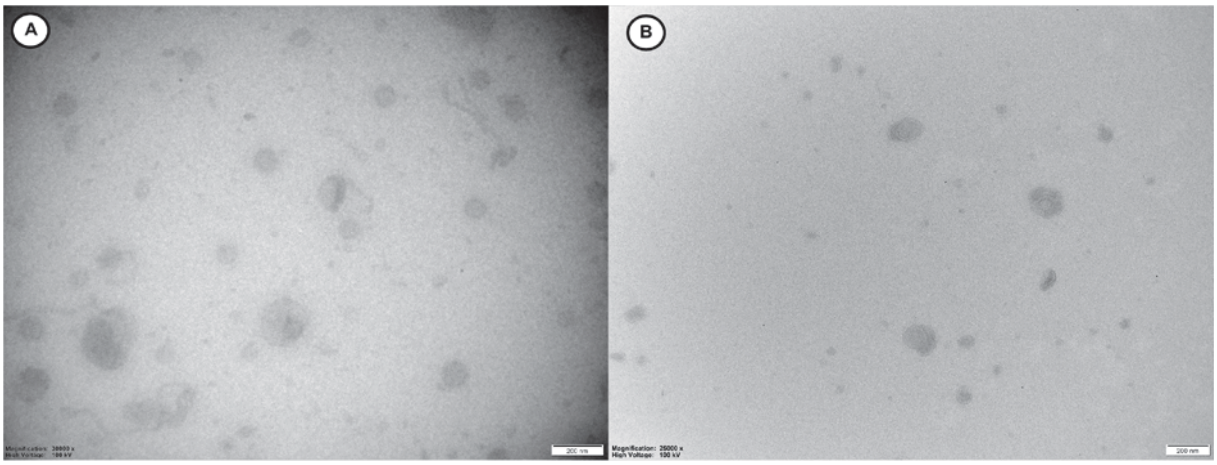

Figure 5.3. TEM images of chitosomes. A) empty chitosomes, B) CHX-chitosomes. Scale bars: 200 nm.

Adapted from Hemmingsen *et al.* (2021c), reproduced under Creative Commons Licence (CC BY).

In the last stage of the first part of the project involving CHX (paper III), we aimed to find new modes to associate chitosan with liposomes; two new protocols were implemented, namely hydration with chitosan solution (Shukla et al., 2020) and coating with chitosan solution (Jøraholmen et al., 2014). As liposomes need a secondary vehicle to be administered onto skin, we chose to use chitosan of a smaller M_w to be associated with liposomes, and rather utilize medium M_w chitosan hydrogel as the secondary vehicle to potentially take advantage of the two previously described antimicrobial mechanisms of chitosan. As seen in Table 5.3, most liposomes were of the targeted size range and maintained an acceptable PI. The surface charge of the CHX-chitosan-containing and CHX-chitosan-coated liposomes was higher than observed for the CHX-chitosomes (paper II). This can be contributed to altered CHX and chitosan accommodation within or on the liposomal bilayers. Furthermore, the entrapment was also slightly lower, however, not to a significant level.

Table 5.3. Chitosan-containing liposomes and chitosan-coated liposomes characteristics: mean diameter, polydispersity index (PI), zeta potential, entrapment efficacy (EE%), and pH in aqueous medium.

	Mean diameter (80%, nm)	PI	Zeta potential (mV)	EE (%)	pH
Empty lipid carrier	308 ± 22	0.37 ± 0.04	-1.6 ± 1.4	-	5.8 ± 0.5
CHX-lipid carrier	305 ± 14	0.38 ± 0.03	42.9 ± 5.9	63.2 ± 4.8	8.5 ± 0.1
Chitosan-containing liposomes	303 ± 18	0.32 ± 0.01	12.4 ± 0.4	-	3.6 ± 0.0
CHX-chitosan-containing liposomes	300 ± 24	0.34 ± 0.07	94.9 ± 2.2	65.7 ± 4.8	3.7 ± 0.0
Chitosan-coated liposomes	325 ± 23	0.35 ± 0.01	13.0 ± 0.4	-	3.7 ± 0.0
CHX-chitosan-coated liposomes	393 ± 23	0.39 ± 0.02	83.3 ± 3.1	70.4 ± 3.9	3.8 ± 0.0

Results of size measurements are expressed as means of cumulative size ≤80% of vesicle populations (weight-intensity distribution) with their respective SD, while the rest of the results are expressed as means with their respective SD (n=3).

5.1.2 CHX-liposomes-in-hydrogel characteristics (papers I-II)

To evaluate the suitability of the hydrogels and liposomes-in-hydrogels, texture analysis was utilized to assess user-friendliness and applicability of the formulations (Hurler et al., 2012). In this method, the formulation is described through the following parameters: hardness, cohesiveness, and adhesiveness (Hurler et al., 2012). Hardness describes the applicability of formulation onto the skin and ease of removing the formulation from the container, cohesiveness expresses the force required to deform the formulation and therefore level of deformation, while the adhesiveness describes the adhesion or retention to the application area (Amasya et al., 2020; Hurler et al., 2012). Additionally, these instruments could be utilized to evaluate the bioadhesive properties of the formulation, expressed either as retained amount of the formulation on the skin or the detachment force used to remove the formulation from the skin sample (Hurler and Škalko-Basnet, 2012).

The texture analysis of the CHX-liposomes-in-hydrogel (paper I) revealed little to no variations between the texture properties of different hydrogels (Figure 5.4). The addition of liposomes seemingly did not influence the hydrogel network. Our findings were not in direct agreement with the analysis by Hurler *et al.* where all hydrogel properties increased upon addition of liposomes (Hurler et al., 2012). However, results obtained with texture analysis are rather difficult to directly compare, moreover the chitosan source in these studies was different.

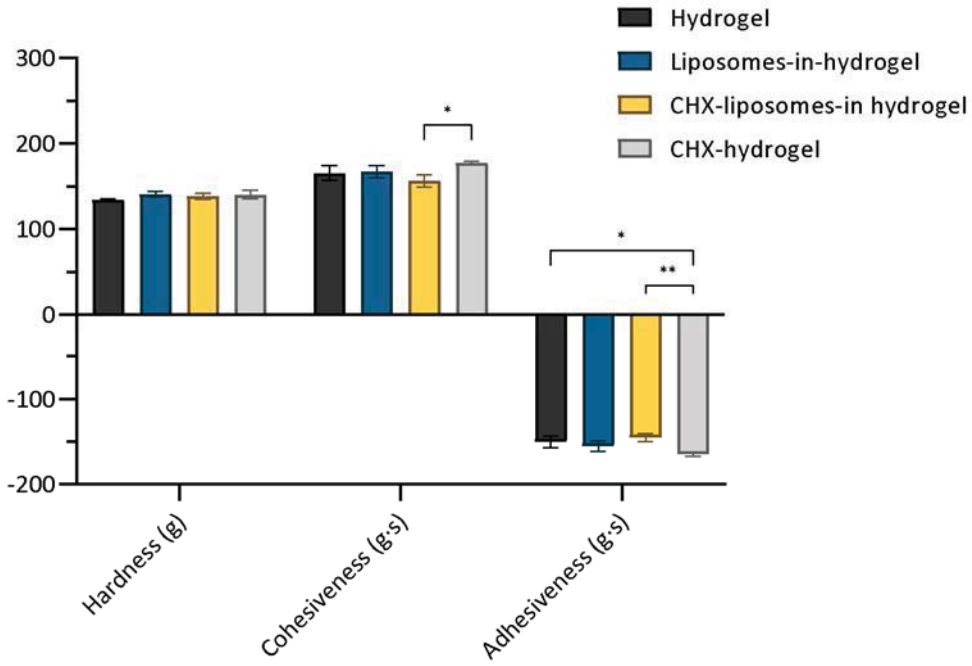

Figure 5.4. The texture properties of chitosan hydrogels measured as hardness, cohesiveness, and adhesiveness. The results are expressed as means with their respective SD (n=3). Hydrogel = plain hydrogel, liposomes-in-hydrogel = liposomes incorporated in hydrogel, CHX-liposomes-in-hydrogel = CHX-liposomes incorporated in hydrogel, and CHX-hydrogel = chlorhexidine (CHX) dispersed in hydrogel. * $p \leq 0.05$, ** $p \leq 0.01$.

Adapted from Hemmingsen et al. (2021a), reproduced under Creative Commons Licence (CC BY).

Along with the texture properties, we evaluated the bioadhesion of the plain hydrogel, liposomes-in-hydrogel, and CHX-liposomes-in-hydrogel (Figure 5.5). The results corresponded to the adhesiveness determined by the texture analysis, showing similar characteristics

between the three hydrogels. Furthermore, the detachment force was also recorded, however this data was not shown in paper I. The detachment force indicated similar trends as both the adhesiveness and amount of retained hydrogels.

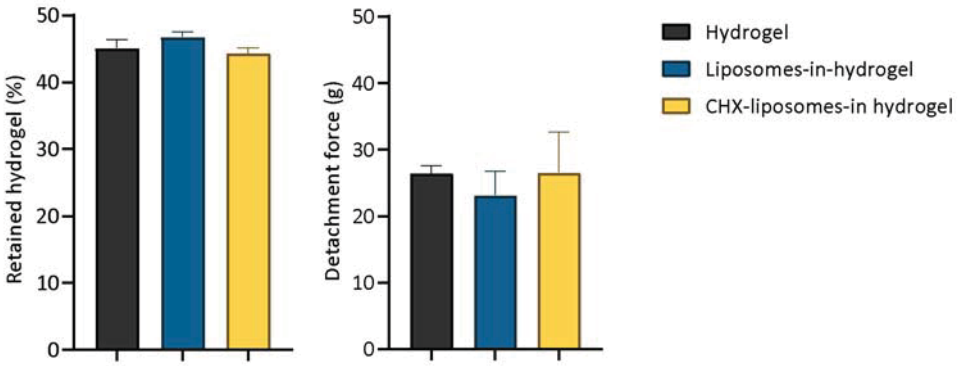

Figure 5.5. Bioadhesive properties, expressed as amount (%) of the plain hydrogel, and hydrogels comprising liposomes remaining on the skin and detachment force upon withdrawal from the skin. The results are expressed as means with their respective SD (n=3). Hydrogel = plain hydrogel, liposomes-in-hydrogel = liposomes incorporated in hydrogel, CHX-liposomes-in-hydrogel = CHX-liposomes incorporated in hydrogel.

Adapted from Hemmingsen *et al.* (2021a), reproduced under Creative Commons Licence (CC BY).

Contrary to the texture properties of CHX-liposomes-in-hydrogels reported in paper I, incorporation of vesicles and chitosomes produced through the one-pot method (paper II) influenced the hydrogel network (Figure 5.6). The hardness increased upon incorporation of vesicles or chitosomes without CHX in the hydrogel, while the hardness of hydrogels with plain CHX-vesicles or CHX-chitosomes did not increase significantly. Furthermore, the cohesiveness decreased for all hydrogels containing vesicles, while adhesiveness was not influenced by the presence of vesicles.

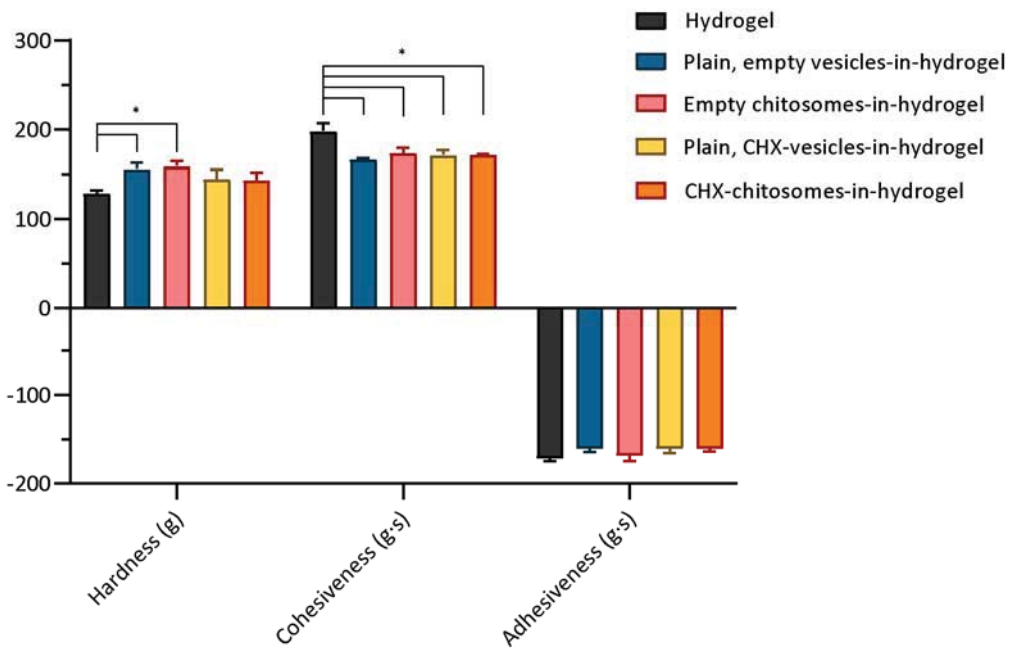

Figure 5.6. The texture properties of chitosan hydrogels measured as hardness, cohesiveness, and adhesiveness. The results are expressed as means with their respective SD (n=3). Hydrogel = plain hydrogel. * $p \leq 0.05$.

Adapted from Hemmingsen *et al.* (2021c), reproduced under Creative Commons Licence (CC BY).

5.1.3 CHX-liposomes and their effects on cells (papers I-III)

One of the most important aspects of skin formulation is its safety and effects on relevant cells. Initially, we intended to evaluate the potential toxicity of CHX-liposomes (paper I, Figure 5.7), and therefore focused on the loaded liposomes since empty liposomes are expected to be safe for keratinocytes (Cauzzo et al., 2020; Ternullo et al., 2018). As in the case of empty liposomes, the CHX-liposomes were proven safe for HaCaT cells in the tested concentrations. Furthermore, the cells seemingly proliferated when treated with CHX-liposomes in a dose-dependent manner. At liposomal lipid concentrations of 10 and 50 µg/mL, the proliferation was significantly improved compared to the non-treated cells. The results of the toxicity evaluation of the CHX-liposomes were promising especially considering that CHX reportedly exhibited cytotoxic effect in keratinocytes (Ortega-Llamas et al., 2022).

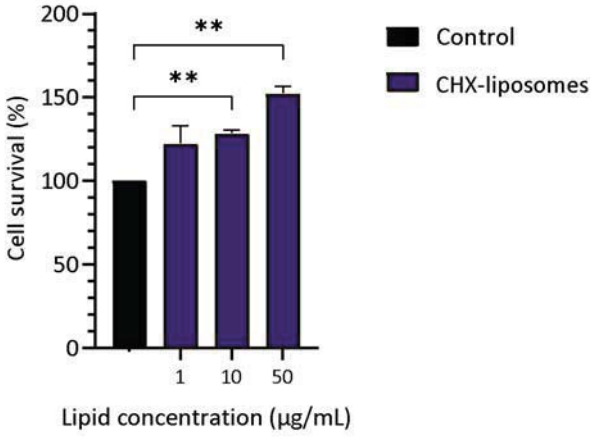

Figure 5.7. Evaluation of cell toxicity of CHX-liposomes in HaCaT cells. Three different concentrations were tested, namely 1, 10, and 50 µg/mL lipid, and the results are presented as cell viability of treated cells compared to control (100%). Control cells were only supplemented with complete medium; the cell viability was thereof considered as 100%. The results are expressed as means with their respective SD (n=3). ** $p \leq 0.01$.

Adapted from Hemmingsen *et al.* (2021a), reproduced under Creative Commons Licence (CC BY).

As previously discussed, the chronic wounds are arrested in the inflammatory stage of the wound healing cascade. Accordingly, we wanted to assess the potential anti-inflammatory activity of our drug delivery system alone as well as CHX-containing systems. Murine macrophages were selected as model cells, in which NO production was induced with LPS. The reduction of NO production was used as an indicator of anti-inflammatory activity (Figure 5.8). Both liposomes and hydrogel formulations reduced the NO production in a dose-dependent manner; however, the strongest effects were seen for macrophages treated with hydrogels. The NO production is measured through nitrate and nitrite, due to the unstable nature of NO. Chitosan is known to remove nitrate from aqueous solutions (Chatterjee and Woo, 2009), suggesting that the anti-inflammatory effects produced by the hydrogels could be overestimated, however, this would require further investigations. Chitosan could also induce anti-inflammatory responses in these cells, as seen in murine wound models (Chen et al., 2018; Xia et al., 2022; Yoon et al., 2007). However, the liposomes and CHX-liposomes

produced a significant anti-inflammatory response without the hydrogels; a potential that was considered encouraging.

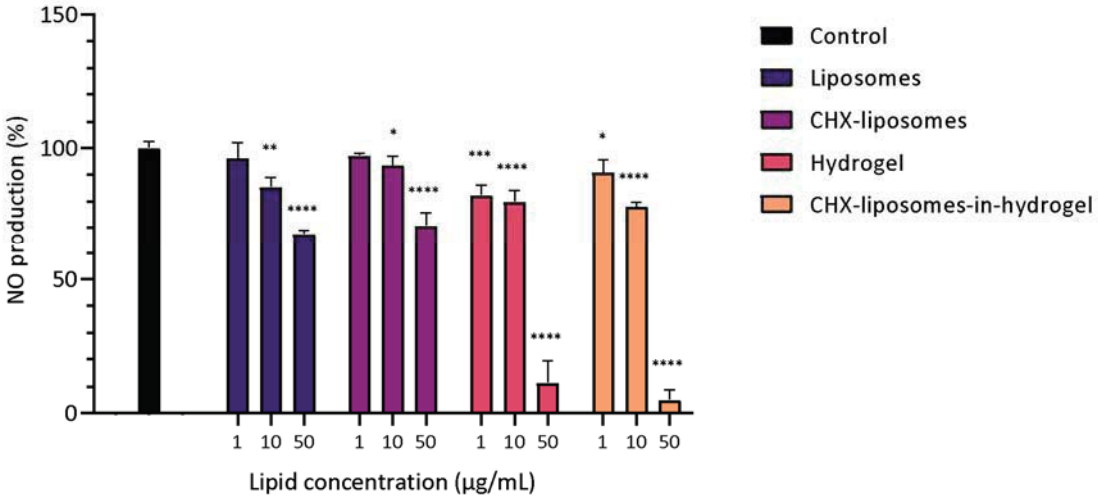

Figure 5.8. Evaluation of anti-inflammatory activity expressed as reduction of nitric oxide (NO) production in RAW 264.7 cells. Three different concentrations were tested, namely 1, 10, and 50 µg/mL lipid, and the results are presented as NO production of treated cells compared to control (100%). Control cells were non-treated lipopolysaccharide (LPS)-induced cells; their production is thereof considered as 100%. The results are expressed as means with their respective SD (n=3). * $p \leq 0.05$, ** $p \leq 0.01$, *** $p \leq 0.001$, **** $p \leq 0.0001$, compared to control.

Adapted from Hemmingsen *et al.* (2021a), reproduced under Creative Commons Licence (CC BY).

To assure the safety also in a formulation with increased cationic properties, the same cell toxicity evaluations were also conducted for the chitosomes (paper II). Cell viability was assessed for vesicles, chitosomes, and hydrogels in HaCaT cells (Figure 5.9). For the vesicles and chitosomes, no toxicity was observed; moreover, for the highest lipid concentration of chitosomes and CHX-chitosomes the cell viability improved. The viability of cells treated with hydrogels was similar to the viability of non-treated cells. Chitosan is considered safe and biocompatible; however, the safety of chitosan *in vitro* could be linked to the cell line and properties of chitosan and need to be assessed for chitosan formulations (Lima and Passos, 2021; Nafee et al., 2009; Wiegand et al., 2010). Our formulations were proven safe in HaCaT cells in the tested concentration range.

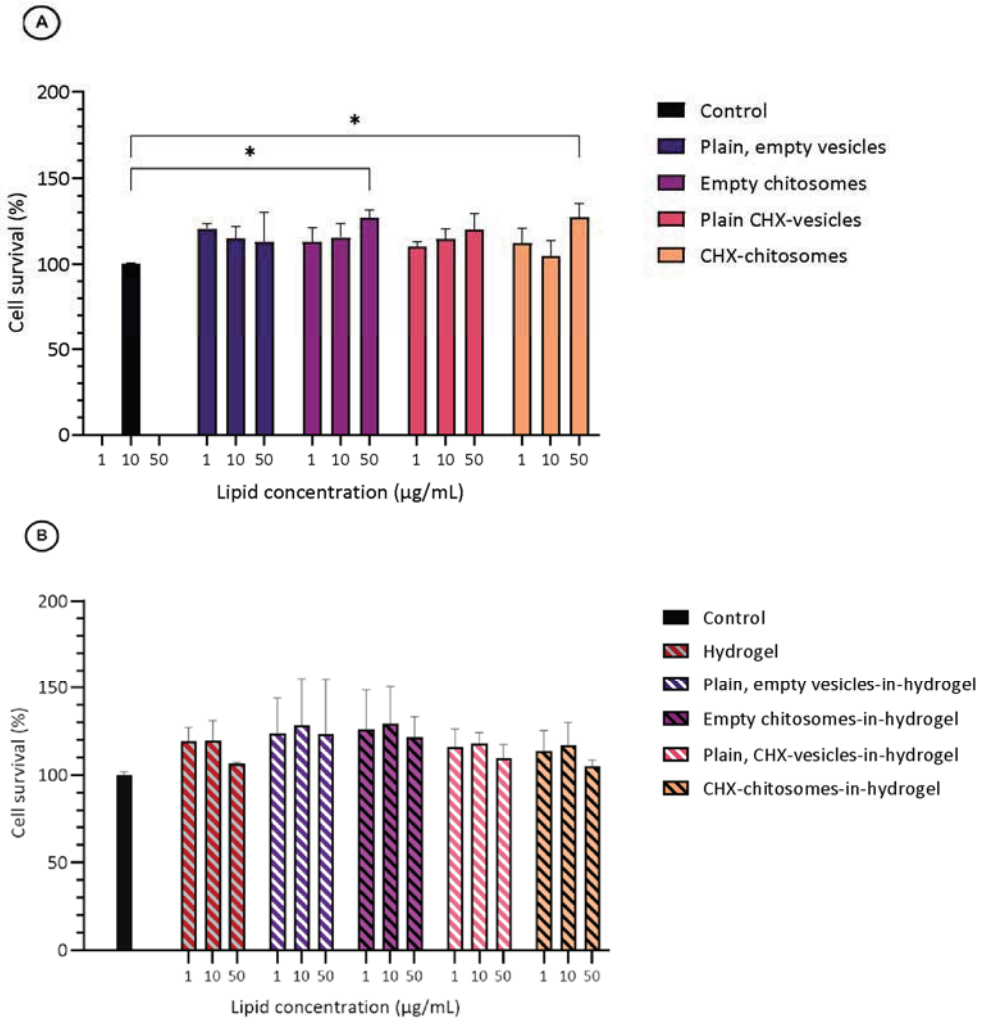

Figure 5.9. Evaluation of cell toxicity of A) vesicles and chitosomes and B) their respective hydrogels (B) in HaCaT cells. Three different concentrations were tested, namely 1, 10, and 50 µg/mL lipid (or the corresponding concentrations of hydrogels), and the results are presented as cell viability of treated cells compared to control (100%). Control cells were only supplemented with complete medium; the cell viability is thereof considered as 100%. The results are expressed as means with their respective SD (n=3). * $p \leq 0.05$.

Adapted from Hemmingsen *et al.* (2021c), reproduced under Creative Commons Licence (CC BY).

In the anti-inflammatory evaluation, the same trends as in paper I were observed for the empty and loaded vesicles and chitosomes (paper II); however, the plain vesicles seemingly exhibited a stronger anti-inflammatory effect than the chitosomes (Figure 5.10). Contrary to the chitosan hydrogels (paper I), chitosan in the chitosomes did not seem to provide additional anti-inflammatory potential in these cells, but rather decreased the

activity. The plain CHX-vesicles at the highest lipid concentration were the only formulation significantly reducing the NO production in the murine macrophages. However, the trend of a dose-dependent reduction of inflammation for CHX-vesicles was confirmed as in paper I.

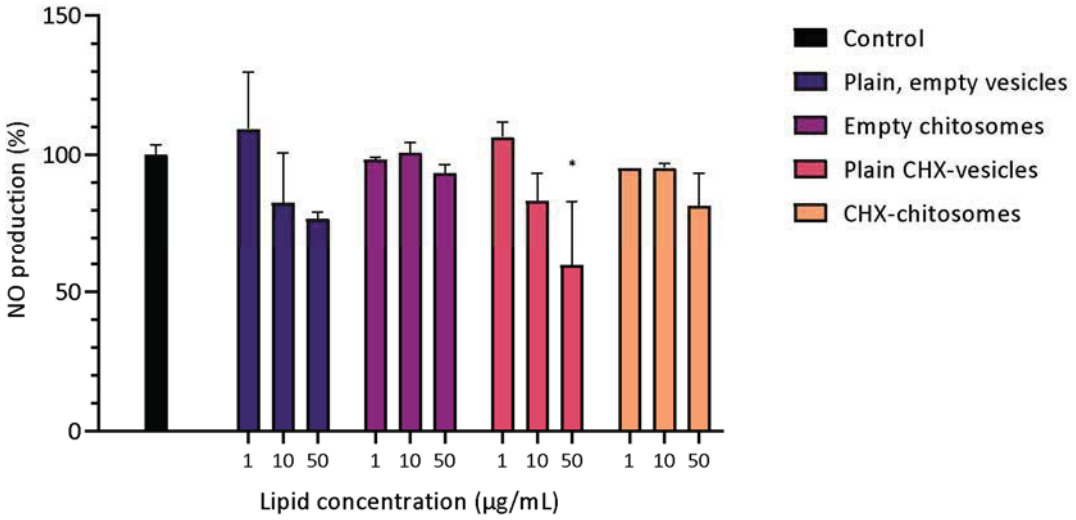

Figure 5.10. Evaluation of anti-inflammatory activity of vesicles and chitosomes expressed as reduction of nitric oxide (NO) production in RAW 264.7 cells. Three different concentrations were tested, namely 1, 10, and 50 µg/mL lipid, and the results are presented as NO production of treated cells compared to control (100%). Control cells were non-treated lipopolysaccharide (LPS)-induced cells; their production is thereof considered as 100%. The results are expressed as means with their respective SD (n=2). * $p \leq 0.05$, compared to control.

Adapted from Hemmingsen *et al.* (2021c), reproduced under Creative Commons Licence (CC BY).

Since the cell toxicity is dependent on the specific cell type and could vary significantly between different cells (Nafee et al., 2009), we included more cells in the toxicity testing of the chitosan-containing and chitosan-coated liposomes. The assessment of safety was extended to include macrophages and fibroblasts in addition to the keratinocytes (paper III). The results were similar to the results for the vesicles and chitosomes (paper II), namely no toxicity was observed in any of the cells (Figure 5.11). However, the proliferative effects were only observed in the macrophages. Interestingly, the highest cell viability was observed for the lowest lipid concentration and gradually decreased upon increasing the concentration.

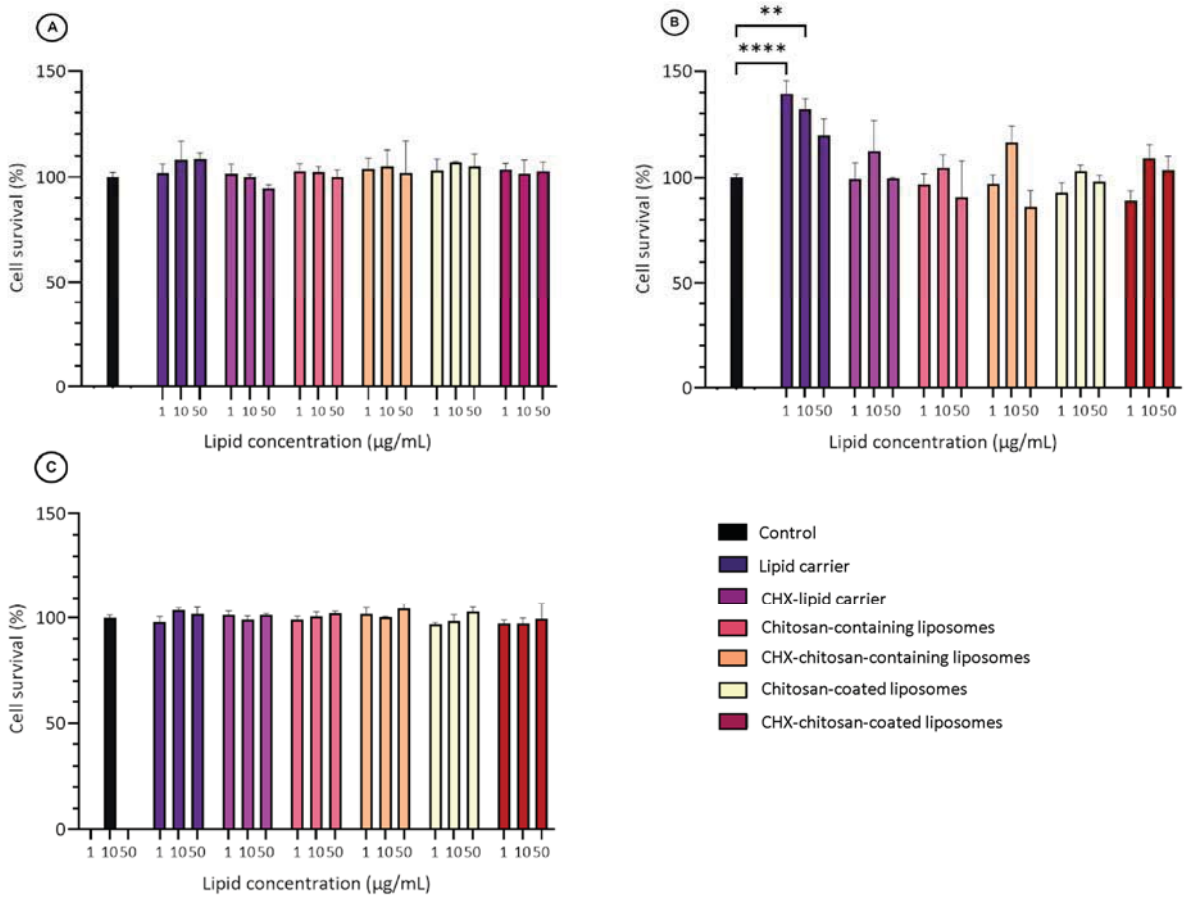

Figure 5.11. Evaluation of cell toxicity of chitosan-containing liposomes and chitosan-coated liposomes in A) HaCaT, B) RAW 264.7 and C) HDF-neo cells. Three different concentrations were tested, namely 1, 10, and 50 µg/mL lipid, and the results are presented as cell viability of treated cells compared to control (100%). Control cells were only supplemented with complete medium; the cell viability is thereof considered as 100%. The results are expressed as means with their respective SD (n=3). ** $p \leq 0.01$, **** $p \leq 0.0001$.

The anti-inflammatory activity of the chitosan-containing and chitosan-coated liposomes was evaluated in paper III. All formulations reduced the NO production (Figure 5.12); however, the reduction was not significant for the lipid carriers (corresponding to liposomes, paper I) compared to the control. Compared to the chitosomes (paper II) and considering the apparent lack of anti-inflammatory activity found for chitosan hydrogel in paper I, the chitosan-containing and chitosan-coated liposomes induced strong anti-inflammatory effects. Furthermore, the CHX-lipid carriers (paper III), exhibited stronger anti-

inflammatory activity than the CHX-liposomes and CHX-vesicles from paper I and II, respectively.

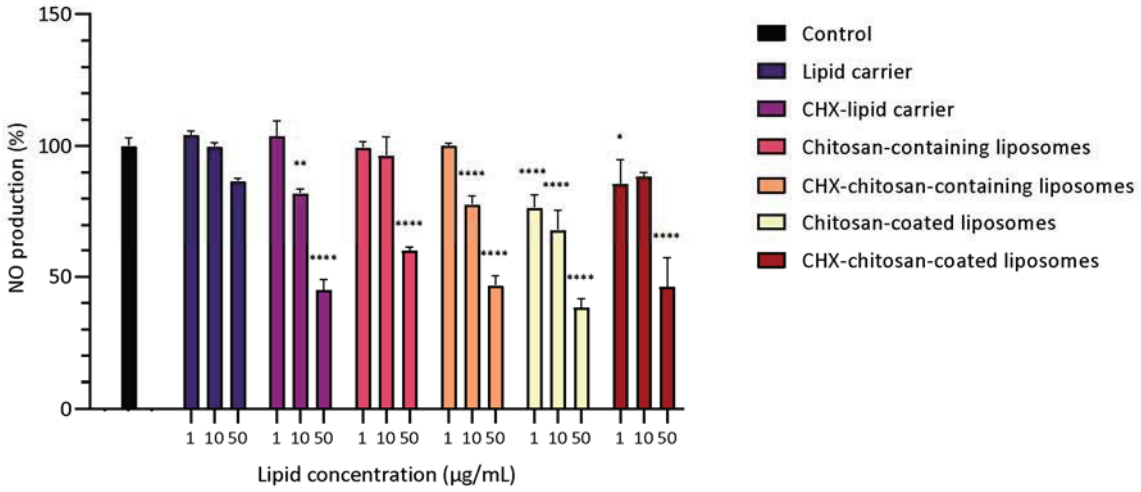

Figure 5.12. Evaluation of anti-inflammatory activity of chitosan-containing and chitosan-coated liposomes expressed as reduction of nitric oxide (NO) production in RAW 264.7 cells. Three different concentrations were tested, namely 1, 10, and 50 µg/mL lipid, and the results are presented as NO production of treated cells compared to control (100%). Control cells were non-treated lipopolysaccharide (LPS)-induced cells; their production is thereof considered as 100%. The results are expressed as means with their respective SD (n=3). * $p \leq 0.05$, ** $p \leq 0.01$, **** $p \leq 0.0001$, compared to control.

5.1.4 CHX-liposomes and their antimicrobial activities (papers I-III)

Since one of the major issues in chronic wounds are the presence of bacteria and biofilms that lead to inflammation responses hampering the healing process, we need to target the underlying causes (Rahim et al., 2017). We therefore evaluated the antimicrobial properties of our delivery systems. For the antimicrobial evaluation of the CHX-liposomes and CHX-liposomes-in-hydrogel (paper I), we selected one antibiotic-sensitive (ATCC29213) and one gentamicin-resistant (SO88) strain of *S. aureus,* one of the most common bacteria found in wounds, as well as *P. aeruginosa*. These species are often partners in crime within wound biofilms. While *S. aureus* is mainly found in the upper layer of the wound, *P. aeruginosa* is usually found in the lower layer of the wound (Serra et al., 2015). First, we evaluated the

minimal lethal concentration (MLC) of both non-formulated and formulated CHX (Table 5.4). The CHX exerted strong activity against all strains; importantly the activity was maintained when CHX was incorporated in liposomes. However, when chitosan was included in the formulation, either as a secondary vehicle for liposomes or dispersed in the hydrogel network (CHX-hydrogel), the MLC was lowered. The antimicrobial effects from both CHX and chitosan included in novel formulations were confirmed.

Table 5.4. MLC of non-formulated and formulated chlorhexidine (CHX) in *S. aureus* ATCC29213, *S. aureus* SO88 and *P. aeruginosa* ATCC10145.

	MLC (μg/mL)		
	***S. aureus* ATCC29213**	***S. aureus* SO88**	***P. aeruginosa* ATCC10145**
CHX-liposomes	0.40	0.80	1.60
CHX-liposomes-in-hydrogel	0.16	0.31	0.63
CHX-hydrogel	0.16	0.31	0.63
CHX	0.40	0.80	1.60

The results are expressed as means with their respective SD (n=3). MLC = minimal lethal concentration. CHX-hydrogel = CHX dispersed in hydrogel network (without liposomes). CHX = non-formulated CHX.

Because of the promising results of MLC testing, we performed time-kill studies of bacterial cultures suspended in SWF. The SWF was used to provide an environment mimicking the wound environment since these formulations are intended for topical treatment of wounds. As seen in Figure 5.13, non-formulated CHX and CHX-hydrogel demonstrated the fastest antimicrobial effects; however, both the CHX-liposomes and CHX-liposomes-in-hydrogel were able to eradicate all bacteria within 24 hours. This delay in the eradication could be related to the CHX release profile from the different formulations. Furthermore, plain chitosan hydrogel also displayed an improved activity compared to the control and empty

liposomes. The inherent antimicrobial activity of chitosan (Kou et al., 2022), was confirmed in our antimicrobial challenge.

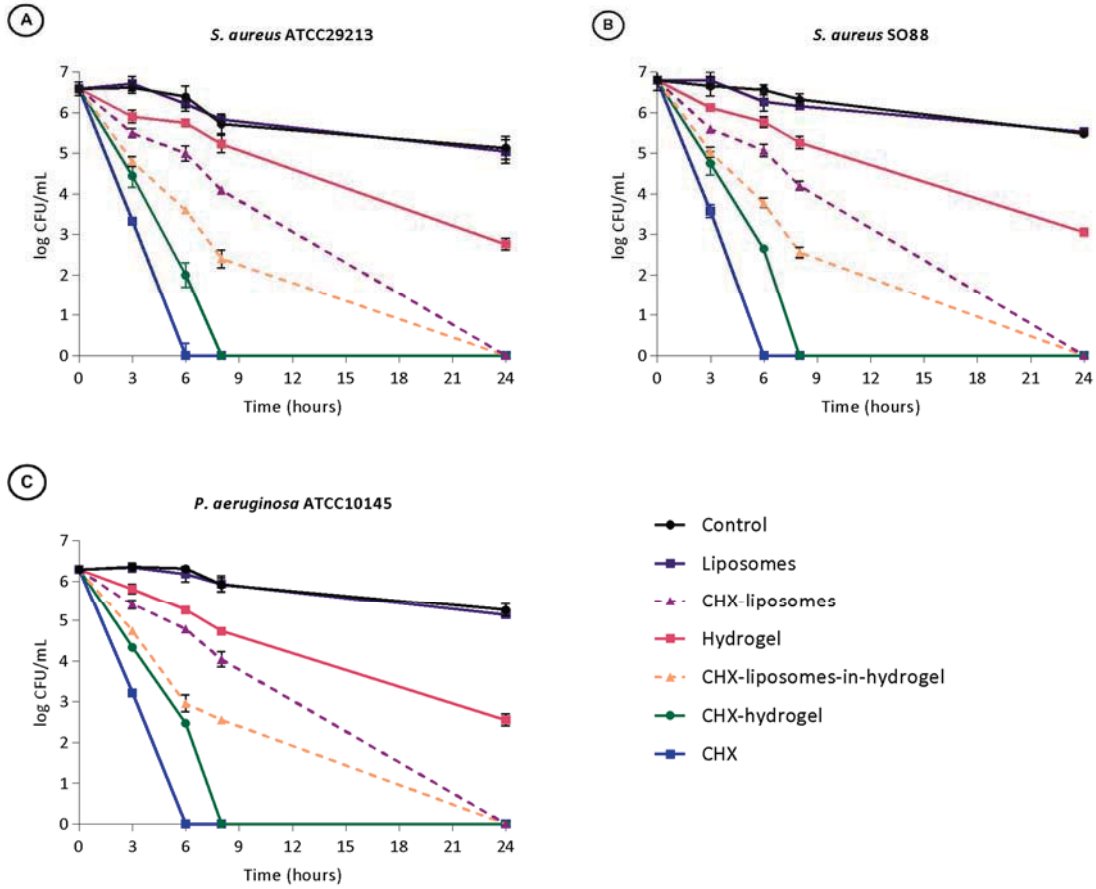

Figure 5.13. Viability (log CFU/mL) of microorganisms (A) *S. aureus* ATCC29213, B) *S. aureus* SO88, and C) *P. aeruginosa* ATCC10145) over the time (up to 24 hours) in presence of non-formulated and formulated chlorhexidine (CHX). The results are expressed as means with their respective SD (n=3). CHX = non-formulated CHX.

Adapted from Hemmingsen *et al.* (2021a), reproduced under Creative Commons Licence (CC BY).

To address the challenges of bacteria in bacterial communities, the biofilms, we sought to assess the anti-biofilm effects, both as the inhibition of biofilm formation and eradication of pre-formed biofilms. The non-formulated and formulated CHX were therefore challenged against biofilm-embedded *S. aureus* and *P. aeruginosa*. As depicted in Figure 5.14, non-formulated CHX had a moderate effect on both biofilm inhibition and biofilm eradication in all strains; however, the inhibition of biofilm formation reached 100% in *S. aureus* ATCC29213

and *P. aeruginosa* ATCC10145 and 92% in the clinical, gentamicin-resistant strain of *S. aureus* SO88 when these were treated with CHX-liposomes-in-hydrogel. Regarding the eradication of pre-formed biofilm, the CHX-liposomes-in-hydrogel reached 82-98% biofilm eradication in *S. aureus* biofilm and 64% in *P. aeruginosa* biofilm, respectively. These results are promising for further development, since we confirmed that delivery system enhanced the anti-biofilm potential of CHX. Considering that Bonez *et al*. previously reported that the anti-biofilm activities of non-formulated CHX were limited in biofilm-embedded bacteria, especially *P. aeruginosa*, even when the activity in planktonic bacteria proved excellent (Bonez et al., 2013), our findings are highly relevant.

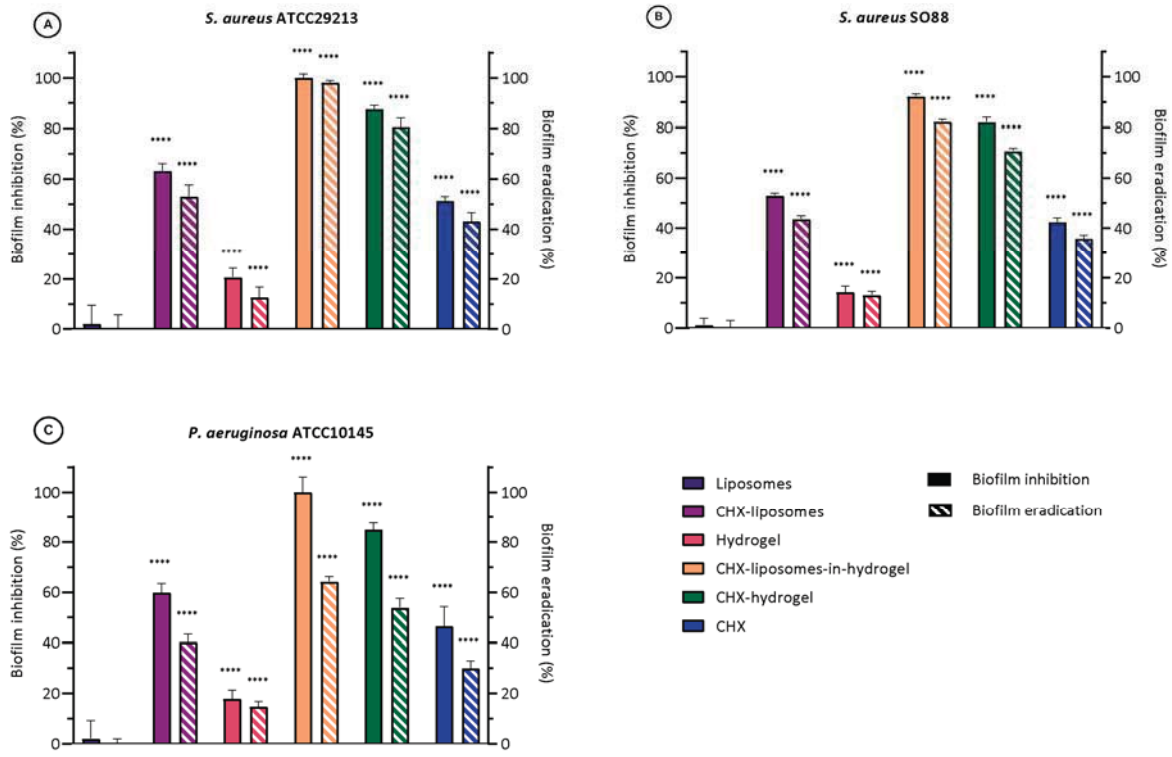

Figure 5.14. Anti-biofilm activity in biofilms of A) *S. aureus* ATCC29213, B) *S. aureus* SO88, and C) *P. aeruginosa* ATCC10145: inhibition of biofilm formation (%) on left Y-axis (solid bars), eradication of pre-formed biofilm (%) on right Y-axis (patterned bars). The results are expressed as means with their respective SD (n=3). CHX = non-formulated chlorhexidine (CHX). **** $p \leq 0.0001$, compared to control.

Adapted from Hemmingsen *et al.* (2021a), reproduced under Creative Commons Licence (CC BY).

We also evaluated weather the activity of CHX was maintained or improved when CHX was incorporated in vesicles and chitosomes produced through the one-pot method and their respective hydrogels (paper II). As expected, the plain, empty vesicles did not exhibit any antimicrobial activity against neither *S. aureus* nor *S. epidermidis* (Table 5.5). However, the empty chitosomes (free of CHX) exhibited antimicrobial activity; although the activity improved when CHX was incorporated into the formulation. CHX-chitosomes exhibited the strongest activity against both bacterial strains, suggesting that both the membrane-active CHX and chitosan acted on the bacteria.

Table 5.5. MLC of non-formulated and formulated chlorhexidine (CHX) in in *S. aureus* MSSA476 (ATCC® BAA-1721™) and *S. epidermidis* 13–67.

	Lipid concentration (mg/mL)	
	***S. aureus* MSSA476**	***S. epidermidis* 13-67**
Plain, empty vesicles	-	-
Empty chitosomes	1.25	0.625
Plain CHX-vesicles	0.32	0.039
CHX-chitosomes	0.078	<0.005

All results are expressed as the liposomal lipid concentration upon reaching MLC. The results are expressed as means with their respective SD (n=3). MLC = minimal lethal concentration, MSSA = methicillin-sensitive *S. aureus*.

The hydrogel formulations were also assessed for their antimicrobial potential (paper II, Table 5.6). The hydrogels, both a plain chitosan hydrogel and hydrogel incorporating vesicles and chitosomes, displayed a strong effect in both strains. Yet, the MLC of all hydrogel formulations were the same against *S. aureus*, except the MLC of hydrogel with CHX-chitosomes that were slightly lower. The antimicrobial effects against *S. epidermidis* were confirmed for chitosomes, CHX-vesicles, and CHX-chitosomes. However, the most potent

formulation was hydrogel with CHX-chitosomes, followed by hydrogel with CHX-vesicles and hydrogels with empty chitosomes.

Table 5.6. MLC of non-formulated and hydrogel-formulated chlorhexidine (CHX) in in *S. aureus* MSSA476 (ATCC® BAA-1721™) and *S. epidermidis* 13–67.

	Lipid concentration (mg/mL)	
	***S. aureus* MSSA476**	***S. epidermidis* 13-67**
Hydrogel	1.56×10^{-2}	0.10×10^{-2}
Plain, empty vesicles-in-hydrogel	1.56×10^{-2}	0.10×10^{-2}
Empty chitosomes-in-hydrogel	1.56×10^{-2}	0.03×10^{-2}
Plain, CHX-vesicles-in-hydrogel	1.56×10^{-2}	0.006×10^{-2}
CHX-chitosomes-in-hydrogel	0.78×10^{-2}	0.003×10^{-2}

All results are expressed as the liposomal lipid concentration upon reaching MLC. The results are expressed as means with their respective SD (n=3). MLC = minimal lethal concentration.

Adapted from Hemmingsen *et al.* (2021c), reproduced under Creative Commons Licence (CC BY).

To improve the comparisons between the different formulations, the lipid carrier, chitosan-containing liposomes, and chitosan-coated liposomes (paper III) were tested at the same concentration (lipid concentration of 0.3125 mg/mL). The results demonstrated the same trends as the trends observed for the vesicles and chitosomes (paper II), namely an increasing activity upon inclusion of CHX and chitosan (Figure 5.15). The chitosan-containing liposomes and chitosan-coated liposomes exhibited a significant improvement of the bacterial eradication compared to the empty lipid carriers ($p < 0.0001$). The antimicrobial activity improved even more upon incorporation of CHX, in CHX-lipid carrier, compared to chitosan-containing and chitosan-coated liposomes without CHX ($p = 0.0003$ and $p < 0.0001$, respectively). The activity was further improved when the liposomes contained both CHX and chitosan ($p < 0.0001$). The most potent formulation was CHX-chitosan-containing liposomes, upon which treatment no bacterial growth was observed, followed by CHX-chitosan-coated-

liposomes and CHX-lipid carrier. The enhanced antimicrobial effect could be linked to the surface charge (Table 5.3).

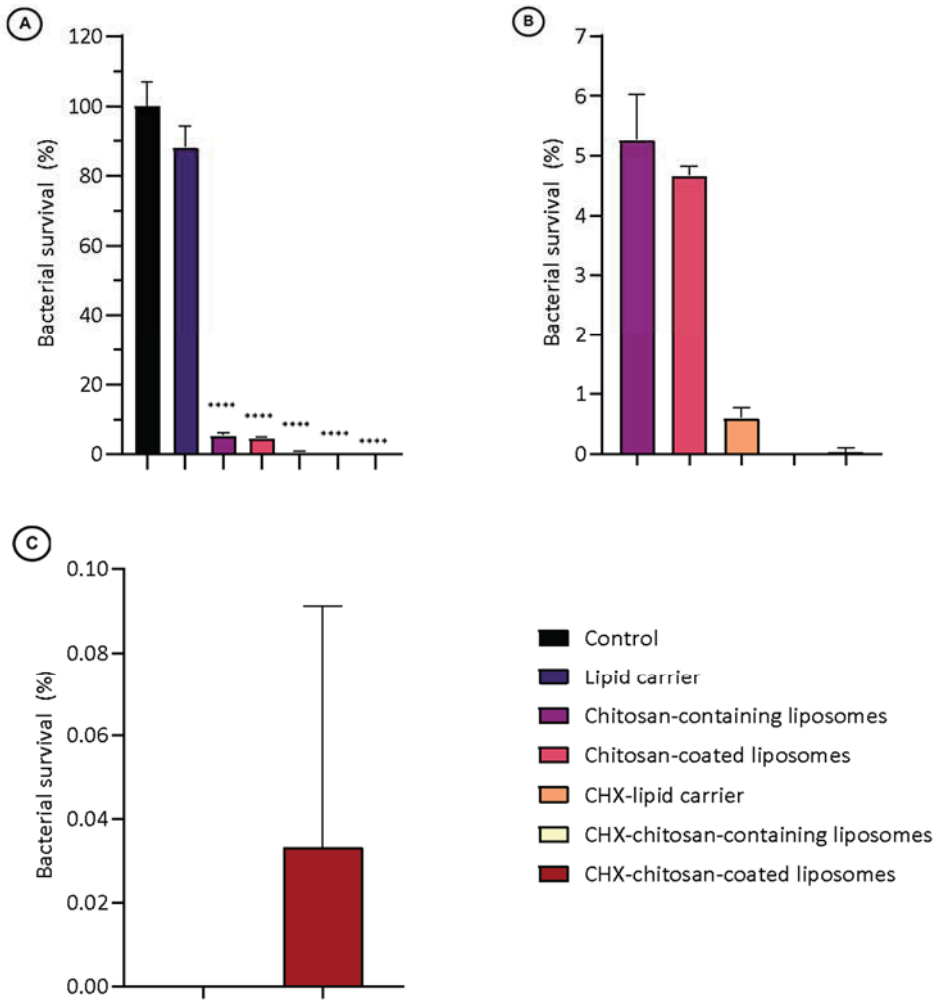

Figure 5.15. Bacterial survival (%) of *S. aureus* MSSA476 (ATCC® BAA-1721™) in the presence of non-formulated and formulated chlorhexidine (CHX) at a lipid concentration of 0.3125 mg/mL. A) Full scale graph with all formulations, B) Enlarged graph (zoomed) to depict the chitosan- and/or CHX-containing/coated liposomes, C) Enlarged graph (zoomed) to depict the CHX-containing liposomes. The results are expressed as means with their respective SD (n=3). **** $p \leq 0.0001$, compared to control.

Chitosan improved the antimicrobial effects both as a hydrogel vehicle and when inserted in liposomes, however, the conventional liposomes incorporated in chitosan hydrogel were selected as the most suitable system to be used as a general platform for formulation of other MAAs. This formulation required rather simple production procedure, its characteristics such

as the textural properties, bioadhesion potential were deemed reproducible, and the antimicrobial and anti-inflammatory activities were promising. Moreover, rather simple liposomal membrane would enable relative control over the carrier system.

5.2 Synthetic mimics of antimicrobial peptides (SMAMPs) and liposomes (papers IV-V)

In the second part of the project, the knowledge acquired in the studies involving CHX, liposomes, and chitosan was utilized to tailor liposomes or liposomes-in-hydrogels for novel 7e-SMAMP (paper IV) and 7a-SMAMP (paper V), respectively. The delivery systems used in the second stage of the project are summarized in Figure 5.16.

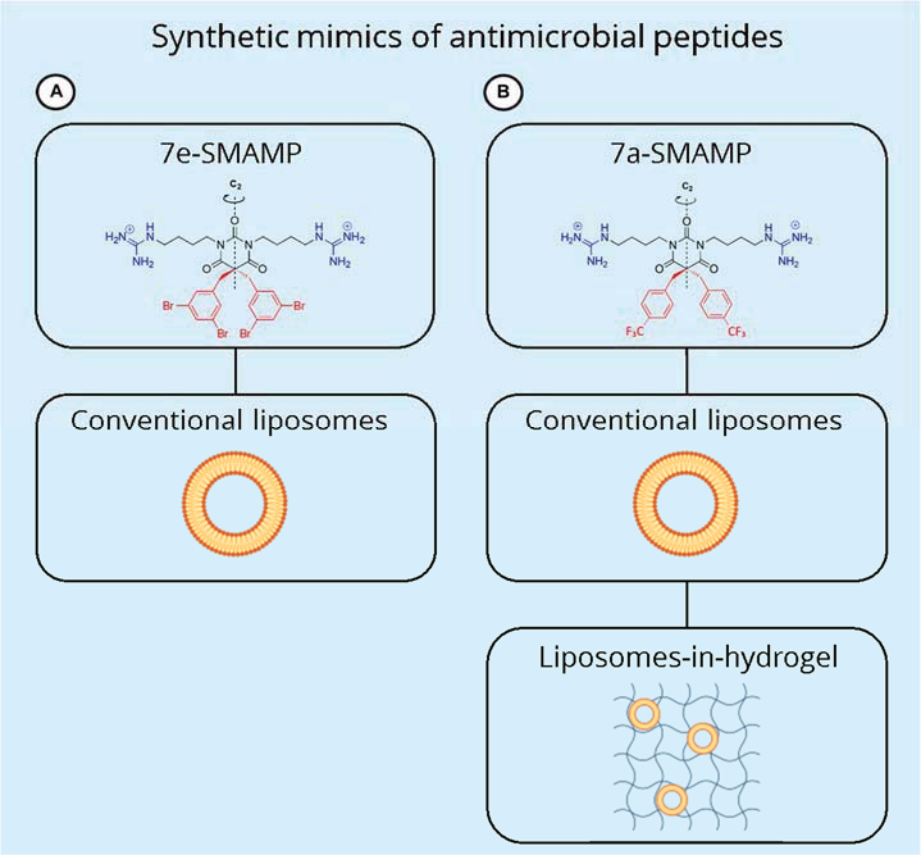

Figure 5.16. Schematic representation of delivery systems in the second part of the project. A) Paper IV and B) paper V. Created with BioRender.com.

5.2.1 7e-SMAMP-liposomes (paper IV)

5.2.1.1 7e-SMAMP-liposome characteristics (paper IV)

As the first stage in development of novel formulations for the SMAMPs, we selected 7e-SMAMP, known for strong antimicrobial activities. This MAAs was, according to the study by Paulsen e*t al*., the most potent membrane-active SMAMP in their selection (Paulsen et al., 2021). Due to its strong membrane activity, the compound was expected to interact with liposomal bilayers; therefore, the first challenge was to develop stable 7e-SMAMP-containing liposomes. We aimed, as for CHX-liposomes (paper I), to prepare liposomes of around 300 nm in size and a PI below 0.3 (Table 5.7). Novel liposomes were characterized exhibiting cationic surface that was highly positive, confirming that at least parts of the 7e-SMAMP molecule were surface-available to interact with bacterial membranes, similarly as confirmed for the CHX-liposomes (paper I).

Table 5.7. Liposome characteristics: mean diameter, polydispersity index (PI), zeta potential, entrapment efficacy (EE%), and pH in aqueous medium.

	Mean diameter (nm)	**PI**	**Zeta potential (mV)**	**EE (%)**	**pH**
Empty liposomes	269 ± 42	0.44 ± 0.05	-0.4 ± 0.2	-	6.3 ± 0.0
7e-SMAMP-liposomes	276 ± 16	0.20 ± 0.01	58.7 ± 1.6	78.1 ± 2.2	4.9 ± 0.1

Results are expressed as means with their respective SD (n=3). The mean diameter represents the weight-intensity distribution of the liposomes.

The TEM image (Figure 5.17 A) confirms spherical structures that were in the size range found using dynamic light scattering (Table 5.7). The results were encouraging considering that Omardien *et al*. demonstrated that amphipathic cationic AMPs could increase membrane fluidity and therefore destabilize membranes (Omardien et al., 2018). We further evaluated membrane elasticity to gain insight on potential destabilization of the liposomal membranes

in presence of the 7e-SMAMP. As seen in Figure 5.17 B, the rigidity of the 7e-SMAMP-liposomes was higher than of the empty liposomes, indicating that the integrity of the membrane was maintained; 7e-SMAMP did not impart destabilizing effects when associated with phosphatidylcholine liposomes.

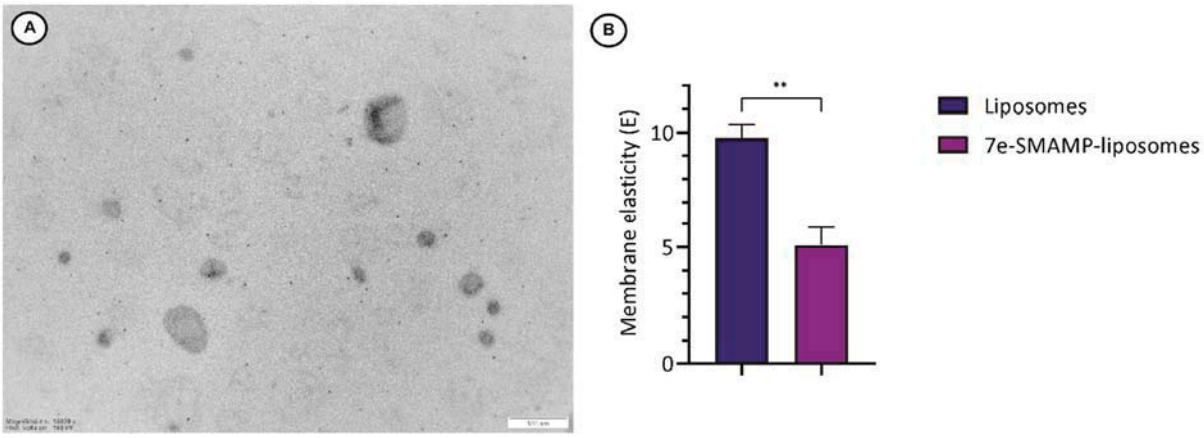

Figure 5.17. A) TEM image of 7e-SMAMP-liposomes. Scale bar 500 nm. B) Membrane elasticity of liposomes and 7e-SMAMP-liposomes. The results are expressed as means with their respective SD (n=3). **) $p > 0.001$.

5.2.1.2 7e-SMAMP-liposomes and their effects on cells (paper IV)

The SMAMPs are often modified in structure to increase the antimicrobial potential, but also to lower the potential toxicity, improving their selectivity (Gera et al., 2021). However, their success is still limited due to toxicity issues (Jiang et al., 2021). The toxicity of AMPs and SMAMPs is often high against erythrocytes, especially for more hydrophobic compounds, and should therefore be monitored for a variety of cells (Gera et al., 2021). Paulsen *et al*. reported haemolytic activity of both 7e-SMAMP and 7a-SMAMP, however, the effect of 7e-SMAMP was more pronounced than 7a-SMAMP (Paulsen et al., 2021). Consequently, we aimed to evaluate the potential toxicity of 7e-SMAMP-liposomes against important cells involved in skin wound healing. We focused on keratinocytes and macrophages. It was evident that neither liposomes nor 7e-SMAMP-liposomes exhibited toxic effects in the tested concentration range (Figure 5.18). On the contrary, at the highest lipid concentration, empty liposomes had a proliferative effect in both cell lines. Furthermore, at the highest lipid concentration, 7e-SMAMP-liposomes

also exhibited proliferative effects on keratinocytes. The findings are in agreement with literature reporting reduced toxicity of active compounds upon their incorporation in liposomes. However, toxicity can also depend on the properties of the compound. Ron-Doitch *et al.* found that the toxicity of the AMP LL-37 was reduced in HaCaT cells when it was incorporated in liposomes compared to free compound, whereas the opposite was observed for indolicidin (Ron-Doitch et al., 2016).

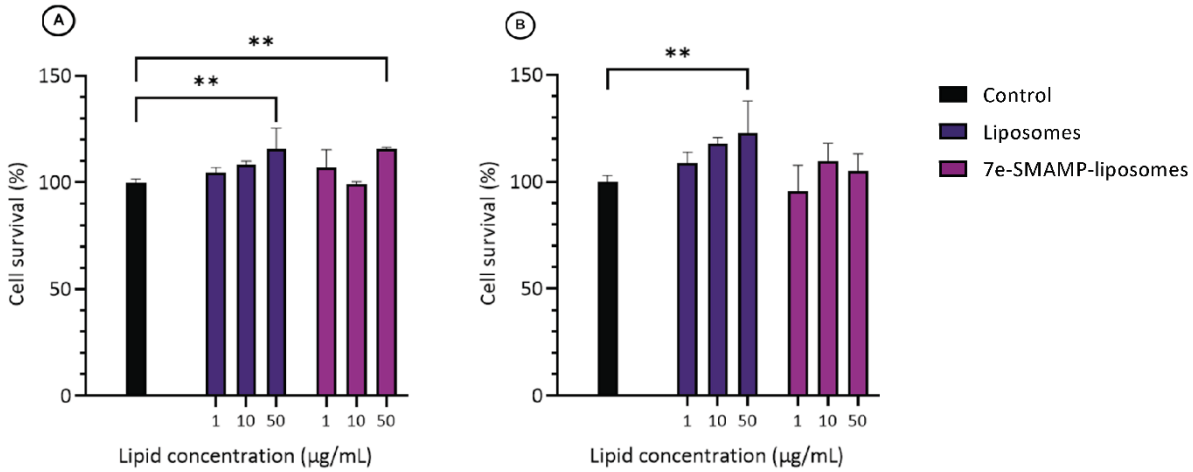

Figure 5.18. Evaluation of cell toxicity of liposomes and 7e-SMAMP-liposomes in A) HaCaT cells and B) RAW 264.7 cells. Three different concentrations were tested, namely 1, 10, and 50 µg/mL lipid, and the results are presented as cell viability of treated cells compared to control (100%). Control cells were only supplemented with complete medium; the cell viability is thereof considered as 100%. The results are expressed as means with their respective SD (n=3). ** $p \leq 0.01$.

As for the formulations with CHX (papers I-III), we also evaluated whether the 7e-SMAMP-liposomes could alleviate the inflammatory responses in macrophages. The human AMPs are, as discussed, known for their involvement in many cellular tasks in the body, including in wound healing. They participate in the inflammatory, proliferative, and remodelling phase, exhibiting pronounced effects on the immune cells (Petkovic et al., 2021). Murugan *at al.* proved anti-inflammatory activity of non-formulated ultra-short peptidomimetics in RAW 264.7 cells by measuring both NO and TNF-α. Furthermore, these ultra-short peptidomimetics exhibited superior antimicrobial activity compared to the AMP

LL-37 (Murugan et al., 2013). The 7e-SMAMP-liposomes were indeed able to reduce the NO production in murine macrophages at the highest lipid concentration (Figure 5.19).

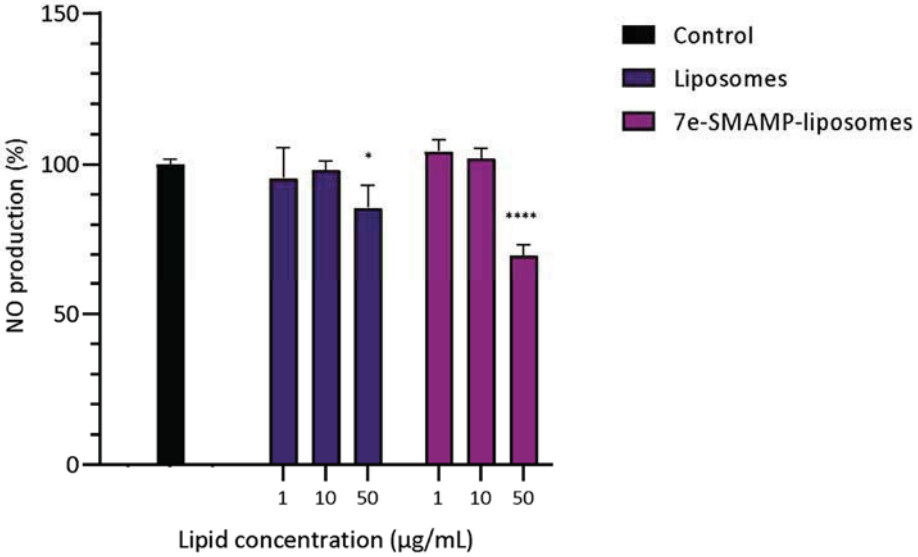

Figure 5.19. Evaluation of anti-inflammatory activity of liposomes and 7e-SMAMP-liposomes expressed as reduction of nitric oxide (NO) production in RAW 264.7 cells. Three different concentrations were tested, namely 1, 10, and 50 µg/mL lipid, and the results are presented as NO production of treated cells compared to control (100%). Control refers to non-treated lipopolysaccharide (LPS)-induced cells; their production is thereof considered as 100%. The results are expressed as means with their respective SD (n=3). * $p \leq 0.05$, **** $p \leq 0.0001$, compared to control.

5.2.1.3 Insight on antimicrobial mechanisms of novel SMAMPs (paper IV)

After establishing the cell compatibility and anti-inflammatory properties of the 7e-SMAMP-liposomes, we aimed to attain an indication of the antimicrobial mechanism of 7e-SMAMP and 7e-SMAMP-liposomes. Artificial membranes are useful tools to gain insight on mechanisms behind the activity of membrane-active compounds, therefore we employed two different protocols. First, we prepared B3M-liposomes mimicking either *S. aureus* or *P. aeruginosa* and loaded these liposomes with FITC-dextrans of two different M_ws, namely 4400 and 20 400 Da. These B3M-liposomes were treated with non-formulated or formulated 7e-SMAMP, and the potential leakage of encapsulated FITC was measured as an indicator of membrane destabilization. Second, we prepared inner-leaflet labelled B3M-liposomes and

challenged these with non-formulated or formulated 7e-SMAMP. Flipping of lipids could be an indicator of membrane destabilization due to increased stress (Sreekumari and Lipowsky, 2022).

In the *S. aureus*-mimicking B3M-liposomes, both non-formulated and formulated 7e-SMAMP induced leakage in a dose-dependent manner, however, the non-formulated 7e-SMAMP seemingly induced a stronger effect (Figure 5.20 A and B). In the *P. aeruginosa*-mimicking B3M-liposomes, non-formulated 7e-SMAMP induced a strong leakage in the B3M-liposomes loaded with FITC-4400, however, the leakage was significantly reduced in B3M-liposomes loaded with FITC-20 400, indicating that the destabilization of the mimicked *P. aeruginosa* membrane was not complete, permitting leakage of smaller but not larger molecules (Figure 5.20 C and D). The formulated 7e-SMAMP induced leakage in the *P. aeruginosa*-mimicking B3M-liposomes loaded with FITC 4400, however this effect was detected between concentration of 0.5 and 2 µg/mL. Interestingly, in the B3M-liposomes loaded with FITC-20 400, the formulated 7e-SMAMP induced more FITC leakage than the non-formulated 7e-SMAMP and maintained the dose-dependent effect. This suggests that formulated 7e-SMAMP could assure stronger interaction with the *P. aeruginosa* B3M-liposomes, and therefore assert stronger destabilizing effect on the membrane. The improved interaction with 7e-SMAMP-liposomes can be contributed to the additional lipid-lipid interactions between the B3M-liposomes and 7e-SMAMP-liposomes, in addition to the electrostatic interactions originating from 7e-SMAMP. These results also confirmed the luciferase-based biosensor assays results on membrane disrupting activity of SMAMPs reported by Paulsen *et al*. (Paulsen et al., 2021).

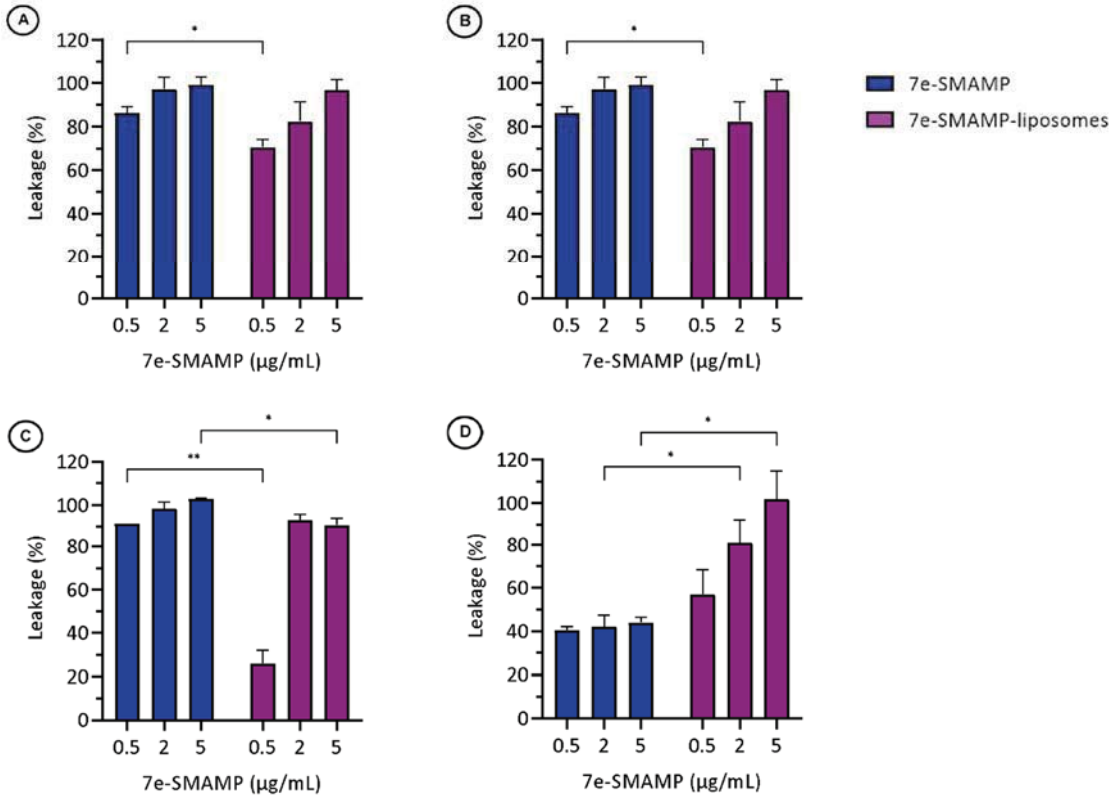

Figure 5.20. Bacterial Membrane-Mimic Liposomes Models (B3M-liposomes) loaded with FITC-dextran 4400 or 20 400 (molecular weight = M_w) treated with 7e-SMAMP or 7e-SMAMP-liposomes. The leakage is expressed as percentage compared to the control (Triton X-100). Concentrations of 7e-SMAMP were 0.5, 2, and 5 µg/mL for both non-formulated and formulated 7e-SMAMP. Different B3M-liposome mimics were prepared and challenged, namely A) *S. aureus* with FITC-4400, B) *S. aureus* with FITC-20 400, C) *P. aeruginosa* with FITC-4400, and D) *P. aeruginosa* with FITC-20 400. Results are presented as means with their respective SD (n=3). *) $p < 0.05$, **) $p < 0.01$.

The second approach to evaluate the SMAMP's effect on membranes, involved assessing the lipid flip-flop within bilayers of B3M-liposomes treated with non-formulated or formulated 7e-SMAMP. The lipid flip-flop represents pore-mediated transmembrane lipid translocation (Gurtovenko and Vattulainen, 2007). Upon treating the *S. aureus*-mimicking B3M-liposomes, formulated 7e-SMAMP in the highest concentration inflicted the strongest lipid flip-flop, initially stronger than the control (Triton X-100) and the non-formulated 7e-SMAMP (Figure 5.21 A). However, in lower concentration the formulated 7e-SMAMP exhibited low destabilizing activity, while the non-formulated 7e-SMAMP maintained strong activity in all concentrations in a dose-dependent manner. Except for the strong activity

observed for formulated 7e-SMAMP at 5 µg/mL, the results were in agreement with the results from the FITC-dextran leakage assay (Figure 5.20 A and B). In the *P. aeruginosa*-mimicking B3M-liposomes, Triton X-100 induced stronger lipid flip-flop than both non-formulated and formulated 7e-SMAMP (Figure 5.21 B). However, in agreement with the results for the FITC-dextran leakage assay, the stress effect inflicted by formulated 7e-SMAMP was higher than for non-formulated 7e-SMAMP suggesting that the formulated 7e-SMAMP exhibited much greater pore-forming and stress-inducing activity in *P. aeruginosa* membrane mimics than non-formulated 7e-SMAMP in all the tested concentrations. The finding is highly encouraging considering antibacterial potential.

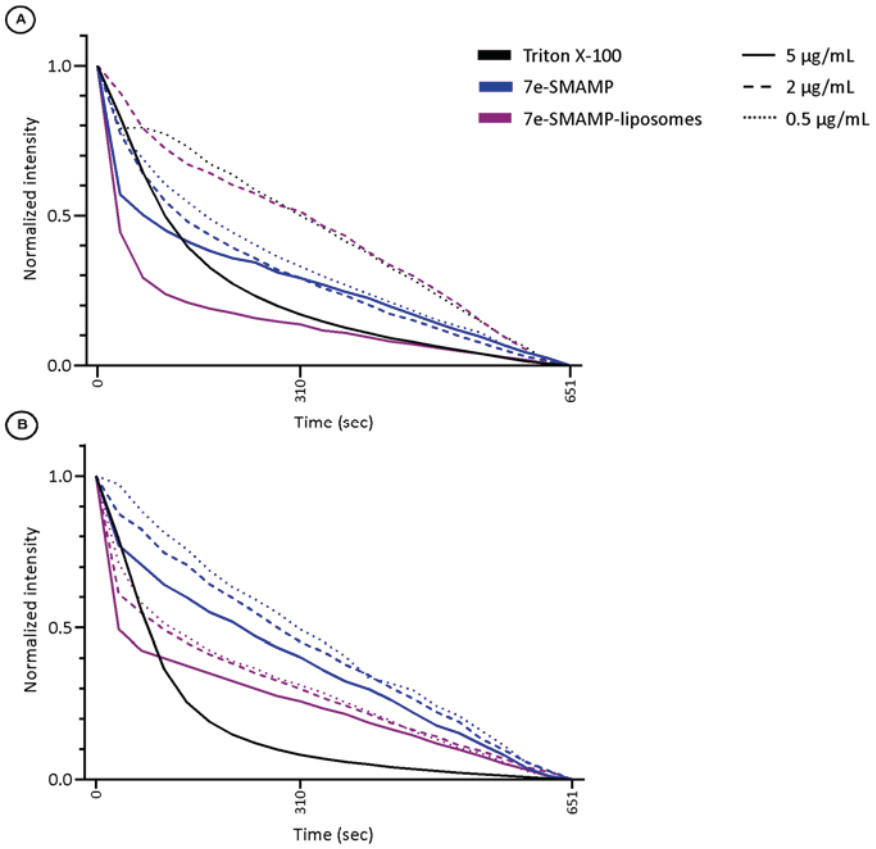

Figure 5.21. Lipid flip-flop in Bacterial Membrane-Mimic Liposomes Models (B3M-liposomes) of bacterial membranes with C6-NBD-PG inner leaflet labelling. The B3M-liposomes were treated with non-formulated and formulated 7e-SMAMP and monitored for 650 sec. Two different B3M-liposome mimics were prepared and challenged, namely A) *S. aureus* and B) *P. aeruginosa* B3M-liposome mimics. Concentrations of 7e-SMAMP were 0.5, 2, and 5 µg/mL were chosen for both non-formulated and formulated 7e-SMAMP. Results are presented as means of the normalized fluorescence intensity (0-1, n=3).

5.2.1.4 Antimicrobial potential of non-formulated and formulated 7e-SMAMP (paper IV)

Several studies have proven the potential of AMPs and SMAMPs against biofilms in infected wounds (Batoni et al., 2021). Furthermore, their potential against resistant bacterial strains based on their broad-spectrum activity and unspecific, rapid onset of action further leading to lowered tendencies to resistance, are key aspects of their promise as candidates in the fight against resistant and biofilm-producing bacteria, especially in topical antimicrobial therapy (Vanzolini et al., 2022). Due to the alarming situation regarding wound infections and the resistance patterns seen today, we assessed the antimicrobial potential of non-formulated and formulated 7e-SMAMP against a variety of bacteria commonly found in wounds including both gram-positive and gram-negative bacteria as well as MDR strains. Furthermore, we needed to assure that the antimicrobial effect of 7e-SMAMP was not hampered by its association with liposomes. Initially, we assessed the antimicrobial activity by attaining the MIC and MLC of both non-formulated and formulated 7e-SMAMP in seven different bacterial cultures (Table 5.8). From these results we observed that MIC and MLC values were the same for non-formulated and formulated 7e-SMAMP, confirming that the antimicrobial activities were maintained upon incorporation of the SMAMP in liposomes. This was deemed highly encouraging since 7e-SMAMP (non-formulated) reportedly exhibited strong antimicrobial activity in a study by Paulsen *et al.* (Paulsen et al., 2021). The 7e-SMAMP exhibited strong activity against both resistant and susceptible strains of *S. aureus*, however, the MDR *S. aureus* SO2 required higher concentrations for the same effects. The 7e-SMAMP activity was also strong against gram-negative *E. coli* ATCC11105, though, *P. aeruginosa* ATCC10145 was more challenging than all other bacteria (Table 5.8).

Table 5.8. The MIC and MLC of non-formulated and formulated 7e-SMAMP in five strains of *S. aureus*, *E. coli* ATCC11105, and *P. aeruginosa* ATCC10145. Resistance is also denoted for the different strains.

	Susceptibility	MIC (µg/mL)		MLC (µg/mL)	
		7e-SMAMP	7e-SMAMP-liposomes	7e-SMAMP	7e-SMAMP-liposomes
S. aureus ATCC29213	S	0.78	0.78	3.13	3.13
S. aureus SO2	MDR	12.50	12.50	25.00	25.00
S. aureus SO83	MDR	6.25	6.25	12.50	12.50
S. aureus SO86	MDR	3.13	3.13	6.25	6.25
S. aureus SO88	Gentamicin	1.56	1.56	6.25	6.25
E. coli ATCC11105	S	3.13	3.13	6.25	6.25
P. aeruginosa ATCC10145	S	25.00	25.00	50.00	50.00

MIC = minimal inhibitory concentration, MLC = minimal lethal concentration, MDR = multidrug resistant, S = susceptible, 7e-SMAMP = non-formulated 7e-SMAMP (n=3).

As for the CHX-liposomes (paper I), we evaluated the activity of non-formulated and formulated 7e-SMAMP in a wound-like environment (SWF). Consequently, we attained time-kill curves for all bacterial cultures treated with non-formulated and formulated 7e-SMAMP in SWF (Figure 5.22) The *S. aureus* ATCC29213, SO83, SO86, and SO88 were readily inhibited by both the non-formulated and formulated 7e-SMAMP, demonstrating only slightly lower inhibition for the resistant strains compared to the susceptible *S. aureus* ATCC29213. However, viability of *S. aureus* SO2 and *P. aeruginosa* ATCC10145 was higher than for the other bacteria; moreover, the non-formulated 7e-SMAMP needed 12 hours to eradicate these strains. For the formulated 7e-SMAMP a delay in activity was observed, in accordance with prolonged release from liposomes. Nevertheless, a pronounced effect was observed against all bacteria after treatment with the formulated 7e-SMAMP, reaching at least 3 log CFU/mL reduction within 8 hours. In *in vitro* conditions, AMPs and SMAMPs often exhibit fast onset of action therefore eradicating bacteria within a short time (Dewangan et al., 2018; Tague et al., 2019). However, Svenson *et al.* demonstrated that short SMAMPs can be affected by the

presence of albumin. Their binding to albumin could lead to a slower bacterial eradication and higher MIC values (Svenson et al., 2007) that might be reflected in our results.

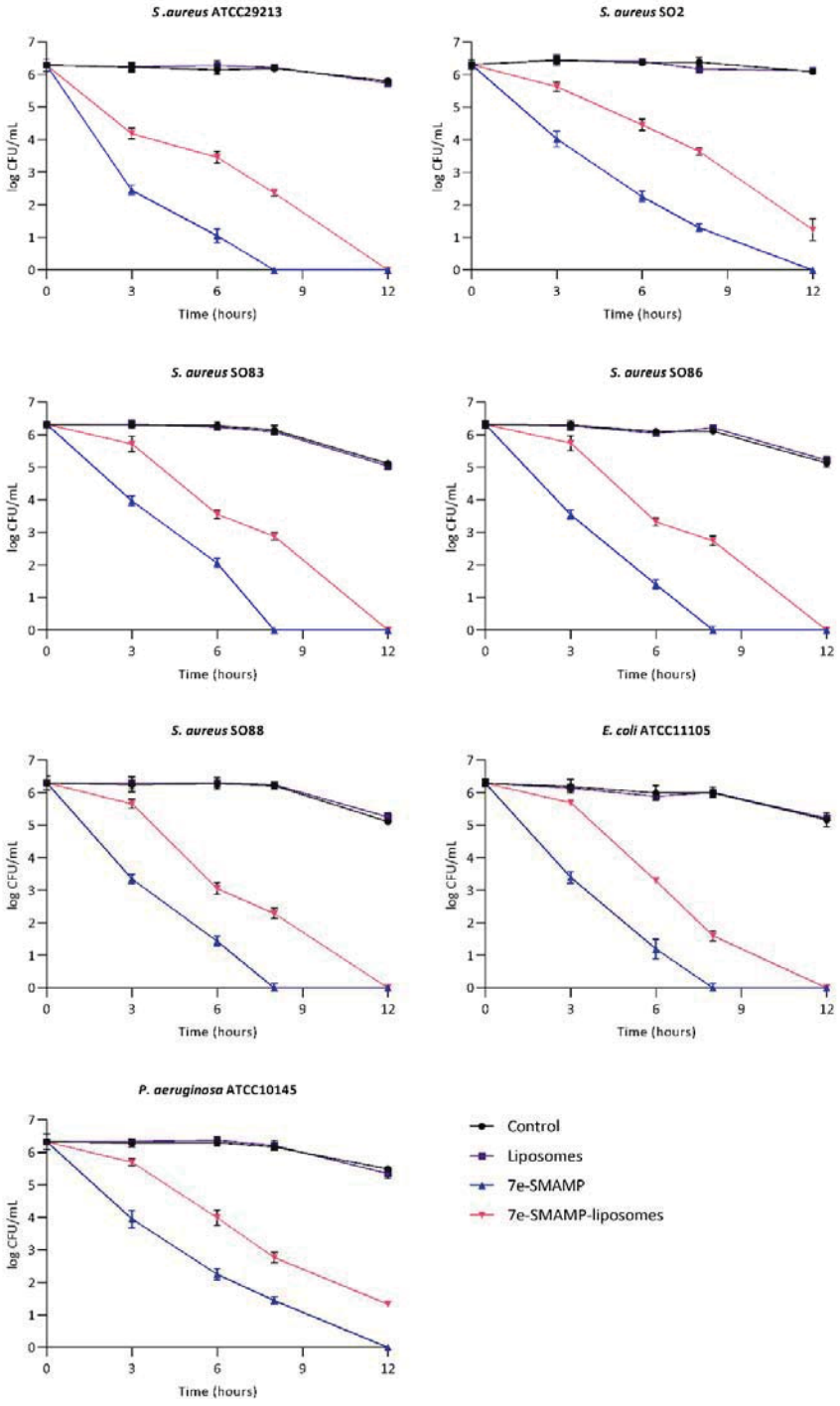

Figure 5.22. Viability (log CFU/mL) of five strains of *S. aureus*, *E. coli* ATCC11105, and *P. aeruginosa* ATCC10145 over the time (up to 12 hours) in presence of non-formulated and formulated 7e-SMAMP (50 µg/mL, 7e-SMAMP concentration). The results are expressed as means with their respective SD (n=3). 7e-SMAMP = non-formulated 7e-SMAMP.

After confirming a very promising bacterial eradication of planktonic bacteria in SWF, we challenged the non-formulated and formulated 7e-SMAMP against bacterial biofilms. The SMAMPs have in previous studies demonstrated both abilities to inhibit the formation of biofilms and eradicate pre-formed biofilms (Kuppusamy et al., 2018; Nizalapur et al., 2017; Zhu et al., 2022). First, we evaluated the abilities to inhibit biofilm formation (Figure 5.23). The non-formulated and formulated 7e-SMAMP effectively inhibited biofilm formation in the tested bacteria, especially in *S. aureus* ATCC29213 and SO88. The biofilm formation in all bacteria were completely inhibited, but in concentrations higher than the MIC values, except from *P. aeruginosa* ATCC10145. Encouragingly, the inhibition of biofilm formation in all bacteria was more effective when 7e-SMAMP was associated with liposomes. This confirmed that liposomes were suitable carriers for 7e-SMAMP that could improve the therapeutic outcome. The effect was always stronger for the 7e-SMAMP-liposomes than the non-formulated 7e-SMAMP in the lower concentrations.

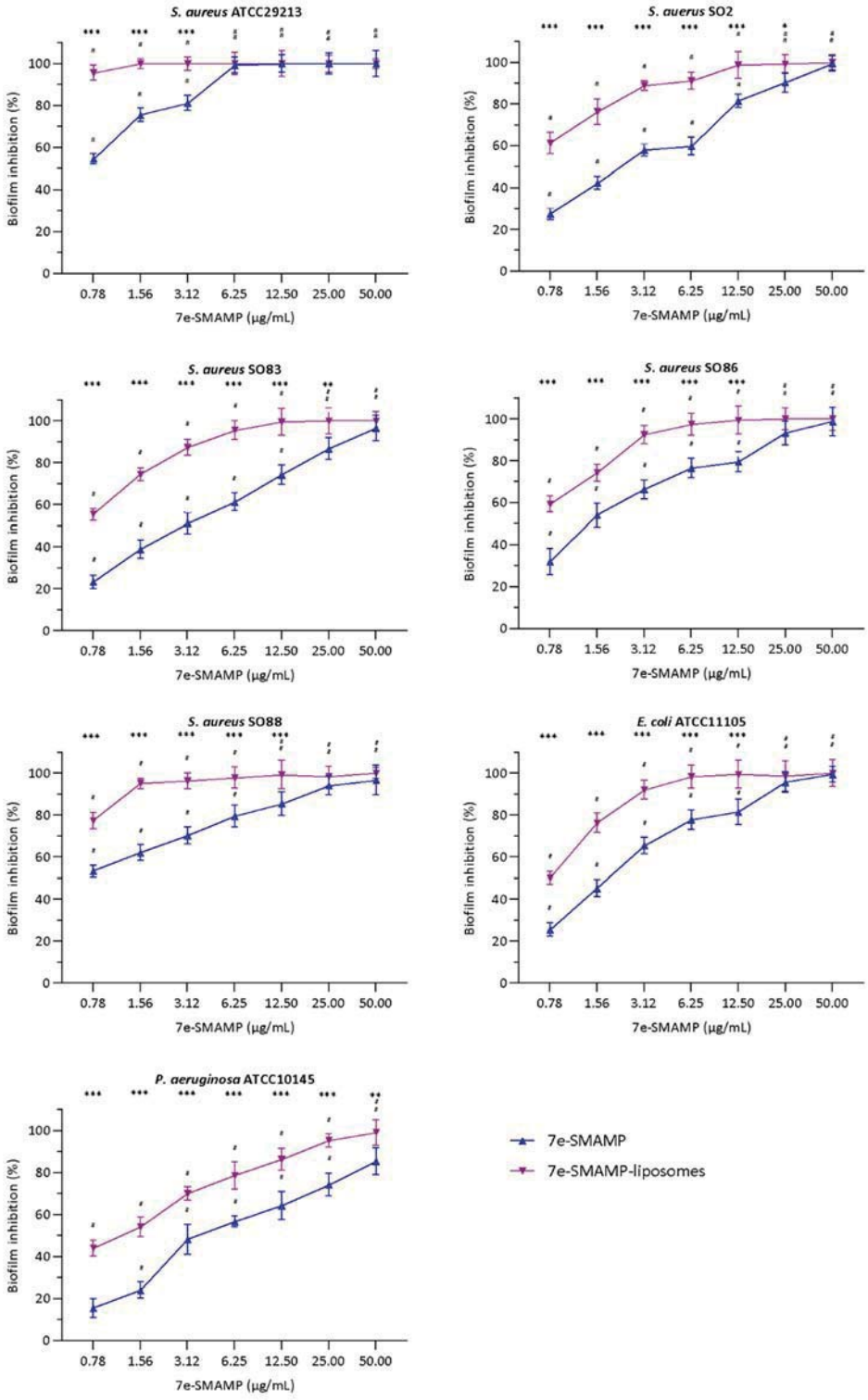

Figure 5.23. Inhibition of biofilm formation (%) by non-formulated and formulated 7e-SMAMP in five strains of *S. aureus*, *E. coli* ATCC11105, and *P. aeruginosa* ATCC10145. Concentrations of 7e-SMAMP were 0.78, 1.56, 3.12, 6.25, 12.5, 25.0, and 50.0 µg/mL were tested for both non-formulated and formulated 7e-SMAMP.The results are expressed as means with their respective SD (n=3). 7e-SMAMP = non-formulated 7e-SMAMP. #) $p < 0.05$ compared to control. Significant differences between non-formulated and formulated 7e-SMAMP were also reported: * $p \leq 0.05$, ** $p \leq 0.01$, *** $p \leq 0.001$.

The second evaluation focused on the ability to eradicate pre-formed biofilms. The strongest eradication of pre-formed biofilm was again observed against *S. aureus* ATCC29213, with complete eradication at a concentration of 12.5 µg/mL (Figure 5.24). Even though the non-formulated 7e-SMAMP was not able to completely eradicate all of the pre-formed bacterial biofilm, the results are fairly promising for antimicrobial therapy. When the biofilms were treated with formulated 7e-SMAMP, the anti-biofilm activity was significantly improved, even if the concentrations needed to eradicate pre-formed biofilms were higher than the concentrations needed to inhibit biofilm formation. The biofilms in all bacteria were completely abolished at concentrations above MIC values, except for the biofilms produced by *P. aeruginosa* ATCC10145. The 7e-SMAMP exhibited evidently stronger effect against gram-positive bacteria, even against most of the resistant bacteria. Yet, the confirmed activity against the gram-negative bacteria calls for optimism.

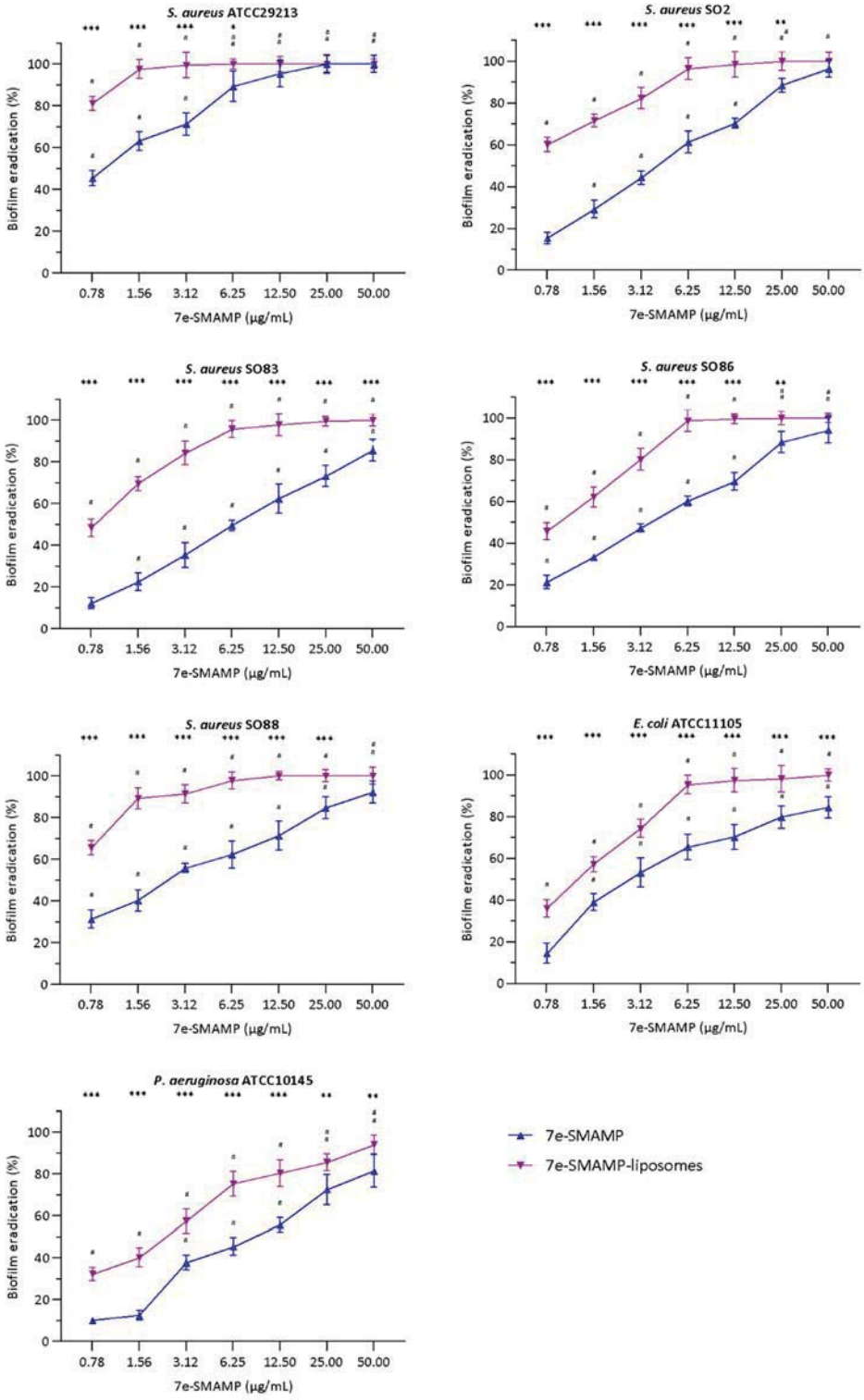

Figure 5.24. Eradication of pre-formed biofilm (%) by non-formulated and formulated 7e-SMAMP in five strains of *S. aureus*, *E. coli* ATCC11105, and *P. aeruginosa* ATCC10145. Concentrations of 7e-SMAMP were 0.78, 1.56, 3.12, 6.25, 12.5, 25.0, and 50.0 µg/mL for both non-formulated and formulated 7e-SMAMP.The results are expressed as means with their respective SD (n=3). 7e-SMAMP = non-formulated 7e-SMAMP. #) $p < 0.05$ compared to control. Significant differences between non-formulated and formulated 7e-SMAMP were also reported: * $p \leq 0.05$, ** $p \leq 0.01$, *** $p \leq 0.001$.

5.2.2 7a-SMAMP-liposomes (paper V)

5.2.2.1 7a-SMAMP-liposome characteristics (paper V)

After establishing that liposomes incorporating 7e-SMAMP remained stable and had promise as efficient antimicrobials were formulated in liposomes, we focused on the potential of SMAMPs in enhanced wound healing. Although highly relevant, bacterial eradication and infection control are not sufficient for successful wound management (Wilkinson and Hardman, 2020). The AMPs have previously been described to be highly promising in wound healing (Thapa et al., 2020). The 7a-SMAMP used in this study has previously exhibited a slightly lower antimicrobial capacity than 7e-SMAMP, but a higher cell compatibility (Paulsen et al., 2021). To develop wound dressing with multitargeting potential, we co-entrapped 7a-SMAMP and chlorogenic acid (CGA) in liposomes expecting to exhibit enhanced anti-inflammatory and proliferative activities. Moreover, CGA is polar and water soluble (Wianowska and Gil, 2019), and would therefore likely accommodate itself in the cores of the liposomes. Thus, it would not sterically affect the liposomal membrane and therefore the stability of bilayers. We focused on the biological properties related to wound healing rather than the antimicrobial potential of 7a-SMAMP-liposomes. Additionally, we sought to assess whether co-entrapped CGA could improve the wound healing properties. The novel liposomes (Table 5.9) were slightly smaller and exhibiting lower surface charge than the 7e-SMAMP-liposomes (Table 5.7). However, the liposomes still maintained a positive surface charge.

Table 5.9. Liposome characteristics: mean diameter, polydispersity index (PI), zeta potential, entrapment efficacy (EE%), and pH in aqueous medium.

	Mean diameter (nm)	PI	Zeta potential (mV)	EE (%) CGA / 7a-SMAMP	pH
Empty liposomes	260 ± 16	0.22 ± 0.15	-2.9 ± 2.4	- / -	6.8 ± 0.2
CGA-liposomes	224 ± 4	0.24 ± 0.06	-6.8 ± 7.5	30.2 ± 3.8 / -	3.2 ± 0.0
7a-SMAMP-liposomes	216 ± 18	0.13 ± 0.05	46.0 ± 1.0	- / 54.5 ± 3.4	5.5 ± 0.2
CGA/7a-SMAMP-liposomes	208 ± 2	0.08 ± 0.02	40.0 ± 1.3	43.5 ± 3.4 / 80.2 ± 5.2	3.0 ± 0.0

Results are expressed as means with their respective SD (n=3). The mean diameter represents the weight-intensity distribution of the liposomes.

5.2.2.2 7a-SMAMP-liposomes-in-hydrogel characteristics (paper V)

The 7a-SMAMP-liposomes where further incorporated into chitosan hydrogels as the secondary vehicle aiming at a suitable wound dressing. The novel formulation was characterized (Figure 5.25) following the methods applied in paper II. The hydrogel hardness was similar to what was reported in paper II, namely it increased upon incorporation of liposomes in hydrogel. On the other hand, the cohesiveness slightly increased when the liposomes were incorporated into hydrogels. This is the opposite effect as observed for vesicles and chitosomes in paper II, but rather more in line with the results the conventional liposomes in paper I. Furthermore, these results are similar to the ones obtained by Hurler *et al.* that reported an increase in the cohesiveness upon incorporation of liposomes in hydrogel (Hurler et al., 2012). The same effects were also observed in a study by Jøraholmen *et al.* (Jøraholmen et al., 2019). Again, it is important to remember that the sources of chitosan as well as its degree of deacetylation and M_w need to be the same for direct comparison.

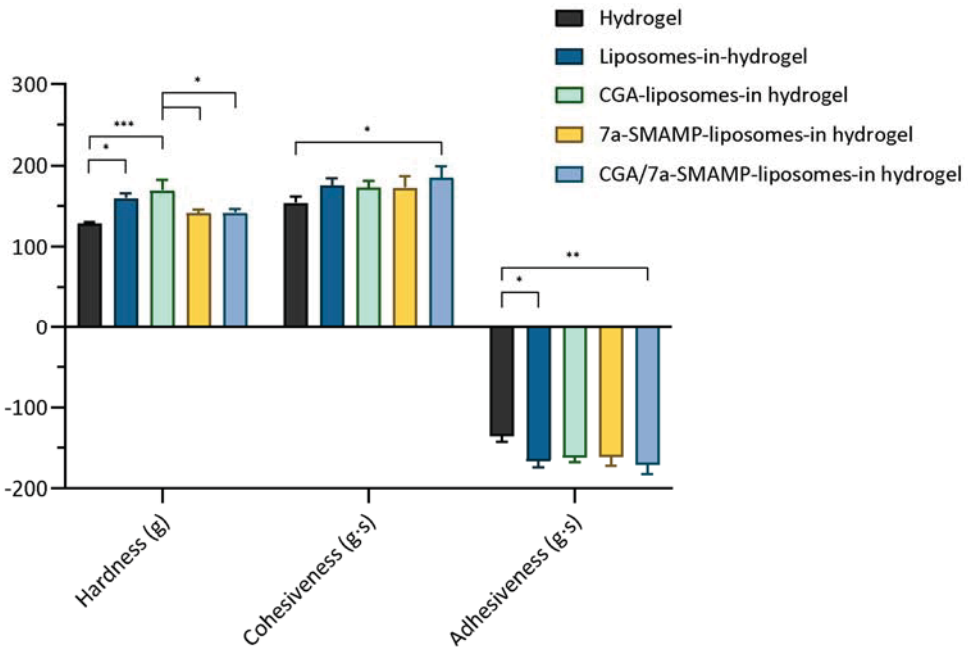

Figure 5.25. The texture properties of chitosan hydrogels measured as hardness, cohesiveness, and adhesiveness. The results are expressed as means with their respective SD (n=3). Hydrogel = plain hydrogel. * $p \leq 0.05$, ** $p \leq 0.01$, *** $p \leq 0.001$.

5.2.2.3 7a-SMAMP-liposomes and their effects on cells (paper V)

The potential cell toxicity was evaluated for the novel 7a-SMAMP-liposomes and their corresponding hydrogels (Figure 5.26). As in paper III, we included keratinocytes, fibroblasts, and macrophages in this evaluation. For both the keratinocytes and fibroblasts, the viability of treated cells was unaffected throughout the whole concentration range. For the macrophages treated with plain hydrogel or CGA-liposomes-in-hydrogel, the viability was reduced to 76 and 82%, respectively. However, according to ISO standard 10993-5:2009, reduction of viability with more that 30% is considered a cytotoxic effect (ISO, 2009). Therefore, the reduction in viability of cells was not considered a toxic effect, and the formulations were deemed safe. Importantly, for the 7a-SMAMP-liposomes-in-hydrogel and CGA/7a-SMAMP-liposomes-in-hydrogel, this reduced cell viability was not observed.

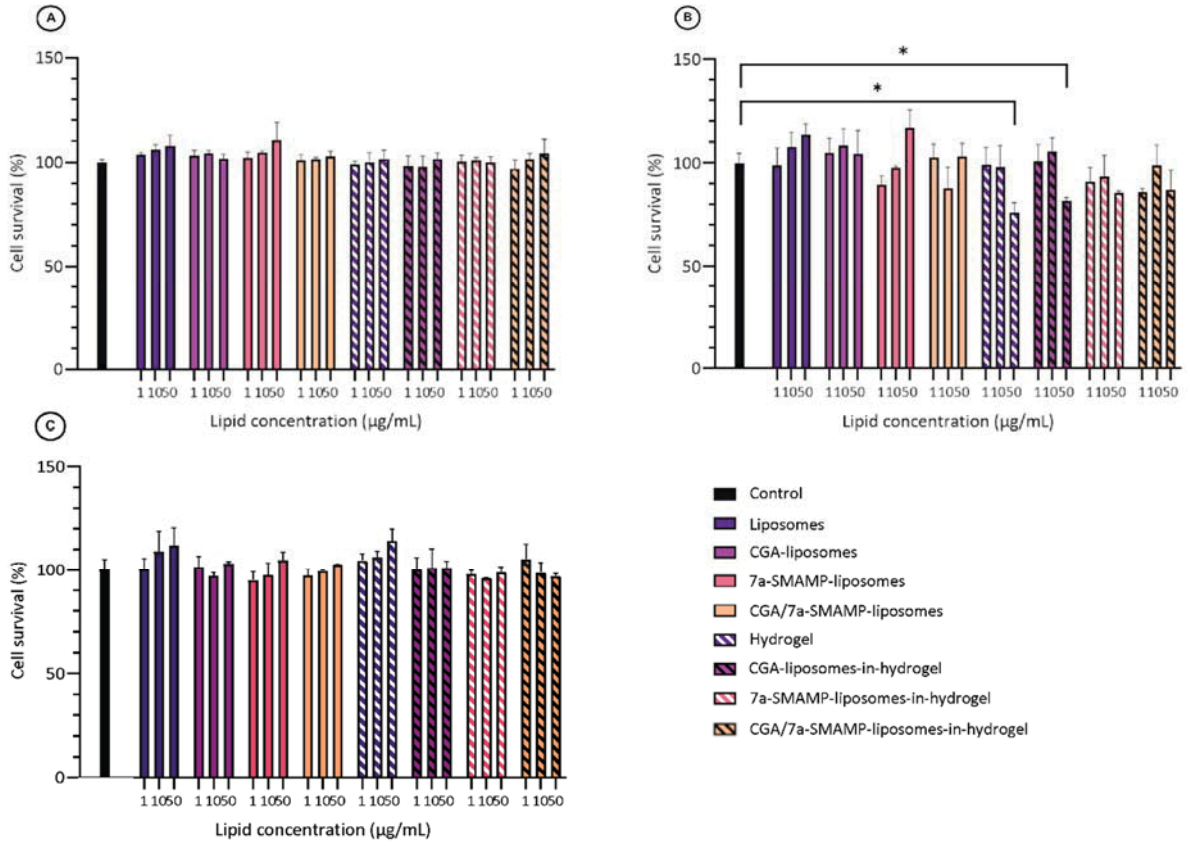

Figure 5.26. Evaluation of cell toxicity of liposomes, CGA-liposomes, 7a-SMAMP-liposomes, CGA/7a-SMAMP-liposomes and their respective hydrogels in A) HaCaT, B) RAW 264.7, and C) HDF-neo cells. Three different concentrations were tested, namely 1, 10, and 50 µg/mL lipid (or the corresponding concentrations of hydrogels), and the results are presented as cell viability of treated cells compared to control (100%). Control cells were only supplemented with complete medium; the cell viability is thereof considered as 100%. The results are expressed as means with their respective SD (n=3). * $p \leq 0.05$.

The anti-inflammatory activity (Figure 5.27) of the 7a-SMAMP-liposomes and their corresponding hydrogels was assessed in murine macrophages as for the CHX-formulations and 7e-SMAMP-liposomes in the papers I-IV. A dose-dependent reduction in NO production was observed when macrophages were treated with 7a-SMAMP-liposomes. Moreover, the hydrogels also reduced the NO production, in line with results for the CHX-liposomes-in-hydrogel (paper I). Interestingly, CGA is known for its anti-inflammatory activity that is thought to originate from the reduction of ROS (Naveed et al., 2018), while looking at the NO production the opposite effect was observed for the CGA-liposomes and CGA/7a-SMAMP-liposomes. At the highest lipid concentration, the production of NO was significantly higher

than for non-treated LPS-induced macrophages. This effect needs to be further assessed, however, increased inflammation upon treatment have previously been reported by Du *et al.* (Du et al., 2013). Nevertheless, the effect was not observed when the liposomes containing CGA were incorporated into hydrogels.

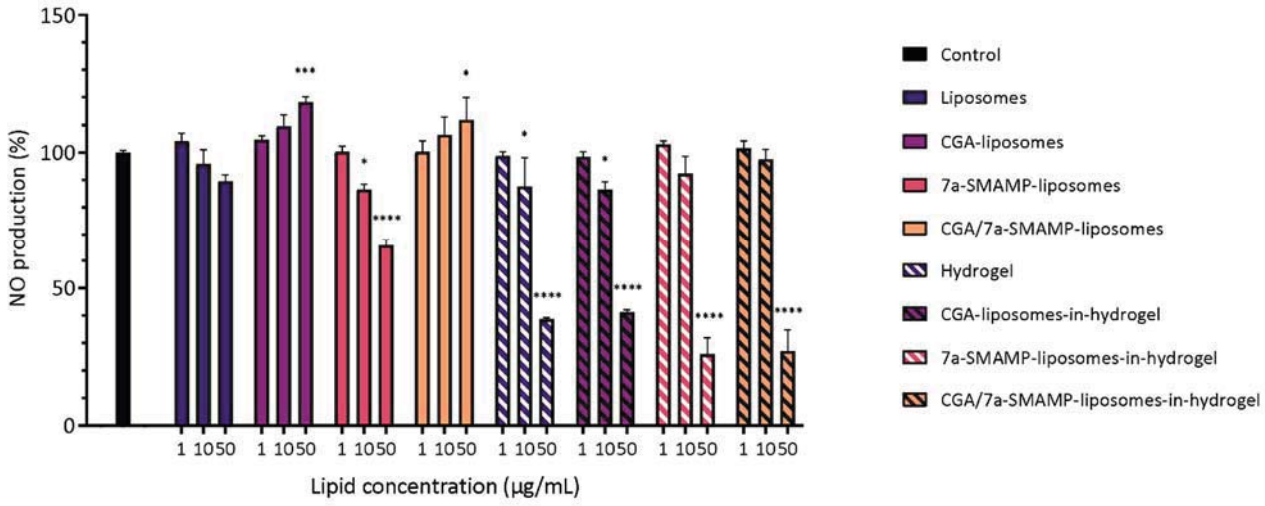

Figure 5.27 Anti-inflammation, CGA/7a-SMAMP-liposomes-in-hydrogel. Evaluation of potential anti-inflammatory activity of liposomes, CGA-liposomes, 7a-SMAMP-liposomes, CGA/7a-SMAMP-liposomes and their respective hydrogels expressed as reduction of nitric oxide (NO) production of formulations in RAW 264.7 cells. Three different concentrations were tested, namely 1, 10, and 50 µg/mL lipid (or the corresponding concentrations of hydrogels), and the results are presented as NO production of treated cells compared to control (100%). Control cells were non-treated lipopolysaccharide (LPS)-induced cells; their production is thereof considered as 100%. The results are expressed as means with their respective SD (n=3). * $p \leq 0.05$, *** $p \leq 0.001$, **** $p \leq 0.0001$, compared to control.

Another important function of keratinocytes and fibroblasts in wound healing is their migration to close off the wounded area and repair the skin (Kwiecien et al., 2019). Consequently, we investigated if the empty liposomes and CGA/7a-SMAMP-liposomes could have modulatory effects on cell migration in an *in vitro* scratch assay (Figure 5.28). In the keratinocytes, the cell migration over the first 7 hours was similar in all treated and non-treated cells. However, after 24 hours the gap in the cells treated with CGA/7a-SMAMPs-

liposomes was significantly smaller than for the other groups. Furthermore, after 30 hours the mean gap closure in the cells treated with CGA/7a-SMAMP-liposomes were smaller than the other group, although not significantly. This reduction of the gap confirmed improved cell migration. In the fibroblasts, the migration of all cells, both treated and non-treated, was approximately the same over the whole test period; however, the gap closure of cells treated with 10 µg/mL of CGA/7a-SMAMP-liposomes was smaller after 7 hours than in the control, which would suggest that these liposomes improved wound closure.

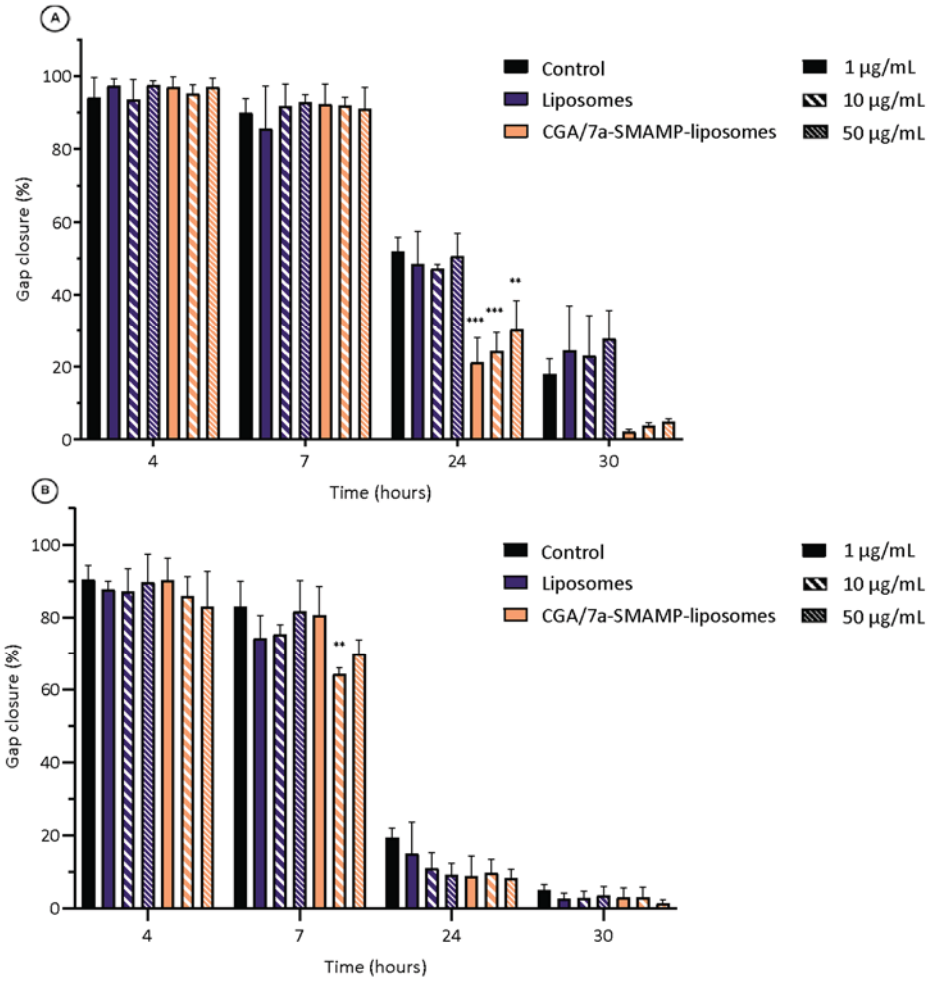

Figure 5.28. Evaluation of cell migration in the *in vitro* scratch assay upon treatment with liposomes or CGA/7a-SMAMP-liposomes in A) HaCaT and B) HDF-neo cells. Three different concentrations were tested, namely 1, 10, and 50 µg/mL lipid, and the results are presented as gap closure (%) in treated cells and control compared to the initial gap opening (0 hours, 100%). Control cells were only supplemented with complete medium. The results are expressed as means with their respective SD (n=3). ** $p \leq 0.01$, *** $p \leq 0.001$, compared to control.

There are not many reports on the role of CGA in enhanced wound healing after topical administration, however, non-formulated CGA was reported to effectively improve cell migration both in keratinocytes and fibroblasts (Moghadam et al., 2017). Song *et al.* very recently demonstrated both improved *in vitro* migration and wound healing of full-thickness diabetic wounds in mice treated with a CGA-hydrogel (Song et al., 2022). The AMPs could also play a vital role in wound closure, for example Park *et al.* reported enhanced gap closure rates in fibroblasts treated with the SMAMP KSL-W (Park et al., 2017). Furthermore, liposomes have also previously improved cell migratory effects of associated active compounds in both keratinocytes and fibroblasts (Allaw et al., 2021). It remains to be further investigated why the improvement in cell migration was only observed in keratinocytes.

6. Conclusions

We developed drug delivery systems for MAAs, namely CHX and two novel SMAMPs. The newly developed systems comprising MAAs exhibited improved antimicrobial properties and could serve as a platform for innovative formulations for management of infected skin wounds. Liposomes-in-hydrogels were deemed the most suitable system for these MAAs.

Conventional phosphatidylcholine-liposomes comprising the MAAs were tailored for topical skin therapy. Furthermore, we also proved that liposomes containing the most membrane-active SMAMP, 7e-SMAMP, remained stable and were not affected by the inclusion of this SMAMP.

The liposomes were further incorporated in chitosan hydrogels to produce a patient-friendly, applicable formulation with improved anti-inflammatory and antimicrobial activities. We confirmed that chitosan had the ability to reduce NO production in macrophages, indicating anti-inflammatory activity. Additionally, both the liposomes, hydrogels, and liposomes-in-hydrogels proved safe in cells relevant for the wound healing process, namely keratinocytes, fibroblasts, and macrophages. The CGA/7a-SMAMP-liposomes also enhanced keratinocyte migration, even though the effect was absent in fibroblasts.

We confirmed enhanced antimicrobial potential of CHX-liposomes and their respective hydrogels as well as 7e-SMAMP-liposomes. Indeed, these formulations were able to eradicate planktonic bacteria in wound-mimicked environment. Furthermore, both the biofilm inhibition and biofilm eradication improved as the MAAs were incorporated in the delivery systems. The incorporation of MAAs into liposomes and liposomes-in-chitosan hydrogel resulted in a formulation with good cell compatibility, anti-inflammatory activity, and antimicrobial effects desired in management of chronic wounds.

7. Perspectives

Considering the multitargeting effects of AMPs and SMAMPs, their biological targets should be further examined. The mechanistic studies should be expanded to include further evaluations in molecular dynamic simulations, artificial membranes, and *in vitro* bacterial membrane integrity assays. Furthermore, studies on gene-expression related to bacterial biofilms, e.g., genomics or proteomics studies, should be conducted to find potential alteration in expressions between treated and non-treated bacteria.

Due to the polymicrobial nature and complexity of biofilms, more bacterial species should be included in biofilms, along with fungi, to better mimic the environment of wound biofilms. The studies could further be extended to include *ex vivo* and *in vivo* biofilm studies in animal models, and wound healing models with histological examinations.

To fully utilize the proven antimicrobial potential of chitosan, chitosans with various M_ws should be investigated. These investigations should focus on cell compatibility, antimicrobial activities, and effects on immune responses.

Further studies of biocompatibility should be conducted to assess cell responses, such as ATP assays, cellular protease assays, or real-time cell monitoring. Additionally, the compatibility needs to be evaluated in more complex models, such as 3D-cell models and *in vivo* evaluations. Other markers to indicate inflammatory responses should also be included in the assessment of anti-inflammatory activity, such as ILs and TNF-α, and histological evaluation to assess the formulations effect on other immune cells should be included in studies. Furthermore, real-time cell monitoring could also provide a deeper understanding of cell migration.

8. References

Abdel-Sayed, P., Tornay, D., Hirt-Burri, N., de Buys Roessingh, A., Raffoul, W., Applegate, L.A., 2020. Implications of chlorhexidine use in burn units for wound healing. Burns 46, 1150-1156. doi: https://doi.org/10.1016/j.burns.2019.12.008.

Aiello, S., Pagano, L., Ceccacci, F., Simonis, B., Sennato, S., Bugli, F., Martini, C., Torelli, R., Sanguinetti, M., Ciogli, A., Bombelli, C., Mancini, G., 2021. Mannosyl, glucosyl or galactosyl liposomes to improve resveratrol efficacy against Methicillin Resistant Staphylococcus aureus biofilm. Colloids Surf. A Physicochem. Eng. Asp. 617, 126321. doi: https://doi.org/10.1016/j.colsurfa.2021.126321.

Akhtar, F., Khan, A.U., Misba, L., Akhtar, K., Ali, A., 2021. Antimicrobial and antibiofilm photodynamic therapy against vancomycin resistant Staphylococcus aureus (VRSA) induced infection in vitro and in vivo. Eur. J. Pharm. Biopharm. 160, 65-76. doi: https://doi.org/10.1016/j.ejpb.2021.01.012.

Al-Obaidy, S.S.M., Greenway, G.M., Paunov, V.N., 2021. Enhanced Antimicrobial Action of Chlorhexidine Loaded in Shellac Nanoparticles with Cationic Surface Functionality. Pharmaceutics 13, 1389. doi: https://doi.org/10.3390/pharmaceutics13091389.

Allaw, M., Manconi, M., Caboni, P., Bacchetta, G., Escribano-Ferrer, E., Peris, J.E., Nacher, A., Diez-Sales, O., Manca, M.L., 2021. Formulation of liposomes loading lentisk oil to ameliorate topical delivery, attenuate oxidative stress damage and improve cell migration in scratch assay. Biomed. Pharmacother. 144, 112351. doi: https://doi.org/10.1016/j.biopha.2021.112351.

Amasya, G., Inal, O., Sengel-Turk, C.T., 2020. SLN enriched hydrogels for dermal application: Full factorial design study to estimate the relationship between composition and mechanical properties. Chem. Phys. Lipids 228, 104889. doi: https://doi.org/10.1016/j.chemphyslip.2020.104889.

Andersen, T., Vanić, Ž., Flaten, G.E., Mattsson, S., Tho, I., Škalko-Basnet, N., 2013. Pectosomes and chitosomes as delivery systems for metronidazole: the one-pot preparation method. Pharmaceutics 5, 445-456. doi: https://doi.org/10.3390/pharmaceutics5030445.

Antimisiaris, S.G., Marazioti, A., Kannavou, M., Natsaridis, E., Gkartziou, F., Kogkos, G., Mourtas, S., 2021. Overcoming barriers by local drug delivery with liposomes. Adv. Drug Deliv. Rev. 174, 53-86. doi: https://doi.org/10.1016/j.addr.2021.01.019.

Arango Duque, G., Descoteaux, A., 2014. Macrophage Cytokines: Involvement in Immunity and Infectious Diseases. Front. Immunol. 5, 491. doi: https://doi.org/10.3389/fimmu.2014.00491.

Arora, D., Nanda, S., 2019. Quality by design driven development of resveratrol loaded ethosomal hydrogel for improved dermatological benefits via enhanced skin permeation and retention. Int. J. Pharm. 567, 118448. doi: https://doi.org/10.1016/j.ijpharm.2019.118448.

Bagdas, D., Etoz, B.C., Gul, Z., Ziyanok, S., Inan, S., Turacozen, O., Gul, N.Y., Topal, A., Cinkilic, N., Tas, S., Ozyigit, M.O., Gurun, M.S., 2015. In vivo systemic chlorogenic acid therapy under diabetic conditions: Wound healing effects and cytotoxicity/genotoxicity profile. Food Chem. Toxicol. 81, 54-61. doi: https://doi.org/10.1016/j.fct.2015.04.001.

Ballén, V., Cepas, V., Ratia, C., Gabasa, Y., Soto, S.M., 2022. Clinical Escherichia coli: From Biofilm Formation to New Antibiofilm Strategies. Microorganisms 10, 1103. doi: https://doi.org/10.3390/microorganisms10061103.

Balouiri, M., Sadiki, M., Ibnsouda, S.K., 2016. Methods for in vitro evaluating antimicrobial activity: A review. J. Pharm. Anal. 6, 71-79. doi: https://doi.org/10.1016/j.jpha.2015.11.005.

Bangham, A.D., Horne, R.W., 1964. Negative staining of phospholipids and their structural modification by surface-active agents as observed in the electron microscope. J. Mol. Biol. 8, 660-668. doi: https://doi.org/10.1016/S0022-2836(64)80115-7.

Barbosa, J.N., Amaral, I.F., Águas, A.P., Barbosa, M.A., 2010. Evaluation of the effect of the degree of acetylation on the inflammatory response to 3D porous chitosan scaffolds. J. Biomed. Mater. Res. A 93A, 20-28. doi: https://doi.org/10.1002/jbm.a.32499.

Barrett, J.P., Raby, E., Wood, F., Coorey, R., Ramsay, J.P., Dykes, G.A., Ravensdale, J.T., 2022. An in vitro study into the antimicrobial and cytotoxic effect of Acticoat™ dressings supplemented with chlorhexidine. Burns 48, 941-951. doi: https://doi.org/10.1016/j.burns.2021.09.019.

Batoni, G., Maisetta, G., Esin, S., 2021. Therapeutic Potential of Antimicrobial Peptides in Polymicrobial Biofilm-Associated Infections. Int. J. Mol. Sci. 22, 482. doi: https://doi.org/10.3390/ijms22020482.

Benson, H.A.E., Grice, J.E., Mohammed, Y., Namjoshi, S., Roberts, M.S., 2019. Topical and Transdermal Drug Delivery: From Simple Potions to Smart Technologies. Curr. Drug Deliv. 16, 444-460. doi: https://doi.org/10.2174/1567201816666190201143457.

Bi, Y., Xia, G., Shi, C., Wan, J., Liu, L., Chen, Y., Wu, Y., Zhang, W., Zhou, M., He, H., Liu, R., 2021. Therapeutic strategies against bacterial biofilms. Fundam. Res. 1, 193-212. doi: https://doi.org/10.1016/j.fmre.2021.02.003.

Bochicchio, S., Lamberti, G., Barba, A.A., 2021. Polymer–Lipid Pharmaceutical Nanocarriers: Innovations by New Formulations and Production Technologies. Pharmaceutics 13, 198. doi: https://doi.org/10.3390/pharmaceutics13020198.

Bonez, P.C., dos Santos Alves, C.F., Dalmolin, T.V., Agertt, V.A., Mizdal, C.R., Flores, V.d.C., Marques, J.B., Santos, R.C.V., Anraku de Campos, M.M., 2013. Chlorhexidine activity against bacterial biofilms. Am. J. Infect. Control 41, e119-e122. doi: https://doi.org/10.1016/j.ajic.2013.05.002.

Borges, G.Á., Elias, S.T., da Silva, S.M.M., Magalhães, P.O., Macedo, S.B., Ribeiro, A.P.D., Guerra, E.N.S., 2017. In vitro evaluation of wound healing and antimicrobial potential of ozone therapy. J. Craniomaxillofac. Surg. 45, 364-370. doi: https://doi.org/10.1016/j.jcms.2017.01.005.

Cañedo-Dorantes, L., Cañedo-Ayala, M., 2019. Skin Acute Wound Healing: A Comprehensive Review. Int. J. Inflam. 2019, 3706315. doi: https://doi.org/10.1155/2019/3706315.

Carita, A.C., Eloy, J.O., Chorilli, M., Lee, R.J., Leonardi, G.R., 2018. Recent Advances and Perspectives in Liposomes for Cutaneous Drug Delivery. Curr. Med. Chem. 25, 606-635. doi: https://doi.org/10.2174/0929867324666171009120154.

Cauzzo, J., Nystad, M., Holsæter, A.M., Basnet, P., Škalko-Basnet, N., 2020. Following the Fate of Dye-Containing Liposomes In Vitro. Int. J. Mol. Sci. 21, 4847. doi: https://doi.org/10.3390/ijms21144847.

Cerchiara, T., Giordani, B., Melgoza, L.M., Prata, C., Parolin, C., Dalena, F., Abruzzo, A., Bigucci, F., Luppi, B., Vitali, B., 2020. New Spanish Broom dressings based on Vitamin E and Lactobacillus plantarum for superficial skin wounds. J. Drug Deliv. Sci. Technol. 56, 101499. doi: https://doi.org/10.1016/j.jddst.2020.101499.

Chang, R.Y.K., Nang, S.C., Chan, H.K., Li, J., 2022. Novel antimicrobial agents for combating antibiotic-resistant bacteria. Adv. Drug Deliv. Rev. 187, 114378. doi: https://doi.org/10.1016/j.addr.2022.114378.

Chatterjee, S., Woo, S.H., 2009. The removal of nitrate from aqueous solutions by chitosan hydrogel beads. J. Hazard. Mater. 164, 1012-1018. doi: https://doi.org/10.1016/j.jhazmat.2008.09.001.

Chen, C., Liu, Y., Wang, H., Chen, G., Wu, X., Ren, J., Zhang, H., Zhao, Y., 2018. Multifunctional Chitosan Inverse Opal Particles for Wound Healing. ACS Nano 12, 10493-10500. doi: https://doi.org/10.1021/acsnano.8b06237.

Chen, S.X., Zhang, L.J., Gallo, R.L., 2019. Dermal White Adipose Tissue: A Newly Recognized Layer of Skin Innate Defense. J. Invest. Dermatol. 139, 1002-1009. doi: https://doi.org/10.1016/j.jid.2018.12.031.

Chen, W.C., Liou, S.S., Tzeng, T.F., Lee, S.L., Liu, I.M., 2013. Effect of Topical Application of Chlorogenic Acid on Excision Wound Healing in Rats. Planta Med. 79, 616-621. doi: https://doi.org/10.1055/s-0032-1328364.

Chessa, C., Bodet, C., Jousselin, C., Wehbe, M., Lévêque, N., Garcia, M., 2020. Antiviral and Immunomodulatory Properties of Antimicrobial Peptides Produced by Human Keratinocytes. Front. Microbiol. 11, 1155. doi: https://doi.org/10.3389/fmicb.2020.01155.

Chiewchalermsri, C., Sompornrattanaphan, M., Wongsa, C., Thongngarm, T., 2020. Chlorhexidine Allergy: Current Challenges and Future Prospects. J. Asthma Allergy 13, 127-133. doi: https://doi.org/10.2147/jaa.S207980.

Ciofu, O., Moser, C., Jensen, P.Ø., Høiby, N., 2022. Tolerance and resistance of microbial biofilms. Nat. Rev. Microbiol. doi: https://doi.org/10.1038/s41579-022-00682-4.

Ciofu, O., Rojo-Molinero, E., Macià, M.D., Oliver, A., 2017. Antibiotic treatment of biofilm infections. APMIS 125, 304-319. doi: https://doi.org/10.1111/apm.12673.

Coates, M., Blanchard, S., MacLeod, A.S., 2018. Innate antimicrobial immunity in the skin: A protective barrier against bacteria, viruses, and fungi. PLoS Pathog. 14, e1007353. doi: https://doi.org/10.1371/journal.ppat.1007353.

da Silva, R.A.G., Afonina, I., Kline, K.A., 2021. Eradicating biofilm infections: an update on current and prospective approaches. Curr. Opin. Microbiol. 63, 117-125. doi: https://doi.org/10.1016/j.mib.2021.07.001.

Danaei, M., Dehghankhold, M., Ataei, S., Hasanzadeh Davarani, F., Javanmard, R., Dokhani, A., Khorasani, S., Mozafari, M.R., 2018. Impact of Particle Size and Polydispersity Index on the Clinical Applications of Lipidic Nanocarrier Systems. Pharmaceutics 10, 57. doi: https://doi.org/10.3390/pharmaceutics10020057.

Darwin, E., Tomic-Canic, M., 2018. Healing Chronic Wounds: Current Challenges and Potential Solutions. Curr. Dermatol. Rep. 7, 296-302. doi: https://doi.org/10.1007/s13671-018-0239-4.

de la Fuente-Núñez, C., Korolik, V., Bains, M., Nguyen, U., Breidenstein, E.B.M., Horsman, S., Lewenza, S., Burrows, L., Hancock, R.E.W., 2012. Inhibition of Bacterial Biofilm Formation and Swarming Motility by a Small Synthetic Cationic Peptide. Antimicrob. Agents Chemother. 56, 2696-2704. doi: https://doi.org/10.1128/AAC.00064-12.

Değim, Z., Çelebi, N., Alemdaroğlu, C., Deveci, M., Öztürk, S., Özoğul, C., 2011. Evaluation of chitosan gel containing liposome-loaded epidermal growth factor on burn wound healing. Int. Wound J. 8, 343-354. doi: https://doi.org/10.1111/j.1742-481X.2011.00795.x.

Dewangan, R.P., Bisht, G.S., Singh, V.P., Yar, M.S., Pasha, S., 2018. Design and synthesis of cell selective α/β-diastereomeric peptidomimetic with potent in vivo antibacterial activity against methicillin resistant S. Aureus. Bioorg. Chem. 76, 538-547. doi: https://doi.org/10.1016/j.bioorg.2017.12.020.

Dey, R., De, K., Mukherjee, R., Ghosh, S., Haldar, J., 2019. Small antibacterial molecules highly active against drug-resistant Staphylococcus aureus. MedChemComm 10, 1907-1915. doi: https://doi.org/10.1039/C9MD00329K.

Dias, C., Rauter, A.P., 2019. Membrane-targeting antibiotics: recent developments outside the peptide space. Future Med. Chem. 11, 211-228. doi: https://doi.org/10.4155/fmc-2018-0254.

Díez-Pascual, A.M., 2020. Recent Progress in Antimicrobial Nanomaterials. Nanomaterials 10, 2315. doi: https://doi.org/10.3390/nano10112315.

Dijksteel, G.S., Ulrich, M.M.W., Middelkoop, E., Boekema, B.K.H.L., 2021. Review: Lessons Learned From Clinical Trials Using Antimicrobial Peptides (AMPs). Front. Microbiol. 12, 616979. doi: https://doi.org/10.3389/fmicb.2021.616979.

Divyashree, M., Mani, M.K., Reddy, D., Kumavath, R., Ghosh, P., Azevedo, V., Barh, D., 2020. Clinical Applications of Antimicrobial Peptides (AMPs): Where do we Stand Now? Protein Pept. Lett. 27, 120-134. doi: https://doi.org/10.2174/0929866526666190925152957.

Drago, F., Gariazzo, L., Cioni, M., Trave, I., Parodi, A., 2019. The microbiome and its relevance in complex wounds. Eur. J. Dermatol. 29, 6-13. doi: https://doi.org/10.1684/ejd.2018.3486.

du Plessis, J., Ramachandran, C., Weiner, N., Müller, D.G., 1994. The influence of particle size of liposomes on the deposition of drug into skin. Int. J. Pharm. 103, 277-282. doi: https://doi.org/10.1016/0378-5173(94)90178-3.

Du, W.Y., Chang, C., Zhang, Y., Liu, Y.Y., Sun, K., Wang, C.S., Wang, M.X., Liu, Y., Wang, F., Fan, J.Y., Li, P.T., Han, J.Y., 2013. High-dose chlorogenic acid induces inflammation reactions and oxidative stress injury in rats without implication of mast cell degranulation. J. Ethnopharmacol. 147, 74-83. doi: https://doi.org/10.1016/j.jep.2013.01.042.

Epand, R.F., Mowery, B.P., Lee, S.E., Stahl, S.S., Lehrer, R.I., Gellman, S.H., Epand, R.M., 2008. Dual Mechanism of Bacterial Lethality for a Cationic Sequence-Random Copolymer that Mimics Host-Defense Antimicrobial Peptides. J. Mol. Biol. 379, 38-50. doi: https://doi.org/10.1016/j.jmb.2008.03.047.

Erdem Büyükkiraz, M., Kesmen, Z., 2022. Antimicrobial peptides (AMPs): A promising class of antimicrobial compounds. J. Appl. Microbiol. 132, 1573-1596. doi: https://doi.org/10.1111/jam.15314.

Eriksson, E., Liu, P.Y., Schultz, G.S., Martins-Green, M.M., Tanaka, R., Weir, D., Gould, L.J., Armstrong, D.G., Gibbons, G.W., Wolcott, R., Olutoye, O.O., Kirsner, R.S., Gurtner, G.C., 2022. Chronic wounds: Treatment consensus. Wound Repair Regen. 30, 156-171. doi: https://doi.org/10.1111/wrr.12994.

EUCAST—the European Committee on Antimicrobial Susceptibility Testing, 2020. EUCAST reading guide for broth microdilution.

Falcone, M., De Angelis, B., Pea, F., Scalise, A., Stefani, S., Tasinato, R., Zanetti, O., Dalla Paola, L., 2021. Challenges in the management of chronic wound infections. J. Glob. Antimicrob. Resist. 26, 140-147. doi: https://doi.org/10.1016/j.jgar.2021.05.010.

Farha, M.A., Brown, E.D., 2019. Drug repurposing for antimicrobial discovery. Nat. Microbiol. 4, 565-577. doi: https://doi.org/10.1038/s41564-019-0357-1.

Farha, M.A., El-Halfawy, O.M., Gale, R.T., MacNair, C.R., Carfrae, L.A., Zhang, X., Jentsch, N.G., Magolan, J., Brown, E.D., 2020. Uncovering the Hidden Antibiotic Potential of Cannabis. ACS Infect. Dis. 6, 338-346. doi: https://doi.org/10.1021/acsinfecdis.9b00419.

Farkas, E., Zelkó, R., Török, G., Rácz, I., Marton, S., 2001. Influence of chlorhexidine species on the liquid crystalline structure of vehicle. Int. J. Pharm. 213, 1-5. doi: https://doi.org/10.1016/S0378-5173(00)00575-5.

Fasiku, V.O., Omolo, C.A., Devnarain, N., Ibrahim, U.H., Rambharose, S., Faya, M., Mocktar, C., Singh, S.D., Govender, T., 2021. Chitosan-Based Hydrogel for the Dual Delivery of Antimicrobial Agents Against Bacterial Methicillin-Resistant Staphylococcus aureus Biofilm-Infected Wounds. ACS Omega 6, 21994-22010. doi: https://doi.org/10.1021/acsomega.1c02547.

Feng, P., Luo, Y., Ke, C., Qiu, H., Wang, W., Zhu, Y., Hou, R., Xu, L., Wu, S., 2021. Chitosan-Based Functional Materials for Skin Wound Repair: Mechanisms and Applications. Front. Bioeng. Biotechnol. 9, 650598. doi: https://doi.org/10.3389/fbioe.2021.650598.

Feng, Y., Sun, C., Yuan, Y., Zhu, Y., Wan, J., Firempong, C.K., Omari-Siaw, E., Xu, Y., Pu, Z., Yu, J., Xu, X., 2016. Enhanced oral bioavailability and in vivo antioxidant activity of chlorogenic acid via liposomal formulation. Int. J. Pharm. 501, 342-349. doi: https://doi.org/10.1016/j.ijpharm.2016.01.081.

Ferreira, M., Pinto, S.N., Aires-da-Silva, F., Bettencourt, A., Aguiar, S.I., Gaspar, M.M., 2021. Liposomes as a Nanoplatform to Improve the Delivery of Antibiotics into Staphylococcus aureus Biofilms. Pharmaceutics 13, 321. doi: https://doi.org/10.3390/pharmaceutics13030321.

Firlar, I., Altunbek, M., McCarthy, C., Ramalingam, M., Camci-Unal, G., 2022. Functional Hydrogels for Treatment of Chronic Wounds. Gels 8, 127. doi: https://doi.org/10.3390/gels8020127.

Flemming, H.C., Wingender, J., Szewzyk, U., Steinberg, P., Rice, S.A., Kjelleberg, S., 2016. Biofilms: an emergent form of bacterial life. Nat. Rev. Microbiol. 14, 563-575. doi: https://doi.org/10.1038/nrmicro.2016.94.

Fong, D., Hoemann, C.D., 2017. Chitosan immunomodulatory properties: perspectives on the impact of structural properties and dosage. Future Sci. OA 4, FSO225. doi: https://doi.org/10.4155/fsoa-2017-0064.

Frapwell, C.J., Skipp, P.J., Howlin, R.P., Angus, E.M., Hu, Y., Coates, A.R.M., Allan, R.N., Webb, J.S., 2020. Antimicrobial Activity of the Quinoline Derivative HT61 against Staphylococcus aureus Biofilms. Antimicrob. Agents Chemother. 64, e02073-19. doi: https://doi.org/10.1128/AAC.02073-19.

Frykberg, R.G., Banks, J., 2015. Challenges in the Treatment of Chronic Wounds. Adv. Wound Care 4, 560-582. doi: https://doi.org/10.1089/wound.2015.0635.

Fuster, M.G., Montalbán, M.G., Carissimi, G., Lima, B., Feresin, G.E., Cano, M., Giner-Casares, J.J., López-Cascales, J.J., Enriz, R.D., Víllora, G., 2020. Antibacterial Effect of Chitosan–Gold Nanoparticles and Computational Modeling of the Interaction between Chitosan and a Lipid Bilayer Model. Nanomaterials 10, 2340. doi: https://doi.org/10.3390/nano10122340.

Gajula, B., Munnamgi, S., Basu, S., 2020. How bacterial biofilms affect chronic wound healing: a narrative review. Int. J. Surg. Glob. Health 3, e16. doi: https://doi.org/10.1097/GH9.0000000000000016.

Gan, B.H., Gaynord, J., Rowe, S.M., Deingruber, T., Spring, D.R., 2021. The multifaceted nature of antimicrobial peptides: current synthetic chemistry approaches and future directions. Chem. Soc. Rev. 50, 7820-7880. doi: https://doi.org/10.1039/D0CS00729C.

Gao, W., Vecchio, D., Li, J., Zhu, J., Zhang, Q., Fu, V., Li, J., Thamphiwatana, S., Lu, D., Zhang, L., 2014. Hydrogel Containing Nanoparticle-Stabilized Liposomes for Topical Antimicrobial Delivery. ACS Nano 8, 2900-2907. doi: https://doi.org/10.1021/nn500110a.

Gera, S., Kankuri, E., Kogermann, K., 2021. Antimicrobial peptides – Unleashing their therapeutic potential using nanotechnology. Pharmacol. Ther. 232, 107990. doi: https://doi.org/10.1016/j.pharmthera.2021.107990.

Ghosh, C., Haldar, J., 2015. Membrane-Active Small Molecules: Designs Inspired by Antimicrobial Peptides. ChemMedChem 10, 1606-1624. doi: https://doi.org/10.1002/cmdc.201500299.

Ghosh, C., Sarkar, P., Issa, R., Haldar, J., 2019. Alternatives to Conventional Antibiotics in the Era of Antimicrobial Resistance. Trends Microbiol. 27, 323-338. doi: https://doi.org/10.1016/j.tim.2018.12.010.

Giordani, B., Basnet, P., Mishchenko, E., Luppi, B., Škalko-Basnet, N., 2019. Utilizing Liposomal Quercetin and Gallic Acid in Localized Treatment of Vaginal Candida Infections. Pharmaceutics 12, 9. doi: https://doi.org/10.3390/pharmaceutics12010009.

Gonzalez Gomez, A., Hosseinidoust, Z., 2020. Liposomes for Antibiotic Encapsulation and Delivery. ACS Infect. Dis. 6, 896-908. doi: https://doi.org/10.1021/acsinfecdis.9b00357.

Guimarães, D., Cavaco-Paulo, A., Nogueira, E., 2021a. Design of liposomes as drug delivery system for therapeutic applications. Int. J. Pharm. 601, 120571. doi: https://doi.org/10.1016/j.ijpharm.2021.120571.

Guimarães, I., Baptista-Silva, S., Pintado, M., L. Oliveira, A., 2021b. Polyphenols: A Promising Avenue in Therapeutic Solutions for Wound Care. Appl. Sci. 11, 1230. doi: https://doi.org/10.3390/app11031230.

Guo, S., Yao, M., Zhang, D., He, Y., Chang, R., Ren, Y., Guan, F., 2022. One-Step Synthesis of Multifunctional Chitosan Hydrogel for Full-Thickness Wound Closure and Healing. Adv. Healthc. Mater. 11, 2101808. doi: https://doi.org/10.1002/adhm.202101808.

Gurtovenko, A.A., Vattulainen, I., 2007. Molecular Mechanism for Lipid Flip-Flops. J. Phys. Chem. B 111, 13554-13559. doi: https://doi.org/10.1021/jp077094k.

Hajiahmadi, F., Alikhani, M.Y., Shariatifar, H., Arabestani, M.R., Ahmadvand, D., 2019. The bactericidal effect of lysostaphin coupled with liposomal vancomycin as a dual combating system applied directly on methicillin-resistant Staphylococcus aureus infected skin wounds in mice. Int. J. Nanomed. 14, 5943-5955. doi: https://doi.org/10.2147/IJN.S214521.

Hamedi, H., Moradi, S., Hudson, S.M., Tonelli, A.E., 2018. Chitosan based hydrogels and their applications for drug delivery in wound dressings: A review. Carbohydr. Polym. 199, 445-460. doi: https://doi.org/10.1016/j.carbpol.2018.06.114.

Hamedi, H., Moradi, S., Hudson, S.M., Tonelli, A.E., King, M.W., 2022. Chitosan based bioadhesives for biomedical applications: A review. Carbohydr. Polym. 282, 119100. doi: https://doi.org/10.1016/j.carbpol.2022.119100.

Hao, M., Peng, X., Sun, S., Ding, C., Liu, W., 2022. Chitosan/Sodium Alginate/Velvet Antler Blood Peptides Hydrogel Promoted Wound Healing by Regulating PI3K/AKT/mTOR and SIRT1/NF-κB Pathways. Front. Pharmacol. 13, 913408. doi: https://doi.org/10.3389/fphar.2022.913408.

Hassan, D., Omolo, C.A., Fasiku, V.O., Mocktar, C., Govender, T., 2020. Novel chitosan-based pH-responsive lipid-polymer hybrid nanovesicles (OLA-LPHVs) for delivery of vancomycin against methicillin-resistant Staphylococcus aureus infections. Int. J. Biol. Macromol. 147, 385-398. doi: https://doi.org/10.1016/j.ijbiomac.2020.01.019.

Hemmingsen, L.M., Giordani, B., Pettersen, A.K., Vitali, B., Basnet, P., Škalko-Basnet, N., 2021a. Liposomes-in-chitosan hydrogel boosts potential of chlorhexidine in biofilm eradication in vitro. Carbohydr. Polym. 262, 117939. doi: https://doi.org/10.1016/j.carbpol.2021.117939.

Hemmingsen, L.M., Škalko-Basnet, N., Jøraholmen, M.W., 2021b. The Expanded Role of Chitosan in Localized Antimicrobial Therapy. Mar. Drugs 19, 697. doi: https://doi.org/10.3390/md19120697.

Hemmingsen, L.M., Julin, K., Ahsan, L., Basnet, P., Johannessen, M., Škalko-Basnet, N., 2021c. Chitosomes-In-Chitosan Hydrogel for Acute Skin Injuries: Prevention and Infection Control. Mar. Drugs 19, 269. doi: https://doi.org/10.3390/md19050269.

Hirschman, W.R., Wheater, M.A., Bringas, J.S., Hoen, M.M., 2012. Cytotoxicity Comparison of Three Current Direct Pulp-capping Agents with a New Bioceramic Root Repair Putty. J. Endod. 38, 385-388. doi: https://doi.org/10.1016/j.joen.2011.11.012.

Hoang, T.P., Ghori, M.U., Conway, B.R., 2021. Topical Antiseptic Formulations for Skin and Soft Tissue Infections. Pharmaceutics 13, 558. doi: https://doi.org/10.3390/pharmaceutics13040558.

Hua, S., 2015. Lipid-based nano-delivery systems for skin delivery of drugs and bioactives. Front. Pharmacol. 6, 219. doi: https://doi.org/10.3389/fphar.2015.00219.

Huh, A.J., Kwon, Y.J., 2011. "Nanoantibiotics": A new paradigm for treating infectious diseases using nanomaterials in the antibiotics resistant era. J. Control. Release 156, 128-145. doi: https://doi.org/10.1016/j.jconrel.2011.07.002.

Hurler, J., Engesland, A., Kermany, B.P., Škalko-Basnet, N., 2012. Improved texture analysis for hydrogel characterization: Gel cohesiveness, adhesiveness, and hardness. J. Appl. Polym. Sci. 125, 180-188. doi: https://doi.org/10.1002/app.35414.

Hurler, J., Škalko-Basnet, N., 2012. Potentials of chitosan-based delivery systems in wound therapy: Bioadhesion study. J. Funct. Biomater. 3, 37-48. doi: https://doi.org/10.3390/jfb3010037.

Hurler, J., Sørensen, K.K., Fallarero, A., Vuorela, P., Škalko-Basnet, N., 2013. Liposomes-in-hydrogel delivery system with mupirocin: in vitro antibiofilm studies and in vivo evaluation in mice burn model. Biomed Res. Int. 2013, 498485. doi: https://doi.org/10.1155/2013/498485.

Ibaraki, H., Kanazawa, T., Chien, W.Y., Nakaminami, H., Aoki, M., Ozawa, K., Kaneko, H., Takashima, Y., Noguchi, N., Seta, Y., 2020. The effects of surface properties of liposomes on their activity against Pseudomonas aeruginosa PAO-1 biofilm. J. Drug Deliv. Sci. Technol. 57, 101754. doi: https://doi.org/10.1016/j.jddst.2020.101754.

Intini, C., Elviri, L., Cabral, J., Mros, S., Bergonzi, C., Bianchera, A., Flammini, L., Govoni, P., Barocelli, E., Bettini, R., McConnell, M., 2018. 3D-printed chitosan-based scaffolds: An in vitro study of human skin cell growth and an in-vivo wound healing evaluation in experimental diabetes in rats. Carbohydr. Polym. 199, 593-602. doi: https://doi.org/10.1016/j.carbpol.2018.07.057.

ISO, 2009. 10993-5:2009 Biological evaluation of medical devices, Part 5: Tests for in vitro cytotoxicity. International Organization for Standardization - ISO.

Jain, S., Patel, N., Shah, M.K., Khatri, P., Vora, N., 2017. Recent Advances in Lipid-Based Vesicles and Particulate Carriers for Topical and Transdermal Application. J. Pharm. Sci. 106, 423-445. doi: https://doi.org/10.1016/j.xphs.2016.10.001.

Jiang, Y., Chen, Y., Song, Z., Tan, Z., Cheng, J., 2021. Recent advances in design of antimicrobial peptides and polypeptides toward clinical translation. Adv. Drug Deliv. Rev. 170, 261-280. doi: https://doi.org/10.1016/j.addr.2020.12.016.

Joo, H.S., Otto, M., 2012. Molecular Basis of In Vivo Biofilm Formation by Bacterial Pathogens. Chem. Biol. 19, 1503-1513. doi: https://doi.org/10.1016/j.chembiol.2012.10.022.

Jung, S.H., Ryu, C.M., Kim, J.S., 2019. Bacterial persistence: Fundamentals and clinical importance. J. Microbiol. 57, 829-835. doi: https://doi.org/10.1007/s12275-019-9218-0.

Jøraholmen, M.W., Bhargava, A., Julin, K., Johannessen, M., Škalko-Basnet, N., 2020. The Antimicrobial Properties of Chitosan Can be Tailored by Formulation. Mar. Drugs 18, 96. doi: https://doi.org/10.3390/md18020096.

Jøraholmen, M.W., Basnet, P., Tostrup, M.J., Moueffaq, S., Škalko-Basnet, N., 2019. Localized Therapy of Vaginal Infections and Inflammation: Liposomes-In-Hydrogel Delivery System for Polyphenols. Pharmaceutics 11, 53. doi: https://doi.org/10.3390/pharmaceutics11020053.

Jøraholmen, M.W., Škalko-Basnet, N., Acharya, G., Basnet, P., 2015. Resveratrol-loaded liposomes for topical treatment of the vaginal inflammation and infections. Eur. J. Pharm. Sci. 79, 112-121. doi: https://doi.org/10.1016/j.ejps.2015.09.007.

Jøraholmen, M.W., Vanić, Ž., Tho, I., Škalko-Basnet, N., 2014. Chitosan-coated liposomes for topical vaginal therapy: Assuring localized drug effect. Int. J. Pharm. 472, 94-101. doi: https://doi.org/10.1016/j.ijpharm.2014.06.016.

Kabir, F., Katayama, S., Tanji, N., Nakamura, S., 2014. Antimicrobial effects of chlorogenic acid and related compounds. J. Korean Soc. Appl. Biol. Chem. 57, 359-365. doi: https://doi.org/10.1007/s13765-014-4056-6.

Karaiskos, I., Lagou, S., Pontikis, K., Rapti, V., Poulakou, G., 2019. The “Old” and the “New” Antibiotics for MDR Gram-Negative Pathogens: For Whom, When, and How. Front. Public Health 7, 151. doi: https://doi.org/10.3389/fpubh.2019.00151.

Kettel, M.J., Heine, E., Schaefer, K., Moeller, M., 2017. Chlorhexidine Loaded Cyclodextrin Containing PMMA Nanogels as Antimicrobial Coating and Delivery Systems. Macromol. Biosci. 17, 1600230. doi: https://doi.org/10.1002/mabi.201600230.

Konai, M.M., Barman, S., Issa, R., MacNeil, S., Adhikary, U., De, K., Monk, P.N., Haldar, J., 2020. Hydrophobicity-Modulated Small Antibacterial Molecule Eradicates Biofilm with Potent Efficacy against Skin Infections. ACS Infect. Dis. 6, 703-714. doi: https://doi.org/10.1021/acsinfecdis.9b00334.

Kou, S., Peters, L., Mucalo, M., 2022. Chitosan: A review of molecular structure, bioactivities and interactions with the human body and micro-organisms. Carbohydr. Polym. 282, 119132. doi: https://doi.org/10.1016/j.carbpol.2022.119132.

Kuppusamy, R., Yasir, M., Berry, T., Cranfield, C.G., Nizalapur, S., Yee, E., Kimyon, O., Taunk, A., Ho, K.K.K., Cornell, B., Manefield, M., Willcox, M., Black, D.S., Kumar, N., 2018. Design and synthesis of short amphiphilic cationic peptidomimetics based on biphenyl backbone as antibacterial agents. Eur. J. Med. Chem. 143, 1702-1722. doi: https://doi.org/10.1016/j.ejmech.2017.10.066.

Kutsevol, N., Virych, P., Nadtoka, O., Virych, P., Krysa, V., 2021. Synthesis of polymeric hydrogels incorporating chlorhexidine as potential antibacterial wound dressings. Mol. Cryst. Liq. Cryst. 720, 65-71. doi: https://doi.org/10.1080/15421406.2021.1905283.

Kwiecien, K., Zegar, A., Jung, J., Brzoza, P., Kwitniewski, M., Godlewska, U., Grygier, B., Kwiecinska, P., Morytko, A., Cichy, J., 2019. Architecture of antimicrobial skin defense. Cytokine Growth Factor Rev. 49, 70-84. doi: https://doi.org/10.1016/j.cytogfr.2019.08.001.

Lam, P.L., Lee, K.K.H., Wong, R.S.M., Cheng, G.Y.M., Bian, Z.X., Chui, C.H., Gambari, R., 2018. Recent advances on topical antimicrobials for skin and soft tissue infections and their safety concerns. Crit. Rev. Microbiol. 44, 40-78. doi: https://doi.org/10.1080/1040841x.2017.1313811.

Large, D.E., Abdelmessih, R.G., Fink, E., Auguste, D.T., 2021. Liposome composition in drug delivery design, synthesis, characterization, and clinical application. Adv. Drug Deliv. Rev. 176, 113851. doi: https://doi.org/10.1016/j.addr.2021.113851.

Las Heras, K., Igartua, M., Santos-Vizcaino, E., Hernandez, R.M., 2020. Chronic wounds: Current status, available strategies and emerging therapeutic solutions. J. Control. Release 328, 532-550. doi: https://doi.org/10.1016/j.jconrel.2020.09.039.

Levin-Reisman, I., Brauner, A., Ronin, I., Balaban, N.Q., 2019. Epistasis between antibiotic tolerance, persistence, and resistance mutations. Proc. Natl. Acad. Sci. 116, 14734-14739. doi: https://doi.org/10.1073/pnas.1906169116.

Li, G., Wang, X., Xu, Y., Zhang, B., Xia, X., 2014. Antimicrobial effect and mode of action of chlorogenic acid on Staphylococcus aureus. Eur. Food Res. Technol. 238, 589-596. doi: https://doi.org/10.1007/s00217-013-2140-5.

Li, R., Liu, K., Huang, X., Li, D., Ding, J., Liu, B., Chen, X., 2022. Bioactive Materials Promote Wound Healing through Modulation of Cell Behaviors. Adv. Sci. 9, 2105152. doi: https://doi.org/10.1002/advs.202105152.

Liang, C.C., Park, A.Y., Guan, J.L., 2007. In vitro scratch assay: a convenient and inexpensive method for analysis of cell migration in vitro. Nat. Protoc. 2, 329-333. doi: https://doi.org/10.1038/nprot.2007.30.

Lima, T.d.P.d.L., Passos, M.F., 2021. Skin wounds, the healing process, and hydrogel-based wound dressings: a short review. J. Biomater. Sci. Polym. Ed. 32, 1910-1925. doi: https://doi.org/10.1080/09205063.2021.1946461.

Lin, Y.K., Yang, S.C., Hsu, C.Y., Sung, J.T., Fang, J.Y., 2021. The Antibiofilm Nanosystems for Improved Infection Inhibition of Microbes in Skin. Molecules 26, 6392. doi: https://doi.org/10.3390/molecules26216392.

Liu, H., Wang, C., Li, C., Qin, Y., Wang, Z., Yang, F., Li, Z., Wang, J., 2018. A functional chitosan-based hydrogel as a wound dressing and drug delivery system in the treatment of wound healing. RSC Adv. 8, 7533-7549. doi: https://doi.org/10.1039/C7RA13510F.

Liu, J., Li, X., Liu, L., Bai, Q., Sui, N., Zhu, Z., 2021b. Self-assembled ultrasmall silver nanoclusters on liposome for topical antimicrobial delivery. Colloids Surf. B 200, 111618. doi: https://doi.org/10.1016/j.colsurfb.2021.111618.

Liu, Y., Shi, L., Su, L., van der Mei, H.C., Jutte, P.C., Ren, Y., Busscher, H.J., 2019. Nanotechnology-based antimicrobials and delivery systems for biofilm-infection control. Chem. Soc. Rev. 48, 428-446. doi: https://doi.org/10.1039/c7cs00807d.

Liu, Y., Sun, M., Wang, T., Chen, X., Wang, H., 2021a. Chitosan-based self-assembled nanomaterials: Their application in drug delivery. VIEW 2, 20200069. doi: https://doi.org/10.1002/VIW.20200069.

Lombardi, L., Stellato, M.I., Oliva, R., Falanga, A., Galdiero, M., Petraccone, L., D'Errico, G., De Santis, A., Galdiero, S., Del Vecchio, P., 2017. Antimicrobial peptides at work: interaction of myxinidin and its mutant WMR with lipid bilayers mimicking the P. aeruginosa and E. coli membranes. Sci. Rep. 7, 44425. doi: https://doi.org/10.1038/srep44425.

Lou, Z., Wang, H., Zhu, S., Ma, C., Wang, Z., 2011. Antibacterial Activity and Mechanism of Action of Chlorogenic Acid. J. Food Sci. 76, M398-M403. doi: https://doi.org/10.1111/j.1750-3841.2011.02213.x.

Mahmoudi, M., Gould, L.J., 2020. Opportunities and challenges of the management of chronic wounds: A multidisciplinary viewpoint. Chronic Wound Care Manag. Res. 7, 27-36. doi: https://doi.org/10.2147/CWCMR.S260136.

Maja, L., Željko, K., Mateja, P., 2020. Sustainable technologies for liposome preparation. J. Supercrit. Fluids 165, 104984. doi: https://doi.org/10.1016/j.supflu.2020.104984.

Malone, M., Bjarnsholt, T., McBain, A.J., James, G.A., Stoodley, P., Leaper, D., Tachi, M., Schultz, G., Swanson, T., Wolcott, R.D., 2017. The prevalence of biofilms in chronic wounds: a systematic review and meta-analysis of published data. J. Wound Care 26, 20-25. doi: https://doi.org/10.12968/jowc.2017.26.1.20.

Mascarenhas-Melo, F., Gonçalves, M.B.S., Peixoto, D., Pawar, K.D., Bell, V., Chavda, V.P., Zafar, H., Raza, F., Paiva-Santos, A.C., Veiga, F., 2022. Application of nanotechnology in management and treatment of diabetic wound. J. Drug Target. doi: https://doi.org/10.1080/1061186X.2022.2092624.

Matar, D.Y., Ng, B., Darwish, O., Wu, M., Orgill, D.P., Panayi, A.C., 2022. Skin Inflammation with a Focus on Wound Healing. Adv. Wound Care. doi: https://doi.org/10.1089/wound.2021.0126.

Matica, M.A., Aachmann, F.L., Tøndervik, A., Sletta, H., Ostafe, V., 2019. Chitosan as a Wound Dressing Starting Material: Antimicrobial Properties and Mode of Action. Int. J. Mol. Sci. 20, 5889. doi: https://doi.org/10.3390/ijms20235889.

McKnight, G., Shah, J., Hargest, R., 2022. Physiology of the skin. Surgery (Oxford) 40, 8-12. doi: https://doi.org/10.1016/j.mpsur.2021.11.005.

Meers, P., Neville, M., Malinin, V., Scotto, A.W., Sardaryan, G., Kurumunda, R., Mackinson, C., James, G., Fisher, S., Perkins, W.R., 2008. Biofilm penetration, triggered release and in vivo activity of inhaled liposomal amikacin in chronic Pseudomonas aeruginosa lung infections. J. Antimicrob. Chemother. 61, 859-868. doi: https://doi.org/10.1093/jac/dkn059.

Mezei, M., Gulasekharam, V., 1980. Liposomes - a selective drug delivery system for the topical route of administration I. Lotion dosage form. Life Sci. 26, 1473-1477. doi: https://doi.org/10.1016/0024-3205(80)90268-4.

Miao, F., Li, Y., Tai, Z., Zhang, Y., Gao, Y., Hu, M., Zhu, Q., 2021. Antimicrobial Peptides: The Promising Therapeutics for Cutaneous Wound Healing. Macromol. Biosci. 21, 2100103. doi: https://doi.org/10.1002/mabi.202100103.

Moghadam, S.E., Ebrahimi, S.N., Salehi, P., Moridi Farimani, M., Hamburger, M., Jabbarzadeh, E., 2017. Wound Healing Potential of Chlorogenic Acid and Myricetin-3-O-β-Rhamnoside Isolated from Parrotia persica. Molecules 22, 1501. doi: https://doi.org/10.3390/molecules22091501.

Mojsoska, B., Zuckermann Ronald, N., Jenssen, H., 2015. Structure-Activity Relationship Study of Novel Peptoids That Mimic the Structure of Antimicrobial Peptides. Antimicrob. Agents Chemother. 59, 4112-4120. doi: https://doi.org/10.1128/AAC.00237-15.

Montefusco-Pereira, C.V., Formicola, B., Goes, A., Re, F., Marrano, C.A., Mantegazza, F., Carvalho-Wodarz, C., Fuhrmann, G., Caneva, E., Nicotra, F., Lehr, C.M., Russo, L., 2020. Coupling quaternary ammonium surfactants to the surface of liposomes improves both antibacterial efficacy and host cell biocompatibility. Eur. J. Pharm. Biopharm. 149, 12-20. doi: https://doi.org/10.1016/j.ejpb.2020.01.013.

Moore, Z., Dowsett, C., Smith, G., Atkin, L., Bain, M., Lahmann, N.A., Schultz, G.S., Swanson, T., Vowden, P., Weir, D., Zmuda, A., Jaimes, H., 2019. TIME CDST: an updated tool to address the current challenges in wound care. J. Wound Care 28, 154-161. doi: https://doi.org/10.12968/jowc.2019.28.3.154.

Municoy, S., Antezana, P.E., Pérez, C.J., Bellino, M.G., Desimone, M.F., 2021. Tuning the antimicrobial activity of collagen biomaterials through a liposomal approach. J. Appl. Polym. Sci. 138, e50330. doi: https://doi.org/10.1002/app.50330.

Murray, C.J.L., Ikuta, K.S., Sharara, F., Swetschinski, L., Robles Aguilar, G., Gray, A., Han, C., Bisignano, C., Rao, P., Wool, E., et al., 2022. Global burden of bacterial antimicrobial resistance in 2019: a systematic analysis. Lancet 399, 629-655. doi: https://doi.org/10.1016/S0140-6736(21)02724-0.

Murugaiyan, J., Kumar, P.A., Rao, G.S., Iskandar, K., Hawser, S., Hays, J.P., Mohsen, Y., Adukkadukkam, S., Awuah, W.A., Jose, R.A., Sylvia, N., Nansubuga, E.P., Tilocca, B., Roncada, P., Roson-Calero, N., Moreno-Morales, J., Amin, R., Kumar, B.K., Kumar, A., Toufik, A.R., Zaw, T.N., Akinwotu, O.O., Satyaseela, M.P., van Dongen, M.B.M., 2022. Progress in Alternative Strategies to Combat Antimicrobial Resistance: Focus on Antibiotics. Antibiotics 11, 200. doi: https://doi.org/10.3390/antibiotics11020200.

Murugan, R.N., Jacob, B., Ahn, M., Hwang, E., Sohn, H., Park, H.N., Lee, E., Seo, J.H., Cheong, C., Nam, K.Y., Hyun, J.K., Jeong, K.W., Kim, Y., Shin, S.Y., Bang, J.K., 2013. De Novo Design and Synthesis of Ultra-Short Peptidomimetic Antibiotics Having Dual Antimicrobial and Anti-Inflammatory Activities. PLoS One 8, e80025. doi: https://doi.org/10.1371/journal.pone.0080025.

Nafee, N., Schneider, M., Schaefer, U.F., Lehr, C.M., 2009. Relevance of the colloidal stability of chitosan/PLGA nanoparticles on their cytotoxicity profile. Int. J. Pharm. 381, 130-139. doi: https://doi.org/10.1016/j.ijpharm.2009.04.049.

Naveed, M., Hejazi, V., Abbas, M., Kamboh, A.A., Khan, G.J., Shumzaid, M., Ahmad, F., Babazadeh, D., FangFang, X., Modarresi-Ghazani, F., WenHua, L., XiaoHui, Z., 2018. Chlorogenic acid (CGA): A pharmacological review and call for further research. Biomed. Pharmacother. 97, 67-74. doi: https://doi.org/10.1016/j.biopha.2017.10.064.

Neff, J.A., Bayramov, D.F., Patel, E.A., Miao, J., 2020. Novel Antimicrobial Peptides Formulated in Chitosan Matrices are Effective Against Biofilms of Multidrug-Resistant Wound Pathogens. Mil. Med. 185, 637-643. doi: https://doi.org/10.1093/milmed/usz222.

Nguyen, A.V., Soulika, A.M., 2019. The Dynamics of the Skin's Immune System. Int. J. Mol. Sci. 20, 1811. doi: https://doi.org/10.3390/ijms20081811.

Nguyen, M.H., Vu, N.B.D., Nguyen, T.H.N., Le, H.S., Le, H.T., Tran, T.T., Le, X.C., Le, V.T., Nguyen, T.T., Bui, C.B., Park, H.J., 2019. In vivo comparison of wound healing and scar treatment effect between curcumin–oligochitosan nanoparticle complex and oligochitosan-coated curcumin-loaded-liposome. J. Microencapsul. 36, 156-168. doi: https://doi.org/10.1080/02652048.2019.1612476.

NICE guideline, 2015. Diabetic foot problems: prevention and management - NG19. Public Health England.

NICE guideline, 2020. Leg ulcer infection: antimicrobial prescribing - NG152. Public Health England.

Nizalapur, S., Kimyon, O., Yee, E., Ho, K., Berry, T., Manefield, M., Cranfield, C.G., Willcox, M., Black, D.S., Kumar, N., 2017. Amphipathic guanidine-embedded glyoxamide-based peptidomimetics as novel antibacterial agents and biofilm disruptors. Org. Biomol. Chem. 15, 2033-2051. doi: https://doi.org/10.1039/C7OB00053G.

Nwabuife, J.C., Pant, A.M., Govender, T., 2021. Liposomal delivery systems and their applications against Staphylococcus aureus and Methicillin-resistant Staphylococcus aureus. Adv. Drug Deliv. Rev. 178, 113861. doi: https://doi.org/10.1016/j.addr.2021.113861.

Omardien, S., Drijfhout, J.W., Vaz, F.M., Wenzel, M., Hamoen, L.W., Zaat, S.A.J., Brul, S., 2018. Bactericidal activity of amphipathic cationic antimicrobial peptides involves altering the membrane fluidity when interacting with the phospholipid bilayer. Biochim. Biophys. Acta Biomembr. 1860, 2404-2415. doi: https://doi.org/10.1016/j.bbamem.2018.06.004.

Ong, T.H., Chitra, E., Ramamurthy, S., Siddalingam, R.P., Yuen, K.H., Ambu, S.P., Davamani, F., 2017. Chitosan-propolis nanoparticle formulation demonstrates anti-bacterial activity against Enterococcus faecalis biofilms. PLoS One 12, e0174888. doi: https://doi.org/10.1371/journal.pone.0174888.

Orioni, B., Bocchinfuso, G., Kim, J.Y., Palleschi, A., Grande, G., Bobone, S., Park, Y., Kim, J.I., Hahm, K.S., Stella, L., 2009. Membrane perturbation by the antimicrobial peptide PMAP-23: A fluorescence and molecular dynamics study. Biochim. Biophys. Acta Biomembr. 1788, 1523-1533. doi: https://doi.org/10.1016/j.bbamem.2009.04.013.

Ortega-Llamas, L., Quiñones-Vico, M.I., García-Valdivia, M., Fernández-González, A., Ubago-Rodríguez, A., Sanabria-de la Torre, R., Arias-Santiago, S., 2022. Cytotoxicity and Wound Closure Evaluation in Skin Cell Lines after Treatment with Common Antiseptics for Clinical Use. Cells 11, 1395. doi: https://doi.org/10.3390/cells11091395.

Parhi, R., 2020. Drug delivery applications of chitin and chitosan: a review. Environ. Chem. Lett. 18, 577-594. doi: https://doi.org/10.1007/s10311-020-00963-5.

Park, H.-J., Salem, M., Semlali, A., Leung, K.P., Rouabhia, M., 2017. Antimicrobial peptide KSL-W promotes gingival fibroblast healing properties in vitro. Peptides 93, 33-43. doi: https://doi.org/10.1016/j.peptides.2017.05.003.

Paulsen, M.H., Engqvist, M., Ausbacher, D., Anderssen, T., Langer, M.K., Haug, T., Morello, G.R., Liikanen, L.E., Blencke, H.M., Isaksson, J., Juskewitz, E., Bayer, A., Strøm, M.B., 2021. Amphipathic Barbiturates as Mimics of Antimicrobial Peptides and the Marine Natural Products Eusynstyelamides with Activity against Multi-resistant Clinical Isolates. J. Med. Chem. 64, 11395-11417. doi: https://doi.org/10.1021/acs.jmedchem.1c00734.

Peers, S., Alcouffe, P., Montembault, A., Ladavière, C., 2020. Embedment of liposomes into chitosan physical hydrogel for the delayed release of antibiotics or anaesthetics, and its first ESEM characterization. Carbohydr. Polym. 229, 115532. doi: https://doi.org/10.1016/j.carbpol.2019.115532.

Pellá, M.C.G., Lima-Tenório, M.K., Tenório-Neto, E.T., Guilherme, M.R., Muniz, E.C., Rubira, A.F., 2018. Chitosan-based hydrogels: From preparation to biomedical applications. Carbohydr. Polym. 196, 233-245. doi: https://doi.org/10.1016/j.carbpol.2018.05.033.

Petkovic, M., Mouritzen, M.V., Mojsoska, B., Jenssen, H., 2021. Immunomodulatory Properties of Host Defence Peptides in Skin Wound Healing. Biomolecules 11, 952. doi: https://doi.org/10.3390/biom11070952.

Piipponen, M., Li, D., Landén, N.X., 2020. The Immune Functions of Keratinocytes in Skin Wound Healing. Int. J. Mol. Sci. 21, 8790. doi: https://doi.org/10.3390/ijms21228790.

Pinheiro, M., Magalhães, J., Reis, S., 2019. Antibiotic interactions using liposomes as model lipid membranes. Chem. Phys. Lipids 222, 36-46. doi: https://doi.org/10.1016/j.chemphyslip.2019.05.002.

Pourshahrestani, S., Zeimaran, E., Kadri, N.A., Mutlu, N., Boccaccini, A.R., 2020. Polymeric Hydrogel Systems as Emerging Biomaterial Platforms to Enable Hemostasis and Wound Healing. Adv. Healthc. Mater. 9, 2000905. doi: https://doi.org/10.1002/adhm.202000905.

Rahim, K., Saleha, S., Zhu, X., Huo, L., Basit, A., Franco, O.L., 2017. Bacterial Contribution in Chronicity of Wounds. Microb. Ecol. 73, 710-721. doi: https://doi.org/10.1007/s00248-016-0867-9.

Rata, D.M., Cadinoiu, A.N., Popa, M., Atanase, L.I., Daraba, O.M., Popescu, I., Romila, L.E., Ichim, D.L., 2021. Biocomposite Hydrogels for the Treatment of Bacterial Infections: Physicochemical Characterization and In Vitro Assessment. Pharmaceutics 13, 2079. doi: https://doi.org/10.3390/pharmaceutics13122079.

Reygaert, W.C., 2018. An overview of the antimicrobial resistance mechanisms of bacteria. AIMS Microbiol. 4, 482-501. doi: https://doi.org/10.3934/microbiol.2018.3.482.

Riaz Rajoka, M.S., Zhao, L., Mehwish, H.M., Wu, Y., Mahmood, S., 2019. Chitosan and its derivatives: synthesis, biotechnological applications, and future challenges. Appl. Microbiol. Biotechnol. 103, 1557-1571. doi: https://doi.org/10.1007/s00253-018-9550-z.

Ribeiro, J.C.V., Forte, T.C.M., Tavares, S.J.S., Andrade, F.K., Vieira, R.S., Lima, V., 2021. The effects of the molecular weight of chitosan on the tissue inflammatory response. J. Biomed. Mater. Res. A 109, 2556-2569. doi: https://doi.org/10.1002/jbm.a.37250.

Ribeiro, M.P., Espiga, A., Silva, D., Baptista, P., Henriques, J., Ferreira, C., Silva, J.C., Borges, J.P., Pires, E., Chaves, P., Correia, I.J., 2009. Development of a new chitosan hydrogel for wound dressing. Wound Repair Regen. 17, 817-824. doi: https://doi.org/10.1111/j.1524-475X.2009.00538.x.

Rodrigues, M., Kosaric, N., Bonham, C.A., Gurtner, G.C., 2018. Wound Healing: A Cellular Perspective. Physiol. Rev. 99, 665-706. doi: https://doi.org/10.1152/physrev.00067.2017.

Rodríguez-Acosta, H., Tapia- Rivera, J.M., Guerrero-Guzmán, A., Hernández-Elizarraráz, E., Hernández- Díaz, J.A., Garza- García, J.J.O., Pérez- Ramírez, P.E., Velasco- Ramírez, S.F., Ramírez- Anguiano, A.C., Velázquez- Juárez, G., et al., 2022. Chronic wound healing by controlled release of chitosan hydrogels loaded with silver nanoparticles and calendula extract. J. Tissue Viability 31, 173-179. doi: https://doi.org/10.1016/j.jtv.2021.10.004.

Romanova, O.A., Grigor'ev, T.E., Goncharov, M.E., Rudyak, S.G., Solov'yova, E.V., Krasheninnikov, S.T., Saprykin, V.P., Sytina, E.V., Chvalun, S.N., Pal'tsev, M.A., Panteleev, A.A., 2015. Chitosan as a Modifying Component of Artificial Scaffold for Human Skin Tissue Engineering. Bull. Exp. Biol. Med. 159, 557-566. doi: https://doi.org/10.1007/s10517-015-3014-6.

Ron-Doitch, S., Sawodny, B., Kuhbacher, A., David, M.M.N., Samanta, A., Phopase, J., Burger-Kentischer, A., Griffith, M., Golomb, G., Rupp, S., 2016. Reduced cytotoxicity and enhanced bioactivity of cationic antimicrobial peptides liposomes in cell cultures and 3D epidermis model against HSV. J. Control. Release 229, 163-171. doi: https://doi.org/10.1016/j.jconrel.2016.03.025.

Roope, L.S.J., 2022. The economic challenges of new drug development. J. Control. Release 345, 275–277. doi: https://doi.org/10.1016/j.jconrel.2022.03.023.

Rossi, S., Marciello, M., Sandri, G., Ferrari, F., Bonferoni, M.C., Papetti, A., Caramella, C., Dacarro, C., Grisoli, P., 2007. Wound Dressings Based on Chitosans and Hyaluronic Acid for the Release of Chlorhexidine Diacetate in Skin Ulcer Therapy. Pharm. Dev. Technol. 12, 415-422. doi: https://doi.org/10.1080/10837450701366903.

Rousselle, P., Braye, F., Dayan, G., 2019. Re-epithelialization of adult skin wounds: Cellular mechanisms and therapeutic strategies. Adv. Drug Deliv. Rev. 146, 344-365. doi: https://doi.org/10.1016/j.addr.2018.06.019.

Rozenbaum, R.T., Su, L., Umerska, A., Eveillard, M., Håkansson, J., Mahlapuu, M., Huang, F., Liu, J., Zhang, Z., Shi, L., van der Mei, H.C., Busscher, H.J., Sharma, P.K., 2019. Antimicrobial synergy of monolaurin lipid nanocapsules with adsorbed antimicrobial peptides against Staphylococcus aureus biofilms in vitro is absent in vivo. J. Control. Release 293, 73-83. doi: https://doi.org/10.1016/j.jconrel.2018.11.018.

Rubey, K.M., Brenner, J.S., 2021. Nanomedicine to fight infectious disease. Adv. Drug Deliv. Rev. 179, 113996. doi: https://doi.org/10.1016/j.addr.2021.113996.

Rukavina, Z., Šegvić Klarić, M., Filipović-Grčić, J., Lovrić, J., Vanić, Ž., 2018. Azithromycin-loaded liposomes for enhanced topical treatment of methicillin-resistant Staphyloccocus aureus (MRSA) infections. Int. J. Pharm. 553, 109-119. doi: https://doi.org/10.1016/j.ijpharm.2018.10.024.

Rukavina, Z., Vanić, Ž., 2016. Current Trends in Development of Liposomes for Targeting Bacterial Biofilms. Pharmaceutics 8, 18. doi: https://doi.org/10.3390/pharmaceutics8020018.

Rumbaugh, K.P., Sauer, K., 2020. Biofilm dispersion. Nat. Rev. Microbiol. 18, 571-586. doi: https://doi.org/10.1038/s41579-020-0385-0.

Rzycki, M., Drabik, D., Szostak-Paluch, K., Hanus-Lorenz, B., Kraszewski, S., 2021. Unraveling the mechanism of octenidine and chlorhexidine on membranes: Does electrostatics matter? Biophys. J. 120, 3392-3408. doi: https://doi.org/10.1016/j.bpj.2021.06.027.

Römling, U., Balsalobre, C., 2012. Biofilm infections, their resilience to therapy and innovative treatment strategies. J. Intern. Med. 272, 541-561. doi: https://doi.org/10.1111/joim.12004.

Raafat, D., Otto, M., Reppschläger, K., Iqbal, J., Holtfreter, S., 2019. Fighting Staphylococcus aureus Biofilms with Monoclonal Antibodies. Trends Microbiol. 27, 303-322. doi: https://doi.org/10.1016/j.tim.2018.12.009.

Sandri, G., Rossi, S., Bonferoni, M.C., Miele, D., Faccendini, A., Del Favero, E., Di Cola, E., Icaro Cornaglia, A., Boselli, C., Luxbacher, T., Malavasi, L., Cantu', L., Ferrari, F., 2019. Chitosan/glycosaminoglycan scaffolds for skin reparation. Carbohydr. Polym. 220, 219-227. doi: https://doi.org/10.1016/j.carbpol.2019.05.069.

Schneider, C.A., Rasband, W.S., Eliceiri, K.W., 2012. NIH Image to ImageJ: 25 years of image analysis. Nat. Methods 9, 671-675. doi: https://doi.org/10.1038/nmeth.2089.

Schröter, D., Neugart, S., Schreiner, M., Grune, T., Rohn, S., Ott, C., 2019. Amaranth's 2-Caffeoylisocitric Acid—An Anti-Inflammatory Caffeic Acid Derivative That Impairs NF-κB Signaling in LPS-Challenged RAW 264.7 Macrophages. Nutrients 11, 571. doi: https://doi.org/10.3390/nu11030571.

Sen, C.K., 2021. Human Wound and Its Burden: Updated 2020 Compendium of Estimates. Adv. Wound Care 10, 281-292. doi: https://doi.org/10.1089/wound.2021.0026.

Serra, R., Grande, R., Butrico, L., Rossi, A., Settimio, U.F., Caroleo, B., Amato, B., Gallelli, L., de Franciscis, S., 2015. Chronic wound infections: The role of Pseudomonas aeruginosa and Staphylococcus aureus. Expert Rev. Anti Infect. Ther. 13, 605-613. doi: https://doi.org/10.1586/14787210.2015.1023291.

Sgolastra, F., deRonde, B.M., Sarapas, J.M., Som, A., Tew, G.N., 2013. Designing Mimics of Membrane Active Proteins. Acc. Chem. Res. 46, 2977-2987. doi: https://doi.org/10.1021/ar400066v.

Shahzadi, L., Bashir, M., Tehseen, S., Zehra, M., Mehmood, A., Chaudhry, A.A., Rehman, I.U., Yar, M., 2020. Thyroxine impregnated chitosan-based dressings stimulate angiogenesis and support fast wounds healing in rats: Potential clinical candidates. Int. J. Biol. Macromol. 160, 296-306. doi: https://doi.org/10.1016/j.ijbiomac.2020.05.127.

Shariatinia, Z., 2019. Pharmaceutical applications of chitosan. Adv. Colloid Interface Sci. 263, 131-194. doi: https://doi.org/10.1016/j.cis.2018.11.008.

Sharifi, S., Hajipour, M.J., Gould, L., Mahmoudi, M., 2021. Nanomedicine in Healing Chronic Wounds: Opportunities and Challenges. Mol. Pharm. 18, 550-575. doi: https://doi.org/10.1021/acs.molpharmaceut.0c00346.

Shen, T., Dai, K., Yu, Y., Wang, J., Liu, C., 2020. Sulfated chitosan rescues dysfunctional macrophages and accelerates wound healing in diabetic mice. Acta Biomater. 117, 192-203. doi: https://doi.org/10.1016/j.actbio.2020.09.035.

Shukla, S.K., Chan, A., Parvathaneni, V., Gupta, V., 2020. Metformin-loaded chitosomes for treatment of malignant pleural mesothelioma – A rare thoracic cancer. Int. J. Biol. Macromol. 160, 128-141. doi: https://doi.org/10.1016/j.ijbiomac.2020.05.146.

Sinsinwar, S., Vadivel, V., 2021. Development and characterization of catechin-in-cyclodextrin-in-phospholipid liposome to eradicate MRSA-mediated surgical site infection: Investigation of their anti-infective efficacy through in vitro and in vivo studies. Int. J. Pharm. 609, 121130. doi: https://doi.org/10.1016/j.ijpharm.2021.121130.

Song, J., Remmers, S.J., Shao, J., Kolwijck, E., Walboomers, X.F., Jansen, J.A., Leeuwenburgh, S.C., Yang, F., 2016. Antibacterial effects of electrospun chitosan/poly(ethylene oxide) nanofibrous membranes loaded with chlorhexidine and silver. Nanomedicine 12, 1357-1364. doi: https://doi.org/10.1016/j.nano.2016.02.005.

Song, L., Yang, H., Liang, D., Chu, D., Yang, L., Li, M., Yang, B., Shi, Y., Chen, Z., Yu, Z., Guo, J., 2022. A chlorogenic acid-loaded hyaluronic acid-based hydrogel facilitates anti-inflammatory and pro-healing effects for diabetic wounds. J. Drug Deliv. Sci. Technol. 70, 103232. doi: https://doi.org/10.1016/j.jddst.2022.103232.

Song, X., Liu, P., Liu, X., Wang, Y., Wei, H., Zhang, J., Yu, L., Yan, X., He, Z., 2021. Dealing with MDR bacteria and biofilm in the post-antibiotic era: Application of antimicrobial peptides-based nano-formulation. Mater. Sci. Eng. C 128, 112318. doi: https://doi.org/10.1016/j.msec.2021.112318.

Sreekumari, A., Lipowsky, R., 2022. Large stress asymmetries of lipid bilayers and nanovesicles generate lipid flip-flops and bilayer instabilities. Soft Matter. doi: https://doi.org/10.1039/D2SM00618A.

Stoica, A.E., Chircov, C., Grumezescu, A.M., 2020. Hydrogel Dressings for the Treatment of Burn Wounds: An Up-To-Date Overview. Materials 13, 2853. doi: https://doi.org/10.3390/ma13122853.

Strøm, M.B., Bayer, A., Engqvist, S.O.M., Paulsen, M.H., Ausbacher, D., 2018. Barbituric acid derivatives comprising cationic and lipophilic groups, Patent Number: WO/2018/178198. UiT The Arctic University of Norway.

Su, Y., Mainardi, V.L., Wang, H., McCarthy, A., Zhang, Y.S., Chen, S., John, J.V., Wong, S.L., Hollins, R.R., Wang, G., Xie, J., 2020. Dissolvable Microneedles Coupled with Nanofiber Dressings Eradicate Biofilms via Effectively Delivering a Database-Designed Antimicrobial Peptide. ACS Nano 14, 11775-11786. doi: https://doi.org/10.1021/acsnano.0c04527.

Suarez-Arnedo, A., Torres Figueroa, F., Clavijo, C., Arbeláez, P., Cruz, J.C., Muñoz-Camargo, C., 2020. An image J plugin for the high throughput image analysis of in vitro scratch wound healing assays. PLoS One 15, e0232565. doi: https://doi.org/10.1371/journal.pone.0232565.

Sun, Y., Dong, W., Sun, L., Ma, L., Shang, D., 2015. Insights into the membrane interaction mechanism and antibacterial properties of chensinin-1b. Biomaterials 37, 299-311. doi: https://doi.org/10.1016/j.biomaterials.2014.10.041.

Svenson, J., Brandsdal, B.O., Stensen, W., Svendsen, J.S., 2007. Albumin Binding of Short Cationic Antimicrobial Micropeptides and Its Influence on the in Vitro Bactericidal Effect. J. Med. Chem. 50, 3334-3339. doi: https://doi.org/10.1021/jm0703542.

Tague, A.J., Putsathit, P., Hammer, K.A., Wales, S.M., Knight, D.R., Riley, T.V., Keller, P.A., Pyne, S.G., 2019. Cationic biaryl 1,2,3-triazolyl peptidomimetic amphiphiles: synthesis, antibacterial evaluation and preliminary mechanism of action studies. Eur. J. Med. Chem. 168, 386-404. doi: https://doi.org/10.1016/j.ejmech.2019.02.013.

Teot, L., Ohura, N., 2021. Challenges and Management in Wound Care. Plast. Reconstr. Surg. 147, 9S-15S. doi: https://doi.org/10.1097/PRS.0000000000007628.

Thapa, R.K., Diep, D.B., Tønnesen, H.H., 2020. Topical antimicrobial peptide formulations for wound healing: Current developments and future prospects. Acta Biomater. 103, 52-67. doi: https://doi.org/10.1016/j.actbio.2019.12.025.

Theuretzbacher, U., Van Bambeke, F., Cantón, R., Giske, C.G., Mouton, J.W., Nation, R.L., Paul, M., Turnidge, J.D., Kahlmeter, G., 2015. Reviving old antibiotics. J. Antimicrob. Chemother. 70, 2177-2181. doi: https://doi.org/10.1093/jac/dkv157.

Ternullo, S., Basnet, P., Holsæter, A.M., Flaten, G.E., de Weerd, L., Škalko-Basnet, N., 2018. Deformable liposomes for skin therapy with human epidermal growth factor: The effect of liposomal surface charge. Eur. J. Pharm. Sci. 125, 163-171. doi: https://doi.org/10.1016/j.ejps.2018.10.005.

Ternullo, S., Gagnat, E., Julin, K., Johannessen, M., Basnet, P., Vanić, Ž., Škalko-Basnet, N., 2019. Liposomes augment biological benefits of curcumin for multitargeted skin therapy. Eur. J. Pharm. Biopharm. 144, 154-164. doi: https://doi.org/10.1016/j.ejpb.2019.09.016.

Tottoli, E.M., Dorati, R., Genta, I., Chiesa, E., Pisani, S., Conti, B., 2020. Skin Wound Healing Process and New Emerging Technologies for Skin Wound Care and Regeneration. Pharmaceutics 12, 735. doi: https://doi.org/10.3390/pharmaceutics12080735.

Vanzolini, T., Bruschi, M., Rinaldi, A.C., Magnani, M., Fraternale, A., 2022. Multitalented Synthetic Antimicrobial Peptides and Their Antibacterial, Antifungal and Antiviral Mechanisms. Int. J. Mol. Sci. 23, 545. doi: https://doi.org/10.3390/ijms23010545.

Velnar, T., Bailey, T., Smrkolj, V., 2009. The Wound Healing Process: An Overview of the Cellular and Molecular Mechanisms. J. Int. Med. Res. 37, 1528-1542. doi: https://doi.org/10.1177/147323000903700531.

Verma, K.D., Lewis, F., Mejia, M., Chalasani, M., Marcus, K.A., 2022. Food and Drug Administration perspective: Advancing product development for non-healing chronic wounds. Wound Repair Regen. 30, 299-302. doi: https://doi.org/10.1111/wrr.13008.

Vipin, C., Mujeeburahiman, M., Ashwini, P., Arun, A.B., Rekha, P.D., 2019. Anti-biofilm and cytoprotective activities of quercetin against Pseudomonas aeruginosa isolates. Lett. Appl. Microbiol. 68, 464-471. doi: https://doi.org/10.1111/lam.13129.

Wang, D.Y., van der Mei, H.C., Ren, Y., Busscher, H.J., Shi, L., 2020. Lipid-Based Antimicrobial Delivery-Systems for the Treatment of Bacterial Infections. Front. Chem. 7, 872. doi: https://doi.org/10.3389/fchem.2019.00872.

Wang, L., Zhou, M., Xu, T., Zhang, X., 2022. Multifunctional hydrogel as wound dressing for intelligent wound monitoring. Chem. Eng. J. 433, 134625. doi: https://doi.org/10.1016/j.cej.2022.134625.

Wang, M., Feng, X., Gao, R., Sang, P., Pan, X., Wei, L., Lu, C., Wu, C., Cai, J., 2021a. Modular Design of Membrane-Active Antibiotics: From Macromolecular Antimicrobials to Small Scorpionlike Peptidomimetics. J. Med. Chem. 64, 9894-9905. doi: https://doi.org/10.1021/acs.jmedchem.1c00312.

Wang, W., Lu, K. j., Yu, C. h., Huang, Q. l., Du, Y. Z., 2019. Nano-drug delivery systems in wound treatment and skin regeneration. J. Nanobiotechnology 17, 82. doi: https://doi.org/10.1186/s12951-019-0514-y.

Wang, X., Cheng, F., Wang, X., Feng, T., Xia, S., Zhang, X., 2021b. Chitosan decoration improves the rapid and long-term antibacterial activities of cinnamaldehyde-loaded liposomes. Int. J. Biol. Macromol. 168, 59-66. doi: https://doi.org/10.1016/j.ijbiomac.2020.12.003.

Wianowska, D., Gil, M., 2019. Recent advances in extraction and analysis procedures of natural chlorogenic acids. Phytochem. Rev. 18, 273-302. doi: https://doi.org/10.1007/s11101-018-9592-y.

Wiegand, C., Winter, D., Hipler, U.C., 2010. Molecular-Weight-Dependent Toxic Effects of Chitosans on the Human Keratinocyte Cell Line HaCaT. Skin Pharmacol. Physiol. 23, 164-170. doi: https://doi.org/10.1159/000276996.

Wilkinson, H.N., Hardman, M.J., 2020. Wound healing: cellular mechanisms and pathological outcomes. Open Biol. 10, 200223. doi: https://doi.org/10.1098/rsob.200223.

Williamson, D.A., Carter, G.P., Howden, B.P., 2017. Current and Emerging Topical Antibacterials and Antiseptics: Agents, Action, and Resistance Patterns. Clin. Microbiol. Rev. 30, 827-860. doi: https://doi.org/10.1128/CMR.00112-16.

Wu, Y.K., Cheng, N.C., Cheng, C.M., 2019. Biofilms in Chronic Wounds: Pathogenesis and Diagnosis. Trends Biotechnol. 37, 505-517. doi: https://doi.org/10.1016/j.tibtech.2018.10.011.

Xia, Y., Wang, D., Liu, D., Su, J., Jin, Y., Wang, D., Han, B., Jiang, Z., Liu, B., 2022. Applications of Chitosan and its Derivatives in Skin and Soft Tissue Diseases. Front. Bioeng. Biotechnol. 10, 894667. doi: https://doi.org/10.3389/fbioe.2022.894667.

Xiong, Y.Q., Mukhopadhyay, K., Yeaman, M.R., Adler-Moore, J., Bayer, A.S., 2005. Functional Interrelationships between Cell Membrane and Cell Wall in Antimicrobial Peptide-Mediated Killing of Staphylococcus aureus. Antimicrob. Agents Chemother. 49, 3114-3121. doi: https://doi.org/10.1128/AAC.49.8.3114-3121.2005.

Xu, J.G., Hu, Q.P., Liu, Y., 2012. Antioxidant and DNA-Protective Activities of Chlorogenic Acid Isomers. J. Agric. Food Chem. 60, 11625-11630. doi: https://doi.org/10.1021/jf303771s.

Yamamoto, N., Tamura, A., 2010. Designed low amphipathic peptides with α-helical propensity exhibiting antimicrobial activity via a lipid domain formation mechanism. Peptides 31, 794-805. doi: https://doi.org/10.1016/j.peptides.2010.01.006.

Yamasaki, K., Gallo, R.L., 2008. Antimicrobial peptides in human skin disease. Eur. J. Dermatol. 18, 11-21. doi: https://doi.org/10.1684/ejd.2008.0304.

Yang, X., Guo, J.L., Han, J., Si, R.J., Liu, P.P., Zhang, Z.R., Wang, A.M., Zhang, J., 2020. Chitosan hydrogel encapsulated with LL-37 peptide promotes deep tissue injury healing in a mouse model. Mil. Med. Res. 7, 20. doi: https://doi.org/10.1186/s40779-020-00249-5.

Yoon, H.J., Moon, M.E., Park, H.S., Im, S.Y., Kim, Y.H., 2007. Chitosan oligosaccharide (COS) inhibits LPS-induced inflammatory effects in RAW 264.7 macrophage cells. Biochem. Biophys. Res. Commun. 358, 954-959. doi: https://doi.org/10.1016/j.bbrc.2007.05.042.

Zhang, N., Ma, S., 2019. Recent development of membrane-active molecules as antibacterial agents. Eur. J. Med. Chem. 184, 111743. doi: https://doi.org/10.1016/j.ejmech.2019.111743.

Zheng, X., Zhang, X., Zhou, B., Liu, S., Chen, W., Chen, L., Zhang, Y., Liao, W., Zeng, W., Wu, Q., Xu, C., Zhou, T., 2022. Clinical characteristics, tolerance mechanisms, and molecular epidemiology of reduced susceptibility to chlorhexidine among Pseudomonas aeruginosa isolated from a teaching hospital in China. Int. J. Antimicrob. Agents 60, 106605. doi: https://doi.org/10.1016/j.ijantimicag.2022.106605.

Zhou, M., Zheng, M., Cai, J., 2020. Small Molecules with Membrane-Active Antibacterial Activity. ACS Appl. Mater. Interfaces 12, 21292-21299. doi: https://doi.org/10.1021/acsami.9b20161.

Zhu, C., Zhao, Y., Zhao, X., Liu, S., Xia, X., Zhang, S., Wang, Y., Zhang, H., Xu, Y., Chen, S., Jiang, J., Wu, Y., Wu, X., Zhang, G., Bai, Y., Hu, J., Fotina, H., Wang, L., Zhang, X., 2022. The Antimicrobial Peptide MPX Can Kill Staphylococcus aureus, Reduce Biofilm Formation, and Effectively Treat Bacterial Skin Infections in Mice. Front. Vet. Sci. 9, 819921. doi: https://doi.org/10.3389/fvets.2022.819921.

Öhnstedt, E., Lofton Tomenius, H., Vågesjö, E., Phillipson, M., 2019. The discovery and development of topical medicines for wound healing. Expert Opin. Drug Discov. 14, 485-497. doi: https://doi.org/10.1080/17460441.2019.1588879.

Paper I

Carbohydrate Polymers 262 (2021) 117939

Contents lists available at ScienceDirect

Carbohydrate Polymers

journal homepage: www.elsevier.com/locate/carbpol

Liposomes-in-chitosan hydrogel boosts potential of chlorhexidine in biofilm eradication *in vitro*

Lisa Myrseth Hemmingsen [a], Barbara Giordani [b], Ann Kristin Pettersen [a], Beatrice Vitali [b], Purusotam Basnet [c,d], Nataša Škalko-Basnet [a,*]

[a] Drug Transport and Delivery Research Group, Department of Pharmacy, University of Tromsø, The Arctic University of Norway, Universitetsvegen 57, 9037, Tromsø, Norway
[b] Molecular and Applied Microbiology, Department of Pharmacy and Biotechnology, University of Bologna, Via San Donato 19/2, 40127, Bologna, Italy
[c] IVF Clinic, Department of Obstetrics and Gynecology, University Hospital of North Norway, Sykehusvegen 38, 9019, Tromsø, Norway
[d] Women's Health and Perinatology Research Group, Department of Clinical Medicine, University of Tromsø, The Arctic University of Norway, Universitetsveien 57, 9037, Tromsø, Norway

ARTICLE INFO

Keywords:
Chitosan
Bacterial eradication
Lipid-based vesicle
Skin therapy
Membrane active antimicrobials

ABSTRACT

Successful treatment of skin infections requires eradication of biofilms found in up to 90 % of all chronic wounds, causing delayed healing and increased morbidity. We hypothesized that chitosan hydrogel boosts the activity of liposomally-associated membrane active antimicrobials (MAA) and could potentially improve bacterial and biofilm eradication. Therefore, liposomes (~300 nm) bearing chlorhexidine (CHX; ~50 μg/mg lipid) as a model MAA were incorporated into chitosan hydrogel. The novel CHX-liposomes-in-hydrogel formulation was optimized for skin therapy. It significantly inhibited the production of nitric oxide (NO) in lipopolysaccharide (LPS)-induced macrophage and almost completely reduced biofilm formation. Moreover, it reduced *Staphylococcus aureus* and *Pseudomonas aeruginosa* adherent bacterial cells in biofilm by 64.2–98.1 %. Chitosan hydrogel boosted the anti-inflammatory and antimicrobial properties of CHX.

1. Introduction

Antimicrobial resistance is currently a serious medical threat, especially because of the decelerated and unsuccessful pipeline of antimicrobial candidates (Hall et al., 2020). Although bacterial resistance often derives from genetic mutations, the biofilm formation and increased inflammatory cascades are also known to be strong contributors (Balaure & Grumezescu, 2020; Cepas et al., 2018; Romana-Souza, Santos, Bandeira, & Monte-Alto-Costa, 2016). Biofilms are found in between 60 and 90 % of all chronic wounds, delaying healing and leading to increased morbidity and costs (Kadam, Shai, Shahane, & Kaushik, 2019; Matos de Opitz & Sass, 2020). Novel approaches for biofilm eradication and efficient wound therapy are urgently needed as skin and soft tissue infections are among the most common infections in humans (Poulakou, Lagou, & Tsiodras, 2019). These infections exhibit a polymicrobial nature and cleaver, novel strategies to eradicate multiple bacteria are necessary for their treatment.

Among the most common bacteria embedded in wound matrices are *Staphylococcus aureus* and *Pseudomonas aeruginosa* (Balaure & Grumezescu, 2020; Kadam et al., 2019). These bacteria display multiple mechanisms of resistance, rendering their eradication particularly challenging. Treating wound biofilms requires innovative approaches. Novel drug delivery systems comprising cationic polymers (Guo et al., 2018) offer potential solutions. Chitosan has attracted a lot of interest due to its broad range of beneficial effects and biodegradability (Ambrogi et al., 2017; Islam, Shahruzzaman, Biswas, Nurus Sakib, & Rashid, 2020). The intrinsic antimicrobial and anti-inflammatory properties are highly relevant for wound therapy (Islam et al., 2020). Several antimicrobial mechanisms are proposed for chitosan; its interaction with negatively charged bacterial membranes leading to possible

Abbreviations: BHI, Brain Heart Infusion Broth; CHX, chlorhexidine; DMEM, Dulbecco's Modified Eagle Medium; EE, entrapment efficiency; FBS, fetal bovine serum; LPS, lipopolysaccharide; MAA, membrane active antimicrobials; MLC, minimal lethal concentration; MW, molecular weight; NB, Nutrient Broth; NO, nitric oxide; PBS, Phosphate Buffer Saline; PI, polydispersity index; RPMI, Roswell Park Memorial Institute; SWF, Simulated Wound Fluid; TEM, transmission electron microscopy.

* Corresponding author.
E-mail address: natasa.skalko-basnet@uit.no (N. Škalko-Basnet).

https://doi.org/10.1016/j.carbpol.2021.117939
Received 9 October 2020; Received in revised form 16 February 2021; Accepted 11 March 2021
Available online 16 March 2021

lysis being the main mechanism (Matica, Aachmann, Tøndervik, Sletta, & Ostafe, 2019). Other mechanisms include interruption of microbial protein synthesis, chelation of metal ions and formation of an envelope on the microbial surface (Matica et al., 2019). In addition, chitosan can influence the haemostasis, inflammatory stage and proliferation as well as accelerate wound healing (Liu et al., 2018; Moeini, Pedram, Makvandi, Malinconico, & Gomez d'Ayala, 2020). Chitosan hydrogel's three-dimensional network contributes to high water-retaining properties and gas-exchange capacity (Tavakoli & Klar, 2020). However, hydrogels often exhibit rapid drug release from the gel matrix (Peers, Alcouffe, Montembault, & Ladavière, 2020).

Combining hydrogel with a lipid-based carrier, such as liposomes, could prevent this rapid drug release (Grijalvo, Eritja, & Díaz, 2020; Peers et al., 2020). Studies report considerably slower release from liposomes-in-hydrogels compared to plain hydrogels (Jøraholmen, Basnet, Tostrup, Moueffaq, & Škalko-Basnet, 2019). The release will be also influenced by the type of entrapped drug. Antiseptics, such as chlorhexidine (CHX), are commonly used in local treatment of wound infection and reasonable candidates for new topical formulations (Smith, Russo, Fiegel, & Brogden, 2020). CHX acts as a membrane active antimicrobial (MAA) on both the dormant and active bacteria (Hubbard, Coates, & Harvey, 2017). The resistance is generally lower than for more target-specific compound due to the rapid and broad bactericidal effect of MAAs (Hubbard et al., 2017). Their mechanism of action could, in synergy with chitosan, enhance eradication of resistant bacteria.

Several researchers reported promising results on the antimicrobial effects of chitosan hydrogel and hydrogels containing carriers or particles. Anjum et al. evaluated a cotton dressing coated with chitosan, polyethylene glycol and polyvinyl pyrrolidone gel loaded with tetracycline against *Escherichia coli* and *S. aureus* (Anjum, Arora, Alam, & Gupta, 2016). In another study, the authors showed effect in the same species of both chitosan and a multi-network hydrogel based on chitosan (Zou et al., 2018). Masood and collaborators reviled antimicrobial activity in several species of silver nanoparticles loaded in chitosan and polyethylene glycol hydrogels (Masood et al., 2019). In addition, moxifloxacin entrapped in niosomes loaded into chitosan hydrogel demonstrated an improved antimicrobial activity in *P. aeruginosa* (Sohrabi, Haeri, Mahboubi, Mortazavi, & Dadashzadeh, 2016). The antimicrobial effects of chitosan are often greater in gram-positive bacteria (Moeini et al., 2020). However, a study on *S. aureus* and *P. aeruginosa* co-existing in biofilm exposed increased vulnerability of *P. aeruginosa*. The finding that bacterial membrane exhibited higher fluidity in the presence of MAAs could lead to novel target in biofilm treatment of wounds (Orazi, Ruoff, & O'Toole, 2019). Since these bacteria are often highly abundant in wounds, we aimed to exploit this vulnerability and create a system with synergic effects on the bacterial membrane. The activity of chitosan on the bacterial membrane is often associated with the molecular weight (MW) of the polymer (Tao, Qian, & Xie, 2011), and to achieve the strongest membrane activity on these bacteria in biofilms, we utilized chitosan with higher MW. The action of chitosan combined with the membrane activity of CHX could promote eradication of *S. aureus* and *P. aeruginosa* biofilms.

We therefore hypothesized that chitosan hydrogel can boost the activity of liposomally-associated MAAs. We aimed, for the first time, to investigate potential synergy between CHX, a model MAA, associated with liposomes and chitosan hydrogel against *S. aureus* and *P. aeruginosa* biofilms.

2. Materials and methods

2.1. Materials

Chitopharm™ M - Medium MW chitosan from shrimp (average of 350–600 kDa; and degree of deacetylation of >70 %) was a gift from Chitinor (Tromsø, Norway) and Lipoid S100 (phosphatidylcholine content >94 %) a gift from Lipoid GmbH (Ludwigshafen, Germany). Methanol (≥99.9 %) was purchased from VWR (Fontenay-sous-Bois, France). Acetic acid ≥99.8 %, chlorhexidine >99.5 %, glycerol solution (86–89 %), sodium nitrite, Kollisolv® PEG E 400, Cell Counting Kit – 8, Trizma base, calcium chloride, sodium phosphate dibasic dehydrate, potassium dihydrogen phosphate, sodium chloride and crystal violet were acquired from Sigma-Aldrich (St. Louis, USA). Ortho-phosphoric acid ≥85 % was obtained from Kebo Lab Ab (Oslo, Norway). Uranyless was procured from Electron Microscopy Sciences (Hatfield, PA, USA). Lipopolysaccharide (from *Escherichia coli* 055:B5), sulfanilamide ≥98 % and N-(1-Naphthyl)ethylenediamine dihydrochloride ≥98 % were acquired from Sigma Life Science Norway AS (Oslo, Norway). Roswell Park Memorial Institute (RPMI) medium 1640, bovine serum albumin, penicillin-streptomycin and fetal bovine serum (FBS) were purchased from Sigma-Aldrich (Steinheim, Germany). Nutrient Broth (NB) and Brain Heart Infusion broth (BHI) were supplied by Becton Dickinson and Company (Sparks, MD, USA). Dulbecco's Modified Eagle Medium (DMEM) high glucose w/ L-glutamine and sodium pyruvate was acquired from Biowest (Nuaillé, France). Murine macrophage RAW 264.7 cells, *S. aureus* ATCC29213 and *P. aeruginosa* ATCC10145 were delivered by ATCC (Manassas, VA, USA). *S. aureus* SO88 is a clinical isolate (Ospedale Sant'Orsola-Malpighi, Bologna, Italy) (Giordani et al., 2019). HaCaT cell line (immortalized human keratinocytes) was purchased from CLS Cell Lines Service GmbH (Eppelheim, Germany).

2.2. Preparation of CHX-liposomes and liposomes

CHX-liposomes were prepared by the film method as previously described (Hurler & Škalko-Basnet, 2012). Briefly, Lipoid S100 (200 mg) and CHX (10 mg) were dissolved in methanol. A lipid film was formed after methanol evaporation on a rotavapor (Büchi rotavapor R-124 with vacuum controller B-721, Büchi Vac® V-500, Büchi Labortechnik, Switzerland) at 60 kPa and 45 °C for at least 1 h, and re-suspended in 10 mL distilled water to form CHX-liposomes. Liposomes (without CHX) were made of lipid alone.

The size of CHX-liposomes was reduced by manual extrusion through polycarbonate membranes (Nuclepore Track-Etch Membrane, Whatman House, Maidstone, UK) with average diameter of 0.8 μm and 0.4 μm three and five times, respectively. Liposomes were extruded under same conditions including additional extrusions twice through a 0.2 μm membrane to be of comparable size.

2.3. Characterization of CHX-liposomes and liposomes

The size was measured on a NICOMP Submicron particle sizer (NICOMP Particle Sizing System, Santa Barbara, California, USA) as described by Ternullo, Gagnat et al. (2019). Liposomal suspensions diluted to an attain intensity of 250–350 KHz were measured (weight-intensity distribution) in three cycles of 10 min. The zeta potential was determined with a Zetasizer Nano Zen 2600 (Malvern, Worcestershire, UK, Jøraholmen et al., 2019). The liposomal suspension was diluted with deionized water. The pH of liposomal suspensions was measured using sensION + PH31 pH benchtop meter (Hach, Loveland, Colorado, USA).

CHX entrapped in the liposomes was separated from the unentrapped CHX using dialysis at 24 ± 1 °C (tube cut-off for MW at 12–14 kDa; Medicell International Ltd., London, UK). The CHX entrapment efficiency was determined using Tecan Spark M10 multimode plate reader (Tecan Trading AG, Switzerland) at 261 nm. A standard curve of CHX was prepared in the concentration range of 1.25–40 μg mL^{-1} for the analysis ($R^2 = 0.999$).

2.4. Preparation of hydrogels

2.4.1. Preparation of hydrogel and liposomes-in-hydrogel

Chitosan hydrogel was prepared as described previously (Hurler, Engesland, Kermany, & Škalko-Basnet, 2012). In brief, 4.5 % chitosan

(w/w) was dispersed in 2.5 % acetic acid (w/w) and 9% glycerol (w/w) and hand-stirred stirring at 24 ± 1 °C for 5 min to form hydrogel. The hydrogel was bath sonicated in an ultrasonic bath (Branson, Ultrasonic cleaner 5510E-MT, Danbury, USA) for 30 min (degassed) and permitted to swell at room temperature for 48 h. Glycerol-free hydrogel was prepared in the same manner without glycerol.

CHX-liposomes or liposomes without drug (10 % w/w) were incorporated into hydrogel comprising 5% (w/w) chitosan and 10 % (w/w) glycerol by hand-stirring at 24 ± 1 °C for 5 min to prepare respective liposomes-in-hydrogel. The concentrations of chitosan and glycerol in hydrogels after incorporation of liposomes were 4.5 % and 9% (w/w), respectively.

2.4.2. Preparation of CHX-hydrogel

CHX was dissolved in 2.5 % acetic acid (w/w) and glycerol by mechanical stirring for 2 h. Chitosan (4.5 %, w/w) was dispersed in the CHX solution and hand-stirred stirring at 24 ± 1 °C for 10 min to form hydrogel. The final concentrations of chitosan and glycerol were 4.5 % (w/w) and 9% (w/w), respectively.

2.5. Characterization of hydrogel

Texture properties were evaluated by utilizing a backward extrusion rig set using a Texture Analyser TA.XT Plus (Stable Micro Systems Ltd., Surrey, UK; Hurler et al., 2012a). Hydrogel (65 g) was transferred to the rig set container. A 35 mm disk was fixed to the texture analyser, and compressed into the hydrogel, and redrawn to starting position. The speed was 4 mm s^{-1} and starting position right above the hydrogel surface. The distance and trigger force were 10 mm and 10 g, respectively.

The pH of hydrogels was evaluated using Accumet ® portable pH meter kit AP115 (Fischer Scientific, Massachusetts, USA).

2.6. Release of CHX

The CHX release from formulations (liposomes and hydrogels) and free CHX were evaluated in a Franz cell diffusion system (PermeGear, Hellertown, PA) utilizing cellophane membrane and acceptor cell of 12 mL (1.77 cm^2) as previously described (Jøraholmen et al., 2019). To address low water solubility of CHX base, 10 % polyethylene glycol (v/v) in distilled water was added to the acceptor chamber. The system was kept on constant heating (32 °C) and mechanical stirring. The formulation (600 µL) was added to the donor chamber and samples were withdrawn after 24 h. CHX from both the acceptor chamber and membrane was quantified on a UV–vis plate reader (SpectraMax 190 Microplate Reader, Molecular Devices, CA, USA) at 261 nm. The hydrogels were weighted before and after each experiment to adjust for fluid exchange.

2.7. Bioadhesion studies

The bioadhesive properties of hydrogel formulations were evaluated using the mucoadhesion rig on the Texture Analyser TA.XT Plus (Stable Micro Systems Ltd., Surrey, UK; Hurler & Škalko-Basnet, 2012). The full thickness human skin was obtained from patients undergoing abdominal plastic surgery. Consent from all patients was obtained prior to every surgical procedure. Skin slices (1.26 ± 0.04 mm) were rinsed in Phosphate Buffer Saline (PBS, pH 7.4, 2.98 g L^{-1} $Na_2HPO_4{\cdot}2H_2O$, 0.19 g L^{-1} KH_2PO_4, 8 g L^{-1} NaCl) and stored in −20 °C. Prior to each experiment, the skin slice was thawed in distilled water for 30 min and rinsed thoroughly. Excess liquid was removed and the skin slice was mounted to the mucoadhesion rig. The hydrogel (150 µL) was applied to the die and the die weighed. The die with hydrogel was pressed onto the skin slice for 10 s with a force of 25 g. The speed was set to 1.0, 0.5 and 0.1 mm s^{-1} for the pre-test, test and post-test, respectively. The die was immediately weighed after the test (Ternullo, Schulte Werning, Holsæter, & Škalko-Basnet, 2019).

2.8. Anti-inflammatory activity

The anti-inflammatory activity was expressed through inhibition of NO production in lipopolysaccharide-induced RAW 264.7 murine macrophages (Basnet, Hussain, Tho, & Škalko-Basnet, 2012). CHX-liposomes-in-hydrogel, hydrogel, CHX-liposomes and liposomes were evaluated. Cell suspension (5×10^5 cells mL^{-1}, 1000 µL, in RPMI supplemented with glutamine, 10 % FBS, penicillin and streptomycin) was added to 24-well plates and incubated in humidified 5% CO_2 at 37 °C for 24 h. The medium was removed and 990 µL of LPS (1 µg mL^{-1}) in supplemented RPMI added to each well. The 10 µL of diluted liposomal suspensions (concentrations corresponding to 1, 10 and 50 µg mL^{-1} lipid content, respectively) and hydrogels (corresponding to liposomal suspensions) were added in triplicates. Supplemented RPMI (100 %) and LPS in medium served as normal and controls, respectively. The cells were incubated in humidified 5% CO_2 at 37 °C for 24 h. After incubation, NO released in medium was measured as nitrite concentration using Griess reagent (1:1, v/v) and quantified on a UV–vis plate reader (Tecan Spark M10 multimode plate reader, Tecan Trading AG, Switzerland) at 540 nm.

2.9. Antimicrobial evaluation

2.9.1. Inhibitory activity against planktonic cultures

The free and formulated CHX (liposomes and hydrogels, 2.5 mL) were diluted in water, mixed with an equal volume of Simulated Wound Fluid (SWF, pH 7.4, bovine serum albumin 2% w/v; $CaCl_2$ 0.02 M; NaCl 0.4 M; Trizma base 0.05 M, Cerchiara et al., 2020, final CHX concentration of 0.005 mg mL^{-1}) and inoculated with microbial suspensions (*S. aureus* ATCC239213, *S. aureus* SO88 and *P. aeruginosa* ATCC10145) prepared from a broth culture in log phase of growth (inoculum concentration: 10^6 CFU mL^{-1}). Non-treated suspensions served as a control. Counts of viable cells were carried out on NB (*S. aureus* strains – gram-positive) or BHI (*P. aeruginosa* – gram-negative) plates at the inoculum time and after 3, 6, 8 and 24 h of incubation at 37 °C. Results are expressed as viability (log CFU mL^{-1}) of microorganisms over time in presence of different formulations.

2.9.2. Anti-biofilm activity

The anti-biofilm activity of formulations was assessed against *S. aureus* ATCC239213, *S. aureus* SO88 and *P. aeruginosa* ATCC10145 as described by Giordani et al. (2019). Briefly, two different mechanisms of action were targeted, the inhibition of biofilm formation and eradication of pre-formed biofilm. For the inhibition assay, 100 µL of bacterial suspension (10^6 CFU mL^{-1}) in NB (*S. aureus* strains) or BHI (*P. aeruginosa*) were incubated in 96-multi-well plates together with 100 µL of free or formulated CHX (liposomes and hydrogels). For the eradication assay, the biofilm was first formed for 48 h (200 µL of bacterial suspension 10^6 CFU mL^{-1}) and then treated with 200 µL of free or formulated CHX (liposomes and hydrogels) for 24 h. Crystal violet is a dye commonly employed in microbiology field because it allows staining of the bacterial cell walls. To quantify the biofilm after treatments, the cells adherent to the wells were stained with crystal violet (0.41 %, w/v), dye exhibiting an absorbance peak at 595 nm when dissolved in ethanol. Thus, the higher absorbance (OD_{595}, EnSpire 217 Multimode Plate Reader, PerkinElmer Inc., Waltham, MA) corresponds to a larger number of bacterial cells adherent to the wells of 96-multi-well plates (37 °C, 100 rpm). Results were expressed in percentage relative to the untreated control accordingly to the following equation (Eq. (1), Giordani et al., 2019):

$$\text{Inhibition of biofilm formation/Eradication of pre-formed biofilm (\%)} = [1\text{-}(\text{mean } OD_{595} \text{ sample} / \text{mean } OD_{595} \text{ control})] \times 100 \quad (1)$$

2.10. Statistical analyses

Statistical significance was evaluated by one-way ANOVA followed by Turkey's correction or student's *t*-test. The results are expressed as means ± SD.

3. Results and discussions

The treatment of infected wounds requires careful tailoring of formulation properties to optimize the treatment outcome (Malaekeh-Nikouei, Fazly Bazzaz, Mirhadi, Tajani, & Khameneh, 2020; Tottoli et al., 2020). Moreover, the formulation should offer mechanical stability, moisture maintenance, protection from environmental exposure, promotion of tissue regeneration and biocompatibility (Anjum et al., 2016). Importantly, infected wounds require high local concentrations of antimicrobials over prolonged periods, therefore, formulations increasing the antimicrobial and anti-inflammatory effects while reducing chances for resistance development are preferred (Lam et al., 2018). Liposomes-in-hydrogel for antimicrobials is a promising strategy in treatment of infected wounds. The synergy between formulations and antimicrobials create a potential therapeutic advantage.

3.1. Characteristics of CHX-liposomes and liposomes

Liposomes are extensively used in studies targeting skin therapies. These lipid-based vesicles provide sustained and controlled release of associated antimicrobial compounds from a safe carrier (Filipczak, Pan, Yalamarty, & Torchilin, 2020; Gonzalez Gomez & Hosseinidoust, 2020; Ibaraki et al., 2020). They provide a reservoir for compounds within the skin layers increasing the local concentration (Lai et al., 2020; Peers et al., 2020). The optimal size considering a depot effect should be around 200−300 nm (Ternullo, Schulte Werning et al., 2019). Generally, the size of liposomes is very likely influencing the antibacterial activity (Martin et al., 2015). Indeed, it has been reported that conventional liposomes that were effective in delivery of antimicrobials to biofilms had a size significantly below 500 nm (Rukavina & Vanić, 2016). For example, amikacin-loaded liposomes with a mean diameter of approximately 300 nm penetrated readily into *P. aeruginosa* biofilm and infected mucus (Meers et al., 2008). Similarly, azithromycin-loaded liposomes of about 400 nm were able to reduce the growth of *P. aeruginosa* in biofilm (Solleti, Alhariri, Halwani, & Omri, 2015). However, the liposomes in our study were incorporated in hydrogels and not applied as suspensions; therefore, the effect of their size should be rather limited. We generated liposomes of a homogenous size distribution exhibiting a relatively low polydispersity index (PI, Table 1). The size of CHX-liposomes was confirmed with transmission electron microscopy (TEM, Fig. S1). Moreover, the images showed spherical liposomes with well-defined surfaces. The liposomes, in addition to all other formulations presented in this study, are summarized in Table S1.

The zeta potential of empty liposomes was neutral due to the high content of neutral phosphatidylcholine (>94 %), however, CHX-liposomes exhibited zeta potential of almost 50 mV (Table 1), making them highly cationic due to presence of CHX. The physiochemical nature of CHX and its biguanide groups would point to CHX being incorporated within and onto the bilayer of liposomes, which could further increase potential interactions with bacterial membranes (Farkas, Zelkó, Török, Rácz, & Marton, 2001). Recently, Ibaraki and colleagues reported increased damage to bacterial biofilms by cationic compared to anionic liposomes (Ibaraki et al., 2020). The amphipathic nature of CHX allows its distribution stretched towards the core in the inner layer and the surface and within the bilayer resulting in a considerably high entrapment (Hassan et al., 2013).

We evaluated the stability of liposomal dispersions over 4 weeks and did not detected any significant changes in their characteristics (data not included).

3.2. Characteristics of hydrogel

Liposomes require secondary vehicles such as hydrogels to remain on the skin. A key feature of hydrogels in skin therapy is to offer mechanical stability. Hydrogel′s texture properties are often measured as an indicator of mechanical stability. Texture analyses provide both in-process controls and information on stability (Hurler et al., 2012a). The relevant parameters are hardness, cohesiveness and adhesiveness. The hardness describes the skin applicability of the formulation (Ternullo, Schulte Werning et al., 2019). The cohesiveness defines the recovery of the structural network within hydrogel after application and level of deformation (Amasya, Inal, & Sengel-Turk, 2020). The adhesiveness represents the ability to remain on the skin (Hurler et al., 2012a). These features define the applicability and user-friendliness of hydrogels.

The texture properties are influenced by plasticisers and polymer concentrations and the addition of glycerol increased the hydrogel hardness (Fig. 1). This was evident from the results of the glycerol-free hydrogel and the CHX-liposomes-in-glycerol-free hydrogel. CHX, in liposomes-in-hydrogel or free in the hydrogel, did not affect the hydrogel hardness. The cohesiveness did not follow the same pattern as the hardness; all hydrogels demonstrated similar cohesiveness, except from the glycerol-free hydrogel (4.5 %, Fig. 1) that exhibited a significantly higher cohesiveness compared to other formulations. Glycerol was added to hydrogels to improve the long-term texture properties (Hurler et al., 2012a) as well as the level of deformation within the hydrogel, the cohesiveness. Glycerol could create three hydrogen bonds with the amino sugar unit and subsequently increase the mobility (Chen et al., 2018). The adhesiveness decreased when CHX-liposomes were incorporated into the hydrogel as compared to liposome.

Our results cannot be directly compared to other studies since we applied higher polymer concentrations and modified set-up. For example, Ternullo and colleagues observed reduced texture properties upon addition of liposomes, whereas Jøraholmen and colleagues observed the opposite (Jøraholmen et al., 2019; Ternullo, Schulte Werning et al., 2019).

The pH of hydrogels was also investigated (Table S3) to assure an appropriate pH of the final formulation. Although the CHX-liposomes demonstrated a higher pH, liposomes were merely the primary formulation since the CHX-liposomes were further incorporated within a chitosan hydrogel network. The pH of the hydrogels was significantly lower than the pH of the CHX-liposomes, assuring that externally applied formulation does not elevate the issue of high pH; on the contrary, it acts on lowering pH.

Table 1
Characteristics of liposomes and CHX-liposomes.

Sample	Size (nm)	PI[a]	Zeta (mV)	pH	EE (%)[b]
Liposomes	271 ± 16	0.33 ± 0.07	−0.4 ± 0.3	6.9 ± 0.2	–
CHX-liposomes	318 ± 9*	0.24 ± 0.03*	45.5 ± 1.3*	8.0 ± 0.1	94.7 ± 0.7

Results are expressed as means with their respective SD (n = 3, * n = 6).
[a] Polydispersity index.
[b] Entrapment efficiency (%).

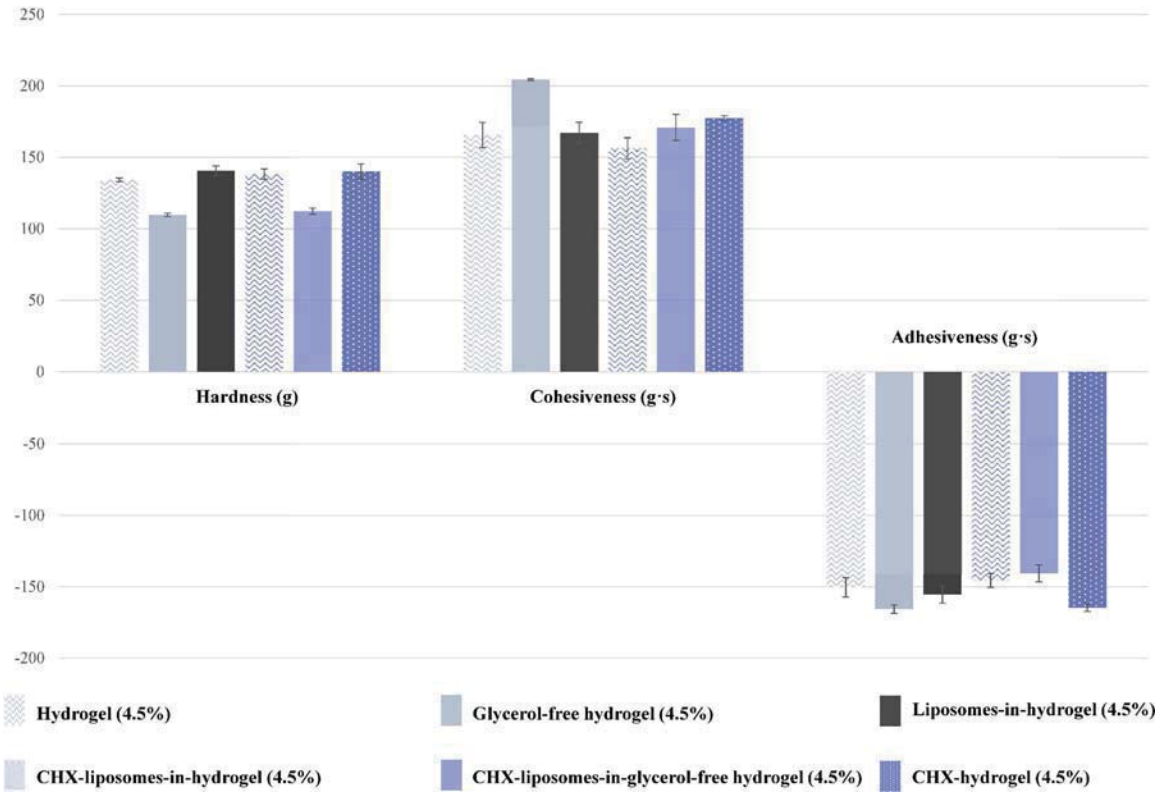

Fig. 1. The texture properties of chitosan hydrogels measured as hardness, cohesiveness and adhesiveness. The values are expressed as mean of three replicates with their respective SD.

3.3. Stability of chitosan hydrogels

The stability testing expressed as the changes of the hydrogels' texture properties (Table S2) indicates that the cohesiveness and adhesiveness of hydrogels comprising glycerol and liposomes remained more stable over a period of 4 weeks than plain hydrogel of the same concentration, probably due to stabilizing effect of both glycerol and liposomes. Additionally, the CHX-liposomes-in-hydrogel exhibited satisfying stability for the evaluation period. This stability could be attributed to the charge of both CHX-liposomes and chitosan, creating repulsive effects through electrostatic forces (Ternullo, Schulte Werning et al., 2019). The liposomal bilayer is electrostatically stabilized and the repulsions might decelerate the release of CHX into the hydrogel network (Grijalvo et al., 2020). The basic CHX is only slowly released into the network, and this would possibly lead to a stable pH in the network. Since liposomes most likely preserve their original size without aggregation, the network mobility would be more stable. In addition, Hurler and colleagues studied the effects of zeta potential of liposomes on the properties of the liposomes-in-hydrogel formulations. The authors postulated that liposomes bearing a positive charge seem to stabilize the chitosan hydrogel network better than neutral or negatively charged liposomes (Hurler et al., 2013). The pH of hydrogels (Table S3) remained stable over four weeks. However, liposomes-in-hydrogels, both with and without CHX, exhibited a small increase in pH.

3.4. Release of CHX

Considering skin therapy, liposomes-in-hydrogel should provide sustained CHX release assuring bacterial eradication without regrowth, reduced administration frequency and improved patient compliance (Smith et al., 2020). Additionally, antimicrobial-liposomes-in-hydrogel formulations prevent burst release from polymeric networks or liposomes alone (Grijalvo et al., 2020).

In Fig. 2, the CHX release (24 h) is presented. CHX-liposomes exhibited sustained release compared to the permeating free CHX ($p < 0.1$). However, incorporation of CHX-liposomes into chitosan hydrogel significantly sustained the release ($p < 0.05$). No differences in release between liposomes-in-hydrogels with and without glycerol were observed. Chitosan hydrogels without liposomes failed to reduce CHX release indicating that liposomes were crucial to provide a sustained release of CHX. Similarly, CHX release from montmorillonite and chitosan composite was reported to be controlled and sustained as compared to free CHX (Onnainty et al., 2016).

These results emphasize the importance of including both systems, liposomes and hydrogel, in the final formulation. In addition to the 24 h endpoint release, we performed preliminary studies on the release profile from CHX-liposomes, CHX-liposomes-in-hydrogel, CHX-liposomes-in-glycerol-free hydrogel and free CHX (Fig. S2). The same patterns as observed in the 24 h endpoint measurements (Fig. 2) were confirmed in hourly release profile; however, we noticed the fluid exchange between the donor and acceptor chamber. Therefore, we proceeded with the endpoint measurement of the release.

3.5. Bioadhesive properties

The efficacy of formulations destined for skin administration is influenced by their bioadhesive properties. Hurler and colleagues developed a method to determine the amount of hydrogel that remained on the skin after compression rather than measuring force of detachment (Hurler & Škalko-Basnet, 2012). The bioadhesive properties of tested hydrogels are found in Fig. 3. All hydrogels were bioadhesive; however, liposomes-in-hydrogel displayed the highest bioadhesive properties.

Most often, reports on bioadhesion refer to mucosal adhesion; however, mechanisms for skin adhesion are also reported (Horstmann, Müller, & Asmussen, 1999; Venkatraman & Gale, 1998). The adhesion to skin is, unlike to the mucosa, more dependent on the surface structure

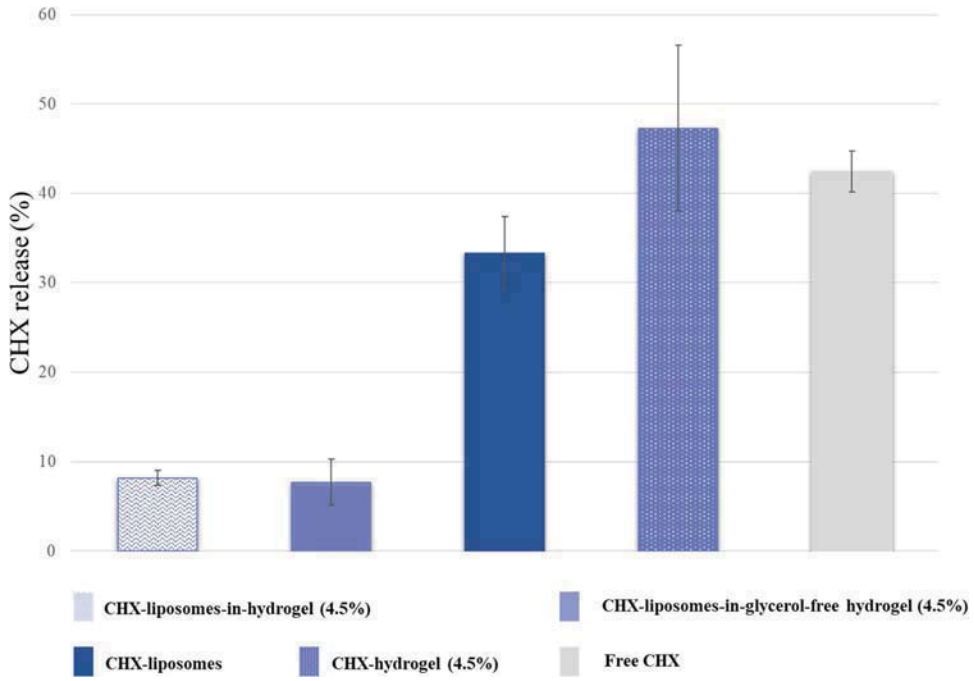

Fig. 2. CHX release or permeation over 24 h at 32 °C. Results are represented as percentage of CHX released compared to the initial concentration. Results are expressed as mean of three replicates with their respective SD.

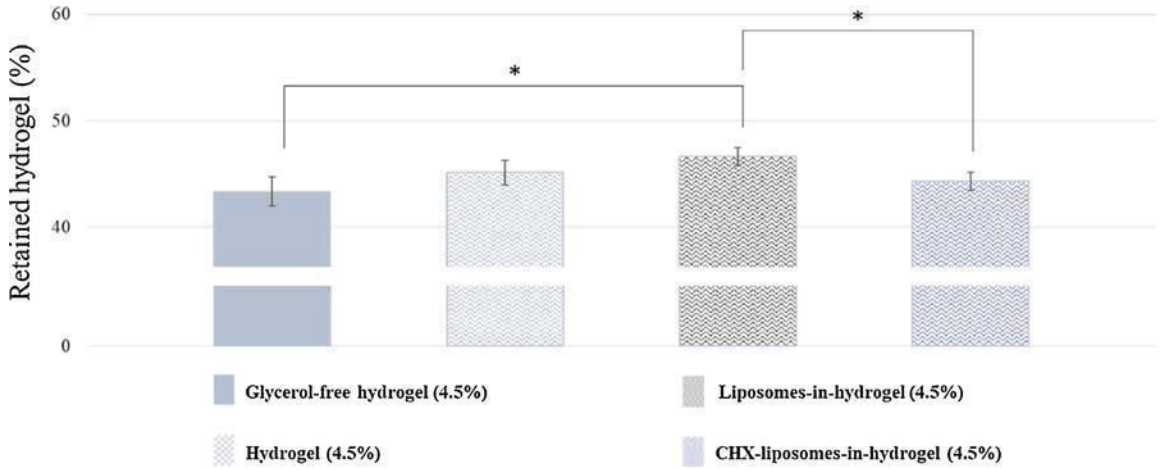

Fig. 3. Bioadhesive properties of chitosan hydrogels and liposomes-in-hydrogel. The bioadhesion is presented as the amount of hydrogel retained on the skin (%) after compression compared to the original amount applied to the die in the rig set to the Texture Analyser. The results are presented as the mean of three replicates with their respective SD.
*) Significantly different ($p < 0.05$).

and size of the surface area (Horstmann et al., 1999). Moreover, the bioadhesion could potentially be affected by interpenetration between the polymer and biological surface (Palacio & Bhushan, 2012), moreover the plasticizer could increase bioadhesion (Horstmann et al., 1999).

3.6. Anti-inflammatory evaluation

Macrophages play an important role in skin infections and inflammations by regulating the production of NO (Kloc et al., 2019). The reduced NO level has been considered beneficial after the inflammatory phase of wound healing. We evaluated the anti-inflammatory effects of chitosan formulations and CHX; CHX is expected to have a mild effect on inflammation in this experimental set-up by neutralizing LPS through binding (Zorko & Jerala, 2008).

Our results confirmed a dose-dependent reduction in NO production (Fig. 4). Even though the difference in production between 1 and 10 μg mL^{-1} was not statistically different except for the CHX-liposomes-in-hydrogel, a clear tendency could be observed. All formulations demonstrated a significant reduction in NO production between 10 and 50 μg mL^{-1}. Furthermore, all formulations at every concentration, except liposomes (1 μg mL^{-1}), demonstrated a significant reduction in NO production compared with the control (non-treated LPS-induced macrophages). The reduction of NO production in the cells treated with hydrogels either with or without CHX liposomes demonstrated a significantly reduced NO production.

Chitosan-based formulations have previously been reported to reduce inflammatory response in macrophages; however, the results were often dependent on MW of chitosan (Chang, Lin, Wu, Huang, & Tsai, 2019). Our group has reported anti-inflammatory activity of liposomes-in-hydrogel formulation with polyphenols (Jøraholmen et al.,

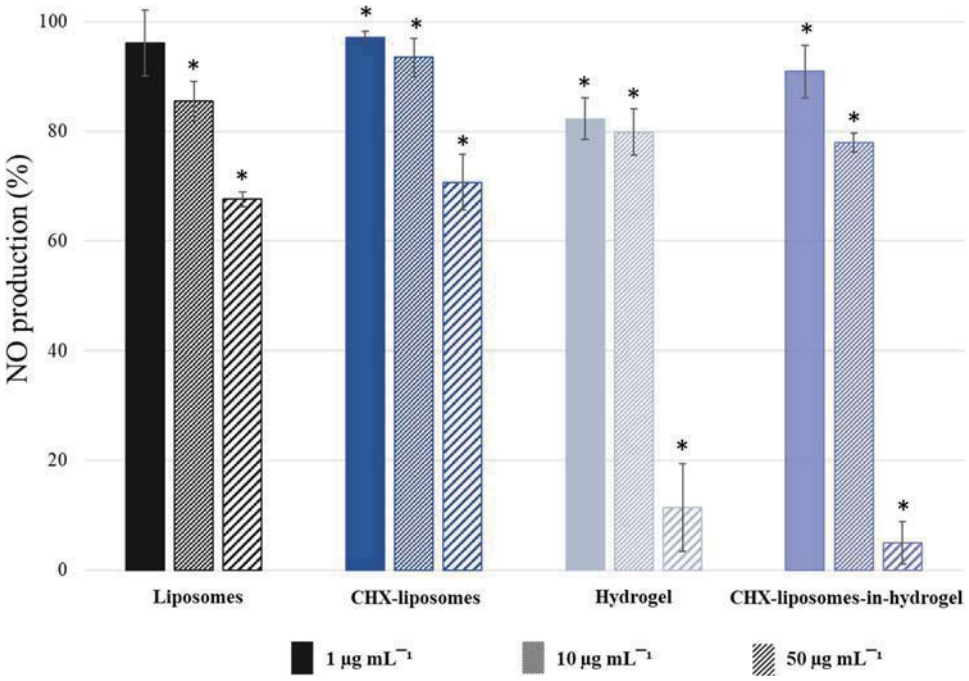

Fig. 4. Anti-inflammatory evaluation on murine macrophages (RAW 264.7). Concentrations refer to the lipid concentration or corresponding concentration where lipids are not present. The NO production is presented as the percentage compared to the NO production in non-treated LPS-induced macrophages (100 %). All results are expressed asmeans of three parallels with their respective SD.
*) Significantly different compared to non-treated LPS-induced macrophages ($p < 0.05$).

2019). In their study, the anti-inflammatory response was lower than we observed, however, the chitosan concentration used in this study was significantly lower than in our study. Since we used higher chitosan concentrations, the differences may indicate that chitosan concentration plays a role in modulating anti-inflammatory response. However, we measured nitrites as an indicator for NO. Due to the anionic nature of nitrites, chitosan might neutralize these inorganic anions (Il'ina & Varlamov, 2016) leading to lower concentration of available nitrites for the Griess reaction. Consequently, the values may be an overestimation of the anti-inflammatory effect and should be further investigated. The most important characteristic to verify is that new formulations for wound therapy do not induce an additional inflammation response, which would lead to impaired healing. Pettinelli and colleagues demonstrated that chitosan hydrogel did not induce any inflammation response in macrophages (Pettinelli et al., 2019). In addition to the evaluation of NO production in macrophages, we evaluated the cell viability of immortalized human keratinocytes treated with CHX-liposomes (Fig. S3). The results demonstrated improved viability of cells treated with CHX-liposomes.

3.7. Antimicrobial evaluation

3.7.1. Minimal lethal concentration (MLC) of formulated and free CHX

The treatment of wound infections is challenging due to the growing problem of antibiotic resistance and tendency of *S. aureus* and *P. aeruginosa* to form biofilms (Serra et al., 2015). Chitosan demonstrates antimicrobial properties towards gram-positive bacteria (Hamedi, Moradi, Hudson, & Tonelli, 2018; Moeini et al., 2020). Since infected wounds comprise polymicrobial manifestation, we aimed to take advantage of the synergic effects of chitosan and CHX to ameliorate the available antibacterial therapies against both bacteria.

We investigated the MLC of free CHX and formulated CHX (liposomes and hydrogels with glycerol) for three bacterial strains (Table S4). As expected, free CHX exerted strong antimicrobial activity against both *S. aureus* and *P. aeruginosa*. The effects were retained in CHX- liposomes, whilst empty liposomes were inactive. Importantly, the incorporation of CHX-liposomes in chitosan hydrogel improved the CHX antibacterial effect, as demonstrated by the lowering of MLC for all tested strains. In addition, hydrogel (4.5 %) revealed an antibacterial activity itself, since it inhibited *S. aureus* ATCC29213, *S. aureus* SO88 and *P. aeruginosa* ATCC10145 at dilutions corresponding to chitosan concentrations of 0.056 %, 1.125 % and 2.25 %, respectively.

3.7.2. Inhibitory activity against planktonic cultures

Considering topical application for the treatment of wounds, the antimicrobial activities towards planktonic culture were evaluated in SWF. The viability of *S. aureus* and *P. aeruginosa* in SWF was compared in the presence of free or formulated CHX (Fig. 5). The untreated bacteria and bacteria exposed to liposomes retained viability. In presence of free CHX, no viable cells were found after 3 h.

CHX-liposomes and CHX-hydrogels both retained antimicrobial activity against planktonic cultures but with delayed effects, due to sustained release of CHX. In particular, CHX-hydrogel completely abolished viability after 9 h, while CHX-liposomes and CHX-liposomes-in-hydrogel required 24 h to achieve a complete depletion of bacterial cells. Interestingly, after 6 and 8 h the antimicrobial effects against all tested microorganisms were more marked for CHX-liposomes-in-hydrogels than for CHX-liposomes ($p < 0.05$), even if release studies showed a reduced release of CHX from CHX-liposomes-in-hydrogels. However, in all cases no viable bacteria were found after 24 h of incubation with formulated CHX (liposomes or hydrogels), as well as with free CHX. It is worth noting that hydrogel without CHX reduced *S. aureus* viability by 1.27–1.55 log CFU after 24 h, while cell viability of *P. aeruginosa* decreased by 1.14 log CFU. This is in agreement with MLC data and suggests that chitosan-based wound treatment improves the antimicrobial potential of CHX.

3.7.3. Anti-biofilm activity

Considering that *S. aureus* and *P. aeruginosa* biofilms are often associated with chronic infections and decreased susceptibility to antimicrobial treatments (Roy, Tiwari, Donelli, & Tiwari, 2018), we focused on anti-biofilm activity of free and formulated CHX against *S. aureus* ATCC29213, *S. aureus* SO88 and *P. aeruginosa* ATCC10145 by means of dispersal and biofilm formation inhibition assays (Fig. 6). Free CHX revealed a moderate anti-biofilm activity, reducing the biofilm formation of all tested microorganisms (inhibition of 42–51 %) and partially eradicating pre-formed biofilm (eradication rate of 29–43 %).

Contrary to what was observed for planktonic cultures, the

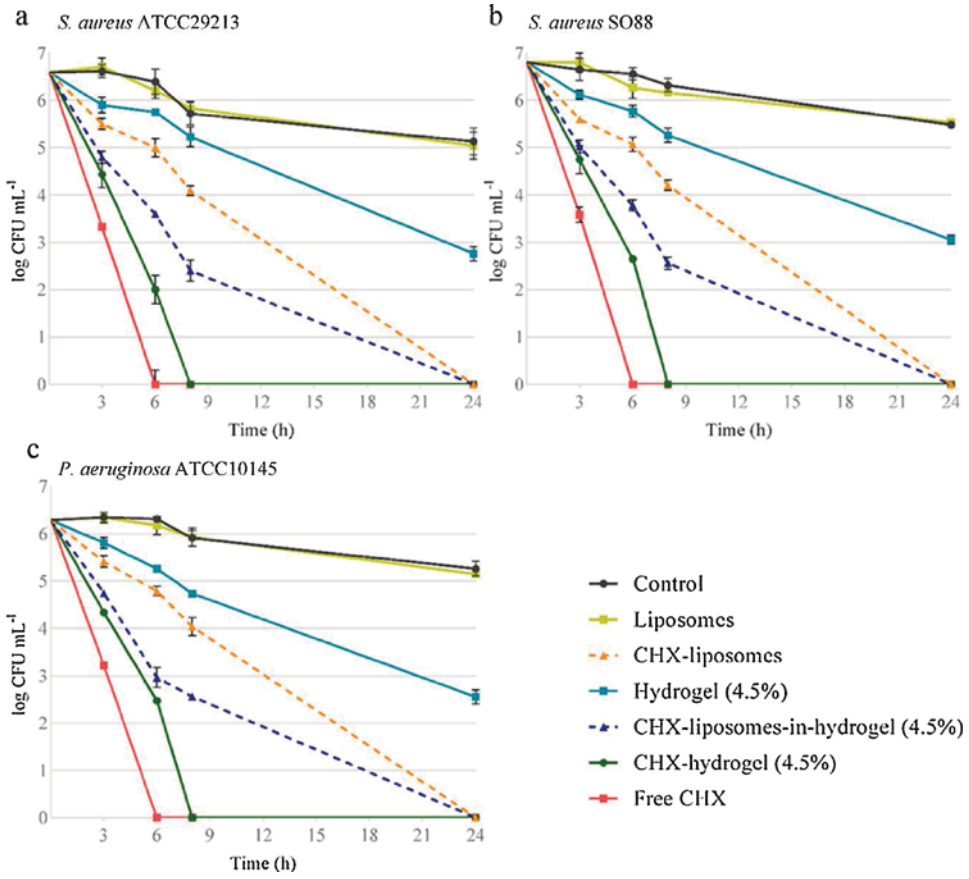

Fig. 5. Viability (log CFU mL^{-1}) of microorganisms over the time (up to 24 h) in presence of different formulations. The results are presented as the mean of three replicates with their respective SD.
a: *S. aureus* ATCC29213; b: *S. aureus* SO88; c: *P. aeruginosa* ATCC10145.

incorporation of CHX inside liposomes significantly enhanced its ability both to counteract biofilm formation (inhibition of 53–63 %) and to disperse pre-formed biofilm (eradication rate of 40–53 %, $p < 0.05$). The increased anti-biofilm activity of CHX-liposomes might be due to a more efficient penetration of positively charged liposomes into the extracellular matrix of biofilms (Rukavina & Vanić, 2016). Our finding is in agreement with data on incorporation of vancomycin (Scriboni et al., 2019) and gentamicin (Alhariri et al., 2017) in liposomes, which improved the penetration of *S. aureus* and *P. aeruginosa* biofilms, respectively. Moreover, reports show that cationic formulations could potentially extend the penetration of active compounds into bacterial biofilm, which are probably negatively charged (Drulis-Kawa et al., 2009; Robinson, Bannister, Creeth, & Jones, 2001). Nevertheless, the composition of external matrix of biofilm is very complex and heterogeneous and can be influenced by numerous factors including surface properties, nutrient availability and microbial species that form the biofilm (Flemming & Wingender, 2010). Thus, we can only make assumptions. However, different authors reported that cationic vesicles showed better performances compared to free active compounds or negatively charged vesicles in targeting biofilm of *Staphylococcus spp.*, including *S. aureus* (Rukavina & Vanić, 2016). Actually, our results support the hypothesis that liposomes and cationic formulations may improve the delivery of active compounds to biofilms.

As expected, liposomes showed no anti-biofilm activity, while hydrogels without CHX exhibited a mild anti-biofilm effect ($p < 0.05$). Consequently, CHX-hydrogel improved activity as compared to free CHX ($p < 0.05$).

Notably, the best anti-biofilm profile was observed for CHX-liposomes-in-hydrogels, and was significantly better than CHX-liposomes. In particular, CHX-liposomes-in-hydrogels almost completely inhibited the formation of *S. aureus* and *P. aeruginosa* biofilm, while the eradication rate was higher for *S. aureus* (82–98 %) than for *P. aeruginosa* (64 %). These results suggest that the insertion of CHX-liposomes inside chitosan hydrogel is a promising and innovative strategy to treat wound infections.

4. Conclusion

To address the challenges related to both treatment of chronic wounds comprising biofilms and increased antimicrobial resistance, we developed novel antimicrobial chitosan-based system. The system comprising liposomally-associated CHX in chitosan hydrogel exhibited superior anti-biofilm activities while maintaining properties relevant for skin administration. In addition, we observed anti-inflammatory effects of the chitosan hydrogel, an important feature considering wound therapy.

CRediT authorship contribution statement

Lisa Myrseth Hemmingsen: Conceptualization, Data curation, Formal analysis, Methodology, Validation, Writing - original draft, Writing - review & editing. **Barbara Giordani:** Data curation, Formal analysis, Methodology, Writing - original draft, Writing - review & editing. **Ann Kristin Pettersen:** Data curation, Formal analysis, Writing - review & editing. **Beatrice Vitali:** Methodology, Writing - original draft, Writing - review & editing. **Purusotam Basnet:** Data curation, Methodology, Writing - review & editing. **Nataša Škalko-Basnet:** Conceptualization, Funding acquisition, Methodology, Supervision, Writing - original draft, Writing - review & editing.

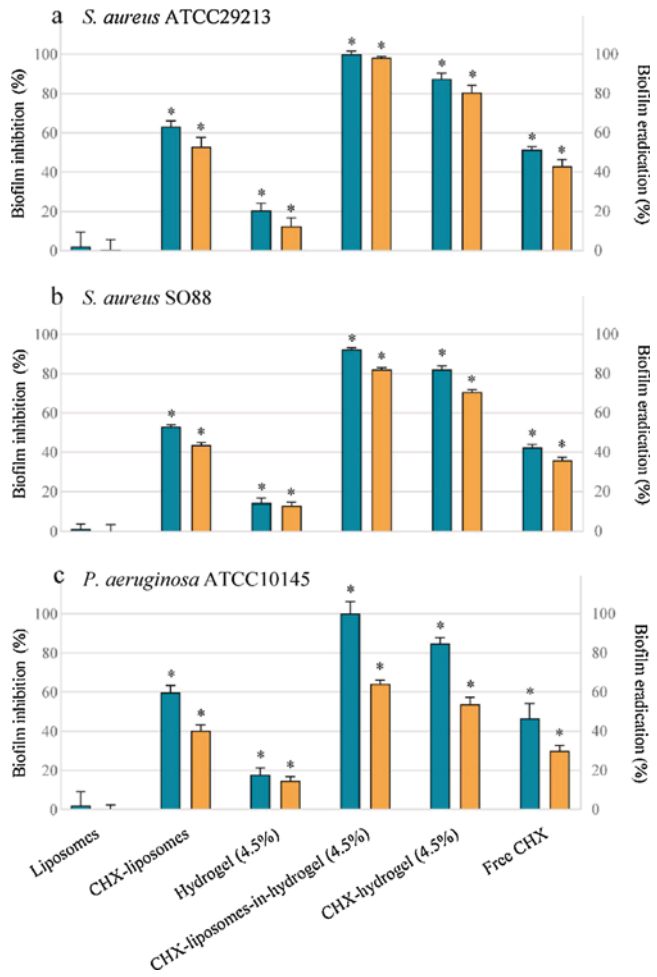

Fig. 6. Anti-biofilm activity: inhibition of biofilm development (%) on left Y-axis (petrol bars), eradication of pre-formed biofilm (%) on the right Y-axis (orange bars). The results are presented as the mean of three replicates with their respective SD.
*) Significantly different from untreated control ($p < 0.05$).
a: *S. aureus* ATCC29213; b: S. aureus SO88; c: P. aeruginosa ATCC10145.

Declaration of Competing Interest

The authors report no declarations of interest.

Acknowledgements

The study was funded by UiT The Arctic University of Norway, Norway (project no. 235569). The authors acknowledge Dr. Selenia Ternullo for skin samples used in the bioadhesion studies. The authors would also like to thank Dr. Sybil Obuobi as well as Augusta Sundbø and Randi Olsen at The Advanced Microscopy Core Facility, Department of Medical Biology, UiT The Arctic University of Norway for the assistance in TEM-imaging.

Appendix A. Supplementary data

Supplementary material related to this article can be found, in the online version, at doi:https://doi.org/10.1016/j.carbpol.2021.117939.

References

Alhariri, M., Majrashi, M. A., Bahkali, A. H., Almajed, F. S., Azghani, A. O., Khiyami, M. A., … Halwani, M. A. (2017). Efficacy of neutral and negatively charged liposome-loaded gentamicin on planktonic bacteria and biofilm communities. *International Journal of Nanomedicine, 12*, 6949–6961.

Amasya, G., Inal, O., & Sengel-Turk, C. T. (2020). SLN enriched hydrogels for dermal application: Full factorial design study to estimate the relationship between composition and mechanical properties. *Chemistry and Physics of Lipids, 228*, Article 104889.

Ambrogi, V., Pietrella, D., Nocchetti, M., Casagrande, S., Moretti, V., De Marco, S., … Ricci, M. (2017). Montmorillonite–chitosan–chlorhexidine composite films with antibiofilm activity and improved cytotoxicity for wound dressing. *Journal of Colloid and Interface Science, 491*, 265–272.

Anjum, S., Arora, A., Alam, M. S., & Gupta, B. (2016). Development of antimicrobial and scar preventive chitosan hydrogel wound dressings. *International Journal of Pharmaceutics, 508*(1), 92–101.

Balaure, P. C., & Grumezescu, A. M. (2020). Recent advances in surface nanoengineering for biofilm prevention and control. Part I: Molecular basis of biofilm recalcitrance. Passive anti-biofouling nanocoatings. *Nanomaterials, 10*(6), 1230.

Basnet, P., Hussain, H., Tho, I., & Škalko-Basnet, N. (2012). Liposomal delivery system enhances anti-inflammatory properties of curcumin. *Journal of Pharmaceutical Sciences, 101*(2), 598–609.

Cepas, V., López, Y., Muñoz, E., Rolo, D., Ardanuy, C., Martí, S., … Soto, S. M. (2018). Relationship between biofilm formation and antimicrobial resistance in gram-negative bacteria. *Microbial Drug Resistance, 25*(1), 72–79.

Cerchiara, T., Giordani, B., Melgoza, L. M., Prata, C., Parolin, C., Dalena, F., … Vitali, B. (2020). New Spanish Broom dressings based on Vitamin E and Lactobacillus plantarum for superficial skin wounds. *Journal of Drug Delivery Science and Technology, 56*, Article 101499.

Chang, S.-H., Lin, Y.-Y., Wu, G.-J., Huang, C.-H., & Tsai, G. J. (2019). Effect of chitosan molecular weight on anti-inflammatory activity in the RAW 264.7 macrophage model. *International Journal of Biological Macromolecules, 131*, 167–175.

Chen, M., Runge, T., Wang, L., Li, R., Feng, J., Shu, X.-L., … Shi, Q.-S. (2018). Hydrogen bonding impact on chitosan plasticization. *Carbohydrate Polymers, 200*, 115–121.

Drulis-Kawa, Z., Dorotkiewicz-Jach, A., Gubernator, J., Gula, G., Bocer, T., & Doroszkiewicz, W. (2009). The interaction between Pseudomonas aeruginosa cells and cationic PC:Chol:DOTAP liposomal vesicles versus outer-membrane structure and envelope properties of bacterial cell. *International Journal of Pharmaceutics, 367*(1), 211–219.

Farkas, E., Zelkó, R., Török, G., Rácz, I., & Marton, S. (2001). Influence of chlorhexidine species on the liquid crystalline structure of vehicle. *International Journal of Pharmaceutics, 213*(1), 1–5.

Filipczak, N., Pan, J., Yalamarty, S. S. K., & Torchilin, V. P. (2020). Recent advancements in liposome technology. *Advanced Drug Delivery Reviews, 156*, 4–22.

Flemming, H.-C., & Wingender, J. (2010). The biofilm matrix. *Nature Reviews Microbiology, 8*(9), 623–633.

Giordani, B., Costantini, P. E., Fedi, S., Cappelletti, M., Abruzzo, A., Parolin, C., & Vitali, B. (2019). Liposomes containing biosurfactants isolated from Lactobacillus gasseri exert antibiofilm activity against methicillin resistant Staphylococcus aureus strains. *European Journal of Pharmaceutics and Biopharmaceutics, 139*, 246–252.

Gonzalez Gomez, A., & Hosseinidoust, Z. (2020). Liposomes for antibiotic encapsulation and delivery. *ACS Infectious Diseases, 6*(5), 896–908.

Grijalvo, S., Eritja, R., & Díaz, D. D. (2020). Liposomes-in-chitosan hydrogels: Challenges and opportunities for biomedical applications. *Materials Science and Technology*, 1–32.

Guo, J., Qin, J., Ren, Y., Wang, B., Cui, H., Ding, Y., & Yan, F. (2018). Antibacterial activity of cationic polymers: Side-chain or main-chain type? *Polymer Chemistry, 9*(37), 4611–4616.

Hall, T. J., Villapún, V. M., Addison, O., Webber, M. A., Lowther, M., Louth, S. E. T., & Cox, S. C. (2020). A call for action to the biomaterial community to tackle antimicrobial resistance. *Biomaterials Science, 8*(18), 4951–4974.

Hamedi, H., Moradi, S., Hudson, S. M., & Tonelli, A. E. (2018). Chitosan based hydrogels and their applications for drug delivery in wound dressings: A review. *Carbohydrate Polymers, 199*, 445–460.

Hassan, K. A., Jackson, S. M., Penesyan, A., Patching, S. G., Tetu, S. G., Eijkelkamp, B. A., & Paulsen, I. T. (2013). Transcriptomic and biochemical analyses identify a family of chlorhexidine efflux proteins. *Proceedings of the National Academy of Sciences of the United States of America, 110*(50), 20254–20259.

Horstmann, M., Müller, W., & Asmussen, B. (1999). Principles of skin adhesion and methods for measuring adhesion of transdermal systems. In E. Mathiowitz, D. E. Chickering, & C. M. Lehr (Eds.), *Bioadhesive drug delivery systems: Fundamentals, novel approaches, and development* (pp. 175–196). New York: Marcel Dekker.

Hubbard, A. T., Coates, A. R., & Harvey, R. D. (2017). Comparing the action of HT61 and chlorhexidine on natural and model Staphylococcus aureus membranes. *The Journal of Antibiotics, 70*(10), 1020–1025.

Hurler, J., & Škalko-Basnet, N. (2012). Potentials of chitosan-based delivery systems in wound therapy: Bioadhesion study. *Journal of Functional Biomaterials, 3*(1), 37–48.

Hurler, J., Engesland, A., Kermany, B. P., & Škalko-Basnet, N. (2012). Improved texture analysis for hydrogel characterization: Gel cohesiveness, adhesiveness, and hardness. *Journal of Applied Polymer Science, 125*(1), 180–188.

Hurler, J., Žakelj, S., Mravljak, J., Pajk, S., Kristl, A., Schubert, R., … Škalko-Basnet, N. (2013). The effect of lipid composition and liposome size on the release properties of liposomes-in-hydrogel. *International Journal of Pharmaceutics, 456*(1), 49–57.

Ibaraki, H., Kanazawa, T., Chien, W.-Y., Nakaminami, H., Aoki, M., Ozawa, K., & Seta, Y. (2020). The effects of surface properties of liposomes on their activity against Pseudomonas aeruginosa PAO-1 biofilm. *Journal of Drug Delivery Science and Technology, 57*, Article 101754.

Il'ina, A. V., & Varlamov, V. P. (2016). Neutralization of reactive oxygen species by chitosan and its derivatives in vitro/in vivo (Review) *Applied Biochemistry and Microbiology, 52*(1), 1–14.
Islam, M. M., Shahruzzaman, M., Biswas, S., Nurus Sakib, M., & Rashid, T. U. (2020). Chitosan based bioactive materials in tissue engineering applications-A review. *Bioactive Materials, 5*(1), 164–183.
Jøraholmen, M. W., Basnet, P., Tostrup, M. J., Moueffaq, S., & Škalko-Basnet, N. (2019). Localized therapy of vaginal infections and inflammation: Liposomes-in-hydrogel delivery system for polyphenols. *Pharmaceutics, 11*(2), 53.
Kadam, S., Shai, S., Shahane, A., & Kaushik, K. S. (2019). Recent advances in non-conventional antimicrobial approaches for chronic wound biofilms: Have we found the 'Chink in the armor'? *Biomedicines, 7*(2), 35.
Kloc, M., Ghobrial, R. M., Wosik, J., Lewicka, A., Lewicki, S., & Kubiak, J. Z. (2019). Macrophage functions in wound healing. *Journal of Tissue Engineering and Regenerative Medicine, 13*(1), 99–109.
Lai, F., Caddeo, C., Manca, M. L., Manconi, M., Sinico, C., & Fadda, A. M. (2020). What's new in the field of phospholipid vesicular nanocarriers for skin drug delivery. *International Journal of Pharmaceutics, 583*, Article 119398.
Lam, P. L., Lee, K. K. H., Wong, R. S. M., Cheng, G. Y. M., Bian, Z. X., Chui, C. H., … Gambari, R. (2018). Recent advances on topical antimicrobials for skin and soft tissue infections and their safety concerns. *Critical Reviews in Microbiology, 44*(1), 40–78.
Liu, H., Wang, C., Li, C., Qin, Y., Wang, Z., Yang, F., … Wang, J. (2018). A functional chitosan-based hydrogel as a wound dressing and drug delivery system in the treatment of wound healing. *RSC Advances, 8*(14), 7533–7549.
Malaekeh-Nikouei, B., Fazly Bazzaz, B. S., Mirhadi, E., Tajani, A. S., & Khameneh, B. (2020). The role of nanotechnology in combating biofilm-based antibiotic resistance. *Journal of Drug Delivery Science and Technology, 60*, Article 101880.
Martin, C., LiLow, W., Gupta, A., Cairul Iqbal Mohd Amin, M., Radecka, I. T., Britland, S., & Kenward, K. (2015). Strategies for antimicrobial drug delivery to biofilm. *Current Pharmaceutical Design, 21*(1), 43–66.
Masood, N., Ahmed, R., Tariq, M., Ahmed, Z., Masoud, M. S., Ali, I., & Hasan, A. (2019). Silver nanoparticle impregnated chitosan-PEG hydrogel enhances wound healing in diabetes induced rabbits. *International Journal of Pharmaceutics, 559*, 23–36.
Matica, M. A., Aachmann, F. L., Tøndervik, A., Sletta, H., & Ostafe, V. (2019). Chitosan as a wound dressing starting material: Antimicrobial properties and mode of action. *International Journal of Molecular Sciences, 20*, 5889.
Matos de Opitz, C. L., & Sass, P. (2020). Tackling antimicrobial resistance by exploring new mechanisms of antibiotic action. *Future Microbiology, 15*(9), 703–708.
Meers, P., Neville, M., Malinin, V., Scotto, A. W., Sardaryan, G., Kurumunda, R., & Perkins, W. R. (2008). Biofilm penetration, triggered release and in vivo activity of inhaled liposomal amikacin in chronic Pseudomonas aeruginosa lung infections. *The Journal of Antimicrobial Chemotherapy, 61*(4), 859–868.
Moeini, A., Pedram, P., Makvandi, P., Malinconico, M., & Gomez d'Ayala, G. (2020). Wound healing and antimicrobial effect of active secondary metabolites in chitosan-based wound dressings: A review. *Carbohydrate Polymers, 233*, Article 115839.
Onnainty, R., Onida, B., Páez, P., Longhi, M., Barresi, A., & Granero, G. (2016). Targeted chitosan-based bionanocomposites for controlled oral mucosal delivery of chlorhexidine. *International Journal of Pharmaceutics, 509*(1), 408–418.
Orazi, G., Ruoff, K. L., & O'Toole, G. A. (2019). Pseudomonas aeruginosa increases the sensitivity of biofilm grown Staphylococcus aureus to membrane-targeting antiseptics and antibiotics. *mBio, 10*(4), e01501–01519.
Palacio, M. L. B., & Bhushan, B. (2012). Bioadhesion: A review of concepts and applications. *Philosophical Transactions of the Royal Society A: Mathematical, Physical and Engineering Sciences, 370*(1967), 2321–2347.
Peers, S., Alcouffe, P., Montembault, A., & Ladavière, C. (2020). Embedment of liposomes into chitosan physical hydrogel for the delayed release of antibiotics or anaesthetics, and its first ESEM characterization. *Carbohydrate Polymers, 229*, Article 115532.
Pettinelli, N., Rodríguez-Llamazares, S., Abella, V., Barral, L., Bouza, R., Farrag, Y., … Lago, F. (2019). Entrapment of chitosan, pectin or κ-carrageenan within methacrylate based hydrogels: Effect on swelling and mechanical properties. *Materials Science and Engineering C, 96*, 583–590.
Poulakou, G., Lagou, S., & Tsiodras, S. (2019). What's new in the epidemiology of skin and soft tissue infections in 2018? *Current Opinion in Infectious Diseases, 32*(2), 77–86.
Robinson, A. M., Bannister, M., Creeth, J. E., & Jones, M. N. (2001). The interaction of phospholipid liposomes with mixed bacterial biofilms and their use in the delivery of bactericide. *Colloids and Surfaces A: Physicochemical and Engineering Aspects, 186*(1), 43–53.
Romana-Souza, B., Santos, J. S. D., Bandeira, L. G., & Monte-Alto-Costa, A. (2016). Selective inhibition of COX-2 improves cutaneous wound healing of pressure ulcers in mice through reduction of iNOS expression. *Life Sciences, 153*, 82–92.
Roy, R., Tiwari, M., Donelli, G., & Tiwari, V. (2018). Strategies for combating bacterial biofilms: A focus on anti-biofilm agents and their mechanisms of action. *Virulence, 9*(1), 522–554.
Rukavina, Z., & Vanić, Ž. (2016). Current trends in development of liposomes for targeting bacterial biofilms. *Pharmaceutics, 8*(2), 18.
Scriboni, A. B., Couto, V. M., Ribeiro, L. N. D. M., Freires, I. A., Groppo, F. C., de Paula, E., & Cogo-Müller, K. (2019). Fusogenic liposomes increase the antimicrobial activity of vancomycin against Staphylococcus aureus biofilm. *Frontiers in Pharmacology, 10*(1401).
Serra, R., Grande, R., Butrico, L., Rossi, A., Settimio, U. F., Caroleo, B., & de Franciscis, S. (2015). Chronic wound infections: The role of Pseudomonas aeruginosa and Staphylococcus aureus. *Expert Review of Anti-Infective Therapy, 13*(5), 605–613.
Smith, R., Russo, J., Fiegel, J., & Brogden, N. (2020). Antibiotic delivery strategies to treat skin infections when innate antimicrobial defense fails. *Antibiotics, 9*(2), 56.
Sohrabi, S., Haeri, A., Mahboubi, A., Mortazavi, A., & Dadashzadeh, S. (2016). Chitosan gel-embedded moxifloxacin niosomes: An efficient antimicrobial hybrid system for burn infection. *International Journal of Biological Macromolecules, 85*, 625–633.
Solleti, V. S., Alhariri, M., Halwani, M., & Omri, A. (2015). Antimicrobial properties of liposomal azithromycin for Pseudomonas infections in cystic fibrosis patients. *The Journal of Antimicrobial Chemotherapy, 70*(3), 784–796.
Tao, Y., Qian, L.-H., & Xie, J. (2011). Effect of chitosan on membrane permeability and cell morphology of Pseudomonas aeruginosa and Staphyloccocus aureus. *Carbohydrate Polymers, 86*(2), 969–974.
Tavakoli, S., & Klar, A. S. (2020). Advanced hydrogels as wound dressings. *Biomolecules, 10*(8), 1169.
Ternullo, S., Gagnat, E., Julin, K., Johannessen, M., Basnet, P., Vanić, Ž., … Škalko-Basnet, N. (2019). Liposomes augment biological benefits of curcumin for multitargeted skin therapy. *European Journal of Pharmaceutics and Biopharmaceutics, 144*, 154–164.
Ternullo, S., Schulte Werning, L. V., Holsæter, A. M., & Škalko-Basnet, N. (2019). Curcumin-in-deformable liposomes-in-chitosan-hydrogel as a novel wound dressing. *Pharmaceutics, 12*(1), 8.
Tottoli, E. M., Dorati, R., Genta, I., Chiesa, E., Pisani, S., & Conti, B. (2020). Skin wound healing process and new emerging technologies for skin wound care and regeneration. *Pharmaceutics, 12*(8), 735.
Venkatraman, S., & Gale, R. (1998). Skin adhesives and skin adhesion: 1. Transdermal drug delivery systems. *Biomaterials, 19*(13), 1119–1136.
Zorko, M., & Jerala, R. (2008). Alexidine and chlorhexidine bind to lipopolysaccharide and lipoteichoic acid and prevent cell activation by antibiotics. *The Journal of Antimicrobial Chemotherapy, 62*(4), 730–737.
Zou, W., Chen, Y., Zhang, X., Li, J., Sun, L., Gui, Z., … Chen, S. (2018). Cytocompatible chitosan based multi-network hydrogels with antimicrobial, cell anti-adhesive and mechanical properties. *Carbohydrate Polymers, 202*, 246–257.

Supporting Information

Liposomes-in-chitosan hydrogel boosts potential of chlorhexidine in biofilm eradication *in vitro*

Lisa Myrseth Hemmingsen[a], Barbara Giordani[b], Ann Kristin Pettersen[a], Beatrice Vitali[b], Purusotam Basnet[c,d] and Nataša Škalko-Basnet[a*]

[a] Drug Transport and Delivery Research Group, Department of Pharmacy, University of Tromsø The Arctic University of Norway, Universitetsvegen 57, 9037 Tromsø, Norway

[b] Molecular and applied microbiology, Department of Pharmacy and Biotechnology, University of Bologna, Via San Donato 19/2, 40127 Bologna, Italy

[c] IVF Clinic, Department of Obstetrics and Gynecology, University Hospital of North Norway, Sykehusvegen 38, 9019 Tromsø, Norway

[d] Women's Health and Perinatology Research Group, Department of Clinical Medicine, University of Tromsø The Arctic University of Norway, Universitetsveien 57, 9037 Tromsø, Norway

*Corresponding author: Nataša Škalko-Basnet at Drug Transport and Delivery Research Group, Department of Pharmacy, University of Tromsø The Arctic University of Norway, Universitetsvegen 57, 9037 Tromsø, Norway.

E-mail: natasa.skalko-basnet@uit.no, phone: +47 77646640

S1 Supplementary methods

S1.1 *Transmission electron microscopy (TEM)*

TEM was performed to confirm the size and evaluate the morphology of the CHX-liposomes. The procedure was conducted as described elsewhere (Obuobi, Julin, Fredheim, Johannessen, & Škalko-Basnet, 2020). The CHX-liposomes were examined on a Hitachi TEM HT7800 (Hitachi High-Tech Corporation, Japan) with accelerated voltage of 20 - 120 kV attached to a Morada camera. Prior to all examinations, the CHX-liposomes were applied to glow discharged carbon-coated 400-mesh grids (5 min) and subsequently stained with either uranyless or 3% uranyl acetate and 2% methylcellulose (Sigma-Aldrich, Steinheim, Germany). The system was air-dried prior to imaging.

S1.2 *Stability studies of hydrogels*

All hydrogels were evaluated over a period of 2-4 weeks for the stability. The evaluated parameters were texture properties and pH as described in Sections 2.5.1.

S1.3 Cell toxicity evaluation

The viability of cells after treatment with CHX-liposomes was evaluated in a HaCaT cell line (Ajayi et al., 2018). The cells were cultured in DMEM high glucose supplemented with 10 % (v/v) FBS and 1 % (v/v) penicillin-streptomycin. Cell suspensions (90 µL, 10^5cells/mL) plated in 96-well plates and incubated at 37 °C in 5 % CO_2 for 24 h. Next, 10 µL of the diluted CHX-liposomes (50, 10 and 1 µg mL^{-1} lipid) were added to the wells and the plates were incubated for another 24 h. Then, the CCK-8 kit reagent (10 µL) was added and the plates were incubated for 4 h. Finally, the absorbance was measured at 450 nm and referenced at 650 nm on the Tecan Spark M10 multimode plate reader (Tecan Trading AG, Switzerland). The toxicity was evaluated by comparing the CHX-liposome treated cells with control (treated with DMEM high glucose, 100 %, Cauzzo, Nystad, Holsæter, Basnet, & Škalko-Basnet, 2020).

S1.4 Determination of minimal lethal concentration (MLC)

The MLC of CHX-liposomes and CHX-liposomes-in-hydrogel, as well as CHX-hydrogel and free CHX, was determined by using the broth microdilution method. *S. aureus* ATCC 239213, *S. aureus* SO88 and *P. aeruginosa* ATCC 10145 were selected for testing. Briefly, all formulations were serially diluted in water in 96-multi-well plates and incubated together with microbial suspension (2×10^6 CFU mL^{-1}) in NB (*S. aureus* strains) or BHI (*P. aeruginosa*) at 37 °C for 24 h. To determine the microbicidal activity, 20 µL from each well were then spotted onto NB or BHI agar plates and further incubated at 37 °C for 48 h. MLC was defined as the minimal concentration that completely inhibited microbial viability. Three batches for each formulation were tested.

S2 Supplementary results

S2.1 *Summarization of all formulations*

All formulations examined in this study, are shown in Table S1.

Table S1. Formulations with their respective designation and composition.

Formulation	Designation	Composition
Empty liposomes	Liposomes	Lipoid S100
CHX loaded liposomes	CHX-liposomes	Lipoid S100 CHX
Chitosan (4.5%) hydrogel without glycerol	Glycerol-free hydrogel	Chitosan (4.5% w/w)
Chitosan (4.5%) hydrogel with glycerol	Hydrogel (4.5%)	Chitosan (4.5% w/w) Glycerol (9% w/w)
Empty liposomes in hydrogel with glycerol	Liposome-in-hydrogel	Lipoid S100 Chitosan (4.5% w/w) Glycerol (9% w/w)
CHX loaded liposomes in hydrogel without glycerol	CHX-in-glycerol-free hydrogel	Lipoid S100 CHX Chitosan (4.5% w/w)
CHX loaded liposomes in hydrogel with glycerol	CHX-liposomes-in-hydrogel	Lipoid S100 CHX

		Chitosan (4.5% w/w) Glycerol (9% w/w)
CHX in hydrogel with glycerol	CHX-hydrogel	CHX Chitosan (4.5% w/w) Glycerol (9% w/w)
Non-entrapped CHX	Free CHX	CHX (dissolved)

Concentrations refers to the concentrations in final formulations.

S2.2 *TEM-imaging*

After the size characterisation of CHX-liposomes, TEM-imaging was performed to confirm the results from the size measurements and investigate the morphology. The results (Figure S1) revealed spherical shapes with clear contours of the surfaces of the CHX-liposomes. The size of liposomes in the images was in agreement with the results obtained with photon correlation spectroscopy.

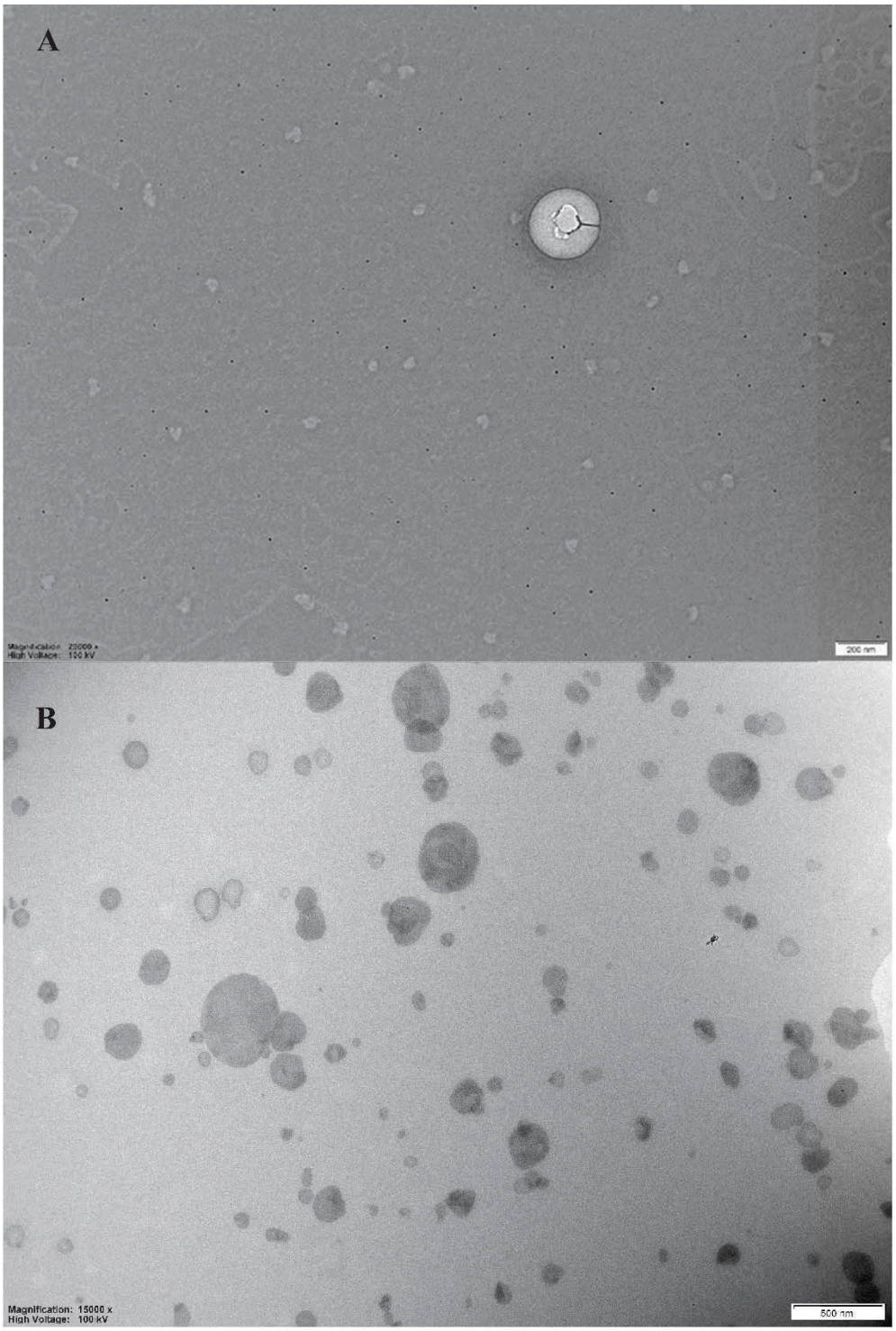

Figure S1.TEM-image of CHX-liposomes.

A: Scale bar: 200 nm, prepared uranyless. B: Scale bar: 500 nm, prepared utilizing uranyl acetate and methylcellulose.

S2.3 *Stability studies of hydrogels*

Table S2. Stability of chitosan hydrogels measured as the mechanical properties initially (0) and after two and four weeks.

Week	Glycerol-free hydrogel (4.5%)			Hydrogel (4.5%)			Liposomes-in-hydrogel (4.5%)			CHX-liposomes-in-glycerol-free hydrogel (4.5%)			CHX-liposomes-in-hydrogel (4.5%)		
	H	C	A	H	C	A	H	C	A	H	C	A	H	C	A
0	110 ± 1	205 ± 1	-166 ± 3	134 ± 1	166 ± 9	-150 ± 7	141 ± 3	167 ± 7	-155 ± 6	113 ± 2	171 ± 9	-141 ± 6	138 ± 4	156 ± 7	-145 ± 5
2	110 ± 6	165 ± 10	-135 ± 3	140 ± 6	149 ± 4	-138 ± 6	152 ± 4	166 ± 2	-160 ± 3	122 ± 8	162 ± 7	-141 ± 9	138 ± 5	159 ± 6	-148 ± 6
4	110 ± 7	193 ± 12	-153 ± 14	139 ± 7	155 ± 17	-145 ± 15	156 ± 9	158 ± 5	-152 ± 6	117 ± 8	166 ± 7	-139 ± 1	140 ± 8	156 ± 11	-144 ± 11

H = hardness (g), C = cohesiveness (g·s) and A = adhesiveness (g·s). The values are presented as a mean between three replicates with their respective SD.

Table S3. pH of the chitosan hydrogels initially (0) and two and four weeks after production.

Week	Glycerol-free hydrogel (4.5%)	Hydrogel (4.5%)	Liposomes-in-hydrogel (4.5%)	CHX-liposomes-in-glycerol-free hydrogel (4.5%)	CHX-liposomes-in-hydrogel (4.5%)
	pH				
0	4.5 ± 0.0	4.6 ± 0.0	4.7 ± 0.0	4.7 ± 0.0	4.6 ± 0.0
2	4.5 ± 0.0	4.6 ± 0.0	4.7 ± 0.0	4.6 ± 0.0	4.7 ± 0.0
4	4.4 ± 0.0	4.6 ± 0.0	4.7 ± 0.0	4.6 ± 0.0	4.7 ± 0.0

The results are expressed as means of three replicates with their respective standard SD.

S2.4 *CHX release profile*

In the initial trials, we conducted *in vitro* release studies over 24 h with intermediate (hourly) sampling to generate release profiles of formulated CHX. In the process, we noticed the fluid exchange between the donor and acceptor chamber in the Franz diffusion system. Consequently, the procedure was modified as to measure the release at the endpoint, as shown in Figure 2. However, the hourly release profiles of the investigated formulations are presented in Figure S2. We decided to proceed with the 24 h endpoint release measurements to assure the accuracy of final data. Since the main purpose of the experiment was to directly compare the different formulations, the endpoint values might be more reliable.

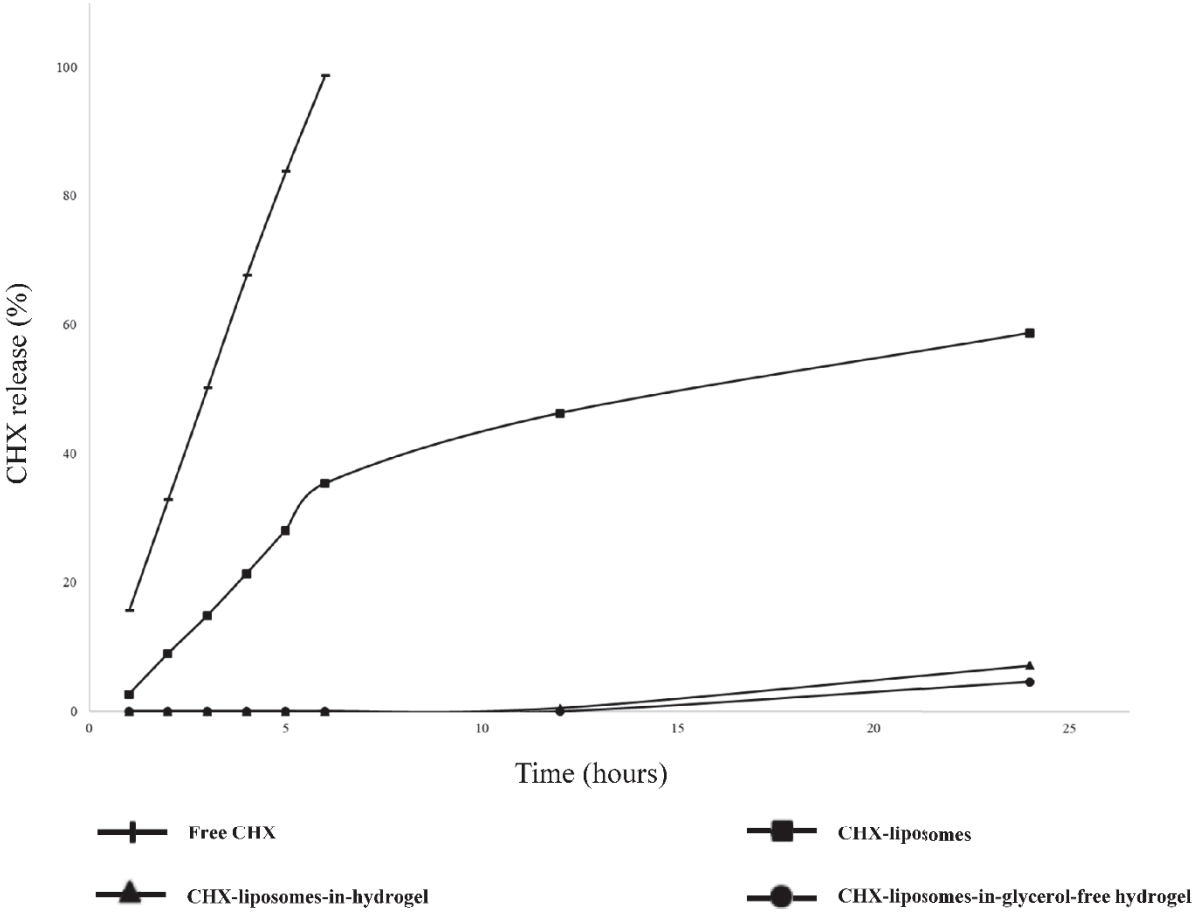

Figure S2. CHX release or permeation profile over 24 h at 32 °C. Results are represented as percentage of CHX released compared to the initial concentration. Results are expressed as means (n=2).

S2.5 *Cell toxicity evaluation*

In addition to the anti-inflammatory effects on macrophages, we sought to investigate the effects of the CHX-liposomes on the viability of immortalized human keratinocytes. It is important to evaluate the composition and preparation method to assure the safety of the carrier and immunological influences (Inglut et al., 2020). Both empty liposomes and chitosan intended for topical therapy have been evaluated in HaCaT cell lines previously (Kang et al., 2015; Lu et al., 2010). However, the CHX-liposomes have not been tested in human keratinocytes. The results from the toxicity evaluation (Figure S2) showed improved cell viability of the CHX-liposomes. The highest concentration showed the highest cell survival and both 50 and 10 μg mL^{-1} displayed a significantly higher survival than the control ($p < 0.05$). The difference between 1 and 10 μg mL^{-1} was not significant, however, the results could indicate trend in the concentration range evaluated in the current study. The cell toxicity of CHX has previously been reported (Borges et al., 2017; Hidalgo & Dominguez, 2001) in the same cell line. However, previous reports also show that liposomes are able to reduce the toxicity of other MAAs (Ron-Doitch et al., 2016).

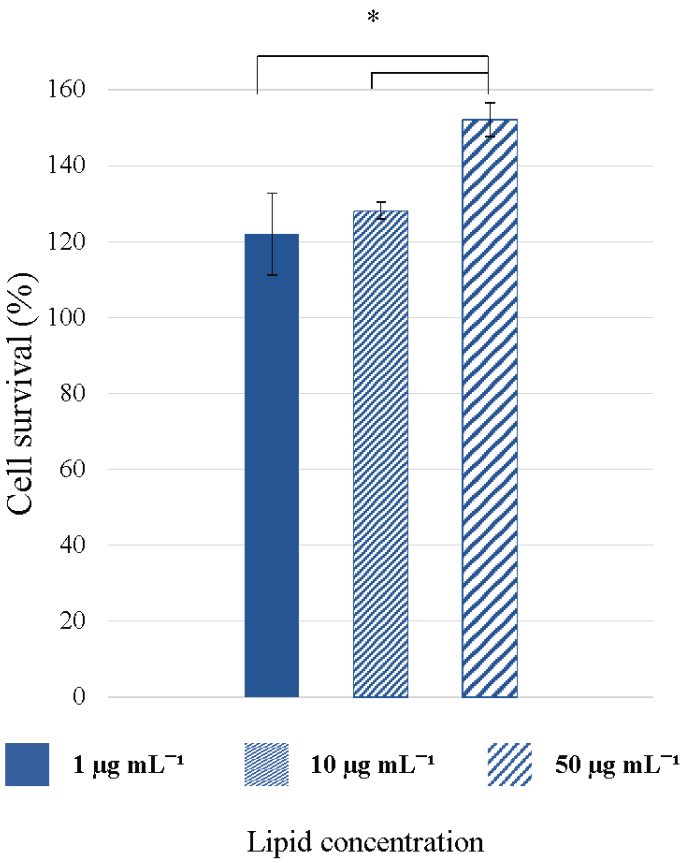

Figure S3. Toxicity evaluation of CHX-liposomes in HaCaT cell line. The results are expressed as the percentage of surviving cells in the treated group compared to control (100 %). The tested concentrations correspond to 1, 10 and 50 µg mL^{-1} lipid. All results are expressed as means of three parallels with their respective SD.

*) Significantly different ($p < 0.05$).

S2.6 *MLC of formulated and free CHX*

The MLC of CHX-liposomes and CHX-liposomes-in-hydrogel, as well as CHX-hydrogel and free CHX, was determined by using the broth microdilution method. Liposomes and hydrogels (4.5%) were also tested (section 3.7.1).

Table S4. MLC of formulated and free CHX in *S. aureus* ATCC29213, *S. aureus* SO88 and *P. aeruginosa* ATCC10145.

	MLC (μg mL^{-1})		
	S. aureus ATCC29213	*S. aureus* SO88	*P. aeruginosa* ATCC10145
CHX-liposomes	0.40	0.80	1.60
CHX-liposomes-in-hydrogel (4.5%)	0.16	0.31	0.63
CHX-hydrogel (4.5%)	0.16	0.31	0.63
Free CHX	0.40	0.80	1.60

MLC: minimal lethal concentration (n=3).

Supplementary references

Ajayi, C., Åberg, E., Askarian, F., Sollid, J. U. E., Johannessen, M., & Hanssen, A.-M. (2018). Genetic variability in the sdrD gene in Staphylococcus aureus from healthy nasal carriers. *BMC Microbiology*, 18(1), 34.

Borges, G. Á., Elias, S. T., da Silva, S. M. M., Magalhães, P. O., Macedo, S. B., Ribeiro, A. P. D., & Guerra, E. N. S. (2017). In vitro evaluation of wound healing and antimicrobial potential of ozone therapy. *Journal of Cranio-Maxillofacial Surgery*, 45(3), 364-370.

Cauzzo, J., Nystad, M., Holsæter, A. M., Basnet, P., & Škalko-Basnet, N. (2020). Following the Fate of Dye-Containing Liposomes In Vitro. *International Journal of Molecular Sciences*, 21(14), 4847.

Hidalgo, E., & Dominguez, C. (2001). Mechanisms underlying chlorhexidine-induced cytotoxicity. *Toxicology in Vitro*, 15(4), 271-276.

Inglut, C. T., Sorrin, A. J., Kuruppu, T., Vig, S., Cicalo, J., Ahmad, H., & Huang, H.-C. (2020). Immunological and Toxicological Considerations for the Design of Liposomes. *Nanomaterials*, 10(2), 190.

156 Kang, M. H., Yoo, H. J., Kwon, Y. H., Yoon, H. Y., Lee, S. G., Kim, S. R., . . . Choi, Y. W.
157 (2015). Design of Multifunctional Liposomal Nanocarriers for Folate Receptor-
158 Specific Intracellular Drug Delivery. *Molecular Pharmaceutics*, 12(12), 4200-4213.

159 Lu, G., Ling, K., Zhao, P., Xu, Z., Deng, C., Zheng, H., . . . Chen, J. (2010). A novel in situ
160 -formed hydrogel wound dressing by the photocross-linking of a chitosan derivative.
161 *Wound Repair and Regeneration*, 18(1), 70-79.

162 Obuobi, S., Julin, K., Fredheim, E. G. A., Johannessen, M., & Škalko-Basnet, N. (2020).
163 Liposomal delivery of antibiotic loaded nucleic acid nanogels with enhanced drug
164 loading and synergistic anti-inflammatory activity against S. aureus intracellular
165 infections. *Journal of Controlled Release*, 324, 620-632.

166 Ron-Doitch, S., Sawodny, B., Kuhbacher, A., David, M. M. N., Samanta, A., Phopase, J., . . .
167 Rupp, S. (2016). Reduced cytotoxicity and enhanced bioactivity of cationic
168 antimicrobial peptides liposomes in cell cultures and 3D epidermis model against
169 HSV. *Journal of Controlled Release*, 229, 163-171.

Paper II

marine drugs

MDPI

Article

Chitosomes-In-Chitosan Hydrogel for Acute Skin Injuries: Prevention and Infection Control

Lisa Myrseth Hemmingsen [1], Kjersti Julin [2], Luqman Ahsan [1], Purusotam Basnet [3,4], Mona Johannessen [2] and Nataša Škalko-Basnet [1,*]

[1] Drug Transport and Delivery Research Group, Department of Pharmacy, University of Tromsø The Arctic University of Norway, Universitetsvegen 57, 9037 Tromsø, Norway; lisa.m.hemmingsen@uit.no (L.M.H.); luqmaan.ahsan@gmail.com (L.A.)

[2] Research Group for Host-Microbe Interaction, Department of Medical Biology, University of Tromsø The Arctic University of Norway, Sykehusvegen 44, 9037 Tromsø, Norway; kjersti.julin@uit.no (K.J.); mona.johannessen@uit.no (M.J.)

[3] IVF Clinic, Department of Obstetrics and Gynecology, University Hospital of North Norway, Sykehusvegen 38, 9019 Tromsø, Norway; purusotam.basnet@uit.no

[4] Women's Health and Perinatology Research Group, Department of Clinical Medicine, University of Tromsø The Arctic University of Norway, Universitetsvegen 57, 9037 Tromsø, Norway

* Correspondence: natasa.skalko-basnet@uit.no; Tel.: +47-77646640

Abstract: Burns and other skin injuries are growing concerns as well as challenges in an era of antimicrobial resistance. Novel treatment options to improve the prevention and eradication of infectious skin biofilm-producing pathogens, while enhancing wound healing, are urgently needed for the timely treatment of infection-prone injuries. Treatment of acute skin injuries requires tailoring of formulation to assure both proper skin retention and the appropriate release of incorporated antimicrobials. The challenge remains to formulate antimicrobials with low water solubility, which often requires carriers as the primary vehicle, followed by a secondary skin-friendly vehicle. We focused on widely used chlorhexidine formulated in the chitosan-infused nanocarriers, chitosomes, incorporated into chitosan hydrogel for improved treatment of skin injuries. To prove our hypothesis, lipid nanocarriers and chitosan-comprising nanocarriers (≈250 nm) with membrane-active antimicrobial chlorhexidine were optimized and incorporated into chitosan hydrogel. The biological and antibacterial effects of both vesicles and a vesicles-in-hydrogel system were evaluated. The chitosomes-in-chitosan hydrogel formulation demonstrated promising physical properties and were proven safe. Additionally, the chitosan-based systems, both chitosomes and chitosan hydrogel, showed an improved antimicrobial effect against *S. aureus* and *S. epidermidis* compared to the formulations without chitosan. The novel formulation could serve as a foundation for infection prevention and bacterial eradication in acute wounds.

Keywords: chitosan-infused liposomes; chitosan hydrogel; membrane-active antimicrobials; bacterial eradication; acute wound management; *Staphylococcaceae*

Citation: Hemmingsen, L.M.; Julin, K.; Ahsan, L.; Basnet, P.; Johannessen, M.; Škalko-Basnet, N. Chitosomes-In-Chitosan Hydrogel for Acute Skin Injuries: Prevention and Infection Control. *Mar. Drugs* **2021**, *19*, 269. https://doi.org/10.3390/md19050269

Academic Editor: Soo Jin Heo

Received: 21 April 2021
Accepted: 10 May 2021
Published: 12 May 2021

1. Introduction

Acute skin injuries, such as burns, cuts, or other trauma, are painful breaches of the skin. With the growing numbers of resistant pathogens, we need to prevent bacterial infections and treat these breaches timely and efficiently. Larger skin injuries such as burn trauma cause destruction of the first line of defence, impairing both the physical barrier and the immune system [1]. These entry points are leaving the patients more vulnerable to bacterial colonisation and infections [1]. Additionally, it is estimated that as much as 75% of attributable mortality in this patient group is linked to infections, making this the primary cause of death [2]. Here, skin and soft tissue infections (SSTIs) are the second leading healthcare-associated class following burn injuries [3] and one of the most common bacterial infections in the human population [4]. The burns are often prone to biofilm

formation, increasing the complexity of the wounds and leading to chronicity [5]. The escalating threat of antimicrobial resistance and biofilm-producing strains influence the treatment outcome [6]. The incidents of burn injuries are ostensibly decreasing [7]; however, nearly 9 million injuries globally were related to fire, heat, or hot substances, according to the Global Burden of Disease 2017 study [8].

In pursuance of novel treatment options for burns and other acute wounds, formulations aiding both microbial eradication and the wound-healing process are highly desirable. Pharmaceutical technology and nanotechnology could be utilized to increase both these processes [9]. Herein, the selection of the materials exhibiting intrinsic wound healing, as well as antimicrobial properties, is fundamental. Chitosan, a natural, cationic polymer, derived from the deacetylation of chitin [10], has attracted attention as a biomaterial for wound management [11]. This bioactive polymer, found in marine crustaceans, fungi, and insects, is regarded both biocompatible and biodegradable [12,13] with confirmed intrinsic antimicrobial [14] and wound-healing properties [15]. As a result, chitosan has been utilized in the preparation of various pharmaceutical formulations, ranging from solid and semi-solid to liquid forms [16]. However, in topical skin therapy, lipid-based delivery systems, such as liposomes, are often particularly interesting because of their potential interaction with the skin structure [17] as well as being a solubilizer for substances with lowered solubility [18]. Moreover, the antimicrobial potential of the lipid-based vesicles, liposomes, can be enhanced by coating of their surface or inclusion of the bioactive polymers to both improve wound healing and antimicrobial properties [19]. The possibility to infuse liposomes with chitosan forming chitosomes was previously proposed by our group [20]. These novel vesicles were challenged against vaginal *Candida* infections and both chitosomes alone and chitosomes with incorporated metronidazole eradicated *Candida* [20]. These chitosomes, unlike many other nanoparticle-based formulations, were prepared through a rapid one-step method.

Considering the improved antibacterial action, combining chitosomes with membrane targeting antimicrobials could further increase the antimicrobial capacity through synergic effects on the bacterial membrane [21]. Chlorhexidine (CHX), a membrane active antimicrobial (MAA), is frequently used in the prevention of SSTIs and commonly used in burn units [22]. The main antibacterial mechanism of CHX is proposed to be destruction of the bacterial membrane; however, precipitation of the cytoplasm has been observed when CHX is administered in higher concentrations [23]. Furthermore, topical formulations of CHX are commonly used in combinational therapy for chronic wounds [24]. Exploiting the activity of MAAs, such as CHX, in combination with chitosan of higher molecular weight, affecting the bacterial membrane [25], could prove beneficial in bacterial prevention and eradication.

Liposomal suspensions are not suitable for direct application onto the skin due to low viscosity and retention; this limitation is often solved by incorporating the vesicles into hydrogels [26]. In addition to serving as a vehicle for liposomes, the hydrogel could also provide an improved release profile and further increase accumulation of the antimicrobial compound in the wound area [27]. In this study, chitosan was selected as a hydrogel base due to its bioadhesive and biocompatible properties, which are suitable for pharmaceutical applications [28,29]. Moreover, we aimed to tailor the release of CHX to assure rapid and efficient microbial prevention and eradication. Although the hydrogel would swell to a certain degree in physiological fluids [30], to assure the fast release as well as prolonged retention on the skin, we combined chitosomes with chitosan hydrogels (Figure 1).

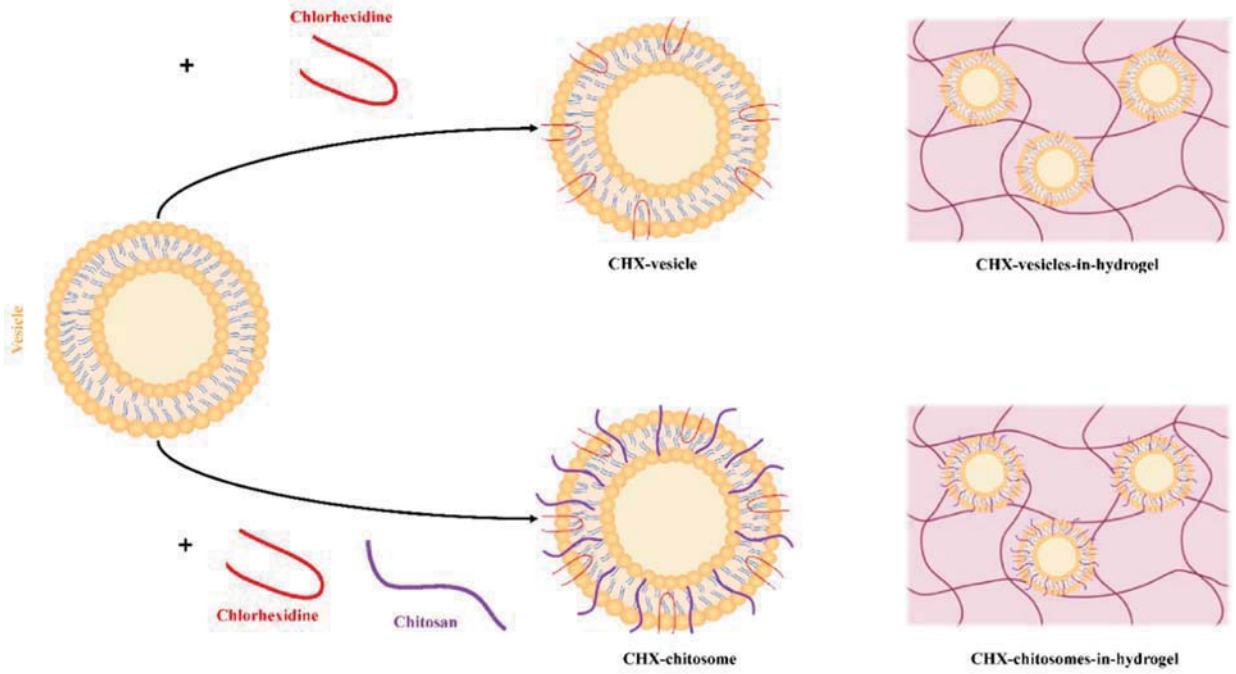

Figure 1. Illustration of the two types of vesicles utilized in the current study. In the top-half of the illustration, the CHX-vesicles (chitosan-free) both as vesicle alone and incorporated in hydrogel network are presented. In the bottom-half of the illustration, the chitosan-infused vesicles, chitosomes, with entrapped CHX are presented both as vesicles alone and incorporated in hydrogel.

In our previous study, we utilized conventional liposomes as primary vesicles for CHX further incorporated in chitosan hydrogel for the treatment of chronic wounds. The novel formulation assured sustained CHX release [18]. However, that formulation would not be optimal for acute wound treatment. To modify the rate of the CHX release to achieve faster and efficient antimicrobial action, we propose chitosomes as primary vesicles for CHX. Andersen et al. showed an initial burst-release from their chitosomes and postulated that this effect might be due to the arrangement of the pharmaceutical compound in the bilayer [31]. In chitosomes, CHX is most likely incorporated within the bilayer and associated with the surface of chitosomes, allowing a faster initial release of CHX. Additionally, chitosan infused in the vesicles (chitosomes) is surface-available and has the possibility of closely interacting with the bacterial membrane immediately (Figure 1). These two factors could act in synergy, providing a faster onset of the antimicrobial action. Since most of the CHX is preserved within the bilayer of chitosomes, it could contribute to the long-term effect, similar to what has been previously confirmed for conventional CHX liposomes [18]. We hypothesized that combining CHX with chitosan-infused vesicles, chitosomes, could improve microbial eradication, and in a combination with the hydrogel network, serve as a promising platform for the prevention of bacterial colonization of acute wounds.

2. Results and Discussions

2.1. Vesicle Characteristics

Chitosan-based formulations could potentially support the wound-healing process in all stages of the complex healing cascade [32]. Additionally, hydrogels comprising this bioactive polymer could counteract the factors impairing healing processes by anti-inflammatory and antimicrobial actions [33]. Among all biomaterials, chitosan is one of the most frequently used ingredients in hydrogel preparation [34,35]; however, other formulations are also reported such as nanofibers [36] and nanoparticles [37]. Moreover, chitosan is often used as a coating material for vesicles [14]. In this study, we intended to exploit chitosan's beneficial intrinsic properties in both the primary and secondary vehicle

to maximize the potential treatment outcome. As this formulation is intended for topical therapy of skin burns and other acute wounds, lipid-based vesicles were selected as the primary vesicle.

2.1.1. Vesicle Characteristics

The size and zeta potential of vesicles are known to influence the characteristics of the hydrogel [38] and the treatment outcome. Consequently, we evaluated the size, zeta potential, CHX entrapment, and pH of the vesicles (Table 1). These properties are influenced by the method of preparation. The one-pot method generates larger vesicles with broader size distribution [31]; therefore, probe sonication was utilized to reduce the vesicle size. The vesicle size was additionally influenced by the incorporation of CHX. A single sonication cycle was sufficient to reach the intended size. For comparison, to reach the same vesicle size, the empty vesicles required several sonication cycles. Our targeted vesicle size was around 200 nm, which was the lower end of the optimal vesicle size range intended for dermal delivery [39].

Table 1. Vesicle characteristics.

	Size (nm)						
	Peak 1 **%**	**Peak 2** **%**	**Peak 3** **%**	**PI** [1]	**Zeta Potential (mV)**	**EE** [2] **%**	**pH**
PL-EMP	31 ± 9 5 ± 3	62 13	169 ± 18 90 ± 4	0.18 ± 0.01	0.6 ± 0.0	-	5.6 ± 0.0
CHI-EMP	14 ± 4 5 ± 4	41 ± 4 30 ± 12	150 ± 3 65 ± 16	0.22 ± 0.01	11.5 ± 0.3	-	4.4 ± 0.0
PL-CHX	16 ± 7 2 ± 1	66 ± 15 16 ± 5	243 ± 13 81 ± 6	0.32 ± 0.03	53.6 ± 2.0	68 ± 5	7.0 ± 0.3
CHI-CHX	14 ± 1 3 ± 1	79 ± 5 29 ± 15	260 ± 3 69 ± 16	0.30 ± 0.00	79.0 ± 3.7	74 ± 2	5.5 ± 0.1

Results are expressed as means with their respective SD (n = 3). PL-EMP = plain, empty vesicles, CHI-EMP = empty chitosomes, PL-CHX = plain, CHX-vesicles, CHI-CHX = CHX-chitosomes. [1] Polydispersity index. [2] Entrapment efficiency (%).

The empty vesicles displayed a slightly smaller size; however, these vesicles served as controls, and the difference would have limited effect on the overall comparison as all vesicles were loaded into hydrogel networks [38]. To confirm the size and to investigate the morphology, we utilized transmission electron microscopy (TEM, Figure 2). Both the empty and CHX-chitosomes were found to be spherical. The size distribution corresponded to the results obtained with the particle sizer. Considering conventional liposomes, the infusion of chitosan did not significantly alter the shape of the vesicles.

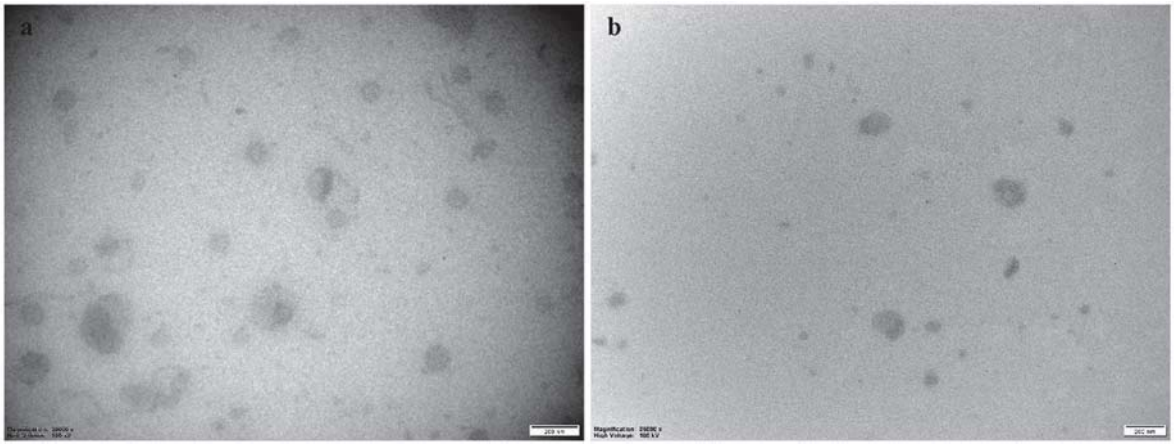

Figure 2. TEM images of chitosomes. (**a**) CHI-EMP, (**b**) CHI-CHX. CHI-EMP = empty chitosomes, CHI-CHX = CHX-chitosomes. Scale bars: 200 nm.

The zeta potential of vesicles was highly influenced by both chitosan and CHX (Table 1). Plain, empty vesicles were, due to the high content of phosphatidylcholine, exhibiting neutral surface; the addition of chitosan (chitosomes) augmented the zeta potential by almost 11 mV (Table 1), as expected. The incorporation of CHX in plain vesicles contributed to increased surface charge to 53 mV due to its incorporation within and on the vesicles (Figure 1). The vesicles comprised of both chitosan and CHX (CHX-chitosomes) exhibited the highest zeta potential, indicating that chitosan and CHX have synergic effects on the surface charge. Moreover, these results indicate that both chitosan and CHX are available on the surface of the vesicles or partially stretches out to the surface from within the bilayer. The amphipathic nature of CHX would also substantiate this postulation; however, the substantial increase might suggest that CHX is positioned even further out within the surface of the chitosan-infused vesicles. The zeta potential of plain, empty vesicles and empty chitosomes is directly comparable to the results of Andersen et al. [20]. In topical antimicrobial therapy, positively charged vesicles could be beneficial in bacterial eradication in wounds. Bacterial membranes are slightly negatively charged, whereas mammalian membranes are closer to neutral [40]; therefore, the potential interaction between a positively charged formulation and the bacteria could improve both efficacy and safety [41]. As reported by Ahani and colleagues, where cationic liposomes were proven beneficial in bacterial eradication [42].

The pH of vesicle suspensions was also influenced by CHX presence; an increased pH of more than one unit was determined for CHX-formulations as compared with the corresponding formulation without CHX. Additionally, the effect of acetic acid used in the production of chitosomes was detected in the pH values.

Due to the interactions between CHX and the vesicles and the increased zeta potential, we anticipated a relatively high drug entrapment. However, chitosan could potentially influence the accommodation of CHX within or on the bilayer. High entrapment is important in the development of novel antibacterial formulations to ensure sufficient bacterial eradication and avoid bacteria regrowth. The entrapment efficiencies for both the plain vesicles and chitosomes were relatively high (Table 1). Remarkably, the entrapment was not influenced by the inclusion of chitosan in the vehicles. The high entrapment could also be a result of the interaction between the lipids of the vesicular bilayer and CHX.

2.1.2. Surface-Available Chitosan

The presence of chitosan on the surface of the chitosomes is indicated by the rise of the zeta potential as compared to the plain vesicles. We sought to compare the initial chitosan concentration with the amount available on the chitosome surface. In addition, we investigated whether the concentration of surface-available chitosan would be affected by the incorporation of CHX within the vesicles. The percentage of surface-available chitosan is presented in Table 2. As seen in the table, the surface-available chitosan for chitosomes both with and without CHX was approximately the same. The zeta potential indicates that CHX was positioned within the bilayer; however, the co-accommodation of chitosan was not influenced by the presence of CHX. In antimicrobial therapy, the aim is to preserve chitosan on the surface of the vesicles, allowing chitosan to interact with the bacteria and cause disturbance to the bacterial membrane, since this is considered crucial for its antimicrobial effects [25]. Additionally, we wanted to exploit the potential anti-inflammatory properties of chitosan hydrogel as well as the chitosomes [43]. As indicated in Table 2, approximately 50% of the initial chitosan concentration was present on the vesicle surface, as expected considering the molecular size of chitosan. Moreover, chitosan was accessible to interact with both bacteria and macrophages, therefore improving the healing.

Table 2. Surface-available chitosan of the empty and loaded chitosan-infused vesicles.

	Surface-Available Chitosan (%) [3]
CHI-EMP	50.2 ± 2.9
CHI-CHX	48.5 ± 5.6

Results are expressed as means with their respective SD (n = 3). CHI-EMP = empty chitosomes, CHI-CHX = CHX-chitosomes. [3] Percentage of initial chitosan concentration (%).

2.1.3. Vesicle Stability

Vesicle stability should be improved upon their incorporation in hydrogel; nevertheless, we evaluated the stability of the vesicle suspensions two and four weeks after preparation to assure that even suspensions are stable (Table 3). The stability of these suspensions is influenced by the zeta potential. Two formulations, namely PL-CHX and CHI-CHX, had a zeta potential above 30 mV, which is expected to stabilize vesicles and preserve their homogeneity [41]. The vesicle size and zeta potential of CHX-loaded formulations did not change significantly (defining significant over 95%) throughout these four weeks, as expected, indicating that the repulsing effects of the CHX-chitosomes and CHX-vesicles are strong enough to stabilize the suspension. However, the empty chitosomes had a significant increase in zeta potential between the second and fourth week (p = 0.0005), which would imply that hydrogels are needed to preserve the stability of drug-free chitosomes. In addition, the empty, plain vesicles also exhibited a significant change in the zeta potential between preparation and second week (p = 0.009), displaying less stability of these vesicles with surfaces closer to neutral. The pH of all formulations was unaffected during the four weeks of the stability evaluation.

Table 3. Surface-available chitosan on the empty and CHX-loaded chitosomes.

	Week	Size (nm) Peak 1 %	Peak 2 %	Peak 3 %	PI [1]	Zeta Potential (mV)	pH
PL-EMP	2	33 ± 3 6 ± 2	133 ± 36 72 ± 35	331 ± 246 33 ± 39	0.20 ± 0.02	−1.7 ± 0.4	5.6 ± 0.1
	4	17 ± 1 2 ± 1	69 ± 21 26 ± 27	229 ± 49 62 ± 31	0.21 ± 0.02	−3.1 ± 1.0	5.6 ± 0.4
CHI-EMP	2	18 ± 2 3 ± 1	58 ± 9 15 ± 2	152 ± 3 82 ± 1	0.22 ± 0.01	12.0 ± 0.2	4.4 ± 0.0
	4	18 ± 5 4 ± 1	56 ± 6 23 ± 23	144 ± 24 86 ± 1	0.22 ± 0.01	14.4 ± 0.5	4.5 ± 0.1
PL-CHX	2	11 ± 0 1 ± 1	64 ± 8 18 ± 4	254 ± 21 81 ± 4	0.33 ± 0.03	55.9 ± 0.9	6.9 ± 0.2
	4	22 ± 13 4 ± 3	101 ± 76 43 ± 43	225 ± 11 82 ± 5	0.32 ± 0.03	55.7 ± 1.0	7.2 ± 0.1
CHI-CHX	2	14 ± 3 3 ± 3	54 ± 9 21 ± 20	222 ± 41 75 ± 22	0.30 ± 0.01	79.8 ± 4.5	5.5 ± 0.1
	4	12 ± 1 2 ± 1	64 ± 17 21 ± 7	215 ± 49 76 ± 8	0.30 ± 0.02	83.0 ± 1.7	5.5 ± 0.1

Vesicle characteristics evaluated 2 and 4 weeks after preparation. Results are expressed as means with their respective SD (n = 3). PL-EMP = plain, empty vesicles, CHI-EMP = empty chitosomes, PL-CHX = plain, CHX-vesicles, CHI-CHX = CHX-chitosomes. [1] Polydispersity index.

2.2. Hydrogel Characterization

2.2.1. Hydrogel Characterization

Texture analysis is an easy method to monitor the hydrogel production, both as an in-process control as well as a method to determine the effects of modifications in the

hydrogel composition [44]. Moreover, it can be utilized for the monitoring of long-term hydrogel stability [45]. Considering the use of hydrogels as skin formulations, this method has been utilized to assess the user-friendliness of both conventional and physical chitosan hydrogels [45,46]. We aimed to utilize the procedure as an in-process control and examine the texture properties upon incorporation of the different vesicles into the original chitosan network. This analysis generates the hardness, cohesiveness, and adhesiveness as quality attributes of the hydrogels. The hardness is expressed as the maximum force required for compressing the hydrogel. The cohesiveness is the level of deformation to the hydrogel upon compression, whereas the adhesiveness describes the hydrogel's adhesion to the probe compressed into the hydrogel [44]. All parameters for all five hydrogel formulations are presented in Figure 3.

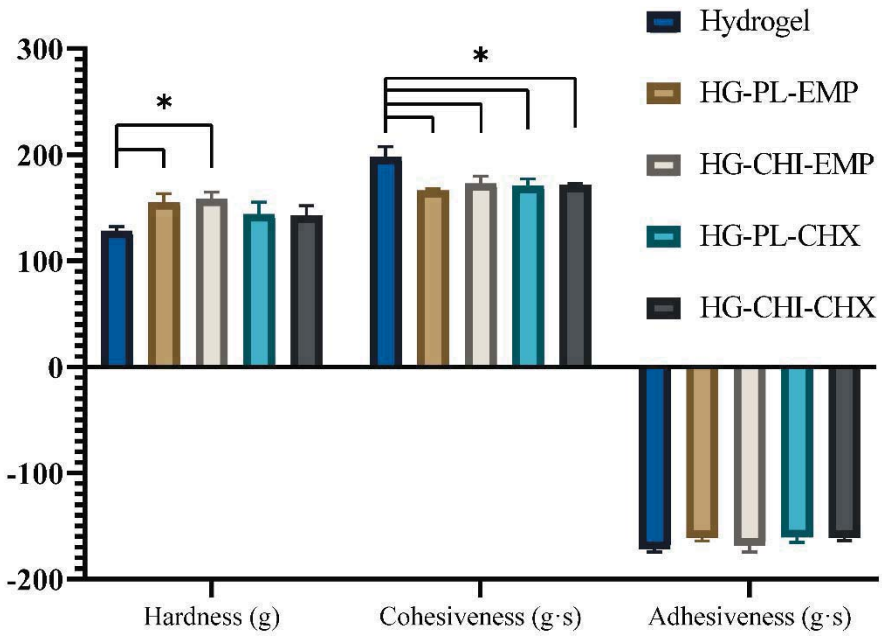

Figure 3. Texture properties of the different chitosan hydrogel formulations All results are expressed as means with their respective SD (n = 3). Hydrogel = plain hydrogel, HG-PL-EMP = plain, empty vesicles-in-hydrogel, HG-CHI-EMP = empty chitosomes-in-hydrogel, HG-PL-CHX = plain, CHX-vesicles-in-hydrogel, HG-CHI-CHX = CHX-chitosomes-in-hydrogel. * $p < 0.05$.

The hardness of the hydrogels incorporating empty vesicles, both plain vesicles and chitosomes, increased compared to the plain (vesicle free) chitosan hydrogel. This increased hardness is in accordance with the findings by Jøraholmen et al. [45]; however, the slight increase in the mean hardness of the CHX-vesicles-containing hydrogels is not significant compared to the plain hydrogel or the hydrogels without CHX. The cohesiveness of the plain chitosan hydrogel was significantly higher than all other formulations (Figure 3). These findings are deviating from our previously reported results on conventional liposomes incorporated in hydrogel. However, the adhesiveness data were in agreement with our previous findings [18]. Moreover, we used texture analysis to determine the stability of the hydrogel formulations; all hydrogels proved to remain relatively stable over a period of four weeks (Table S1).

Considering the pH measurements, no larger variations between the different hydrogels were observed. The values were ranging between the plain hydrogel, with the lowest pH at 4.6, to HG-PL-EMP, displaying the highest pH of 4.9. The rest of the hydrogels had a pH of 4.7. Normal, intact human skin has a pH between 4 and 6 [47], while wounds often display a more alkaline environment [48]. It was suggested that wound healing is improved under more acidic conditions [49], and that the optimal growth conditions of many common skin pathogens are closer to neutral [48]. Therefore, restoring the acidic

wound environment would be considered advantageous. Our hydrogels would clearly restore the acidic environment and potentially enhance the healing process. Nevertheless, it is important to state that an acidic pH of skin dressings alone is not sufficient to maintain proper healing cascades [50]. Therefore, we utilized chitosan and CHX to enhance the antimicrobial and anti-inflammatory properties.

2.2.2. Viscosity Evaluation

In addition to the texture analysis, we sought to investigate the rheological behavior of the plain hydrogel and hydrogels comprising CHX-vesicles. The rheological behavior could elucidate the applicability and therefore the user-friendliness of semi-solid formulations [51]. These properties could be influenced by the temperature. Consequently, we evaluated the hydrogels at 25 °C (Figure 4a,b) and 32 °C (Figure 4c,d), corresponding to dermal application. As seen in Figure 4, the shear stress increased (Figure 4a,c) and viscosity decreased (Figure 4b,d) with increasing shear rate. All hydrogels demonstrated pseudoplastic flow with shear thinning behavior. The rheological behavior was seemingly not influenced by the incorporation of CHX-chitosomes or plain vesicles with CHX. We did not observe any differences in viscosity between different hydrogels as we did for the cohesiveness determined in the texture analysis. Kaplan and colleagues incorporated liposomes in chitosan hydrogel and observed decreased viscosity upon the incorporation of liposomes [52]. However, in their study, the chitosan concentration was significantly lower than in our study. Phospholipids are known to act as plasticizers [53]; therefore, they could increase the mobility within the hydrogel network, leading to a decreased viscosity. Yet, this was not observed in our study. The rheological behavior of vesicles-in-hydrogel is highly influenced by the composition of carriers, lipid concentration, type of polymer, and polymer concentration [54].

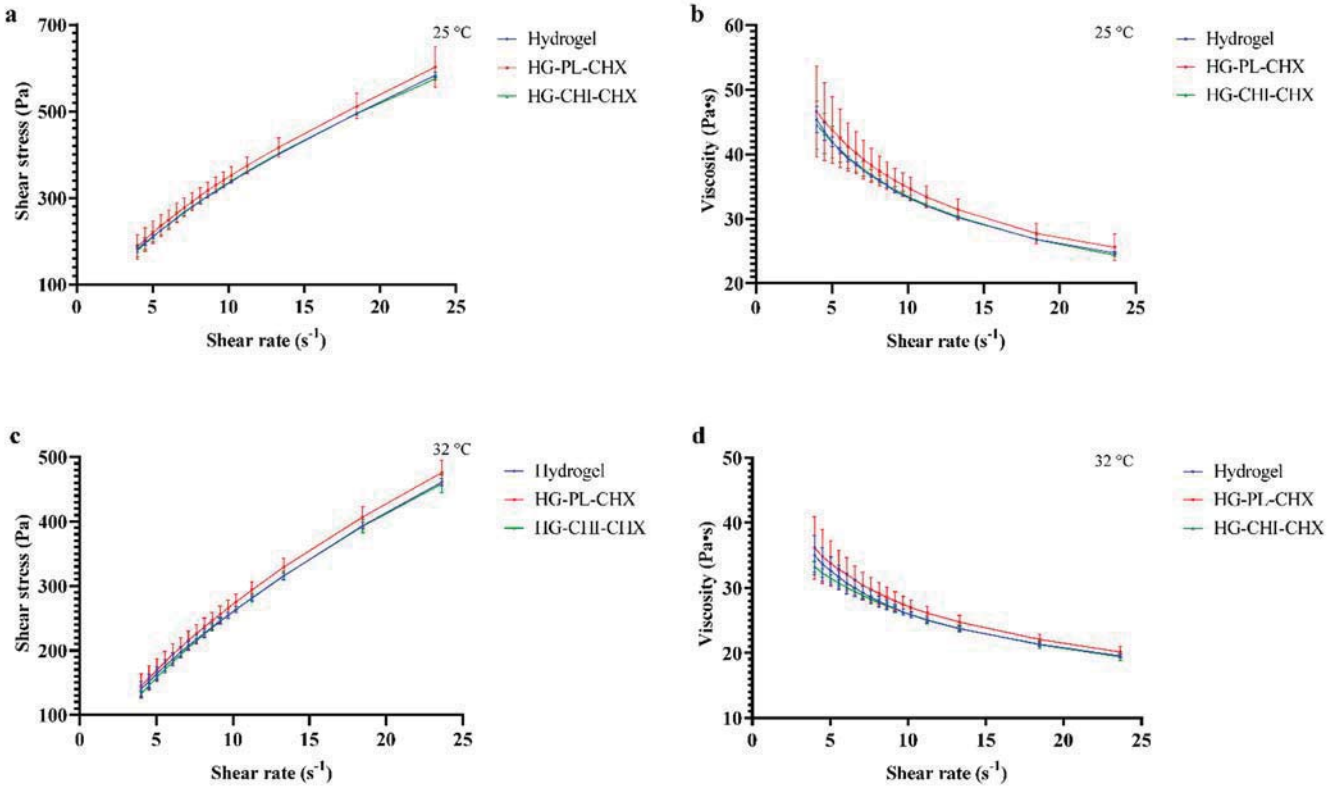

Figure 4. Rheological characteristics. Shear rate was plotted against shear stress (**a**,**c**) and viscosity (**b**,**d**) at 25 °C (**a**,**b**) and 32 °C (**c**,**d**). The results are expressed as means with their respective SD (n = 3). Hydrogel = plain hydrogel, HG-PL-CHX = plain, CHX-vesicles-in-hydrogel, HG-CHI-CHX = CHX-chitosomes-in-hydrogel.

Contrary to the effect of incorporation of vesicles into the hydrogel network, the temperature affected the rheological behavior of all hydrogels. The same trends observed at 25 °C were observed at 32 °C as well; however, shear stress and viscosity were significantly lowered at 32 °C. In pharmaceutical formulations, both the shear thinning behavior and the lowered viscosity at application-site temperature (32 °C for skin) could improve the user-friendliness upon administration [51].

2.3. CHX Release

Topical, localized treatment of burn injuries and acute wounds is preferred, as this provides sufficient concentration of the antimicrobial compound in the infected area [55]. Consequently, patients could avoid both bacterial regrowth and unnecessary adverse systemic effects. We compared the CHX release and permeation from formulated CHX, both the vesicles and vesicles-in-hydrogel, to CHX dissolved in the acceptor medium (Figure 5). As anticipated, the dissolved CHX permeated faster than CHX from all other formulations. Only the CHX-chitosomes released a significantly greater amount than both vesicles-in-hydrogel formulations under the tested conditions. The CHX-chitosomes seemingly had a higher mean release than the plain vesicles with CHX. This might be due to the competition between CHX and chitosan within the lipid bilayer of the vesicles, as CHX might be expelled. Interestingly, comparing the vesicles-in-hydrogel, the CHX release from the formulation comprising chitosomes displayed sustained release; however, it was not significantly relevant. We postulate that this effect might be due to the effect of the positive charge of the surrounding chitosan hydrogel network. The zeta potential of CHX-chitosomes was significantly higher than the zeta potential of plain vesicles with CHX (Table 1), which might lead to stronger repulsion between the hydrogel and the CHX-chitosomes. This similar effect has previously been demonstrated by Hurler and colleagues [38]. This repulsive effect could also stabilize the vesicles incorporated in the hydrogel network. However, the effect of the wound exudate should not be neglected [18]. Moreover, in an in vivo challenge, the hydrogel would be exposed to wound bed comprising exudates and blood components resulting in its swelling [30].

Vesicles-in-hydrogels often offer a prolonged drug release profile, important for chronic wound treatment [56].

2.4. Evaluation of Potential Toxicity

The biocompatibility of any formulation intended for burns and other wounds is essential for a successful treatment outcome. Reduced cell compatibility could prevent or delay the intricate healing cascade. After skin disruption, keratinocytes migrate and proliferate to close the wound area and are, together with fibroblasts, fundamental in the healing process [57]. Therefore, cell toxicity studies were performed for both vesicles (Figure 6) and hydrogels (Figure 7) after 24 h exposure of each formulation to keratinocytes. The treated cells were compared with non-treated cells to assess the safety and compatibility of each formulation. As seen in Figure 6, the vesicles did not impair the cell survival, regardless of their concentration. Additionally, the highest lipid concentration (50 µg/mL) of chitosomes exhibited a significantly improved cell proliferation as compared to the cells treated with only medium (control). Both empty chitosomes ($p = 0.02$) and CHX-chitosomes ($p = 0.01$) improved cell survival in the highest lipid concentration. The improved proliferation of keratinocytes exposed to chitosan can be attributed to its positive effects on cell growth. The vesicles and chitosomes with CHX appeared to display a concentration-dependent trend with improved cell viability in the highest concentrations. Other chitosan-comprising formulations such as chitosan-coated liposomes have been evaluated in various cell lines. Mengoni and colleagues demonstrated compatible chitosan-coated liposomes in keratinocytes (HaCaT cells) [58]. Phetdee and colleagues investigated the proliferation in HaCaT cells treated with chitosan-coated liposomes and reported no negative proliferative effects [59]. Additionally, proliferative effects have been reported in fibroblasts treated with chitosan [60]. On the other hand, CHX has been shown

to demonstrate toxicity in both fibroblasts [61] and keratinocytes [62]; however, we did not detect any toxicity issues with CHX-chitosomes (Figure 6).

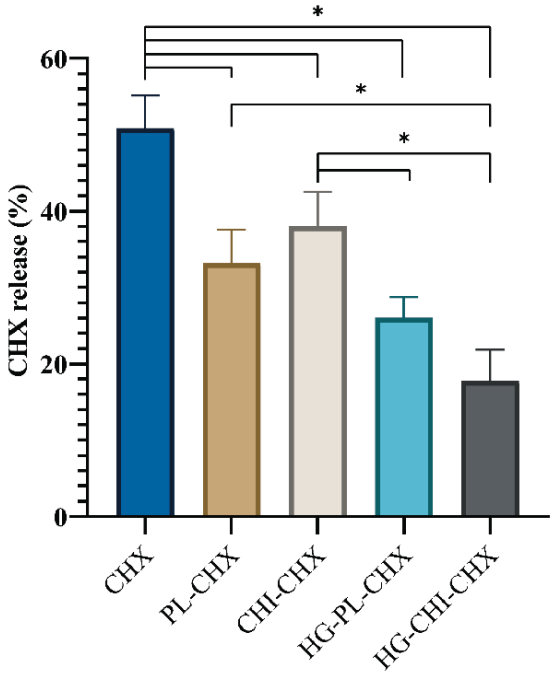

Figure 5. CHX release and permeation from formulated and free CHX after 24 h utilizing the Franz diffusion system (32 °C). The release is presented as the percentage of the initial concentration and all formulations were adjusted to the same initial concentration. All results are expressed as means with their respective SD (n = 3). CHX = dissolved CHX, PL-CHX = plain, CHX-vesicles, CHI-CHX = CHX-chitosomes, HG-PL-CHX = plain, CHX-vesicles in hydrogel, HG-CHI-CHX = CHX-chitosomes in hydrogel. * $p < 0.05$.

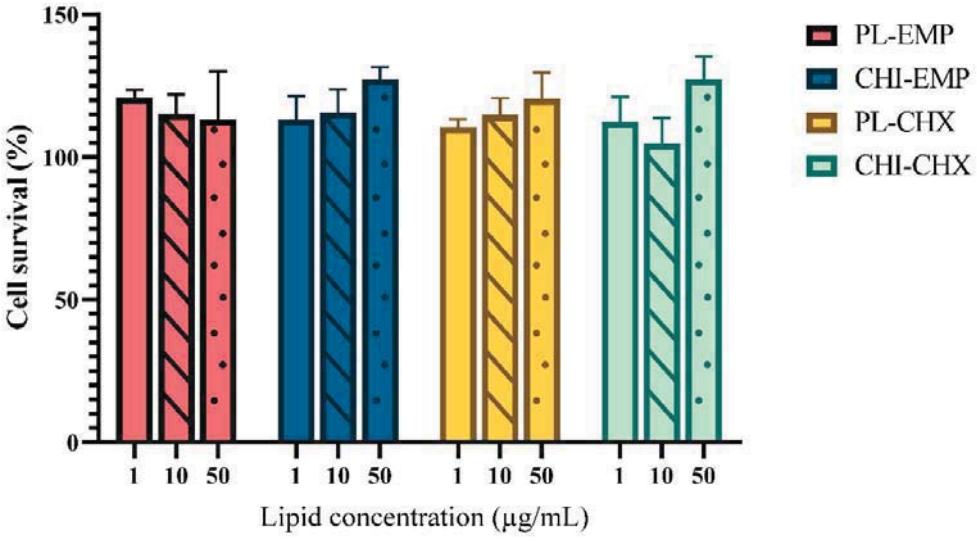

Figure 6. Evaluation of vesicles cell toxicity in HaCaT cells. Three different concentrations were tested, namely 1 (no pattern), 10 (stripes), and 50 (dots) µg/mL lipid, and the results are presented as cell viability of treated cells compared to control (100%). Control was only supplemented with complete medium; the cell viability is thereof considered as 100%. All results are expressed as means with their respective SD (n = 3). PL-EMP = plain, empty vesicles, CHI-EMP = empty chitosomes, PL-CHX = plain, CHX-vesicles, CHI-CHX = CHX-chitosomes.

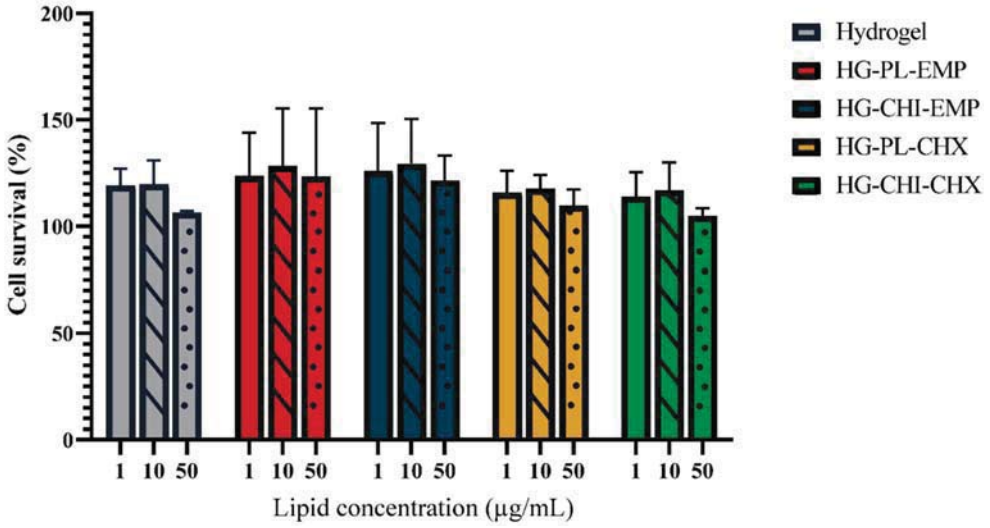

Figure 7. Evaluation of cell toxicity of hydrogels on HaCaT cells. Three different concentrations were tested, namely 1 (no pattern), 10 (stripes), and 50 (dots) µg/mL lipid (or the corresponding chitosan concentration), and the results are presented as cell viability of treated cells compared to control (100%). Control was only supplemented with complete medium; the cell viability is thereof considered as 100%. All results are expressed as means with their respective SD (n = 3). Hydrogel = plain hydrogel, HG-PL-EMP = plain, empty vesicles-in-hydrogel, HG-CHI-EMP = empty chitosomes-in-hydrogel, HG-PL-CHX = plain, CHX-vesicles-in-hydrogel, HG-CHI-CHX = CHX-chitosomes-in-hydrogel.

In addition to the evaluation of the vesicles compatibility, we investigated the cell compatibility of hydrogels (Figure 7). The hydrogels did not exhibit any toxicity toward the keratinocytes; however, none of the hydrogels significantly improved cell survival. The cell compatibility of hydrogels or other wound dressing materials has previously been reported in both keratinocytes and fibroblasts [63–65]. Additionally, Hurler and colleagues demonstrated in a murine burn model that liposomes-in-hydrogel formulations with mupirocin were safe [66]. Chitosan is generally regarded as both safe and biocompatible [12]. However, the degree of deacetylation and chitosan concentration play an important role in cell compatibility. Due to the complex process of wound healing, the full extent of the underlying mechanisms responsible for the effects of chitosan on keratinocytes or fibroblasts are not fully elucidated [60,67]. However, chitosan appears to support granulation and remodeling through its effects on the inflammatory cells and growth factors [68]. Certain growth factors are important in the migration and proliferation of keratinocytes [69]. Consequently, the effects of chitosan-based formulations on inflammatory cells are important to monitor.

In the inflammation phase, immune cells are requited to the wound bed, and some cells differentiate into macrophages. These cells initiate a process that coordinates other cells in the overlapping phases in the healing process as well as combats microorganisms in the injured area [70]. The involvement of macrophages in the wound-healing cascade is extensive and not fully elucidated [71]. We have previously confirmed a decreased inflammatory activity in cells treated with chitosan formulations [18]. The CHX-chitosomes have not been evaluated for their potential effect on macrophages earlier. Figure S1 indicates that chitosan-infused vesicles did not potentiate immune response. Interestingly, the plain vesicles demonstrated a dose-dependent reduction of the inflammatory response in lipopolysaccharide (LPS)-induced murine macrophages compared to untreated activated cells. These results are promising considering application in wound therapy.

In the wound-healing process, both cell compatibility and inflammatory responses are important factors. Additionally, the ability of cells to migrate into the wound bed to close the wound area is equally important for the wound-healing process. The impact of chitosan on the migratory abilities of different cell lines was previously evaluated [35], and the re-

sults are encouraging for our system. Formulations containing chitosan have demonstrated improved cell migration in fibroblasts [72], macrophages [73], and keratinocytes [74].

2.5. Antimicrobial Evaluation

Tailoring drug delivery systems comprising chitosan to optimize its intrinsic antimicrobial activity could improve the effect of the formulation itself [14]. Chitosan is known to act against *Staphylococcus aureus*, which is one of the most common skin pathogens [75] as previously reported [76,77]. Although the mechanisms of the antimicrobial activity of chitosan are not fully elucidated, the electrostatic interaction between the slightly negatively charged bacterial membrane and the positively charged chitosan groups is the most common explanation [76]. In addition, reports suggest that chitosan, especially higher molecular weight chitosan, could form an envelope around the bacteria, depriving them of nutrients and closing of the exchange with the surrounding environment [78]. These strong effects on the bacteria could act in synergy with MAAs such as CHX. Therefore, we sought to compare plain vesicles and chitosomes both with and without CHX to assess the potential antimicrobial effects. Through the modified broth dilution method, we demonstrated a lowered minimum bactericidal concentration (MBC) in both *S. aureus* and *Staphylococcus epidermidis* cultures from formulations comprising both CHX and chitosan compared to their respective controls (Table 4). Chitosomes without CHX and CHX-vesicles displayed improved activity compared to the plain, empty vesicles. As expected, plain, empty vesicles did not eradicate a sufficient number of bacteria to reach MBC, neither with *S. aureus* nor *S. epidermidis*. However, in the highest concentration, the plain-empty vesicles reduced the *S. epidermidis* colony count by approximately 50%. The antimicrobial activity of CHX-chitosomes against both bacteria was proven to be superior to the other vesicles, indicating that there is a synergetic effect between CHX, our model MAA, and chitosan, as hypothesized.

Table 4. MBC of vesicles in *S. aureus* and *S. epidermidis*.

	Lipid Concentration (mg/mL) ***S. aureus***	**Lipid Concentration (mg/mL)** ***S. epidermidis***
PL-EMP	-	-
CHI-EMP	1.25	0.625
PL-CHX	0.32	0.039
CHI-CHX	0.078	<0.005

All results are expressed as the lipid concentration upon reaching MBC (n = 3). PL-EMP = plain, empty vesicles, CHI-EMP = empty chitosomes, PL-CHX = plain, CHX-vesicles, CHI-CHX = CHX-chitosomes.

Alshamsan and colleagues evaluated the antibacterial efficacy of chitosan-coated and non-coated liposomes loaded with dicloxacillin against methicillin-resistant *S. aureus*. Dicloxacillin, commonly used in skin infections, demonstrated improved activity of non-coated liposomes; however, the activity of coated liposomes was retained compared to dicloxacillin in solution [79]. Chitosan-coated liposomes have also demonstrated promising antimicrobial effects in colistin-resistant *Pseudomonas aeruginosa* [80]. Sacco and colleagues evaluated a physical chitosan hydrogel against *S. epidermidis* and revealed promising antimicrobial activity [81]. These results along with other reports [82] demonstrate the promising antimicrobial effects of chitosan-coated or infused vesicles in antimicrobial treatment.

Since secondary vehicles are required in wound therapy, we aimed to investigate whether chitosan hydrogel could further improve the effect of chitosan-infused vesicles with CHX. Jøraholmen and colleagues compared the antimicrobial effects of both chitosan hydrogel and chitosan-coated liposomes against both *S. aureus* and *S. epidermidis* and reported promising effects of chitosan in low concentrations [14]. As seen in Table 5, for *S. aureus*, almost all hydrogels exhibited a similar antimicrobial effect; only the CHX-chitosomes-in-hydrogel showed slightly lowered MBC compared to the other hydrogel formulations. However, the MBC for all hydrogels was lowered as compared to the

vesicular suspensions. For *S. epidermidis*, the effects of different vesicles incorporated in the hydrogel were more evident (Table 5). The activity increased upon the addition of CHX, chitosan, and their combination. The most potent formulation was CHX-chitosomes-in-hydrogel. Moreover, these results indicate that even a diluted hydrogel with a modified chitosan network structure acts on improving the antimicrobial activity. The findings confirmed that vesicle surface-available chitosan in combination with CHX induces the strongest activity also when those vesicles were arranged within a chitosan network.

Table 5. MBC of vesicles in *S. aureus* and *S. epidermidis*.

	Lipid Concentration (mg/mL) [4] ***S. aureus***	**Lipid Concentration (mg/mL)** [4] ***S. epidermidis***
Hydrogel	1.56×10^{-2}	0.10×10^{-2}
HG-PL-EMP	1.56×10^{-2}	0.10×10^{-2}
HG-CHI-EMP	1.56×10^{-2}	0.025×10^{-2}
HG-PL-CHX	1.56×10^{-2}	0.0063×10^{-2}
HG-CHI-CHX	0.78×10^{-2}	0.0031×10^{-2}

All results are expressed as the lipid concentration upon reaching MBC (n = 3). Hydrogel = plain hydrogel, HG-PL-EMP = plain, empty vesicles-in-hydrogel, HG-CHI-EMP = empty chitosomes-in-hydrogel, HG-PL-CHX = plain, CHX-vesicles-in-hydrogel, HG-CHI-CHX = CHX-chitosomes-in-hydrogel. [4] Lipid concentration or the corresponding concentration of hydrogel.

3. Materials and Methods

3.1. Materials

Chitopharm™ M-Chitosan with medium molecular weight (average of 350–600 kDa) and degree of deacetylation of >70% from shrimp was kindly provided by Chitinor (Tromsø, Norway). Lipoid S100 was kindly provided by Lipoid GmbH (Ludwigshafen, Germany). Methanol $\geq$ 99.9%, HiPerSolv CHROMANORM® for LC-MS and acetic acid (>99.9%) were purchased from VWR International (Fontenay-sous-Bois, France). Cibacron Brilliant Red 3B-A was procured from Santa Cruz Biotechnology (Dallas, TX, USA). Chlorhexidine > 99.5%, glycerol solution (86–89%), glycine hydrochloride $\geq$ 99% (HPLC), sodium chloride, hydrochloric acid, Cell Counting Kit-8 (CCK-8), and Kollisolv® PEG E 400 were acquired from Sigma-Aldrich (St. Louis, MO, USA). 1-Propanol, penicillin–streptomycin, and fetal bovine serum (FBS) were purchased from Sigma-Aldrich (Steinheim, Germany). Blood agar plates, saline solution, and Mueller–Hinton broth were delivered by University Hospital of North Norway (Tromsø, Norway). Dulbecco's Modified Eagle Medium high glucose (DMEM HG) w/l-glutamine and sodium pyruvate was purchased from Biowest (Nuaillé, France). HaCaT cell line (immortalized human keratinocytes) was purchased from CLS Cell Lines Service GmbH (Eppelheim, Germany). *Staphylococcus aureus* (ATCC® BAA-1721™) MSSA 476 was purchased from LGC standards AB (Borås, Sweden). *Staphylococcus epidermidis* (13–67) was delivered by University Hospital of Northern Norway (Tromsø, Norway).

3.2. Vesicle Preparation

3.2.1. Vesicle Preparation

The preparation of chitosomes was based on the one-pot method previously described by Andersen et al. [31]. In short, Lipoid S100 (200 mg) and CHX (10 mg) were dissolved in methanol and a lipid film was formed by evaporation of the solvent in a rotoevaporator (Büchi rotavapor R-124, with vacuum controller B-721, Büchi vac V-500, Büchi Labortechnik, Flawil, Switzerland) at 60 mBar and 45 °C for 1 h. A micro syringe (Innovative Labor Systeme GmBH, Stutzerbach, Germany) filled with 150 µL 1-propanol was used to disperse the lipid film. The 1-propanol/lipid dispersion was further injected into a chitosan dispersion (0.17%, w/w, 2 mL) in acetic acid (0.1%, v/v) under continuous mechanical stirring. Finally, the resulting suspension was stirred for another 2 h at room temperature (24 $\pm$ 1 °C) and stored in the refrigerator (4 °C) prior to size reduction. Formulations without chitosan were prepared in the same manner; however, the 1-propanol/lipid dispersion was injected into distilled water (2 mL) instead of the chitosan dispersion. Formulations without CHX

was prepared in the same way but without CHX. All vesicle designations and constituents are included in Table 6.

Table 6. Designation and constituents of all vesicles.

	Composition
PL-EMP	Lipoid S100
CHI-EMP	Lipoid S100 Chitosan
PL-CHX	Lipoid S100 CHX
CHI-CHX	Lipoid S100 Chitosan CHX

3.2.2. Size Reduction

Prior to size reduction, all vesicle suspensions were diluted with distilled water to a lipid concentration of 20 mg/mL. The samples were probe sonicated (SONICS high-intensity ultrasonic processor, 500-watt model, 13 mm probe diameter, Sonics & Materials Inc., Newtown, CT, USA) at 40% amplitude for 10 s and ten times 10 s for the CHX-containing and the empty vesicles, respectively. The sample containers were placed in an ice bath throughout the sonication to avoid extensive heating.

3.3. Characterization of Chitosomes

3.3.1. Vesicle Size and Morphology

The size of vesicles was measured on a NICOMP Submicron particle sizer model 370 (NICOMP Particle Sizing system, Santa Barbara, CA, USA) described elsewhere [14]. The suspensions were diluted in filtered (0.2 μm) distilled water to reach an intensity of 250–350 KHz and measured for three cycles of 10 min. The scattering angle of every measurement was 90°, and the temperature was 24 ± 1 °C. The results are expressed as the weight-intensity distribution.

Prior to the morphological investigations, empty chitosomes and CHX-chitosomes were deposited onto carbon-coated grids for 5 min, washed with double-distilled water, and stained with 3% uranyl acetate and 2% methylcellulose (1:9) for 2 min. The samples were picked up with a loop and dried on the loop holder. The images were obtained with a transmission electron microscope HT7800 Series (Hitachi High-Tech Corp., Tokyo, Japan) operating at an accelerated voltage of 100 kV coupled with a Morada camera.

3.3.2. Zeta Potential and pH of the Vesicles

The zeta potential was determined with a Malvern Zetasizer Nano Zen 2600 (Malvern, Worcestershire, UK) as described earlier [83]. Zeta cells were rinsed three times with methanol and filtered, deionized water prior to the measurements. The suspensions were measured in three replicates at room temperature (24 ± 1 °C).

Determination of the pH was carried out with an Accumet®, Portable pH meter AP115 (Fischer Scientific, MA, USA) at room temperature (24 ± 1 °C).

3.3.3. Separation and Entrapment Efficiency

The free CHX was separated from the entrapped CHX by centrifugation [84]. The chitosomes were centrifuged at 4000× *g* and 4 °C for 30 min on the Biofuge Stratos centrifuge (Heraeus Instruments GmbH, Hanau, Germany). Entrapment analysis was carried out on the SPARK® multimode microplate reader (Tecan Trading AG, Männedorf, Switzerland) at 261 nm.

3.3.4. Determination of Availability of Chitosan on the Surface

The determination of surface-available chitosan was based on a method described by Muzzarelli [85]. Prior to the determination, the chitosomes were centrifuged in a centrifugal filter (Amicon Ultra-2 Centrifugal Filter Unit Ultracel-10, Sigma-Aldrich, St. Louis, MI, USA) at 3118× *g* for 15 min on the Biofuge Stratos centrifuge (Heraeus Instruments GmbH, Hanau, Germany) [86]. First, glycine and NaCl was dissolved in distilled water in concentrations of 0.748% (*w*/*v*) and 0.584% (*w*/*v*), respectively. A glycine buffer with pH 3.2 was prepared by diluting 81 mL of the glycine and NaCl solution with 0.1 M HCl to a total volume of 100 mL. Next, a dye solution was prepared by dissolving Cibacron Brilliant Red 3B-A (0.15%, *w*/*v*) in distilled water and 5 mL of this solution was diluted in glycine buffer to a total volume of 100 mL. The centrifuged chitosomes were diluted (1:1, *v*/*v*) in distilled water. An aliquot of 3 mL of the dye solution was added to 300 µL of the diluted chitosomes, and the samples were analyzed on a UV-vis plate reader (Tecan Trading AG, Männedorf, Switzerland) at 575 nm [87].

3.3.5. Chitosome and Vesicle Stability

The physical properties of chitosomes and plain vesicles (stored at 4 °C) were evaluated after storage for two and four weeks after preparation. Properties evaluated were size, PI, zeta potential, and pH as described in Sections 3.3.1 and 3.3.2.

3.4. Preparation and Characterization of Hydrogels

3.4.1. Preparation of Chitosan Hydrogel

Chitosan hydrogels comprising glycerol as a plasticizer were prepared in 2.5% (*w*/*w*) acetic acid in distilled water. The dispersions were mixed with a Cito Unguator® 2000 (GAKO International AG, Zurich, Switzerland) and degassed by bath sonication (Bransonic® 5510R-MT Ultrasonic cleaner, Branson Ultrasonics Corporation, Danbury, CT, USA) for 30 min. The final concentrations of chitosan and glycerol were 4.5 and 9%, respectively. Hydrogels were allowed to swell for 48 h prior to characterization or the incorporation of vesicles.

The vesicles-in-hydrogel were prepared by incorporating 10% (*w*/*w*) vesicle suspension into chitosan hydrogels of 5% chitosan and 10% glycerol, respectively, by hand-stirring for 5 min. The concentration of chitosan and glycerol after the incorporation of vesicular suspensions were 4.5 and 9%, respectively. All hydrogel designations and their composition are included in Table 7.

Table 7. Designation and constituents of all hydrogels.

	Composition
Hydrogel	Chitosan Glycerol
HG-PL-EMP	Chitosan Glycerol PL-EMP vesicles
HG-CHI-EMP	Chitosan Glycerol CHI-EMP vesicles
HG-PL-CHX	Chitosan Glycerol PL-CHX vesicles
HG-CHI-CHX	Chitosan Glycerol CHI-CHX vesicles

3.4.2. Texture Properties and pH of Hydrogels

Texture properties of hydrogels were evaluated on the TA.XT plus Texture Analyser (Stable Micro Systems Ltd., Surrey, UK) with a backward extrusion rig as previously described by Hurler et al. [44]. The beaker of the rig set was filled with 65 g hydrogel and the disc (35 mm) was compressed into the hydrogel and withdrawn back to the starting position (above the surface). The measuring distance was 10 mm and the trigger force was set to 10 g. The pre-test, test, and post-test speeds were 10, 4, and 4 mm/s, respectively. Hardness, cohesiveness, and adhesiveness were recorded.

The pH of all hydrogels were measured with an Accumet®, Portable pH meter, AP115 (Fisher scientific, Waltham, MA, USA) at room temperature (24 ± 1 °C).

3.4.3. Viscosity Measurements

The measurements of viscosity were performed on a Rotavisc hi-vi II Complete coupled with DINS-1 adapter with spindle DIN-SP-7 and DIN-C-2 chamber (IKA®-Werke GmbH & Co. KG, Staufen, Germany). Both viscosity and shear stress was evaluated as a function of the shear rate [51]. The shear rate range was between 4.0 s^{-1} and 23.63 s^{-1} and the temperature was set to 25 or 32 °C.

3.5. CHX Release Studies

CHX release was determined in a Franz cell diffusion system (PermeGear, Hellertown, PA, USA) with circulating heated water of 32 °C. The diffusion area of the pre-soaked cellophane membrane (Max Bringmann KG, Wendelstein, Germany) was 1.77 cm^2 and the acceptor volume was 12 mL. Due to the lowered water solubility of CHX, the acceptor chamber was filled with polyethylene glycol 400 (10%, *v*/*v*) in distilled water. The formulations (600 µL) were added to the donor chamber. Samples were withdrawn from the donor chamber after 24 h and analyzed as described in Section 3.3.3. The formulations were compared with free CHX dissolved in the acceptor medium (permeation). The donor chamber was weighed before and after every run to adjust for fluid exchange, and therefore, the samples were measured only after 24 h [18].

3.6. Cell Viability Valuation

The cytotoxicity of formulations was evaluated using a Cell counting kit–8 (CCK-8, Sigma-Aldrich Chemie, St. Louise, MI, USA) as described elsewhere [88]. Briefly, an aliquot of 90 µL cell suspension cultured in DMEM HG supplemented with 10% (*v*/*v*) FBS and 1% (*v*/*v*) penicillin–streptomycin (1×10^5 cells/mL) were plated on a 96-well plate and incubated for 24 h at 37 °C with 5% CO_2. Next, 10 µL of medium (control), diluted vesicle suspension, or diluted hydrogel (1, 10, and 50 µg/mL lipid concentration or the corresponding concentration of hydrogels) was added to the wells. The cells were incubated for another 24 h at 37 °C with 5% CO_2. After incubation, 10 µL CCK-8 was added to each well, and the plates were incubated for 4 h. Finally, the plates were evaluated at a UV-vis microplate reader (Tecan Trading AG, Männedorf, Switzerland) at 450 nm with the reference set to 650 nm. All formulations were evaluated in triplicates and the results were expressed as percentage compared to control.

3.7. Antimicrobial Evaluation

In the microbial evaluation, we sought to calculate the MBC for each formulation to compare the effect of every modification for both vesicles and hydrogels. Here, we used a modified broth micro-dilution method [89,90]. Two species were evaluated, namely *S. aureus* MSSA 476 and *S. epidermidis* (13–67). Prior to the experiments, all hydrogels were diluted 1:4 (*v*/*v*) in distilled water. All formulations were two-fold diluted in Mueller–Hinton broth in sterile 96-well plates. Bacterial suspensions were prepared at 0.5 McFarland in 0.85% (*w*/*w*) sodium chloride solutions, corresponding to approximately 10^8 CFU/mL. The bacterial suspensions were further diluted (1:150, *v*/*v*) in Mueller–Hinton broth. The inoculum was added to each well (1:1, *v*/*v*) in the 96-well plate and incubated at 37 °C on a

shaker (100 rpm) for 24 h. The wells with only bacteria and Mueller–Hinton broth served as positive and negative controls, respectively. After 24 h incubation, the bacterial suspensions were 10-fold serial diluted in phosphate-buffered saline, plated on blood agar plates, and incubated at 37 °C overnight [90]. The CFUs of the bacteria treated with formulations were compared to the control (only growth medium) and the MBC (lipid concentration) was determined.

3.8. Statistical Analyses

In general, results are expressed as mean ± SD. Student's t-tests or one-way ANOVA with Tukey post-test were performed to evaluate significance ($p < 0.05$). All statistical analyses were performed in GraphPad Prism version 9.0.0 for Windows (GraphPad Software LLC, San Diego, CA, USA).

4. Conclusions

Novel formulations for prevention and treatment of acute skin injuries prone to infections are highly needed. This study supported the hypothesis that chitosan-infused lipid-based vesicles, chitosomes loaded with CHX and incorporated into chitosan hydrogel network could serve as a suitable formulation for infection control, prevention, and eradication of bacterial infections in acute wounds. The novel formulation displayed safety and superior antimicrobial properties, which are both highly desirable for topical therapy of infected wounds. Additionally, the combination of chitosan and CHX could provide both a faster onset of the antimicrobial action and additionally offer a long-term effect on bacteria in wounds.

Supplementary Materials: The following are available online at https://www.mdpi.com/article/10.3390/md19050269/s1, Table S1: Stability hydrogel measured as texture properties and pH. Figure S1: Evaluation of anti-inflammatory activity of vesicles on RAW 264.7 cells.

Author Contributions: Conceptualization, L.M.H. and N.Š.-B.; methodology, L.M.H., K.J., P.B., M.J. and N.Š.-B.; validation, L.M.H., K.J. and N.Š.-B.; formal analysis, L.M.H., K.J. and L.A.; investigation, L.M.H. and L.A; resources, M.J. and N.Š.-B.; data curation, L.M.H., L.A. and P.B.; writing—original draft preparation, L.M.H., K.J., L.A., P.B., M.J. and N.Š.-B.; writing—review and editing, L.M.H., K.J., P.B., M.J. and N.Š.-B.; visualization, L.M.H.; supervision, N.Š.-B.; project administration, N.Š.-B.; funding acquisition, N.Š.-B. All authors have read and agreed to the published version of the manuscript.

Funding: The study was funded by UiT The Arctic University of Norway, Norway (project no. 235569). The publication fund of UiT The Arctic University of Norway funded the publication charges of this article.

Institutional Review Board Statement: Not applicable.

Informed Consent Statement: Not applicable.

Data Availability Statement: Data is contained within the article and supplementary material.

Acknowledgments: The authors would like to acknowledge Augusta Sundbø at the Advanced Microscopy Core Facility, Department of Medical Biology at the UiT The Arctic University of Norway for the assistance in TEM imaging. We would also like to thank Chitinor (Tromsø, Norway) and Lipoid GmbH (Ludwigshafen, Germany) for providing chitosan and phospholipid, respectively, for this study.

Conflicts of Interest: The authors declare no conflict of interest.

References

1. Salyer, C.E.; Bomholt, C.; Beckmann, N.; Bergmann, C.B.; Plattner, C.A.; Caldwell, C.C. Novel Therapeutics for the Treatment of Burn Infection. *Surg. Infect.* **2020**, *22*, 113–120. [CrossRef]
2. Corcione, S.; Pensa, A.; Castiglione, A.; Lupia, T.; Bortolaso, B.; Romeo, M.R.; Stella, M.; Rosa, F.G.D. Epidemiology, prevalence and risk factors for infections in burn patients: Results from a regional burn centre's analysis. *J. Chemother.* **2020**, *33*, 62–66. [CrossRef]

3. van Duin, D.; Strassle, P.D.; DiBiase, L.M.; Lachiewicz, A.M.; Rutala, W.A.; Eitas, T.; Maile, R.; Kanamori, H.; Weber, D.J.; Cairns, B.A.; et al. Timeline of health care–associated infections and pathogens after burn injuries. *Am. J. Infect. Control* **2016**, *44*, 1511–1516. [CrossRef]
4. Poulakou, G.; Lagou, S.; Tsiodras, S. What's new in the epidemiology of skin and soft tissue infections in 2018? *Curr. Opin. Infect. Dis.* **2019**, *32*, 77–86. [CrossRef] [PubMed]
5. Jabalameli, F.; Mirsalehian, A.; Khoramian, B.; Aligholi, M.; Khoramrooz, S.S.; Asadollahi, P.; Taherikalani, M.; Emaneini, M. Evaluation of biofilm production and characterization of genes encoding type III secretion system among Pseudomonas aeruginosa isolated from burn patients. *Burns* **2012**, *38*, 1192–1197. [CrossRef] [PubMed]
6. Brandenburg, K.S.; Weaver, A.J.; Karna, S.L.R.; You, T.; Chen, P.; Stryk, S.V.; Qian, L.; Pineda, U.; Abercrombie, J.J.; Leung, K.P. Formation of *Pseudomonas aeruginosa* Biofilms in Full-thickness Scald Burn Wounds in Rats. *Sci. Rep.* **2019**, *9*, 13627. [CrossRef] [PubMed]
7. Smolle, C.; Cambiaso-Daniel, J.; Forbes, A.A.; Wurzer, P.; Hundeshagen, G.; Branski, L.K.; Huss, F.; Kamolz, L.-P. Recent trends in burn epidemiology worldwide: A systematic review. *Burns* **2017**, *43*, 249–257. [CrossRef] [PubMed]
8. James, S.L.; Lucchesi, L.R.; Bisignano, C.; Castle, C.D.; Dingels, Z.V.; Fox, J.T.; Hamilton, E.B.; Henry, N.J.; McCracken, D.; Roberts, N.L.S.; et al. Epidemiology of injuries from fire, heat and hot substances: Global, regional and national morbidity and mortality estimates from the Global Burden of Disease 2017 study. *Inj. Prev.* **2019**, 1–10. [CrossRef]
9. Mofazzal Jahromi, M.A.; Sahandi Zangabad, P.; Moosavi Basri, S.M.; Sahandi Zangabad, K.; Ghamarypour, A.; Aref, A.R.; Karimi, M.; Hamblin, M.R. Nanomedicine and advanced technologies for burns: Preventing infection and facilitating wound healing. *Adv. Drug Deliv. Rev.* **2018**, *123*, 33–64. [CrossRef]
10. Khan, F.; Pham, D.T.N.; Oloketuyi, S.F.; Manivasagan, P.; Oh, J.; Kim, Y.-M. Chitosan and their derivatives: Antibiofilm drugs against pathogenic bacteria. *Colloids Surf. B* **2020**, *185*, 110627. [CrossRef]
11. Bakshi, P.S.; Selvakumar, D.; Kadirvelu, K.; Kumar, N.S. Chitosan as an environment friendly biomaterial—A review on recent modifications and applications. *Int. J. Biol. Macromol.* **2020**, *150*, 1072–1083. [CrossRef]
12. Barbosa, A.I.; Coutinho, A.J.; Costa Lima, S.A.; Reis, S. Marine Polysaccharides in Pharmaceutical Applications: Fucoidan and Chitosan as Key Players in the Drug Delivery Match Field. *Mar. Drugs* **2019**, *17*, 654. [CrossRef]
13. Islam, M.M.; Shahruzzaman, M.; Biswas, S.; Nurus Sakib, M.; Rashid, T.U. Chitosan based bioactive materials in tissue engineering applications—A review. *Bioact. Mater.* **2020**, *5*, 164–183. [CrossRef]
14. Jøraholmen, M.W.; Bhargava, A.; Julin, K.; Johannessen, M.; Škalko-Basnet, N. The Antimicrobial Properties of Chitosan Can be Tailored by Formulation. *Mar. Drugs* **2020**, *18*, 96. [CrossRef]
15. Hu, Z.; Zhang, D.-Y.; Lu, S.-T.; Li, P.-W.; Li, S.-D. Chitosan-Based Composite Materials for Prospective Hemostatic Applications. *Mar. Drugs* **2018**, *16*, 273. [CrossRef]
16. Desbrieres, J.; Peptu, C.; Ochiuz, L.; Savin, C.; Popa, M.; Vasiliu, S. Application of Chitosan-Based Formulations in Controlled Drug Delivery. In *Sustainable Agriculture Reviews 36: Chitin and Chitosan: Applications in Food, Agriculture, Pharmacy, Medicine and Wastewater Treatment*; Crini, G., Lichtfouse, E., Eds.; Springer International Publishing: Cham, Switzerland, 2019; pp. 241–314.
17. Vanić, Ž.; Holsæter, A.M.; Škalko-Basnet, N. (Phospho) lipid-based Nanosystems for Skin Administration. *Curr. Pharm. Des.* **2015**, *21*, 4174–4192. [CrossRef] [PubMed]
18. Hemmingsen, L.M.; Giordani, B.; Pettersen, A.K.; Vitali, B.; Basnet, P.; Škalko-Basnet, N. Liposomes-in-chitosan hydrogel boosts potential of chlorhexidine in biofilm eradication in vitro. *Carbohydr. Polym.* **2021**, *262*, 117939. [CrossRef] [PubMed]
19. Kumar, S.; Dutta, J.; Dutta, P.K.; Koh, J. A systematic study on chitosan-liposome based systems for biomedical applications. *Int. J. Biol. Macromol.* **2020**, *160*, 470–481. [CrossRef] [PubMed]
20. Andersen, T.; Mishchenko, E.; Flaten, G.E.; Sollid, J.U.E.; Mattsson, S.; Tho, I.; Škalko-Basnet, N. Chitosan-Based Nanomedicine to Fight Genital Candida Infections: Chitosomes. *Mar. Drugs* **2017**, *15*, 64. [CrossRef] [PubMed]
21. Hurdle, J.G.; O'Neill, A.J.; Chopra, I.; Lee, R.E. Targeting bacterial membrane function: An underexploited mechanism for treating persistent infections. *Nat. Rev. Microbiol.* **2011**, *9*, 62–75. [CrossRef]
22. Abdel-Sayed, P.; Tornay, D.; Hirt-Burri, N.; de Buys Roessingh, A.; Raffoul, W.; Applegate, L.A. Implications of chlorhexidine use in burn units for wound healing. *Burns* **2020**, *46*, 1150–1156. [CrossRef]
23. Hubbard, A.T.M.; Coates, A.R.; Harvey, R.D. Comparing the action of HT61 and chlorhexidine on natural and model *Staphylococcus aureus* membranes. *J. Antibiot.* **2017**, *70*, 1020–1025. [CrossRef]
24. Drago, F.; Gariazzo, L.; Cioni, M.; Trave, I.; Parodi, A. The microbiome and its relevance in complex wounds. *Eur. J. Dermatol.* **2019**, *29*, 6–13. [CrossRef]
25. Matica, M.A.; Aachmann, F.L.; Tøndervik, A.; Sletta, H.; Ostafe, V. Chitosan as a Wound Dressing Starting Material: Antimicrobial Properties and Mode of Action. *Int. J. Mol. Sci.* **2019**, *20*, 5889. [CrossRef]
26. Vanić, Ž.; Škalko-Basnet, N. Chapter 11—Hydrogels as intrinsic antimicrobials. In *Hydrogels Based on Natural Polymers*; Chen, Y., Ed.; Elsevier BV: Amsterdam, The Netherlands, 2020; pp. 309–328.
27. Billard, A.; Pourchet, L.; Malaise, S.; Alcouffe, P.; Montembault, A.; Ladavière, C. Liposome-loaded chitosan physical hydrogel: Toward a promising delayed-release biosystem. *Carbohydr. Polym.* **2015**, *115*, 651–657. [CrossRef] [PubMed]
28. Parhi, R. Chitin and Chitosan in Drug Delivery. In *Sustainable Agriculture Reviews 36: Chitin and Chitosan: Applications in Food, Agriculture, Pharmacy, Medicine and Wastewater Treatment*; Crini, G., Lichtfouse, E., Eds.; Springer International Publishing: Cham, Switzerland, 2019; pp. 175–239.

29. Shariatinia, Z. Pharmaceutical applications of chitosan. *Adv. Colloid Interface Sci.* **2019**, *263*, 131–194. [CrossRef] [PubMed]
30. Zhu, T.; Mao, J.; Cheng, Y.; Liu, H.; Lv, L.; Ge, M.; Li, S.; Huang, J.; Chen, Z.; Li, H.; et al. Recent Progress of Polysaccharide-Based Hydrogel Interfaces for Wound Healing and Tissue Engineering. *Adv. Mater. Interfaces* **2019**, *6*, 1900761. [CrossRef]
31. Andersen, T.; Bleher, S.; Flaten, G.E.; Tho, I.; Mattsson, S.; Škalko-Basnet, N. Chitosan in mucoadhesive drug delivery: Focus on local vaginal therapy. *Mar. Drugs* **2015**, *13*, 222–236. [CrossRef] [PubMed]
32. Jones, M.; Kujundzic, M.; John, S.; Bismarck, A. Crab vs. Mushroom: A Review of Crustacean and Fungal Chitin in Wound Treatment. *Mar. Drugs* **2020**, *18*, 64. [CrossRef]
33. Liu, H.; Wang, C.; Li, C.; Qin, Y.; Wang, Z.; Yang, F.; Li, Z.; Wang, J. A functional chitosan-based hydrogel as a wound dressing and drug delivery system in the treatment of wound healing. *RSC Adv.* **2018**, *8*, 7533–7549. [CrossRef]
34. Mathews, P.D.; Mertins, O. Chapter 9—Chitosan and lipid composites as versatile biomedical material. In *Materials for Biomedical Engineering*; Holban, A.-M., Grumezescu, A.M., Eds.; Elsevier: Amsterdam, The Netherlands, 2019; pp. 259–291.
35. Stoica, A.E.; Chircov, C.; Grumezescu, A.M. Hydrogel Dressings for the Treatment of Burn Wounds: An Up-To-Date Overview. *Materials* **2020**, *13*, 2853. [CrossRef]
36. Amiri, N.; Ajami, S.; Shahroodi, A.; Jannatabadi, N.; Amiri Darban, S.; Fazly Bazzaz, B.S.; Pishavar, E.; Kalalinia, F.; Movaffagh, J. Teicoplanin-loaded chitosan-PEO nanofibers for local antibiotic delivery and wound healing. *Int. J. Biol. Macromol.* **2020**, *162*, 645–656. [CrossRef] [PubMed]
37. El-Alfy, E.A.; El-Bisi, M.K.; Taha, G.M.; Ibrahim, H.M. Preparation of biocompatible chitosan nanoparticles loaded by tetracycline, gentamycin and ciprofloxacin as novel drug delivery system for improvement the antibacterial properties of cellulose based fabrics. *Int. J. Biol. Macromol.* **2020**, *161*, 1247–1260. [CrossRef] [PubMed]
38. Hurler, J.; Žakelj, S.; Mravljak, J.; Pajk, S.; Kristl, A.; Schubert, R.; Škalko-Basnet, N. The effect of lipid composition and liposome size on the release properties of liposomes-in-hydrogel. *Int. J. Pharm.* **2013**, *456*, 49–57. [CrossRef] [PubMed]
39. Ternullo, S.; Schulte Werning, L.V.; Holsæter, A.M.; Škalko-Basnet, N. Curcumin-In-Deformable Liposomes-In-Chitosan-Hydrogel as a Novel Wound Dressing. *Pharmaceutics* **2019**, *12*, 8. [CrossRef] [PubMed]
40. Paulsen, M.H.; Ausbacher, D.; Bayer, A.; Engqvist, M.; Hansen, T.; Haug, T.; Anderssen, T.; Andersen, J.H.; Sollid, J.U.E.; Strøm, M.B. Antimicrobial activity of amphipathic α,α-disubstituted β-amino amide derivatives against ESBL—CARBA producing multi-resistant bacteria; effect of halogenation, lipophilicity and cationic character. *Eur. J. Med. Chem.* **2019**, *183*, 111671. [CrossRef] [PubMed]
41. Wang, D.-Y.; van der Mei, H.C.; Ren, Y.; Busscher, H.J.; Shi, L. Lipid-Based Antimicrobial Delivery-Systems for the Treatment of Bacterial Infections. *Front. Chem.* **2020**, *7*, 1–15. [CrossRef]
42. Ahani, E.; Montazer, M.; Toliyat, T.; Mahmoudi Rad, M.; Harifi, T. Preparation of nano cationic liposome as carrier membrane for polyhexamethylene biguanide chloride through various methods utilizing higher antibacterial activities with low cell toxicity. *J. Microencapsul.* **2017**, *34*, 121–131. [CrossRef]
43. Chang, S.-H.; Lin, Y.-Y.; Wu, G.-J.; Huang, C.-H.; Tsai, G.J. Effect of chitosan molecular weight on anti-inflammatory activity in the RAW 264.7 macrophage model. *Int. J. Biol. Macromol.* **2019**, *131*, 167–175. [CrossRef]
44. Hurler, J.; Engesland, A.; Kermany, B.P.; Škalko-Basnet, N. Improved texture analysis for hydrogel characterization: Gel cohesiveness, adhesiveness, and hardness. *J. Appl. Polym. Sci.* **2012**, *125*, 180–188. [CrossRef]
45. Jøraholmen, M.W.; Basnet, P.; Tostrup, M.J.; Moueffaq, S.; Škalko-Basnet, N. Localized Therapy of Vaginal Infections and Inflammation: Liposomes-In-Hydrogel Delivery System for Polyphenols. *Pharmaceutics* **2019**, *11*, 53. [CrossRef] [PubMed]
46. Djekic, L.; Martinović, M.; Ćirić, A.; Fraj, J. Composite chitosan hydrogels as advanced wound dressings with sustained ibuprofen release and suitable application characteristics. *Pharm. Dev. Technol.* **2020**, *25*, 332–339. [CrossRef] [PubMed]
47. Wallace, L.A.; Gwynne, L.; Jenkins, T. Challenges and opportunities of pH in chronic wounds. *Ther. Deliv.* **2019**, *10*, 719–735. [CrossRef]
48. Kruse, C.R.; Singh, M.; Targosinski, S.; Sinha, I.; Sørensen, J.A.; Eriksson, E.; Nuutila, K. The effect of pH on cell viability, cell migration, cell proliferation, wound closure, and wound reepithelialization: In vitro and in vivo study. *Wound Repair Regen.* **2017**, *25*, 260–269. [CrossRef]
49. Schneider, L.A.; Korber, A.; Grabbe, S.; Dissemond, J. Influence of pH on wound-healing: A new perspective for wound-therapy? *Arch. Dermatol. Res.* **2007**, *298*, 413–420. [CrossRef]
50. Dalisson, B.; Barralet, J. Bioinorganics and Wound Healing. *Adv. Healthc. Mater.* **2019**, *8*, 1900764. [CrossRef] [PubMed]
51. Szymańska, E.; Sosnowska, K.; Miltyk, W.; Rusak, M.; Basa, A.; Winnicka, K. The Effect of β-Glycerophosphate Crosslinking on Chitosan Cytotoxicity and Properties of Hydrogels for Vaginal Application. *Polymers* **2015**, *7*, 2223–2244. [CrossRef]
52. Kaplan, M.; Tuğcu-Demiröz, F.; Vural, İ.; Çelebi, N. Development and characterization of gels and liposomes containing ovalbumin for nasal delivery. *J. Drug Deliv. Sci. Technol.* **2018**, *44*, 108–117. [CrossRef]
53. Szuhaj, B.F. PHOSPHOLIPIDS | Properties and Occurrence. In *Encyclopedia of Food Sciences and Nutrition (Second Edition)*; Caballero, B., Ed.; Academic Press: Oxford, UK, 2003; pp. 4514–4519.
54. Thirumaleshwar, S.K.; Kulkarni, P.V.; Gowda, D. Liposomal Hydrogels: A Novel Drug Delivery System for Wound Dressing. *Curr. Drug Ther.* **2012**, *7*, 212–218. [CrossRef]
55. Souto, E.B.; Ribeiro, A.F.; Ferreira, M.I.; Teixeira, M.C.; Shimojo, A.A.M.; Soriano, J.L.; Naveros, B.C.; Durazzo, A.; Lucarini, M.; Souto, S.B.; et al. New Nanotechnologies for the Treatment and Repair of Skin Burns Infections. *Int. J. Mol. Sci.* **2020**, *21*, 393. [CrossRef]

56. Ciobanu, B.C.; Cadinoiu, A.N.; Popa, M.; Desbrières, J.; Peptu, C.A. Modulated release from liposomes entrapped in chitosan/gelatin hydrogels. *Mater. Sci. Eng. C* **2014**, *43*, 383–391. [CrossRef]
57. Heimbuck, A.M.; Priddy-Arrington, T.R.; Padgett, M.L.; Llamas, C.B.; Barnett, H.H.; Bunnell, B.A.; Caldorera-Moore, M.E. Development of Responsive Chitosan–Genipin Hydrogels for the Treatment of Wounds. *ACS Appl. Bio Mater.* **2019**, *2*, 2879–2888. [CrossRef]
58. Mengoni, T.; Adrian, M.; Pereira, S.; Santos-Carballal, B.; Kaiser, M.; Goycoolea, F.M. A Chitosan—Based Liposome Formulation Enhances the In Vitro Wound Healing Efficacy of Substance P Neuropeptide. *Pharmaceutics* **2017**, *9*, 56. [CrossRef]
59. Phetdee, M.; Polnok, A.; Viyoch, J. Development of chitosan-coated liposomes for sustained delivery of tamarind fruit pulp's extract to the skin. *Int. J. Cosmet. Sci.* **2008**, *30*, 285–295. [CrossRef]
60. Howling, G.I.; Dettmar, P.W.; Goddard, P.A.; Hampson, F.C.; Dornish, M.; Wood, E.J. The effect of chitin and chitosan on the proliferation of human skin fibroblasts and keratinocytes in vitro. *Biomaterials* **2001**, *22*, 2959–2966. [CrossRef]
61. Hidalgo, E.; Dominguez, C. Mechanisms underlying chlorhexidine-induced cytotoxicity. *Toxicol. In Vitro* **2001**, *15*, 271–276. [CrossRef]
62. Boyce, S.T.; Warden, G.D.; Holder, I.A. Cytotoxicity Testing of Topical Antimicrobial Agents on Human Keratinocytes and Fibroblasts for Cultured Skin Grafts. *J. Burn Care Rehabil.* **1995**, *16*, 97–103. [CrossRef] [PubMed]
63. Intini, C.; Elviri, L.; Cabral, J.; Mros, S.; Bergonzi, C.; Bianchera, A.; Flammini, L.; Govoni, P.; Barocelli, E.; Bettini, R.; et al. 3D-printed chitosan-based scaffolds: An in vitro study of human skin cell growth and an in-vivo wound healing evaluation in experimental diabetes in rats. *Carbohydr. Polym.* **2018**, *199*, 593–602. [CrossRef]
64. Lauto, A.; Hook, J.; Doran, M.; Camacho, F.; Poole-Warren, L.A.; Avolio, A.; Foster, L.J.R. Chitosan adhesive for laser tissue repair: In vitro characterization. *Lasers Surg. Med.* **2005**, *36*, 193–201. [CrossRef] [PubMed]
65. Ribeiro, M.P.; Espiga, A.; Silva, D.; Baptista, P.; Henriques, J.; Ferreira, C.; Silva, J.C.; Borges, J.P.; Pires, E.; Chaves, P.; et al. Development of a new chitosan hydrogel for wound dressing. *Wound Repair Regen.* **2009**, *17*, 817–824. [CrossRef] [PubMed]
66. Hurler, J.; Sørensen, K.K.; Fallarero, A.; Vuorela, P.; Škalko-Basnet, N. Liposomes-in-hydrogel delivery system with mupirocin: In vitro antibiofilm studies and in vivo evaluation in mice burn model. *BioMed Res. Int.* **2013**, 498485. [CrossRef]
67. Chatelet, C.; Damour, O.; Domard, A. Influence of the degree of acetylation on some biological properties of chitosan films. *Biomaterials* **2001**, *22*, 261–268. [CrossRef]
68. Gomathysankar, S.; Halim, A.S.; Makhtar, W.R.W.; Saad, A.Z.M.; Yaacob, N.S. Skin Substitutes in Wound Healing and the Stimulatory Effects of Adipose-Derived Stem Cells for the Proliferation of Keratinocytes on Chitosan. In *Chronic Wounds, Wound Dressings and Wound Healing*; Shiffman, M.A., Low, M., Eds.; Springer International Publishing: Cham, Switzerland, 2021; pp. 379–394.
69. Seeger, M.A.; Paller, A.S. The Roles of Growth Factors in Keratinocyte Migration. *Adv. Wound Care* **2014**, *4*, 213–224. [CrossRef] [PubMed]
70. Oishi, Y.; Manabe, I. Macrophages in inflammation, repair and regeneration. *Int. Immunol.* **2018**, *30*, 511–528. [CrossRef] [PubMed]
71. Kloc, M.; Ghobrial, R.M.; Wosik, J.; Lewicka, A.; Lewicki, S.; Kubiak, J.Z. Macrophage functions in wound healing. *J. Tissue Eng. Regen. Med.* **2019**, *13*, 99–109. [CrossRef]
72. Ouyang, Q.-Q.; Hu, Z.; Lin, Z.-P.; Quan, W.-Y.; Deng, Y.-F.; Li, S.-D.; Li, P.-W.; Chen, Y. Chitosan hydrogel in combination with marine peptides from tilapia for burns healing. *Int. J. Biol. Macromol.* **2018**, *112*, 1191–1198. [CrossRef]
73. Parthasarathy, A.; Vijayakumar, S.; Malaikozhundan, B.; Thangaraj, M.P.; Ekambaram, P.; Murugan, T.; Velusamy, P.; Anbu, P.; Vaseeharan, B. Chitosan-coated silver nanoparticles promoted antibacterial, antibiofilm, wound-healing of murine macrophages and antiproliferation of human breast cancer MCF 7 cells. *Polym. Test.* **2020**, *90*, 106675. [CrossRef]
74. Xiao, J.; Zhou, Y.; Ye, M.; An, Y.; Wang, K.; Wu, Q.; Song, L.; Zhang, J.; He, H.; Zhang, Q.; et al. Freeze-Thawing Chitosan/Ions Hydrogel Coated Gauzes Releasing Multiple Metal Ions on Demand for Improved Infected Wound Healing. *Adv. Healthc. Mater.* **2021**, *10*, 2001591. [CrossRef]
75. Sen, C.K. Human Wounds and Its Burden: An Updated Compendium of Estimates. *Adv. Wound Care* **2019**, *8*, 39–48. [CrossRef] [PubMed]
76. Goy, R.C.; Morais, S.T.B.; Assis, O.B.G. Evaluation of the antimicrobial activity of chitosan and its quaternized derivative on *E. coli* and *S. aureus* growth. *Rev. Bras. Farmacogn.* **2016**, *26*, 122–127. [CrossRef]
77. Kim, K.W.; Thomas, R.L.; Lee, C.; Park, H.J. Antimicrobial activity of native chitosan, degraded chitosan, and O-carboxymethylated chitosan. *J. Food Prot.* **2003**, *66*, 1495–1498. [CrossRef] [PubMed]
78. Arkoun, M.; Daigle, F.; Heuzey, M.-C.; Ajji, A. Mechanism of Action of Electrospun Chitosan-Based Nanofibers against Meat Spoilage and Pathogenic Bacteria. *Molecules* **2017**, *22*, 585. [CrossRef] [PubMed]
79. Alshamsan, A.; Aleanizy, F.S.; Badran, M.; Alqahtani, F.Y.; Alfassam, H.; Almalik, A.; Alosaimy, S. Exploring anti-MRSA activity of chitosan-coated liposomal dicloxacillin. *J. Microbiol. Methods* **2019**, *156*, 23–28. [CrossRef] [PubMed]
80. Laverde-Rojas, V.; Liscano, Y.; Rivera-Sánchez, S.P.; Ocampo-Ibáñez, I.D.; Betancourt, Y.; Alhajj, M.J.; Yarce, C.J.; Salamanca, C.H.; Oñate-Garzón, J. Antimicrobial Contribution of Chitosan Surface-Modified Nanoliposomes Combined with Colistin against Sensitive and Colistin-Resistant Clinical *Pseudomonas aeruginosa*. *Pharmaceutics* **2021**, *13*, 41. [CrossRef] [PubMed]
81. Sacco, P.; Travan, A.; Borgogna, M.; Paoletti, S.; Marsich, E. Silver-containing antimicrobial membrane based on chitosan-TPP hydrogel for the treatment of wounds. *J. Mater. Sci. Mater. Med.* **2015**, *26*, 128. [CrossRef]

82. Wang, X.; Cheng, F.; Wang, X.; Feng, T.; Xia, S.; Zhang, X. Chitosan decoration improves the rapid and long-term antibacterial activities of cinnamaldehyde-loaded liposomes. *Int. J. Biol. Macromol.* **2021**, *168*, 59–66. [CrossRef]
83. Wu, I.Y.; Bala, S.; Škalko-Basnet, N.; di Cagno, M.P. Interpreting non-linear drug diffusion data: Utilizing Korsmeyer-Peppas model to study drug release from liposomes. *Eur. J. Pharm. Sci.* **2019**, *138*, 105026. [CrossRef]
84. Maqbool, F.; Moyle, P.M.; Tan, M.S.A.; Thurecht, K.J.; Falconer, J.R. Preparation of albendazole-loaded liposomes by supercritical carbon dioxide processing. *Artif. Cells Nanomed. Biotechnol.* **2018**, *46*, S1186–S1192. [CrossRef] [PubMed]
85. Muzzarelli, R.A.A. Colorimetric Determination of Chitosan. *Anal. Biochem.* **1998**, *260*, 255–257. [CrossRef]
86. Hirsjärvi, S.; Qiao, Y.; Royere, A.; Bibette, J.; Benoit, J.-P. Layer-by-layer surface modification of lipid nanocapsules. *Eur. J. Pharm. Biopharm.* **2010**, *76*, 200–207. [CrossRef]
87. Jøraholmen, M.W.; Škalko-Basnet, N.; Acharya, G.; Basnet, P. Resveratrol-loaded liposomes for topical treatment of the vaginal inflammation and infections. *Eur. J. Pharm. Sci.* **2015**, *79*, 112–121. [CrossRef] [PubMed]
88. Cauzzo, J.; Nystad, M.; Holsæter, A.M.; Basnet, P.; Škalko-Basnet, N. Following the Fate of Dye-Containing Liposomes In Vitro. *Int. J. Mol. Sci.* **2020**, *21*, 4847. [CrossRef] [PubMed]
89. Balouiri, M.; Sadiki, M.; Ibnsouda, S.K. Methods for in vitro evaluating antimicrobial activity: A review. *J. Pharm. Anal.* **2016**, *6*, 71–79. [CrossRef]
90. Ternullo, S.; Gagnat, E.; Julin, K.; Johannessen, M.; Basnet, P.; Vanić, Ž.; Škalko-Basnet, N. Liposomes augment biological benefits of curcumin for multitargeted skin therapy. *Eur. J. Pharm. Biopharm.* **2019**, *144*, 154–164. [CrossRef] [PubMed]

Supplementary material

Chitosomes-in-chitosan hydrogel for acute skin injuries: prevention and infection control

Lisa Myrseth Hemmingsen [1], Kjersti Julin [2], Luqman Ahsan [1], Purusotam Basnet [3,4], Mona Johannessen [2] and Nataša Škalko-Basnet [1*]

[1] Drug Transport and Delivery Research Group, Department of Pharmacy, University of Tromsø The Arctic University of Norway, Universitetsvegen 57, 9037 Tromsø, Norway; lisa.m.hemmingsen@uit.no (L.M.H), luqmaan.ahsan@gmail.com (L.A.), natasa.skalko-basnet@uit.no (N.Š-B)

[2] Research Group for Host-Microbe Interaction, Department of Medical Biology, University of Tromsø The Arctic University of Norway, Sykehusvegen 44, 9037 Tromsø, Norway; kjersti.julin@uit.no (K.J), mona.johannessen@uit.no (M.J)

[3] IVF Clinic, Department of Obstetrics and Gynecology, University Hospital of North Norway, Sykehusvegen 38, 9019 Tromsø, Norway; purusotam.basnet@uit.no (P.B)

[4] Women's Health and Perinatology Research Group, Department of Clinical Medicine, University of Tromsø The Arctic University of Norway, Universitetsvegen 57, 9037 Tromsø, Norway; purusotam.basnet@uit.no (P.B)

* Correspondence: natasa.skalko-basnet@uit.no; Tel.: +47 77646640

S1. Supplementary results

S1.1. Hydrogel stability

The stability of the hydrogels both with and without vesicles was evaluated as the texture properties and pH over time. The texture properties of hydrogels with vesicles demonstrated higher stability over a period of four weeks compared to hydrogel without vesicles (Table S1). The parameters cohesiveness and adhesiveness of the plain hydrogel demonstrated significant changes. This might be attributed to the effects of phospholipids. Since phospholipids could act as plasticizers, which could provide an improved long-term effect. Glycerol was added as a plasticizer in all hydrogels, both to improve the mobility in the hydrogel networks and to improve the stability of the hydrogels [44]. The increased mobility in the hydrogels with vesicles was evident from the lowered cohesiveness in these hydrogels compared to the hydrogel without vesicles. Jøraholmen and colleagues did not observe this effect upon addition of liposomes in a concentration of 10 or 20% in chitosan hydrogel [45]. Additionally, Hurler and colleagues suggested that vesicles with positive zeta potential stabilize the chitosan hydrogel network better than neutral vesicles [38], probably due to the repulsive effects.

The pH of all hydrogels proved stable over the whole period and no significant changes were observed (Table S1).

Table S1. Stability hydrogel measured as texture properties and pH.

	Week	Hardness	Cohesiveness	Adhesiveness	pH
		g	g·s	g·s	
Hydrogel	2	143 ± 3	177 ± 2	-164 ± 2	4.6 ± 0.0
	4	144 ± 5	190 ± 5	-174 ± 5	4.6 ± 0.0
HG-PL-EMP	2	153 ± 6	160 ± 5	-155 ± 3	4.9 ± 0.1
	4	164 ± 10	166 ± 8	-162 ± 7	4.9 ± 0.1
HG-CHI-EMP	2	160 ± 9	162 ± 2	-159 ± 3	4.8 ± 0.0
	4	165 ± 11	166 ± 5	-162 ± 6	4.8 ± 0.0

HG-PL-CHX	2	139 ± 6	169 ± 10	-156 ± 9	4.7 ± 0.0
	4	141 ± 3	161 ± 5	-152 ± 2	4.7 ± 0.0
HG-CHI-CHX	2	145 ± 8	169 ± 4	-160 ± 4	4.7 ± 0.0
	4	150 ± 6	174 ± 5	-165 ± 3	4.7 ± 0.0

Hydrogel characteristics were evaluated 2 and 4 weeks after preparation. Hydrogel = plain hydrogel, HG-PL-EMP = plain, empty vesicles in hydrogel, HG-CHI-EMP = empty chitosomes in hydrogel, HG-PL-CHX = plain, CHX-vesicles in hydrogel, HG-CHI-CHX = CHX-chitosomes in hydrogel. Results are expressed as means with their respective SD (n = 3).

S1.2. Anti-inflammatory activity

In Figure S1, the inflammatory responses of both chitosomes and plain vesicles with and without CHX are presented. The plain vesicles demonstrated dose-dependent reduction of the inflammation response in lipopolysaccharide (LPS)-induced murine macrophages compared to untreated activated cells, whereas the chitosan-infused vesicles maintained the same response as the non-treated cells and did not introduce any additional inflammation response. These results are promising for these lipid and chitosan-based vesicles in wound therapy.

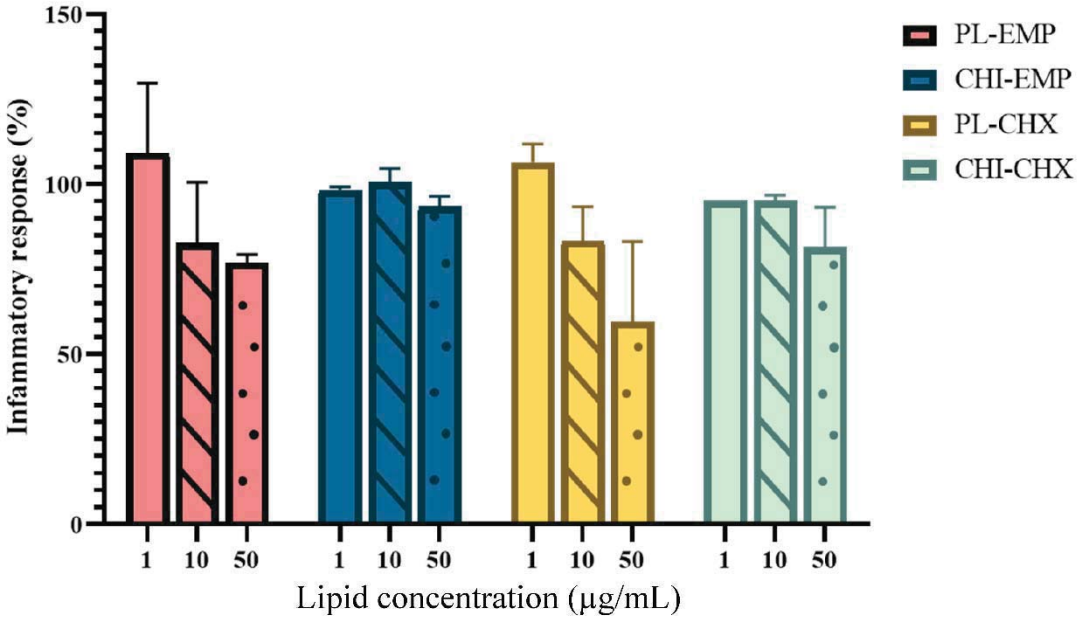

Figure S1. Evaluation of anti-inflammatory activity of vesicles on RAW 264.7 cells. Three different concentrations were tested, namely 1 (no pattern), 10 (stripes) and 50 (dots) µg/mL lipid and the results are presented as inflammatory response of treated cells compared to control (100%). All results are expressed as means with their respective SD (n = 2).

PL-EMP = plain, empty vesicles, CHI-EMP = empty chitosomes, PL-CHX = plain, CHX-vesicles, CHI-CHX = CHX-chitosomes.

S2. Supplementary methods

S2.1. Stability testing of hydrogels

The stability of hydrogels and vesicles-in-hydrogel were evaluated after storage for two and four weeks after preparation. The texture properties and pH were measured as described in section 3.4.2.

S2.2. Anti-inflammatory activity

Anti-inflammatory activity was determined by LPS-induced NO production in murine macrophages RAW 264.7 cells [88]. Cells were cultured in complete RPMI (containing 10 % fetal bovine serum and 1 % penicillin and streptomycin) and seeded in 24 well plates prior to incubation (37 °C /5 % CO_2) for 24 hours. After incubation, the complete medium was replaced with medium containing LPS (1 μg/mL). The cells were then treated with chitosome suspensions of different concentrations (1, 10 and 50 μg/mL lipid concentration) diluted in LPS (1 μg/mL) containing medium. LPS containing medium and complete medium served as positive and negative controls. The cells were then incubated for another 24 hours and the NO production was evaluated on a UV-vis plate reader (Tecan Trading AG, Männedorf, Switzerland) with Griess reagent (2.5 % phosphoric acid with 1 % sulphanilamide and 0.1 % N-(-1-naphthyl)ethylenediamine) at 540 nm.

Supplementary references

38. Hurler, J.; Žakelj, S.; Mravljak, J.; Pajk, S.; Kristl, A.; Schubert, R.; Škalko-Basnet, N., The effect of lipid composition and liposome size on the release properties of liposomes-in-hydrogel. *Int. J. Pharm.* **2013,** 456, 49-57; https://doi.org/10.1016/j.ijpharm.2013.08.033.

44. Hurler, J.; Engesland, A.; Kermany, B. P.; Škalko-Basnet, N., Improved texture analysis for hydrogel characterization: Gel cohesiveness, adhesiveness, and hardness. *J. Appl. Polym. Sci.* **2012,** 125, 180-188; https://doi.org/10.1002/app.35414.

45. Jøraholmen, M. W.; Basnet, P.; Tostrup, M. J.; Moueffaq, S.; Škalko-Basnet, N., Localized Therapy of Vaginal Infections and Inflammation: Liposomes-In-Hydrogel Delivery System for Polyphenols. *Pharmaceutics* **2019,** 11, 53; https://doi.org/10.3390/pharmaceutics11020053.

88. Cauzzo, J.; Nystad, M.; Holsæter, A. M.; Basnet, P.; Škalko-Basnet, N., Following the Fate of Dye-Containing Liposomes In Vitro. *Int. J. Mol. Sci.* **2020,** 21, 4847; https://doi.org/10.3390/ijms21144847.

Paper III

frontiers | Frontiers in Microbiology

TYPE Original Research
PUBLISHED 29 September 2022
DOI 10.3389/fmicb.2022.1023083

OPEN ACCESS

EDITED BY
Nayeli Alva-Murillo,
University of Guanajuato,
Mexico

REVIEWED BY
Guodong Zhao,
Zhejiang University Kunshan Innovation Institute, China
Anita Hafner,
University of Zagreb,
Croatia

*CORRESPONDENCE
Nataša Škalko-Basnet
natasa.skalko-basnet@uit.no

SPECIALTY SECTION
This article was submitted to Infectious Agents and Disease, a section of the journal Frontiers in Microbiology

RECEIVED 19 August 2022
ACCEPTED 15 September 2022
PUBLISHED 29 September 2022

CITATION
Hemmingsen LM, Panchai P, Julin K, Basnet P, Nystad M, Johannessen M and Škalko-Basnet N (2022) Chitosan-based delivery system enhances antimicrobial activity of chlorhexidine. *Front. Microbiol.* 13:1023083. doi: 10.3389/fmicb.2022.1023083

Chitosan-based delivery system enhances antimicrobial activity of chlorhexidine

Lisa Myrseth Hemmingsen[1], Pimmat Panchai[1], Kjersti Julin[2], Purusotam Basnet[3], Mona Nystad[3,4], Mona Johannessen[2] and Nataša Škalko-Basnet[1]*

[1]Drug Transport and Delivery Research Group, Department of Pharmacy, University of Tromsø The Arctic University of Norway, Tromsø, Norway, [2]Research Group for Host-Microbe Interaction, Department of Medical Biology, University of Tromsø The Arctic University of Norway, Tromsø, Norway, [3]Women's Health and Perinatology Research Group, Department of Clinical Medicine, University of Tromsø The Arctic University of Norway, Tromsø, Norway, [4]IVF Clinic, Women's Clinic, University Hospital of North Norway, Tromsø, Norway

Infected chronic skin wounds and other skin infections are increasingly putting pressure on the health care providers and patients. The pressure is especially concerning due to the rise of antimicrobial resistance and biofilm-producing bacteria that further impair treatment success. Therefore, innovative strategies for wound healing and bacterial eradication are urgently needed; utilization of materials with inherent biological properties could offer a potential solution. Chitosan is one of the most frequently used polymers in delivery systems. This bioactive polymer is often regarded as an attractive constituent in delivery systems due to its inherent antimicrobial, anti-inflammatory, anti-oxidative, and wound healing properties. However, lipid-based vesicles and liposomes are generally considered more suitable as delivery systems for skin due to their ability to interact with the skin structure and provide prolonged release, protect the antimicrobial compound, and allow high local concentrations at the infected site. To take advantage of the beneficial attributes of the lipid-based vesicles and chitosan, these components can be combined into chitosan-containing liposomes or chitosomes and chitosan-coated liposomes. These systems have previously been investigated for use in wound therapy; however, their potential in infected wounds is not fully investigated. In this study, we aimed to investigate whether both the chitosan-containing and chitosan-coated liposomes tailored for infected wounds could improve the antimicrobial activity of the membrane-active antimicrobial chlorhexidine, while assuring both the anti-inflammatory activity and cell compatibility. Chlorhexidine was incorporated into three different vesicles, namely plain (chitosan-free), chitosan-containing and chitosan-coated liposomes that were optimized for skin wounds. Their release profile, antimicrobial activities, anti-inflammatory properties, and cell compatibility were assessed *in vitro*. The vesicles comprising chitosan demonstrated slower release rate of chlorhexidine and high cell compatibility. Additionally, the inflammatory responses in murine macrophages treated with these vesicles were reduced by about 60% compared to non-treated cells. Finally, liposomes containing both chitosan and chlorhexidine demonstrated the strongest antibacterial effect against *Staphylococcus aureus*. Both chitosan-containing and

10.3389/fmicb.2022.1023083

chitosan-coated liposomes comprising chlorhexidine could serve as excellent platforms for the delivery of membrane-active antimicrobials to infected wounds as confirmed by improved antimicrobial performance of chlorhexidine.

KEYWORDS

chitosan, chlorhexidine, lipid-based vesicles, membrane-active antimicrobials, skin wound healing, bioactive polymer, antibacterial activity

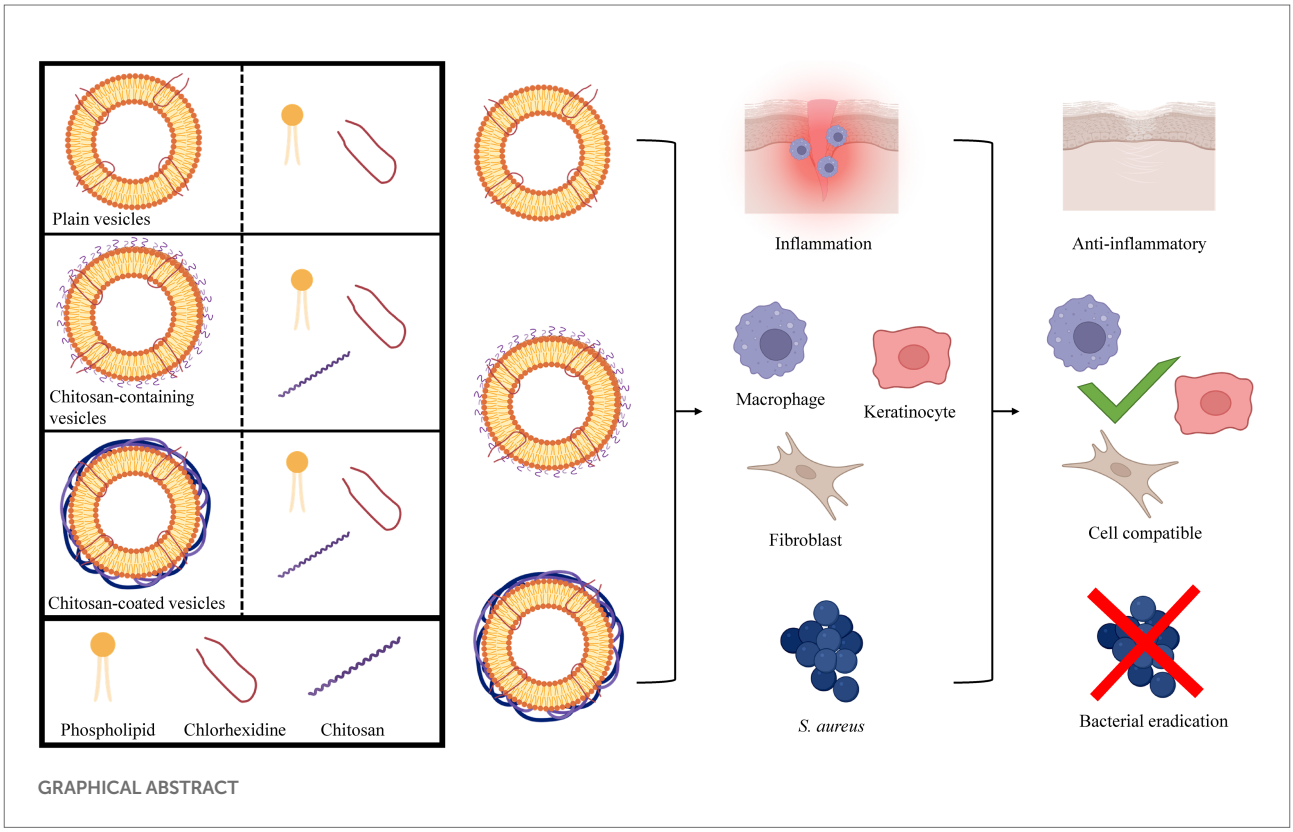

GRAPHICAL ABSTRACT

Introduction

Skin wounds, and particularly chronic wounds, are placing an enormous strain on health care systems worldwide; in 2018 the prevalence of chronic wounds was estimated to be approximately 1–2% in the general population (Kaiser et al., 2021). There is a solid consensus that one of the most important factors permitting wounds to heal properly is the ability to lower the microbial burden and inflammation in the wound bed (Eriksson et al., 2022). However, the rising antimicrobial resistance (AMR) and bacteria's production of biofilms are making this undertaking more challenging, therefore innovative strategies are urgently needed to mend the situation (Barrigah-Benissan et al., 2022). In this scenario, chitosan could play an important role both because of its inherent biological properties, but also its ability to improve efficacy of antimicrobial compounds (Hemmingsen et al., 2021a). Chitosan is among the most frequently used polymers in pharmaceutical technology and drug delivery systems (Pramanik and Sali, 2021). The interest in chitosan emanates from its many beneficial attributes, such as antimicrobial, anti-inflammatory, anti-oxidative, and hemostatic properties (Iacob et al., 2021). Additionally, this polymer, derived from deacetylated chitin found in crab, shrimp, krill shells, and fungi, is biodegradable and biocompatible with generally low toxicity (Bakshi et al., 2020). Numerous studies have confirmed its potential in skin therapy, especially against skin infections (Hemmingsen et al., 2021c). However, lipid-based systems are more frequently used in skin delivery; liposomes are often considered attractive because of their ability to closely interact

Abbreviations: AMR, Antimicrobial resistance; CCK-8, Cell counting kit-8; CFU, Colony-forming units; CHX, chlorhexidine; DMEM-hg, Dulbecco's Modified Eagle Medium high glucose; EE, Entrapment efficiency; FBS, Fetal bovine serum; LPS, Lipopolysaccharide; MAA, Membrane-active antimicrobial; M_w, Molecular weight; NO, Nitric oxide; PBS, Phosphate buffered-saline; PEG, Polyethylene glycol; PI, Polydispersity index; RMPI, Roswell park memorial institute medium.

with the skin structure (Matei et al., 2021). Additionally, liposomes and lipid-based vesicles provide prolonged release, protect the entrapped antimicrobial, and allow high local drug concentrations at the infected site (Nwabuife et al., 2021). To utilize the advantageous attributes from both lipid-based systems and chitosan, they can be combined, as, e.g., in chitosomes (chitosan-containing liposomes) with chitosan on the surface and in the interior of the liposomes or chitosan-coated liposomes (Sebaaly et al., 2021). These vesicles have been investigated for several applications, however, mainly for mucosal delivery (Sebaaly et al., 2021). Additionally, their role in wound healing has also been investigated (Mengoni et al., 2017; Eid et al., 2022), yet their role in antimicrobial wound therapy is not fully explored. We propose that by tailoring chitosan's availability on vesicle surface we could improve the antimicrobial potential of chitosan-comprising vesicles for wound therapy.

Taking advantage of the antimicrobial properties and potentially elevate the effect of chitosan, chitosan-containing or chitosan-coated drug delivery systems could be further combined with membrane-active antimicrobials (MAAs); their combination could generate a synergetic antimicrobial effect (Hemmingsen et al., 2021b). Among antiseptics that are often used to treat skin and soft tissue infections, the MAA chlorhexidine (CHX), is one of the most common (Hoang et al., 2021). Its main mechanism of action is proposed to be a destruction of the bacterial membranes; however, precipitation of the cytoplasm has been observed at higher doses (Hubbard et al., 2017). Unfortunately, studies show growing resistance towards CHX which might affect its future effectiveness in the clinics (Fritz et al., 2013; Cieplik et al., 2019; Abdel-Sayed et al., 2020). Here, the drug delivery systems could play a valuable role. Carefully tailored delivery systems could improve the antimicrobial efficacy of antimicrobial compounds by increasing their local concentration and retention time, protect antimicrobial compounds, and improve interaction with bacterial membranes (Osman et al., 2022). Furthermore, in chronic wounds, the additional beneficial biological properties of chitosan could improve wound healing by directly affecting the healing cascade or reducing inflammation and oxidative radicals (Iacob et al., 2021).

In our previous study, we investigated the effect of medium molecular weight (M_w) chitosan combined with liposomes on inflammatory responses and antimicrobial potential (Hemmingsen et al., 2021b). In the current study, we assessed whether the insertion of chitosan into lipid vesicles, as in chitosan-containing liposomes or chitosomes, or chitosan-coating of pre-made lipid carriers, influenced the CHX release and biological properties of the novel system. Furthermore, we investigated the ability of low M_w chitosan to improve the anti-inflammatory and antimicrobial properties of CHX. The antimicrobial activity of chitosan is not fully elucidated, however, the most common explanations for its antimicrobial properties are proposed to be linked to the interaction between positively charged chitosan and the slightly negatively charged bacterial membrane (Khan et al., 2020; Xia et al., 2022). However, chitosan's biological properties are coupled to its M_w and degree of deacetylation. Chitosans of higher M_w are proposed to form an envelope around the bacterial membrane, limiting nutrient uptake and growth, while chitosans of lower M_w are more prone to penetrate the bacterial membrane and interact with intracellular components (Matica et al., 2019). We aimed to exploit the latter mechanism to improve the antimicrobial potential of CHX.

Materials and methods

Materials

Chitopharm™ S-Chitosan with low M_w (50–1000 kDa), degree of deacetylation >70% was kindly provided by Chitinor (Tromsø, Norway). Lipoid S100 was kindly provided by Lipoid GmbH (Ludwigshafen, Germany). Methanol ≥99.9%, HiPerSolv CHROMANORM® for LC–MS, phosphate buffered-saline (PBS, pH 7.4) tablets and acetic acid glacial were procured from VWR International (Fontenay-sous-Bois, France). Chlorhexidine ≥99.5%, glycerol solution (86–89%), glycine hydrochloride ≥99% (HPLC), sodium chloride, hydrochloric acid, Cell Counting Kit-8 (CCK-8), and Kollisolv® polyethylene glycol (PEG) E 400 were obtained from Sigma-Aldrich (St. Louis, MO, United States). Cibacron Brilliant Red 3BA was a product from Santa Cruz Biotechnology (Dallas, TX, United States). Ortho-phosphoric acid ≥85% was purchased from Kebo Lab Ab (Oslo, Norway). Penicillin–streptomycin and Roswell Park Memorial Institute (RPMI) medium 1640 were purchased from Sigma-Aldrich (Steinheim, Germany). Lipopolysaccharide (LPS, from *Escherichia coli* 055:B5), sulfanilamide ≥98% and N-(1-Naphthyl)ethylenediamine dihydrochloride ≥98% were obtained from Sigma Life Science Norway AS (Oslo, Norway). Dulbecco's Modified Eagle Medium high glucose w/ l-glutamine (DMEM-hg) and sodium pyruvate and fetal bovine serum (FBS) were purchased from Biowest (Nuaillé, France). Blood agar plates, saline solution, and Mueller–Hinton broth were supplied by University Hospital of North Norway (Tromsø, Norway). Murine macrophage RAW 264.7 cells were ordered from ATCC (Manassas, VA, United States). Human Dermal Fibroblasts, Neonatal (NHDF-neo) were obtained from Lonza (Basel, Switzerland), and HaCaT cell line (immortalized human keratinocytes) from CLS Cell Lines Service GmbH (Eppelheim, Germany). *Staphylococcus aureus* (ATCC® BAA-1721™) MSSA476 was ordered from LGC standards AB (Borås, Sweden).

Preparation of vesicles

Preparation of plain lipid carriers or chitosan-containing liposomes

Vesicles were produced by the thin film method as described previously (Shukla et al., 2020; Hemmingsen et al., 2021a). In

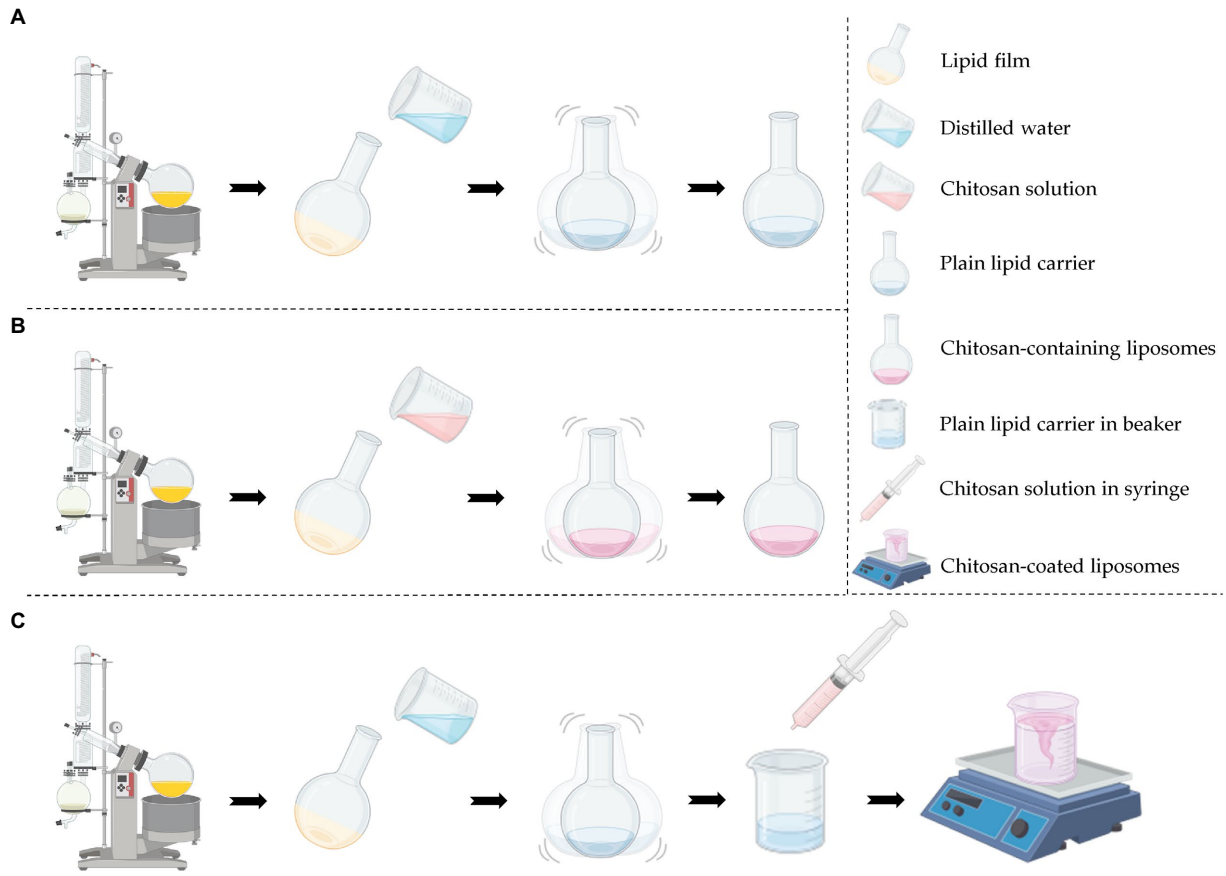

FIGURE 1
Production procedure of the different vesicles. **(A)** Production of plain lipid carrier with or without chlorhexidine. **(B)** Production of chitosan-containing liposomes with or without chlorhexidine. **(C)** Production of chitosan-coated liposomes with or without chlorhexidine. Created with BioRender.com.

brief, Lipoid S100 (200 mg) and CHX (10 mg) were dissolved in methanol; the solvent was removed by evaporation (Büchi rotavapor R-124 with vacuum controller B-721, Büchi Vac® V-500, Büchi Labortechnik, Flawil, Switzerland) at 60 mBar and 45°C for at least 1 h. The lipid film was dislodged with 10 ml distilled water to create plain (chitosan-free) lipid carriers or 10 ml 0.2% (w/v) chitosan solution in 0.1 M acetic acid, to form chitosan-containing liposomes. Both formulations were shaken to anneal vesicles. Empty lipid carriers were prepared in the same manner without CHX present. The vesicles were stored in the refrigerator (4°C) prior to size reduction.

Vesicle coating with chitosan

Plain lipid carriers with or without CHX were coated with 0.2% (w/v) chitosan solution in 0.1 M acetic acid (1:1, v/v, Jøraholmen et al., 2014). The chitosan solution was added dropwise (1.22 min/ml) under continuous stirring (250 rpm). The suspensions were stirred for another hour at 24°C before refrigeration (4°C). The lipid and chitosan concentrations were adjusted to be comparable prior to all further experiments. The production of the different vesicles is depicted in Figure 1.

Vesicle size reduction

The size of the vesicles was reduced using probe sonication and manual extrusion. The amplitude of the probe (SONICS high intensity ultrasonic processor, 500-watt model, 13 mm probe diameter, Sonics & Materials Inc., Newtown, CT, United States) was set to 40% and the samples were kept on ice bath to avoid extensive heating. Extrusion was performed with polycarbonate membranes (Nuclepore Track-Etch Membrane, Whatman House, Maidstone, United Kingdom) with average pore size of 0.4 µm (Cauzzo et al., 2020). The size of the different formulations was reduced as described in Table 1 to attain vesicles of similar sizes.

Vesicle characterization

Vesicle size and zeta potential measurements

The size of vesicles was measured with NICOMP Submicron particle sizer (NICOMP Particle Sizing System, Santa Barbara, CA, United States) at an intensity of 250–350 kHz reached by dilution in filtered (0.2 µm) distilled water (Hemmingsen et al., 2021b). The vesicles were measured in three rounds of 15–20 min

TABLE 1 Vesicle type, designation, and size reduction procedure.

	Sonication time (s)	Sonication intervals	Rounds of extrusion
PL	10	10	3
PL-CHX	5	1	–
CH	10	10	3
CH-CHX	5	2	–
CO	10	18	–
CO-CHX	5	1	–

PL, Plain, empty lipid carrier; PL-CHX, Plain CHX-lipid carrier; CH, Chitosan-containing empty liposomes; CH-CHX, Chitosan-containing CHX-liposomes; CO, Chitosan-coated empty liposomes; CO-CHX, Chitosan-coated CHX-liposomes.

(to attain stable readings) at 22–24°C, and the weight-intensity distribution was recorded (as cumulative size of 80% of the population).

The zeta potential was measured with Zetasizer Nano Zen 2,600 (Malvern, Worcestershire, United Kingdom). The samples were diluted in filtered (0.2 µm) tap water (assuring counter ions) to an appropriate concentration (according to attenuation) and measured at 25°C in three cycles using a DTS1070 cell (Malvern, Worcestershire, United Kingdom, Jøraholmen et al., 2015).

The pH of vesicle suspensions was measured using sensION+ PH31 pH benchtop meter (Hach, Loveland, CO, United States).

Entrapment efficiency

Unentrapped CHX was removed from the vesicle suspension using dialysis tubing with M_w cut-off 12–14 kDa (Spectra/Por®4, Spectrum®, VWR International, Fontenay-sous-Bois, France). An aliquot of 1 ml of vesicle suspension was dialyzed against 1 l distilled water under stirring for 4 h at room temperature. The CHX incorporated in the liposomes was quantified using Spark M10 multimode plate reader (Tecan Trading AG, Männedorf, Switzerland) at 261 nm (Hemmingsen et al., 2021a).

Surface-available chitosan determination

Quantification of surface-available chitosan was performed as previously described (Muzzarelli, 1998; Jøraholmen et al., 2015). In short, glycine buffer (250 ml, pH 3.2) was prepared in distilled water using 1.87 g glycine and 1.46 g NaCl. This buffer (81 ml) was further diluted to a total volume of 100 ml in 0.1 M HCl. To quantify chitosan, a dye solution was prepared. An aliquot of 150 mg Cibacron Brilliant Red 3B-A was dissolved in distilled water (100 ml). The glycine buffer was used to dilute 5 ml of the dye solution to a total volume of 100 ml. An aliquot of 300 µl of diluted vesicle suspensions (distilled water, 1:1, v/v) were mixed with 3 ml of the diluted Cibacron dye and surface-available chitosan was quantified using Spark M10 multimode plate reader (Tecan Trading AG, Männedorf, Switzerland) at 575 nm (Jøraholmen et al., 2015).

Vesicle stability

The stability of the vesicles was evaluated after 2- and 4-week storage at 4°C. The parameters evaluated were the vesicle size, zeta potential, and pH as described in the section Vesicle size and zeta potential measurements.

In vitro chlorhexidine release

In vitro CHX release studies were performed using a Franz cell diffusion system (PermeGear, Hellertown, PA, United States). Pre-soaked cellophane membranes (Max Bringmann KG, Wendelstein, Germany) were used as diffusion barriers with area of 1.77 cm^2 (Jøraholmen et al., 2014). Due to the low water solubility of CHX base (Farkas et al., 2001), the acceptor chamber was filled with PEG E 400 (10%, v/v) in distilled water (12 ml acceptor volume, Hemmingsen et al., 2021b). The temperature was maintained at 32°C with heated circulating water. Vesicle suspensions (600 µl) were added to the donor chamber. Samples were withdrawn after 1, 2, 3, 4, 5, 8, and 24 h, and the sample volume was replaced with fresh medium to maintain sink conditions. The release from vesicles was compared to non-formulated CHX (dissolved in release media). Quantitative analysis was carried out using Spark M10 multimode plate reader (Tecan Trading AG, Männedorf, Switzerland) at 261 nm (Hemmingsen et al., 2021b).

Evaluation of cell viability and anti-inflammatory responses

Assessment of cell viability

Assessment of cell viability was accomplished using the CCK-8 kit according to methods previously described (Hemmingsen et al., 2021b). The cells (HaCaT; Cauzzo et al., 2020, NHDF-neo; Domiński et al., 2022, and murine macrophages RAW 264.7; Basnet et al., 2012; Cauzzo et al., 2020) in complete RPMI medium [containing 10% (v/v) FBS and penicillin–streptomycin; RAW 264.7] or complete DMEM-hg (HaCaT and NHDF-neo) were plated on 96-well plates (90 µl, 1×10^5 cells/ml) and incubated (37°C, 5% CO_2) for 24 h. Diluted vesicle suspensions (10 µl) were added to the wells (final lipid concentration of 1, 10, and 50 µg/ml) and the plates incubated for another 24 h (37°C, 5% CO_2). Next, an aliquot of 10 µl CCK-8 reagent was added to each well and the plates were incubated for 4 h. The cell viability was measured using Spark M10 multimode plate reader (Tecan Trading AG, Männedorf, Switzerland) at 450 nm with the reference set to 650 nm. Treated cells were compared to non-treated cells (only complete RPMI or DMEM-hg).

Anti-inflammatory activity

The anti-inflammatory activity of the vesicles was assessed by inducing nitric oxide (NO) production in murine macrophages using

LPS as previously described (Schulte-Werning et al., 2021). RAW 264.7 cells (Basnet et al., 2012) in complete RPMI medium [containing 10% (v/v) FBS and penicillin–streptomycin] were plated on 24-well plate (1,000 µl, 5×10^5 cells/ml) and incubated (37°C, 5% CO_2) for 24 h. The complete medium was aspirated and LPS (1 µg/ml, 990 µl) in complete RPMI added to each well. Next, diluted vesicle suspensions (10 µl) were added to the wells at final lipid concentration of 1, 10, and 50 µg/ml, and the plates incubated for another 24 h (37°C, 5% CO_2). The NO production was assessed by mixing the cell medium and Griess reagent [1:1, v/v; 2.5% phosphoric acid with 1% sulphanilamide and 0.1% N-(−1-naphthyl)ethylenediamine] and analyzing the mixture with Spark M10 multimode plate reader (Tecan Trading AG, Männedorf, Switzerland) at 560 nm. Only complete medium or LPS (1 µg/ml) in complete RPMI served as controls. The LPS-induced cells treated with vesicles were compared to non-treated LPS-induced cells (100%).

Antimicrobial evaluation

The broth microdilution method was utilized to evaluate the antibacterial properties of the vesicles with or without CHX (Balouiri et al., 2016). Overnight cultures of *S. aureus* MSSA476 were diluted in saline solutions (0.85%, w/w) to a turbidity of 0.5 McFarland; these bacterial suspensions were further diluted (1:150, v/v) in Mueller-Hinton broth. Vesicle suspensions were 2-fold diluted with Mueller-Hinton broth in 96-well plates and the diluted bacterial suspensions added (1:1, v/v). The plates were incubated at 37°C with shaking (100 rpm) for 24 h. Non-treated or treated (with different vesicles) bacteria in suspensions were serially diluted (10-fold) in PBS, plated on blood agar plates and incubated at 37°C overnight. The colony-forming units (CFUs) were counted to evaluate the activity of the tested formulations as compared to non-treated bacteria. Lipid concentrations of 0.3125 mg/ml were used to compare the different vesicle formulations (Ternullo et al., 2019).

Statistical analyses

The results are generally expressed as means ± SD. Statistical significance was evaluated by student's *t*-test or one-way ANOVA followed by Turkey's correction (p at least 0.05). All statistical analyses were performed in GraphPad Prism version 9.3.1 for Windows (GraphPad Software LLC, San Diego, CA, United States).

Results and discussion

Vesicle characteristics

Size is an important parameter in the development of drug delivery systems; considering the dermal administration route it has been proposed that size around 300 nm might be beneficial assuring that the vesicles are able to reach the deeper layers of the skin without advancing too deep (du Plessis et al., 1994). In our previous studies, we have shown that the vesicles in a size range between 250 and 350 nm provide good eradication of common skin pathogens (Hemmingsen et al., 2021a,b). Furthermore, reports indicate that nanoparticles smaller than 350 nm can diffuse through biofilm pores (Makabenta et al., 2021). Therefore, we aimed for the size range of 250–350 nm for our plain and chitosan-comprising formulations (Table 2). We assessed the vesicle size as cumulative size of 80% of the vesicle populations since some of the vesicles exhibited the bi- or multi-modal distributions that were difficult to directly compare. Most vesicles were slightly over 300 nm in diameter; however, the chitosan-coated liposomes displayed a larger size likely due to the coating procedure. Even though the optimal polydispersity index (PI) is suggested to be about 0.3 for lipid-based vesicles destined for skin delivery (Danaei et al., 2018), our vesicles had a PI below 0.4 and that was deemed acceptable. The vesicle size of chitosan-coated liposomes is often larger and harder to control as compared to non-coated liposomes (Jøraholmen et al., 2015).

TABLE 2 Chitosan-containing liposomes and chitosan-coated liposomes characteristics: mean diameter (≤80%, nm), polydispersity index (PI), zeta potential, entrapment efficacy (EE%), and pH in aqueous medium.

	Size (≤80%, nm)	PI	Zeta potential (mV)	EE%	pH
PL	308 ± 22	0.37 ± 0.04	−1.6 ± 1.4	–	5.8 ± 0.5
PL-CHX	305 ± 14	0.38 ± 0.03	42.9 ± 5.9	63.2 ± 4.8	8.5 ± 0.1
CH	303 ± 18	0.32 ± 0.01	12.4 ± 0.4	–	3.6 ± 0.0
CH-CHX	300 ± 24	0.34 ± 0.07	94.9 ± 2.2	65.7 ± 4.8	3.7 ± 0.0
CO	325 ± 23	0.35 ± 0.01	13.0 ± 0.4	–	3.7 ± 0.0
CO-CHX	393 ± 23	0.39 ± 0.02	83.3 ± 3.1	70.4 ± 3.9	3.8 ± 0.0

Results of size measurements are expressed as means of cumulative size ≤ 80% of vesicle populations (weight-intensity distribution) with their respective SD, while the rest of the results are expressed as means with their respective SD ($n = 3$). PL, Plain, empty lipid carrier; PL-CHX, Plain CHX-lipid carrier; CH, Chitosan-containing empty liposomes; CH-CHX, Chitosan-containing CHX-liposomes; CO, Chitosan-coated empty liposomes; and CO-CHX, Chitosan-coated CHX-liposomes.

Tailoring vesicles with chitosan have previously shown to increase the zeta potential of the delivery system (Mady et al., 2009; Park et al., 2014). The increase in surface charge is an indication of successful addition (coating or insertion) of chitosan indicating that chitosan is available on the surface of the vesicles (Jøraholmen et al., 2014). Additionally, nanoparticles with a cationic character are able to distribute within the biofilm after penetration into the matrix (Makabenta et al., 2021). The surface charge increased even more upon incorporation of CHX in the formulations; the fact that both chitosan and CHX are available on the vesicle surface and able to interact with the bacteria is highly encouraging considering antimicrobial potential of novel system. The entrapment of CHX was relatively high; however, lower than the entrapment achieved when

10.3389/fmicb.2022.1023083

TABLE 3 Surface-available chitosan on chitosan-containing liposomes and chitosan-coated liposomes.

	Surface-available chitosan (%)[1]
CH	86.2 ± 16.0
CH-CHX	92.2 ± 3.2
CO	55.1 ± 7.4
CO-CHX	84.4 ± 4.2

Results are expressed as means with their respective SD ($n = 3$). CH, Chitosan-containing empty liposomes; CH-CHX, Chitosan-containing CHX-liposomes; CO, Chitosan-coated empty liposomes; and CO-CHX, Chitosan-coated CHX-liposomes.
[1]Percentage of initial chitosan concentration.

TABLE 4 Chitosan-containing liposomes and chitosan-coated liposomes stability after 2 and 4 weeks of storage: mean diameter (≤80%, nm), polydispersity index (PI), zeta potential, and pH in aqueous medium.

	Week	Size (80%, nm)	PI	Zeta potential (mV)	pH
PL	2	326 ± 54	0.44 ± 0.05	−2.6 ± 0.6	6.0 ± 0.2
	4	298 ± 25	0.39 ± 0.05	−3.9 ± 0.1	5.7 ± 0.3
PL-CHX	2	272 ± 11	0.41 ± 0.02	40.2 ± 7.6	7.7 ± 0.2
	4	259 ± 8	0.40 ± 0.01	42.2 ± 10.5	7.8 ± 0.4
CH	2	307 ± 19	0.32 ± 0.00	11.1 ± 0.9	3.6 ± 0.0
	4	307 ± 24	0.31 ± 0.01	11.1 ± 0.9	3.7 ± 0.0
CH-CHX	2	285 ± 5	0.28 ± 0.01	92.1 ± 7.8	3.8 ± 0.0
	4	280 ± 6	0.29 ± 0.02	91.9 ± 3.3	3.8 ± 0.0
CO	2	316 ± 17	0.36 ± 0.01	12.5 ± 1.0	3.7 ± 0.0
	4	328 ± 25	0.37 ± 0.01	11.8 ± 0.6	3.7 ± 0.0
CO-CHX	2	375 ± 44	0.39 ± 0.02	83.3 ± 3.2	3.8 ± 0.0
	4	371 ± 40	0.42 ± 0.03	78.6 ± 0.9	3.8 ± 0.0

Vesicle stability after 2 and 4 weeks of storage at 4°C. Results of size measurements are expressed as means of cumulative size ≤80% of vesicle populations (weight-intensity distribution) with their respective SD, while the rest of the results are expressed as means with their respective SD ($n = 3$), while the rest of the results are expressed as means with their respective SD ($n = 3$). PL, Plain, empty lipid carrier; PL-CHX, Plain CHX-lipid carrier; CH, Chitosan-containing empty liposomes; CH-CHX, Chitosan-containing CHX-liposomes; CO, Chitosan-coated empty liposomes; and CO-CHX, Chitosan-coated CHX-liposomes.

utilizing the one-pot method which provided a CHX entrapment efficiency of 74% in chitosomes (Hemmingsen et al., 2021b). Nonetheless, a high entrapment and surface-available chitosan and CHX are assuring features for successful antimicrobial therapy. Both compounds are available to interact with the bacteria; moreover, the cationic nature of delivery system will improve the interaction between the vesicles and bacteria since bacterial membranes are slightly negatively changed (Epand and Epand, 2009).

Surface-available chitosan

To confirm that chitosan was available on the vesicle surface and determine to which extent it was available, we quantified the amount of surface-available chitosan on the vesicles using a colorimetric protocol first described by Muzzarelli (Muzzarelli, 1998). The quantity of surface-available chitosan on the vesicles was found to be rather high for all formulations (Table 3). For the empty, chitosan-coated liposomes the amount was comparable to the study of Jøraholmen et al. (2015). However, for the chitosan-containing liposomes, the amount of chitosan that was available on the surface was greater than the amount achieved for the chitosomes prepared with the one-pot method by Andersen et al. (2015). Additionally, contrary to our previous finding (Hemmingsen et al., 2021b), the addition of CHX seemed to increase the amount of surface-available chitosan on the vesicles; however, it was significant only for the chitosan-coated liposomes. Again, it is important to consider the chitosan origin and its M_w when comparing the results. Using a different method, Li et al. reported surface-available chitosan in quantities of up to 89.5% (Li et al., 2009). The surface availability is important not only for potential antimicrobial effects but also considering chitosan's bioadhesive properties that can be beneficial in wound treatment (Hamedi et al., 2022).

Vesicle stability

To assess the vesicle stability the size, PI, zeta potential, and pH of each formulation were evaluated after 2 and 4 weeks of storage at 4°C (Table 4). The size of all vesicles was relatively stable over the 4-week period; however, plain CHX-lipid carriers exhibited a small decrease in size between production and week 2 ($p = 0.0109$) that was not considered as an issue. Furthermore, the size did not change significantly between week 2 and 4; probably due to the surface charge (above 40 mV) and its stabilizing effect. All other parameters remained stable for the entire period. The addition of chitosan to liposomal formulations is often considered to improve the stability of the suspensions, both as a physical measure to maintain the integrity of the bilayers and due to electrostatic effects; however, this seems to be affected by the chitosan concentration (Sebaaly et al., 2021).

In vitro chlorhexidine release

As a result of the physical presence of chitosan and its physiochemical properties, chitosan could affect the release rate of active compounds from the vesicles (Gibis et al., 2016). Therefore, we investigated the CHX release from the plain lipid carriers, chitosan-containing, and chitosan-coated liposomes (Figure 2). Non-formulated CHX, dissolved in the release medium, was used as a control. After 24 h, the plain CHX-lipid carrier had released significantly more CHX than the chitosan-containing liposomes ($p = 0.0371$). However, no difference in the release was observed between the chitosan-containing and chitosan-coated liposomes. All vesicles significantly decreased the rate of release compared with non-formulated CHX at all time points. This prolonged release profile with gradual, long-lasting release of the compounds is highly beneficial for a drug delivery

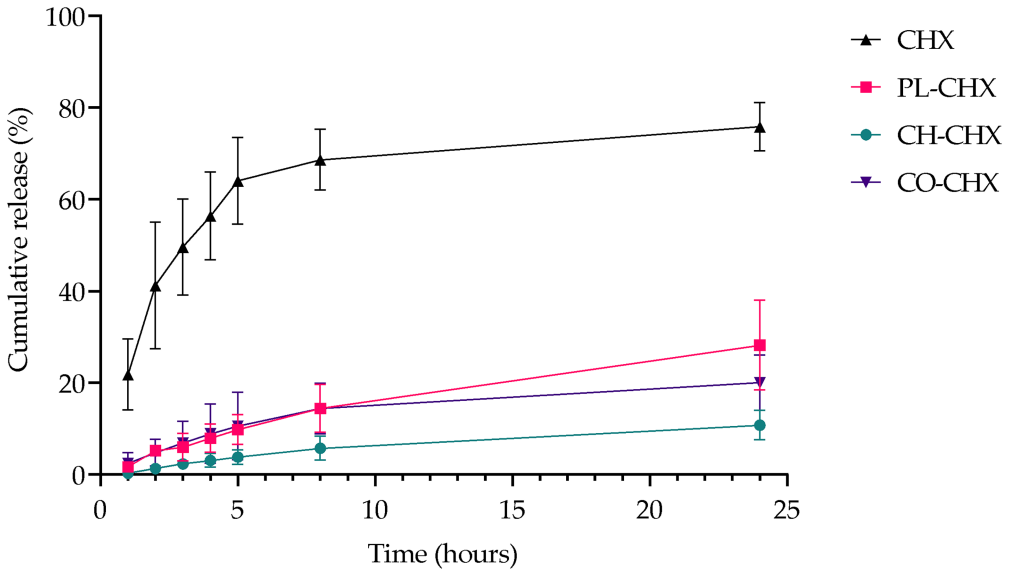

FIGURE 2
Cumulative *in vitro* release of CHX from non-formulated and formulated CHX over 24 h at 32°C. Results are expressed as release percentage compared to entrapped amount of CHX and means with their respective SD (n=3). Chlorhexidine (CHX), non-formulated CHX in media; PL-CHX, Plain CHX-lipid carrier; CH-CHX, Chitosan-containing CHX-liposomes; and CO-CHX, Chitosan-coated CHX-liposomes.

system intended for topical, antimicrobial therapy. First, these delivery systems could provide a high local concentration important for the therapeutic outcome; however, this is depending on whether the concentration reaches an effective concentration limit (Allen and Cullis, 2013). To prove the effect, biological assays are required. Second, drug delivery systems with prolonged release of the antimicrobial compound could help prevent regrowth of bacteria as well as ensure long-lasting antimicrobial effects (Piras et al., 2015). Third, as the compounds are retained onto/in the skin assuring local depot, the potential for reaching the systemic circulation is limited (Cui et al., 2021). The latter is highly relevant when limiting AMR.

Polymyxin B, another MAA, has previously displayed slower release rate from chitosan-modified liposomes. The vesicles released polymyxin B over a period of 24 h, while the non-formulated polymyxin B was completely released already after 12 h (Fu et al., 2019). On the other hand, Park et al. reported faster permeation rate of the MAA nisin from coated liposomes than uncoated liposomes; however, this study was conducted with mouse skin (Park et al., 2014). It is rather challenging to compare the release data from different studies due to the differences in physicochemical properties of active compounds and experimental settings.

Cell viability and anti-inflammatory responses

Liposomes and many other lipid-based delivery systems are generally regarded to be highly biocompatible, biodegradable, and safe. Furthermore, the toxicity of certain pharmaceutical compounds is often reduced when they are entrapped in these drug delivery systems (Liu et al., 2022). Nevertheless, the systems' effect on relevant cells is a critical parameter to be assessed in the development of new carriers or upon entrapment of new pharmaceutical compounds. The safety of these carriers is highly influenced by different features of the systems, such as the composition, size, size distribution, and surface properties (Liu et al., 2022). Consequently, we investigated cell compatibility in relevant cells, namely keratinocytes, fibroblasts, and macrophages, as well as the system's influence on inflammatory responses in macrophages.

Cell viability

As previously mentioned, liposomes can reduce the toxicity of pharmaceutical compounds (Nwabuife et al., 2021). Similarly, chitosan is also regarded biocompatible and biodegradable (Rashki et al., 2021). However, it is known that several alternations could change the properties of the materials, especially in the nano-range. For instance, the safety of chitosan is often considered to be linked to its degree of deacetylation and M_w (Rashki et al., 2021). The MAA, CHX, has in previous studies displayed toxicity in different cells, e.g., macrophages, keratinocytes, and fibroblasts (Li et al., 2014; Borges et al., 2017). Therefore, the potential toxicity of empty and CHX-loaded vesicles was assessed in these cells (Figure 3). In HaCaT and NHDF-neo cells, the viability of cells was unaffected by the treatment with both empty and CHX-loaded vesicles with or without chitosan. This is highly beneficial, as the viability of these cells is crucial for the successful therapy by therapeutics

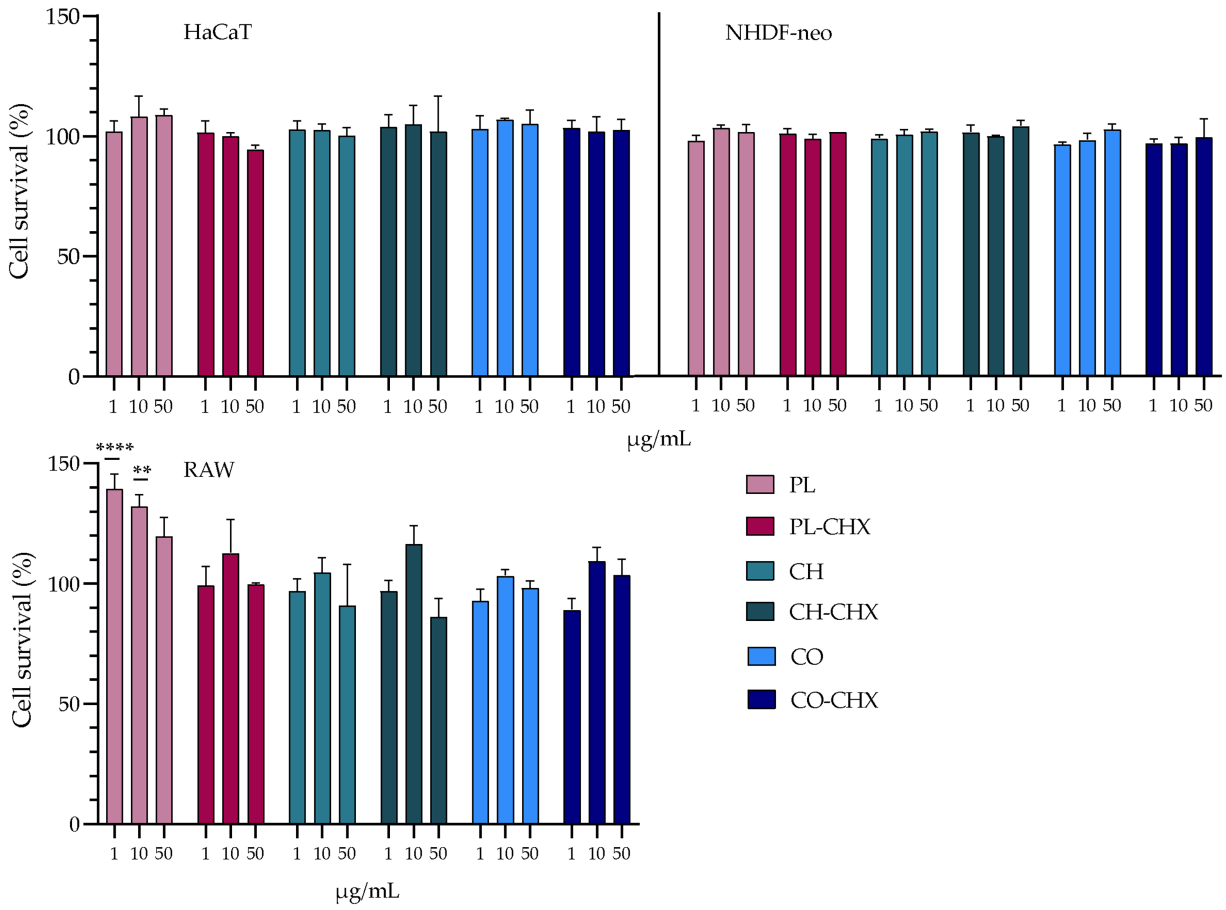

FIGURE 3
Evaluation of cell toxicity of chitosan-containing liposomes and chitosan-coated liposomes in HaCaT, NHDF-neo cells, and RAW 264.7. Three different concentrations were tested, namely 1, 10, and 50 μg/ml lipid, and the results are presented as cell viability of treated cells compared to control (100%). Control cells were only supplemented with complete medium; the cell viability is thereof considered as 100%. The results are expressed as means with their respective SD (n=3). PL, plain, empty lipid carrier; PL-CHX, plain CHX-lipid carrier; CH, chitosan-containing empty liposomes; CH-CHX, chitosan-containing CHX-liposomes; CO, chitosan-coated empty liposomes; and CO-CHX, chitosan-coated CHX-liposomes. **$p \leq 0.01$, ****$p \leq 0.0001$.

intended for wounds. Both keratinocytes and fibroblasts play active roles in the inflammatory phase in wounds; their release of cytokines and growth factors maintains hemostasis and influences other cells to participate in the process of wound closure (Wojtowicz et al., 2014). Moreover, keratinocytes are especially important in our defense against bacterial invasion due to their ability to release the antimicrobial peptides with antibacterial, antifungal, and antiviral activities (Chessa et al., 2020).

In the murine macrophages, no negative effects were observed in the treated cells; however, the empty, plain lipid carriers seemed to improve the viability of the cells, suggesting a proliferative effect. At lipid concentrations of 1 and 10 μg/ml, the viability or cell proliferation was significantly improved compared to control ($p < 0.0001$ and 0.0013, respectively). The proliferative effects of liposomes have previously been demonstrated by Ye et al. (2019); however, in significantly higher concentrations than in the current study. Macrophages play several pivotal roles in the wound healing cascade, for instance, cleaning of pathogens and debris from the wound, activation of immune cells, promotion of migration of other cells, such as keratinocytes and fibroblasts, and breaking down the temporary extracellular matrix (Krzyszczyk et al., 2018). Therefore, their presence and retained viability are of high importance. Furthermore, Hilițanu et al. confirmed the biocompatibility of chitosan-coated liposomes containing erythromycin after oral administration in mice. The authors investigated erythrocyte counts, liver enzyme activity, serum urea plasma levels, immunological biomarkers, and histopathological examinations of liver or kidney, and found no significant changes in the mice (Hilițanu et al., 2021).

Anti-inflammatory activity

Macrophages bear crucial attributes in wound healing; however, in chronic wounds these cells might also be a part of the problem. Chronic wounds are arrested in a state of

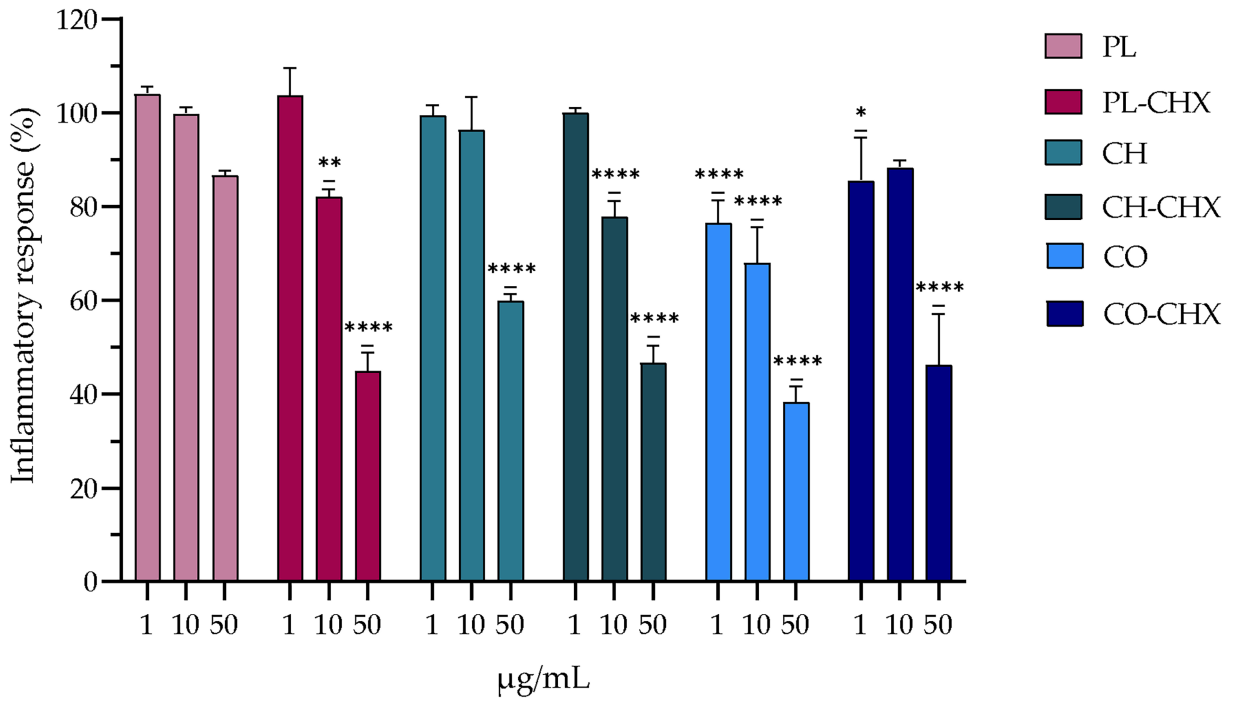

FIGURE 4
Evaluation of anti-inflammatory activity of chitosan-containing and chitosan-coated liposomes expressed as reduction of nitric oxide (NO) production in RAW 264.7 cells. Three different concentrations were tested, namely 1, 10, and 50 µg/ml lipid, and the results are presented as NO production of treated cells compared to control (100%). Control cells were non-treated lipopolysaccharide (LPS)-induced cells; their production is thereof considered as 100%. The results are expressed as means with their respective SD (n=3). PL, Plain, empty lipid carrier; PL-CHX, Plain CHX-lipid carrier; CH, Chitosan-containing empty liposomes; CH-CHX, Chitosan-containing CHX-liposomes; CO, Chitosan-coated empty liposomes; CO-CHX, Chitosan-coated CHX-liposomes. *$p \leq 0.05$, **$p \leq 0.01$, ****$p \leq 0.0001$, compared to control.

inflammation and unable to progress in the healing cascade. This is linked to the presence of pro-inflammatory macrophages (M1-type macrophages) at the site of injury that leads to elevated levels of cytokines and reactive oxygen species, and apoptosis of keratinocytes and fibroblasts (Shamiya et al., 2022). This prolonged state of inflammation is undesirable in wounds as it hinders healing. To evaluate whether novel formulations can act on inflammatory response, we assessed the anti-inflammatory effects in murine macrophages. In macrophages, LPS is recognized by toll-like receptor 4, its binding leading to expression of pro-inflammatory genes. In mice, this leads to overexpression of inducible nitric oxide synthase and subsequent high levels of NO that could serve as an indicator of anti-inflammatory responses. This effect is far greater in mice than in humans, and therefore murine macrophages were utilized to assess the potential anti-inflammatory activity (Krzyszczyk et al., 2018). The results of the inflammatory assessments are presented in Figure 4 and demonstrate a clear dose-dependent anti-inflammatory effect the formulations had on treated cells. The anti-inflammatory activities of the vesicles with chitosan and/or CHX were significantly higher as compared to non-treated LPS-induced macrophages. However, the effects did not seem to be synergetic, namely the presence of both chitosan and CHX did not enhance the effects in synergy. The determined threshold was at about 55–65% reduction. Interestingly, the empty, plain lipid carriers also induced a dose-dependent reduction in inflammatory response; however, this effect was not significant.

Antimicrobial evaluation

In recent years, more focus has been placed on drug delivery systems and nanostructured materials in the development of new therapeutic options for microbial eradication and prevention. These systems and materials, both organic and inorganic, have demonstrated superior antimicrobial activities against a wide variety of microbial strains (Baranwal et al., 2018). Liposomes are among the most frequently used systems while chitosan has generated interest due to its inherent antimicrobial properties (Baranwal et al., 2018). Considering liposomes, their structure and composition is similar to the bacterial membrane; this could lead to a fusion between liposomes and bacteria resulting in delivery of higher antimicrobial payloads. Additionally, liposomes that possess a positively charged surface could interact with bacteria and further improve the antimicrobial effects (Wang et al., 2020). All of this is expected to improve the therapeutic index and make bacteria more susceptible to antimicrobials associated with delivery system as compared to non-formulated antimicrobials (Wang et al., 2020). To further improve the antimicrobial properties of drug delivery systems,

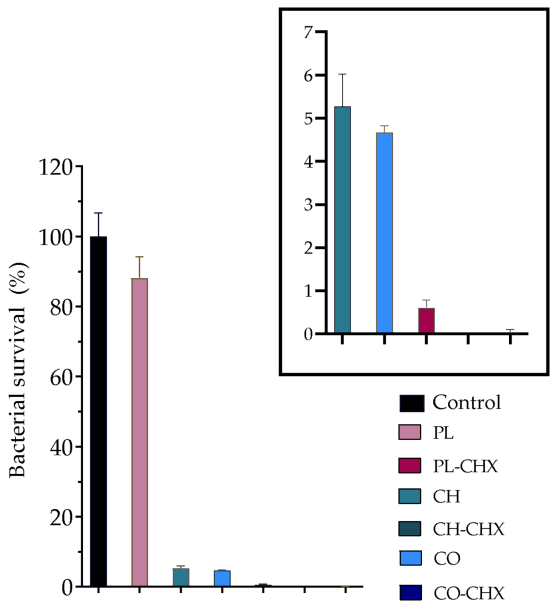

FIGURE 5
Bacterial survival (%) of *Staphylococcus aureus* MSSA476 (ATCC® BAA-1721™) in the presence of non-formulated and formulated chlorhexidine (CHX) at a lipid concentration of 0.3125 mg/ml. The boxed area is enlarged to depict the chitosan- and/or CHX-containing and/or coated vesicles. The results are expressed as means with their respective SD (n=3). PL, Plain, empty lipid carrier; PL-CHX, Plain CHX-lipid carrier; CH, Chitosan-containing empty liposomes; CH-CHX, Chitosan-containing CHX-liposomes; CO, Chitosan-coated empty liposomes; and CO-CHX, Chitosan-coated CHX-liposomes. ****$p \leq 0.0001$, compared to control.

chitosan is often utilized together with other delivery systems. In the current study, we were using an MAA, postulating that chitosan and MAA could act in synergy and enhance the effect on the bacteria. We assessed the antimicrobial activity of our vesicles against *S. aureus*, one of the most common pathogens found in chronic wounds (Alves et al., 2021). As seen in Figure 5, the empty, plain lipid carriers did not display any antimicrobial activity, as expected; however, upon inclusion of chitosan in vesicles, the bacterial survival was dramatically reduced to 5.3 and 4.7% for the chitosan-containing and chitosan-coated liposomes, respectively. Jøraholmen et al. have previously proven that chitosan-coated liposomes exhibit antimicrobial activity against *S. aureus*, even when their corresponding non-coated liposomes did not possess any activities (Jøraholmen et al., 2020).

We were also interested in the activity of plain and chitosan-comprising vesicles with CHX. The plain CHX-lipid carriers reduced the bacterial survival by 99.4%; even more than chitosan-vesicles without CHX. However, the combination of chitosan and CHX in vesicles demonstrated the strongest antimicrobial activity. Chitosan-containing CHX-liposomes completely eradicated *S. aureus*, while the bacterial survival after treatment with chitosan-coated CHX-liposomes was reduced to only 0.03%. These results are in agreement with the results from our previous study where we utilized one-pot method for the production of vesicles; however, chitosan of different M_w (higher M_w) was utilized in that study (Hemmingsen et al., 2021b). Wang et al. also demonstrated improved antimicrobial activity against *S. aureus* of cinnamaldehyde, a MAA, when the compound was entrapped in chitosan-coated liposomes. Furthermore, they also demonstrated that the mechanism behind this action was membrane disruption (Wang et al., 2021). In another study, Hassan et al., proved lowered MIC and faster antimicrobial action of vancomycin when it was entrapped in lipid-chitosan hybrid vesicles. They also established that the effect was due to membrane destruction. Moreover, the authors demonstrated eradication of pre-formed MRSA biofilms (Hassan et al., 2020). These encouraging results highlight the potential of systems combining lipid-based vesicles and chitosan for successful microbial eradication.

Conclusion

In an era of lowered microbial susceptibility to conventional antimicrobial compounds and higher prevalence of chronic wounds, often with high microbial burden, innovative strategies for microbial eradication and improved wound healing are crucially needed. We proposed that combinations of lipid-based vesicles and chitosan could serve as promising delivery systems for MAAs, such as CHX, as confirmed by successful bacterial eradication of the common skin pathogen *S. aureus*. Indeed, we showed that both chitosan-containing liposomes and chitosan-coated liposomes destined to treat infected wounds could successfully improve antimicrobial activity of CHX against *S. aureus*, highlighting their potential in antimicrobial wound therapy.

Data availability statement

The raw data supporting the conclusions of this article will be made available by the authors, without undue reservation.

Author contributions

LH and NŠ-B: conceptualization, formal analysis, and writing—original draft preparation. LH, KJ, PB, MJ, and NŠ-B: methodology. LH, KJ, and NŠ-B: validation. LH and PP: investigation and data curation. MN, MJ, and NŠ-B: resources. LH, PP, KJ, PB, MN, MJ, and NŠ-B: writing—review and editing. LH: visualization. NŠ-B: supervision, project administration, and funding acquisition. All authors contributed to the article and approved the submitted version.

Funding

UiT The Arctic University of Norway, Norway funded this study (project no. 235569). The publication fund of UiT The Arctic

University of Norway funded the publication charges of this article.

Acknowledgments

The authors would like to acknowledge Chitinor (Tromsø, Norway) and Lipoid GmbH (Ludwigshafen, Germany) for providing chitosan and phospholipid, respectively, for this study. The authors would also like to thank Maddhusja Sritharan Nalliah and Nora Hersoug Nedberg at Department of Clinical Medicine, UiT The Arctic University of Norway. Figure 1 and graphical abstract were created with BioRender.com.

Conflict of interest

The authors declare that the research was conducted in the absence of any commercial or financial relationships that could be construed as a potential conflict of interest.

Publisher's note

References

Abdel-Sayed, P., Tornay, D., Hirt-Burri, N., De Buys Roessingh, A., Raffoul, W., and Applegate, L. A. (2020). Implications of chlorhexidine use in burn units for wound healing. *Burns* 46, 1150–1156. doi: 10.1016/j.burns.2019.12.008

Allen, T. M., and Cullis, P. R. (2013). Liposomal drug delivery systems: from concept to clinical applications. *Adv. Drug Deliv. Rev.* 65, 36–48. doi: 10.1016/j.addr.2012.09.037

Alves, P. J., Barreto, R. T., Barrois, B. M., Gryson, L. G., Meaume, S., and Monstrey, S. J. (2021). Update on the role of antiseptics in the management of chronic wounds with critical colonisation and/or biofilm. *Int. Wound J.* 18, 342–358. doi: 10.1111/iwj.13537

Andersen, T., Bleher, S., Flaten, G. E., Tho, I., Mattsson, S., and Škalko-Basnet, N. (2015). Chitosan in mucoadhesive drug delivery: focus on local vaginal therapy. *Mar. Drugs* 13, 222–236. doi: 10.3390/md13010222

Bakshi, P. S., Selvakumar, D., Kadirvelu, K., and Kumar, N. S. (2020). Chitosan as an environment friendly biomaterial – a review on recent modifications and applications. *Int. J. Biol. Macromol.* 150, 1072–1083. doi: 10.1016/j.ijbiomac.2019.10.113

Balouiri, M., Sadiki, M., and Ibnsouda, S. K. (2016). Methods for in vitro evaluating antimicrobial activity: a review. *J. Pharm. Anal.* 6, 71–79. doi: 10.1016/j.jpha.2015.11.005

Baranwal, A., Srivastava, A., Kumar, P., Bajpai, V. K., Maurya, P. K., and Chandra, P. (2018). Prospects of nanostructure materials and their composites as antimicrobial agents. *Front. Microbiol.* 9:422. doi: 10.3389/fmicb.2018.00422

Barrigah-Benissan, K., Ory, J., Sotto, A., Salipante, F., Lavigne, J. P., and Loubet, P. (2022). Antiseptic agents for chronic wounds: a systematic review. *Antibiotics* 11:350. doi: 10.3390/antibiotics11030350

Basnet, P., Hussain, H., Tho, I., and Škalko-Basnet, N. (2012). Liposomal delivery system enhances anti-inflammatory properties of Curcumin. *J. Pharm. Sci.* 101, 598–609. doi: 10.1002/jps.22785

Borges, G. Á., Elias, S. T., Da Silva, S. M. M., Magalhães, P. O., Macedo, S. B., Ribeiro, A. P. D., et al. (2017). In vitro evaluation of wound healing and antimicrobial potential of ozone therapy. *J. Craniomaxillofac. Surg.* 45, 364–370. doi: 10.1016/j.jcms.2017.01.005

Cauzzo, J., Nystad, M., Holsæter, A. M., Basnet, P., and Škalko-Basnet, N. (2020). Following the fate of dye-containing liposomes in vitro. *Int. J. Mol. Sci.* 21:4847. doi: 10.3390/ijms21144847

Chessa, C., Bodet, C., Jousselin, C., Wehbe, M., Lévêque, N., and Garcia, M. (2020). Antiviral and Immunomodulatory properties of antimicrobial peptides produced by human keratinocytes. *Front. Microbiol.* 11:1155. doi: 10.3389/fmicb.2020.01155

Cieplik, F., Jakubovics, N. S., Buchalla, W., Maisch, T., Hellwig, E., and Al-Ahmad, A. (2019). Resistance toward Chlorhexidine in Oral bacteria–is there cause for concern? *Front. Microbiol.* 10:587. doi: 10.3389/fmicb.2019.00587

Cui, M., Wiraja, C., Chew, S. W. T., and Xu, C. (2021). Nanodelivery Systems for Topical Management of skin disorders. *Mol. Pharm.* 18, 491–505. doi: 10.1021/acs.molpharmaceut.0c00154

Danaei, M., Dehghankhold, M., Ataei, S., Hasanzadeh Davarani, F., Javanmard, R., Dokhani, A., et al. (2018). Impact of particle size and Polydispersity index on the clinical applications of Lipidic Nanocarrier systems. *Pharmaceutics* 10:57. doi: 10.3390/pharmaceutics10020057

Domiński, A., Domińska, M., Skonieczna, M., Pastuch-Gawołek, G., and Kurcok, P. (2022). Shell-Sheddable micelles based on poly(ethylene glycol)-hydrazone-poly[RS]-3-hydroxybutyrate copolymer loaded with 8-Hydroxyquinoline Glycoconjugates as a dual tumor-targeting drug delivery system. *Pharmaceutics* 14:290. doi: 10.3390/pharmaceutics14020290

du Plessis, J., Ramachandran, C., Weiner, N., and Müller, D. G. (1994). The influence of particle size of liposomes on the deposition of drug into skin. *Int. J. Pharm.* 103, 277–282. doi: 10.1016/0378-5173(94)90178-3

Eid, H. M., Ali, A. A., Ali, A. M. A., Eissa, E. M., Hassan, R. M., Abo El-Ela, F. I., et al. (2022). Potential use of tailored Citicoline chitosan-coated liposomes for effective wound healing in diabetic rat model. *Int. J. Nanomedicine* 17, 555–575. doi: 10.2147/ijn.S342504

Epand, R. M., and Epand, R. F. (2009). Lipid domains in bacterial membranes and the action of antimicrobial agents. *Biochim. Biophys. Acta Biomembr.* 1788, 289–294. doi: 10.1016/j.bbamem.2008.08.023

Eriksson, E., Liu, P. Y., Schultz, G. S., Martins-Green, M. M., Tanaka, R., Weir, D., et al. (2022). Chronic wounds: treatment consensus. *Wound Repair Regen.* 30, 156–171. doi: 10.1111/wrr.12994

Farkas, E., Zelkó, R., Török, G., Rácz, I., and Marton, S. (2001). Influence of chlorhexidine species on the liquid crystalline structure of vehicle. *Int. J. Pharm.* 213, 1–5. doi: 10.1016/S0378-5173(00)00575-5

Fritz, S. A., Hogan, P. G., Camins, B. C., Ainsworth, A. J., Patrick, C., Martin, M. S., et al. (2013). Mupirocin and Chlorhexidine resistance in Staphylococcus aureus in patients with community-onset skin and soft tissue infections. *Antimicrob. Agents Chemother.* 57, 559–568. doi: 10.1128/AAC.01633-12

Fu, Y. Y., Zhang, L., Yang, Y., Liu, C. W., He, Y. N., Li, P., et al. (2019). Synergistic antibacterial effect of ultrasound microbubbles combined with chitosan-modified polymyxin B-loaded liposomes on biofilm-producing Acinetobacter baumannii. *Int. J. Nanomedicine* 14, 1805–1815. doi: 10.2147/IJN.S186571

Gibis, M., Ruedt, C., and Weiss, J. (2016). In vitro release of grape-seed polyphenols encapsulated from uncoated and chitosan-coated liposomes. *Food Res. Int.* 88, 105–113. doi: 10.1016/j.foodres.2016.02.010

Hamedi, H., Moradi, S., Hudson, S. M., Tonelli, A. E., and King, M. W. (2022). Chitosan based bioadhesives for biomedical applications: a review. *Carbohydr. Polym.* 282:119100. doi: 10.1016/j.carbpol.2022.119100

Hassan, D., Omolo, C. A., Fasiku, V. O., Mocktar, C., and Govender, T. (2020). Novel chitosan-based pH-responsive lipid-polymer hybrid nanovesicles (OLA-LPHVs) for delivery of vancomycin against methicillin-resistant Staphylococcus aureus infections. *Int. J. Biol. Macromol.* 147, 385–398. doi: 10.1016/j.ijbiomac.2020.01.019

Hemmingsen, L. M., Giordani, B., Pettersen, A. K., Vitali, B., Basnet, P., and Škalko-Basnet, N. (2021a). Liposomes-in-chitosan hydrogel boosts potential of chlorhexidine in biofilm eradication in vitro. *Carbohydr. Polym.* 262:117939. doi: 10.1016/j.carbpol.2021.117939

Hemmingsen, L. M., Julin, K., Ahsan, L., Basnet, P., Johannessen, M., and Škalko-Basnet, N. (2021b). Chitosomes-in-chitosan hydrogel for acute skin injuries: prevention and infection control. *Mar. Drugs* 19:269. doi: 10.3390/md19050269

Hemmingsen, L. M., Škalko-Basnet, N., and Jøraholmen, M. W. (2021c). The expanded role of chitosan in localized antimicrobial therapy. *Mar. Drugs* 19:697. doi: 10.3390/md19120697

Hiliţanu, L. N., Mititelu-Tarţău, L., Popa, G. E., Buca, B. R., Pavel, L. L., Pelin, A. M., et al. (2021). The analysis of chitosan-coated Nanovesicles containing erythromycin–characterization and biocompatibility in mice. *Antibiotics* 10:1471. doi: 10.3390/antibiotics10121471

Hoang, T. P., Ghori, M. U., and Conway, B. R. (2021). Topical antiseptic formulations for skin and soft tissue infections. *Pharmaceutics* 13:558. doi: 10.3390/pharmaceutics13040558

Hubbard, A. T. M., Coates, A. R., and Harvey, R. D. (2017). Comparing the action of HT61 and chlorhexidine on natural and model Staphylococcus aureus membranes. *J. Antibiot.* 70, 1020–1025. doi: 10.1038/ja.2017.90

Iacob, A. T., Lupascu, F. G., Apotrosoaei, M., Vasincu, I. M., Tauser, R. G., Lupascu, D., et al. (2021). Recent biomedical approaches for chitosan based materials as drug delivery Nanocarriers. *Pharmaceutics* 13:587. doi: 10.3390/pharmaceutics13040587

Jøraholmen, M. W., Bhargava, A., Julin, K., Johannessen, M., and Škalko-Basnet, N. (2020). The antimicrobial properties of chitosan can be tailored by formulation. *Mar. Drugs* 18:96. doi: 10.3390/md18020096

Jøraholmen, M. W., Škalko-Basnet, N., Acharya, G., and Basnet, P. (2015). Resveratrol-loaded liposomes for topical treatment of the vaginal inflammation and infections. *Eur. J. Pharm. Sci.* 79, 112–121. doi: 10.1016/j.ejps.2015.09.007

Jøraholmen, M. W., Vanić, Ž., Tho, I., and Škalko-Basnet, N. (2014). Chitosan-coated liposomes for topical vaginal therapy: assuring localized drug effect. *Int. J. Pharm.* 472, 94–101. doi: 10.1016/j.ijpharm.2014.06.016

Kaiser, P., Wächter, J., and Windbergs, M. (2021). Therapy of infected wounds: overcoming clinical challenges by advanced drug delivery systems. *Drug Deliv. Transl. Res.* 11, 1545–1567. doi: 10.1007/s13346-021-00932-7

Khan, F., Pham, D. T. N., Oloketuyi, S. F., Manivasagan, P., Oh, J., and Kim, Y. M. (2020). Chitosan and their derivatives: Antibiofilm drugs against pathogenic bacteria. *Colloids Surf. B: Biointerfaces* 185:110627. doi: 10.1016/j.colsurfb.2019.110627

Krzyszczyk, P., Schloss, R., Palmer, A., and Berthiaume, F. (2018). The role of macrophages in acute and chronic wound healing and interventions to promote pro-wound healing phenotypes. *Front. Physiol.* 9:419. doi: 10.3389/fphys.2018.00419

Li, Y. C., Kuan, Y. H., Lee, S. S., Huang, F. M., and Chang, Y. C. (2014). Cytotoxicity and genotoxicity of chlorhexidine on macrophages in vitro. *Environ. Toxicol.* 29, 452–458. doi: 10.1002/tox.21771

Li, N., Zhuang, C., Wang, M., Sun, X., Nie, S., and Pan, W. (2009). Liposome coated with low molecular weight chitosan and its potential use in ocular drug delivery. *Int. J. Pharm.* 379, 131–138. doi: 10.1016/j.ijpharm.2009.06.020

Liu, P., Chen, G., and Zhang, J. (2022). A review of liposomes as a drug delivery system: current status of approved products, regulatory environments, and future perspectives. *Molecules* 27:1372. doi: 10.3390/molecules27041372

Mady, M. M., Darwish, M. M., Khalil, S., and Khalil, W. M. (2009). Biophysical studies on chitosan-coated liposomes. *Eur. Biophys. J.* 38, 1127–1133. doi: 10.1007/s00249-009-0524-z

Makabenta, J. M. V., Nabawy, A., Li, C. H., Schmidt-Malan, S., Patel, R., and Rotello, V. M. (2021). Nanomaterial-based therapeutics for antibiotic-resistant bacterial infections. *Nat. Rev. Microbiol.* 19, 23–36. doi: 10.1038/s41579-020-0420-1

Matei, A. M., Caruntu, C., Tampa, M., Georgescu, S. R., Matei, C., Constantin, M. M., et al. (2021). Applications of Nanosized-lipid-based drug delivery Systems in Wound Care. *Appl. Sci.* 11:4915. doi: 10.3390/app11114915

Matica, M. A., Aachmann, F. L., Tøndervik, A., Sletta, H., and Ostafe, V. (2019). Chitosan as a wound dressing starting material: antimicrobial properties and mode of action. *Int. J. Mol. Sci.* 20:5889. doi: 10.3390/ijms20235889

Mengoni, T., Adrian, M., Pereira, S., Santos-Carballal, B., Kaiser, M., and Goycoolea, F. M. (2017). A chitosan—based liposome formulation enhances the in vitro wound healing efficacy of substance P neuropeptide. *Pharmaceutics* 9:56. doi: 10.3390/pharmaceutics9040056

Muzzarelli, R. R. A. (1998). Colorimetric determination of chitosan. *Anal. Biochem.* 260, 255–257. doi: 10.1006/abio.1998.2705

Nwabuife, J. C., Pant, A. M., and Govender, T. (2021). Liposomal delivery systems and their applications against Staphylococcus aureus and methicillin-resistant Staphylococcus aureus. *Adv. Drug Deliv. Rev.* 178:113861. doi: 10.1016/j.addr.2021.113861

Osman, N., Devnarain, N., Omolo, C. A., Fasiku, V., Jaglal, Y., and Govender, T. (2022). Surface modification of nano-drug delivery systems for enhancing antibiotic delivery and activity. *Wires Nanomed. Nanobi.* 14:e1758. doi: 10.1002/wnan.1758

Park, S. N., Jo, N. R., and Jeon, S. H. (2014). Chitosan-coated liposomes for enhanced skin permeation of resveratrol. *J. Ind. Eng. Chem.* 20, 1481–1485. doi: 10.1016/j.jiec.2013.07.035

Piras, A. M., Maisetta, G., Sandreschi, S., Gazzarri, M., Bartoli, C., Grassi, L., et al. (2015). Chitosan nanoparticles loaded with the antimicrobial peptide temporin B exert a long-term antibacterial activity in vitro against clinical isolates of Staphylococcus epidermidis. *Front. Microbiol.* 6:372. doi: 10.3389/fmicb.2015.00372

Pramanik, S., and Sali, V. (2021). Connecting the dots in drug delivery: a tour d'horizon of chitosan-based nanocarriers system. *Int. J. Biol. Macromol.* 169, 103–121. doi: 10.1016/j.ijbiomac.2020.12.083

Rashki, S., Asgarpour, K., Tarrahimofrad, H., Hashemipour, M., Ebrahimi, M. S., Fathizadeh, H., et al. (2021). Chitosan-based nanoparticles against bacterial infections. *Carbohydr. Polym.* 251:117108. doi: 10.1016/j.carbpol.2020.117108

Schulte-Werning, L. V., Murugaiah, A., Singh, B., Johannessen, M., Engstad, R. E., Škalko-Basnet, N., et al. (2021). Multifunctional Nanofibrous dressing with antimicrobial and anti-inflammatory properties prepared by needle-free electrospinning. *Pharmaceutics* 13:1527. doi: 10.3390/pharmaceutics13091527

Sebaaly, C., Trifan, A., Sieniawska, E., and Greige-Gerges, H. (2021). Chitosan-coating effect on the characteristics of liposomes: a focus on bioactive compounds and essential oils: a review. *Processes* 9:445. doi: 10.3390/pr9030445

Shamiya, Y., Ravi, S. P., Coyle, A., Chakrabarti, S., and Paul, A. (2022). Engineering nanoparticle therapeutics for impaired wound healing in diabetes. *Drug Discov. Today* 27, 1156–1166. doi: 10.1016/j.drudis.2021.11.024

Shukla, S. K., Chan, A., Parvathaneni, V., and Gupta, V. (2020). Metformin-loaded chitosomes for treatment of malignant pleural mesothelioma – a rare thoracic cancer. *Int. J. Biol. Macromol.* 160, 128–141. doi: 10.1016/j.ijbiomac.2020.05.146

Ternullo, S., Gagnat, E., Julin, K., Johannessen, M., Basnet, P., Vanić, Ž., et al. (2019). Liposomes augment biological benefits of curcumin for multitargeted skin therapy. *Eur. J. Pharm. Biopharm.* 144, 154–164. doi: 10.1016/j.ejpb.2019.09.016

Wang, X., Cheng, F., Wang, X., Feng, T., Xia, S., and Zhang, X. (2021). Chitosan decoration improves the rapid and long-term antibacterial activities of cinnamaldehyde-loaded liposomes. *Int. J. Biol. Macromol.* 168, 59–66. doi: 10.1016/j.ijbiomac.2020.12.003

Wang, D. Y., Van Der Mei, H. C., Ren, Y., Busscher, H. J., and Shi, L. (2020). Lipid-based antimicrobial delivery-Systems for the Treatment of bacterial infections. *Front. Chem.* 7:872. doi: 10.3389/fchem.2019.00872

Wojtowicz, A. M., Oliveira, S., Carlson, M. W., Zawadzka, A., Rousseau, C. F., and Baksh, D. (2014). The importance of both fibroblasts and keratinocytes in a bilayered living cellular construct used in wound healing. *Wound Repair Regen.* 22, 246–255. doi: 10.1111/wrr.12154

Xia, Y., Wang, D., Liu, D., Su, J., Jin, Y., Wang, D., et al. (2022). Applications of chitosan and its derivatives in skin and soft tissue diseases. *Front. Bioeng. Biotechnol.* 10:894667. doi: 10.3389/fbioe.2022.894667

Ye, J., Yang, Y., Dong, W., Gao, Y., Meng, Y., Wang, H., et al. (2019). Drug-free mannosylated liposomes inhibit tumor growth by promoting the polarization of tumor-associated macrophages. *Int. J. Nanomedicine* 14, 3203–3220. doi: 10.2147/IJN.S207589

Paper IV

Tailored anti-biofilm activity – liposomal delivery for mimic of small antimicrobial peptide

Lisa Myrseth Hemmingsen[a], Barbara Giordani[b], Marianne H. Paulsen[c,d], Željka Vanić[e], Gøril Eide Flaten[a], Beatrice Vitali[b], Purusotam Basnet[f], Annette Bayer[c], Morten B. Strøm[d], and Nataša Škalko-Basnet[a]*

[a]Drug Transport and Delivery Research Group, Department of Pharmacy, University of Tromsø The Arctic University of Norway, Universitetsvegen 57, N-9037 Tromsø, Norway

[b]Beneficial Microbes Research Group, Department of Pharmacy and Biotechnology, University of Bologna, Via San Donato 19/2, 40127, Bologna, Italy

[c]Department of Chemistry, University of Tromsø The Arctic University of Norway, Universitetsvegen 57, N-9037 Tromsø, Norway

[d]Natural Products and Medicinal Chemistry Research Group, Department of Pharmacy, University of Tromsø The Arctic University of Norway, Universitetsvegen 57, N-9037 Tromsø, Norway

[e]Department of Pharmaceutical Technology, Faculty of Pharmacy and Biochemistry, University of Zagreb, A. Kovačića 1, 10 000 Zagreb, Croatia

[f]Women's Health and Perinatology Research Group, Department of Clinical Medicine, University of Tromsø The Arctic University of Norway, Universitetsveien 57, N-9037 Tromsø, Norway

Corresponding Author:

*Nataša Škalko-Basnet - Drug Transport and Delivery Research Group, Department of Pharmacy, University of Tromsø The Arctic University of Norway, Universitetsvegen 57, N-9037 Tromsø, Norway. E-mail: natasa.skalko-basnet@uit.no, phone: +47 77646640.

Abstract

The eradication of bacteria embedded in biofilms is among the most challenging obstacles in the management of chronic wounds. These biofilms are found in most chronic wounds; moreover, the biofilm-embedded bacteria are considerably less susceptible to conventional antimicrobial treatment than the planktonic bacteria. Antimicrobial peptides and their mimics are considered attractive candidates in the pursuit of novel therapeutic options for the treatment of chronic wounds and general bacterial eradication. However, some limitations linked to these membrane-active antimicrobials are making their clinical use challenging. Novel innovative delivery systems addressing these limitations represent a smart solution. We hypothesized that incorporation of a novel synthetic mimic of an antimicrobial peptide in liposomes could improve its anti-biofilm effect as well as the anti-inflammatory activity. The small synthetic mimic of an antimicrobial peptide, 7e-SMAMP, was incorporated into liposomes (~280 nm) tailored for skin wounds and evaluated for its potential activity against both biofilm formation and eradication of pre-formed biofilms. The 7e-SMAMP-liposomes significantly lowered inflammatory response in murine macrophages (~30% reduction) without affecting the viability of macrophages or keratinocytes. Importantly, the 7e-SMAMP-liposomes completely eradicated biofilms produced by *Staphylococcus aureus* and *Escherichia coli* above concentrations of 6.25 μg/mL, whereas in *Pseudomonas aeruginosa* the eradication reached 75% at the same concentration. Incorporation of 7e-SMAMP in liposomes improved both the inhibition of biofilm formation as well as biofilm eradication *in vitro*, as compared to non-formulated antimicrobial, therefore confirming its potential as a novel therapeutic option for bacteria-infected chronic wounds.

Keywords: peptidomimetics; liposomes; bacterial biofilms; membrane-active antimicrobials; chronic wounds

Abbreviations: AMP, antimicrobial peptide; AMR, antimicrobial resistance; B3M-liposomes, Bacterial Membrane-Mimic Liposomes Model; CCK-8, cell counting kit-8; CFU, colony-forming unit; DMEM-hg, Dulbecco's Modified Eagle Medium high glucose; DMSO, dimethyl sulfoxide; EE, entrapment efficiency; FBS, fetal bovine serum; FITC, fluorescein isothiocyanate; HEPES, N-(2-hydroxyethyl)piperazine-N′-(2-ethanesulfonic acid); LPS, lipopolysaccharide; MAAs, membrane-active antimicrobials; MDR; multidrug-resistant; MIC: minimal inhibiting concentration; MLC, minimal lethal concentration; mQ, milli-Q water; M_w, molecular weight; NB, nutrient broth; PBS, phosphate buffered saline; PI, polydispersity index; RPMI, Roswell Park Memorial Institute; SMAMP, synthetic mimics of antimicrobial peptide; SWF, simulated wound fluid; TEM, transmission electron microscopy.

1. Introduction

As we are entering a post-antibiotic era, antimicrobial resistance (AMR) has become one of the major medical concerns and critical hurdles in medical care, often with fatal consequences [1]. Over the course of time, the inevitable rise of AMR and multidrug-resistant (MDR) pathogens have rendered many infections practically untreatable and potentially life threatening. Moreover, researchers struggle to bring forward novel antimicrobial compounds for new targets, resulting in the clinical pipelines for antimicrobial compounds being rather stagnant [2]. With this upsurge of AMR and limited arsenal of antimicrobial compounds and therapeutic options, chronic wounds and wound management are rapidly growing challenges for both patients and health care providers. Furthermore, due to an aging population and increased prevalence of diabetes and obesity, cases of chronic wounds are increasing and expected to further rise [3]. Amid these challenges of chronic wound treatment, it is essential to focus on biofilms as they are found in up to 80% of all chronic wounds [4]. Bacteria embedded in these bacterial communities often have 1000-fold increased tolerance to antibiotics. Moreover, there are no antimicrobials specifically targeting biofilm eradication approved by the major regulatory agencies [5, 6]. Antimicrobial peptides (AMPs) are often considered promising candidates to mitigate the effects and progression of AMR [7, 8]. The antimicrobial activities of AMPs and other membrane-active antimicrobials (MAAs) reach beyond disruption of bacterial membranes. For instance, many cause alterations of immune responses as well as target the internal components, such as DNA, in bacteria [9, 10]. Besides, AMPs have proven to evoke less resistance due to their fast onset of action and activity against metabolically inactive bacteria [11]. The antimicrobial activity of AMPs is often broad, including gram-positive and gram-negative bacteria, viruses, and fungi [12, 13]. Additionally, AMPs and other MAAs could improve the eradication of biofilm-embedded bacteria compared to the more conventional antimicrobials [6].

All listed properties bear optimism around AMPs as valuable candidates in the path to ease the challenges around AMR and eradication of biofilm-embedded bacteria; however, some frequent drawbacks linked to AMPs require careful consideration. These limitations include their toxicity, haemolytic activity, loss of *in vivo* efficacy, and proteolytic instability [7, 11]. These are amongst the most common reasons for their discontinuation before or in early-stage clinical trials [9]. Researchers have tried to evade these problems, further improving the therapeutic index, by chemically modifying AMPs or creating AMP mimics. A fine-tuned

balance between activity and toxicity or selectivity is vital for the success of these compounds [14]. Development of peptidomimetics or synthetic mimics of antimicrobial peptides (SMAMPs) could overcome the hurdles of instability, lowered bioavailability, and immunogenicity [15]. Although small SMAMPs are especially promising drug candidates, some of the issues considering clinical settings remain, namely, interactions with biomolecules, tendencies to proteolytic degradation, toxicity, and rather low *in vitro*/*in vivo* translation. The remaining issues limit their clinical applicability as well as faster progress in the pipelines [14, 16].

Pursuing topical administration routes such as efficient localized therapy of skin and vaginal infections could help circumvent many of the SMAMPs limitations linked to systemic route; however, certain obstacles remain to be addressed even for topical routes [14]. Drug delivery strategies, using e.g., nanomaterials, could advance the therapeutic index and increase exposure or contact time and retention at the infected area [8, 17, 18]. Lipid-based systems for MAA delivery have previously demonstrated superior antimicrobial activity and could therefore be suitable alternatives for the delivery of these compounds [7, 19, 20]. We have previously established that liposomes associated with MAA chlorhexidine improved biofilm eradication in addition to lower inflammatory responses in macrophages [21]. Moreover, liposomes can facilitate sustained release of the active compound which in turn could lower the risk of bacterial regrowth, improve interaction with the bacterial membrane, and increase the exposure time [17, 22]. Additionally, liposomes enable accumulation of the active compound at the infected site, thus limiting systemic exposure due to their ability to interact with skin lipids, making them suitable for topical skin administration [23, 24].

In the present study, 7e-SMAMP, a novel SMAMP with excellent antimicrobial properties [15], was incorporated into liposomes optimized for treatment of biofilm-infected chronic skin wounds. Development of 7e-SMAMP was inspired by incorporating important properties of AMPs into a cationic and amphipathic scaffold mimicking the marine antimicrobials *Eusynstyelamides* found in bryozoan *Tegella cf. spitzbergensis* [15]. We hypothesized that associating the membrane-active 7e-SMAMP with liposomes could improve *in vitro* biofilm eradication of bacteria commonly found in wounds in addition to lowering the inflammatory activity of macrophages therefore further improving healing. After initial optimization and characterization of 7e-SMAMP-liposomes, the evaluation of *in vitro* performance of the

delivery system focused on cell compatibility, anti-inflammatory properties, and antimicrobial efficacy.

2. Experimental section

2.1. Materials

Lipoid S100 (phosphatidylcholine content >94%) was kindly provided by Lipoid GmbH (Ludwigshafen, Germany). Methanol (≥99.9%), HiPerSolv CHROMANORM® for LC-MS, acetonitrile (≥99.9%), HiPerSolv CHROMANORM®, gradient grade for HPLC and acetic acid (>99.9%) were purchased from VWR International (Fontenay-sous-Bois, France). Phosphoric acid (>85%) was acquired from Kebo lab (Oslo, Norway). Albunorm (200 mg/mL human serum albumin) was acquired from Octapharma AG (Lachen, Switzerland). Sepharose™ CL-4B was purchased from GE Healthcare (Uppsala, Sweden). 1,2-Dioleoyl-*sn*-glycero-3-phospho-*rac*-(1-glycerol) (DOPG), and 1-palmitoyl-2-(6-[(7-nitro-2-1,3-benzoxadiazol-4-yl)amino]hexanoyl)-*sn*-glycero-3-[phospho-*rac*-(1-glycerol)] (ammonium salt) (C_6-NBD-PG) were obtained from Avanti Polar Lipids (Alabaster, AL, USA). 1,2-Dioleoyl-*sn*-glycero-3-phosphoethanolamine (DOPE) was obtained from Lipoid GmbH (Ludwigshafen, Germany). Trifluoroacetic acid (TFA) for HPLC (≥99.0%), chloroform (99.0-99.4%, GC), glycerol solution (86-89%), sodium phosphate dibasic dihydrate, potassium phosphate monobasic, sodium chloride, EDTA sodium, sodium hydrogen carbonate, potassium chloride, calcium chloride dehydrate, cardiolipin sodium salt from bovine heart (≥97%), N-(2-Hydroxyethyl)piperazine-N′-(2-ethanesulfonic acid) (HEPES), sodium dithionite, fluorescein isothiocyanate–dextran average molecular weight (M_w) 3000-5000 Da (FITC–dextran 4400), fluorescein isothiocyanate–dextran average M_w 20 400 Da (FITC–dextran 20 400), Kollisolv® PEG E 400, Phospholipid Assay Kit for colorimetric or fluorometric tests, N-(-1-Naphthyl)ethylenediamine dihydrochloride, sulphanilamide, Triton™ X-100, and Cell Counting Kit-8 (CCK-8) were purchased from Sigma-Aldrich (St. Louis, MO, USA). Penicillin-streptomycin (10 000 units/mL and 10 mg/mL, respectively), lipopolysaccharides (LPS) from *Escherichia coli* O55:B5, RPMI-1640 medium (with L-glutamine and sodium bicarbonate) and fetal bovine serum (FBS) were obtained from Sigma-Aldrich (Steinheim, Germany). Dulbecco's Modified Eagle Medium high glucose (DMEM-hg) w/l-glutamine and sodium pyruvate was purchased from Biowest (Nuaillé, France). Nutrient Broth (NB) was supplied by Becton Dickinson and Company (Sparks, MD, USA). Murine macrophage, RAW

264.7 cell line was obtained from ATCC (Manassas, VA, USA). HaCaT cell line (immortalized human keratinocytes) was purchased from CLS Cell Lines Service GmbH (Eppelheim, Germany). *Staphylococcus aureus* ATCC29213, *Escherichia coli* ATCC11105, *Pseudomonas aeruginosa* ATCC10145 were purchased from American Tissue and Cell Culture Corp. (Manhasset, Virginia, USA). *Staphylococcus aureus* SO2, SO83, SO86, and SO88 are clinical isolates (Ospedale Sant'Orsola-Malpighi, Bologna, Italy) [25].

2.2. SMAMP synthesis

The synthesis of the 7e-SMAMP has been previously described by Paulsen *et al.* including the detailed methodology and materials involved [15]. However, a brief overview of the procedure is provided in Supplementary Material (S1.1.).

2.3. Evaluation of 7e-SMAMP stability

The 7e-SMAMP stock solutions were diluted to 25 and 50 µM with simulated wound fluid (SWF; 5.84 g/L NaCl, 3.36 g/L $NaHCO_3$, 0.3 g/L KCl, 0.35 g/L $CaCl_2 \cdot 2H_2O$, and 33 g/L albumin from Albunorm in milli-Q water (mQ)) [26] or mQ and analysed using reversed-phase chromatography [27] with a Waters e2795 separations module combined with a Waters 2489 UV–VIS detector. The quantification of 7e-SMAMP was carried out using Waters XBridge® C18 column (5 µm, 4.6 x 250 mm) and a Waters XBridge® C18 guard cartridge (5 µm, 4.6 x 20 mm, Waters Corporation, Milford, CT, USA) modified from a method by Paulsen *et al*. [28]. The 7e-SMAMP was eluted with mobile phases comprising mQ and acetonitrile, both with TFA (0.1%, v/v). The gradient starting at 50% acetonitrile followed a linear gradient to 75% acetonitrile over 8 min with a flow of 1 mL/min at detection wavelength set to 231 nm.

Prior to the evaluation of 7e-SMAMP stability, we performed a UV-VIS scan analysis [27]; the detailed procedure can be found in Supplementary Materials (S1.2.). All solutions were stored for 7 days at 4, 25, and 32 °C. Chemical evaluations of stability were performed at preparation time and after 1- and 7-days storage.

2.4. Liposome preparation and size reduction

The thin film method was utilized to prepare liposomes. In short, Lipoid S100 (200 mg) and 7e-SMAMP (20 mg) were dissolved in methanol. Lipid films were created by evaporation on Büchi rotavapor R-124 (equipped with vacuum controller B-721, Büchi Vac® V-500 and Büchi B-480 water bath, Büchi Labortechnik, Flawil, Switzerland) at 60 mBar and 45 °C for at least 1 hour. The lipid film was rehydrated with 10 mL distilled water to form liposomes. Empty liposomes (without 7e-SMAMP) were prepared with only Lipoid S100 in the lipid film. The size of the liposomes was reduced by manual extrusion through polycarbonate membranes (Nuclepore Track-Etch Membrane, Whatman House, Maidstone, UK). The size reduction was achieved by successional manual extrusion through 0.8 µm (three times), 0.4 µm (five times), and 0.2 µm (two times) membranes [21].

2.5. Liposome characterisation - size, zeta potential, pH, and entrapment efficiency determination

The liposome size was determined with a Malvern Zetasizer Nano Zen 2600 (Malvern, Oxford, UK). The liposomes were diluted 1:100 (v/v) with 0.2 µm filtered tap water prior to every measurement and measured in triplicates.

The zeta potential was determined with the Zetasizer Nano Zen 2600 (Malvern, Worcestershire, UK). The liposomes were diluted 1:20 (v/v) in 0.2 µm filtered tap water prior to every measurement and measured in triplicates.

The pH was determined using the Accumet®, Portable pH meter AP115 (Fisher Scientific, MA, USA) at room temperature (21 ± 1 °C). The stability of the 7e-SMAMP-liposomes was evaluated, and the procedure is described in the Supplementary Materials (S1.3.).

Liposomes were dialyzed (tube, MWCO: 12–14 kDa; Spectra/Por®4, Spectrum®, VWR International, Fontenay-sous-Bois, France) for 4 hours (1:1000, v/v) as previously described [21]. HPLC was utilized to determine 7e-SMAMP concentrations as described in section 2.3.

2.6. Morphology studies by transmission electron microscopy

The morphology of 7e-SMAMP-liposomes was investigated using transmission electron microscopy (TEM) as reported earlier [29]. Liposomes were deposited onto carbon-coated grids and stained with 3% uranyl acetate and 2% methylcellulose. The images were acquired with microscope HT7800 Series (Hitachi High-Tech Corp., Tokyo, Japan) at an accelerated voltage of 100 kV coupled with a Morada camera.

2.7. Phospholipid content of liposomes

The phospholipid content of liposomes was measured with Phospholipid Assay Kit according to the technical bulletin provided by the supplier. Prior to the experiment, liposomes (50 µL) were diluted with distilled water to a total volume of 10 mL. Finally, the phospholipid content was measured on a UV–VIS plate reader (Tecan Trading AG, Männedorf, Switzerland) at 570 nm.

2.8. Elasticity of liposomal membranes

The assessment of the elasticity of the liposomal membranes to confirm integrity of liposomes followed a method by Palac *et al*. [30]. The empty and 7e-SMAMP-liposomes were extruded with a constant pressure of 2.5 Bar through a membrane with a pore size of 100 nm. The amount of liposomal suspension passing through the membrane within 5 min and liposomal mean diameter were recorded. Empty liposomes served as control for 7e-SMAMP-liposomes. The elasticity was calculated according to Eq. 1:

$$E = J \times (r_v/r_p)^2$$

where J represents the amount (g) of liposomal suspension passing through the membrane within 5 min, r_v represents mean diameter (nm) after extrusion, and r_p represents pore size of the membrane (nm).

2.9. In vitro release studies

The *in vitro* 7e-SMAMP release from the liposomes was evaluated using tubes of pre-soaked regenerated cellulose (MWCO: 12-14 kDa) membranes (Spectra/Por®4, Spectrum®, VWR International, Fontenay-sous-Bois, France) [31]. The medium (150 mL) used in the experimental setup was PEG E400 (10%, v/v) in distilled water, heated to 32 °C. An aliquot (1.5 mL) of 7e-SMAMP-liposomes or 7e-SMAMP dissolved in acceptor medium was added to the dialysis membrane. Samples were withdrawn after 1, 2, 3, 4, 6, 8, and 24 hours and analysed using HPLC as described in section 2.3. The sample volume was replaced with fresh medium in the acceptor phase after every sampling. The sink conditions were assured. The cumulative release of formulated and non-formulated 7e-SMAMP was compared.

2.10. Evaluation of cell viability

AMPs and their mimics often display certain level of toxicity to eukaryotic cells; therefore, to ensure the safety of the novel formulations we evaluated cytotoxicity using Cell counting kit – 8 (CCK-8) as described previously [32]. Suspensions of HaCaT or RAW 264.7 cells (90 µL, 1×10^5 cells/mL) were plated on 96-well plates and incubated for 24 hours (37 °C /5% CO_2). The macrophages were cultured in complete RPMI (containing 10% FBS, penicillin-streptomycin), while keratinocytes were cultured in complete DMEM-hg (containing 10% FBS, penicillin-streptomycin). The pre-incubated cells were treated with 10 µL of medium (control), diluted liposome suspensions (1, 10, and 50 µg/mL lipid concentration) and incubated for another 24 hours (37 °C/5% CO_2). An aliquot of 10 µL CCK-8 reagent was added to each well and the cells were incubated for 4 hours (37 °C/5% CO_2). To evaluate the cell survival, the cells were assessed using a UV–VIS plate reader (Tecan Trading AG, Männedorf, Switzerland) at 450 nm and referenced at 650 nm. The results were expressed as percentage of surviving cells compared to the non-treated cells (control).

2.11. Assessment of anti-inflammatory activity

Anti-inflammatory activities of empty and 7e-SMAMP-liposomes were determined by assessing lipopolysaccharide (LPS)-induced nitric oxide (NO) production in murine macrophages. Macrophages (RAW 264.7) were cultured in complete RPMI and seeded in 24-

well plates (1 mL, 5×10^5 cells/mL) prior to incubation (37 °C/5% CO_2) for 24 hours. After incubation, the complete medium was replaced with medium containing LPS (1 µg/mL). The cells were then treated with liposomal suspensions (1, 10, and 50 µg/mL lipid concentration). The LPS containing medium and complete medium served as controls. The cells were then incubated for another 24 hours and NO production evaluated on a UV–VIS plate reader (Tecan Trading AG, Männedorf, Switzerland) with Griess reagent (1:1, v/v; 2.5% phosphoric acid with 1% sulphanilamide and 0.1% N-(-1-naphthyl)ethylenediamine) at 540 nm [32].

2.12. Effects of 7e-SMAMP on bacterial membrane-mimic liposomes model

2.12.1. Bacterial Membrane-Mimic Liposomes Model

Bacterial Membrane-Mimic Liposomes Models (B3M-liposomes) mimicking *S. aureus* membranes were tailored according to literature [33, 34]. In brief, DOPG and cardiolipin (20 mg) were dissolved in chloroform and methanol (2:1, v/v) in a molar ratio of 58:42. A lipid film was produced by solvent evaporation on a rotary evaporator at 45 °C, 60 mBar, and 60 rpm for 2 hours to remove the solvents. The lipid films were rehydrated with FITC-dextrans (10 mg/mL, 2 mL) of two different average M_ws, namely 4400 or 20 400 Da, in HEPES buffer (10 mM, with 100 mM NaCl and 1 mM EDTA sodium, pH 7.4). The size of B3M-liposomes was reduced and made uniform by manual extrusion (8 times through 0.8 µm polycarbonate membranes). A Sepharose™ CL-4B column was used for removal of unentrapped FITC-dextran 4400 and 20 400. HEPES buffer (10 mM, with 100 mM NaCl and 1 mM EDTA sodium, pH 7.4) was used for the elution.

The B3M-liposomes mimicking *P. aeruginosa* membranes were tailored similarly to the *S. aureus* membranes mimics; however, the lipid composition was altered. The membrane was composed of DOPE, DOPG, and cardiolipin (20 mg) in a molar ratio of 65:23:12 as described by Lombardi *et al.* [35].

2.12.2. FITC-dextran leakage

FITC-dextrans leakage from B3M-liposomes was assessed following the procedures [34, 36] with minor modifications. The FITC-dextran-loaded B3M-liposomes were diluted 20-fold in the HEPES buffer. The non-formulated and formulated 7e-SMAMP were also diluted in

HEPES buffer (final 7e-SMAMP concentrations corresponding to 0.5, 2, and 5 µg/mL). The leakage from FITC-dextran-loaded B3M-liposomes was measured as a fluorescence intensity at excitation wavelength 485 nm and emission wavelength 530 nm. Triton (10 %, v/v) in HEPES buffer served as control. The leakage was calculated using the following formula (Eq. 2) [37]:

$$\text{Leakage (\%)} = 100 \times [(F - F_0)/(F_T - F_0)]$$

F = fluorescence of treated FITC-dextran B3M-liposomes

F_0 = buffer

F_T = buffer with Triton

2.12.3. Lipid flip-flop

The B3M-liposomes mimicking *S. aureus* or *P. aeruginosa* membranes for the lipid flip-flop assay were tailored in the same manner as for the FITC-dextran leakage assay; however, C_6-NBD-PG was added at 0.5 mol% together with the other lipids [38]. The lipid film was rehydrated with HEPES buffer (10 mM, comprising 100 mM NaCl and 1 mM EDTA sodium, pH 7.4) and the vesicle size reduced in the same manner as for the FITC leakage assay. To achieve only the labelling of the inner leaflet, sodium dithionite (1 M) in 1 M HEPES buffer (pH 7.4) was added to B3M-liposomes that were incubated for 15 min at 24 °C to ensure quenching of C_6-NBD-PG in the outer leaflets. Subsequently, B3M-liposomes and sodium dithionite were separated on PD-10 desalting columns (Cytiva, Marlborough, MA, USA) with HEPES buffer (10 mM, with 100 mM NaCl and 1 mM EDTA, pH 7.4) sodium for the elution. The B3M-liposomes were diluted 50-fold with buffer and incubated with non-formulated or formulated 7e-SMAMP (0.5, 2, and 5 µg/mL, 7e-SMAMP concentration). Finally, sodium dithionite (1 M) was added, and monitored with excitation and emission wavelengths of 460 and 520 nm, respectively, for 650 sec. Triton or buffer served as respective controls [38, 39].

2.13. Antimicrobial evaluation

2.13.1. Determination of MIC and MLC

The antimicrobial activity of 7e-SMAMP-liposomes, as well as 7e-SMAMP and empty liposomes, was evaluated by broth microdilution method following the EUCAST guidelines [40]. Microorganisms were aerobically cultured on nutrient agar plates at 37 °C for 24 hours, and subsequently diluted in nutrient broth (NB) [25, 41] to obtain bacterial suspensions at final concentrations of 2×10^6 CFU/mL. The 7e-SMAMP was solubilized in 100% dimethyl sulfoxide (DMSO, 10 mg/mL) and then diluted in distilled water to assure that the final concentration of DMSO in the test series was <1%. The non-formulated and formulated 7e-SMAMP were diluted in sterile water in a two-fold sequence in 96-well culture plates (Corning Inc., Pisa, Italy) to test 7e-SMAMP concentration ranging from 0.1 to 100 μg/mL. Empty liposomes and DMSO were tested at the same dilutions. The microbial suspension (100 μL) was then inoculated with 100 μL of samples. Wells containing microbial suspension (100 μL) and sterile water (100 μL) served as growth control. Blank control, comprising only a growth medium, and sterility controls, containing samples and sterile medium, were also included. Plates were aerobically incubated at 37 °C for 24 hours. Afterwards, the minimal inhibiting concentrations (MIC) were determined by comparing the turbidity (OD_{600}) of samples with that of growth control by means of EnSpire Multimode Plate Reader (PerkinElmer Inc., Waltham, MA, USA). To determine a microbicidal effect, 20 μL of samples from wells exhibiting no growth were spotted onto nutrient agar plates and incubated at 37 °C for another 48 hours. The minimal lethal concentration (MLC) was defined as the minimal concentration that completely inhibited microbial viability. Three batches for each formulation were tested.

2.13.2. Killing curves in simulated wound fluid

The antimicrobial activity of non-formulated and formulated 7e-SMAMP was also evaluated against planktonic cultures of pathogens in SWF (bovine serum albumin 2% w/v; $CaCl_2$ 0.02 M; NaCl 0.4 M; Trizma base 0.05 M, pH 7.4) [21]. The non-formulated and formulated 7e-SMAMP were diluted in 5 mL of SWF (50 μg/mL, 7e-SMAMP concentration). Empty liposomes were diluted in the same way. Microbial suspensions were prepared in SWF and used to inoculate samples (starting inoculum: 10^6 CFU/mL). Microorganisms inoculated in 1 mL of SWF were used as controls.

Counts of viable cells were carried out on nutrient agar plates at the inoculum time and after 3, 6, 8, and 12 hours of incubation at 32 °C. Three batches for each formulation were tested. Results are expressed as viability (logCFU/mL) of microorganisms over the time in presence of different samples.

2.13.3. Anti-biofilm activity

The non-formulated and formulated 7e-SMAMP were investigated for their ability to inhibit the biofilm formation and eradicate pre-formed biofilms of *S. aureus*, *E. coli*, and *P. aeruginosa*. Microbial suspensions were prepared as previously described (2.13.1) and employed as inocula for both the inhibition and eradication assays. For the inhibition assay, the wells of sterile 96-well flat-bottomed culture plates were filled with 100 µL of microbial suspension and 100 µL of non-formulated and formulated 7e-SMAMP. Both non-formulated and formulated 7e-SMAMP were tested at final concentrations of 0.78, 1.56, 3.12, 6.25, 12.5, 25, and 50 µg/mL. The DMSO and empty liposomes were also tested as controls. The multi-well plates were incubated at 37 °C under shaking (100 rpm) for 48 hours to allow biofilm development.

For the eradication assay, the 96 multi-well plates were inoculated with 200 µL of bacterial suspensions and after 48 hours of incubation (37 °C, 100 rpm), the liquid cultures were removed, leaving only adherent cells. Biofilms were then treated with 100 µL of fresh medium and 100 µL of non-formulated and formulated 7e-SMAMP at the same concentrations as in the inhibition assay. The plates were further incubated (37 °C, 100 rpm) for 24 hours.

Biofilm quantification was performed through crystal violet staining. Briefly, the liquid culture was removed, and adherent cells were washed twice with 200 µL of phosphate-buffered saline (PBS, pH 7.4), fixed with 200 µL of conc. ethanol for 5 min and stained with 180 µL of crystal violet 0.41% (w/v) in 12% ethanol for 5 min. Excess stain was rinsed out by washing the multi-well plate with PBS thrice. Subsequently, the plates were air dried, the dye bound to the adherent microorganisms was resolubilized with 200 µL of acetic acid 30% (v/v) and the optical density measured at 595 nm (OD_{595}). Three batches for each formulation were tested. The anti-biofilm activity was calculated with respect to untreated control, as follows (Eq 3):

Inhibition of biofilm formation/Eradication of pre-formed biofilm (%)
= (1- OD_{595} sample/ OD_{595} control) × 100

2.14. Statistical analyses

In general, results are expressed as mean ± SD. Student's t-tests, one-way ANOVA with Tukey's post-test or two-way ANOVA with Šídák's multiple comparisons post-test were performed to evaluate significance (at least $p < 0.05$). All statistical analyses were performed in GraphPad Prism version 9.3.1 for Windows (GraphPad Software LLC, San Diego, CA, USA).

4. Results and discussions

4.1. 7e-SMAMP stability

AMPs often display instability in different biological fluids; however, this drawback is expected to be addressed by designing SMAMPs. Still, it is important to evaluate the stability of novel SMAMPs as well as their safety prior to the development of pharmaceutical formulations [27].

The chemical stability of 7e-SMAMP was evaluated by analysing the 7e-SMAMP content in fluids after 1- and 7-days storage at 4, 25, and 32 °C. The 7e-SMAMP was stored in either SWF (Fig 1a) or water (Fig.1b) and compared to the initial concentrations. As seen in Fig.1a, the 7e-SMAMP was stable in SWF over the entire period at all temperatures. The stability of the 7e-SMAMP in water (Fig.1b) was in most cases seemingly lower at 25 and 32 °C; however, the deviations within the same measurements were rather large. Despite more variations upon storage in water, the content remained almost constant throughout the stability testing period. Additionally, the 7e-SMAMP is formulated in delivery systems both to maintain over an extended period at wounded site and be protected against degradation. Furthermore, our results were in agreement with the UV-scans analysis data presented in Supplementary Materials (S2.1.), and indicate that 7e-SMAMP should be stored at 4 °C.

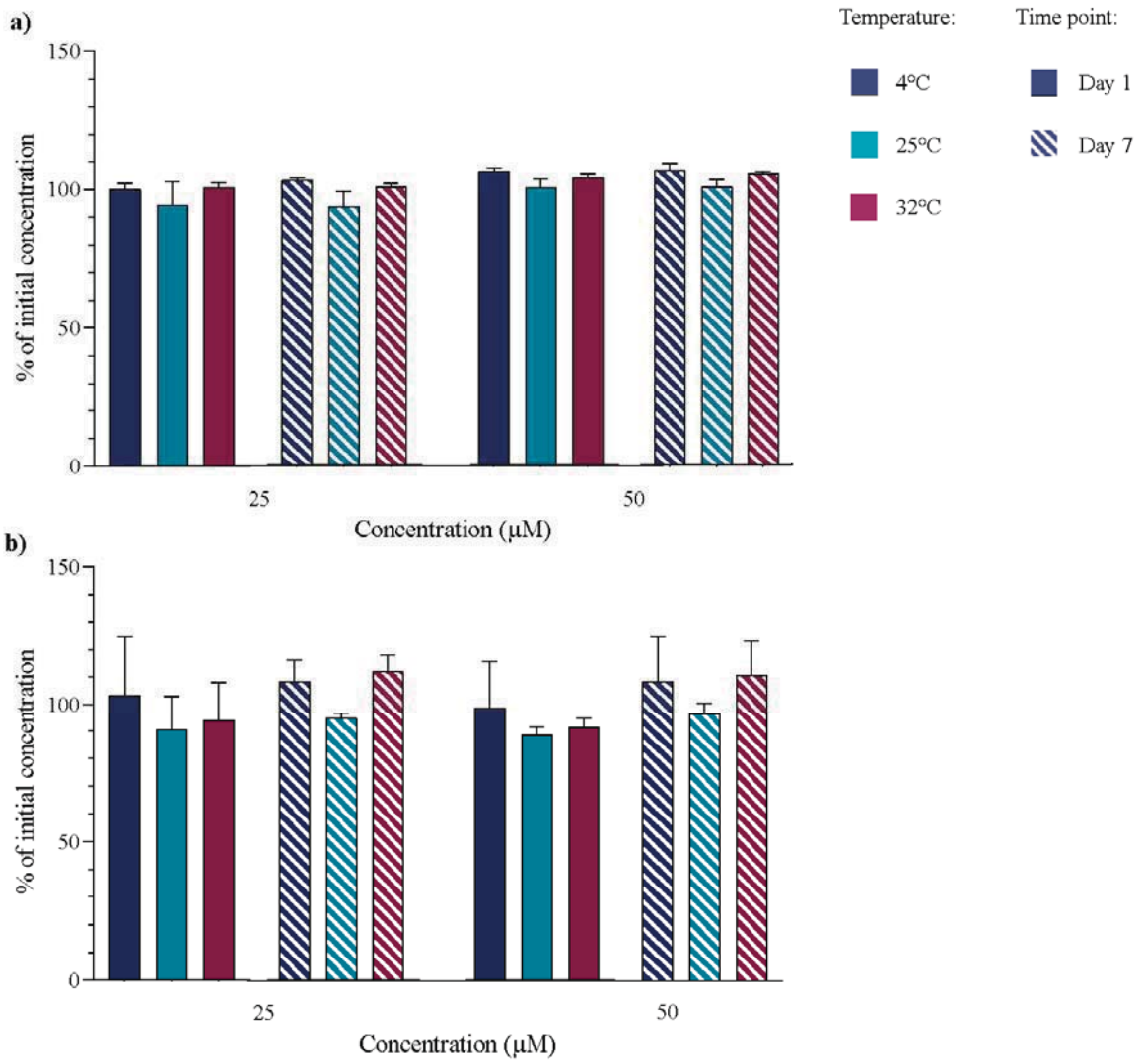

Figure 1. Stability of non-formulated 7e-SMAMP. The changes from initial concentration (25 and 50 µM) when stored in a) simulated wound fluid (SWF) and b) milli-Q (mQ) water at 4, 25, and 32 °C for 1 day (solid colour) and 7 days (pattern). All results are expressed as means with their respective SD (n = 3).

4.2. Liposome characteristics

In the fight against resistant pathogens, new antimicrobial compounds are needed to avoid an even more challenging outcome and further progression of resistance patterns seen today. However, effective means of delivering these active compounds to the targeted site are desired and often necessary to achieve sufficient therapeutic effects. The novel 7e-SMAMP has previously displayed excellent activity against some of the most problematic bacteria; however, its toxicity profile might still limit its applicability in clinical settings [15]. Liposomes are

known to reduce the toxicity of pharmaceutical compounds, including AMPs [23, 42]. Moreover, liposomes are known to be able to improve antimicrobial efficacy of antimicrobial compounds both against planktonic and biofilm-embedded bacteria and it has been shown that they interact with skin and can accumulate active compounds at specific sites [43, 44]. As exemplified by Rukavina *et al.*, incorporating azithromycin in liposomes significantly lowered both MIC and minimum biofilm inhibitory concentration of azithromycin [45]. Our formulation, comprising liposomes and a SMAMP, could fulfil most crucial requirements; increased activity, reduced toxicity, prolonged release, and maintenance of structural integrity, all required for a successful topical delivery system intended for treatment of infected chronic wounds or other topical infections.

The liposome properties are strongly related to the formulation characteristics and, in the extent of that, the biological properties. In topical delivery, sizes in the range of 200-300 nm are found to be suitable for pharmaceutical delivery vesicles [46, 47]. Furthermore, we previously found that liposomes associated with the MAA chlorhexidine, in the same size range, demonstrated promising antimicrobial and anti-biofilm activities against *S. aureus* and *P. aeruginosa* [21]. As illustrated in Table 1, the thin film hydration method followed by extrusion, as a size reduction method, resulted in liposomes smaller than 300 nm. Furthermore, these preparation methods also yielded an acceptable polydispersity index (PI) of 7e-SMAMP-liposomes. For lipid-based systems intended for topical delivery, PIs below 0.3 are considered suitable and represent rather homogenous populations [48]. Generally, an overall positive surface charge of vesicles is preferred when tailoring drug delivery systems for microbial and biofilm eradication [42, 49]. The bacterial membrane is negatively charged, therefore liposomes with a positive surface charge can easily interact with the membrane. A strengthened electrostatic interaction between the bacterial membrane and liposomes could result in a successful outcome [50]. This interaction is potentially stronger with bacterial compared to eukaryotic membranes due to the slightly higher negative charge density on bacterial membranes [51]. This may lead to reduced toxicity and a favourable outcome of treatment with the novel SMAMP; however, the biocompatibility needs to be assessed. Literature also shows that cationic liposomes might improve inhibition of biofilm formation [43]. The high zeta potential of 7e-SMAMP-liposomes (58.7 mV) could most likely be ascribed to 7e-SMAMP association with/in bilayers of liposomes. This indicated that the cationic guanidine groups of 7e-SMAMP (Fig. 2) are accommodated onto/within the lipid bilayer This association also resulted in a rather high entrapment efficiency of 78%, as seen in Table 1.

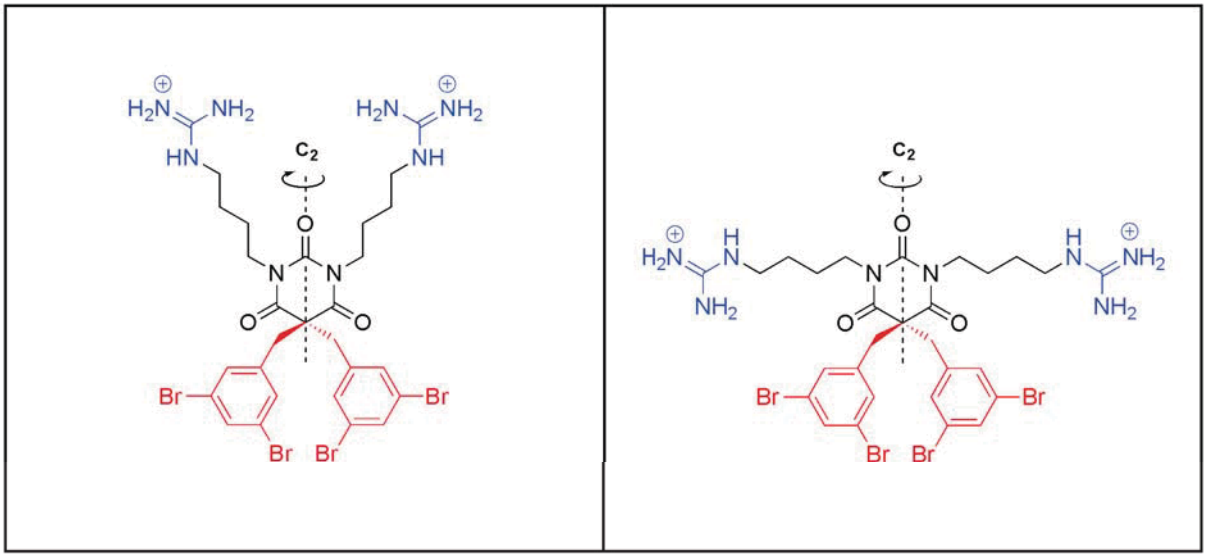

Figure 2. Structure of the 7e-SMAMP. The barbiturate ring ensures an amphipathic and achiral scaffold with C2-symmetry.

Considering wound healing, acidic pH conditions could be advantageous. The most common bacteria have optimal growth at neutral pH conditions, therefore lowered pH could generate less favourable conditions for the bacterial growth [52]. Although this alone is not enough to prevent bacterial growth, acidic pH of 7e-SMAMP is highly beneficial feature considering therapy.

Table 1. Liposome characteristics: mean diameter, polydispersity index (PI), zeta potential, entrapment efficacy (EE%), and pH in aqueous medium.

	Mean diameter (nm)	**PI**	**Zeta potential (mV)**	**EE (%)**	**pH**
7e-SMAMP-liposomes	276 ± 16	0.20 ± 0.01	58.7 ± 1.6	78.1 ± 2.2	4.9 ± 0.1
Empty liposomes	269 ± 42	0.44 ± 0.05	-0.4 ± 0.2	-	6.3 ± 0.0

Results are expressed as means with their respective SD (n=3). The mean diameter represents the weight-intensity distribution of the liposomes.

In the quality control of liposomes or other lipid-based formulations, it is important to monitor the lipid content of formulations, especially when reducing the size of liposomes by extrusion. The phospholipid content of 7e-SMAMP-liposomes was approximately 90% (Table 2), proving limited loss of lipid during the extrusion process. To further examine the stability of liposomes after incorporation of 7e-SMAMP, the membrane elasticity assay was performed. AMPs and SMAMPs are reported to destabilize the bacterial membrane [53]; we therefore sought to investigate if the membrane integrity of liposomes was altered by 7e-SMAMP. As seen in Table 2, the rigidity of the bilayer of 7e-SMAMP-liposomes was higher (p = 0.001) than for the empty liposomes, indicating that the bilayer of the 7e-SMAMP-lipsomes remained stable upon incorporation of 7e-SMAMP. A small increase in fluidity could be linked to the so-called carpet-like model of their antimicrobial mechanisms of action; a contribution because of disruption of lipid packing within the membrane [54]. Furthermore, the 7e-SMAMP-liposomes maintained a stable size, size distribution, surface charge, entrapment efficacy, and pH over a period of 12 weeks (Table S1).

Table 2. Phospholipid content and membrane elasticity of liposomes

	Phospholipid content (%)[a]	**Membrane elasticity (E)**
7e-SMAMP-liposomes	89.9 ± 1.0	5.081 ± 0.785
Empty liposomes	92.6 ± 1.7	9.775 ± 0.581

Results are expressed as means with their respective SD (n = 3).

[a] Phospholipid content (%) of initial concentration (20 mg/mL).

Since liposomes incorporating 7e-SMAMP were prepared for the first time, we utilized TEM to evaluate the morphology and confirm the size of the novel 7e-SMAMP-liposomes. The 7e-SMAMP-liposomes were spherical and in similar size range as determined using dynamic light scattering (Fig. 3a). Additionally, TEM was also used to confirm the formation of

liposomes and their structure, even upon incorporation of 7e-SMAMP. Fig. 3b demonstrates the proposed accommodation of 7e-SMAMP within the liposomal bilayers.

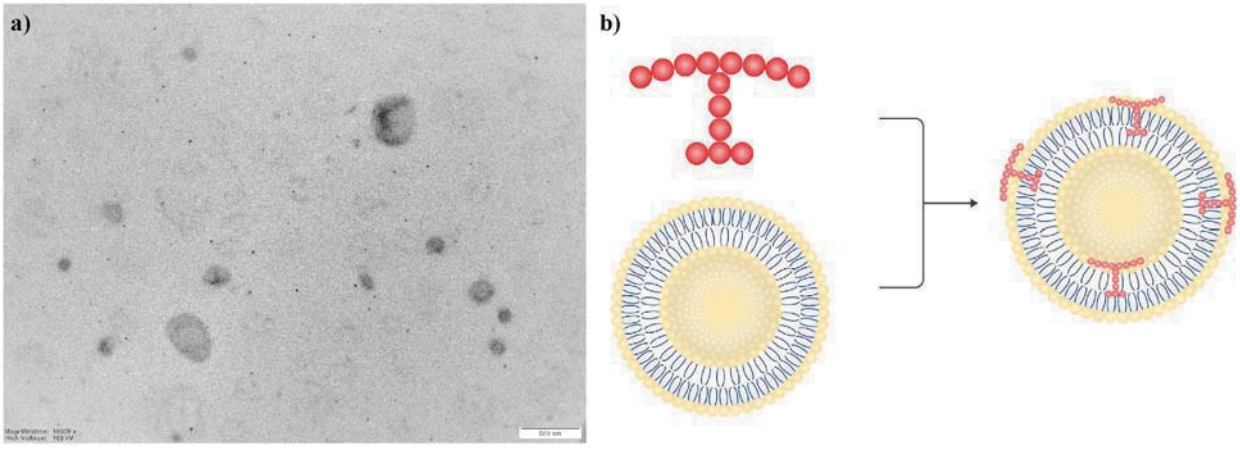

Figure 3. a) TEM image of 7e-SMAMP-liposomes. Scale bar 500 nm. b) Proposed accommodation of 7e-SMAMP in liposomes.

4.3. In vitro release

The conventional formulations for localized antimicrobial therapy of the skin, especially considering wounds, are often associated with serious limitations such as instability of drug at the site of application and/or insufficient drug release leading to low drug concentration at the site of infection [45]. Therefore, the first aim was to tailor a formulation able to remain at the intended site and serves as a depot of the antimicrobial compound assuring its prolonged release. Secondly, the formulation should ensure proper release of the antimicrobial compound to achieve a high local concentration to prevent bacterial growth, eradicate existing bacteria and inhibit biofilm formation or eliminate biofilm-embedded bacteria [55]. As shown in Fig. 4 the release from the 7e-SMAMP-liposomes was approximately 71% (after 12 hours) and 79% (after 24 hours), respectively, while for the free or non-formulated 7e-SMAMP, 94% of the content permeated through the membrane after only 6 hours. The release from liposomes was significantly slowed ($p < 0.0001$ for all time points) as compared to non-formulated 7e-SMAMP (free). Therefore, this rather high initial concentration could boost the immediate eradication, while slower release after 6-8 hours could prevent bacterial regrowth. Furthermore, liposomes could interact with the bacterial membrane and give increased concentration of the antimicrobial compound within bacteria [56].

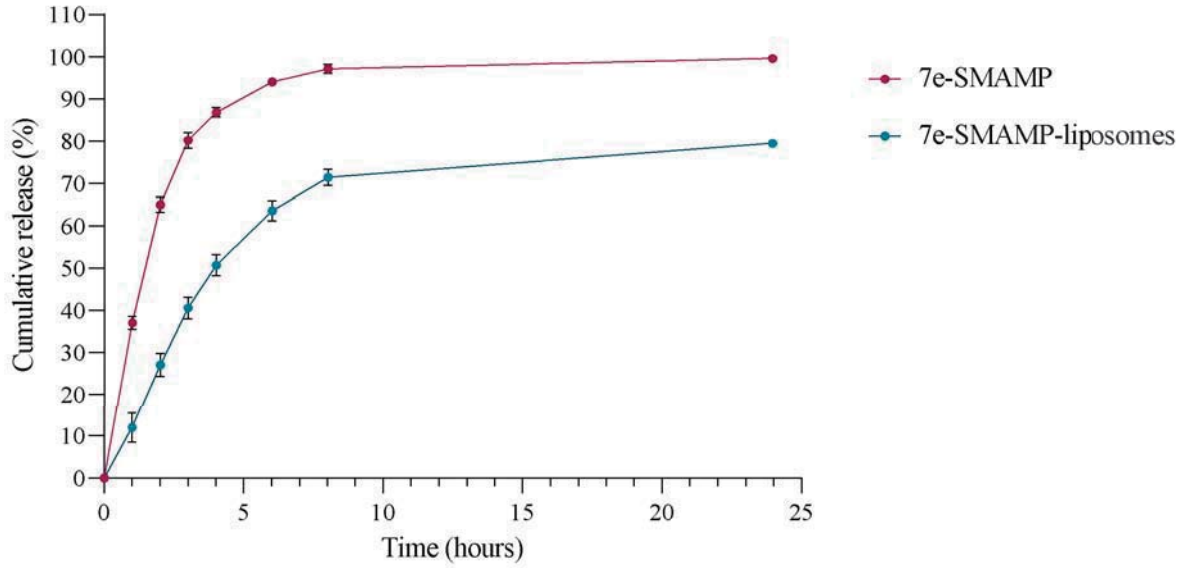

Figure 4. Cumulative release (%) from non-formulated (dissolved in release medium, free) and formulated 7e-SMAMP utilizing dialysis membranes (32 °C, 24 hours). The release is presented as the cumulative percentage of the initial liposomally-associated 7e-SMAMP concentration. All results are expressed as means with their respective SD (n = 3).

Reducing the frequency of formulation application onto an already painful area is considered beneficial in the treatment of chronic wounds [21]. The 7e-SMAMP-liposomes decreased the release rate of 7e-SMAMP enabling less frequent administration onto wounded areas. Furthermore, according to Korrapati and colleagues, ideal biological nanomaterials should be easy to design and modify, originate from natural sources and be biodegradable, biocompatible, and non-toxic [57]. Liposomes possess all these features; namely, are made of lipids originating from natural sources are biodegradable, non-toxic, and biocompatible, especially considering skin and the moist environment in wounds [58]. However, liposomal formulations do not exhibit proper viscosity as well as desired retention and are often incorporated within secondary delivery system (vehicle), such as hydrogels, that can be tailored to improve the healing while treating infection intended for wounds [21].

4.4. Evaluation of cell viability

Biocompatibility of drug formulation is an important issue, especially considering its contact with the wound [3]. Since 7e-SMAMP requires a smart formulation to be administered, the potential cytotoxicity of 7e-SMAMP-liposomes in comparison to empty liposomes was investigated *in vitro* using murine macrophages and keratinocytes. In both cell lines, the cell viability for liposomes-treated cells was similar to the non-treated cells (Fig. 5). However, both macrophages and keratinocytes treated with the highest concentration (50 μg/mL) of empty liposomes demonstrated significantly improved viability ($p < 0.01$), while keratinocyte viability improved at the highest concentration of 7e-SMAMP-liposomes ($p < 0.01$). Highly cationic surfaces of liposomes, as in our case, could alter the safety profile of the formulation [59]. Nevertheless, no negative effects of empty or 7e-SMAMP-liposomes were observed in the current study. The dose-dependent cell compatibility and proliferative effects of empty liposomes have previously been confirmed in both macrophages and keratinocytes [32, 60].

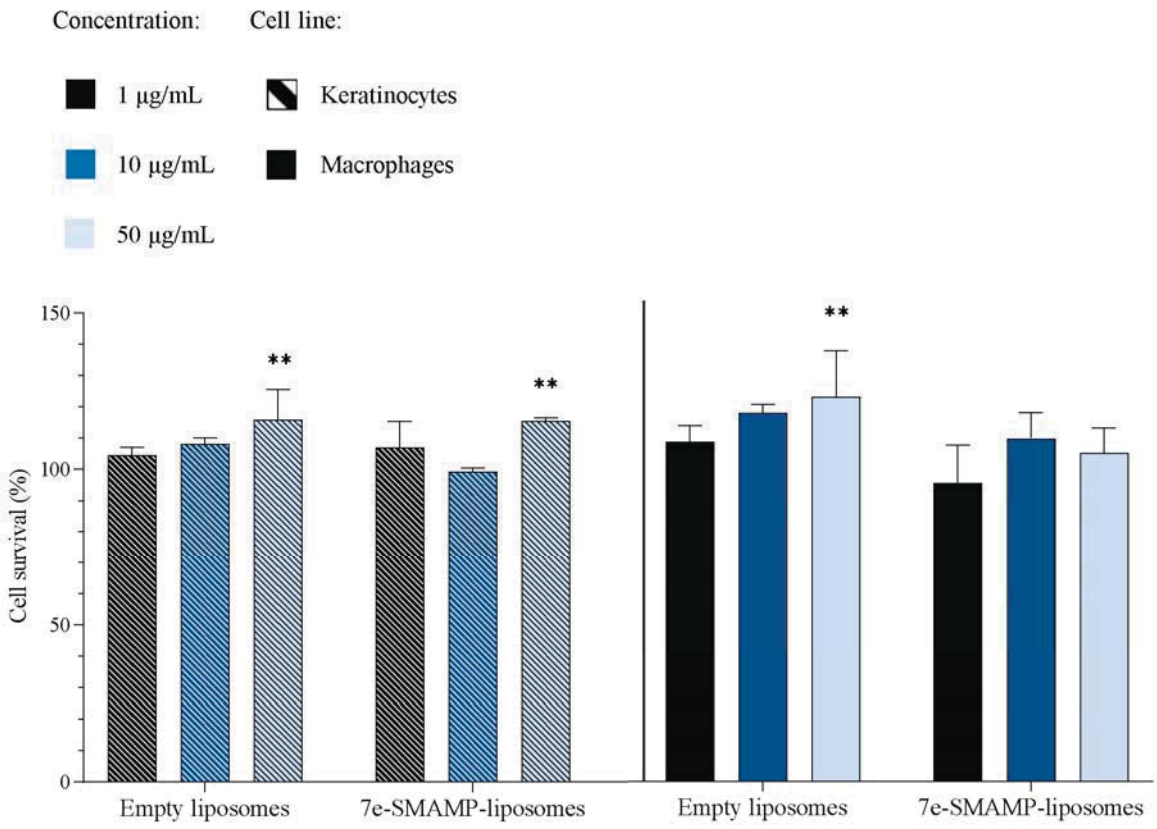

Figure 5. Evaluation of cell toxicity of empty and 7e-SMAMP-liposomes in HaCaT (patterned bars, left) and RAW 264.7 cells (solid bars, right). Three different concentrations were tested, namely 1, 10, and 50 µg/mL lipid, and the results are presented as cell viability of treated cells compared to control (100%). Control cells were only supplemented with complete medium; the cell viability is thereof considered as 100%. The results are expressed as means with their respective SD (n=3). ** $p \leq 0.01$.

4.5. Anti-inflammatory activity

The wound healing cascade is both dynamic and complex, and therefore depends on several intricately tuned events to transpire [61]. In this cascade, macrophages are essential for removal of debris, damaged matrix, microorganisms, and neutrophils from the wound bed in addition to releasing cytokines and growth factors [62]. Throughout wound healing process, pro-inflammatory macrophages transition into an anti-inflammatory macrophage phenotype to initiate healing [63]. However, in chronic wounds, transition to the next stages is hampered and the wound becomes haltered in the inflammatory phase [64]. Furthermore, many chronic wounds exhibit higher levels of NO that could cause damages to the tissue in the later stages of

the cascade [65]. Therefore, we evaluate the anti-inflammatory activity of both empty and 7e-SMAMP-liposomes through their ability to lower inflammatory response by reducing the NO production in LPS-induced murine macrophages as an indicator for the liposomes' anti-inflammatory potential. As shown in Fig. 6, the highest lipid concentration of both empty and 7e-SMAMP-liposomes significantly ($p < 0.05$ and $p < 0.0001$, respectively) reduced the NO production compared to the non-treated cells (control cells).

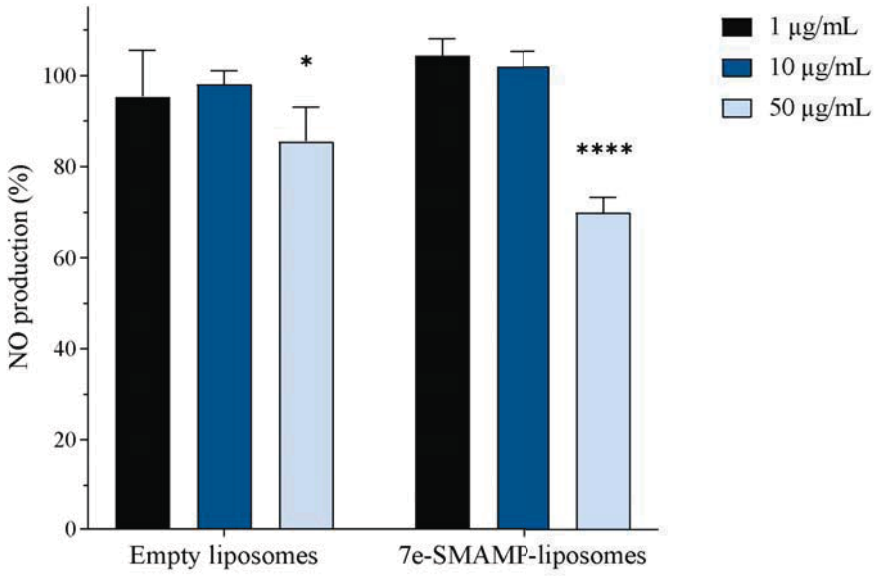

Figure 6. Evaluation of anti-inflammatory activity of empty liposomes and 7e-SMAMP-liposomes expressed as reduction of nitric oxide (NO) production in RAW 264.7 cells. Three different concentrations were tested, namely 1, 10, and 50 µg/mL lipid, and the results are presented as NO production of treated cells compared to control (100%). Control refers to non-treated lipopolysaccharide (LPS)-induced cells; their production is thereof considered as 100%. The results are expressed as means with their respective SD (n=3). * $p \leq 0.05$, **** $p \leq 0.0001$, compared to control.

In the current study, we observed a clear indication of the dose-dependent anti-inflammatory trends when 7e-SMAMP was incorporated within liposomes. The findings are in agreement with the work by Ahn *et al*. who investigated the anti-inflammatory properties of a peptidomimetic in the same cell line as used in our work; the authors also found a dose-dependent reduction in inflammatory response upon treatment with the peptidomimetic [66].

Moreover, we also detected anti-inflammatory activity of empty liposomes, similarly as Giordani *et al*. who reported reduced NO production in LPS-induced macrophages by approximately 20% compared to the non-treated cells evaluated in the same concentration range [67].

4.6. Effect of formulated and non-formulated 7e-SMAMP on Bacterial Membrane-Mimic Liposome Models

Liposomes tailored to mimic bacterial membranes are often utilized to investigate the potential antimicrobial and membrane-activity of MAAs, also termed transient pore formation [35, 68]. We assessed the activity of both non-formulated and formulated 7e-SMAMP on B3M-liposomes mimicking *S. aureus* and *P. aeruginosa* membranes by studying the leakage of liposomally-associated FITC-4400 or FITC-20 400, respectively. As shown in Fig. 7, both non-formulated and formulated 7e-SMAMP induced leakage from mimicked *S. aureus* (Figs. 7a and b) and *P. aeruginosa* (Figs. 7c and d) B3M-liposomes. A dose-dependent leakage was observed; however, it was more pronounced in the mimicked *S. aureus* B3M-liposomes. Stronger antimicrobial activity against gram-positive strains is commonly observed for both AMPs and SMAMPs due to their membrane structure [15, 69]. In our study, the leakage was stronger for non-formulated 7e-SMAMP than formulated 7e-SMAMP, while FITC-4400 leakage was slightly higher than FITC-20 400 leakage, as expected due to smaller M_w. In mimicked *P. aeruginosa* B3M-liposomes, the dose-dependency was not as evident for non-formulated 7e-SMAMP; however, the differences in leakage between the two markers were observed. Leakage of FITC-4400 was greater when the B3M-liposomes were treated with non-formulated 7e-SMAMP; in addition, a clear dose/effect step was observed between 0.5 and 2 µg/mL upon treatment with formulated 7e-SMAMP. Leakage of FITC-20 400 was only about 40% and approximately the same for all concentrations of non-formulated 7e-SMAMP. The mimicked *P. aeruginosa* B3M-liposomes loaded with FITC-20 400 treated with formulated 7e-SMAMP displayed much greater leakage in a dose-dependent manner. Other studies have also confirmed dose-dependent leakage from membrane-mimics, as in the study of Lee *et al.* where they assessed calcein leakage from *Escherichia coli* mimics [68]. Furthermore, Lombardi *et al.* showed dose-dependent leakage of 8-aminonaphtalene-1,3,6-trisulfonic acid disodium salt in membrane-mimics of *E. coli* and *P. aeruginosa* [35].

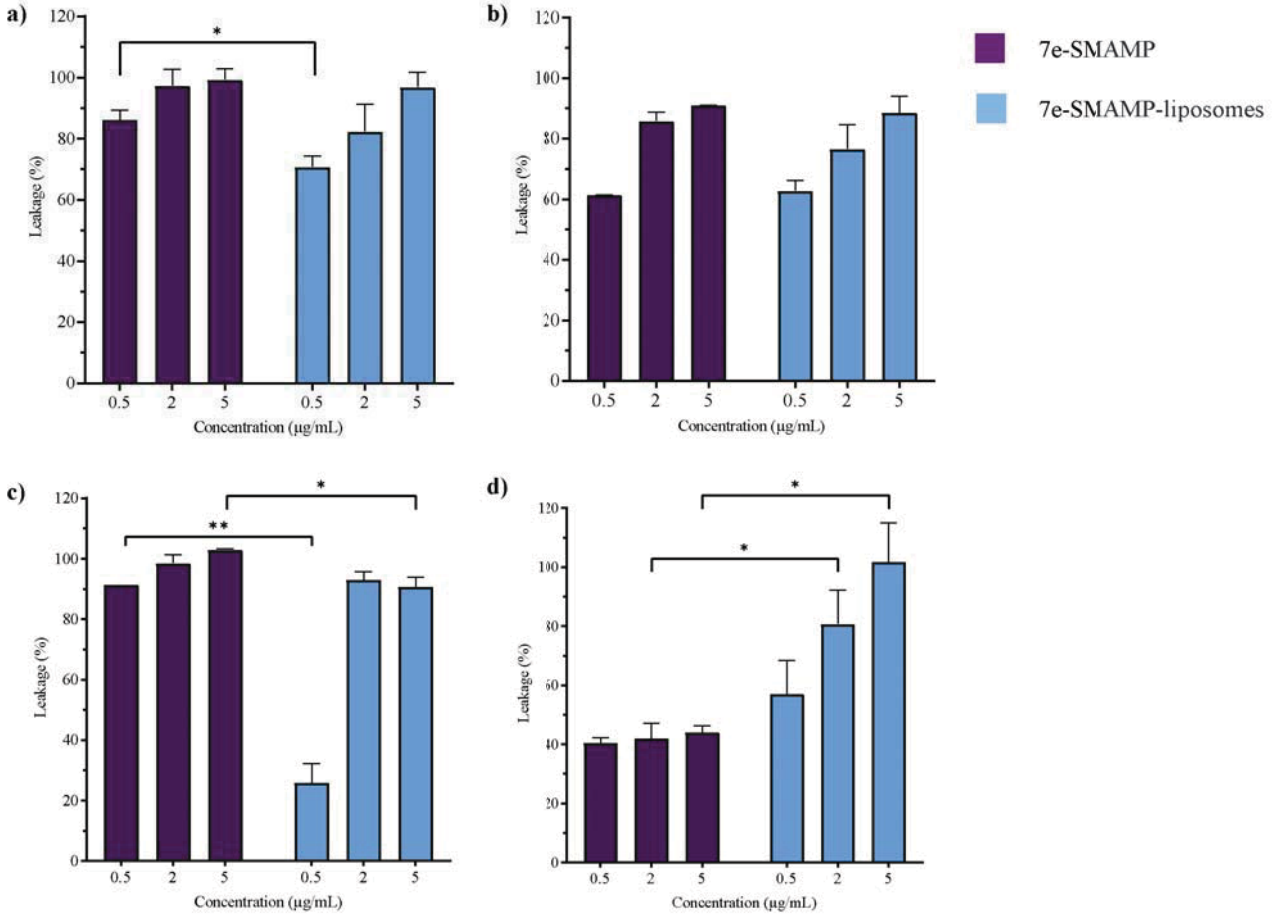

Figure 7. Bacterial Membrane-Mimic Liposomes Models (B3M-liposomes) loaded with FITC-dextran 4400 or 20 400 (molecular weight = M_w) treated with 7e-SMAMP or 7e-SMAMP-liposomes. The leakage is expressed as percentage compared to the control (Triton X-100). Concentrations of 7e-SMAMP were 0.5, 2, and 5 µg/mL for both non-formulated and formulated 7e-SMAMP. Different B3M-liposome mimics were prepared and challenged, namely A) *S. aureus* with FITC-4400, B) *S. aureus* with FITC-20 400, C) *P. aeruginosa* with FITC-4400, and D) *P. aeruginosa* with FITC-20 400. Results are presented as means with their respective SD (n=3). *) $p < 0.05$, **) $p < 0.01$.

Another approach to investigate the membrane-activity of MAAs is to examine the fusion between the inner and outer layer of mimicked B3M-liposomes. Here, the B3M-liposomes were labelled only on the inner leaflet by reducing the labelling on the outer layer using a reducing agent [35]. In the mimicked *S. aureus* B3M-liposomes (Fig 8a), the initial leaflet fusion of mimics treated with non-formulated 7e-SMAMP showed dose-dependent

trends. Mimicked *S. aureus* B3M-liposomes treated with formulated 7e-SMAMP showed different tendencies. At the highest 7e-SMAMP concentrations, the fusion was quite extensive and exhibited an initially stronger effect than the control (Triton); however, the leaflet fusion gradually turned similar for different concentrations. In the mimicked *P. aeruginosa* B3M-liposomes (Fig 8b), Triton exhibited the strongest fusion activity overall. Additionally, both the non-formulated and formulated 7e-SMAMP demonstrated dose-dependent lipid flip-flop activity. Yet, the formulated 7e-SMAMP seemingly had a stronger effect on the inner-outer leaflet fusion than the non-formulated 7e-SMAMP indicating higher stress responses on the membranes. This was in line with the results from the evaluation of FITC leakage from B3M-liposomes. Strong effects on inner-leaflet-labelled liposomes have previously been showed in other studies [70]. Additionally, dose-dependent responses have also earlier been confirmed for AMPs [38, 71].

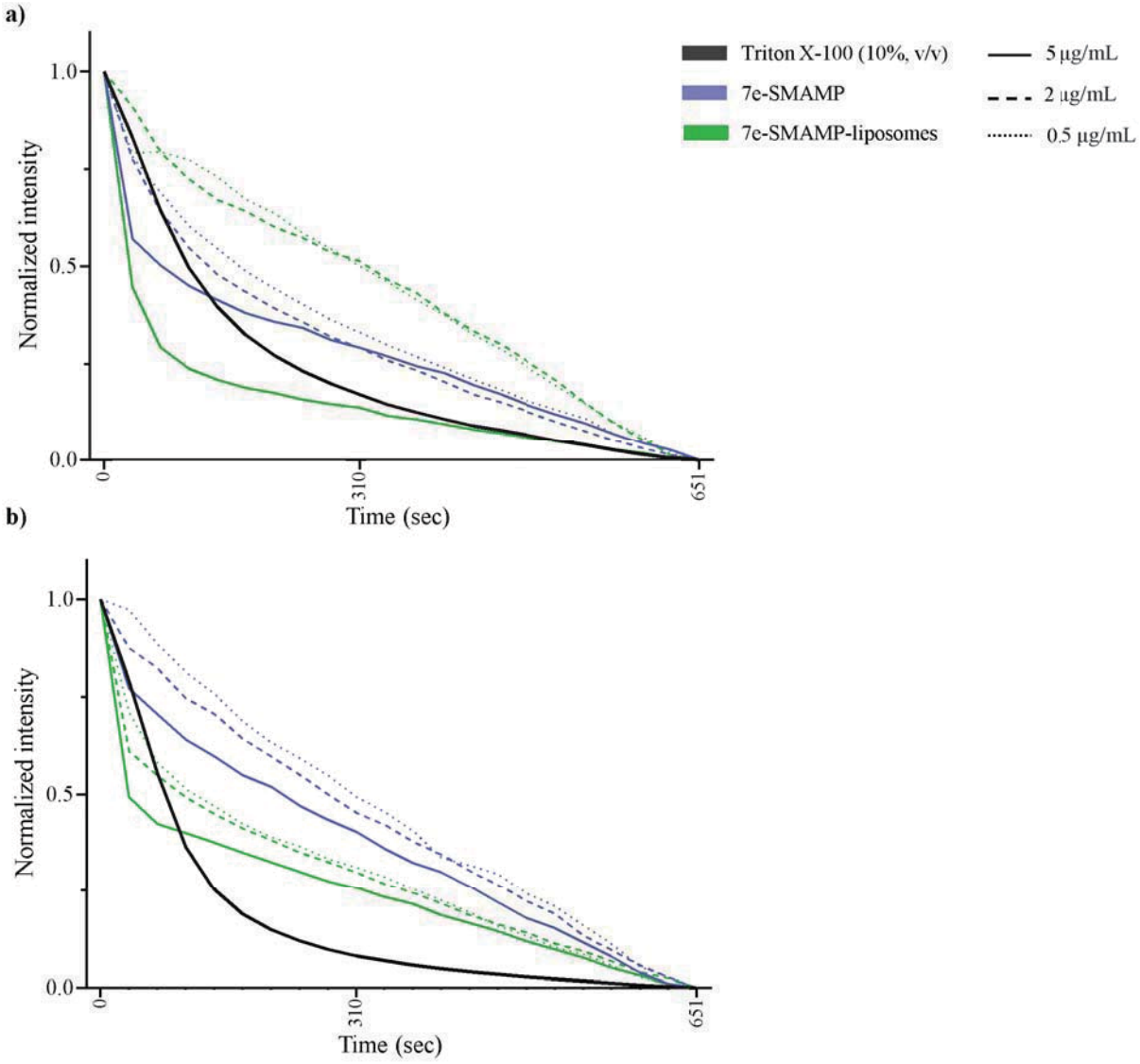

Figure 8. Lipid flip-flop in Bacterial Membrane-Mimic Liposomes Models (B3M-liposomes) of bacterial membranes with C6-NBD-PG inner leaflet labelling. The B3M-liposomes were treated with non-formulated and formulated 7e-SMAMP and monitored for 650 sec. Two different B3M-liposome mimics were prepared and challenged, namely A) *S. aureus* and B*) P. aeruginosa* B3M-liposome mimics. Concentrations of 7e-SMAMP were 0.5, 2, and 5 µg/mL were chosen for both non-formulated and formulated 7e-SMAMP. Results are presented as means of the normalized fluorescence intensity (0-1, n=3).

4.7. Antimicrobial activity

4.7.1. Inhibitory activity towards planktonic cultures

Antimicrobial wound management is a major challenge that highlights the need for new solutions against free-floating pathogens and their biofilms. After a first contamination, the wound microenvironment can be rapidly colonized by gram-positive bacteria, specifically *S. aureus*, followed by gram-negative bacteria, including *P. aeruginosa* and *E. coli*. During acute wound infections, local therapy is highly beneficial to immediately inhibit microbial proliferation, and therefore, prevent the spread and chronification of wounds. Unfortunately, the tendency of microorganisms such as *S. aureus* to easily acquire MDR makes most of the conventional available therapies ineffective [72, 73]. In this regard, AMPs and SMAMPs are intriguing alternatives to counteract bacterial spreading. Paulsen *et al.* have already reported that free 7e-SMAMP possesses promising antibacterial activity both *in vitro* and in a murine model [15]. Considering that delivery system is expected to enhance the activity on incorporated antimicrobial [21], we developed novel 7e-SMAMP liposomes and, tested their antimicrobial activity against planktonic cultures of susceptible bacteria (*S. aureus* ATCC29213, *E. coli* ATCC11105, and *P. aeruginosa* ATCC10145), gentamicin-resistant *S. aureus* (SO88) and MDR *S. aureus* (SO2, SO83, and SO86). The MIC and MLC values are reported in Table 3. Empty liposomes and DMSO did not affect the bacterial growth, as expected (data not shown). We were concern whether liposomal incorporation can hamper the activity of 7e-SMAMP. The 7e-SMAMP-liposomes exhibited the same MIC and MLC values as non-formulated 7e-SMAMP, indicating that neither the delivery system nor the preparation procedure interfered with the biological activity of the payload.

Table 3. Antimicrobial activity (MIC and MLC) of non-formulated and formulated 7e-SMAMP.

	MIC (µg/mL)		MLC (µg/mL)	
	7e-SMAMP	7e-SMAMP-liposomes	7e-SMAMP	7e-SMAMP-liposomes
S. aureus ATCC29213	0.78	0.78	3.13	3.13
S. aureus SO2	12.50	12.50	25.00	25.00
S. aureus SO83	6.25	6.25	12.50	12.50
S. aureus SO86	3.13	3.13	6.25	6.25
S. aureus SO88	1.56	1.56	6.25	6.25
E. coli ATCC11105	3.13	3.13	6.25	6.25
P. aeruginosa ATCC10145	25.00	25.00	50.00	50.00

MIC: minimal inhibitory concentration; MLC: minimal lethal concentration (n=3).

Among tested bacteria, inhibiting *P. aeruginosa* ATCC10145 was the most challenging (MIC: 25.00 µg/mL), whilst *S. aureus* ATCC29213 and *S. aureus* SO88 were very sensitive to the action of 7e-SMAMP-liposomes (MIC: 0.78-1.56 µg/mL). Notably, 7e-SMAMP-liposomes were also effective against MDR *S. aureus*, although MIC values (MIC: 3.13-12.50 µg/mL) were higher than those obtained for the susceptible strain. Overall, the MLC values were only slightly higher than MIC values suggesting that 7e-SMAMP acted as bactericidal compound. This was in full agreement with Paulsen *et al.* who previously demonstrated that 7e-SMAMP possesses membranolytic dose-dependent activity against both gram-positive and gram-negative bacteria [15].

To mimic the microenvironment at the wound site, the viability of *S. aureus, E. coli*, and *P. aeruginosa* was assessed in SWF [74] and compared with that of the same bacteria in the presence of non-formulated and formulated 7e-SMAMP (Fig 9). The 7e-SMAMP concentration was adjusted to 50 µg/mL because it was proven to be bactericidal for all tested microorganisms (Table 3). In the control, cell viability was retained over time, as well as in the presence of empty liposomes. Considering susceptible bacteria, 7e-SMAMP showed high

potency against *S. aureus* ATCC29213 and a slightly lower activity against *E. coli* ATCC11105 and *P. aeruginosa* ATCC10145. Indeed, after 3 hours of incubation, *S. aureus* ATCC29213, *E. coli* ATCC11105, and *P. aeruginosa* ATCC10145 viability was reduced by 3.84, 2.90, and 2.38 logCFU/mL, respectively. This suggested that gram-positive bacteria were more efficiently killed than gram-negative bacteria, possibly because the outer membrane of the latter hindered 7e-SMAMP bacteriolytic effect. Importantly, drug resistant *S. aureus* strains were only slightly more difficult to inhibit compared to sensitive *S. aureus* ATCC29213. Indeed, the viability of *S. aureus* SO2, SO83, SO86, and SO88 decreased by 2.28-2.96 logCFU/mL after 3 hours of incubation and was completely abolished after 12 hours as for sensitive pathogens. An almost complete killing effect was also detected for 7e-SMAMP-liposomes within 12 hours, but with a delayed action, in agreement with the release profile of 7e-SMAMP (section 4.3.). However, already after 8 hours of treatment the bacterial load was reduced by at least 3 logCFU/mL, except for *S. aureus* SO2, indicating that concentration of 7e-SMAMP released in this time-window was enough to elicit a first strong anti-microbial activity. After 12 hours, the inhibition of bacterial growth was even more pronounced, with complete killing of all bacterial strains, except from *S. aureus* SO2 and *P. aeruginosa* ATCC10145. However, the viability of these strains was reduced by at least 4.99 logCFU/mL, thus confirming that the liposome formulation was able to assure a prolonged 7e-SMAMP action.

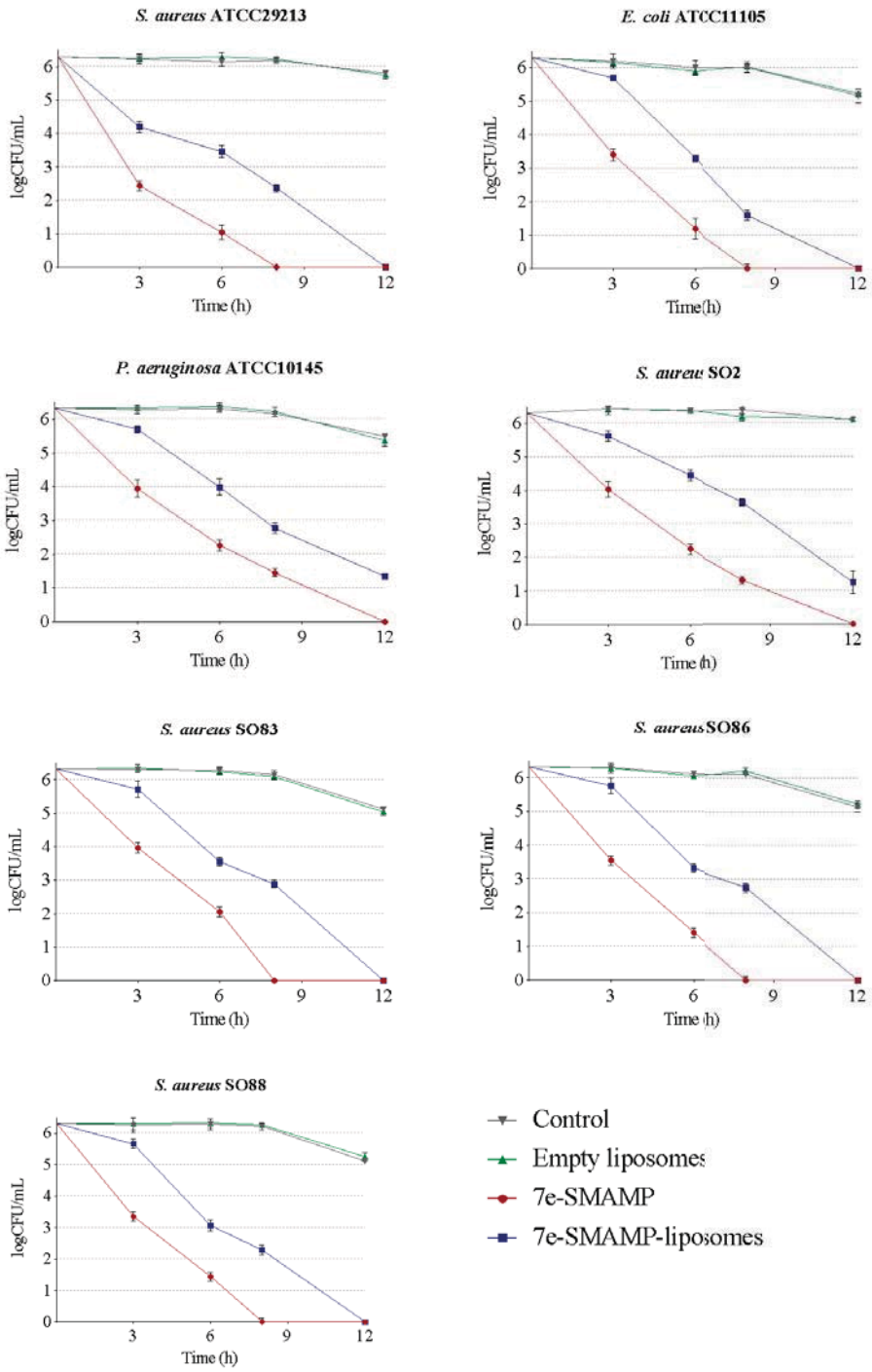

Figure 9. Viability (logCFU/mL) of bacteria over the time in simulated wound fluid (up to 12 hours) in the presence of non-formulated and formulated 7e-SMAMP. The results are presented as the mean of three replicates with their respective SD.

4.7.2. Activity towards biofilms

The formation of biofilms at the infection site can delay/hamper the healing process, which in turn leads to chronic infections [73]. It has been proposed that AMPs and SMAMPs are promising as anti-biofilm compounds as compared to conventional antibiotics since their bactericidal and/or bacteriostatic activities primarily depend on their ability to interact with bacterial membranes or cell walls, regardless of the bacterial metabolic state [53, 75]. Results reported in section 4.6. proved that 7e-SMAMPs, as well as 7e-SMAMPs-liposomes, can interact with *S. aureus* and *P. aeruginosa* membranes. Thus, we also investigated the potential of non-formulated and formulated 7e-SMAMP to inhibit biofilm formation (Fig. 10) and eradicate pre-formed biofilms (Fig. 11). Generally, bacterial biofilms exhibit higher resistance to antimicrobials compared to planktonic bacteria, due to difficulty of penetrating capsular polysaccharides [76]. Non-formulated 7e-SMAMP completely inhibited *S. aureus* ATCC29213 biofilm formation at 6.25 µg/mL (Fig. 10), and eradicated pre-formed biofilms at 12.5 µg/mL (Fig. 10), confirming the promising effect of 7e-SMAMP against this strain. Consistent with what has been previously observed for planktonic cultures (Fig. 9), the biofilm of *S. aureus* ATCC29213 was the most sensitive to 7e-SMAMP.

The non-formulated 7e-SMAMP exerted anti-biofilm activity even towards MDR *S. aureus* strains (SO2, SO83, and SO86). However, concentrations above MIC values were required and their eradication was more challenging than the sensitive *S. aureus* ATCC29213. The same trends were observed for gentamicin-resistant *S. aureus* SO88, *E. coli*, and *P. aeruginosa*. Even though, inhibition of biofilm formation in *P. aeruginosa* reached only 86% at 7e-SMAMP concentration of 50 µg/mL.

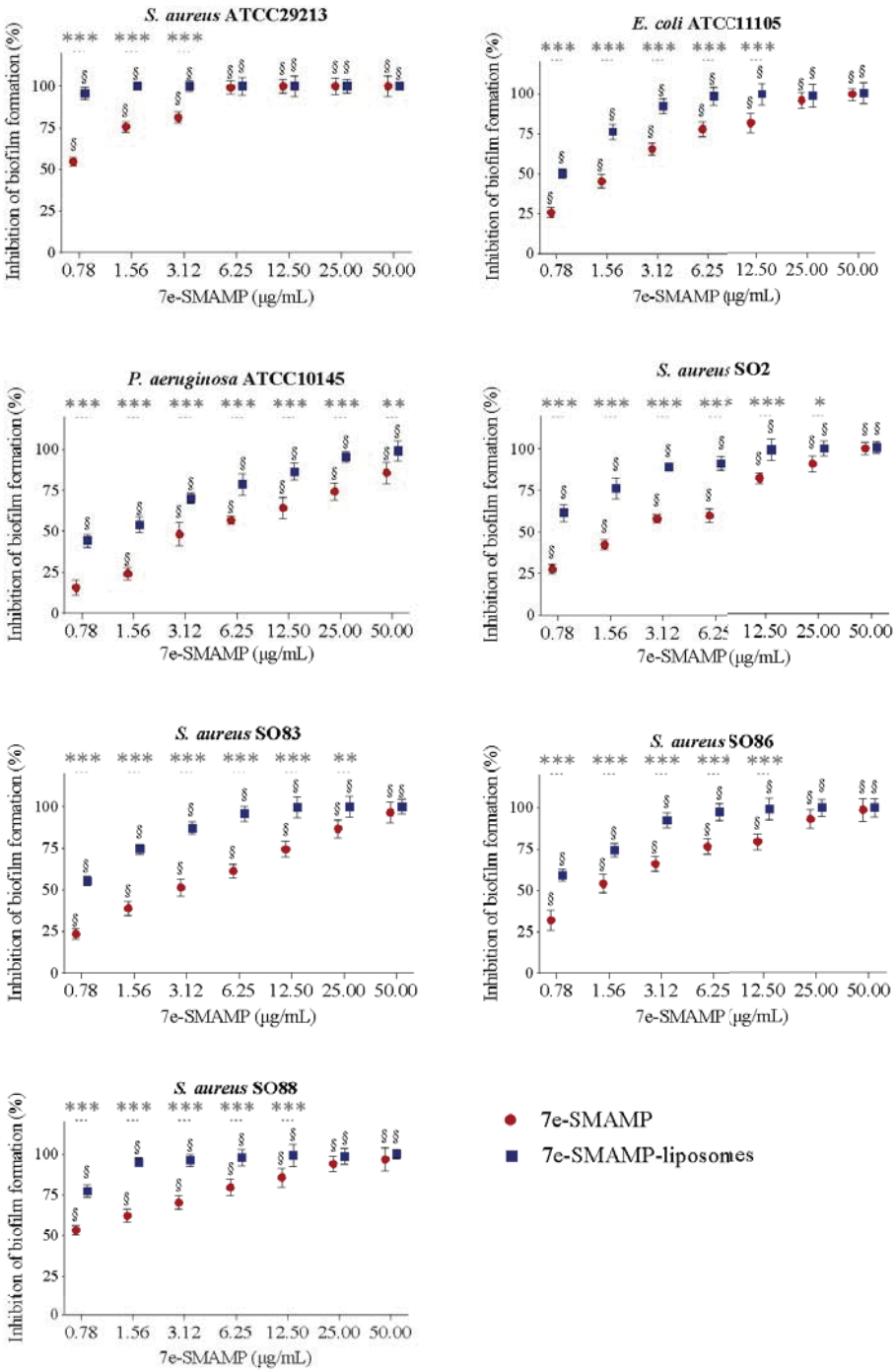

Figure 10. Anti-biofilm activity: inhibition of the biofilm development (%). The results are presented as the mean of three replicates with their respective SD. §: $p < 0.05$ compared to control. Significant differences between non-formulated and formulated 7e-SMAMP were also reported: *** $p < 0.001$, ** $p < 0.005$.

As demonstrated in Figs. 10 and 11, association of 7e-SMAMP within bilayers of phosphatidylcholine liposomes significantly improved its anti-biofilm activity, particularly against *S. aureus* SO88 and ATCC29213 biofilms, thus preventing the biofilm formation even at the SMAMP concentrations close to MIC values (Fig. 10). Similar patterns were also confirmed for eradication ability of 7e-SMAMP-liposomes towards pre-formed bacterial biofilms (Fig. 11), although the effective 7e-SMAMP concentrations were significantly higher than for biofilm inhibition (Fig. 10). In MDR strains, the 7e-SMAMP-liposomes (formulated) were able to inhibit biofilm formation and eradicate pre-formed biofilms at concentrations close to MIC values, however, slightly higher concentrations were required for *S. aureus* SO86. We confirmed the superiority of formulated 7e-SMAMP's as compared to non-formulated 7e-SMAMP. The inhibition and eradication of gram-negative bacterial biofilms were more challenging than for the gram-positive bacteria, especially for *P. aeruginosa* ATCC10145. In *E. coli* ATCC11105, biofilm inhibition and eradication required concentrations above MIC values (6.25 μg/mL, Figs. 10 and 11). The most challenging bacteria, *P. aeruginosa* ATCC10145, required even higher concentrations for the same activity, in line with the higher MIC values (Table 3).

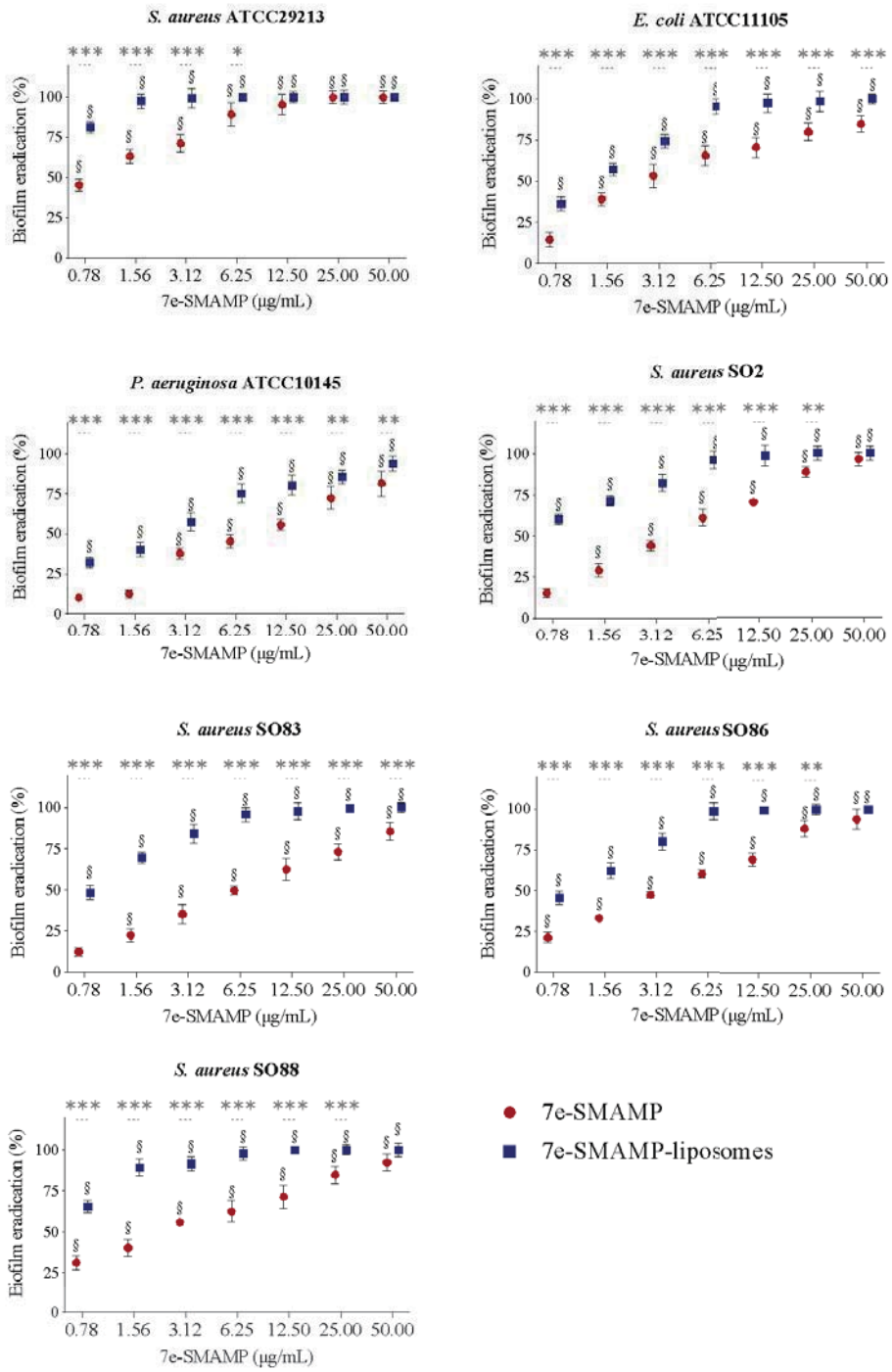

Figure 11. Anti-biofilm activity: eradication of pre-formed biofilm (%). The results are presented as the mean of three replicates with their respective SD. §: $p < 0.05$ compared to control. Significant differences between non-formulated and formulated 7e-SMAMP were also reported: *** $p < 0.001$, ** $p < 0.005$, * $p < 0.01$.

Many relevant medical pathogens, including *S. aureus*, *E. coli*, and *P. aeruginosa*, comprise negatively charged biofilm extracellular matrix due to the presence of anionic exopolysaccharide and extracellular DNA [77, 78]. In this regard, the incorporation of 7e-SMAMP inside liposomes resulted in positive surface charge (Table 1), which can aid the penetration into the extracellular matrix of the biofilm, thus increasing the anti-biofilm capability of the payload [49]. Conventional liposomes have been shown to successfully improve cellular uptake [79]. Moreover, liposomes prepared with the phosphatidylcholine revealed optimal ability to enhance the anti-biofilm activity of chlorhexidine [21]. Here, we confirmed that phosphatidylcholine liposomes were effectively suitable as nanocarrier to target pathogens' biofilms. Indeed, 7e-SMAMP exerted a significantly more efficient anti-biofilm activity when delivered in liposomes than when applied in its non-formulated form. In particular, the capability to eradicate pre-formed biofilms was greatly improved as demonstrated by the complete eradication of biofilms for 7e-SMAMP-liposomes concentrations above 6.25 μg/mL, with the only exception for *P. aeruginosa* ATCC10145. However, even this biofilm was reduced by 75% when treated with 6.25 μg/mL 7e-SMAMP-liposomes, compared to 45% eradication in the presence of non-formulated 7e-SMAMP at the same concentration. Moreover, 7e-SMAMP-liposomes strongly hampered pathogens' biofilm formation, with inhibition efficacy close to 100%, for concentrations at least equal to MIC, especially for gram-positive strains. At the lower tested concentrations, 7e-SMAMP-liposomes were always more efficient in inhibiting the development of biofilms than non-formulated 7e-SMAMP ($p < 0.05$). Taken together these results suggest that 7e-SMAMP-liposomes can be employed both for the prevention of the onset of severe infections and treatment of chronic wound infections.

5. Conclusion

Antimicrobial peptides and their mimics are regarded valuable alternatives in the battle against resistant bacteria and biofilm-embedded bacteria; however, some of their limitations require careful consideration to reach therapeutic use. Addressing these issues, a novel antimicrobial, 7e-SMAMP, was incorporated in liposomes destined for the treatment of biofilm-infected chronic wounds. The 7e-SMAMP-liposomes were evaluated for their *in vitro* biological and antimicrobial activities. The newly developed formulation displayed superior *in vitro* anti-inflammatory responses and had no negative effect on the cellular viability as

confirmed in macrophages and keratinocytes. Additionally, the anti-biofilm activities of 7e-SMAMP liposomes against *S. aureus*, *E. coli*, and *P. aeruginosa* were improved as compared to the non-formulated 7e-SMAMP. These superior anti-biofilm effects were proven in both biofilm formation and eradication of pre-formed biofilms. The results supported our hypothesis that 7e-SMAMP-liposomes could serve as a novel platform in the development of antimicrobial therapeutic options for the treatment of biofilm-infected chronic wounds.

Credit authorship contribution statement

Lisa Myrseth Hemmingsen: Conceptualization, Data curation, Formal analysis, Investigation, Methodology, Visualization, Validation, Writing - original draft, Writing - review & editing. **Barbara Giordani**: Data curation, Formal analysis, Investigation, Methodology, Validation, Writing - original draft, Writing - review & editing. **Marianne H. Paulsen**: Writing - review & editing. **Željka Vanić**: Data curation, Formal analysis, Investigation, Methodology, Writing - review & editing. **Gøril Eide Flaten**: Conceptualization, Writing - review & editing. **Beatrice Vitali**: Methodology, Validation, Resources, Writing - review & editing. **Purusotam Basnet**: Methodology, Validation, Writing - review & editing. **Annette Bayer**: Conceptualization, Writing - review & editing. **Morten B. Strøm**: Conceptualization, Funding acquisition, Project administration, Writing - review & editing. **Nataša Škalko-Basnet**: Conceptualization, Funding acquisition, Methodology, Resources, Supervision, Writing - original draft, Writing - review & editing.

Data availability

The data supporting conclusions of this manuscript will be made available by requests.

Declaration of interest

The authors declare no competing financial interest.

Acknowledgements

The authors would also like to thank Manuel K. Langer at Department of Chemistry, UiT The Arctic University of Norway for assistance in SMAMP synthesis and Randi Olsen at The Advanced Microscopy Core Facility, Department of Medical Biology, UiT The Arctic University of Norway for the assistance in TEM-imaging The graphical abstract and figures were created with BioRender.com.

Funding Sources

The study was funded by UiT The Arctic University of Norway, Norway (project no. 235569). The publication fund of UiT The Arctic University of Norway covered the publication charges of this article.

References

[1] C.J.L. Murray, K.S. Ikuta, F. Sharara, L. Swetschinski, G. Robles Aguilar, A. Gray, C. Han, C. Bisignano, P. Rao, E. Wool, et al., Global burden of bacterial antimicrobial resistance in 2019: a systematic analysis, Lancet, 399 (2022) 629-655; https://doi.org/10.1016/S0140-6736(21)02724-0.
[2] P. Beyer, S. Paulin, The Antibacterial Research and Development Pipeline Needs Urgent Solutions, ACS Infect. Dis., 6 (2020) 1289-1291; https://doi.org/10.1021/acsinfecdis.0c00044.
[3] B. Blanco-Fernandez, O. Castaño, M.Á. Mateos-Timoneda, E. Engel, S. Pérez-Amodio, Nanotechnology Approaches in Chronic Wound Healing, Adv. Wound Care, 10 (2020) 234-256; https://doi.org/10.1089/wound.2019.1094.
[4] M. Malone, T. Bjarnsholt, A.J. McBain, G.A. James, P. Stoodley, D. Leaper, M. Tachi, G. Schultz, T. Swanson, R.D. Wolcott, The prevalence of biofilms in chronic wounds: a systematic review and meta-analysis of published data, J. Wound Care, 26 (2017) 20-25; https://doi.org/10.12968/jowc.2017.26.1.20.
[5] S. Darvishi, S. Tavakoli, M. Kharaziha, H.H. Girault, C.F. Kaminski, I. Mela, Advances in the Sensing and Treatment of Wound Biofilms, Angew. Chem. Int. Ed., 61 (2022) e202112218; https://doi.org/10.1002/anie.202112218.
[6] X. Song, P. Liu, X. Liu, Y. Wang, H. Wei, J. Zhang, L. Yu, X. Yan, Z. He, Dealing with MDR bacteria and biofilm in the post-antibiotic era: Application of antimicrobial peptides-based nano-formulation, Mater. Sci. Eng. C, 128 (2021) 112318; https://doi.org/10.1016/j.msec.2021.112318.
[7] L. Boge, K. Hallstensson, L. Ringstad, J. Johansson, T. Andersson, M. Davoudi, P.T. Larsson, M. Mahlapuu, J. Håkansson, M. Andersson, Cubosomes for topical delivery of the antimicrobial peptide LL-37, Eur. J. Pharm. Biopharm., 134 (2019) 60-67; https://doi.org/10.1016/j.ejpb.2018.11.009.

[8] S. Singh, A. Numan, H.H. Somaily, B. Gorain, S. Ranjan, K. Rilla, H.R. Siddique, P. Kesharwani, Nano-enabled strategies to combat methicillin-resistant Staphylococcus aureus, Mater. Sci. Eng. C, 129 (2021) 112384; https://doi.org/10.1016/j.msec.2021.112384.
[9] C.D. Fjell, J.A. Hiss, R.E.W. Hancock, G. Schneider, Designing antimicrobial peptides: form follows function, Nat. Rev. Drug Discov., 11 (2012) 37-51; https://doi.org/10.1038/nrd3591.
[10] A.T.Y. Yeung, S.L. Gellatly, R.E.W. Hancock, Multifunctional cationic host defence peptides and their clinical applications, Cell. Mol. Life Sci., 68 (2011) 2161-2176; https://doi.org/10.1007/s00018-011-0710-x.
[11] C. Ghosh, P. Sarkar, R. Issa, J. Haldar, Alternatives to Conventional Antibiotics in the Era of Antimicrobial Resistance, Trends Microbiol., 27 (2019) 323-338; https://doi.org/10.1016/j.tim.2018.12.010.
[12] D. Ciumac, H. Gong, X. Hu, J.R. Lu, Membrane targeting cationic antimicrobial peptides, J. Colloid Interface Sci., 537 (2019) 163-185; https://doi.org/10.1016/j.jcis.2018.10.103.
[13] U. Piotrowska, M. Sobczak, E. Oledzka, Current state of a dual behaviour of antimicrobial peptides-Therapeutic agents and promising delivery vectors, Chem. Biol. Drug Des., 90 (2017) 1079-1093; https://doi.org/10.1111/cbdd.13031.
[14] Y. Jiang, Y. Chen, Z. Song, Z. Tan, J. Cheng, Recent advances in design of antimicrobial peptides and polypeptides toward clinical translation, Adv. Drug Deliv. Rev., 170 (2021) 261-280; https://doi.org/10.1016/j.addr.2020.12.016.
[15] M.H. Paulsen, M. Engqvist, D. Ausbacher, T. Anderssen, M.K. Langer, T. Haug, G.R. Morello, L.E. Liikanen, H.M. Blencke, J. Isaksson, E. Juskewitz, A. Bayer, M.B. Strøm, Amphipathic Barbiturates as Mimics of Antimicrobial Peptides and the Marine Natural Products Eusynstyelamides with Activity against Multi-resistant Clinical Isolates, J. Med. Chem., 64 (2021) 11395-11417; https://doi.org/10.1021/acs.jmedchem.1c00734.
[16] S.C. Park, C. Ko, H. Hyeon, M.K. Jang, D. Lee, Imaging and Targeted Antibacterial Therapy Using Chimeric Antimicrobial Peptide Micelles, ACS Appl. Mater. Interfaces, 12 (2020) 54306-54315; https://doi.org/10.1021/acsami.0c13083.
[17] K. Forier, K. Raemdonck, S.C. De Smedt, J. Demeester, T. Coenye, K. Braeckmans, Lipid and polymer nanoparticles for drug delivery to bacterial biofilms, J. Control. Release, 190 (2014) 607-623; https://doi.org/10.1016/j.jconrel.2014.03.055.
[18] J. Ndayishimiye, T. Kumeria, A. Popat, J.R. Falconer, M.A.T. Blaskovich, Nanomaterials: The New Antimicrobial Magic Bullet, ACS Infect. Dis., 8 (2022) 693-712; https://doi.org/10.1021/acsinfecdis.1c00660.
[19] A.A. Aytekin, S. Tuncay Tanrıverdi, F. Aydın Köse, D. Kart, İ. Eroğlu, Ö. Özer, Propolis loaded liposomes: evaluation of antimicrobial and antioxidant activities, J. Liposome Res., 30 (2020) 107-116; https://doi.org/10.1080/08982104.2019.1599012.
[20] E. Bhatia, S. Sharma, K. Jadhav, R. Banerjee, Combinatorial liposomes of berberine and curcumin inhibit biofilm formation and intracellular methicillin resistant Staphylococcus aureus infections and associated inflammation, J. Mater. Chem. B, 9 (2021) 864-875; https://doi.org/10.1039/D0TB02036B.
[21] L.M. Hemmingsen, B. Giordani, A.K. Pettersen, B. Vitali, P. Basnet, N. Škalko-Basnet, Liposomes-in-chitosan hydrogel boosts potential of chlorhexidine in biofilm eradication in vitro, Carbohydr. Polym., 262 (2021) 117939; https://doi.org/10.1016/j.carbpol.2021.117939.
[22] N. Škalko-Basnet, Ž. Vanić, Chapter 5 - Lipid-Based Nanopharmaceuticals in Antimicrobial Therapy, in: R. Boukherroub, S. Szunerits, D. Drider (Eds.) Functionalized Nanomaterials for the Management of Microbial Infection, Elsevier, Boston, US, 2017, pp. 111-152.

[23] M. Cui, C. Wiraja, S.W.T. Chew, C. Xu, Nanodelivery Systems for Topical Management of Skin Disorders, Mol. Pharm., 18 (2021) 491–505; https://doi.org/10.1021/acs.molpharmaceut.0c00154.
[24] M. Sguizzato, E. Esposito, R. Cortesi, Lipid-Based Nanosystems as a Tool to Overcome Skin Barrier, Int. J. Mol. Sci., 22 (2021) 8319; https://doi.org/10.3390/ijms22158319.
[25] B. Giordani, P.E. Costantini, S. Fedi, M. Cappelletti, A. Abruzzo, C. Parolin, C. Foschi, G. Frisco, N. Calonghi, T. Cerchiara, F. Bigucci, B. Luppi, B. Vitali, Liposomes containing biosurfactants isolated from Lactobacillus gasseri exert antibiofilm activity against methicillin resistant Staphylococcus aureus strains, Eur. J. Pharm. Biopharm., 139 (2019) 246-252; https://doi.org/10.1016/j.ejpb.2019.04.011.
[26] C. Bradford, R. Freeman, S.L. Percival, In Vitro Study of Sustained Antimicrobial Activity of a New Silver Alginate Dressing, J. Am. Col. Certif. Wound Spec., 1 (2009) 117-120; https://doi.org/10.1016/j.jcws.2009.09.001.
[27] R.K. Thapa, H.C. Winther-Larsen, D.B. Diep, H.H. Tønnesen, Preformulation studies on novel garvicin KS peptides for topical applications, Eur. J. Pharm. Sci., 151 (2020) 105333; https://doi.org/10.1016/j.ejps.2020.105333.
[28] M.H. Paulsen, M. Engqvist, D. Ausbacher, M.B. Strøm, A. Bayer, Efficient and scalable synthesis of alpha,alpha-disubstituted beta-amino amides, Org. Biomol. Chem., 14 (2016) 7570-7578; https://doi.org/10.1039/c6ob01219a.
[29] L.M. Hemmingsen, K. Julin, L. Ahsan, P. Basnet, M. Johannessen, N. Škalko-Basnet, Chitosomes-In-Chitosan Hydrogel for Acute Skin Injuries: Prevention and Infection Control, Mar. Drugs, 19 (2021) 269; https://doi.org/10.3390/md19050269.
[30] Z. Palac, A. Engesland, G.E. Flaten, N. Škalko-Basnet, J. Filipović-Grčić, Ž. Vanić, Liposomes for (trans)dermal drug delivery: the skin-PVPA as a novel in vitro stratum corneum model in formulation development, J. Liposome Res., 24 (2014) 313-322; https://doi.org/10.3109/08982104.2014.899368.
[31] X. Liu, Z. Li, X. Wang, Y. Chen, F. Wu, K. Men, T. Xu, Y. Luo, L. Yang, Novel antimicrobial peptide-modified azithromycin-loaded liposomes against methicillin-resistant Staphylococcus aureus, Int. J. Nanomed., 11 (2016) 6781-6794; https://doi.org/10.2147/ijn.S107107.
[32] J. Cauzzo, M. Nystad, A.M. Holsæter, P. Basnet, N. Škalko-Basnet, Following the Fate of Dye-Containing Liposomes In Vitro, Int. J. Mol. Sci., 21 (2020) 4847; https://doi.org/10.3390/ijms21144847.
[33] R.F. Epand, B.P. Mowery, S.E. Lee, S.S. Stahl, R.I. Lehrer, S.H. Gellman, R.M. Epand, Dual Mechanism of Bacterial Lethality for a Cationic Sequence-Random Copolymer that Mimics Host-Defense Antimicrobial Peptides, J. Mol. Biol., 379 (2008) 38-50; https://doi.org/10.1016/j.jmb.2008.03.047.
[34] Y. Sun, W. Dong, L. Sun, L. Ma, D. Shang, Insights into the membrane interaction mechanism and antibacterial properties of chensinin-1b, Biomaterials, 37 (2015) 299-311; https://doi.org/10.1016/j.biomaterials.2014.10.041.
[35] L. Lombardi, M.I. Stellato, R. Oliva, A. Falanga, M. Galdiero, L. Petraccone, G. D'Errico, A. De Santis, S. Galdiero, P. Del Vecchio, Antimicrobial peptides at work: interaction of myxinidin and its mutant WMR with lipid bilayers mimicking the P. aeruginosa and E. coli membranes, Sci. Rep., 7 (2017) 44425; https://doi.org/10.1038/srep44425.
[36] Y.Q. Xiong, K. Mukhopadhyay, M.R. Yeaman, J. Adler-Moore, A.S. Bayer, Functional Interrelationships between Cell Membrane and Cell Wall in Antimicrobial Peptide-Mediated Killing of Staphylococcus aureus, Antimicrob. Agents Chemother., 49 (2005) 3114-3121; https://doi.org/10.1128/AAC.49.8.3114-3121.2005.

[37] S. Kobayashi, K. Takeshima, C.B. Park, S.C. Kim, K. Matsuzaki, Interactions of the Novel Antimicrobial Peptide Buforin 2 with Lipid Bilayers: Proline as a Translocation Promoting Factor, Biochemistry, 39 (2000) 8648-8654; https://doi.org/10.1021/bi0004549.
[38] B. Orioni, G. Bocchinfuso, J.Y. Kim, A. Palleschi, G. Grande, S. Bobone, Y. Park, J.I. Kim, K.S. Hahm, L. Stella, Membrane perturbation by the antimicrobial peptide PMAP-23: A fluorescence and molecular dynamics study, Biochim. Biophys. Acta Biomembr., 1788 (2009) 1523-1533; https://doi.org/10.1016/j.bbamem.2009.04.013.
[39] N. Yamamoto, A. Tamura, Designed low amphipathic peptides with α-helical propensity exhibiting antimicrobial activity via a lipid domain formation mechanism, Peptides, 31 (2010) 794-805; https://doi.org/10.1016/j.peptides.2010.01.006.
[40] EUCAST—the European Committee on Antimicrobial Susceptibility Testing, EUCAST reading guide for broth microdilution, 2020.
[41] A. Zajmi, N.M. Hashim, M.I. Noordin, S.A.M. Khalifa, F. Ramli, H. Mohd Ali, H.R. El-Seedi, Ultrastructural Study on the Antibacterial Activity of Artonin E versus Streptomycin against Staphylococcus aureus Strains, PLoS One, 10 (2015) e0128157; https://doi.org/10.1371/journal.pone.0128157.
[42] S. Ron-Doitch, B. Sawodny, A. Kuhbacher, M.M.N. David, A. Samanta, J. Phopase, A. Burger-Kentischer, M. Griffith, G. Golomb, S. Rupp, Reduced cytotoxicity and enhanced bioactivity of cationic antimicrobial peptides liposomes in cell cultures and 3D epidermis model against HSV, J. Control. Release, 229 (2016) 163-171; https://doi.org/10.1016/j.jconrel.2016.03.025.
[43] A.M. Robinson, M. Bannister, J.E. Creeth, M.N. Jones, The interaction of phospholipid liposomes with mixed bacterial biofilms and their use in the delivery of bactericide, Colloids Surf. A Physicochem. Eng. Asp., 186 (2001) 43-53; https://doi.org/10.1016/S0927-7757(01)00481-2.
[44] M. Elmowafy, Skin penetration/permeation success determinants of nanocarriers: Pursuit of a perfect formulation, Colloids Surf. B, 203 (2021) 111748; https://doi.org/10.1016/j.colsurfb.2021.111748.
[45] Z. Rukavina, M. Šegvić Klarić, J. Filipović-Grčić, J. Lovrić, Ž. Vanić, Azithromycin-loaded liposomes for enhanced topical treatment of methicillin-resistant Staphyloccocus aureus (MRSA) infections, Int. J. Pharm., 553 (2018) 109-119; https://doi.org/10.1016/j.ijpharm.2018.10.024.
[46] M.J. Choi, H.I. Maibach, Liposomes and niosomes as topical drug delivery systems, Skin Pharmacol. Physiol., 18 (2005) 209-219; https://doi.org/10.1159/000086666.
[47] J. Hurler, O.A. Berg, M. Skar, A.H. Conradi, P.J. Johnsen, N. Škalko-Basnet, Improved burns therapy: liposomes-in-hydrogel delivery system for mupirocin, J. Pharm. Sci., 101 (2012) 3906-3915; https://doi.org/10.1002/jps.23260.
[48] M. Danaei, M. Dehghankhold, S. Ataei, F. Hasanzadeh Davarani, R. Javanmard, A. Dokhani, S. Khorasani, M.R. Mozafari, Impact of Particle Size and Polydispersity Index on the Clinical Applications of Lipidic Nanocarrier Systems, Pharmaceutics, 10 (2018) 57; https://doi.org/10.3390/pharmaceutics10020057.
[49] Z. Rukavina, Ž. Vanić, Current Trends in Development of Liposomes for Targeting Bacterial Biofilms, Pharmaceutics, 8 (2016) 18; https://doi.org/10.3390/pharmaceutics8020018.
[50] H.J. Kim, E.L.M. Gias, M.N. Jones, The adsorption of cationic liposomes to Staphylococcus aureus biofilms, Colloids Surf. A Physicochem. Eng. Asp., 149 (1999) 561-570; https://doi.org/10.1016/S0927-7757(98)00765-1.
[51] S. Sandreschi, A.M. Piras, G. Batoni, F. Chiellini, Perspectives on polymeric nanostructures for the therapeutic application of antimicrobial peptides, Nanomedicine, 11 (2016) 1729-1744; https://doi.org/10.2217/nnm-2016-0057.

[52] L.A. Wallace, L. Gwynne, T. Jenkins, Challenges and opportunities of pH in chronic wounds, Ther. Deliv., 10 (2019) 719-735; https://doi.org/10.4155/tde-2019-0066.
[53] N. Mookherjee, M.A. Anderson, H.P. Haagsman, D.J. Davidson, Antimicrobial host defence peptides: functions and clinical potential, Nat. Rev. Drug Discov., 19 (2020) 311-332; https://doi.org/10.1038/s41573-019-0058-8.
[54] A. Alghalayini, A. Garcia, T. Berry, C.G. Cranfield, The Use of Tethered Bilayer Lipid Membranes to Identify the Mechanisms of Antimicrobial Peptide Interactions with Lipid Bilayers, Antibiotics, 8 (2019) 12; https://doi.org/10.3390/antibiotics8010012.
[55] L.M. Hemmingsen, N. Škalko-Basnet, M.W. Jøraholmen, The Expanded Role of Chitosan in Localized Antimicrobial Therapy, Mar. Drugs, 19 (2021) 697; https://doi.org/10.3390/md19120697.
[56] Y. Liu, Y. Li, L. Shi, Controlled drug delivery systems in eradicating bacterial biofilm-associated infections, J. Control. Release, 329 (2021) 1102-1116; https://doi.org/10.1016/j.jconrel.2020.10.038.
[57] P.S. Korrapati, K. Karthikeyan, A. Satish, V.R. Krishnaswamy, J.R. Venugopal, S. Ramakrishna, Recent advancements in nanotechnological strategies in selection, design and delivery of biomolecules for skin regeneration, Mater. Sci. Eng. C, 67 (2016) 747-765; https://doi.org/10.1016/j.msec.2016.05.074.
[58] K. Shanmugapriya, H.W. Kang, Engineering pharmaceutical nanocarriers for photodynamic therapy on wound healing: Review, Mater. Sci. Eng. C, 105 (2019) 110110; https://doi.org/10.1016/j.msec.2019.110110.
[59] P. Méndez-Samperio, Peptidomimetics as a new generation of antimicrobial agents: current progress, Infect. Drug Resist., 7 (2014) 229-237; https://doi.org/10.2147/IDR.S49229.
[60] S. Ternullo, P. Basnet, A.M. Holsæter, G.E. Flaten, L. de Weerd, N. Škalko-Basnet, Deformable liposomes for skin therapy with human epidermal growth factor: The effect of liposomal surface charge, Eur. J. Pharm. Sci., 125 (2018) 163-171; https://doi.org/10.1016/j.ejps.2018.10.005.
[61] H.N. Wilkinson, M.J. Hardman, Wound healing: cellular mechanisms and pathological outcomes, Open Biol., 10 (2020) 200223; https://doi.org/10.1098/rsob.200223.
[62] J. Larouche, S. Sheoran, K. Maruyama, M.M. Martino, Immune Regulation of Skin Wound Healing: Mechanisms and Novel Therapeutic Targets, Adv. Wound Care, 7 (2018) 209-231; https://doi.org/10.1089/wound.2017.0761.
[63] K. Las Heras, M. Igartua, E. Santos-Vizcaino, R.M. Hernandez, Chronic wounds: Current status, available strategies and emerging therapeutic solutions, J. Control. Release, 328 (2020) 532-550; https://doi.org/10.1016/j.jconrel.2020.09.039.
[64] S. Ellis, E.J. Lin, D. Tartar, Immunology of Wound Healing, Curr. Dermatol. Rep., 7 (2018) 350-358; https://doi.org/10.1007/s13671-018-0234-9.
[65] A. Soneja, M. Drews, T. Malinski, Role of nitric oxide, nitroxidative and oxidative stress in wound healing, Pharmacol. Rep., 57 Suppl (2005) 108-119
[66] M. Ahn, P. Gunasekaran, G. Rajasekaran, E.Y. Kim, S.J. Lee, G. Bang, K. Cho, J.K. Hyun, H.J. Lee, Y.H. Jeon, N.H. Kim, E.K. Ryu, S.Y. Shin, J.K. Bang, Pyrazole derived ultra-short antimicrobial peptidomimetics with potent anti-biofilm activity, Eur. J. Med. Chem., 125 (2017) 551-564; https://doi.org/10.1016/j.ejmech.2016.09.071.
[67] B. Giordani, P. Basnet, E. Mishchenko, B. Luppi, N. Škalko-Basnet, Utilizing Liposomal Quercetin and Gallic Acid in Localized Treatment of Vaginal Candida Infections, Pharmaceutics, 12 (2019) 9; https://doi.org/10.3390/pharmaceutics12010009.
[68] M.Y. Lee, S.C. Park, M. Jung, M.K. Shin, H.L. Kang, S.C. Baik, G.W. Cheong, M.K. Jang, W.K. Lee, Cell-selectivity of tryptophan and tyrosine in amphiphilic alpha-helical antimicrobial peptides against drug-resistant bacteria, Biochem. Biophys. Res. Commun., 505 (2018) 478-484; https://doi.org/10.1016/j.bbrc.2018.09.095.

[69] M.B. Strøm, B.E. Haug, M.L. Skar, W. Stensen, T. Stiberg, J.S. Svendsen, The Pharmacophore of Short Cationic Antibacterial Peptides, J. Med. Chem., 46 (2003) 1567-1570; https://doi.org/10.1021/jm0340039.
[70] C. Mazzuca, L. Stella, M. Venanzi, F. Formaggio, C. Toniolo, B. Pispisa, Mechanism of Membrane Activity of the Antibiotic Trichogin GA IV: A Two-State Transition Controlled by Peptide Concentration, Biophys. J., 88 (2005) 3411-3421; https://doi.org/10.1529/biophysj.104.056077.
[71] A. Patrzykat, L. Friedrich Carol, L. Zhang, V. Mendoza, R.E.W. Hancock, Sublethal Concentrations of Pleurocidin-Derived Antimicrobial Peptides Inhibit Macromolecular Synthesis in Escherichia coli, Antimicrob. Agents Chemother., 46 (2002) 605-614; https://doi.org/10.1128/AAC.46.3.605-614.2002.
[72] A.F. Cardona, S.E. Wilson, Skin and Soft-Tissue Infections: A Critical Review and the Role of Telavancin in Their Treatment, Clin. Infect. Dis., 61 (2015) S69-S78; https://doi.org/10.1093/cid/civ528.
[73] G. Daeschlein, Antimicrobial and antiseptic strategies in wound management, Int. Wound J., 10 (2013) 9-14; https://doi.org/10.1111/iwj.12175.
[74] K. Vowden, P. Vowden, Understanding exudate management and the role of exudate in the healing process, Br. J. Community Nurs., 8 (2003) S4-S13; https://doi.org/10.12968/bjcn.2003.8.Sup5.12607.
[75] P. Cardoso, H. Glossop, T.G. Meikle, A. Aburto-Medina, C.E. Conn, V. Sarojini, C. Valery, Molecular engineering of antimicrobial peptides: microbial targets, peptide motifs and translation opportunities, Biophys. Rev., 13 (2021) 35-69; https://doi.org/10.1007/s12551-021-00784-y.
[76] T.F.C. Mah, G.A. O'Toole, Mechanisms of biofilm resistance to antimicrobial agents, Trends Microbiol., 9 (2001) 34-39; https://doi.org/10.1016/S0966-842X(00)01913-2.
[77] L.R. Mulcahy, V.M. Isabella, K. Lewis, Pseudomonas aeruginosa Biofilms in Disease, Microb. Ecol., 68 (2014) 1-12; https://doi.org/10.1007/s00248-013-0297-x.
[78] M. Okshevsky, R.L. Meyer, The role of extracellular DNA in the establishment, maintenance and perpetuation of bacterial biofilms, Crit. Rev. Microbiol., 41 (2015) 341-352; https://doi.org/10.3109/1040841X.2013.841639.
[79] M.E. van Gent, M. Ali, P.H. Nibbering, S.N. Kłodzińska, Current Advances in Lipid and Polymeric Antimicrobial Peptide Delivery Systems and Coatings for the Prevention and Treatment of Bacterial Infections, Pharmaceutics, 13 (2021) 1840; https://doi.org/10.3390/pharmaceutics13111840.

Supplementary Material

Tailored anti-biofilm activity – liposomal delivery for mimic of small antimicrobial peptide

Lisa Myrseth Hemmingsen[a], Barbara Giordani[b], Marianne H. Paulsen[c,d], Željka Vanić[e], Gøril Eide Flaten[a], Beatrice Vitali[b], Purusotam Basnet[f], Annette Bayer[c], Morten B. Strøm[d], and Nataša Škalko-Basnet[a]*

S1. Supplementary methods

S1.1. 7e-SMAMP synthesis

Firstly, disubstituted malonate (diethyl 2,2-bis(3,5-dibromobenzyl)malonate) was synthesized by dialkylation of diethyl malonate with 1,3-dibromo-5(bromomethyl)benzene. Urea was then used for cyclization of diethyl 2,2-bis(3,5-dibromobenzyl)malonate yielding 5,5-bis(3,5-dibromobenzyl)pyrimidine-2,4,6-(1H,3H,5H)-trione. 1,4-dibromobutane was used for *N*-alkylation under basic conditions followed by bromine substitution with azide to produce 1,3-bis(4-azidobutyl)-5,5-bis(3,5-dibromobenzyl)pyrimidine-2,4,6-(1H,3H,5H)-trione. Finally, azide reduction to amine using 1,3-propanedithiol and sodium borohydride was performed prior to guanidinylation to the guanylated barbiturate 1,1′-((5,5-bis(3,5-dibromobenzyl)-2,4,6-trioxodihydropyrimidine1,3(2H,4H)-diyl)bis(butane-4,1-diyl))diguanidine (7e-SMAMP) [15].

S1.2. UV-VIS scan analysis

Stock solutions of 7e-SMAMP (100 μM) were prepared in 1% (v/v) glycerol in milli-Q water (mQ) and stirred mechanically overnight at room temperature (21 ± 1°C). These stock solutions were diluted to 10, 25, and 50 μM in mQ and scanned using absorbance scan (200-800 nm) on a UV–VIS plate reader (Tecan Trading AG, Männedorf, Switzerland) together with the stock solution (100 μM) [27]. All solutions were stored for 7 days at 4, 25, or 32 °C. UV-VIS analysis was performed at preparation and after 1- and 7-days storage.

S1.3. Liposome stability

The liposomes were evaluated for a period of 12 weeks (2, 4, and 12 weeks, 4 °C) for conformation of the stability. The evaluated parameters were the size, PI, zeta potential, pH, and entrapment efficiency as described in the section 2.5.

S2. Supplementary results and discussions

S2.1. 7e-SMAMP UV-VIS analysis

Typically, the AMPs have distinct UV absorption at 180-230 nm and 230–300 nm, and therefore analysed within these ranges. The first absorption range is mediated by $\pi \rightarrow \pi*$ transitions of the peptide bonds or peptide backbone and in our case, amide bonds in the SMAMP, while the second absorption range originates from aromatic side chains [S1, 27]. These aromatic side chains are important to ensure that the facially amphiphilic character is maintained and are therefore often preserved in the mimics [S2]. Consequently, the range 250–300 nm is most often used in analysis; however, we assessed the range 260-320 nm in this study due to the disubstitution with bromide on the side chains where these could be followed and are important features of the SMAMP structure (Fig. 2) [S3, S4].

Fig. S1 presents 7e-SMAMP absorbance scans following preparation and after storage at three different temperatures, namely 4 (Fig. S1a), 25 (Fig S1b), and 32 °C (Fig S1c), and at four different concentrations (10, 25, 50, and 100 μM). A peak around 280 nm is evident for all conditions. As seen in the Fig. 1a, there were no changes in the peak wavelength over time or at different concentrations. However, small deviations in the absorbance peaks were observed when 7e-SMAMP was stored at 25 or 32 °C compared to storage temperature of 4 °C. These results indicate that 7e-SMAMP is relatively stable while stored at 4 °C.

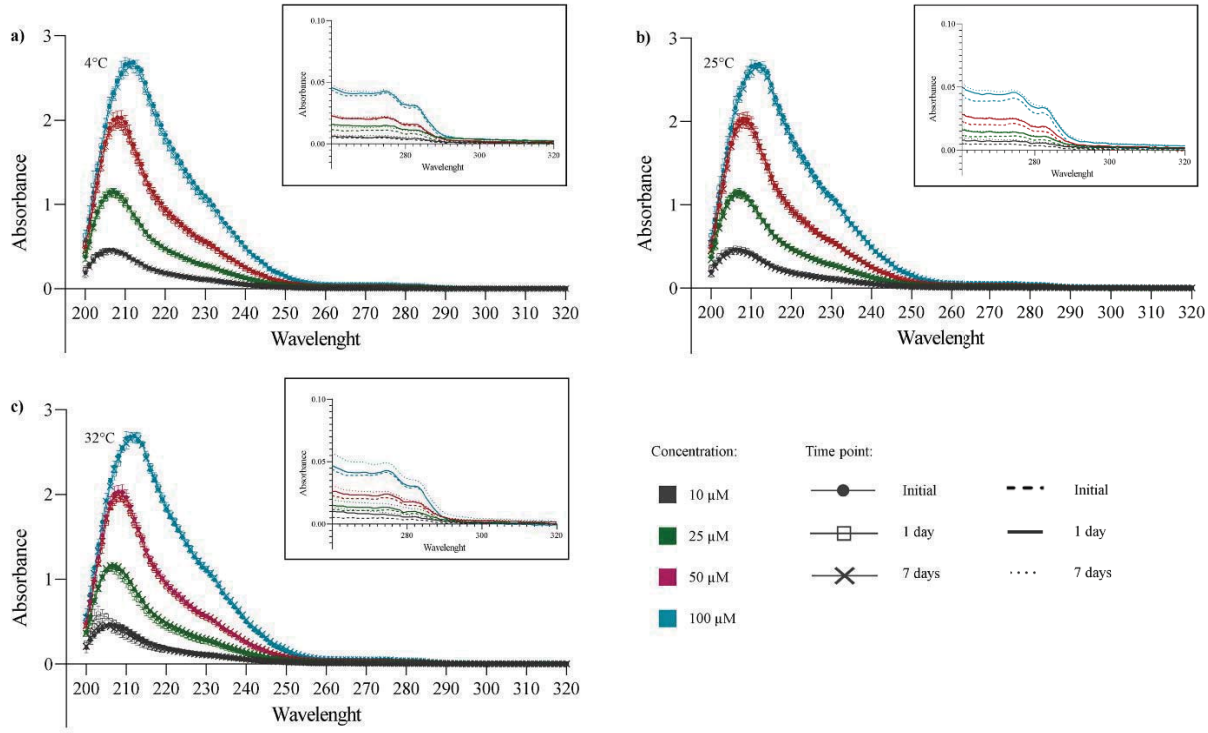

Figure S1. Absorbance scan (200-320 nm) of non-formulated 7e-SMAMP in concentration range of 10 to 100 µM. The 7e-SMAMP was assessed under different temperature conditions, namely a) 4 °C, b) 25 °C, and c) 32 °C. The boxed areas (figure zoom) highlights wavelength ranging between 260 and 320 nm. The absorbance scan was performed upon initial preparation and after 1- and 7-days storage (n=3).

S2.2. Liposome stability

The stability of 7e-SMAMP-liposomes was examined to ensure that the liposomes maintained the acceptable size, size distribution, zeta potential, entrapment, and pH. The liposomes were stored at 4 °C and the stability was determined after 2-, 4-, and 12-weeks storage. The characteristics of the formulation demonstrated no significant changes ($p < 0.05$) in any of the parameters as presented in Table S1.

Table S1. Stability of 7e-SMAMP-liposomes: mean diameter, polydispersity index (PI), zeta potential, entrapment efficacy (EE%), and pH in aqueous medium.

Week	Size (nm)	PI[a]	Zeta potential (mV)	EE%[b]	pH
2	291 ± 33	0.19 ± 0.02	61.2 ± 5.1	73.1 ± 7.1	5.2 ± 0.2
4	314 ± 35	0.19 ± 0.01	59.0 ± 1.1	73.8 ± 8.1	5.1 ± 0.3
12	310 ± 26	0.20 ± 0.01	65.5 ± 4.7	71.4 ± 8.8	4.9 ± 0.1

Liposome characteristics evaluated 2, 4, and 12 weeks after preparation.

Results are expressed as means with their respective SD (n = 3).

S3. Supplementary references

[S1] J.M. Antosiewicz, D. Shugar, UV–Vis spectroscopy of tyrosine side-groups in studies of protein structure. Part 2: selected applications, Biophys. Rev., 8 (2016) 163-177; https://doi.org/10.1007/s12551-016-0197-7.

[S2] F. Sgolastra, B.M. deRonde, J.M. Sarapas, A. Som, G.N. Tew, Designing Mimics of Membrane Active Proteins, Acc. Chem. Res., 46 (2013) 2977-2987; https://doi.org/10.1021/ar400066v.

[S3] W.F. Forbes, Light absorption studies. Part XVIII. The ultraviolet absorption spectra of bromobenzenes, Can. J. Chem., 39 (1961) 1131-1142; https://doi.org/10.1139/v61-140.

[S4] M.R. Liyanage, K. Bakshi, D.B. Volkin, C.R. Middaugh, Ultraviolet absorption spectroscopy of peptides, in: A.E. Nixon (Ed.) Therapeutic Peptides: Methods and Protocols, Methods in Molecular Biology, Humana Press, Totowa, NJ, USA, 2014, pp. 225-236.

Paper V

Towards multitarget approach in chronic wound healing – Synthetic mimic of antimicrobial peptide combined with polyphenol in liposomes-in-hydrogel dressing

Lisa Myrseth Hemmingsen[a], Mari Salamonsen[a], Marianne H. Paulsen[b,c], Purusotam Basnet[d], Mona Nystad[d,e], Anette Bayer[b], Morten B. Strøm[c] and Nataša Škalko-Basnet[a*]

[a] Drug Transport and Delivery Research Group, Department of Pharmacy, University of Tromsø The Arctic University of Norway, Universitetsvegen 57, N-9037 Tromsø, Norway

[b] Department of Chemistry, University of Tromsø The Arctic University of Norway, Universitetsvegen 57, N-9037 Tromsø, Norway

[c] Natural Products and Medicinal Chemistry Research Group, Department of Pharmacy, Faculty of Health Sciences, University of Tromsø The Arctic University of Norway, N-9037 Tromsø, Norway

[d] Women's Health and Perinatology Research Group, Department of Clinical Medicine, University of Tromsø The Arctic University of Norway, Universitetsvegen 57, N-9037 Tromsø, Norway

[e] IVF Clinic, Women's Clinic, University Hospital of North Norway, Sykehusvegen 38, N-9038 Tromsø, Norway

*Corresponding author: Nataša Škalko-Basnet at Drug Transport and Delivery Research Group, Department of Pharmacy, University of Tromsø The Arctic University of Norway, Universitetsvegen 57, 9037 Tromsø, Norway.

E-mail: natasa.skalko-basnet@uit.no, phone: +47 77646640

Abstract

Chronic wounds are a major burden for patients and health care providers, both from the medical as well as economical perspectives. Due to the complexity of unhealing wounds and their management, novel and multitarget approaches are necessary to ease the burden. Antimicrobial peptides and their mimics are considered promising candidates in therapeutic management of chronic wounds; however, some limitations are hindering their clinical translation. Moreover, a combination with active compounds offering additional improvement of healing, serving as multitargeted therapy, is gaining attention. We therefore proposed dual loading of a novel synthetic mimic of an antimicrobial peptide, 7a-SMAMP, and chlorogenic acid in liposomes incorporated in chitosan hydrogels. Antimicrobial peptides are expected to contribute to antimicrobial and wound healing potential as well as immunomodulation, while chlorogenic acid and chitosan should enhance both antimicrobial and wound healing potential of the novel dressing. Liposomes containing 7a-SMAMP and chlorogenic acid (~200 nm, 40 mV) were incorporated into chitosan hydrogels, that was further characterized for its anti-inflammatory activity, biocompatibility, and effect on cell migration. The novel dual system exhibited excellent cell compatibility. Additionally, 7a-SMAMP and chitosan demonstrated significant reduction in nitric oxide production in macrophages, indicating a potent anti-inflammatory activity. All of these contributions could help facilitate healing of a chronic wound. The novel dressing could serve as an innovative and multitargeting formulation for chronic wound management.

Keywords: peptidomimetic; polyphenol; chitosan; liposomes; non-healing wounds; biocompatibility

Abbreviations: ABTS, 2,2'-azino-bis (3-ethylbenzothiazoline-6-sulfonic acid) diammonium salt; AMP, antimicrobial peptide; CCK-8, cell counting kit-8; CGA, chlorogenic acid; DMEM, Dulbecco's Modified Eagle Medium high glucose; DPPH, 2,2-diphenyl-1picylhydrazyl; FBS, fetal bovine serum; LPS, lipopolysaccharide; NO, nitric oxide; PBS, phosphate buffered saline; PI, polydispersity index; RPMI, Roswell Park Memorial Institute; SMAMP, synthetic mimic of antimicrobial peptide

1. Introduction

Chronic wounds are major burden for health care providers and patients world-wide, for example about 2% of the population in the United States are affected (Sen, 2021). The quality of life of these patients is significantly reduced due to pain, loss of function, social restriction and isolation, economic burden, morbidity, and death (Järbrink et al., 2016). Furthermore, the numbers of patients with chronic wounds are expected to rise due to an aging population, prevalence of diseases, such as diabetes, and overweight (Gorain et al., 2022). The current available treatment options are limited and the clinical challenges in wound management are numerous (Monika et al., 2022). For many of these patients, a single therapeutic strategy is not adequate to cope with their condition and strategies are often combined to achieve treatment goals. Among these strategies, infection control and microbial eradication is often necessary if the bacterial burden causes delayed healing and the wound is critically colonized (Singh et al., 2013). Infection is one of the major factors leading to healing impairment. Moreover, the bacteria embedded in biofilms are found in up to 80% of infected chronic wounds (Drago et al., 2019). Biofilms are increasing the challenge of managing chronic wounds due to heightened resistance of bacteria embedded in the biofilm matrix. These bacteria are between 4 and 1000-fold more resistant to antimicrobial compounds than their planktonic counterparts (Ciofu et al., 2022). Additionally, bacteria cultured from patients with chronic wounds are often found to exhibit higher tolerance towards antimicrobial compounds, increasing the risk of resistance development (Wangoye et al., 2022). Antimicrobial resistance is one of the most important challenges as we are entering a post-antibiotic era accompanied by the decline of new antimicrobials approved for the market (Pfalzgraff et al., 2018; Ventola, 2015). Bacterial wound infections additionally contribute to prolonged inflammatory phase in natural healing process, hampering healing. Consequently, high levels of reactive oxygen species (ROS) could cause oxidative damage and cell death, further hampering the healing process (Xu et al., 2021). Treating patients with antioxidants could help resolve the ROS imbalance and therefore improve wound healing (Comino-Sanz et al., 2021). Additionally, nitric oxide (NO) plays a significant role in inflammatory pathways, leading to impaired healing (Basnet et al., 2012). To address such a complex challenge, wound dressing should, ideally, control the microbial challenge, mediate the inflammatory response, and assist in healing, while being biocompatible and safe.

As a novel approach to address the therapy of chronic wounds, antimicrobial peptides (AMPs) are often considered promising candidates. In addition to their antimicrobial activity against a wide range of microorganisms, these compounds could serve as immunomodulators and accelerate wound healing (Thapa et al., 2020). Despite their clear advantages, their clinical success is still limited by instability and degradation, toxicity, and lowered bioavailability (Zhang et al., 2021). One of the most common strategies to circumvent the mentioned drawbacks is the synthesis of synthetic mimics of antimicrobial peptides (SMAMPs). These compounds often demonstrate improved bioavailability, higher stability, and less toxicity. However, their toxicity is often linked to the concentration; therefore, a second strategy could rely on combining AMPs and SMAMPs with other compounds with antimicrobial or other beneficial properties for wound healing (Sierra and Viñas, 2021). Often, although improved, the stability, efficacy and toxicity issues need to be overcome by their entrapped within drug delivery systems tailored for wound therapy (Divyashree et al., 2020).

In our previous study, we confirmed the improved bacterial eradication, excellent anti-inflammatory activity, and no cytotoxicity upon incorporation of the membrane-active antimicrobial, chlorhexidine, in liposomes-in-chitosan hydrogels (Hemmingsen et al., 2021a). In this work, we intended to further improve biological properties, particularly the anti-oxidative and wound healing properties, by co-entrapping a novel SMAMP with the polyphenol chlorogenic acid (CGA) within liposomes. Indeed, CGA is known for its numerous biological properties, such as anti-oxidative, anti-inflammatory, and antimicrobial properties, that could facilitate wound healing. (Naveed et al., 2018). The novel 7a-SMAMP, has previously exhibited excellent antimicrobial properties; however, its other biological properties are not well-elucidated (Paulsen et al., 2021). The aim of this study was therefore to assess the biocompatibility and anti-inflammatory properties of 7a-SMAMP entrapped or co-entrapped with CGA in liposomes-in-hydrogel formulations. We also assessed the anti-oxidative effects of CGA. Chitosan was selected as a hydrogel vehicle for its antimicrobial, anti-inflammatory, anti-oxidative, and wound healing properties (Hemmingsen et al., 2021c).

2. Materials and methods

2.1 Materials

Chitopharm™ M – Chitosan from shrimp, medium molecular weight (average of 350 – 600 kDa) and degree of deacetylation of >70% was kindly provided by Chitinor (Tromsø, Norway). Lipoid S100 was a gift from Lipoid GmbH (Ludwigshafen, Germany). Methanol ≥99.9%, HiPerSolv CHROMANORM® for LC-MS, acetonitrile ≥99.9% HiPerSolv CHROMANORM®, gradient grade for HPLC, acetic acid (>99.9%), and glycerol solution (86%) were purchased from VWR International (Fontenay-sous-Bois, France). Chlorogenic acid ≥95% (titration), trifluoroacetic acid for HPLC, ≥99.0%, acetic acid ≥99.8%, sodium nitrite, 2,2-diphenyl-1picylhydrazyl (DPPH), α-tocopherol, L-ascorbic acid, 2,2'-azino-bis (3-ethylbenzothiazoline-6-sulfonic acid) diammonium salt (ABTS), potassium peroxodisulfate puriss. p.a., ACS reagent, ≥99.0%, Phospholipid Assay Kit, Bovine serum albumin, Dulbecco′s Phosphate Buffered Saline (PBS, modified) without calcium chloride and magnesium chloride, Fibronectin; bovine plasma, and Cell Counting Kit-8 (CCK-8) were acquired from Sigma-Aldrich (St. Louis, MO, USA). Ortho-phosphoric acid ≥85% was purchased from Kebo Lab Ab (Oslo, Norway). Penicillin-streptomycin, Dulbecco's Modified Eagle Medium high glucose w/ l-glutamine and sodium pyruvate (DMEM) and Roswell Park Memorial Institute (RPMI) medium 1640 were purchased from Sigma-Aldrich (Steinheim, Germany). Lipopolysaccharide (from *Escherichia coli* 055:B5), sulphanilamide ≥98% and N-(1-Naphthyl)ethylenediamine dihydrochloride ≥98% were obtained from Sigma Life Science Norway AS (Oslo, Norway). Fetal bovine serum (FBS) was purchased from Biowest (Nuaillé, France). Murine macrophage RAW 264.7 cells were bought from ATCC (Manassas, VA, USA), Human Dermal Fibroblasts, Neonatal (HDF-neo) from Lonza (Basel, Switzerland) andHaCaT cell line (immortalized human keratinocytes) was acquired from CLS Cell Lines Service GmbH (Eppelheim, Germany).

2.2 Synthesis of 7a-SMAMP

A detailed description of the synthesis of 7a-SMAMP has previously been published by Paulsen *et al.* (Paulsen et al., 2021). However, in Supplementary Materials (S1.1.) we have provided a short description and the structure of 7a-SMAMP (Figure S1).

2.3 Liposome preparation and characterisation

2.3.1 Liposome preparation and size reduction

Lipid films were created by dissolving Lipoid S100 (200 mg) and 7a-SMAMP (10 mg) in methanol followed by subsequent evaporation of the solvent on a rotary evaporator (Büchi rotavapor R-124 with vacuum controller B-721, Büchi Vac® V-500, Büchi Labor-technik, Flawil, Switzerland) for minimum 1 hour at 60 mBar and 45 °C (Hemmingsen et al., 2021a). Liposomes were formed by rehydration of lipid films with 10 mL CGA (20 mg) in distilled water. Liposomes with only 7a-SMAMP or CGA were prepared in the same manner, however, without CGA and 7a-SMAMP, respectively. Empty liposomes were prepared without both CGA and 7a-SMAMP. The liposome size was reduced using manual extrusion with polycarbonate membranes (Nuclepore Track-Etch Membrane, Whatman House, Maidstone, UK; 800 nm thrice, 400 nm five times, and 200 nm once).

2.3.2 Liposome size, zeta potential, and pH determination

Size and size distribution were determined using a NICOMP Submicron particle sizer (NICOMP Particle Sizing System, Santa Barbara, CA, USA) as previously described (Hemmingsen et al., 2021a). The liposomes were diluted in distilled water to reach an intensity of 250-350 kHz and the weight-intensity distribution was recorded after three cycles of 15 min. Zeta potential was determined using Zetasizer Nano Zen 2600 (Malvern, Worcestershire, UK). The liposomes were diluted in 0.2 µm filtered water (1:20, v/v). The pH was measured at 24 ± 1 °C on a sensION + PH31 pH benchtop meter (Hach, Loveland, CO, USA).

2.3.3 Entrapment efficiency

Unentrapped CGA and 7a-SMAMP were separated from the liposomal suspensions by dialysis (Spectra/Por®4, Spectrum®, MWCO: 12-14 kDa, VWR International, Fontenay-sous-Bois, France) against distilled water (1:500, v/v) for 4 hours at 24 ± 1 °C. The quantification of CGA and 7a-SMAMP was performed with a reversed-phase Waters Nova-Pak C18 Column (4 µm, 3.9 x 150 mm) with a Waters C18 guard cartridge (5 µm, 3.9 x 20 mm, Waters Corporation, Milford, CT, USA) on Waters Alliance 2690 separation module coupled to Waters 996 Photodiode Array Detector (Waters Corporation, Milford, CT, USA) for high performance

liquid chromatography (HPLC) systems. The compounds were eluted with mobile phases comprising of milli-Q water and acetonitrile both with trifluoroacetic acid (0.1%, v/v). The gradient started at 90% acetonitrile followed a linear gradient to 35% acetonitrile over 27.5 min with a flow of 0.5 mL/min. The 7a-SMAMP and CGA were detected at 231 nm and 325 nm, respectively.

2.3.4 Liposome stability

The stability of the liposomes was evaluated by measuring the size, size distribution, zeta potential, pH, and entrapment efficiency, as described in sections 2.3.2 and 2.3.3, after 2-, 4-, and 12-weeks storage at 4 °C.

2.4 Preparation and characterisation of hydrogels

2.4.1 Preparation of chitosan hydrogel

Chitosan hydrogels were prepared with 4.5 % (w/w) chitosan and 9% (w/w) glycerol in 2.5% (w/w) acetic acid in distilled water (Hemmingsen et al., 2021b). The Cito Unguator® 2000 (GAKO International AG, Zurich, Switzerland) was utilized to homogenize hydrogels (24 ± 1 °C). The hydrogels were degassed in a bath sonicator (Bransonic® 5510R-MT Ultrasonic cleaner, Branson Ultrasonics Corporation, Danbury, CT, USA) for 30 min prior to 48-hour swelling. Hydrogels comprising liposomes (10%, w/w) were adjusted to have the same final concentrations of chitosan (4.5 % (w/w) and glycerol (9% (w/w)) as the plain hydrogels. Upon addition of liposomes, the liposomes-in-hydrogels were hand-stirred for 5 min.

2.4.2 Characterisation of hydrogels

Texture analysis was performed on all hydrogels and liposomes-in-hydrogels as previously described by Hurler *et al*. (Hurler et al., 2012). The analysis was performed on the TA.XT plus Texture Analyser (Stable Micro Systems Ltd., Surrey, UK) with a backward extrusion rig and a 35 mm disk. Hydrogels (65 g) was carefully transferred to the container of the rig set and tested at pre-test, test, and post-test speeds of 10, 4, and 4 mm/s, respectively. The trigger force was 10 g, and the distance was set to 10 mm. Obtaining the hardness,

cohesiveness, and adhesiveness, the disk was compressed into the hydrogels and withdrawn back to the starting position.

The pH of hydrogels was measured at 24 ± 1 °C with Accumet®, Portable pH meter, AP115 (Fisher scientific, Waltham, MA, USA).

Viscosities of hydrogel, hydrogel with 7a-SMAMP-liposomes and hydrogel with CGA/7a-SMAMP-liposomes were recoded with Rotavisc hi-vi II Complete coupled with DINS-1 adapter with spindle DIN-SP-7 and DIN-C-2 chamber (IKA®-Werke GmbH & Co. KG, Staufen, Germany). The measurements were performed at two different temperatures, namely 25 and 32 °C, to simulate room temperature and the skin temperature. The shear rate range was set between 4.0 s^{-1} and 23.63 s^{-1}.

2.4.3 Stability testing of hydrogels and liposomes-in-hydrogel

The stability of the hydrogels and liposomes-in- hydrogels was evaluated by measuring the texture properties and pH, as described in section 2.4.2, after 2-, 4-, and 12-weeks storage.

2.5 In vitro release studies

The *in vitro* release of formulated 7a-SMAMP from both liposomes and hydrogels was assessed utilizing the Franz cell diffusion system (PermeGear, Hellertown, PA, USA) with cellophane membrane and acceptor cell volume of 5 mL. As acceptor medium, β-cyclodextrin (2%, w/v) in distilled water was used to assure sink conditions (Chaudhari et al., 2007). The system was maintained on circulating heat (32 °C) and stirring with a stirring bar. The formulated 7a-SMAMP (600 µL) was added to the donor chamber. Samples (250 µL) were collected after 1, 2, 3, 4, 5, 8, and 24 hours and equal volumes of fresh acceptor media was added to maintain sink conditions. For quantification, HPLC was utilized as described in section 2.3.3.

2.6 Anti-oxidative activity of chlorogenic acid

Measurement of $ABTS^{\bullet+}$ and $DPPH^{\bullet}$ radical scavenging activity was based on methods described by Jøraholmen *et al*. (Jøraholmen et al., 2019). To generate and stabilize $ABTS^{\bullet+}$

radicals, ABTS (7.4 mM, 3 mL) and potassium peroxodisulphate (2.6 mM, 3 mL) were mixed and kept at room temperature overnight and subsequently diluted to 100 mL with ethanol. The CGA solution (5, 10, 25, and 50 µM) was mixed with $ABTS^{\bullet+}$ radical ethanolic solution (1:1, v/v) and kept at room temperature for 30 min protected for light. The $ABTS^{\bullet+}$ scavenging activity was measured using the UV–VIS plate reader (Tecan Spark M10 multimode plate reader, Tecan Trading AG, Männedorf, Switzerland) at 731 nm.

Stock solutions of CGA were diluted to 5, 10, 25, and 50 µM and mixed (1:1, v/v) with DPPH (60 µM) in ethanol and kept in room temperature for 30 min shielded for light. The DPPH scavenging activity was determined using the UV–VIS plate reader (Tecan Spark M10 multimode plate reader, Tecan Trading AG, Männedorf, Switzerland) at 519 nm. The $ABTS^{\bullet+}$ and DPPH radical scavenging activity of CGA was compared to the activity of vitamin C and E in corresponding concentrations.

2.7 Biological activity

2.7.1 Anti-inflammatory activity

The NO production in murine macrophages (RAW 264.7 cells) was used as an indicator of the anti-inflammatory activities of liposomes and hydrogels (Basnet et al., 2012). The RAW 264.7 cells were cultured in RPMI with 10% (v/v) FBS and penicillin-streptomycin, seeded (5×10^5 cells/mL, 1 mL) in 24-well plates and incubated (37 °C/5% CO_2) for 24 hours. Next, the medium was replaced with medium containing LPS (1 µg/mL) to induce NO production. Cells were treated with liposomes (with concentrations corresponding to 1, 10, or 50 µg/mL lipid content) or hydrogels (corresponding to liposome concentrations). Additionally, cells treated with only LPS containing medium or RPMI served as control cells. Subsequently, the cells were incubated for another 24 hours. Finally, the NO production was evaluated on the UV-vis plate reader (Tecan Trading AG, Männedorf, Switzerland) with Griess reagent (1:1, v/v; 2.5% phosphoric acid with 1% sulphanilamide and 0.1% N-(-1-naphthyl)ethylenediamine) at 540 nm.

2.7.2 Cell compatibility evaluation

Cell compatibility was evaluated in keratinocytes (HaCaT), fibroblasts (HDF-neo), and macrophages (RAW 264.7). The cells were cultured in DMEM (HaCaT and NDF-neo) or RPMI (RAW 264.7) with 10% (v/v) FBS and penicillin-streptomycin, seeded (1×10^5 cells/mL, 90 µL) in 96-well plates, and incubated (37 °C/5% CO_2) for 24 hours. Next, 10 µL liposomes (with concentrations corresponding to 1, 10, or 50 µg/mL lipid content) or hydrogels (corresponding to liposome concentrations) were added to the wells and plates were incubated for 24 hours. The CCK-8 kit reagent was added in aliquots of 10 µL, and the plates were incubated for 4 hours. Finally, the cells were measured at 450 nm and referenced at 650 nm on the UV-vis plate reader (Tecan Trading AG, Männedorf, Switzerland). The cell survival was expressed as percentage of survival compared to cells treated with complete medium (Hemmingsen et al., 2021b).

2.7.3 Cell migration – *in vitro* scratch assay

Cell migration was evaluated in keratinocytes and fibroblasts cultured in DMEM with 10% (v/v) FBS and penicillin-streptomycin. The 6-well plates were coated with fibronectin (2.1 µg/cm^2) as previously described by Liang *et al*. (Liang et al., 2007). The cells were seeded (1.2×10^6 cells/well, 2 mL) in the pre-coated 6-well plates and incubated (37 °C/5% CO_2) to obtain a confluent cell monolayer (Borges et al., 2017). A scratch was made in the cell monolayer with a p200 pipette tip and debris was removed by washing with PBS. Fresh medium containing treatment (2 mL, liposomes or CGA/7a-SMAMP-liposomes, 1, 10, or 50 µg/mL lipid concentration) was added to the wells. Only medium served as control. The cells were incubated (37 °C/5% CO_2) and evaluated under an Eclipse Ts2 inverted microscope (Nikon Corporation, Tokyo, Japan) coupled to an HDMI microscope camera (DeltaPix, Smorum, Denmark) after 4, 7, 24, and 30 hours. The images were analysed using ImageJ (Schneider et al., 2012) with the Wound_healing_size_tool plugin developed by Suarez-Arnedo *et al*. (Suarez-Arnedo et al., 2020). Representative images are presented in Supplementary Materials (Figures S2 and S3).

2.8 Statistical analysis

Generally, results are expressed as mean ± SD. Student's t-tests or one-way ANOVA with Tukey's post-test were performed to evaluate significance ($p < 0.05$). All statistical analyses were performed in GraphPad Prism version 9.3.1 for Windows (GraphPad Software LLC, San Diego, CA, USA).

3. Results and discussions

There are numerous factors affecting the wound healing process, and different strategies have been proposed to improve wound healing (Mirhaj et al., 2022). The role and use of antimicrobial treatment to treat infected wounds are frequently discussed (Chen et al., 2022; Eriksson et al., 2022; Malone and Schultz, 2022; Siddiqui and Bernstein, 2010). Generally, administering antimicrobials is favourable in cases of infection; however, the antimicrobial compounds commonly used in topical treatment of skin and wound infections could impair healing and cause toxic effects on cells responsible for repairing the skin structure (Punjataewakupt et al., 2019). In this context, nanomaterials and delivery systems could improve the therapeutic outcome by enhancing the activity while controlling potential toxicity. Delivery systems could assure increased concentration of antimicrobials at the infection site, influence/modulate cellular responses, and reduce toxicity (Naskar and Kim, 2020). Liposomes are considered highly promising in topical formulations intended for skin. These systems could improve penetration into/across the skin and skin partitioning, solubilize pharmaceutical compounds, closely interact with the skin structure and microorganisms, as well as decrease toxicity of pharmaceutical compounds (Kushwaha et al., 2021). We have previously demonstrated improved microbial eradication upon incorporation of membrane-active antimicrobials in liposomes (Hemmingsen et al., 2021a). Liposomes were therefore selected as the primary delivery system for the novel 7a-SMAMP and CGA.

3.1 Liposome characteristics

In our previous study, we targeted a size around 300 nm, however, in the current study, we aimed at liposomes smaller than 300 nm to potentially improve biofilm penetration and therefore the antimicrobial efficacy (Hemmingsen et al., 2021a; Meers et al., 2008). Liposomes

containing 7a-SMAMP were generally smaller than the empty liposomes, while all formulations exhibited relatively narrow size distribution (Table 1). Liposomes and CGA-liposomes possessed neutral surfaces, however, upon through incorporation of 7a-SMAMP, the surface charge increased substantially (>45 mV). The cationic liposome surface indicates that 7a-SMAMP is accommodated within or onto the surface of liposomes, enabling its closer interaction with bacteria. The cationic nature of the SMAMPs is one of the most important features for selectivity towards bacterial membranes as well as for their effect on the bacterial membrane destabilization (Lin et al., 2021). Positively charged liposomes have reportedly showed improved biofilm penetration, contributed to closer interaction between the liposomes and biofilm matrix (Alhajlan et al., 2013).

Table 1. Mean diameter, polydispersity index (PI), zeta potential, and pH of all liposomal formulations.

	Size (nm)	PI	Zeta potential (mV)	pH
Liposomes	260 ± 16	0.22 ± 0.15	-2.9 ± 2.4	6.5 ± 0.2
CGA-liposomes	224 ± 4	0.24 ± 0.06	-6.8 ± 7.5	3.2 ± 0.0
7a-SMAMP-liposomes	216 ± 18	0.13 ± 0.05	46.0 ± 1.0	5.5 ± 0.2
CGA/7a-SMAMP-liposomes	208 ± 2	0.08 ± 0.02	40.0 ± 1.3	3.0 ± 0.0

Results are expressed as means with their respective SD (n = 3).

Considering a novel delivery system destined for antimicrobial therapy of skin infections, high entrapment efficiency is important to achieve a high local concentration of the antimicrobial compound. The entrapment of both CGA and 7a-SMAMP was evaluated using dialysis, followed by HPLC. Interestingly, the entrapment of CGA and 7a-SMAMP increased when the compounds were co-incorporated in the liposomes (Table 2). The entrapment of CGA and 7a-SMAMP increased by approximately 13 and 26%, respectively. This could potentially be ascribed to more favourable conditions for 7a-SMAMP accommodation within liposomal bilayers, (Figure S1) when entrapped together with CGA (Gomaa et al., 2017). The improved accommodation within bilayers can also be seen in the different surface charge for liposomes with co-entrapped compounds.

Table 2. Entrapment efficiency (EE%) of CGA and 7a-SMAMP in liposomal formulations.

	CGA EE%	7a-SMAMP EE%
CGA-liposomes	30.2 ± 3.8	-
7a-SMAMP-liposomes	-	54.5 ± 3.4
CGA/7a-SMAMP-liposomes	43.5 ± 3.4	80.2 ± 5.2

Results are expressed as means with their respective SD (n = 3).

3.1.3 Vesicle stability

The AMPs and SMAMPs exert their antimicrobial action through interaction and destabilization of bacterial membranes; since we incorporate the novel SMAMP in liposomes with bilayer structures, we needed to evaluate if the liposomes remained stable after the incorporation of 7a-SMAMP. We evaluated the stability of liposomes (Figure 1) by monitoring their size, size distribution, zeta potential, pH, and entrapment efficiency over a period of 12 weeks. As seen in the Figure 1, all characteristics remained relatively stable over the whole testing period. However, not unexpectedly, the liposomes size increased after two weeks of storage. Additionally, the CGA/7a-SMAMP-liposomes exhibited a small decrease in size after 12 weeks as well as a fluctuation in surface charge at week four. Furthermore, there was no leakage of either 7a-SMAMP or CGA from the liposomal formulations. These results were promising permitting us to further incorporate novel liposomes into hydrogels to formulate wound dressing.

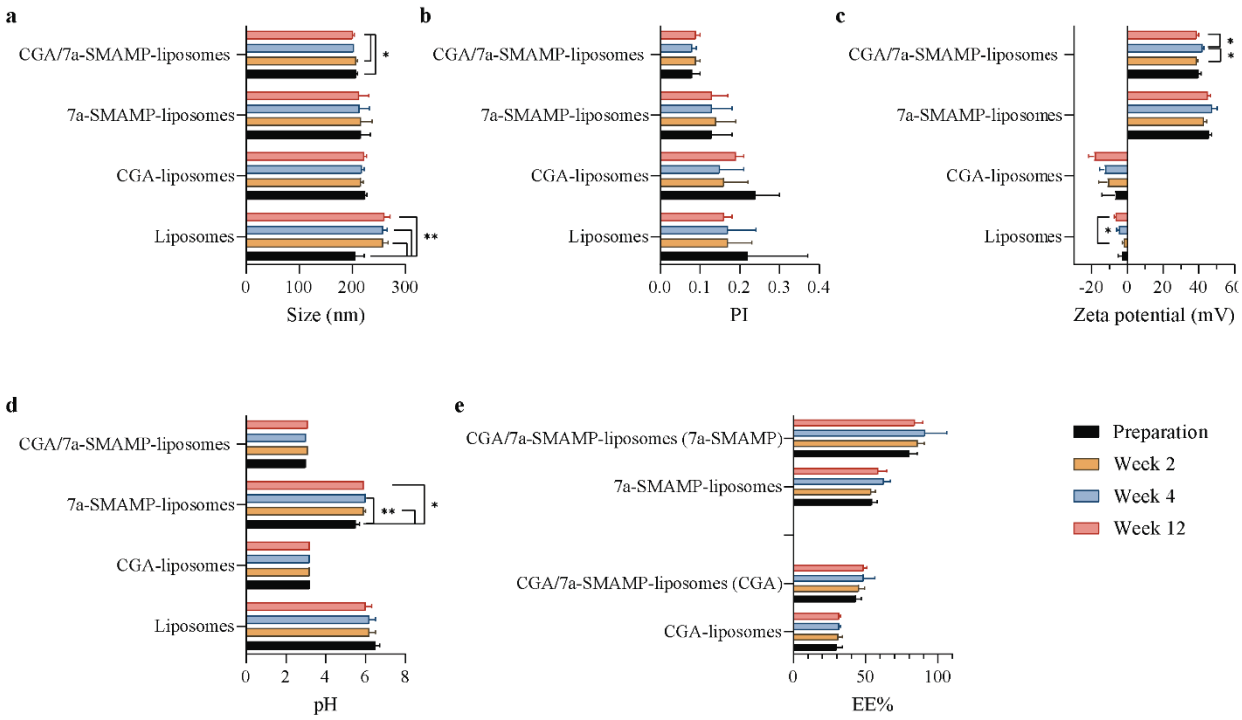

Figure 1. Liposome stability 2, 4, and 12 weeks after preparation evaluated as liposome characteristics. a) size, b) PI, c) zeta potential, d) pH, and e) EE%. PI = polydispersity index and EE% = entrapment efficiency (%). Results are expressed as means with their respective SD (n = 3).

* $p \leq 0.05$, ** $p \leq 0.01$.

3.2 Hydrogel characterisation

Due to the low viscosity and limited retention of liposomes at skin site, we utilized chitosan hydrogel as a secondary vehicle in our final formulation. The inclusion of both liposomes as primary and hydrogel as secondary delivery system could prevent a burst release of antimicrobials and create a more user-friendly formulation for the patients (Maja et al., 2020). Additionally, hydrogels are often preferred as wound dressings due to their three-dimensional network resembling extracellular matrix, and ability to maintain moisture balance and gas exchange in the wound bed (Hemmingsen et al., 2021a; Liang et al., 2021; Rezaei et al., 2020). Moreover, utilizing chitosan as a hydrogel vehicle, we could improve the treatment outcome, based on its s antimicrobial, anti-inflammatory, anti-oxidative, and wound healing properties (Hemmingsen et al., 2021c). Additionally, chitosan hydrogels have previously

exhibited promising antimicrobial effects and biocompatibility in combination with AMPs (Neff et al., 2020; Qianqian et al., 2021; Rezaei et al., 2020).

3.2.1 Hydrogel characteristics

We utilized an easy method to evaluate the mechanical properties of hydrogels, namely texture analysis. Texture analysis generates information about the hardness, cohesiveness, and adhesiveness of the hydrogels, which further describes the skin applicability, deformation, and adhesion, respectively. These parameters define the user-friendliness and general applicability of the hydrogels (Hurler et al., 2012). The incorporation of liposomes and CGA-liposomes increased the hydrogel hardness; however, the cohesiveness approximately remained the same (Figure 2). Interestingly, addition of 7a-SMAMP-liposomes and CGA/7a-SMAMP-liposomes did not impose similar effects, the cohesiveness increased upon incorporation of CGA/7a-SMAMP-liposomes. The adhesiveness also slightly increased when liposomes or CGA/7a-SMAMP-liposomes were incorporated within the hydrogel network. Jøraholmen *et al.* observed an increase in all textural properties when they incorporated liposomes into to a chitosan hydrogel. Additionally, the parameters increased by an increase in liposome concentrations (Jøraholmen et al., 2019). Similar trends were observed in the current study; however, the cohesiveness was not affected by the presence of liposomes containing 7a-SMAMP.

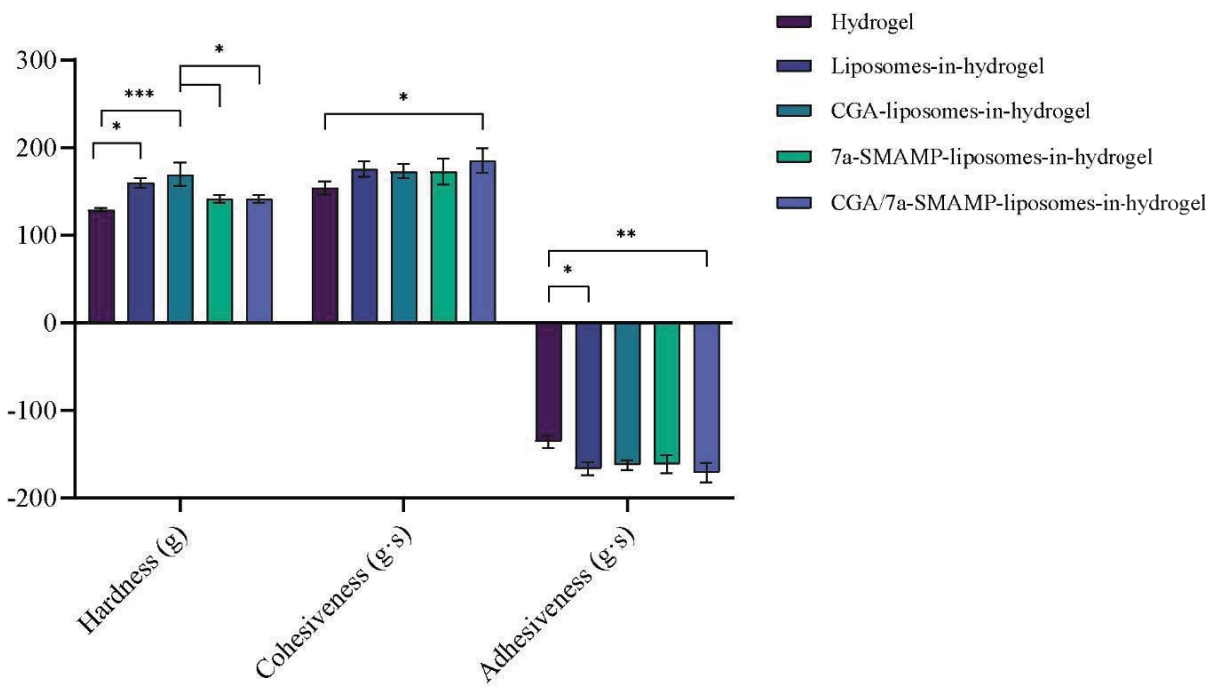

Figure 2. Texture properties of hydrogels measured as the hardness, cohesiveness, and adhesiveness. The results are expressed as means with their respective SD (n = 3).

* $p \leq 0.05$, ** $p \leq 0.01$, *** $p \leq 0.001$.

Another useful technique utilized to evaluate hydrogel properties, is by following rheological behaviour. Here, the viscosity and shear stress of hydrogels are assessed under increasing shear stress. Therefore, we followed the hydrogel, 7a-SMAMP-liposomes-in-hydrogel, and CGA/7a-SMAMP-liposomes-in-hydrogel. Furthermore, to evaluate the properties of hydrogel under storage and application conditions, we assessed the rheological behaviour at two temperatures, namely 25 and 32 °C, since temperature is known to affect the behaviour (Figure 3). All three hydrogels exhibited pseudoplastic flow and shear thinning behaviour. As the shear rate increased, the shear stress increased, and the viscosity decreased. Additionally, temperature influenced the rheological behaviour of the hydrogels; both viscosity and shear stress were significantly higher at 25 °C than at 32 °C. This temperature effect could be favourable for the hydrogels' user-friendliness since the at the skin temperature their flow improved, easing the administration.

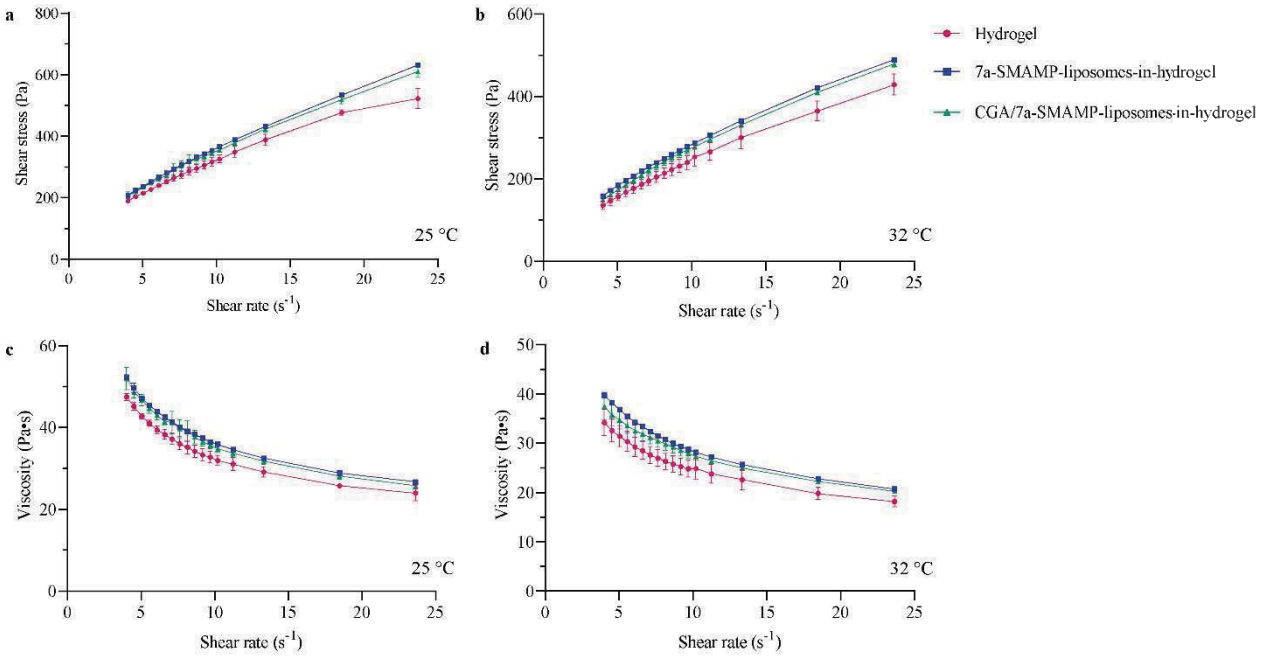

Figure 3. Viscosity of hydrogel, 7a-SMAMP-liposomes-in-hydrogel and CGA/7a-SMAMP-liposomes-in-hydrogel. Shear rate was plotted against shear stress (a, b) and viscosity (c, d) at 25 ◦C (a, c) and 32 ◦C (b, d). The results are expressed as means with their respective SD (n = 3).

Contrary to our previous study (Hemmingsen et al., 2021b) where the incorporation of liposomes into the hydrogel network did not influence the rheological behaviour, in the current study shear stress increased at both 25 and 32 °C when 7a-SMAMP-liposomes (p = 0.002 and 0.009 at 23.6 s^{-1} respectively) or CGA/7a-SMAMP-liposomes (p = 0.007 and 0.019 at 23.6 s^{-1}, respectively) were incorporated to the hydrogel. Additionally, the viscosity increased at 32 °C when 7a-SMAMP-liposomes (p = 0.009 at 23.6 s^{-1}) or CGA/7a-SMAMP-liposomes (p = 0.021 at 23.6 s^{-1}) were present in hydrogels.

3.2.2 Hydrogel stability

The storage stability of the hydrogels with and without liposomes were evaluated as the mechanical properties and pH over a time period of 12 weeks (Figure 4). Throughout the first four weeks, all hydrogels were relatively stable; however, on week 12, both hardness and cohesiveness increased significantly for the hydrogels comprising CGA-liposomes or CGA/7a-SMAMP-liposomes (p = <0.0001). This might be an indication that CGA is leaking into the

hydrogel network after some time. However, this effect requires further investigations. The 7a-SMAMP-liposomes-in-hydrogels were the most stable, and except for a small increase in their hardness, no other changes were observed throughout the whole test period. The adhesiveness and pH were stable for all hydrogels throughout the whole period.

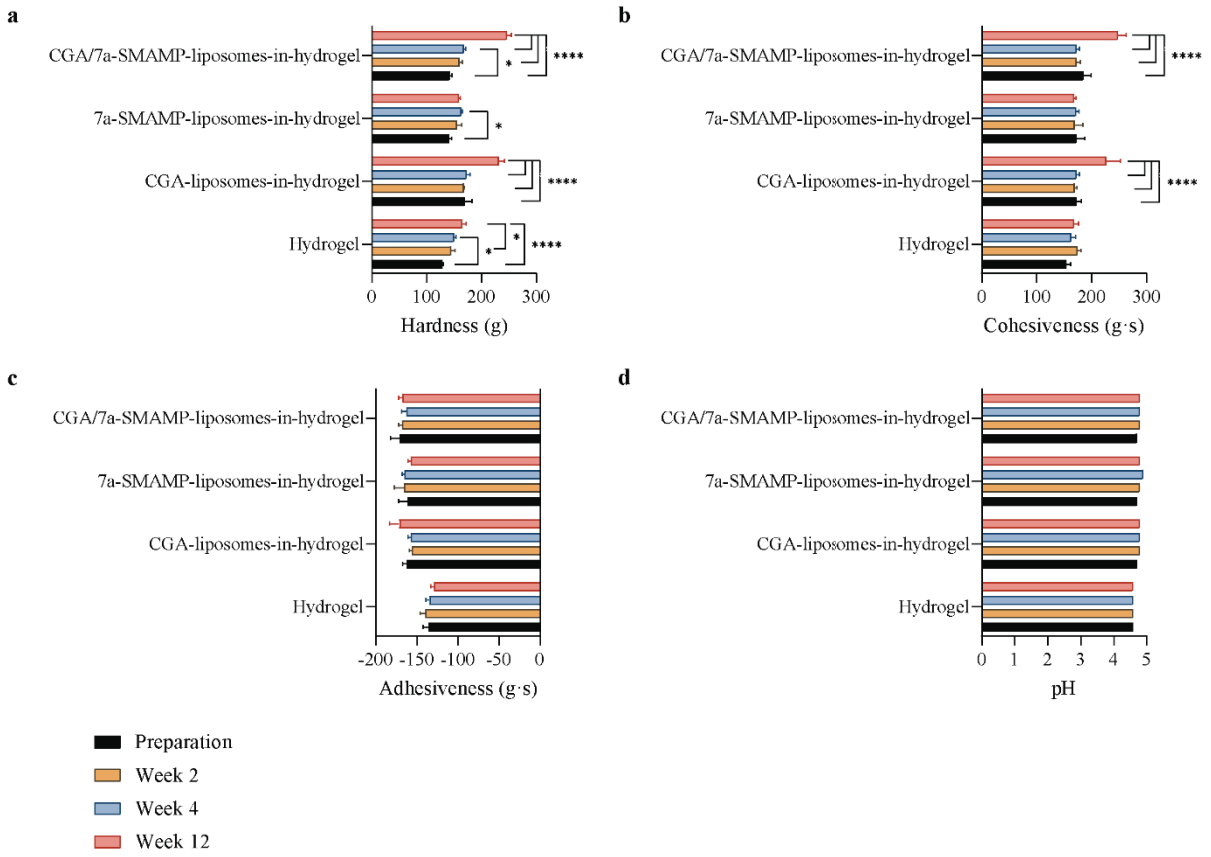

Figure 4. Stability of hydrogels measured as the mechanical properties and pH 2, 4, and 12 weeks after preparation. a) hardness, b) cohesiveness, c) adhesiveness, and d) pH. The results are expressed as means with their respective SD (n = 3).

* $p \leq 0.05$, **** $p \leq 0.0001$.

3.3 In vitro 7a-SMAMP release

The *in vitro* 7a-SMAMP release from liposomes and liposomes-in-hydrogels is presented in Figure 5. Interestingly, the liposomes-in-hydrogels released significantly more of 7a-SMAMP than the 7a-SMAMP-liposomes. Release of 7a-SMAMP into the hydrogel network

containing glycerol might be more favourable than to the water phase surrounding the liposomes. However, all formulations provided sustained release over 24 hours. This indicates that the formulation might be suitable for a once daily administration to wounded area. Application to the wounded skin area more frequently than once daily could lead to more discomfort for the patients, which is common for many topical antimicrobial treatments available today (Ray et al., 2019). Sustained release could also reduce the probability of bacterial regrowth and is therefore often desired for topical antimicrobial formulations (Zhu et al., 2010).

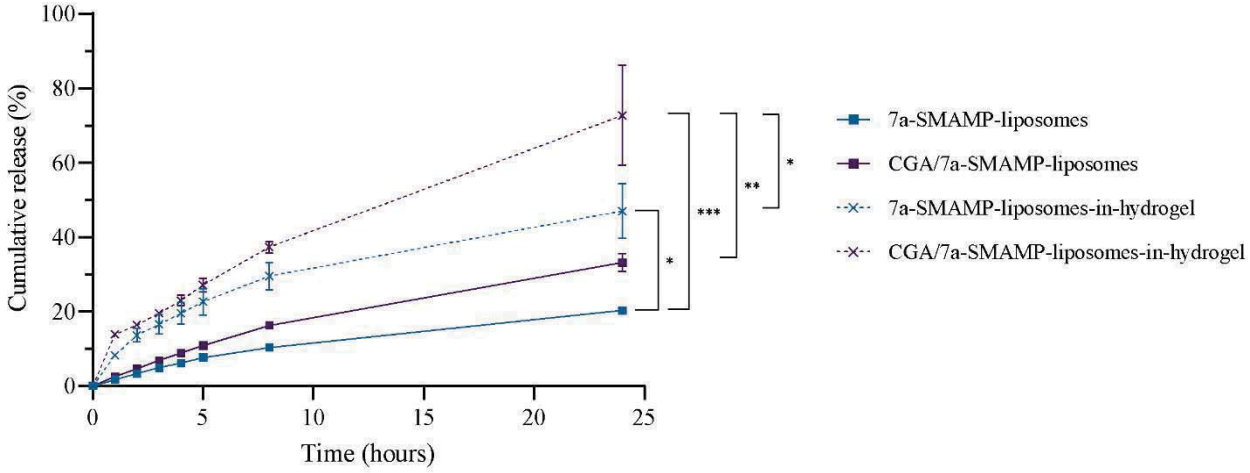

Figure 5. *In vitro* 7a-SMAMP release over 24 hours at 32 °C. The results are expressed as percentage of 7a-SMAMP released compared to the initial concentration. The results are expressed as means with their respective SD (n = 3).

* $p \leq 0.05$, ** $p \leq 0.01$, *** $p \leq 0.001$ compared at the 24-hour time point.

3.4 Anti-oxidative activity of chlorogenic acid

The presence of ROS in wounds is beneficial as is could protect against infections and assist in wound healing. However, an ROS imbalance could lead to cell damage and impaired healing (Comino-Sanz et al., 2021). In chronic wounds that are arrested in the inflammatory state, it is often vital that ROS are removed to permit proper wound healing. The most important reason for the inclusion of CGA in our formulation was its ability scavenge radicals. Therefore, we assessed CGA's ability to scavenge ABTS and DPPH radicals. We compared its scavenging

activity to two compounds known for their anti-oxidative activities, namely vitamin C and E (Jøraholmen et al., 2015). As seen in Figure 6, the scavenging activity of CGA was similar or greater than the activity of vitamin C and E at all concentrations in respect to both ABTS and DPPH radicals. Previous studies have also confirmed the high anti-oxidative activity of CGA against both ABTS and DPPH radicals (Oboh et al., 2013; Ohnishi et al., 1994), in agreement with the result of the current study. Furthermore, these results could indicate that CGA could help improve wound healing and decrease potential cell damage in the wounded area. In addition, by including chitosan, the anti-oxidative effect could potentially increase even further (Comino-Sanz et al., 2021).

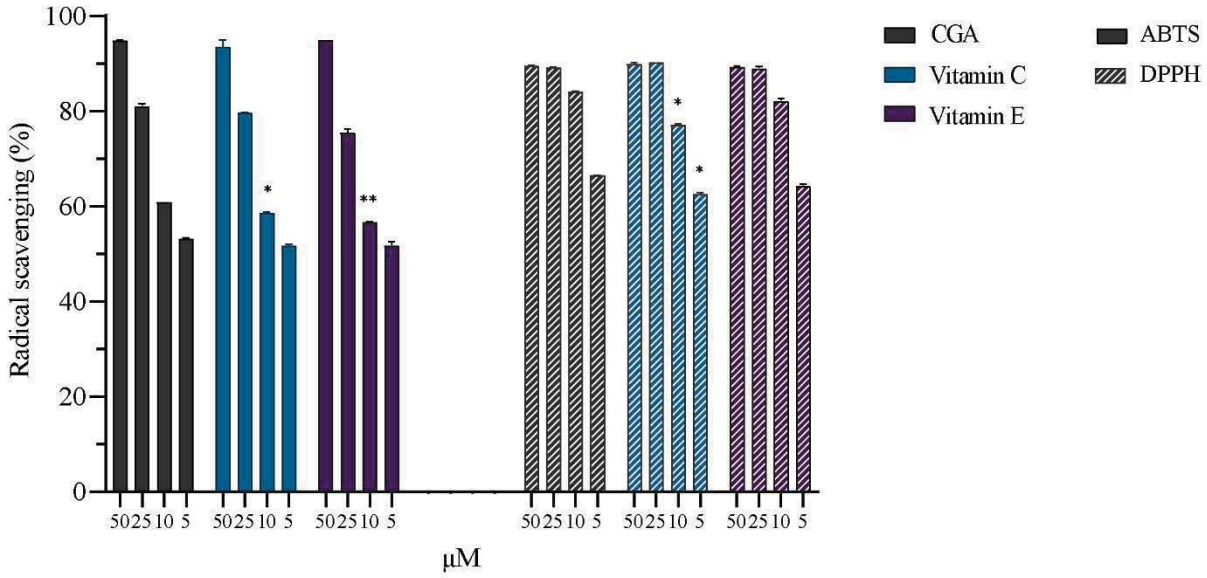

Figure 6. Radical scavenging by CGA compared to vitamin C and E assessed as scavenging of ABTS (solid) and DPPH radicals (pattern) as percentage compared to no radicals available (100%). The tested concentrations corresponded to 5, 10, 25, and 50 μM of the compounds. The results are expressed as means with their respective SD (n = 2).

* $p \leq 0.05$, ** $p \leq 0.01$ compared to CGA at the same concentration.

3.5 Anti-inflammatory response, cell compatibility, and migration

3.5.1 Anti-inflammatory responses in murine macrophages

Elevated and prolonged inflammation could generate imbalance of ROS. Since chronic wounds are haltered in the inflammatory phase, reduced inflammation and controlled overexpression of ROS are important features to be considered for improved healing (Zhao et al., 2016). Polyphenols are frequently also used to provide additional anti-inflammatory activity in formulations (Liang et al., 2021). Indeed, CGA has also been described to possess anti-inflammatory properties (Bagdas et al., 2020; Naveed et al., 2018). Therefore, we assessed the effect of novel formulations on NO production in LPS-induced macrophages as an indicator of their anti-inflammatory properties (Figure 7). We have, in our previous study, established that both liposomes and chitosan hydrogel could reduce the NO production in murine macrophages (Hemmingsen et al., 2021a). In the current study, for all formulations, except from the ones containing CGA, we could observe a dose-dependent trend of reduction in NO production, indicating anti-inflammatory activity. The 7a-SMAMP-liposomes exhibited a significant reduction of the NO production, confirming anti-inflammatory activity of the novel SMAMP. Anti-inflammatory activity of SMAMPs has previously been reported by Lior *et al.* (Lior et al., 2022). Additionally, all chitosan hydrogels demonstrated strong anti-inflammatory activity at the highest tested concentrations (50 μg/mL).

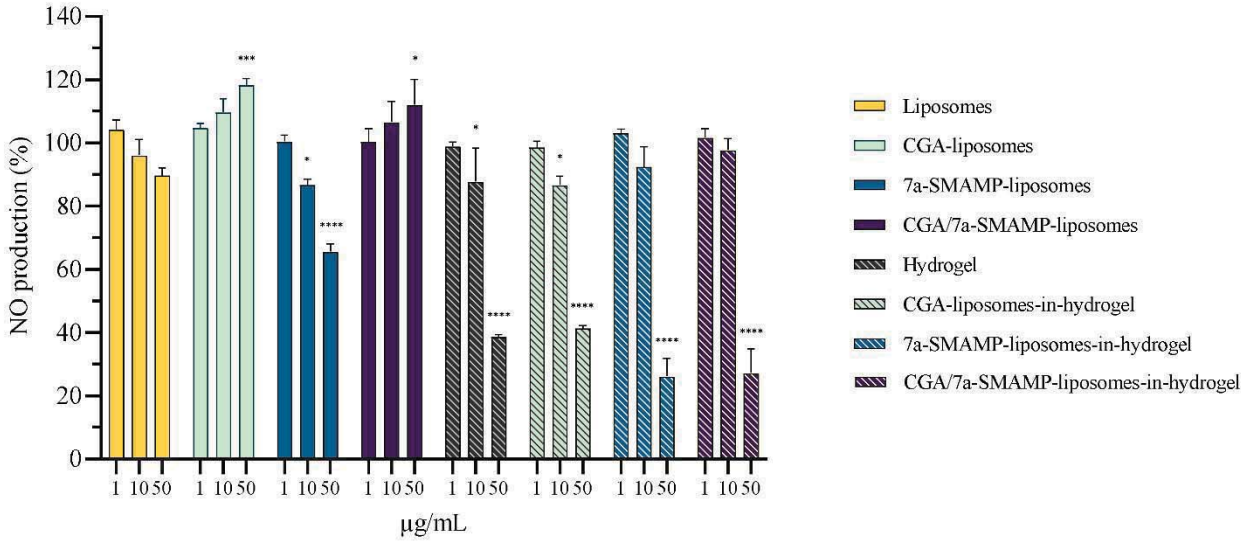

Figure 7. Anti-inflammatory response expressed as reduction in nitric oxide (NO) production in RAW 264.7 cells. Three different concentrations were tested, namely 1, 10, and 50 µg/mL lipid (or the corresponding concentrations of hydrogels). The results are expressed as the percentage of NO production in treated cells compared to production in non-treated LPS-induced RAW 264.7 cells (100 %). The results are expressed as means with their respective SD (n = 3).

* $p \leq 0.05$, *** $p \leq 0.001$, **** $p \leq 0.0001$ compared to control (100%).

Despite the fact that CGA has been described as a strong anti-inflammatory compound in literature, we found pro-inflammatory activity of CGA-liposomes and CGA/7a-SMAMP-liposomes. This effect was only significant at the highest concentration (50 µg/mL lipid). The anti-inflammatory activity of CGA is proposed to originate from the downregulation of the nuclear factor kappa B signalling pathway (Bagdas et al., 2020). However, Du *et al.* demonstrated that higher doses of CGA could induce inflammation in rats. It has also previously been shown that antioxidants could become prooxidants under certain conditions, which could further lead to increased inflammation (Du et al., 2013). When looking at NO production in the current study, the inflammatory activity increased, however, the effect was ameliorated when CGA-liposomes and CGA/7a-SMAMP-liposomes were incorporated in chitosan hydrogels. This finding again confirmed that by smart tailoring of a wound dressing we can gain more control over the therapy outcome.

3.5.2 Cell compatibility

The toxicity of AMPs is often limiting their progression into the clinics and delays the development of new therapeutic alternatives. The modification of their structure, as synthesizing mimics of AMPs, or utilizing drug delivery systems, could be suitable strategies to improve their toxicity profile (Divyashree et al., 2020). Yet, even with these modifications, both AMPs and SMAMPs occasionally exhibit toxicity towards mammalian cells (Svenson et al., 2022). In this study, we selected the macrophages, keratinocytes, and fibroblasts as the cells of interest for wound healing. These cells are important actors in the wound healing cascade, and their viability is of great importance in chronic wounds (Delavary et al., 2011). As seen in Figure 8, the cell viability of all cells was maintained upon treatment with both liposomes and hydrogels. The exception were the hydrogel and CGA-liposomes-in-hydrogel at the highest tested concentrations in the RAW 264.7 cells. In these two instances, the viability was reduced to approximately 76 and 82% compared to the control, respectively. However, according to ISO standards, the material that retains the cell viability over 70% is considered as a non-toxic (ISO, 2009). therefore, the hydrogels were deemed non-toxic. Additionally, these results indicate that the anti-inflammatory activity of the chitosan hydrogels can be contributed to reduction of NO production and not due to reduced macrophage viability. Moreover, most liposomal formulations exhibited a proliferative trend. This trend has been observed in other studies (Cauzzo et al., 2020; Giordani et al., 2019).

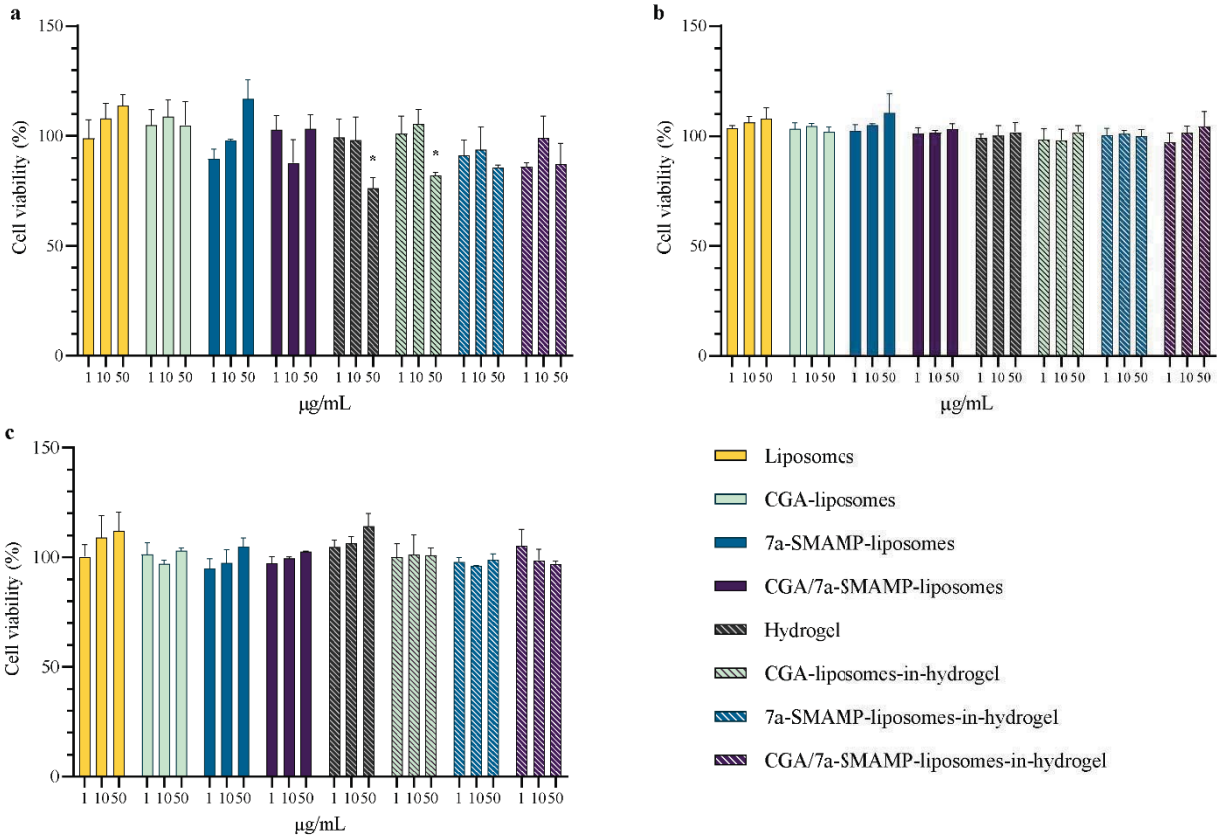

Figure 8. Cell compatibility assessment of liposomes and hydrogels in a) RAW 264.7 cells, b) HaCaT cells, and c) HDF-neo cells. The results are expressed as the percentage of surviving cells in the treated group compared to control (100 %). Control cells were only supplemented with complete medium; the cell viability is thereof considered as 100%. Three different concentrations were tested, namely 1, 10, and 50 µg/mL lipid (or the corresponding concentrations of hydrogels). The results are expressed as means with their respective SD (n = 3).

* $p \leq 0.05$ compared to control (100%).

3.5.3 *In vitro* scratch assay – cell migration

In wound healing, migration of cells to close the breach in the skin structure is vital to restore normal structure and integrity after an injury. In this process, keratinocytes and fibroblasts are strong contributors to skin restoration. Keratinocytes are important for the re-epithelialization and migrates to the wound edge to close the wound, while fibroblasts act to repair the loss of connective tissue (Shaw and Martin, 2016). Therefore, we assessed the effects of liposomes and CGA/7a-SMAMP-liposomes on migration of these cells. The *in vitro* scratch

assay is a well-known, straightforward, and fast method used to investigate the migration of cells to close artificial gaps or wounds in cell monolayers (Liang et al., 2007). In the HaCaT cell line the migration of the treated and non-treated cells was initially similar, however, after 24 hours the cells treated with CGA/7a-SMAMP-liposomes had migrated faster than the other groups (Figure 9). Even though the mean gap remained smaller after 30 hours, the difference was not significant compared to the other groups. In the HDF-neo cell line, the migration was similar in all groups indicating that treatment with liposomes or CGA/7a-SMAMP-liposomes did not impede the migration process.

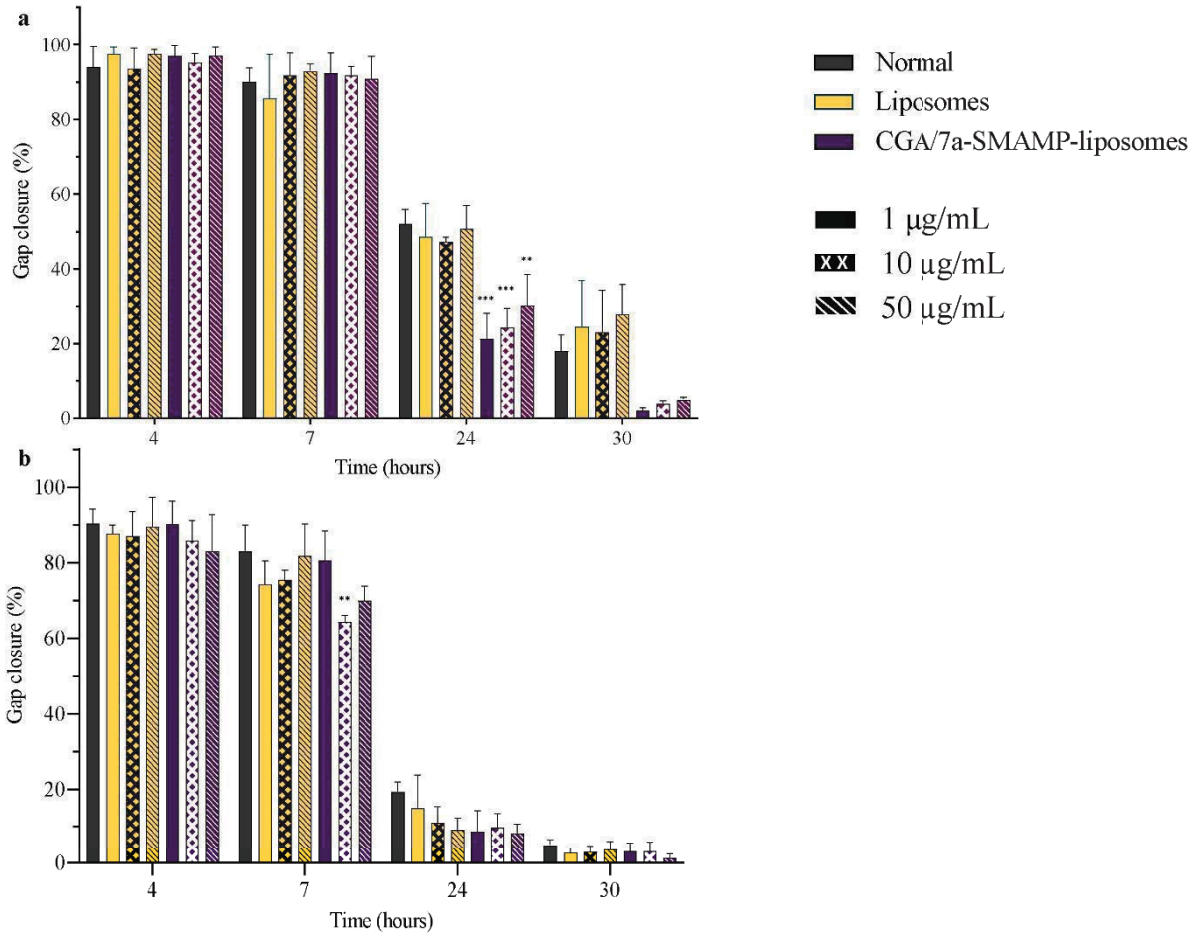

Figure 9. Cell migration (scratch assay) expressed as gap closure in a) HaCaT cell line and b) HDF-neo cells after treatment with liposomes or CGA/7a-SMAMP-liposomes. Three different concentrations were tested, namely 1 (solid), 10 (x-pattern), and 50 (striped) µg/mL lipid. Normal refers *c*ontrol cells *that* were only supplemented with complete medium. The results are expressed as the percentage of gap closure after 7, 24, and 30 hours compared gap in cell monolayer at the starting point of the scratch assay (0 hours, 100 %). The results are expressed as means with their respective SD (n = 3).

** $p \leq 0.01$, *** $p \leq 0.001$ compared to normal (control).

The *in vitro* scratch assay has been utilized to investigate the effect of various drug delivery systems and formulations intended for wound therapy. Ma and colleagues evaluated the effect of the non-formulated SMAMP MSI-1 on the migration of HaCaT cells. In this study, the SMAMP did not improve cell migration, however, the SMAMP still improved wound healing in mice (Ma et al., 2020). In another study, Manca *et al*. assessed the effects of

liposomes on fibroblast and keratinocyte migration. Especially in the fibroblasts, liposomes significantly improved migration (Manca et al., 2021). Ouyang *et al.* investigated migratory activity of fibroblasts treated with a marine peptide and chitosan hydrogel. Here, the peptide, chitosan, and their combination substantially improved the migration. Moreover, the novel formulation improved wound healing in rabbits (Ouyang et al., 2018). Zhao *et al.* did not observe improved migration of chitosan hydrogel in dermal fibroblasts, however, this study only lasted for 12 hours (Zhao et al., 2021), and these interpretations should be considered with care (Johnston et al., 2014).

4. Conclusion

To address the challenges in the complex therapeutic management of chronic wounds, we tailored a delivery system comprising chitosan hydrogels with liposomes bearing the novel 7a-SMAMP and CGA. We confirmed anti-oxidative activity of CGA. Moreover, both 7a-SMAMP-liposomes and chitosan hydrogels were able to significantly reduce NO production in macrophages, indicating strong anti-inflammatory activity. Additionally, CGA/7a-SMAMP-liposomes were able to improve keratinocytes cell migration, while remining a safe formulation, namely no toxicity was observed in any of tested cells. The results indicate the potential of novel delivery system to serve as a multitargeted therapeutic option in therapeutic management of chronic wounds.

Funding

The study was funded by UiT The Arctic University of Norway, Norway [project no. 235569]. The publication fund of UiT The Arctic University of Norway funded the publication charges of this article.

Acknowledgements

The authors would also like to Maddhusja Sritharan Nalliah and Nora Hersoug Nedberg at Department of Clinical Medicine, UiT The Arctic University of Norway for assistance in cell work. The graphical abstract was created with BioRender.com.

Declaration of interest

None.

CRediT authorship contribution statement

Lisa Myrseth Hemmingsen: Conceptualization, Data curation, Formal analysis, Investigation, Methodology, Visualization, Validation, Writing - original draft, Writing - review & editing. **Mari Salamonsen**: Investigation, Data curation, Writing - review & editing. **Marianne H. Paulsen**: Validation, Writing - review & editing. **Purusotam Basnet**: Methodology, Validation, Writing - review & editing. **Mona Nystad**: Resources, Writing - review & editing. **Annette Bayer**: Conceptualization, Writing - review & editing. **Morten B. Strøm**: Conceptualization, Methodology, Resources, Funding acquisition, Project administration, Writing - review & editing. **Nataša Škalko-Basnet**: Conceptualization, Funding acquisition, Methodology, Resources, Supervision, Project administration, Writing - original draft, Writing - review & editing.

References

Alhajlan, M., Alhariri, M., Omri, A., 2013. Efficacy and Safety of Liposomal Clarithromycin and Its Effect on Pseudomonas aeruginosa Virulence Factors. Antimicrob. Agents Chemother. 57, 2694-2704. doi: https://doi.org/10.1128/AAC.00235-13.

Bagdas, D., Gul, Z., Meade, J.A., Cam, B., Cinkilic, N., Gurun, M.S., 2020. Pharmacologic Overview of Chlorogenic Acid and its Metabolites in Chronic Pain and Inflammation. Curr. Neuropharmacol. 18, 216-228. doi: https://doi.org/10.2174/1570159X17666191021111809.

Basnet, P., Hussain, H., Tho, I., Škalko-Basnet, N., 2012. Liposomal Delivery System Enhances Anti-Inflammatory Properties of Curcumin. J. Pharm. Sci. 101, 598-609. doi: https://doi.org/10.1002/jps.22785.

Borges, G.Á., Elias, S.T., da Silva, S.M.M., Magalhães, P.O., Macedo, S.B., Ribeiro, A.P.D., Guerra, E.N.S., 2017. In vitro evaluation of wound healing and antimicrobial potential of ozone therapy. J. Craniomaxillofac. Surg. 45, 364-370. doi: https://doi.org/10.1016/j.jcms.2017.01.005.

Cauzzo, J., Nystad, M., Holsæter, A.M., Basnet, P., Škalko-Basnet, N., 2020. Following the Fate of Dye-Containing Liposomes In Vitro. Int. J. Mol. Sci. 21, 4847. doi: https://doi.org/10.3390/ijms21144847.

Chaudhari, P., Sharma, P., Barhate, N., Kulkarni, P., Mistry, C., 2007. Solubility enhancement of hydrophobic drugs using synergistically interacting cyclodextrins and cosolvent. Curr. Sci. 92, 1586-1591.

Chen, V., Burgess, J.L., Verpile, R., Tomic-Canic, M., Pastar, I., 2022. Novel Diagnostic Technologies and Therapeutic Approaches Targeting Chronic Wound Biofilms and Microbiota. Curr. Dermatol. Rep. 11, 60-72. doi: https://doi.org/10.1007/s13671-022-00354-9.

Ciofu, O., Moser, C., Jensen, P.Ø., Høiby, N., 2022. Tolerance and resistance of microbial biofilms. Nat. Rev. Microbiol. doi: https://doi.org/10.1038/s41579-022-00682-4.

Comino-Sanz, I.M., López-Franco, M.D., Castro, B., Pancorbo-Hidalgo, P.L., 2021. The Role of Antioxidants on Wound Healing: A Review of the Current Evidence. J. Clin. Med. 10, 3558. doi: https://doi.org/10.3390/jcm10163558.

Delavary, B.M., van der Veer, W.M., van Egmond, M., Niessen, F.B., Beelen, R.H.J., 2011. Macrophages in skin injury and repair. Immunobiology 216, 753-762. doi: https://doi.org/10.1016/j.imbio.2011.01.001.

Divyashree, M., Mani, M.K., Reddy, D., Kumavath, R., Ghosh, P., Azevedo, V., Barh, D., 2020. Clinical Applications of Antimicrobial Peptides (AMPs): Where do we Stand Now? Protein Pept. Lett. 27, 120-134. doi: https://doi.org/10.2174/0929866526666190925152957.

Drago, F., Gariazzo, L., Cioni, M., Trave, I., Parodi, A., 2019. The microbiome and its relevance in complex wounds. Eur. J. Dermatol. 29, 6-13. doi: https://doi.org/10.1684/ejd.2018.3486.

Du, W.Y., Chang, C., Zhang, Y., Liu, Y.Y., Sun, K., Wang, C.S., Wang, M.X., Liu, Y., Wang, F., Fan, J.Y., Li, P.T., Han, J.Y., 2013. High-dose chlorogenic acid induces inflammation reactions and oxidative stress injury in rats without implication of mast cell degranulation. J. Ethnopharmacol. 147, 74-83. doi: https://doi.org/10.1016/j.jep.2013.01.042.

Eriksson, E., Liu, P.Y., Schultz, G.S., Martins-Green, M.M., Tanaka, R., Weir, D., Gould, L.J., Armstrong, D.G., Gibbons, G.W., Wolcott, R., Olutoye, O.O., Kirsner, R.S., Gurtner, G.C., 2022. Chronic wounds: Treatment consensus. Wound Repair Regen. 30, 156-171. doi: https://doi.org/10.1111/wrr.12994.

Giordani, B., Basnet, P., Mishchenko, E., Luppi, B., Škalko-Basnet, N., 2019. Utilizing Liposomal Quercetin and Gallic Acid in Localized Treatment of Vaginal Candida Infections. Pharmaceutics 12, 9. doi: https://doi.org/10.3390/pharmaceutics12010009.

Gomaa, A.I., Martinent, C., Hammami, R., Fliss, I., Subirade, M., 2017. Dual Coating of Liposomes as Encapsulating Matrix of Antimicrobial Peptides: Development and Characterization. Front. Chem. 5, 103. doi: https://doi.org/10.3389/fchem.2017.00103.

Gorain, B., Pandey, M., Leng, N.H., Yan, C.W., Nie, K.W., Kaur, S.J., Marshall, V., Sisinthy, S.P., Panneerselvam, J., Molugulu, N., Kesharwani, P., Choudhury, H., 2022. Advanced drug delivery systems containing herbal components for wound healing. Int. J. Pharm. 617, 121617. doi: https://doi.org/10.1016/j.ijpharm.2022.121617.

Hemmingsen, L.M., Giordani, B., Pettersen, A.K., Vitali, B., Basnet, P., Škalko-Basnet, N., 2021a. Liposomes-in-chitosan hydrogel boosts potential of chlorhexidine in biofilm eradication in vitro. Carbohydr. Polym. 262, 117939. doi: https://doi.org/10.1016/j.carbpol.2021.117939.

Hemmingsen, L.M., Julin, K., Ahsan, L., Basnet, P., Johannessen, M., Škalko-Basnet, N., 2021b. Chitosomes-In-Chitosan Hydrogel for Acute Skin Injuries: Prevention and Infection Control. Mar. Drugs 19, 269. doi: https://doi.org/10.3390/md19050269.

Hemmingsen, L.M., Škalko-Basnet, N., Jøraholmen, M.W., 2021c. The Expanded Role of Chitosan in Localized Antimicrobial Therapy. Mar. Drugs 19, 697. doi: https://doi.org/10.3390/md19120697.

Hurler, J., Engesland, A., Kermany, B.P., Škalko-Basnet, N., 2012. Improved texture analysis for hydrogel characterization: Gel cohesiveness, adhesiveness, and hardness. J. Appl. Polym. Sci. 125, 180-188. doi: https://doi.org/10.1002/app.35414.

ISO, 10993-5:2009, 2009. Biological evaluation of medical devices, Part 5: Tests for in vitro cytotoxicity. International Organization for Standardization - ISO, Geneva, Switzerland.

Johnston, S.T., Simpson, M.J., McElwain, D.L.S., 2014. How much information can be obtained from tracking the position of the leading edge in a scratch assay? J. R. Soc. Interface 11, 20140325. doi: https://doi.org/10.1098/rsif.2014.0325.

Järbrink, K., Ni, G., Sönnergren, H., Schmidtchen, A., Pang, C., Bajpai, R., Car, J., 2016. Prevalence and incidence of chronic wounds and related complications: a protocol for a systematic review. Syst. Rev. 5, 152. doi: https://doi.org/10.1186/s13643-016-0329-y.

Jøraholmen, M.W., Basnet, P., Tostrup, M.J., Moueffaq, S., Škalko-Basnet, N., 2019. Localized Therapy of Vaginal Infections and Inflammation: Liposomes-In-Hydrogel Delivery System for Polyphenols. Pharmaceutics 11, 53. doi: https://doi.org/10.3390/pharmaceutics11020053.

Jøraholmen, M.W., Škalko-Basnet, N., Acharya, G., Basnet, P., 2015. Resveratrol-loaded liposomes for topical treatment of the vaginal inflammation and infections. Eur. J. Pharm. Sci. 79, 112-121. doi: https://doi.org/10.1016/j.ejps.2015.09.007.

Kushwaha, P., Saxena, S., Shukla, B., 2021. A Recent Overview on Dermatological Applications of Liposomes. Recent Pat. Nanotechnol. 15, 310-321. doi: https://doi.org/10.2174/1872210514666201021145233.

Liang, C.C., Park, A.Y., Guan, J.L., 2007. In vitro scratch assay: a convenient and inexpensive method for analysis of cell migration in vitro. Nat. Protoc. 2, 329-333. doi: https://doi.org/10.1038/nprot.2007.30.

Liang, Y., He, J., Guo, B., 2021. Functional Hydrogels as Wound Dressing to Enhance Wound Healing. ACS Nano 15, 12687-12722. doi: https://doi.org/10.1021/acsnano.1c04206.

Lin, L., Chi, J., Yan, Y., Luo, R., Feng, X., Zheng, Y., Xian, D., Li, X., Quan, G., Liu, D., Wu, C., Lu, C., Pan, X., 2021. Membrane-disruptive peptides/peptidomimetics-based therapeutics: Promising systems to combat bacteria and cancer in the drug-resistant era. Acta Pharm. Sin. B. 11, 2609-2644. doi: https://doi.org/10.1016/j.apsb.2021.07.014.

Lior, Y., Shtriker, E., Kahremany, S., Lewis, E.C., Gruzman, A., 2022. Development of anti-inflammatory peptidomimetics based on the structure of human alpha1-antitrypsin. Eur. J. Med. Chem. 228, 113969. doi: https://doi.org/10.1016/j.ejmech.2021.113969.

Ma, L., Xie, X., Liu, H., Huang, Y., Wu, H., Jiang, M., Xu, P., Ye, X., Zhou, C., 2020. Potent antibacterial activity of MSI-1 derived from the magainin 2 peptide against drug-resistant bacteria. Theranostics 10, 1373-1390. doi: https://doi.org/10.7150/thno.39157.

Maja, L., Željko, K., Mateja, P., 2020. Sustainable technologies for liposome preparation. J. Supercrit. Fluids 165, 104984. doi: https://doi.org/10.1016/j.supflu.2020.104984.

Malone, M., Schultz, G., 2022. Challenges in the diagnosis and management of wound infection. Br. J. Dermatol. 187, 159-166. doi: https://doi.org/10.1111/bjd.21612.

Manca, M.L., Manconi, M., Meloni, M.C., Marongiu, F., Allaw, M., Usach, I., Peris, J.E., Escribano-Ferrer, E., Tuberoso, C.I., Gutierrez, G., Matos, M., Ghavam, M., 2021. Nanotechnology for Natural Medicine: Formulation of Neem Oil Loaded Phospholipid Vesicles Modified with Argan Oil as a Strategy to Protect the Skin from Oxidative Stress and Promote Wound Healing. Antioxidants 10, 670. doi: https://doi.org/10.3390/antiox10050670.

Meers, P., Neville, M., Malinin, V., Scotto, A.W., Sardaryan, G., Kurumunda, R., Mackinson, C., James, G., Fisher, S., Perkins, W.R., 2008. Biofilm penetration, triggered release and in vivo activity of inhaled liposomal amikacin in chronic Pseudomonas aeruginosa lung infections. J. Antimicrob. Chemother. 61, 859-868. doi: https://doi.org/10.1093/jac/dkn059.

Mirhaj, M., Labbaf, S., Tavakoli, M., Seifalian, A.M., 2022. Emerging treatment strategies in wound care. Int. Wound J. doi: https://doi.org/10.1111/iwj.13786.

Monika, P., Chandraprabha, M.N., Rangarajan, A., Waiker, P.V., Chidambara Murthy, K.N., 2022. Challenges in Healing Wound: Role of Complementary and Alternative Medicine. Front. Nutr. 8, 791899. doi: https://doi.org/10.3389/fnut.2021.791899.

Naskar, A., Kim, K.S., 2020. Recent Advances in Nanomaterial-Based Wound-Healing Therapeutics. Pharmaceutics 12, 499. doi: https://doi.org/10.3390/pharmaceutics12060499.

Naveed, M., Hejazi, V., Abbas, M., Kamboh, A.A., Khan, G.J., Shumzaid, M., Ahmad, F., Babazadeh, D., FangFang, X., Modarresi-Ghazani, F., WenHua, L., XiaoHui, Z., 2018. Chlorogenic acid (CGA): A pharmacological review and call for further research. Biomed. Pharmacother. 97, 67-74. doi: https://doi.org/10.1016/j.biopha.2017.10.064.

Neff, J.A., Bayramov, D.F., Patel, E.A., Miao, J., 2020. Novel Antimicrobial Peptides Formulated in Chitosan Matrices are Effective Against Biofilms of Multidrug-Resistant Wound Pathogens. Mil. Med. 185, 637-643. doi: https://doi.org/10.1093/milmed/usz222.

Oboh, G., Agunloye, O.M., Akinyemi, A.J., Ademiluyi, A.O., Adefegha, S.A., 2013. Comparative Study on the Inhibitory Effect of Caffeic and Chlorogenic Acids on Key Enzymes Linked to Alzheimer's Disease and Some Pro-oxidant Induced Oxidative Stress in Rats' Brain-In Vitro. Neurochem. Res. 38, 413-419. doi: https://doi.org/10.1007/s11064-012-0935-6.

Ohnishi, M., Morishita, H., Iwahashi, H., Toda, S., Shirataki, Y., Kimura, M., Kido, R., 1994. Inhibitory effects of chlorogenic acids on linoleic acid peroxidation and haemolysis. Phytochemistry 36, 579-583. doi: https://doi.org/10.1016/S0031-9422(00)89778-2.

Ouyang, Q.Q., Hu, Z., Lin, Z.P., Quan, W.Y., Deng, Y.F., Li, S.D., Li, P.W., Chen, Y., 2018. Chitosan hydrogel in combination with marine peptides from tilapia for burns healing. Int. J. Biol. Macromol. 112, 1191-1198. doi: https://doi.org/10.1016/j.ijbiomac.2018.01.217.

Paulsen, M.H., Engqvist, M., Ausbacher, D., Anderssen, T., Langer, M.K., Haug, T., Morello, G.R., Liikanen, L.E., Blencke, H.M., Isaksson, J., Juskewitz, E., Bayer, A., Strøm, M.B., 2021. Amphipathic Barbiturates as Mimics of Antimicrobial Peptides and the Marine Natural Products Eusynstyelamides with Activity against Multi-resistant Clinical Isolates. J. Med. Chem. 64, 11395-11417. doi: https://doi.org/10.1021/acs.jmedchem.1c00734.

Pfalzgraff, A., Brandenburg, K., Weindl, G., 2018. Antimicrobial Peptides and Their Therapeutic Potential for Bacterial Skin Infections and Wounds. Front. Pharmacol. 9, 281. doi: https://doi.org/10.3389/fphar.2018.00281.

Punjataewakupt, A., Napavichayanun, S., Aramwit, P., 2019. The downside of antimicrobial agents for wound healing. Eur. J. Clin. Microbiol. Infect. Dis. 38, 39-54. doi: https://doi.org/10.1007/s10096-018-3393-5.

Qianqian, O., Songzhi, K., Yongmei, H., Xianghong, J., Sidong, L., Puwang, L., Hui, L., 2021. Preparation of nano-hydroxyapatite/chitosan/tilapia skin peptides hydrogels and its burn wound treatment. Int. J. Biol. Macromol. 181, 369-377. doi: https://doi.org/10.1016/j.ijbiomac.2021.03.085.

Ray, P., Singh, S., Gupta, S., 2019. Topical Antimicrobial Therapy: Current Status and Challenges. Indian J. Med. Microbiol. 37, 299-308. doi: https://doi.org/10.4103/ijmm.IJMM_19_443.

Rezaei, N., Hamidabadi, H.G., Khosravimelal, S., Zahiri, M., Ahovan, Z.A., Bojnordi, M.N., Eftekhari, B.S., Hashemi, A., Ganji, F., Darabi, S., Gholipourmalekabadi, M., 2020. Antimicrobial peptides-loaded smart chitosan hydrogel: Release behavior and antibacterial potential against antibiotic resistant clinical isolates. Int. J. Biol. Macromol. 164, 855-862. doi: https://doi.org/10.1016/j.ijbiomac.2020.07.011.

Schneider, C.A., Rasband, W.S., Eliceiri, K.W., 2012. NIH Image to ImageJ: 25 years of image analysis. Nat. Methods 9, 671-675. doi: https://doi.org/10.1038/nmeth.2089.

Sen, C.K., 2021. Human Wound and Its Burden: Updated 2020 Compendium of Estimates. Adv. Wound Care 10, 281-292. doi: https://doi.org/10.1089/wound.2021.0026.

Shaw, T.J., Martin, P., 2016. Wound repair: a showcase for cell plasticity and migration. Curr. Opin. Cell Biol. 42, 29-37. doi: https://doi.org/10.1016/j.ceb.2016.04.001.

Siddiqui, A.R., Bernstein, J.M., 2010. Chronic wound infection: Facts and controversies. Clin. Dermatol. 28, 519-526. doi: https://doi.org/10.1016/j.clindermatol.2010.03.009.

Sierra, J.M., Viñas, M., 2021. Future prospects for Antimicrobial peptide development: peptidomimetics and antimicrobial combinations. Expert Opin. Drug Discov. 16, 601-604. doi: https://doi.org/10.1080/17460441.2021.1892072.

Singh, M.R., Saraf, S., Vyas, A., Jain, V., Singh, D., 2013. Innovative approaches in wound healing: trajectory and advances. Artif. Cells Nanomed. Biotechnol. 41, 202-212. doi: https://doi.org/10.3109/21691401.2012.716065.

Suarez-Arnedo, A., Torres Figueroa, F., Clavijo, C., Arbeláez, P., Cruz, J.C., Muñoz-Camargo, C., 2020. An image J plugin for the high throughput image analysis of in vitro scratch wound healing assays. PLoS One 15, e0232565. doi: https://doi.org/10.1371/journal.pone.0232565.

Svenson, J., Molchanova, N., Schroeder, C.I., 2022. Antimicrobial Peptide Mimics for Clinical Use: Does Size Matter? Front. Immunol. 13, 915368. doi: https://doi.org/10.3389/fimmu.2022.915368.

Thapa, R.K., Diep, D.B., Tønnesen, H.H., 2020. Topical antimicrobial peptide formulations for wound healing: Current developments and future prospects. Acta Biomater. 103, 52-67. doi: https://doi.org/10.1016/j.actbio.2019.12.025.

Ventola, C.L., 2015. The antibiotic resistance crisis: part 1: causes and threats. Pharm. Ther. 40, 277-283.

Wangoye, K., Mwesigye, J., Tungotyo, M., Twinomujuni Samba, S., 2022. Chronic wound isolates and their minimum inhibitory concentrations against third generation cephalosporins at a tertiary hospital in Uganda. Sci. Rep. 12, 1195. doi: https://doi.org/10.1038/s41598-021-04722-6.

Xu, Z., Liang, B., Tian, J., Wu, J., 2021. Anti-inflammation biomaterial platforms for chronic wound healing. Biomater. Sci. 9, 4388-4409. doi: https://doi.org/10.1039/D1BM00637A.

Zhang, Q.Y., Yan, Z.B., Meng, Y.M., Hong, X.Y., Shao, G., Ma, J.J., Cheng, X.R., Liu, J., Kang, J., Fu, C.Y., 2021. Antimicrobial peptides: mechanism of action, activity and clinical potential. Mil. Med. Res. 8, 48. doi: https://doi.org/10.1186/s40779-021-00343-2.

Zhao, R., Liang, H., Clarke, E., Jackson, C., Xue, M., 2016. Inflammation in Chronic Wounds. Int. J. Mol. Sci. 17, 2085. doi: https://doi.org/10.3390/ijms17122085.

Zhao, X., Liu, Y., Jia, P., Cheng, H., Wang, C., Chen, S., Huang, H., Han, Z., Han, Z.C., Marycz, K., Chen, X., Li, Z., 2021. Chitosan hydrogel-loaded MSC-derived extracellular vesicles promote skin rejuvenation by ameliorating the senescence of dermal fibroblasts. Stem Cell. Res. Ther. 12, 196. doi: https://doi.org/10.1186/s13287-021-02262-4.

Zhu, C.T., Xu, Y.Q., Shi, J., Li, J., Ding, J., 2010. Liposome combined porous β-TCP scaffold: Preparation, characterization, and anti-biofilm activity. Drug Deliv. 17, 391-398. doi: https://doi.org/10.3109/10717541003762870.

Supplementary Materials

Towards multitarget approach in chronic wound healing – Synthetic mimic of antimicrobial peptide combined with polyphenol in liposomes-in-hydrogel dressing

Lisa Myrseth Hemmingsen[a], Mari Salamonsen[a], Marianne H. Paulsen[b,c], Purusotam Basnet[d], Mona Nystad[d,e], Anette Bayer[b], Morten B. Strøm[c] and Nataša Škalko-Basnet[a*]

[a] Drug Transport and Delivery Research Group, Department of Pharmacy, University of Tromsø The Arctic University of Norway, Universitetsvegen 57, N-9037 Tromsø, Norway

[b] Department of Chemistry, University of Tromsø The Arctic University of Norway, Universitetsvegen 57, N-9037 Tromsø, Norway

[c] Natural Products and Medicinal Chemistry Research Group, Department of Pharmacy, Faculty of Health Sciences, University of Tromsø The Arctic University of Norway, N-9037 Tromsø, Norway

[d] Women's Health and Perinatology Research Group, Department of Clinical Medicine, University of Tromsø The Arctic University of Norway, Universitetsvegen 57, N-9037 Tromsø, Norway

[e] IVF Clinic, Women's Clinic, University Hospital of North Norway, Sykehusvegen 38, 9038 Tromsø, Norway

*Corresponding author: Nataša Škalko-Basnet at Drug Transport and Delivery Research Group, Department of Pharmacy, University of Tromsø The Arctic University of Norway, Universitetsvegen 57, 9037 Tromsø, Norway.

E-mail: natasa.skalko-basnet@uit.no, phone: +47 77646640

S1.1 Synthesis *of 7a-SMAMP*

Initial, disubstituted malonate (diethyl 2,2-bis(4-(trifluoromethyl)benzyl)malonate) was synthesized by dialkylation of diethyl malonate with 1-(bromomethyl)-4-(trifluoromethyl)benzene. Cyclization of diethyl 2,2-bis(3,5-dibromobenzyl)malonate with urea yielded 5,5-bis(4-trifluoromethylbenzyl)pyrimidine-2,4,6(1H,3H,5H)-trione. Next, 1,4-dibromobutane was utilized for *N*-alkylation under basic conditions followed by bromine substitution with azide to generate 1,3-bis(4-azidobutyl)-5,5-bis(4trifluoromethylbenzyl)pyrimidine-2,4,6(1H,3H,5H)-trione. Lastly, azide reduction to amine with 1,3-propanedithiol and sodium borohydride was performed prior to guanidinylation to the guanylated barbiturate 1,1′-((2,4,6-trioxo5,5-bis(4-(trifluoromethyl)benzyl)dihydropyrimidine-1,3(2H,4H)diyl)bis(butane-4,1-diyl))diguanidine (7a-SMAMP, Figure S1) (Paulsen et al., 2021).

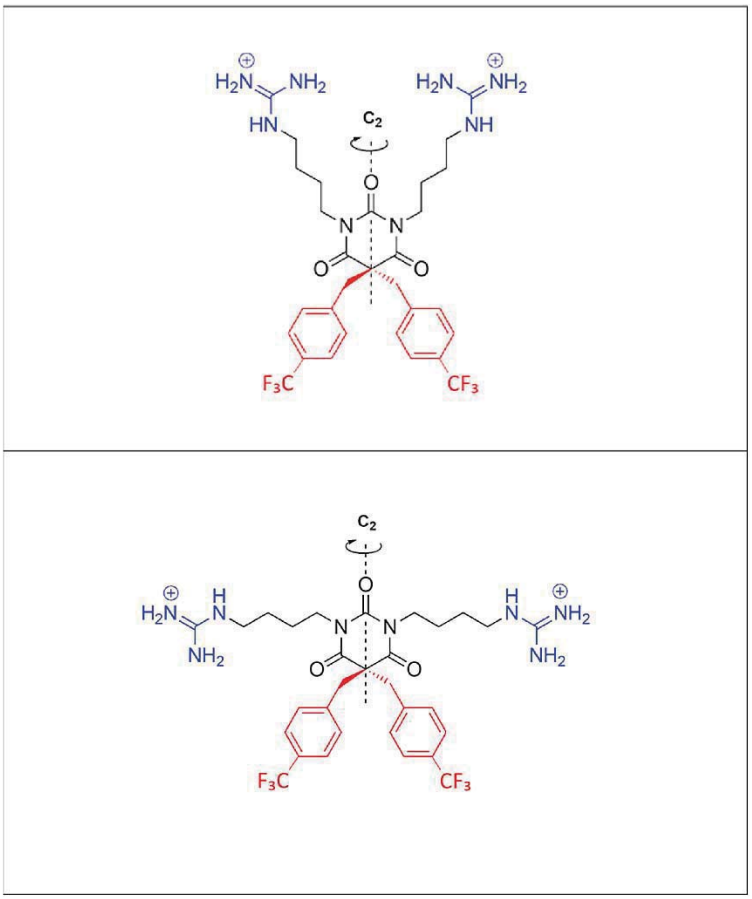

Figure S1. Structure of 7a-SMAMP.

S2.1 *In vitro* scratch assay – cell migration

In Figure S2 and S3, the images of HaCaT and HDF-neo cells, respectively, obtained during the scratch assay, are presented.

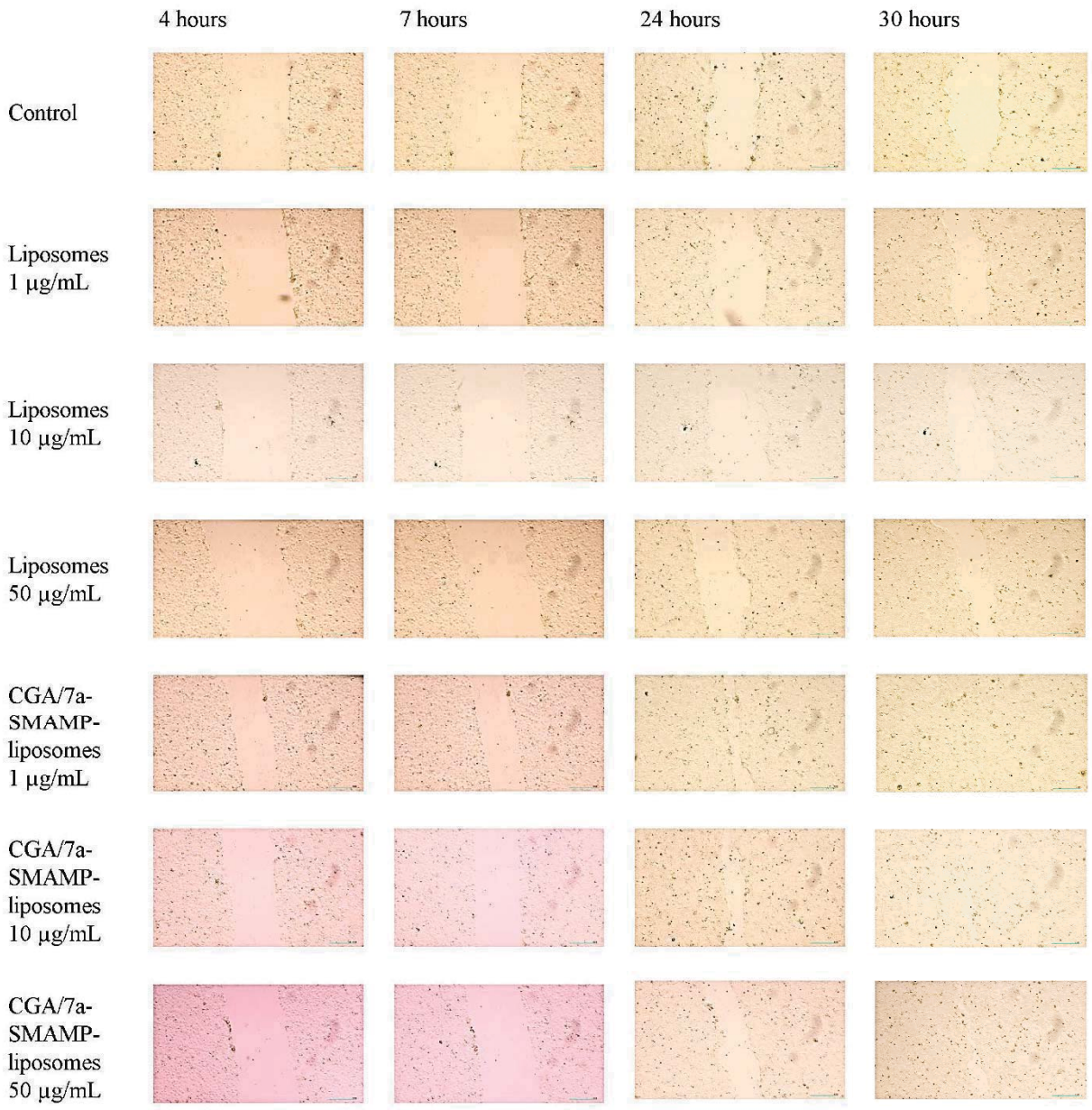

Figure S2. Scratch assay depicting the migration of HaCaT cells after treatment with liposomes or CGA/7a-SMAMP-liposomes. The tested concentrations corresponded to 1, 10, and 50 µg/mL lipid. Control (normal) refers to cells only treated with medium. The time refers to the recording time after creation of the scratch (4, 7, 24, and 30 hours).

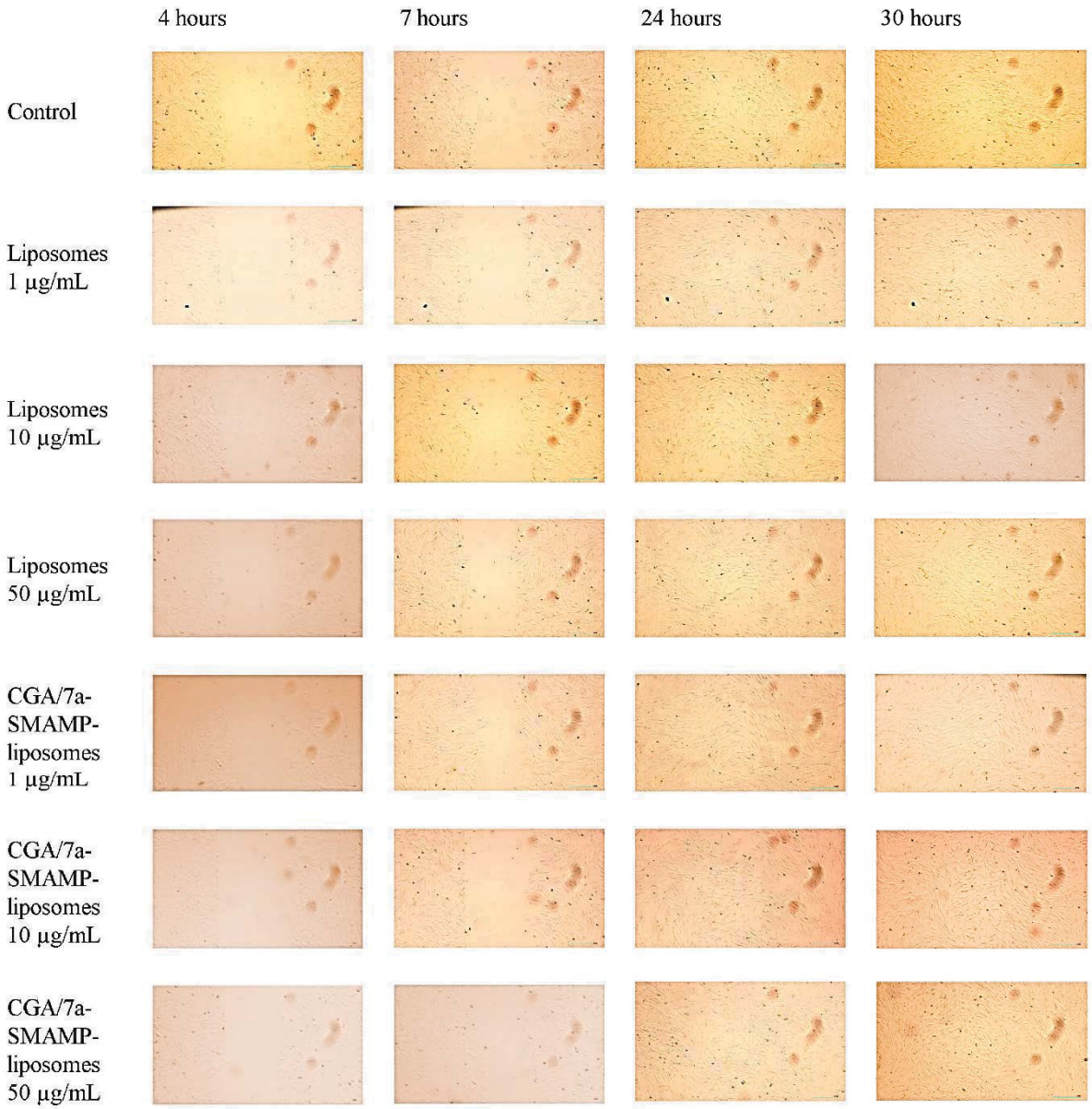

Figure S3. Scratch assay depicting the migration of HDF-neo cell after treatment with liposomes or CGA/7a-SMAMP-liposomes. The tested concentrations corresponded to 1, 10, and 50 µg/mL lipid. Control (normal) refers to cells only treated with medium. The time refers to the recording time after creation of the scratch (4, 7, 24, and 30 hours).

S3.1 Supplementary references

Paulsen, M.H., Engqvist, M., Ausbacher, D., Anderssen, T., Langer, M.K., Haug, T., Morello, G.R., Liikanen, L.E., Blencke, H.-M., Isaksson, J., Juskewitz, E., Bayer, A., Strøm, M.B., 2021. Amphipathic Barbiturates as Mimics of Antimicrobial Peptides and the Marine Natural Products Eusynstyelamides with Activity against Multi-resistant Clinical Isolates. J. Med. Chem. 64, 11395-11417. doi: https://doi.org/10.1021/acs.jmedchem.1c00734.